University of Southampton
Faculty of Medicine

MicroRNAs in Osteoarthritis and Chondrogenesis

Emma Budd

Thesis for the degree of Doctor of Philosophy
August 2016

Supervised by Professor Richard Oreffo and Dr Tilman Sanchez-Elsner

Institute of Developmental Health,
Bone and Joint research group,
University of Southampton

Abstract

Loss of chondrocytes along with diminishment of specialised extracellular matrix (ECM) is often the outcome of articular cartilage injury and can progress to the onset of osteoarthritis (OA). OA is typically seen as an age related disease and with the changing world demographic, the fastest growing age category is the elderly population. Cartilage injury, which may result in OA, results in the clinical requirement for replacement of degenerated tissues and with an ageing population the demand for clinical replacement of degenerated tissue is set to dramatically increase posing socio-economic burdens. MicroRNAs are a class of small non-coding single stranded RNA which regulate gene expression post transcriptionally. MicroRNAs could be directly administered to articular cartilage, having direct effect upon resident articular chondrocytes, as a form of treatment for cartilage injury and OA. Exogenous microRNAs could be used in combination with isolated skeletal stem cells and transplanted to defective articular sites to induce articular cartilage regeneration. The identification and function of dysregulated microRNAs in OA and identification of microRNAs which govern chondrogenic differentiation may help the development of novel strategies to enhance cartilage formation and possibly in the treatment of cartilage injury and OA.

The work in this thesis has looked to identify if specific microRNAs are dysregulated in OA. Specifically the expression of miR-146b in human OA articular chondrocytes was investigated. MiR-146b shares close sequence homology to miR-146a and was hypothesised to exhibit similar expression in OA chondrocytes and be receptive to IL-1β stimulation. Using TaqMan qPCR, the expression of miR-146b-5p was found to be significantly up-regulated in human articular OA chondrocytes, with a fold change of ~123. Treatment of human chondrocytes with pro-inflammatory IL-1β did not induce miR-146b up-regulation, but did induce miR-146a up-regulation. Specific microRNAs were also hypothesised to be involved with chondrogenic differentiation of human stem cells. Specifically, miR-34a was hypothesised to target specific chondrogenic associated genes in human fetal femur-derived cells and miR-146b was hypothesised to target chondrogenic associated genes in human bone marrow derived skeletal stem cells.

Skeletal stem cell chondrogenic differentiation can be conducted *in vitro* with the use of chemical cues and a three dimensional micromass culture system. Despite the identification that miR-34a was found to be significantly up-regulated during chondrogenic differentiation of fetal femur-derived cells, no effect was observed following modulation of miR-34a levels on the selected predicted mRNA target; *TGIF2*. MiR-146b was found to be significantly down-regulated during chondrogenic differentiation of human bone marrow derived skeletal stem cells and both *SMAD4* and *SOX5* were identified as predicted targets of miR-146b. Overexpression of miR-146b resulted in the significant down-regulation of SOX5. SOX5 is required for early chondrogenic differentiation. MiR-146b is suggested to be down-regulated during chondrogenesis to prevent the inhibitory effects upon SOX5 expression. Future studies to modulate anti-chondrogenic miR-146b through stable transfection and future *in vivo* studies will assess the ability of miR-146b to modulate chondrogenic differentiation *in vivo*.

Identification of miR-146b, which was shown to display dysregulated expression in human OA articular chondrocytes, could be used as a potential therapeutic target in the future, as a potential anti-inflammatory therapeutic. Identification of miR-146b down-regulation during the chondrogenic differentiation of human bone marrow derived skeletal stem cells may enable the potential use of miR-146b modulation in combination with skeletal stem cell therapy to induce articular cartilage regeneration at articular cartilage defect sites, which may prevent to the onset of OA.

Contents

List of Figures

List of Tables

Author's Declaration

I, Emma Budd

Declare that this thesis and the work presented in it are my own and has been generated by me as the result of my own original research.

MicroRNAs in Osteoarthritis and Chondrogenesis

I confirm that:

1. This work was done wholly or mainly while in candidature for the research degree at this University;
2. Where any part of this thesis has previously been submitted for a degree or any other qualification at this University or any other institution, this has been clearly stated;
3. Where I have consulted the published work of others, this is always clearly attributed;
4. Where I have quoted from the work of others, the source is always given. With exception of such quotations, this thesis is entirely my own work;
5. I have acknowledged all main sources of help;
6. Where the thesis is based on work done by myself jointly with others, I have made clear exactly what was done by others and what I have contributed myself;
7. None of this work has been published before submission.

Signed……..

Date…06/09/2016….

Acknowledgements

I would like to thank my supervisors Professor Richard Oreffo and Dr Tilman Sanchez-Elsner for giving me the opportunity to undertake my doctoral research at the University of Southampton. I am extremely grateful for the time you have taken to support me with my work and also sharing your academic expertise.

Many thanks to various members of the Bone and Joint research group, including Julia Wells, Stef Inglis, Carol Roberts, Kate Wright and Janos Kanczler for the organisation and training given at the beginning of my doctoral research and the laboratory support throughout the three years. I would also like to thank Dr May De Andreas Gonzalez for sharing with me much of her expertise on osteoarthritis and molecular biology.

I am immensely grateful for the full support that my family has given to me across the last four years. From the doctoral interview process right through to completion of my doctoral thesis, with your complete understanding, moral and financial support I have been able to complete my doctoral research, for which I am eternally thankful.

Nomenclature

2D	Two-dimensional
3D	Three-dimensional
AA	Attendance allowance
ACI	Autologous chondrocyte implantation
ACL	Anterior cruciate ligament
ACVR2A	Activin A type II receptor
ACVR2B	Activin A receptor type 2 B
ADAM17	Disintegrin and metalloproteinase domain-containing protein 17
ADAMTS	A disintegrin and metalloproteinase with thrombospondin motifs
ADAMTS4	A disintegrin and metalloproteinase with thrombospondin motifs 4
ADAMTS5	A disintegrin and metalloproteinase with thrombospondin motifs 5
AGCAN	Aggrecan
ALP	Alkaline phosphatase
AP-1	Activator protein 1
APA	Alternative polyadenylation
APC	Adenomatous polyposis coli
AREs	Adenylate-uridylate (AU)-rich elements
BCA	Bicinchoninic acid
BCL2	B cell lymphoma 2
BMP	Bone morphogenetic protein
BMP2	Bone morphogenetic protein 2
BMP7	Bone morphogenetic protein 7
BMPR	Bone morphogenetic protein receptor
BSA	Bovine serum albumin
CARD10	Caspase recruitment domain-containing protein 10
CARD11	Caspase recruitment domain-containing protein 11
CARD8	Caspase recruitment domain-containing protein 8
CASP-10	Caspase 10
CASP-7	Caspase 7
CASP-9	Caspase 9
Cat	Catalytic domain
CAT1	Cationic acid transporter 1
Cbfa-1	Core-binding factor alpha 1
CCL2	Chemokine (C-C motif) ligand 2
CCL5	Chemokine (C-C motif) ligand 5
CCN2	Connective tissue growth factor

CD28	Cluster of differentiation factor 28
CD40	Cluster of differentiation factor 40
CD80	Cluster of differentiation factor 80
CD86	Cluster of differentiation factor 86
CDK	Cyclin dependent kinase
CDK4	Cyclin dependent kinase 4
CDK6	Cyclin dependent kinase 6
cDNA	Complimentary deoxyribonucleic acid
CFU-F	Colony forming unit- fibroblastic
CHRDL1	Chordin like 1
COL2A1	Collagen, type II, alpha I
COL9A1	Collagen, type IX, alpha 1
COX-2	Cyclooxygenase-2
CPC	Cardiac progenitor cells
CpG	-C-phosphate-G- (Cytosine-phosphate-Guanine)
Cx43	Connexion 43
CXCL12	Stromal cell-derived factor 1
DAAM1	Dishevelled associated activator of morphogenesis 1
DAMPs	Danger associated molecular pathogens
DAPI	4’,6-diamidino-2-phenylindole
Dex	Dexamethasone
DLA	Disability living allowance
DLL4	Delta-like ligand 4
DNA	Deoxyribonucleic acid
DND1	Dead end protein 1
DNMT	Deoxyribonucleic acid methyltransferases
DNPEP	Aspartyl Aminopeptidase
DSH	Dishevelled
DTT	Dithiothreitol
ECL	Enhanced chemiluminescence
ECM	Extracellular matric
Edu	5-ethyl-2’-deoxyuridine
EGR	Epidermal growth factor
ERK	Extracellular signal regulated kinase
FAF1	FAS associated factor 1
FAK	Focal adhesion kinase
FBS	Fetal bovine serum
FCS	Fetal calf serum

FGF	Fibroblast growth factor
FOXO3A	Forkhead box O3
FOXP1	Forkhead box protein P1
FRS2	Fibroblast growth factor receptor substrate 2
GAG	Glycosaminoglycan
GPR75	G-protein coupled receptor 75
Grb2	Growth factor receptor bound protein
GSK-3β	Glycogen synthase kinase 3 beta
H_2O	Water
HA	Hydroxyapatite
HATs	Histone acetyltransferases
HBMSC	Human bone marrow derived stem cell
HDACs	Histone deacetylases
HIF3A	Hypoxia inducible factor 3 alpha
HK	Human keratinocytes
HLA class I	Human leukocyte antigen class I
HLA class II	Human leukocyte antigen class II
HLA	Human leukocyte antigen
HMTs	Histone methyl transferases
Hpx	Hemopexin chemoattractant protein
HRP	Horseradish peroxidase
HuR	Human antigen R
IFNAR1	Interferon alpha/beta receptor 1
IFN-γ	Interferon gamma
IGF	Insulin-like growth factor
iHEP	Induced hepatocytes
Ihh	Indian hedgehog
IL-10	Interleukin 10
IL-18	Interleukin 18
IL-1Ra	Interleukin 1 receptor antagonist
IL-1RAcP	Interleukin 1 receptor accessory protein
IL-1RI	Type I Interleukin 1 receptor
IL-1RII	Type II Interleukin 1 decoy receptor
IL-1β	Interleukin 1 beta
IL-6	Interleukin 6
iNOS	induced nitric oxide synthase
IRAK1	Interleukin 1 receptor associated kinase 1
IRAK4	Interleukin 1 receptor associated kinase 4

IRF5	Interferon regulatory factor 5
ITS	Insulin-Transferrin-Selenium
JAK	Janus kinase
JNK	c-Jun N-terminal kinase
lnRNAs	Long non-coding RNAs
LRP	Low density lipoprotein receptor related protein
MACS	Magnetic activated cell sorting
MALT1	Mucosa-associated lymphoid tissue lymphoma translocation protein 1
MAPK	Mitogen activated protein kinase
MCP	Monocyte chemoattractant protein
MCPIP1	Monocyte chemotactic protein-1-induced protein-1
MCSF	Macrophage-colony stimulating factor
MDM2	Mouse double minute 2 homolog
MEK1	Mitogen activated kinase kinase 1
MH1	MAD homology 1
MHC	Major Histocompatibility complex
MIP-1α	Macrophage inflammatory protein
miRNA	MicroRNA
MMP	Metalloproteinase
MSM	Methylsufonylmethane
NATs	Natural antisense transcripts
NC	Negative control
NF-κB	Nuclear factor kappa-light-chain-enhancer of activated B cells
NHS	National Health Service
NO	Nitric Oxide
NOF	Neck of Femur
NSAIDs	Non-steroidal anti-inflammatory drugs
OA	Osteoarthritis
P/S	Penicillin/Streptomycin
P38 MAPK	p38 mitogen activated protein kinase
PBS	Phosphate buffered saline
PCL	Posterior cruciate ligament
PFA	Paraformaldehyde
PGE_2	Prostaglandin E2
PI3K	Phosphatidylinositol 3 kinase
PK3	Protein kinase 3
PPAR γ	Peroxisome proliferator-activated receptor gamma
PRG2	Proteoglycan 2

PRMTs	Protein arginine methyltransferases
PTGS1	Prostaglandin G/H synthase 1 or cyclooxygenase-1
PTH	Parathyroid hormone
PTHrP	Parathyroid hormone related peptide
PVDF	Polyvinylidene fluoride
RA	Rheumatoid arthritis
RAC1	Ras-related C3 botulinum toxin substrate 1
RALA	Ras related protein Rel-A
RANTES	Regulates on activation, normal T expressed and secreted
RBPs	RNA binding proteins
RHOA	Ras homolog gene family, member A
RISC	Ribonucleic acid induced silencing complex
ROCK1	Rho-associated, coiled-coil containing protein kinase 1
RUNX2	Runt related transcription factor 2
SBE	Sterol binding element
SDS	Sodium dodecyl sulphate
SDS-PAGE	Sodium dodecyl sulphate-polyacrylamide gel electrophoresis
SEC	Synovio-entheal complex
SIRT1	NAD-dependent deacetylase sirtuin-1
SMAD2	Mothers against decapentaplegic homolog 2
SMAD3	Mothers against decapentaplegic homolog 3
SMAD4	Mothers against decapentaplegic homolog 4
SMAD7	Mothers against decapentaplegic homolog 7
snoRNAs	Small nucleolar RNAs
SOS	Son of sevenless protein
SOX	Sex determining region Y related HMG box
SOX5	Sex determining region Y (SRY)-Box 5
SOX6	Sex determining region Y (SRY)-Box 6
SOX9	Sex determining region Y (SRY)-Box 9
SREBP1	Sterol regulatory element binding transcription factor 1
SSC	Skeletal stem cell
STAT	Signal transducer and activator of transcription
TANK	TRAF family member-associated NF-κB activator
TCP	Tri-calcium phosphate
TGF-β	Transforming growth factor beta
TGIF2	Transforming growth factor-beta-induced factor 2
TIFA	TRAF interacting protein with forkhead associated domain
TIMPs	Tissue inhibitors of metalloproteinases

TIRAP	Toll/interleukin 1 receptor domain containing adaptor protein
TLR4	Toll-like receptor 4
TLR8	Toll-like receptor 8
TNF-α	Tumour necrosis factor alpha
TRAF2	TNF receptor associated factor 2
TRAF6	TNF receptor associated factor 6
TuD	Tough Decoy
UDPGD	Uridine diphosphate-glucose dehydrogenase
UK	United Kingdom
UTR	Untranslated region
VEGF	Vascular endothelial growth factor
Wnts	Wingless-int family members
YLD	Years lived with disability
YY1	Yin Yang 1
α-MEM	Minimum essential medium eagle, alpha modification
β-actin	Beta actin
β-catenin	Beta catenin

Chapter 1.1
Introduction
Articular Cartilage; function, structure and disease

1.1.1 Cartilage

Cartilage can be defined as a connective tissue made up of a matrix of predominantly collagen fibres along with elastin fibres and accompanied by several differing specialised proteoglycans which reside within the ECM. The chondrocyte is the cell responsible for synthesising the cartilage matrix. Cartilage is part of the skeletal system, an important organ which has several fundamental functions. Cartilage can be sub-categorised into three types of cartilage; elastic, hyaline and fibrocartilage cartilage and each type is determined by the differing amounts of the three main components; collagenous fibres, proteoglycans and elastin. Elastic cartilage is flexible and as the name suggests is elastic, as a result of dense mesh works of elastic fibres located between typical ECM arrangements. Elastic cartilage is found in the Eustachian tubes, external auditory canal and pinna of the ear and epiglottis. Fibrocartilage has densely packed collagen fibres with little ECM making it resilient and strong and is found in the meniscus of the knee, the intervertebral disks of the spine and covers the mandibular condyle of the temporomandibular joint [1].

The most common cartilage in the body; hyaline cartilage comprises, a mesh work of thin collagen fibres together with proteoglycan complexes. Collagen provides the cartilage with tensile strength and the proteoglycan complex is able to bind water therefore making it fluid and resistant to compressive forces. Thus cartilage is ideal for absorbing shock at the surfaces of moveable joints. Hyaline cartilage is found in the nose, within the walls of the trachea and larynx, anterior parts of the ribs and at the articular surface of bones; forming part of the synovial joint. In addition to the role that cartilage plays in the adult skeleton, hyaline cartilage forms the cartilage anlage during fetal skeletal development. Hyaline cartilage present within fetal long bone development undergoes endochondral ossification at the primary ossification centre, a process in which the chondrocytes undergo hypertrophic differentiation in order to induce bone formation. Additionally, hyaline cartilage is present at the epiphyseal growth plate in long bones, which induces longitudinal lengthening of long bones through endochondral ossification until bone maturity is reached [1] [2].

1.1.1.1 Articular cartilage function, structure and composition

Hyaline cartilage located at the articular surfaces of bone is commonly referred to as articular cartilage. Articular cartilage is essential for proper functioning of the skeleton, enabling load bearing and shock absorbance as well as near frictionless movement preventing bone deterioration [1]. Articular cartilage is viscoelastic and biphasic; collagens, proteoglycans and non-collagenous proteins comprise the solid phase and high water content which confers the fluid phase. Interaction of the solid and fluid phase is critical for the biochemical properties of articular cartilage [3]. Cartilage does not contain blood vessels, lymphatics or nerves and cells receive nutrients and oxygen by means of diffusion. Due to the lack of blood vessels in this specialised connective tissue, cartilage is slow growing and repairs slowly [2]. Articular cartilage at the synovial joint interface is comprised of articular chondrocytes which maintain a stable phenotype and do not undergo hypertrophy, calcification or apoptosis. The mechanisms which govern the articular chondrocyte in maintaining this phenotype remain unknown.

Articular cartilage comprises of four zones (Figure 1); the superficial zone which is the outermost layer which is in contact with the synovial fluid within the synovial joint space, the middle zone, the deep zone and the calcified zone which resides next to the subchondral bone [4]. The outermost superficial zone comprises approximately 10-20% of the articular cartilage thickness and protects the other layers from shear, compressive and tensile stress induced by joint articulation and is composed predominantly of type II and type IX collagen. The middle transitional zone which is located beneath the superficial zone comprises 40-60% of the articular cartilage thickness, providing the connection to the deep zone. Approximately 30% of articular cartilage thickness is composed of the deep zone which provides the highest resistance to compressive forces. The deep zone contains the lowest water content and the highest proteoglycan content, and thickest collagen fibrils. The deep zone can be distinguished from the deepest calcified zone through the presence of the tide mark. The calcified zone contains hypertrophic chondrocytes and the collagen fibrils located in the deep zone are connected to subchondral bone. The four distinct zones of articular cartilage are organised differently. The superficial zone contains tightly packed collagen fibres, parallel to the articular surface and also contains flattened chondrocytes. The middle zone contains thicker collagen fibrils which are arranged diagonally, with a low density of chondrocytes spherical in shape. The thickest collagen fibrils of the deep zone are organised perpendicular to the articular surface, with chondrocytes arranged in a parallel manner to the collagen fibres [4].

In addition to the presence of each zone within articular cartilage, each zone contains three distinct regions in proximity to chondrocytes which differ by matrix composition, known as the pericellular, territorial and inter-territorial regions (Figure 1). The pericellular region comprised of matrix is directly in contact with the chondrocyte membrane and contains predominantly proteoglycans. The territorial region completely surrounds the pericellular matrix region and contains predominantly fine collagen fibrils and is speculated to protect chondrocytes from mechanical stress. The inter-territorial

region is the largest matrix region and contains collagen fibrils and abundant proteoglycans and confers the biomechanical properties of the articular cartilage [4].

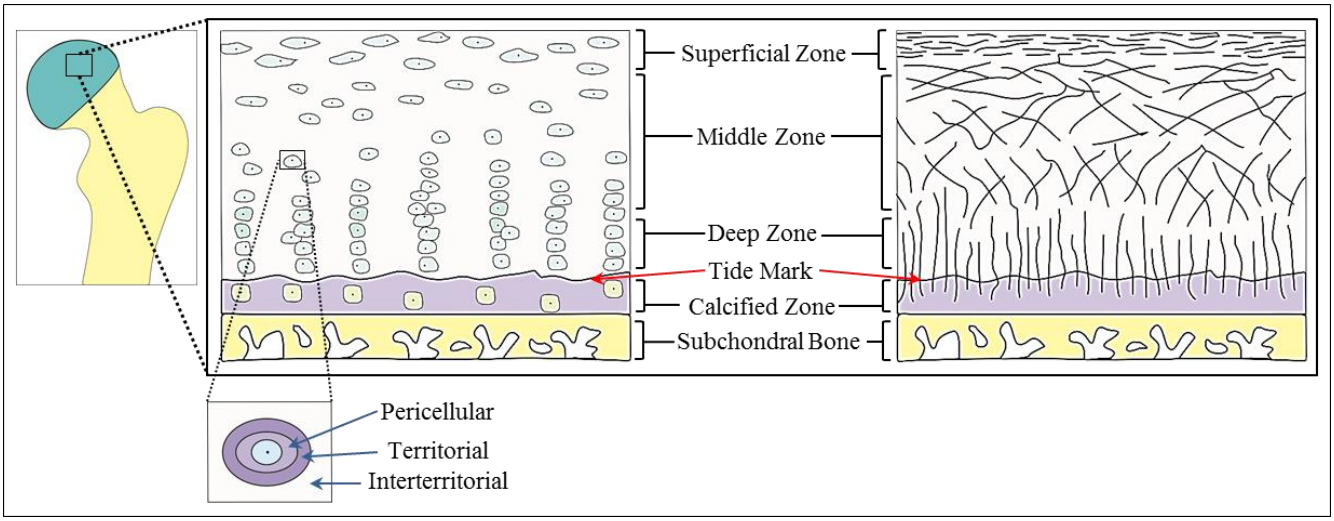

Figure 1. Articular cartilage zones and compartments. Articular cartilage located at the ends of long bones, for example the femoral head, is organised into zones. The superficial zone contains small and flattened chondrocytes and collagen fibrils aligned parallel to the surface. The middle zone contains rounded chondrocytes which are randomly orientated. The deep zone contains chondrocytes which are grouped in columns. The collagen fibrils aggregate into larger bundles in the middle and deep zones and are aligned more perpendicular to the surface. The articular cartilage is also organised into pericellular, territorial and inter-territorial compartments with respect to the location of chondrocytes. (Figure adapted from Buckwater *et al*, Restoration of Injured or Damaged Articular Cartilage, Journal of the American Academy of Orthopaedic Surgeons- July/August 1994 - Volume 2 - Issue 4 - p 192–201)

Despite the significant role chondrocytes play in articular cartilage homeostasis, only 10% of the total volume of cartilage is occupied by chondrocytes [3]. The predominant function of chondrocytes is in the development and maintenance of the specialised cartilage ECM, critical for articulation of the skeleton. Chondrocytes are located within the pericellular region within the specified zone of articular cartilage and are metabolically active, controlling ECM turnover. The space occupied by chondrocytes is referred to as lacunae. The size, shape and number of chondrocytes is dependent upon the zonal region that chondrocytes are located within in the articular cartilage [4].

Chondrocytes do not participate in cell-cell communication but are, however, receptive to other stimuli, such as mechanical sensing, hydrostatic pressures, soluble mediators such as growth factors and piezoelectric forces. Chondrocytes cannot migrate and therefore cannot move to damaged areas following injury and have a limited capacity for replication. Currently chondrocyte survival is dependent upon an optimal mechanical and chemical environment, an imbalance is likely to induce aberrant chondrocyte signalling and ultimately cartilage degradation [4].

80% of the wet weight of articular cartilage is water, with approximately 30% of the water being associated with collagen intrafibrillar space, a small proportion located within chondrocytes and the largest remaining proportion contained in the ECM molecular pore space [4], [3]. The presence of water in the articular joint is essential in conferring articular cartilage properties and also for the transportation and distribution of nutrients required by chondrocytes, by means of diffusion from the synovial fluid. The most abundant macromolecule in the ECM is collagen, with the dry weight of articular cartilage consisting of approximately 60% collagen. 90-95% of the collagen found within the articular cartilage is type II collagen. Other collagens present in low abundance include collagen type I, IV, V, IX and XI [4]. Three polypeptide chains, known as alpha chains, form a tripe helix comprising collagen. The variation in amino acid sequence of the alpha chain determines the different properties of different types of collagen. Type II collagen found in articular cartilage is a homotrimeric molecule which consists of collagen fibrils which are made up of tropocollagen consisting of three α1 chains [5].

Type II collagen is synthesised by chondrocytes and given the abundance of type II collagen in articular cartilage, type II collagen serves as a marker for chondrocyte health and also an indication of differentiation of stem cells to chondrocytes during hyaline cartilage development. Collagen synthesis involves several steps, illustrated in Figure 2. Following transcription and translation of appropriate alpha chains, pre-pro-peptide formation ensues. The N terminal of the peptide sequence contains a signal sequence recognised by the endoplasmic reticulum; where it is directed to for post-translational processing. Post-translational processing includes three modifications to the pre-pro-peptide; the signal on the N terminus is dissolved, hydroxylation of prolines and lysines produces hydroxyproline and hydroxylysine which aids with cross linking of alpha peptides and glycosylation of hydroxyl group of the hydroxylysines. Hydroxylation and glycosylation enables the pro-peptide to twist tightly and allow for the formation of a triple helix by addition of two more pro-peptides forming procollagen, consisting of a twisted centre and loose ends on each side of the centre. After transportation to the golgi apparatus where oligosaccharides are added, procollagen is secreted from the cell. Membrane bound enzymes cleave the loose ends of the procollagen molecule forming tropocollagen. In the ECM, lysyl oxidase oxidises the lysines and hydroxylysines to induce covalent bonding between tropocollagen molecules resulting in the formation of a collagen fibril [5].

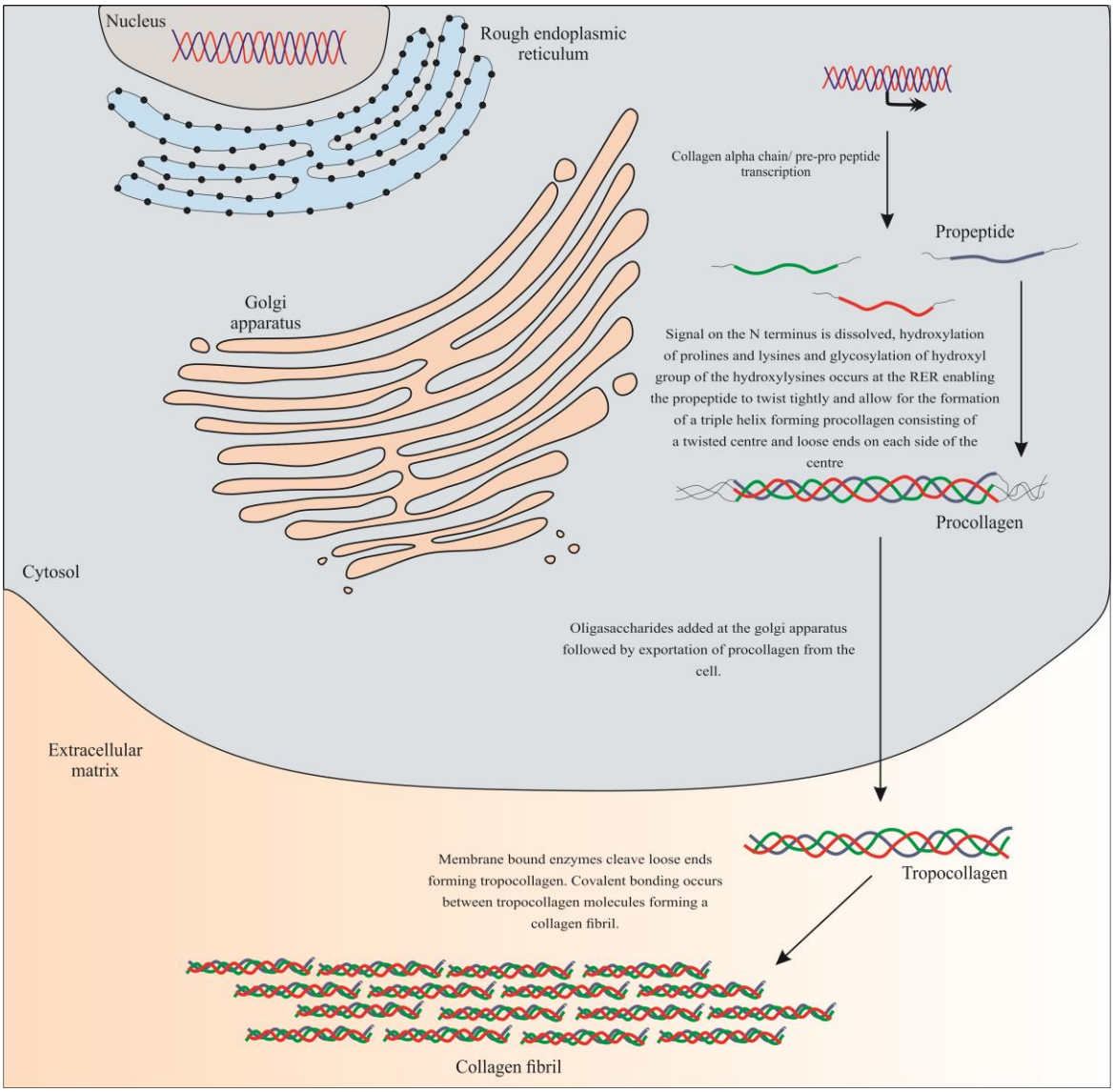

Figure 2. Collagen synthesis. The process by which collagen is synthesised involving the formation of a procollagen from three pro-peptides. Procollagen undergoes various translation modifications steps before exportation from the cell. Collagen peptidases on the cell surface cleave the loose ends of procollagen forming tropocollagen. Covalent bonding between tropocollagen molecules creates a collagen fibril. (Figure adapted from Myllyharju and Kivirikko, Collagens, modifying enzymes and their mutation from human, flies and worms, Trends in Genetics, doi:10.1016/j.tig.2003.11.004).

The presence of collagens in articular cartilage and the cross-linking of collagen fibrils, particularly type II collagen, provide tensile strength and stiffness. Collagens can entrap proteoglycans, which enable proteoglycan aggregates to remain intact under compression [6]. Mutation of the *COL2A1* gene encoding the collagen type II, alpha 1 chain which forms a homotrimeric molecule with two additional alpha 1 chains to ultimately from type II collagen, highlights the importance of type II collagen. Hypochondroplasia, achondrogenesis, Kniest syndrome, Stickler syndrome and spondyloepiphyseal dysplasia congenital are skeletal dysplasias which result due to mutations in the *COL2A1* gene [7].

Approximately 10-15% of the wet weight of articular cartilage is comprised of proteoglycans which make up the second largest group of macromolecules in the ECM. Glycosylated protein monomers; proteoglycans are synthesised by chondrocytes. A central protein core is covalently attached to linear glycosaminoglycan (GAG) side chains. A single GAG is comprised of repeating disaccharide units which contain either a negatively charged carboxylate or sulphate group. The negative charged GAG side chains repel other negatively charged GAG side chains creating proteoglycans with expanded side chains which do not interact, which causes proteoglycans to be easily entrapped in the collagen framework. Large osmotic swelling pressure is created by high concentrations of proteoglycans, which induces water to move into the ECM as a result of the presence of the negatively charged GAG side chains and mobile counter ions such as Na^+, which creates differences in ion concentration between the articular cartilage and the surrounding tissue. Water diffuses into the articular cartilage as a result of the osmotic imbalance and the inability of proteoglycans such as aggrecan to move within the matrix and redistribute, the presence of water induces expansion [8]. The anionic property of proteoglycans and the resultant presence of water provide resistance to compression. The presence of several proteoglycans within the articular cartilage include aggrecan, decorin, fibromodulin and biglycan [4]. The proteoglycan aggrecan (Figure 3) is the most abundant proteoglycan in articular cartilage and many aggrecan molecules can bind through the presence of link protein to a hyaluronan chain creating large aggregates. The central core protein of aggrecan has 100-150 GAG side chains which are predominantly chondroitin or dermatan sulphate [8].

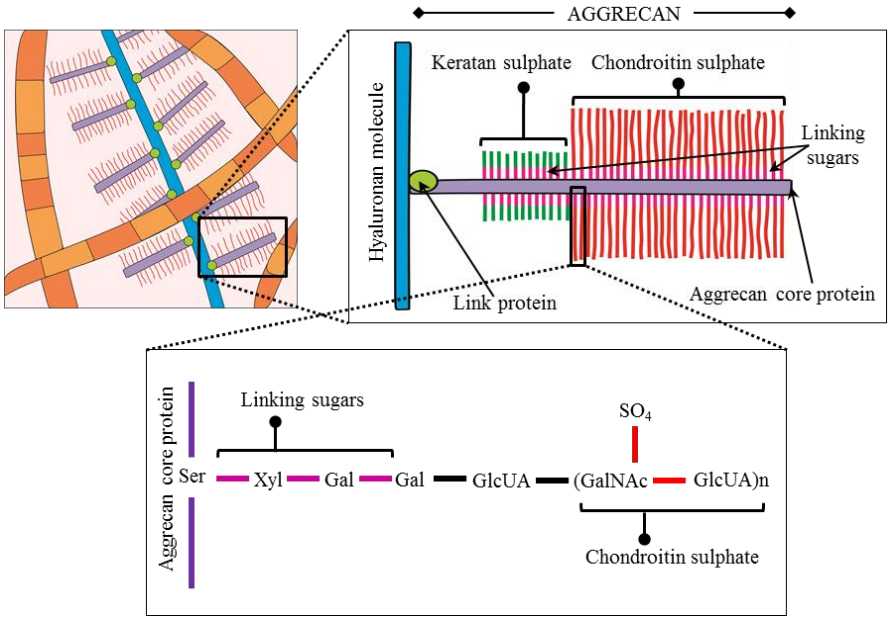

Figure 3. Structure of Aggrecan. Proteoglycan aggregates such as aggregates of aggrecan are entrapped in the collagen fiber network. A single aggrecan molecule binds to hyaluronan and is composed of a central core protein and sulphated glycosaminoglycan (GAG) side chains including keratin sulphate and chondroitin sulphate. The negatively charged glycosaminoglycan side chains induce repulsion against neighbouring molecules and attract water. (Figure adapted from Aspberg, The different roles of aggrecan interaction domains, J Histochem Cytochem 2012; 60(12):987–96, doi: 10.1369/0022155412464376)

1.1.1.2 Long bone formation, synovial joint formation and articular chondrocyte differentiation

Articular cartilage allows for near frictionless articulation of limbs and is formed during fetal synovial joint formation. The process of fetal long bone formation (Figure 4 & Figure 5) is distinct from synovial joint formation (Figure 6), both processes essential for limb development and articulation in adult life. Fetal skeletal development proceeds by skeletal morphogenesis and skeletogenesis, resulting in skeletal formation in vertebrates which occur during embryogenesis from mesodermal sources. Skeletal morphogenesis is the process during the embryonic phase by which the skeletal anatomical structure is generated and organised [9]. The first stage of skeletal development is the migration of mesenchymal cells derived from the sclerotomes, lateral plate mesoderm or neural crest, followed by mesenchymal condensation whereby mesenchymal stem cells accumulate to areas of future skeletal locations in high density and condense into mesenchymal precursors of cartilage or bone [10]. When and where the mesenchymal cells condense is determined by early patterning events. The majority of genes that are involved in skeletal morphogenesis encode transcription factors (Figure 5) which regulate migratory and cellular determination events [10].

Long bone formation is a distinct process from synovial joint formation. The long bones of the appendicular and axial skeletons form through endochondral ossification, illustrated below in Figures 4 and 5. Endochondral bone formation requires the proliferation and hypertrophy of differentiated chondrocytes which provide a template for perspective bone [11]. Long bone elongation proceeds due to the location of differentiated chondrocytes in distinct zones along the longitudinal axis. In the centre of mesenchymal condensation, what will become the primary ossification centre, mesenchymal cells differentiate into chondrocytes and at the periphery of the condensations the perichondrium is formed by undifferentiated cells. The bone collar is formed as a result of the differentiation of perichondrial cells into osteoblasts at the same time as chondrocyte hypertrophy occurs [12]. *ColII* is expressed by proliferating, differentiating chondrocytes, when proliferation ceases chondrocytes enlarge and *ColX* is expressed, indicating that chondrocytes have become hypertrophic. The surrounding matrix of hypertrophic chondrocytes is mineralized, osteoclasts are derived from the haematopoietic lineage which invade and reabsorb the calcified matrix produced by hypertrophic chondrocytes. Following resorption by osteoclasts, osteoblast differentiation occurs in the area to form a layer of woven bone above the remaining cartilage; initiation of the formation of the primary spongiosa occurs due to vascularization and invasion of osteoblasts into the cartilage [13]. It is hypertrophic chondrocytes that signal to perichondrial cells which induces progenitor cell differentiation into osteoblasts. Away from the border of cartilage and primary spongiosa proliferation of round chondrocytes continues to occur, the chondrocytes then flatten out forming columns of proliferating cells, after these cells have ceased proliferating, they enlarge. An increase in synthesis of chondrocyte matrix, the increase in number of chondrocytes and the size of chondrocytes result in bone lengthening. Interstitial growth is responsible for long bone growth.

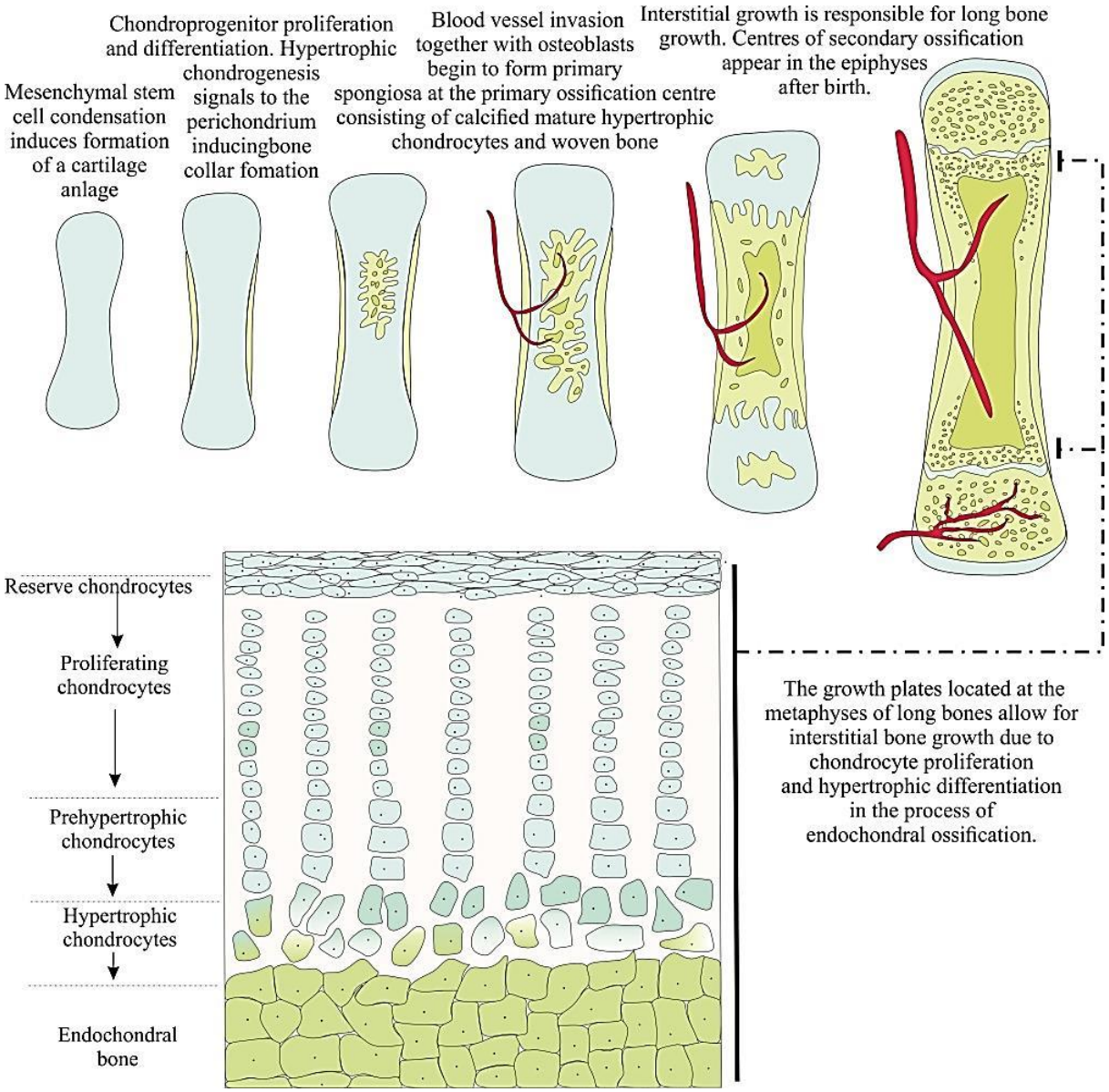

Figure 4. Endochondral bone formation in long bones. The process begins with the condensation of stem cells resulting in the formation of a cartilage anlage followed by chondrogenic differentiation to produce prehypertrophic and hypertrophic chondrocytes which produce Ihh, which induces osteoblast differentiation at the perichondrium resulting in formation of the bone collar. Blood vessel invasion together with osteoblasts begin to form primary spongiosa at the primary ossification centre consisting of calcified mature hypertrophic chondrocytes and woven bone. (Figure adapted from Richette *et al*, Achondroplasia: From genotype to phenotype, Joint, spine, bone, doi:10.1016/j.jbspin.2007.06.007).

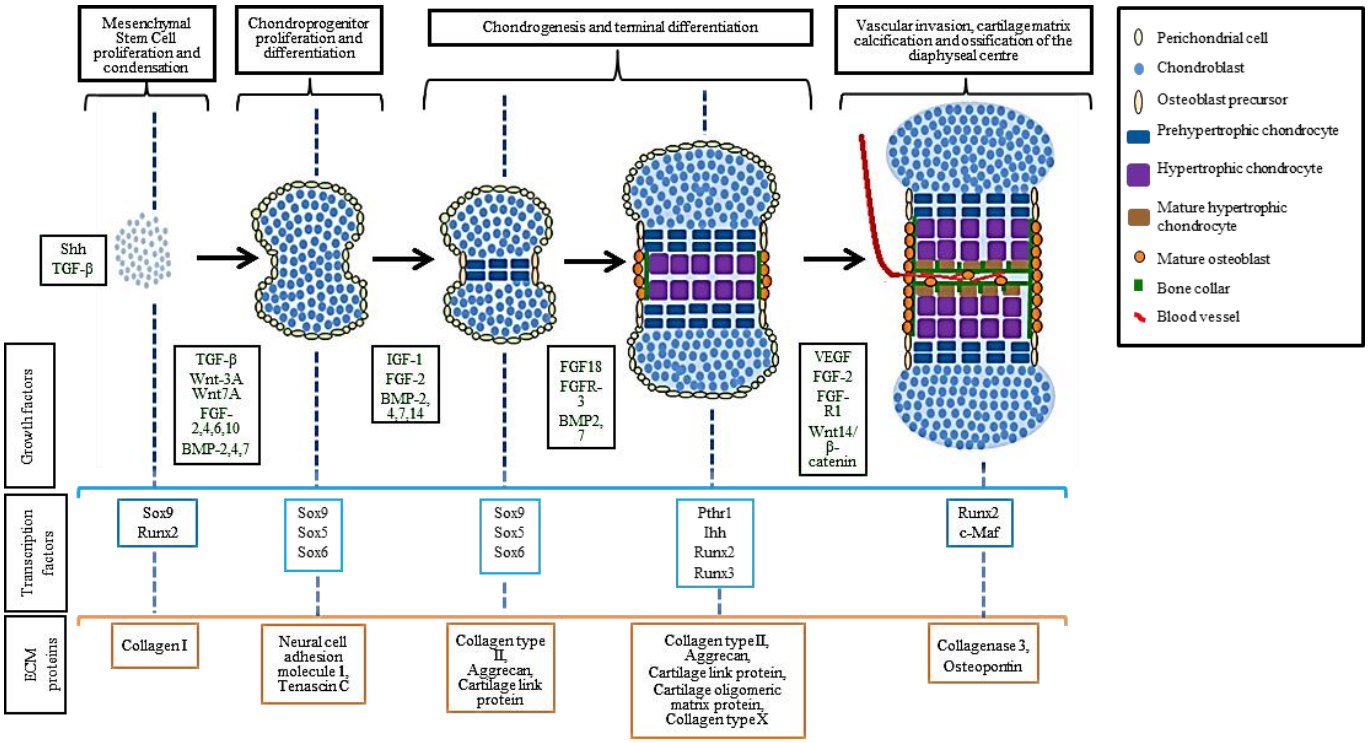

Figure 5. Endochondral bone formation in long bones. Condensation of stem cells results in the formation of a cartilage anlage followed by chondrogenic differentiation to produce prehypertrophic and hypertrophic chondrocytes which produce Ihh, which induces osteoblast differentiation at the perichondrium resulting in formation of the bone collar. Blood vessel invasion together with osteoblasts begin to form primary spongiosa at the primary ossification centre consisting of calcified mature hypertrophic chondrocytes and woven bone. Throughout the process of endochondral ossification a number of key growth factors are present at the differing stages which induce differing transcription factors which in turn induce the synthesis of differing ECM proteins. (Figure adapted from schematic of endochondral bone formation by Christine Hartmann, Transcriptional networks controlling skeletal development, DOI: 10.1016/j.gde.2009.09.001).

Formation of the arthrodial or synovial joint requires the formation of an interzone which is followed by a process known as cavitation (Figure 6). During fetal development, mesenchymal progenitor cells aggregate and condensate as a result of differing growth factors. The synovial joints within vertebrate limbs are composed of the ends of two long bones reciprocal in shape covered by articular cartilage and stabilised by peri-joint and intra-joint ligaments and encapsulated by a synovial membrane and a fibrous synovial capsule, with a synovial fluid contained joint cavity. Articular cartilage located within the synovial joint space has a complex structure, subdivided into four distinct zones, as described previously [14]. Hox genes may be responsible for the patterning mechanisms which determine the location for joint development. The first sign of joint formation is the further condensation of a high density of cells which is known as the interzone. The process of cavitation occurs within the interzone whereby a physical separation of the adjacent skeletal anlagen and the formation of the synovial space

and mesenchymal cells present in the condensations differentiate into chondrocytes and form the articular cartilage which will cover the ends of adjacent developing long bones [2] [15].

The importance of the interzone was first identified when the interzone was microsurgically removed from a prospective chick elbow joint *in ovo*, resulting in the fusion of the humerus to the radius and ulna [16]. The interzonal cells and the process of cavitation give rise to the synovial joint and all of the essential joint components. The development of the joint cavity which is filled with synovial fluid following formation is critical to limb articulation. The interzone can be divided into three layers; the central layer comprising cells in low density which is known as the central intermediate lamina and two areas on either side of the central intermediate lamina consisting of cells in high density which form the articular cartilage on corresponding long bone epiphyses. Cells which compose the central intermediate lamina eventually undergo apoptosis in the process of cavitation, creating the joint cavity [17], illustrated in Figure 6.

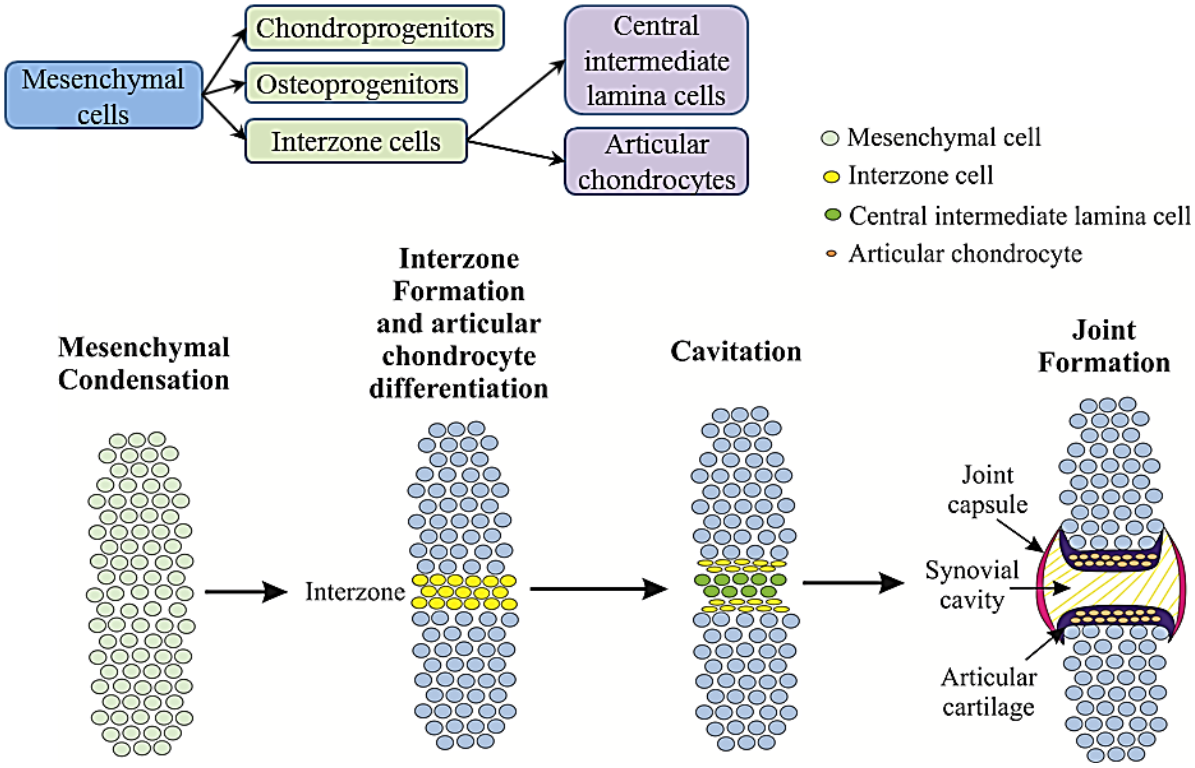

Figure 6. Interzone formation, cavitation and joint formation. Condensation of mesenchymal cells induces formation of interzone cells which can further condensate and differentiate into either articular chondrocytes or form central intermediate lamina cells. Cavitation involves apoptosis of central intermediate lamina cells and creation of the joint cavity. (Figure adapted from Pacifici and Koyama, Mechanisms of synovial joint and articular cartilage formation: Recent advances, but many lingering mysteries, Birth Defects Research Part C: Embryo Today: Reviews Volume 75, Issue 3, pages 237–248, September 2005, DOI: 10.1002/bdrc.20050)

The formation of the interzone mediates formation of the synovial joint, part of which involves the differentiation of cells into articular chondrocytes. Unlike chondrocytes within the cartilage anlage, articular chondrocyte differentiation is less well defined in terms of the molecular pathways which govern interzonal cells to differentiate into articular chondrocytes and maintain a stable phenotype which does not undergo hypertrophy. The antagonism of BMP signalling has been indicated to have a role in joint formation. The expression of *NOG* encoding Noggin, a BMP antagonist, is thought to play a role in the initial formation of the joint, in the absence of Noggin, initiation of joint development failed in mice [18]. The BMP antagonist *CHRD*, encoding chordin has also been shown to be expressed in the joint interzone. It has been speculated that antagonists of BMP signalling in the interzone may prevent BMPs from inducing endochondral ossification and therefore initiating joint formation [19]. *Wnt14* expression was identified in the interzone and overexpression of *Wnt14* resulted in the formation of a non-cartilaginous skeletal structure believed to be the interzone. *Wnt-14* is able to block chondrogenic differentiation which is likely attributable in enabling mesenchymal cells to follow down an alternative interzone differentiation pathway [20].

The expression of *Gdf-5*, which encodes growth differentiating factor 5, is present within the interzone and lack of *Gdf-5* has been shown to result in defects in the ankle, wrist and digit joints in mice [21]. Articular chondrocytes have been shown to be derived from *Gdf-5* expressing progenitor cells, while cells of the shaft and growth plate cartilage have been shown to be *Gdf-5* negative [22]. Chondrogenesis has been shown to be stimulated in chick limb mesenchymal cells treated with GDF-5 *in vitro* [23]. Pacifici *et al* propose a model whereby *Gdf-5* expression stimulates chondrogenesis of cells on the distal sides of the interzone adjacent to the prospective epiphysis thereby inducing the formation of articular cartilage [15]. Additional to the expression of *Gdf-5*, articular chondrocytes have been shown to be distinguishable from growth plate chondrocytes through the expression of *Matn1* which encode matrillin-1. Chondrocytes of the growth plate have been shown to express matrillin-1, whereas articular chondrocytes were shown not to express matrilin-1 [24]. Despite the differences in matrilin-1 expression, matrilin-1 has been shown not to be essential for skeletal or joint formation or cartilage structure [25], [26], regardless, the expression of matrilin-1 shows a distinction between the two types of chondrocytes.

TGF-β signalling has also been shown to be a critical mediator. Mice with a TGF-β signalling downstream disruption of *Smad3* resulted in loss of articular cartilage, decreased synthesis of proteoglycans and an increase in type X collagen expression indicative of hypertrophic differentiation, with an OA phenotype. TGF-β signalling acts to inhibit hypertrophic differentiation in articular chondrocytes [27]. The initial steps in chondrogenesis are shared by growth plate chondrocytes and articular chondrocytes, however, growth plate cartilage undergoes hypertrophic differentiation and articular cartilage remains permanent which lacks vasculature and hypertrophy, perhaps in the absence of BMP6 or Indian Hedgehog (Ihh) [28]. The molecular mechanisms which direct interzone cells to differentiate into articular cartilage still remain undefined. It is likely that a cascade of signalling

pathways work to induce differentiation. TGF-β signalling induces Wnt signalling, including Wnt14 up-regulation which activates GDF-5 [29]. The transcription factor SOX-9 is required for chondrocyte differentiation, Sox9 inactivation in mice limb bud mesenchymal cells prior to condensation resulted in absence of cartilage and bone, while inactivation of Sox9 following mesenchymal cell condensation resulted in a cessation of chondrogenic differentiation and defective joint formation [30].

The distinct cellular layers which comprise the interzone are defined by cell density, origin with respect to adjacent cartilage anlage which will undergo endochondral ossification and gene expression. In addition to the expression of specific genes during joint cavitation, are other factors which are believed to contribute to the process, including skeletal movement and ECM production. Osborne *et al* showed that *in ovo* immobilisation prior to joint cavitation affected interzone differentiation and induced fusion between the opposing cartilage anlagen [31]. Extrinsic stimuli are likely to be provided by mechanical influences which mediates the behaviour of interzone cells [32]. Joint cavitation also brings about changes within the ECM. A major constituent of synovial fluid is hyaluronan (HA). Joint cavitation has been proposed to be dependent in part upon the expression of hyaluronan which may mediate fluidity within the developing interzone and subsequent formation of the synovial cavity [32].

Chondrocytes which form articular cartilage are believed to be from a distinct origin and initially originate from the interzone as opposed to chondrocytes which form the cartilage anlage of prospective long bones. There are distinctive differences in the functions of the chondrocytes which are located within the shaft and growth plate which undergo proliferation, maturation and hypertrophy and apoptosis as part of the endochondral ossification process of longitudinal lengthening of bones. In comparison, chondrocytes which form the articular cartilage maintain a stable function and phenotype, mediating the production of the articular cartilage ECM in response to chemical and mechanical stimuli and do not undergo hypertrophy. The differentiation of cells from the interzone to chondrocytes and subsequent formation of articular cartilage at epiphyseal ends of long bone may be controlled by mechanisms to maintain the distinct phenotype and function [33]. The transcription factor ERG has been speculated as playing role in the maintenance of the articular chondrocyte phenotype and function throughout life, preventing hypertrophy. Overexpression of ERG chondrocytes exhibit immature articular phenotypes, expression of cartilage matrix components inclusive of aggrecan and tenascin-C [33]. Despite the differences in function and phenotype observed in growth plate chondrocytes and articular cartilage chondrocytes in healthy individuals, articular cartilage chondrocytes may still undergo hypertrophy and apoptosis reminiscent of growth plate chondrocytes, which is often observed in osteoarthritis.

1.1.2 Articular Cartilage Injury and Osteoarthritis

1.1.2.1 Osteoarthritis

Skeletal disease and injury is prevalent in society, posing a great burden upon individual sufferers affecting quality of life. Osteoarthritis (OA) is a prevalent chronic disease which causes socio-economic burden to society as well as reducing quality of life for the individual affected. Osteoarthritis can be described as a heterogeneous group of conditions which result in joint signs and symptoms associated with changes to bone at joint margins and defective integrity of articular cartilage; degeneration of the articular cartilage and subchondral bone. The exact causes of OA are unknown but there are several factors which are thought to increase the likelihood of development of the condition including; tendon or ligament problems, inflammation of the joint as a result of joint damage through injury or an operation and damage to cartilage. The risk of OA increases with age due to weakened muscles and worn joints and also in overweight individuals who put more strain on their joints due to increased body mass and in particular the knees and hips which bear most of the weight. OA symptoms include; joint tenderness, pain, crepitus, limited movement and local inflammation therefore reducing quality of life. 45% of women over the age of 65 have symptoms of OA. Radiological evidence shows that OA is found in over 70% of women over the age of 65 with OA of the knee being the most prevalent cause of immobility [34].

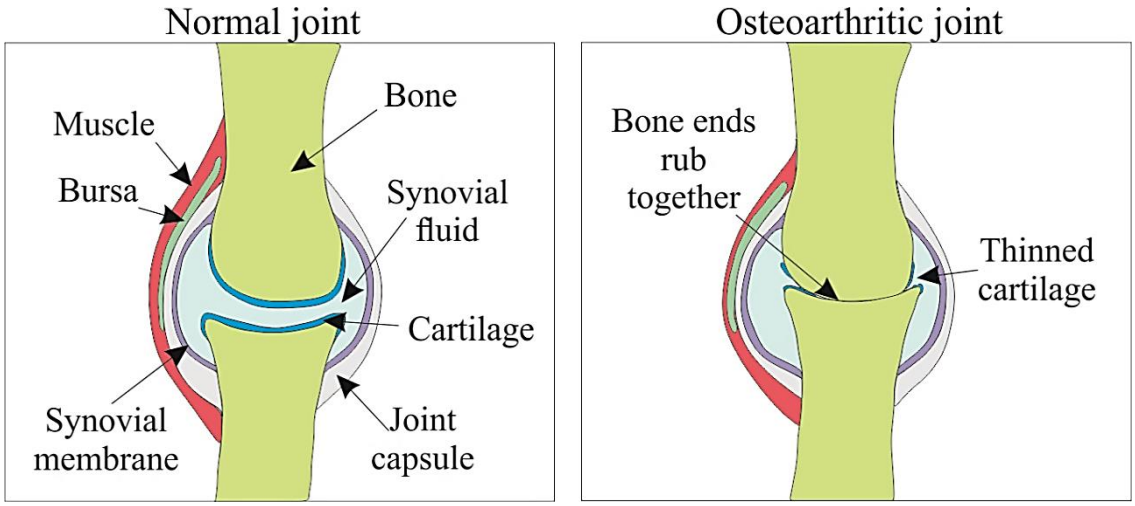

Figure 7. Normal and Osteoarthritic knee joints. Compared to the normal joint, in OA joints, cartilage fibrillation and erosion occurs. Loss of joint space can induce the exposed subchondral bones to rub together. (Figure adapted from Sharma and Rathore, Potential Role of Nutraceuticals in the Management of Knee and Hip Joint Osteoarthritis, Biomedical Science and Engineering Vol. 3, No. 1,2015,pp 23-29.doi:10.12691/bse-3-1-5).

1.1.2.2 Articular Cartilage Injury

Articular cartilage as indicated earlier is avascular, aneural and alymphatic, with embedded non-proliferating and non-migratory chondrocytes in a specialised ECM, factors which likely contribute to the limited capacity articular cartilage has for intrinsic healing and repair. Therefore for articular cartilage to retain homeostasis, the preservation and health of articular cartilage is critical. Therefore, trauma to articular cartilage often results in the need of operative treatment [35]. Focal cartilage injury is damage to cartilage as a result of fall, twist or direct blow to the joint and can also extend to damage involving underlying bone (osteochondral defect). The affected area of articular cartilage which is injured is unlikely to repair. Cartilage injury as a result of torsion or intensive axial load and shear stress which induces chondral damage can also be the first stage of OA. Chondral defects which extend to the subchondral bone are likely to mediate repair with fibrocartilage which is inferior to hyaline cartilage which can ultimately result in OA.

1.1.2.3 Injury to Adjacent Joint Tissues

End stage OA generally affects the whole joint and subchondral bone, the commencement of OA with regards to anatomical site may however differ. OA is often believed to be as a result of underlying articular cartilage damage with secondary synovitis. However, recent developments have shown that intra-articular pathology which originates in adjacent structures to the articular cartilage may participate in the early OA disease process, proposing that OA can be a disorder of the ligaments, tendons or joint capsule. Initiation of OA as a result of trauma may initiate in differing sites including the anterior cruciate ligament, the meniscus and also the articular cartilage. In nodal OA of the interphalangeal joints of the hands, ligamentous thickening of the collateral ligaments occurs. Following injury, inflammation occurs in the collateral ligaments and also extracapsular tissues. Degenerative changes ensue inclusive of fibrocartilage fibrillation, chondrocyte hypertrophy and subchondral cystic changes. Ligament damage which initiates inflammation can therefore induce inflammatory changes in nearby joint tissues [36].

A functional complex, termed the synovio-entheseal complex (SEC), is a region in which a ligament, tendon or joint capsule attaches to bone and includes the adjacent synovium and bony tuberosities. The attachment or insertion sites, formerly recognised as focal attachments which are composed of fibrocartilage at the location of bony insertion, involve the extension of fibrocartilage into joint cavities to disperse stress away from the site of attachment [37]. The SEC formed at the tibial insertion of the posterior cruciate ligament (PCL) has been implicated in OA. Binks *et al* have shown that the PCL-SEC plays a role in joint inflammation and as an initiator of the early OA disease process [38]. Inflammation of the joint capsule, ligaments or tendons can induce enthetitis. McGonagle *et al* have proposed a concept in which OA may be as a consequence of damage and degeneration to ligaments or tendons which may directly affect the synovial-entheseal complex.

Release of pro-inflammatory mediators as result of damage may trigger inflammation in nearby tissue including the adjacent synovium and the articular cartilage [39].

1.1.2.4 Inflammation

OA is often referred to as a non-inflammatory disease to discriminate it from 'inflammatory arthritis' such as rheumatoid arthritis (RA); which can be defined as an autoimmune disease. Despite OA being commonly described as a 'non-inflammatory' disease, inflammation is very much present in OA and likely to contribute to the aetiology and progression of OA. Inflammation of articular cartilage usually ensues following cartilage injury. Pro-inflammatory cytokines including IL-1β, TNF-α and IL-6 have been found to have significant implications in OA [40], Figure 8 illustrates the effects of pro-inflammatory mediators on articular chondrocytes and cartilage. Persistent pro-inflammation may also induce up-regulation of anti-inflammatory mediators. However, anti-inflammatory mediators may be insufficient to overcome the negative destructive effects of pro-inflammatory mediators upon articular cartilage integrity.

1.1.2.4.1 Interleukin-1 Beta (IL-1β)

IL-1β is one of the most significant cytokines involved with the pathogenesis of OA. Elevated levels of IL-1β in the cartilage, subchondral bone, synovial membrane and synovial fluid have been identified in patients with OA [41], [42], [43], [44], [45]. Saha *et al* identified that the enzyme interleukin-1 converting enzyme (ICE) was significantly increased in OA human synovial membrane and cartilage, with the production of ICE predominantly located to the superficial and upper intermediate zones of articular cartilage. Immunostaining for IL-1β was observed at the same topographical location of ICE [46]. Articular chondrocytes are receptive to IL-1β, expressing the IL-1 receptor [47] and also express IL-1β. LPS treated chondrocytes have been shown to express IL-1β, but the expression of IL-1β has also been observed in untreated chondrocytes suggesting that normal articular chondrocytes produce a basal level of IL-1β. Secretion of IL-1β from chondrocytes has been shown to occur in an LPS dose dependent manner [48]. Chondrocytes located adjacent to OA lesions were found to bind more IL-1β compared to chondrocytes isolated from cartilage deemed morphologically normal from the same joint. TNF-α stimulation induced an up-regulation of IL-1β and also the IL-1 receptor, suggesting that chondrocytes express more IL-1β as a result of increased surface receptor expression, inducing a amplification of IL-1β expression [49].

The observed marked up-regulation of IL-1β in OA pathogenesis has led to the use of exogenous IL-1β to induce the pro-inflammatory environment identified in OA *in vitro* and *in vivo*. IL-1β induces chondrocytes to mediate biochemical changes and therefore use of exogenous IL-1β in an experimental setting can mimic the molecular mechanism and pathology associated with OA. Transgenic mice with an inducible IL-1β transcription unit in the temporomandibular joints, when activated were found to exhibit joint pain with accompanied pathogenic associated changes including articular surface fibrillations and cartilage remodelling, many of the structural changes associated with

OA [50]. Intra-articular injection of IL-1β to the knee joints of pigs has been shown to induce OA associated changes including induction of matrix metalloproteinase and critical decrease in proteoglycan content [51]. Chondrocytes isolated from healthy equine articular cartilage and treated with IL-1β induced down-regulation of type II collagen and aggrecan mRNA [52]. Intra-articular injection of IL-1β into murine knee joints have also been shown to induce inhibition of proteoglycan synthesis [53].

Many *in vitro* and *in vivo* studies have identified that IL-β is responsible for proteoglycan loss in articular cartilage and is partly responsible for the loss of articular cartilage in OA. The role that IL-1β has in mediating proteoglycan degradation is as an inducer of proteolytic enzymes and other pro-inflammatory molecules. Synthesis of pro-IL-1β is cleaved by intracellular caspase-1 or IL-1β-converting enzyme (ICE) which generates a mature and active cytokine. Natural inhibitors of IL-1β can bind to and inhibit IL-1β, inhibitors include IL-1 receptor antagonist (IL-Ra) and type 2 IL-1 decoy receptor (IL-1RII) [54]. Interaction of IL-1β with the type I receptor (IL-1RI) on the membrane surface can induce several intracellular signalling pathways including ERK1/2, JNK, PKC and NF-κB [54]. The importance of these intracellular pathways mediated by IL-1β is the convergence at pro-inflammatory inducing transcription factors mediating the up-regulation of pro-inflammatory associated genes and proteolytic mediators involved with articular cartilage catabolism.

A disintegrin and metalloproteinase with thrombospondin motifs (ADAMTS) or aggrecanases, which mediate the degradation of aggrecans, have been shown to be up-regulated by IL-1β. Bovine articular chondrocytes treated with IL-1β resulted in the up-regulation of both ADAMTS-4 and ADAMTS-5 expression [55]. Treatment of human articular chondrocytes with IL-1β was shown to up-regulate *ADAMTS-4* expression [56]. Healthy equine chondrocytes treated with IL-1β induced matrix metalloproteinase (MMP) -1, -3 and -13 expression by approximately 100 fold [52]. An *in vitro* study of human chondrocytes treated with IL-1β, identified that MMP-1, MMP-3 and MMP-13 were up-regulated with MMP-3 exhibiting the strongest expression. However, comparison of OA articular cartilage and normal articular cartilage identified that MMP-1 exhibited low levels of expression and MMP-13 exhibited the strongest up-regulation in OA articular cartilage, especially in late stage OA specimens. The study by Bau *et al* suggests MMP13 as the most critical collagenase in OA cartilage [57]. IL-1 receptor antagonist added to explant cultures of human OA articular cartilage was found to inhibit cleavage of type II collagen, increase proteoglycan content and induce down-regulation of MMP-1, MMP-3 AND MMP-13 expression, this reinforces the significance of IL-1β signalling on the expression of MMP expression [58].

MMPs or collagenases initiate matrix degradation which are secreted in latent form and activated through propeptide cleavage. Type II collagen is the preferred substrate of MMP-13, a zinc dependent collagenase, which recognises a specific site within the tropocollagen molecule and induces disruption to the triple helix which enables enzymatic cleavage to ensue at Gly775-Leu776. The different domains of MMP initiate binding and cleavage of the tropocollagen molecule. The C-terminal 4

bladed β propeller hemopexin-like domain (Hpx) relaxes the tropocollagen helix and the catalytic domain (Cat) hydrolyses specific bonds [59]. Aberrant up-regulation of pro-inflammatory IL-1β induces the upregulation of MMPs which induce articular cartilage degradation through the cleavage of critical ECM proteoglycans, observed as fissuring fibrillation of articular cartilage.

Human articular chondrocytes cultured in the presence of IL-1β have been shown to induce IL-6 production [60] [61], IL-8 production [62], RANTES or CCL5 chemokine [63] monocyte chemoattractant protein (MCP-1) and macrophage inflammatory protein (MIP-1alpha) [64]. IL-1β can be defined as one of the most critical pro-inflammatory mediators in OA as a result of the autocrine manner in which IL-1β is regulated. Articular chondrocytes produce IL-1β and are receptive to IL-1β, therefore in the presence of aberrant elevated levels of IL-1β, articular chondrocytes function to exhibit a catabolic phenotype of which function through an IL-1β positive feedback mechanism, by which IL-1β is able to induce highly inflammatory conditions and articular cartilage degradation.

1.1.2.4.2 Tumour Necrosis Factor Alpha (TNF-α)

TNF-α is considered another key inflammatory cytokine which is involved with the underlying pathophysiology of OA. TNF-α is initially formed as a transmembrane protein and requires cell membrane TACE or ADAM17 metalloproteinase activity for cleavage of pro-TNF-α and release of soluble TNF-α through a process known as 'shedding' [65]. Intra-articular injection of TNF-α in combination with IL-1β was found to induce a marked synergistic effect on induction of polymorphonuclear leukocyte infiltration in the knee joints of rabbits [66]. The creation of a transgenic mice overexpressing human TNF-α resulted in mice which developed a chronic inflammatory polyarthritis with articular cartilage destruction. Use of a monoclonal antibody against the human TNF-α was able to prevent development of disease symptoms [67]. Following the induction of OA in dogs, immunostaining identified chondrocytes positive for both TNF-α and TNF receptors in articular cartilage [68]. Self-administration of a TNF-α inhibitor, Adalimumab, in a patient with OA resulted in a reduction in pain, synovitis and bone marrow oedema [69]. Like IL-1β, TNF-α has been shown to induce ECM degradation through the up-regulation of proteolytic enzymes [70], [71], [72].

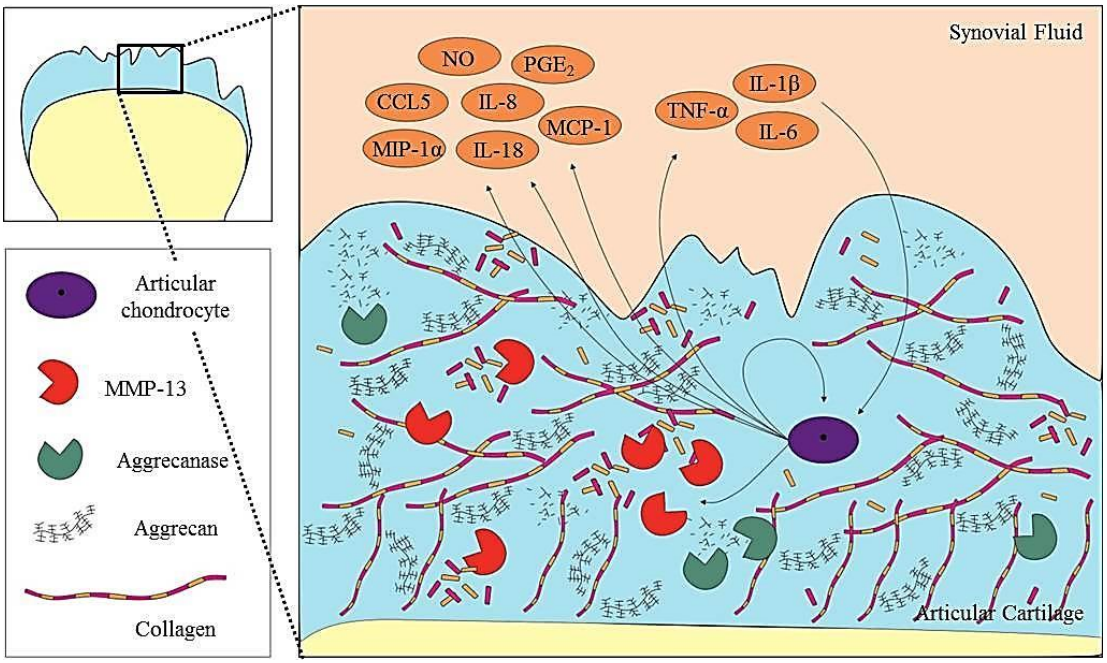

Figure 8. Inflammation of the articular cartilage in osteoarthritis. Chondrocytes which reside in the articular cartilage are receptive to IL-1β, TNF-α and IL-6, which induces up-regulation of other pro-inflammatory mediators including IL-8, IL-18, CCL5, MCP-1, MIP-1α, NO and PGE_2, further up-regulation of IL-1β and TNF-α in an autocrine manner and also up-regulation of MMP-13 and aggrecanases including ADAMTS-4 and ADAMTS-5. Up-regulation of MMP-13 and aggrecanases initiates breakdown of collagen fibers and aggrecan in the articular cartilage. (Figure adapted from Sellam and Berenbaum, The role of synovitis in pathophysiology and clinical symptoms of osteoarthritis, Nature Reviews Rheumatology 6, 625-635 (November 2010) doi:10.1038/nrrheum.2010.159).

1.1.2.5 Articular Cartilage Homeostatic Imbalance

The articular cartilage is maintained by metabolically active articular chondrocytes. Articular chondrocytes can be induced by catabolic and anabolic mediators. Catabolic mediators include pro-inflammatory cytokines and proteolytic enzymes as described previously which induce chondrocytes to mediate articular cartilage degradation. Anabolic mediators act upon chondrocytes and induce chondrocytes to synthesize ECM molecules. An imbalance in catabolic and anabolic signalling upon chondrocytes can therefore initiate degradative changes to the ECM which may lead to the onset and progression of OA. While the role of pro-inflammatory cytokines has been discussed previously and the catabolic role associated with pro-inflammatory cytokines in OA, a down-regulation of anabolic signalling may also initiate OA onset. A downregulation in mediators which induce chondrocytes to produce and maintain the ECM which comprises the articular cartilage could therefore result in a degeneration of the articular cartilage ECM.

TGF-β signalling has been shown to exhibit several anabolic associated functions in articular chondrocytes. Transgenic lapine articular chondrocytes which produced high levels of TGF-β1 were found to increase levels of proteoglycan and type II collagen synthesis [73]. Type II collagen was found to be elevated following treatment of articular chondrocytes with exogenous TGF-β1 [74]. TGF-β signalling may also function to down-regulate collagenase through the expression of tissue inhibitors of metalloproteinases (TIMPs). TIMPs are natural inhibitors of MMPs. Articular chondrocytes have been shown to induce TIMP-1 expression up-regulation in response to TGF-β1 treatment [75]. TGF-β has also been shown to induce TIMP-3 expression in bovine and human chondrocytes [76]. Quereshi *et al* investigated the pathway by which TGF-β signalling up-regulates *TIMP-3* expression in chondrocytes, identifying that activation of the ERK-MAPK intracellular pathway and resultant activation of Sp1 transcription factor act to induce TIMP-3 [77].

Epiphyseal chondrocyte differentiation in an *in vitro* model has shown that use of exogenous TGF-β1 prevents epiphyseal chondrocytes from undergoing terminal differentiation into hypertrophic chondrocytes [78]. Overexpression of a dominant negative TGF-β type II receptor in the skeletal tissues of mice resulted in the joints with the resemblance of human OA [79]. Mutant Smad3 mice with chondrocytes which lacked responsiveness to the TGF-β signalling pathway resulted in terminal hypertrophic differentiation with an osteoarthritis phenotype. TGF-β signalling was believed to be responsible for the inhibition of terminal hypertrophic differentiation in chondrocytes and therefore responsible in maintaining articular cartilage integrity [27]. The two studies of aberrant TGF-β signalling in mice indicate the need of TGF-β to prevent hypertrophic chondrocyte terminal differentiation and the prevention of OA development. The expression of TGF-β -2 and -3 and TGF-β receptors was found to be reduced with age in mice. Old mice were found to have a limited response to TGF-β induced IL-1 counteraction and exhibited reduced levels of proteoglycan synthesis. Lack of TGF-β responsiveness with age was suggested to be the cause of OA development [80]. Reduced responsiveness of aged articular chondrocytes to anabolic TGF-β signalling may therefore contribute to the higher level of articular cartilage degradation subsequently resulting in OA onset and progression.

In epidemiological studies a polymorphism in asporin, which exhibited increased inhibition of the TGF-β signalling pathway and suppression of cartilage ECM components compared to the common asporin, was found at a higher frequency in patients with OA [81], [82]. SMAD3 is a key intracellular molecule of the TGF-β signalling pathway and a single nucleotide polymorphism mapped to intron 1 of *SMAD3* has been found at high frequency in knee and hip OA in a European cohort [83]. Mutations in *SMAD3* have been identified in patients with aneurysm-osteoarthritis syndrome whereby osteoarthritis manifests early [84]. Osteoarthritis is also a clinical feature in some individuals of the connective tissue disorder, Loeys-Dietz syndrome which is caused by mutations in any of *TGFβR1*, *TGFβR2*, *TGFβ2* and *SMAD3* genes [85]. The studies indicate that supressed TGF-β signalling as a

result of either direct TGF-β de-regulation or a component of TGF-β intracellular signalling is positively related to the development of OA.

Additional to the potential dysregulation of TGF-β signalling, the up-regulation of catabolic mediators may far outweigh the neutralising effects of anabolic mediators. In addition to the role in inducing cartilage catabolism, IL-1β has also been found to suppress cartilage anabolism. IL-1β can down-regulate anabolic TGF-β intracellular signalling. A genome wide gene expression study conducted by Takahashi *et al* in a murine chondrocytic cell line in response to IL-1 and TGF-β treatment alone and in combination found that antagonism was the dominant mode of interaction between TGF-β and IL-1β upon pro-inflammatory genes [86]. IL-1β has been found to repress TGF-β signalling by down-regulation of TGF-βRII expression and also up-regulation of SMAD7 expression [87], [88] . SMAD7 was first found to inhibit TGF-β signalling by prevention of receptor SMAD activation and phosphorylation by binding to the TGF-β type I receptor [89]. SMAD7 has also been shown to interact with other molecules forming ubiquitin ligase complexes which consequently degrade the TGF-β type I receptor [90], [91], [92]. SMAD7 has also been found to bind to DNA in the nucleus, preventing formation of the TGF-β induced R-SMAD-SMAD4-DNA complex [93]. SMAD7 has also been found to interact with Yin Yang 1 (YY1) to inhibit TGF-β activated SMAD induced transcription [94].

Articular cartilage homeostasis is maintained by an anabolic-catabolic balance. Perturbation to the anabolic-catabolic balance is likely to result in the onset of articular cartilage degenerative changes. It is apparent that catabolic associated activity is substantially increased in osteoarthritis, with chondrocytes unable to compensate for loss of ECM components. Additionally, and just as important, is the disruption to anabolism in articular cartilage homeostasis, which may be either as a result of anabolic down-regulation with age and/or as a consequence of catabolic influences upon anabolic signalling. It is apparent that signalling network which controls the catabolic and anabolic balance is complex and interconnected.

1.1.2.6 Genetic predisposition

While injury and inflammation mediate the break-down of articular cartilage and therefor the onset of OA, there has been a number of candidate genes identified which indicate a genetic predisposition for certain forms of OA. Individuals with mutations in genes which encode for example articular cartilage ECM proteins or genes encoding proteins involved with chondrocyte and cartilage homeostasis have been identified as causative of diseases with which OA is a clinical manifestation. For example a missense mutation in the gene encoding cartilage ECM matrix protein aggrecan, results in amino acid substitution in the aggrecan G3 domain C-type lectin, preventing interaction with ECM proteins upon cell secretion, inducing loss of aggrecan interaction with fibulin-1, fibulin-2 and tenascin-R. The missense mutation in the *AGCAN* gene results in the disease known as osteochondritis dissecans, short stature and early onset osteoarthritis [95]. Table 1 lists some examples of genes identified amongst

groups of individuals which contain mutations which cause disease with an OA phenotype as one of the symptoms of the disease. Gene mutation may lead to amino acid substitution, deletion or duplication which ultimately affects tertiary protein conformational structure and protein function. Any change in protein function required for articular chondrocyte function and cartilage homeostasis is likely to induce pathological changes to the articular cartilage which manifests as OA.

Gene	Disease	Mutation	Reference
COL2A1	**Czech dysplasia** (autosomal dominant)	c.823C>T nucleotide substitution mutation inducing amino acid substitution p.R75C or p.R275C. c.4172A>G nucleotide substitution mutation inducing amino acid substitution p.Y1391C.	[96], [97]
	Osteoarthritis associated with chondrodysplasia (autosomal dominant)	Amino acid substitution p.R519C	[98], [99], [100]
	Otospondylomegaepiphyseal Dysplasia (autosomal dominant)	Mutation in the splice-acceptor site of intron 10 - c.709-2A>G inducing in-frame deletion through skipping of exon 11 and exons 11 and 13.	[101]
AGCAN	**Osteochondritis Dissecans, Short stature and Early Onset Osteoarthritis (**autosomal dominant)	c.6907G>A nucleotide substitution mutation inducing amino acid substitution p.V2303M .	[95]
SMAD3	**Loeys-dietz syndrome with osteoarthritis** (autosomal dominant)	c.859C>T nucleotide substitution mutation in exon 6 inducing amino acid substitution p.R287W. c.741_742delAT 2 nucleotide deletion in exon 6 inducing frameshift and a premature termination sequence. c.783C>T nucleotide substitution mutation in exon 6 inducing amino acid substitution p.T261I. c.652delA nucleotide deletion mutation in exon 5 inducing frameshift and premature termination following asparagine-218 (p.N218fs). c.836G>A nucleotide substitution mutation in exon 6 inducing amino acid substitution p.R279K. c.715G>A nucleotide substitution mutation in exon 6 inducing amino acid substitution p.E239K. c.313delG nucleotide deletion inducing frameshift p.(Ala105ProfsTer11). c.788C>T nucleotide substitution mutation inducing amino acid substitution p.2263L. c.1080dupT nucleotide duplication inducing amino acid substitution p.E361X.	[84], [102], [103]

Table 1. Examples of gene mutations which cause diseases which result in an OA phenotype

In addition to changes as a result of mutation inducing disease, individuals with certain polymorphic variants of a gene may have a predisposition for developing OA. Recently Wang *et al* listed many single nucleotide polymorphisms associated with OA and calculated the odds ratio of the SNPs with OA susceptibility [104]. There are numerous studies which have looked to investigate candidate genes which have been found to contain polymorphisms which modulate gene and ultimately protein activity and function in articular cartilage development and homeostasis. For example Valdes *et al* investigated the role of genetic variation in *SMAD3* in the risk of hip and knee OA in individuals of European descent. Polymorphisms identified were tested for presence within cohorts of individuals with hip OA and knee OA. Four SNPs: rs266335, rs6494629 and rs2289263 were found to be associated with knee OA and rs12901499: which maps to intron 1 of *SMAD3*, was found to be associated with both knee and hip OA. Signalling through the TGF-β pathway involving SMAD3 induces chondrocyte anabolism and helps in maintaining the articular chondrocyte phenotype and loss of SMAD3 leads to hypertrophy and OA associated changes. The SNP rs12901499, a genetic variation of *SMAD3*, is therefore involved with genetic susceptibility to inducing both knee and hip OA [83]. Identification of gene polymorphisms and the prevalence in the wider community enable links to be made between disease susceptibility as a result of having a particular genetic variant. To date there have been many gene polymorphisms identified which relate to increase risk of OA and there are likely to be many still to be discovered.

1.1.3 Osteoarthritis and Disease Burden

The risk of OA increases with age due to weakened muscles and worn joints and also in overweight individuals who put more strain on their joints. More than 6 million people in the UK have painful OA in one or both knees, more than 650,000 people in the UK have painful OA in one or both hips and with X-ray evidence it has been estimated that 8.5 million people have OA of the spine [105]. In 1990 it was estimated that OA was the tenth leading cause of non-fatal encumbrance in the world. In the 2000 study for the Global Burden of Disease OA was ranked 4th for the cause of years lived with disability (YLD) at a global level [106].

In the UK medical costs associated with OA are high requiring referral which is estimated to cost approximately £500 a case per year and the cost of joint replacement varies depending on the centre from £5000 to £10,000 and annual costs for OA in 1998 had been calculated at £320 million by the NHS executive [107]. It was estimated that 10 million working days were lost in 2006/7 as a result of musculoskeletal conditions [108]. From February 2011 until February 2012 of the claims made for Disability Living Allowance (DLA) and Attendance Allowance (AA) the largest type of main disabling condition was claims arising from individuals with musculoskeletal conditions with approximately 120,420 new claims in that year period [109].

Understandably the number of skeletal diseases, including OA, will increase proportionally as the world population increases but also the changing world population demographic means that the elderly are in fact the fastest growing age category in the UK; in 2008 it was estimated that there were 323 million over the age of 65 years which is expected to increase to 1555 million by the year 2050 [110]. Figure 9 shows the estimated and projected age structure in the UK. The elderly are the fastest growing age category as a result of the period of population growth and social change between 1946 and 1964 particularly in those more developed countries who participated in the World War, after which time there was a baby boom. The following decades will see the retirement of the baby boom generation from work creating an ageing population whereby the number of elderly people in society will outweigh the number of young people. In addition to the baby boom generation, advances in healthcare as a result of scientific research means that increased longevity can be expected. Therefore the prevalence of skeletal disease will increase given that these skeletal diseases affect mainly older people.

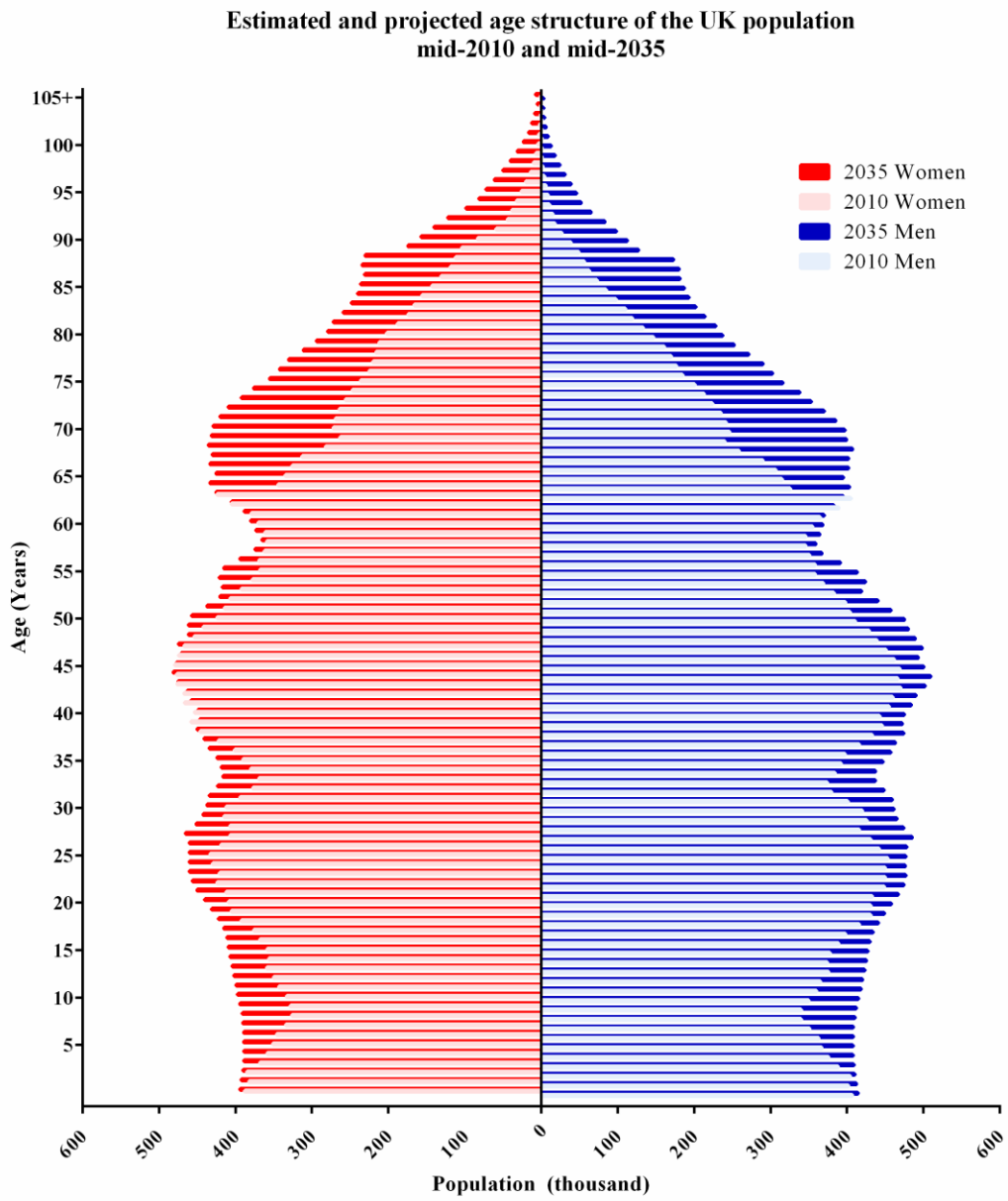

Figure 9. Estimated and projected age structure of the UK population in mid-2010 and mid-2035. The median age of 39.7 years in 2010 is predicted to rise to 39.9 years in 2020 and up to 42.2 years by 2035. (Population pyramid generated using GraphPad Prism software version 6.0, using data taken from the UK office for national statistics, released 26 October 2011, UK population projected to reach 70 million by mid-2027, nationalarchives.gov.uk).

1.1.4 Articular Cartilage Restoration following injury

1.1.4.1 Conservative treatment for Articular Cartilage injury

Treatment selection for chondral lesions depends upon patient age, daily and sporting activities, the potential underlying aetiology causative for the chondral lesion and the grade of the lesion. Conservative treatment of chondral lesions does not involve surgery and aims to reduce symptoms. Conservative treatment is generally considered when chondral lesions are small. Conservative treatment includes medications including non-steroidal anti-inflammatory drugs (NSAIDs) and analgesics. Mechanical treatments look to reduce load upon the injured site and includes weight loss, rest, use of canes and braces and physical therapy. Nutritional supplementation includes the use of chondro-protective agents such as glucosamine sulphate, chondroitin phosphate, methylsulfonylmethane (MSM) and Omega-3. Intra-articular injections of steroids and viscosupplementation such as Hylan GF20 or Ostenil which is synthetic hyaluronic acid, may also be considered [111].

In a study of 28 athletes with isolated chondral lesions, the majority of patients did not require treatment. However, after 14 years, radiographic findings identified that 12 of the athletes had a reduction of the joint space, indicating that whilst the initial chondral lesions were asymptomatic, degradation of the articular cartilage ensued leading to permanent knee damage [112]. Despite conservative treatment providing therapy for small chondral lesions and potentially reducing any symptoms, conservative treatment does not improve the structure of the articular cartilage or the chondral lesion and in the long term, articular cartilage deterioration is likely to ensue. Conservative treatment may be short term therapy after which operative treatment may be required.

1.1.4.2 Operative treatment for articular cartilage injury and OA

Large chondral lesions cannot be intrinsically regenerated and operative treatment is required. Surgical intervention can either be restorative or reparative. Reparative techniques of surgical intervention does not induce complete re-establishment of the articular cartilage, but looks to treat osteochondral defects by means of enabling full function of the joint. Restorative techniques of surgery, however, attempt to regenerate the articular cartilage [113]. Despite the differing operative techniques in place to treat large cartilage lesions and OA, and to prevent cartilage induced injury from further deterioration and onset of OA, techniques have limitations, Figure 10 illustrates the operative treatment techniques used to treat or alleviate cartilage injury and OA.

1.1.4.2.1 Restorative surgical intervention

Large focal cartilage injuries are currently treated by either: debridement, autologous chondrocyte implantation, bone marrow stimulation or osteochondral grafts. In terms of articular cartilage damage the major issue is that unlike other connective tissue and bone, cartilage is avascular, lack of blood vessels means that chondrocytes get their nutrients and oxygen by means of diffusion and this also

means that it lacks the regenerative capacity of bone due to lack of nutrients required for tissue reparation. There are currently several surgical techniques used to help restore the surface and increase mobility which include debridement, autologous chondrocyte implantation, osteochondral grafts or bone marrow stimulation.

Bone marrow stimulation

Bone marrow stimulation involves the removal of damaged articular cartilage to expose the subchondral bone followed by either drilling, microfracture or arthroscopic abrasion in hope that blood and bone marrow infiltrate into the defect site and chondroprogenitors will undergo differentiation and therefore repair the defect area [114]. The limitation of bone marrow stimulation is that fibrocartilage can be generated and not the regeneration of native articular cartilage. Fibrocartilage can deteriorate and also incomplete filling of the defect site can occur.

Mosaicplasty

Osteochondral grafts otherwise known as mosaicplasty, involves the transfer of healthy cartilage and bone to the damaged area. The technique involves the harvesting of small cylinders of bone and cartilage from areas that are generally underused and transplanted into the defect area to restore the area. The concept is to restore the original contour of the articular surface. Limitations to this technique include availability of osteochondral plugs, size of the defect, donor site morbidity, and disintegration between the plugs and defect area. The majority of successful treatments are in young patients with initial defect areas being under $4cm^2$ [115].

Autologous Chondrocyte Implantation

Autologous chondrocyte implantation (ACI) involves the implantation of *in vitro* expanded chondrocytes from healthy cartilage from a non-weight bearing area injected into the defect site under a periosteal cover. Limitations to this type of technique are that it is most successful in young patients and one study shows that mid-term results of autologous transplant implantation in patients who took part in high impact activity following surgery area not as good as mid-term results from other techniques. Those with well-established disability, failed previous cartilage techniques and large defects are not likely to benefit from an ACI [116]. Additionally the chondrocytes cultured in vitro from donor healthy cartilage requires prolonged expansion over several weeks in monolayer culture to have a sufficient number of cells to inject into the defect site. During this time the cell phenotype and morphology changes. Chondrocytes are known to dedifferentiate in monolayer culture and display fibroblastic phenotype and morphology [117]. It is likely that fibrous tissue is formed in the defect area rather than hyaline tissue.

1.1.4.2.2 Reparative surgical intervention

Some full thickness articular cartilage lesions and cartilage and subchondral bone deterioration as a result of OA results in the need for joint replacement by means of prosthesis when symptoms cannot be alleviated by less invasive forms of therapy. Limitations of prosthetic joints include aseptic

loosening and periprosthetic bone loss. Early loosening of prostheses is related to poor fixation and design and late loosening is due to wear of prosthetic components which would require the patient to undergo revision of the joint replacement. It has been shown that after 15-20 years approximately 10-20% of joints need to be replaced which includes the need for bone grafting as a result of osteolysis with significantly higher rates of morbidity [118]. Periprosthetic bone loss is generally as a result of prostheses wear believed to be as a result of implant derived wear particles which induces an inflammatory response along implant bone interfaces and the joint capsule resulting in loosening and bone loss [118].

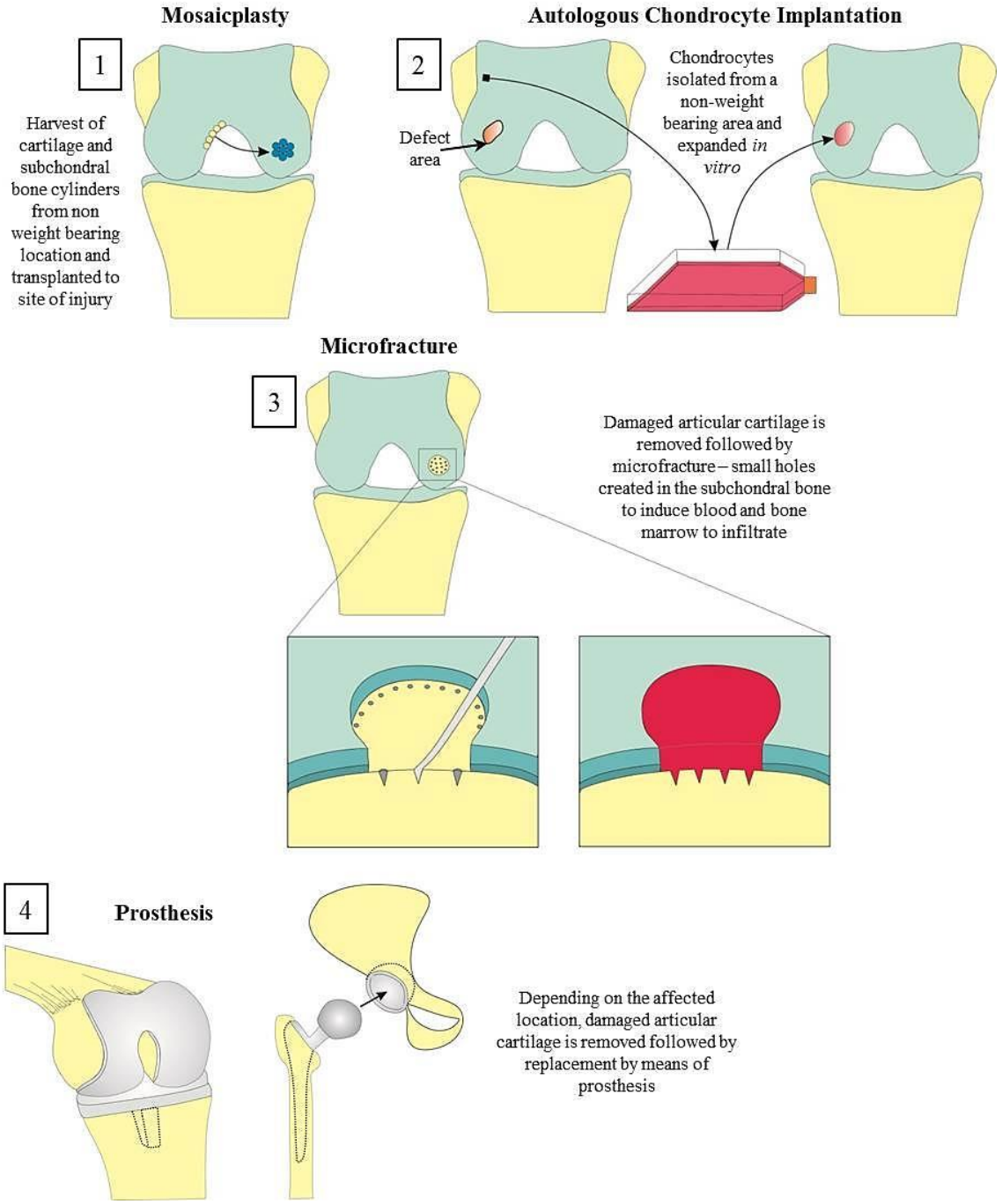

Figure 10. Restorative and reparative methods of surgical intervention for articular cartilage damage. Restorative methods include 1) mosaicplasty, 2) autologous chondrocyte implantation and 3) microfracture. 4) Reparative surgical intervention as a result of full thickness cartilage injury is in the form of prosthesis. The image depicts a prosthetic knee and prosthetic hip following arthroplasty procedure. The method chosen depends upon the size of injury and extent of damage. (Figure adapted from Hunziker et al, An Educational Review of Cartilage Repair: Precepts & Practice - Myths & Misconceptions - Progress & Prospects, Osteoarthritis and Cartilage 12/2014; 23(3). doi: 10.1016/j.joca.2014.12.011, Baugé and Boumédiene, Use of Adult Stem Cells for Cartilage Tissue Engineering:: Current Status and Future Developments, Volume 2015 (2015), Article ID 438026, 14 pages, doi.10.1155/2015/438026 and Mithoefer et al, Clinical Efficacy of the Microfracture Technique for Articular Cartilage Repair in the Knee, Am J Sports Med October 2009vol. 37 no. 10 2053-2063, doi:10.1177/0363546508328414).

1.1.5 Chondroprogenitor Cells and Articular Regeneration

Once a healthy adult human articular chondrocyte has reached a fully differentiated state it remains quiescent, maintaining the constituents of the articular cartilage ECM, remaining metabolically active but is not mitotically active, does not continue to differentiate to hypertrophy or senesce. Fully differentiated articular chondrocytes can be defined as resting cells with low synthetic activity to maintain the ECM. Unlike the majority of other tissues, articular cartilage has minimal numbers of resident mesenchymal progenitors for differentiation of new articular chondrocytes to replace injured chondrocytes following trauma. Unlike other cartilaginous structures, the articular cartilage does not have a perichondrium. The perichondrium has been shown to provide a dual role during non-articular cartilage wound healing. The inner layer of the perichondrium has been shown to provide cells for novel cartilage formation [119]. The perichondrium contains chondroprogenitors which can differentiate into chondrocytes and allow for the formation of new cartilage. Articular cartilage lacks a perichondrium and therefore cannot repair through appositional growth, which may be a confounding factor in the limited ability of articular cartilage to repair following extensive injury.

The articular chondrocyte is a derivative of the interzone, a unique mesenchymal cell population. The interzone cells can therefore be regarded as the progenitor cells for articular chondrocytes, however, the interzone is only present during embryogenesis and undergoes distinct differentiation pathways to form the components of the synovial joint, inclusive of articular cartilage and does not exist in adult life. Tissues of the adult human body and especially tissues which renew frequently contain a pool of stem cells which reside within a stem cell niche, which provide cells for differentiation and replenish cells lost due to senescence or injury. Schofield *et al* first proposed the 'niche' hypothesis to define and describe the microenvironment which supports stem cells [120]. The bone marrow serves as a niche for haematopoietic stem cells, the epithelial stem cell niche is located within the bulge area of hair follicles, intestinal stem cells are located adjacent to paneth cells in intestinal crypts and the subgranular zone of the hippocampus serves as a niche for neuronal stem cells [121]. There is much deliberation as to whether there is a local stem cell niche which provides progenitor cells for articular cartilage differentiation in adult life.

Various cell labelling studies of stem cells within the developing synovial joint have endeavoured to identify the residence of stem cells in the adult joint. Use of bromodeoxyuridine (BrdU) can be used to identify slow cycling stem cells. Karlsson *et al* exposed New Zealand white rabbits with BrdU and found that cells located within the perichondrial groove of Ranvier retained BrdU labelling after a long duration. Cells located within the groove of Ranvier also exhibited cell immunoreactivity to antibodies against mesenchymal progenitor markers including the Stro-1 antigen and Jagged-1. Karlsson *et al* proposed that progenitor cells identified in the groove of Ranvier have the ability to migrate to the articular surface [122]. Candela *et al* also conducted slow cycling cell labelling with 5-ethynyl-2′-deoxyuridine (EdU) in mice, identifying that after 6 weeks from the last intraperitoneal

EdU injection, EdU labelled cells were detected in the ligament attachment sites, intrapatellar fat pad, perichondrium, synovium and the articular cartilage, predominantly the articular surface of the articular cartilage [123]. Slow-cycling cells identified in the articular cartilage and adjacent joint tissues may be progenitor cells, however, articular chondrocytes are not mitotically active and therefore are likely to retain EdU, therefore limiting the use of cell labelling for articular cartilage studies.

Isolation of cells from the superficial zone of postnatal articular cartilage have been identified to exhibit progenitor cell characteristics [124], [125] and have been shown to express stem cells markers including *Sox2, CD34* and *CD105* [126]. The use of Hoechst 33342 dye and flow cytometry have also been employed to distinguish a 'side population' of cells which are not permanently stained by the dye as a result of a subpopulation of cells expressing a multi-drug transporter. Certain stem cells and non-differentiated cells have been shown to express the multi-drug transporter and therefore can be isolated [127]. A small population of cells isolated from the superficial zone of calf cartilage were shown to exclude Hoechst 33342 dye [125] and also exclusion of Hoechst dye was found in a small population of cells isolated from human articular cartilage [128]. Cells isolated from human articular cartilage were found to express cell surface markers which are normally expressed by mesenchymal stem cells in bone marrow and the perichondrium. The mean percentage of cells which expressed both *CD105* and *CD166* was 4% of total isolated cartilage cells. The subpopulation of CD105+/CD166+ isolated cells were found not to express markers of differentiated chondrocytes and were able to undergo successful multilineage differentiation including osteogenesis, adipogenesis and chondrogenesis. The presence of a small subpopulation of CD105+/CD166+ cells isolated from articular cartilage indicate the presence of multipotential mesenchymal progenitor cells in the human articular cartilage [129]. Seol *et al* induced injury in bovine osteochondral explants and found that migrating cells, which expressed *Notch1* and *ABCG2* homed to the site of injury. The presence of migrating cells were believed to include a subpopulation of chondrogenic progenitor cells [130].

Other adjacent joint tissues to articular cartilage have also been shown to contain cells with mesenchymal stem cells properties. Cells isolated from the fat pad stroma of the infrapatellar fat pad of human knee were found to exhibit cell surface molecules similar to those observed from bone marrow derived mesenchymal stem cells. Fat pad stromal cells were also able to undergo multilineage differentiation, forming osteoblasts, adipocytes and chondrocytes under appropriate culture conditions [131]. Mesenchymal stem cells have been found in bovine synovial fluid; cells exhibited CD44 and CD166 cell surface markers and could undergo multilineage differentiation. Synovial fluid derived MSCs have been proposed to originate from the synovium [132]. Cells isolated from human synovial membrane have been shown to undergo multilineage differentiation *in vitro* [133] and in an *in vivo* murine study, MSC markers were identified in cells in the lining layer and subsynovial tissue of joint synovium [134].

Chondroprogenitors have been identified in differing tissues of the synovial joint, including the articular cartilage superficial zone, the synovium, the groove of Ranvier and the fat pad. However, despite evidence that chondroprogenitors exist within these locations, there is little evidence that the chondroprogenitors mediate self-renewal and intrinsic repair of articular cartilage. OA incidence within the community and the phenomenon of the likely onset of OA following cartilage injury indicate that the existence of chondroprogenitors do not mediate healing or at least not at the rate at which articular cartilage deterioration takes place.

1.1.6 Skeletal Stem Cells: a source for Articular Cartilage Regeneration

1.1.6.1 Skeletal Stem Cells

A stem cell is characterized by its ability to self-renew by means of mitotic cell division and its potential to differentiate into differing specialised types of cells, through asymmetrical cell division, therefore retaining a pool of stem cells and also simultaneously producing transit amplifying cells [135]. Adult stem cells replace degenerating cells and thereby ensure that tissue is normally maintained which is turn allows for normal functioning of tissue in the body. Adult stem cells can therefore be thought as the regenerators that follow the degeneration process which may occur due to age, trauma or pathogenic conditions such as disease [135]. Given the limited capacity for endogenous regeneration of articular chondrocytes and the deterioration of specialised ECM, collectively the articular cartilage, following injury there is a need for alternative methods to regenerate articular cartilage.

Mesenchymal stem cells and chondroprogenitors have been shown to be resident in tissues of the synovial joint, but the use of these cells for regeneration of articular cartilage would require the harvest of joint tissue which would result in greater damage. However, the use of skeletal stem cells for articular cartilage regeneration is a propitious option. Given the availability of autologous skeletal stem cells from patients, the relatively easy method of harvest from bone marrow, the plasticity and non-immunogenic properties of skeletal stem cells, makes skeletal stem cells a promising candidate for therapeutic therapy in clinical application. Skeletal stem cell therapy could therefore be potentially used as therapy to regenerate cartilage tissue at joints in diseases such as OA and focal cartilage damage which have been previously discussed. Current stem cell research looks to delineate skeletal stem cells, allowing a more thorough comprehension of their differentiation process in terms of cell signalling pathways, epigenetic regulation, optimal growth conditions including stem cell niche. Understanding these processes will allow for better application of skeletal stem cells to regenerate and repair articular cartilage.

Stromal precursor cells, mesenchymal stem cells, bone marrow stromal stem cells, osteogenic stem cells [136] and skeletal stem cells are all names commonly used that refer to stem cells derived from bone marrow. Skeletal progenitor cells were first isolated by in 1966 by Friedenstein, who isolated colony forming unit-fibroblasts (CFU-F), progenitor cells, which had replicative capacity *in vitro* and capacity to differentiate into adipocytes, chondrocytes, haematopoietic supporting stroma and osteoblasts following transplantation of a single CFU-F *in vivo*. Friedenstein suggested that during postnatal life the bone marrow serves as a receptacle for stem cells which will generate mesenchymal tissues [137].

Multipotent mesenchymal stem cells are most commonly isolated from the bone marrow but have also been reported to be isolated from connective tissues such as periosteum, adipose tissue and synovial membrane [138] and have the potential to differentiate into various somatic cell types of the

mesenchymal cell lineage including; osteoblasts, chondrocytes, adipocytes, marrow stromal cells, myoblasts and tendonoblasts (Figure 11). Skeletal stem cells can also be isolated from developing fetal bones [139] and can be produced by differentiating isolated embryonic stem cells down the mesenchymal lineage and also induced pluripotent stem cells. The definitive cell type that a skeletal stem cell will terminally differentiate into depends upon the exposure to regulators specific to a certain lineage which includes growth factors and culture conditions [140]. Pittenger *et al* demonstrated that the osteoblastic, chondrocytic and adipocytic lineages could be established from human iliac crest bone marrow derived progenitor cells *in vitro* by isolation, expansion and characterization. The cells were characterized by the presence of marker proteins on their cell surface by flow cytometric analysis, their ability to proliferate in culture; exhibiting an attached and spread morphology by means of microscopy, and by their ability to continuously differentiate into the mesenchymal lineages [141].

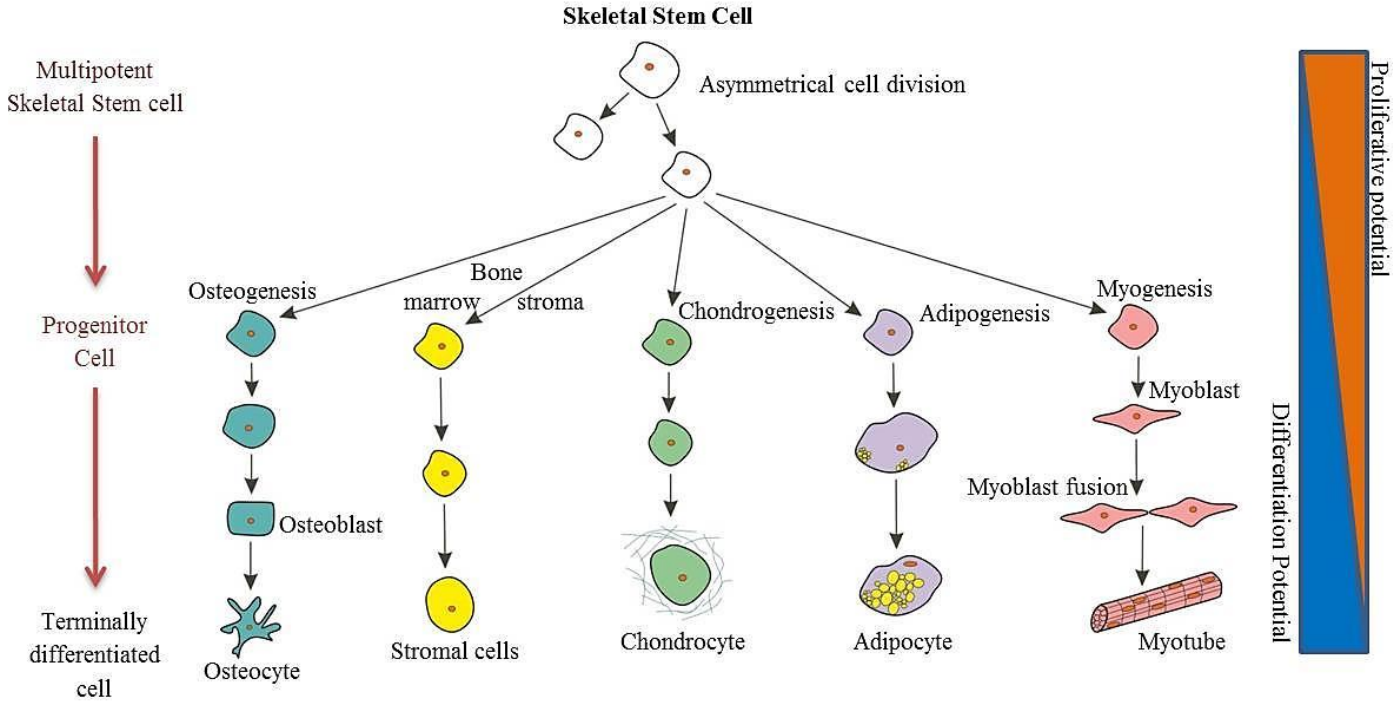

Figure 11. Skeletal stem cell proliferation and differentiation. Skeletal stem cells undergo asymmetrical cell division, retaining a pool of multipotent skeletal stem cells and also having the ability to differentiate along differing mesenchymal lineages. Skeletal stem cells can differentiate into differing fully differentiated cell types including osteoblasts and osteocytes, chondrocytes, adipocytes, myocytes and stromal cells which ultimately function as part of mesenchyme tissue including bone, cartilage, adipose tissue and muscle. (Image adapted from Bonfield, Adult Mesenchymal Stem Cells: An innovative therapy for Lung Diseases, 2010).

In addition to the regenerative capacity that bone marrow derived stem cells possess, skeletal progenitor cells have also been shown to possess immuno-modulatory properties which have been shown to regulate autoimmunity, tumour evasion and regulation of transplantation tolerance [142]. A combination of regulatory mechanisms exist which act upon several immune cells including T lymphocytes, B lymphocytes, Natural Killer cells and monocytes [143]. Skeletal progenitor cells also been shown to express no major histocompatibility complex (MHC) class II molecules and express only very low levels of MHC class I molecules. Skeletal progenitor cells have also been shown to lack the cell surface antigens including CD80, CD40 and CD86; the co-stimulatory molecules that have been shown to be involved in transplant rejection due to T lymphocyte activation [143].

The German pathologist Cohnheim was the first to hypothesize that fibroblast like cells derived from bone marrow were able to migrate to distal sites of injury [144]. Stem cells have homing potential to injured sites and likely to induce repair either through direct differentiation to replace damaged cells and/or have an ability to secrete mediators which create a reparative environment with immuno-regulatory function and anti-apoptotic regulation. Mesenchymal stem cells have been shown to express several chemokine receptors including CCR1, CCR7, CX3CR1 and CXCR4 and have been shown to migrate in response to chemokine ligand CX3CL1 and CXCL12 [145].

The formation of the mesenchymal tissues from skeletal stem cells is as a result of lineage commitment and maturation of the transit amplifying cells towards a somatic cell fate that no longer possesses the ability to self-renew indefinitely and exhibits the specialised features and functions of the particular specialised cell type. The ultimate differentiated cell type produced depends upon regulators such as growth factors and cell culture conditions which are specific to a certain lineage. A combination of extrinsic and intrinsic factors cause skeletal stem cells to differentiate into a specific cell type which follows a complex pathway with multiple cell intermediates; which themselves produce and secrete matrix proteins and factors which are essential for differentiation of the cell, along with environmental cues and available nutrients. *In vivo* a balance between skeletal stem cell self-renewal and differentiation is maintained [146] in post-natal life. *In vitro* stem cell differentiation can be manipulated by modifying the cell culture conditions and addition of certain growth regulators.

1.1.6.2 Skeletal Stem Cells and Chondrogenic Differentiation

Human bone marrow derived skeletal stem cells have the ability to undergo chondrogenesis. Culture expanded human skeletal stem cells have been shown to undergo chondrogenesis in micromass pellet culture in the presence of transforming growth factor beta 3 (TGF-β3). After 14 days of culture, cells secreted an ECM comprising of aggrecan, type II collagen and anionic proteoglycans [147]. The knowledge regarding mechanisms responsible for chondrogenesis have primarily focused on the process of chondrogenic differentiation of mesenchymal precursors during long bone development. The presence of a cartilage anlage and process of long bone development is distinct from the process of articular chondrocyte differentiation and articular cartilage development during synovial joint

formation as discussed previously. Despite the differences in the distinct developmental processes which both involve chondrogenic differentiation of mesenchymal cells, both processes are believed to initially share many of the same molecular mechanisms which regulate the differentiation process. Microaaray analyses have enabled the identification of certain genes involved in chondrogenesis, including genes encoding transcription factors, ECM genes and growth factors [148], [149]. Mechanisms which govern chondrogenic differentiation include both autonomous components which are stem-cell intrinsic and also non-cell autonomous which include components of the extracellular microenvironment. Chondrogenesis is mediated by a co-ordinated effect of hormones, cytokines, ECM proteins and cell adhesion proteins [149].

Chondrogenic differentiation is initiated through the condensation of mesenchymal cells, which can be replicated *in vitro* through the formation of high density micromass cultures. Yoo *et al* were the first to apply the use of a three dimensional micromass culture system for investigating the chondrogenic differentiation of adult human bone marrow derived stem cells [150]. Failure of the induction of chondrogenesis in monolayer culture of adult human bone marrow derived stem cells was demonstrated, but induction of chondrogenesis in adult human bone marrow derived stem cells cultured as aggregates highlighted the importance of high cell density and cell interaction, reminiscent of pre-cartilaginous condensation of cells *in vivo* [150]. Condensation of mesenchymal cells increases cell to cell contact and also cell-ECM interaction. Following condensation, chondroblasts undergo a phase of proliferation, within which phase the expression of cartilaginous ECM matrix proteins are up-regulated. Chondroblasts synthesise type II, type IX and type XI collagen, cartilage oligomeric matrix protein-1 and aggrecan [151]. Transcription factors mediate intracellular signalling, SOX5, SOX6 and SOX9 are the most studied in chondrogenesis.

Several growth factors, hormones and cytokines have been shown to influence chondrogenic differentiation, promoting cartilaginous ECM production and a chondrogenic phenotype. The TGF-β superfamily includes BMPs, TGF-βs, activins and inhibins. TGF-β is a significant factor in chondrogenesis, acting as a powerful stimulator of type II collagen and proteoglycan synthesis [152]. The expression of transcription factor *SOX9* is induced by TGF-β signalling [153]. All three isoforms of TGF-β have the ability to induce chondrogenic differentiation in MSCs, however, Barry *et al* have shown that TGF-β2 and TGF-β3 induce greater glycosaminoglycan accumulation and increased deposition of type II collagen in comparison to TGF-β1 [154]. BMP-2, -4, -6, -7, -13 and -14 have been shown to induce chondrogenic differentiation of MSCs. BMP-2 and BMP-4 have both been shown to induce up-regulation of type II collagen expression as well as hyaline cartilage proteins in MSCs [155]. Despite the role that BMPs have been shown to play during chondrogenic differentiation of MSCs, BMPSs may also induce hypertrophic differentiation and subsequent ossification [156]. BMP2 transfected MSCs were injected into thigh muscles of mice and shown to induce ectopic bone formation [157]. Therefore the role that certain mediators have in inducing chondrogenesis may induce hypertrophic chondrogenic differentiation and consequently induce endochondral ossification.

Depicting the factors involved primarily with non-hypertrophic differentiation will enable a better understanding of the differentiation of skeletal stem cells to chondrocytes with a hyaline or articular phenotype. Danisovic *et al* have reviewed the recent knowledge about growth factors and the effect upon MSC chondrogenic differentiation [158].

SRY (sex determining region Y)-box 9 (SOX9) transcription factor is the one of the earliest markers of chondrogenic differentiation. The importance of SOX9 during chondrogenic differentiation is highlighted by the hypoplasia of skeletal structures derived from cartilage precursors identified in a *Sox9* mutant mouse model [159]. SOX9 induces the up-regulation of cartilage specific genes including *Col2a1, Col9a2, Col11a2* and *Agcan* [160]. SOX9 was found to interact with the transcriptional coactivators CBP and p300, the interaction was shown to enhance SOX9-dependent *COL2A1* promoter activity. *COL2A1* expression was also found to be inhibited and chondrogenic differentiation of MSCs was inhibited following disruption of the CBP-SOX9 complex [161].

SRY (sex determining region Y)-box 5 (SOX5) transcription factor and SRY (sex determining region Y)-box 6 (SOX6) were found to be co-expressed with SOX9 during chondrogenic differentiation to enhance *Col2a1* expression [162]. The importance of the two transcription factors were shown by Sox5 and Sox6 mutant mice studies. *Sox5/Sox6* double null fetuses died *in utero* and an absence of cartilage was observed [163]. Chondrogenic differentiation was only found to be successful when Sox5, Sox6 and Sox9 were combined when investigated in differing cell types compared to the action of each Sox gene individually [164]. Han *et al* have shown that the action of the 'sox trio' inclusive of SOX5, SOX6 and SOX9 is required for aggrecan expression. SOX9 binds to the *Agc1* enhancer only in the presence of SOX5 and SOX6 [165].

1.1.6.3 The use of Skeletal Stem Cells for Articular Cartilage Repair

The use of cell based therapies to repair articular cartilage defects with the aim to allow a fully functional joint surface, which is capable of tolerating the stresses and strains induced in joint loading is a promising ideal for the regeneration of cartilaginous tissue. The properties of skeletal stem cells make them a viable and promising cell source to help regenerate articular cartilage. Skeletal stem cells have been shown to be regulated in part by microRNAs which regulate different genes involved with the differentiation process post-transcriptionally. The use of skeletal stem cells in combination with microRNA modulation could provide a new approach to skeletal tissue reparation. Endogenous regeneration of cartilage does not occur spontaneously resulting in the loss of chondrocytes and diminishment of the surrounding specialised extracellular matrix, use of autologous skeletal stem cells for cartilage repair is one a proposed method for cartilaginous tissue reparation. Im *et al* induced osteochondral defects in to the patella grooves of a rabbits, following isolation of MSCs from the marrows of rabbits, MSCs were applied to the defect sites. Im *et al* identified that the histological score of the MSC treated group was higher than untreated controls concluding that MSCs implantation could enhance the cartilage defect [166]. Non-operative administration of MSCs in

animal studies has also shown the beneficial effect of MSCs in experimentally induced OA joints [167], [168].

Murphy *at al* injected autologous bone marrow derived MSCs in a hyaluronan solution directly into the medial compartment of OA induced caprine knee joints and found a reduction in degeneration to the articular cartilage [167]. Comparison of intra-articular injection of autologous culturally expanded bone marrow derived MSCs and autologous culturally expanded and chondrogenic induced bone marrow derived MSCs into the knee joints of sheep were both found to slow the progression of deterioration of cartilage in experimentally induced OA. Regeneration of the articular cartilage was observed in the sheep knee joints which had been administered chondrogenically induced MSCs [168].

Transplantation of MSCs combined with a scaffold has been a popular choice amongst many research groups for investigating articular cartilage regeneration. However, unlike intra-articular injection of MSCs, the use of a scaffold generally involves operative surgery. Bone marrow derived cells were isolated and expanded *in vitro* and then dispersed into a type-1 collagen gel, which was then transplanted into a full thickness surgically induced articular cartilage defect in rabbits. Following implantation cells differentiated into chondrocytes and at 24 weeks post operation, subchondral bone was fully repaired with overlying articular cartilage [169]. Berninger *et al* have suggested a method combining MSCs in fibrin clots and the transplantation of the pre-established fibrin cell clot into osteochondral defects in rabbit knee joints. Preliminary results indicated that following implantation of the fibrin-MSC-clot into defect sites, at post-operative inspection an intact and homogenous surface was observed [170]. MSCs seeded onto a hyaluronan based scaffold was transplanted to an OA induced defect site in the knees of rabbits, 6 months post-operative inspection found that regenerated tissue had formed [171].

Previous studies in humans have reported the therapeutic effect of skeletal stem cells administration in patients; Nejadnik *et al* found that patients administered with bone marrow stem cells into chondral lesions were found to have better physical chondrocyte implantation [172]. Autologous expansion of bone marrow derived MSCs following combination with platelet-rich fibrin glue were transplanted to full thickness cartilage defects of the femoral condyle of 5 patients. Follow up inspection found improvement to symptoms in all patients, with MRI revealing complete defect filling and surface conformity with native cartilage in 3 patients [173].

Kasemkijwattana *et al* found that patients who were administered autologous bone marrow mesenchymal stem cell exhibited significant improvement in knee function with good defect filling [174]. Davatchi *et al* found that patients with moderate to severe osteoarthritis who were administered autologous mesenchymal stem cells showed a reduction in pain [175]. Kuroda *et al* showed that a young male athlete treated with autologous bone marrow stromal cells to a articular cartilage defect in the medial femoral condyle, seven months post-surgery histological analysis

showed the defect was filled with hyaline like cartilage and one year after surgery the returned to his previous sporting activity and experienced no pain with significant improvement in clinical symptoms [176].

1.1.7 Chondrogenesis and Epigenetics

The process by which skeletal stem cells differentiate is complex; different growth factors, signalling pathways and transcription factors are involved and these are all regulated at different levels. There are several levels of control that are responsible for regulating skeletal stem cell differentiation which all fall under the study of heritable changes in gene expression which does not involve changes to Watson-Crick base pairing of DNA; which is known as epigenetics. To fully elucidate the cell regulatory mechanisms which regulate the differentiation of a skeletal stem cell to a chondrocyte, comprehension of the mechanisms of epigenetic regulation of gene expression is fundamental.

Differing parts of the genome can be switched on and off at specific locations and times; the reactions that initiate these switches and the factors that influence them can be studied. As progression of developmental stages occurs in stem cell genes that would have been active in earlier stages of differentiation for example in the earlier progenitors are gradually down regulated at later stages of development. The progression of developmental stages is due to expression of select transcription factors accordant with chromatin remodelling and histone modification [177]. Understanding how DNA is packaged into chromosomes is key to understanding epigenetic regulation. Chromatin consists of both DNA and proteins and generally exists in a condensed form known as heterochromatin which is transcriptionally silent, whereas euchromatin is less condensed and exposes active transcription sites. Histone proteins and DNA can be modified which influences the chromatin structure by altering the affinity of chromatin binding proteins and also altering its electrostatic nature determining whether it exists as heterochromatin or euchromatin.

1.1.7.1 Mechanism of Epigenetic regulation of gene expression during differentiation

Epigenetic changes include chromatin remodelling and modification, DNA methylation of CpG dinucleotides, covalent histone modification and positioning of chromatin to distinct nuclear domains. These mechanisms allow for cells to retain their identity, for example when cells are exposed to environments which may induce cells to alter their definitive cell fate and these mechanisms are also in place to ensure stem cell maintenance over time [177].

The best characterised example of epigenetics is DNA methylation; the process by which a methyl group is added to either the 5 position of a cytosine pyrimidine ring or the 6 nitrogen of an adenine purine ring. DNA methyltransferases (DNMTs) regulate DNA methylation patterns by catalysing the transfer of a methyl group from an S-adenosyl methionine donor to DNA. The three DNMTs which catalyse this reaction include DNMT1, DNMT3A and DNMT3B. The DNA methylation process allows for stable change of gene expression so that cells can either acquire a memory allowing them to remember where they have been or allows for a decrease in gene expression as a result of inhibition of transcription factor binding [178]. Often CpG sequences (regions of DNA where a cytosine nucleotide resides next to a guanine nucleotide) are cumulated in islands located near to the promoters to approximately a third of genes. It is the cytosines in CpG dinucleotides which are methylated and

the methylation process outlined above correlates with gene expression down regulation, DNA methylation stably alters gene expression during stem cell differentiation, the change is generally permanent and therefore prevents the cells from de-differentiating or trans-differentiating. Methylated DNA attracts methylcytosine binding proteins which promote the condensation of chromatin preventing exposure of transcription sites. In addition to CpG islands that exist there are also regions which are located close to CpG islands but have a lower CpG density; these regions are known as shores where tissue specific transcriptional repression occurs [178].

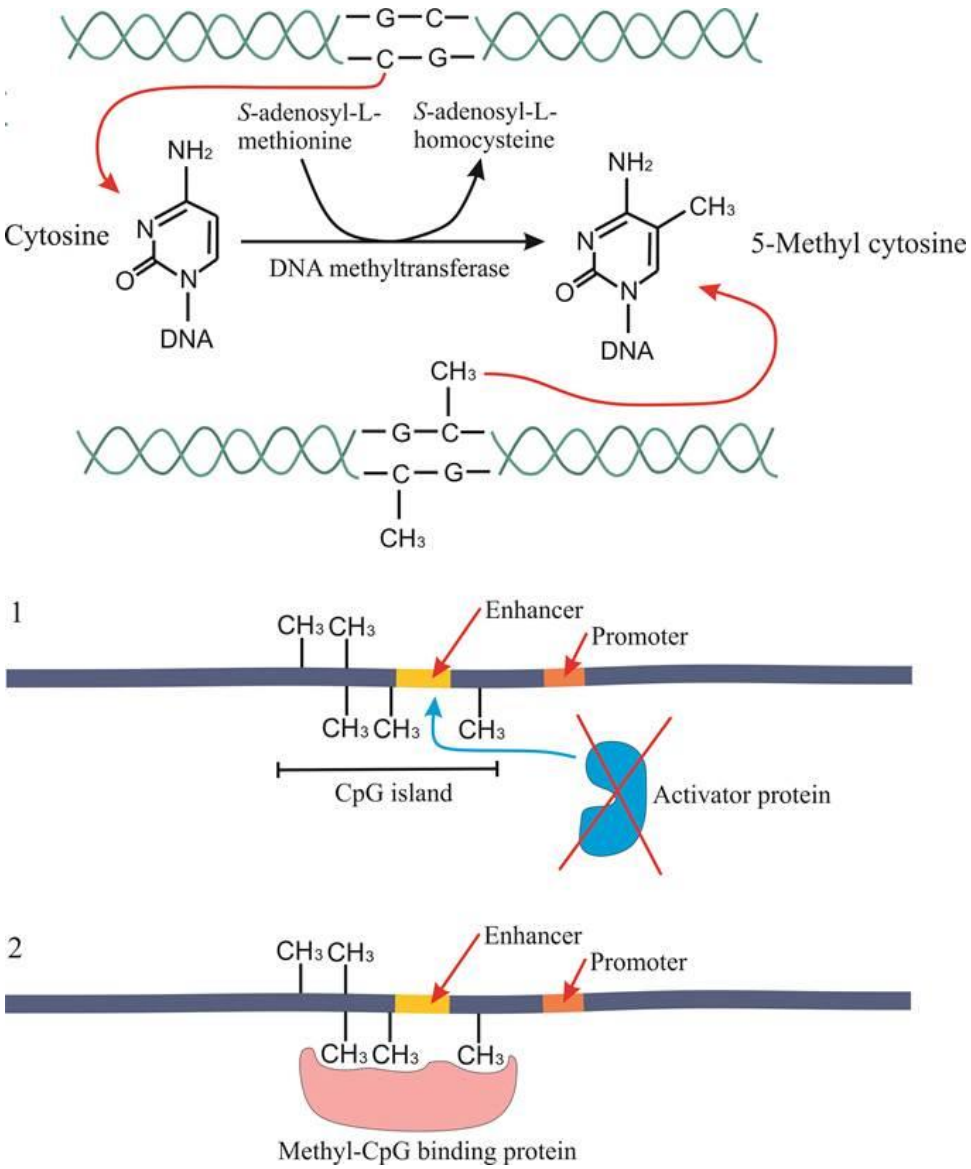

Figure 12. DNA methylation. Cytosine groups are methylated forming 5-Methyl cytosine by DNA methyltransferase at CpG islands. 1) Methylation at CpG islands can prevent activator proteins from binding to the enhancer element, inducing transcription repression. 2) Methylation can recruit methyl-CpG binding proteins, which can recruit other proteins such as histone deacetylase which induces chromatin condensation. (Figure adapted from DNA Methylation: Fingerprints of the (epi)genome, https://www.caymanchem.com/article/2153).

DNA is packaged into nucleosomes. A single nucleosome is made up of 8 histone protein cores around which a segment of DNA sequence is wound (Figure 13). The core histones carry covalent modifications which is another type of epigenetic mechanism which regulates gene expression. Histones can be enzymatically post-transcriptionally modified at their amino terminal tails through processes such as methylation, acetylation, phosphorylation and ubiquitination. The formation of inactive and active genomic regions is regulated by these histone modifications which is related to transcriptional silencing and activation [178].

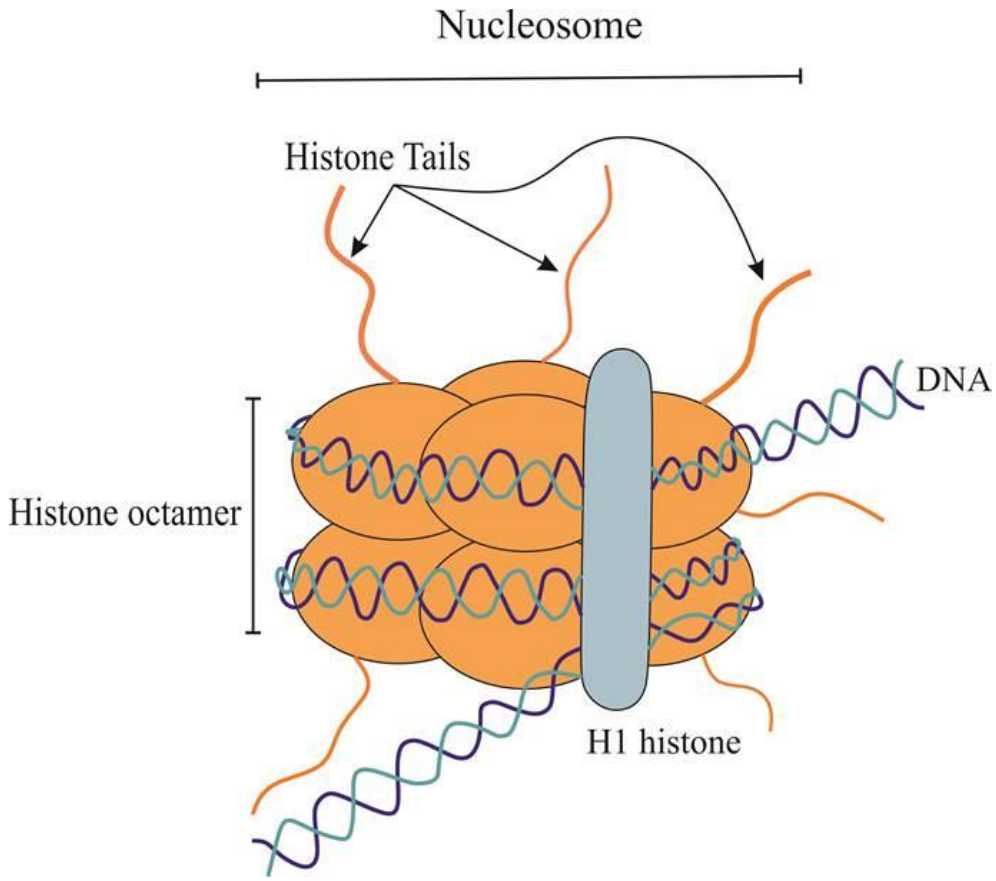

Figure 13. Nucleosome structure. The nucleosome is comprised of 8 histone proteins around which DNA are wrapped around. Histone tails can be modified through processes such as methylation, acetylation, phosphorylation and ubiquitination, which can repress and activate gene transcription. (Figure adapted from Catalano *et al*, Epigenetics modifications and therapeutic prospects in human thyroid cancer, Frontiers in Endocrinology, http://dx.doi.org/10.3389/fendo.2012.00040).

Histone modification by acetylation is mediated by histone acetyltransferases (HATs) which takes place at specific lysine residues at the amino terminal tail and catalyses the addition of an acetyl group which results in the slackening of the nucleosome as a result of weakened charge attraction between the histone and the DNA which allows for transcriptional machinery to access. In contrast, histone modification by deacetylases (HDACs), catalyse the reverse reaction and is associated with transcriptional repression. Deacetylases include the zinc catalysed mechanism of deacetylation and

sirtuin deacetylases which needs NAD^{+}[42] to function both of which catalyse the removal of an acetyl group from histones. Many transcriptional repressors either have or recruit HDAC activity and many transcriptional activators either have or recruit HAT activity [178]. Histone tails can be methylated on arginine or lysine residues, the reaction is catalysed by protein arginine methyltransferases (PRMTs) and histone methyl transferases (HMTs). Histone methylation is a reversible reaction which requires the action of histone demethylases [178].

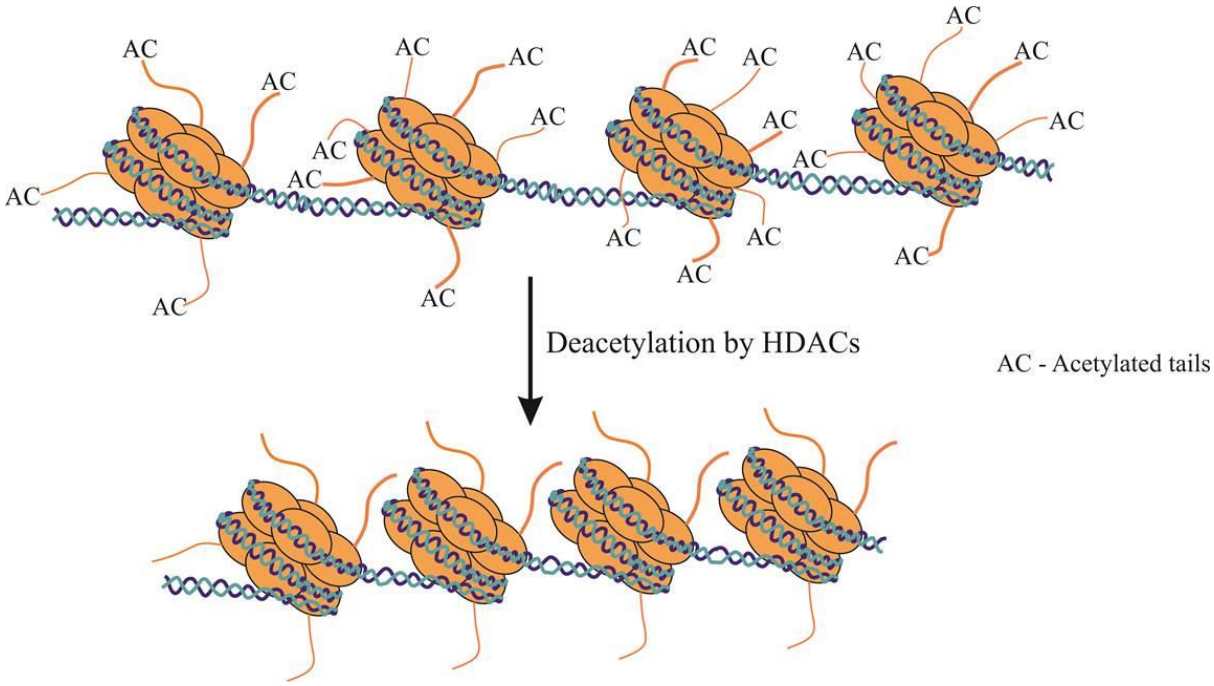

Figure 14. Histone deacetylation. Histone tails can be deacetylated by histone deacetylases (HDACs) which remove acetyl groups, which increases the positive charge of histone tails and induces high affinity biding between the histone tails and the negatively charges phosphate groups on the DNA backbone, causing chromatin condensation and transcription repression. (Figure adapted from Pons *et al*, Epigenetic histone acetylation modifiers in vascular remodelling: new targets for therapy in cardiovascular disease, European Heart Journal, doi: http://dx.doi.org/10.1093/eurheartj/ehn603).

1.1.7.2 Epigenetics and microRNAs

Gene regulatory processes are responsible for the expression of genes; which include the processes of epigenetics such as DNA methylation and histone modifications. MicroRNAs can alter gene expression by acting as post transcriptional regulators; they allow for gene transcription but can prevent the translation of the gene transcript. It is predicted that a single microRNA may target many genes and it is also thought that approximately a third of human messenger RNA is regulated by miRNAs [179]. The expression of specific microRNAs during stem cell differentiation may determine the lineage which the stem cell will differentiate towards.

MicroRNAs are noncoding single stranded RNAs which range in length from 20 to 25 nucleotides and regulate gene expression. MiRNAs are expressed in a tissue specific and developmentally

regulated modus. MiRNAs are processed from longer primary transcripts which undergo processing in the nucleus and the cytoplasm to form small coding single stranded RNA. MiRNAs are transcribed from either part of a gene or from an intergenic region whereby the miRNA has its own promoter. Following transcription, the primary transcript it is cleaved into a 60-75 nucleotide hairpin [180]. Further processing results in a double stranded duplex which eventually forms the mature single-stranded microRNA. Single stranded mature microRNA targets messenger RNA which contains complimentary sequences within the 3' untranslated region (UTR). Sequence complimentarity between miRNA and its target mRNA determines whether or not the miRNA induces posttranscriptional repression of the mRNA and therefore determines whether protein translation proceeds. Degradation of the target mRNA occurs as a result of complete complimentarity between miRNA and target mRNA and inhibition of the target mRNA results due to incomplete complimentarity between miRNA and target mRNA [181].

During the process of stem cell differentiation there is a requirement to down-regulate stem cell maintenance genes and up-regulate lineage-specific genes in order for a cell to progress along a certain lineage and ultimately reach terminal differentiation. Throughout the process of differentiation through which the cell transits, the transcription pool is replaced simultaneously when a new stage of differentiation occurs; whereby new genes are activated but this also means that transcripts may remain from the previous stage and therefore need to be silenced to allow for the progression of differentiation. One way of silencing the remaining transcripts is through the transcription of microRNAs which can bind to mRNA transcripts and prevent their downstream translation and therefore prevent protein expression. It is predicted that a single miRNA can target many different genes and that a least thirty percent of human messenger RNAs may be regulated by miRNAs [179].

Chapter 1.2
Introduction
The role of MicroRNAs in Osteoarthritis and Chondrogenesis

1.2.1 MicroRNA discovery and Biogenesis

1.2.1.1 MicroRNA discovery

The first microRNA was discovered in 1993 which involved a study on *lin-4* small RNA in *Caenorhabditis elegans.* Lee *et al* showed that *lin-4* negatively regulated the level of the protein Lin-14 in *C.elegans*, which caused a decrease in the Lin-14 protein in the first larval stage of *C.elegans* development. Regulation of Lin-14 was suggested to be controlled by two small transcripts which were complimentary to sequences in the 3' untranslated region (UTR) of the *lin-14* messenger RNA and therefore suggested that *lin-14* translation was regulated by *lin-4*; which encodes the small transcripts observed, via an interaction involving antisense RNA-RNA base pairing [182]. This finding by Lee *et al* showed that the miRNA lin-4 regulated the level of the Lin-14, which had previously been shown by Ambros and Horvitz to play a role in *C.elegans* lateral hypodermal cell lineage development [183].

Lagos-Quintana *et al* went on to show that many 21 and 22 nucleotide RNAs, known as microRNAs, were found to exist in both invertebrate and vertebrates, with many which exhibited high conservation [184]. It was the initial work on lin-4 which opened up a vast area of potential to look at cellular processes in a different light; predicting that miRNAs may greatly contribute to the control of differing regulatory processes. From the initial discovery outlined above, the roles and functions of differing miRNAs, has been broadly studied in recent years across differing models. The study by Lee *et al*, in addition to the discovery of microRNA, also highlighted the importance of microRNA during development. Research into small non-coding RNAs established a novel group of post-transcriptional regulators of gene expression. It was also predicted that if small non-coding RNAs could regulate gene expression, it could be possible that the dysregulation of microRNA expression may result in aberrant gene expression and potentially disease outcome. The first study to link microRNA dysregulation with human disease was conducted by Calin *et al*, who showed that miR-15 and miR-16 were deleted or down-regulated in the majority of B-cell chronic lymphocytic leukemias [185].

1.2.1.2 MicroRNA biogenesis

MicroRNAs are expressed in a tissue specific and developmentally regulated modus. MicroRNAs are processed from longer primary transcripts, which like classic RNA polymerase II yields, possess polyA tails and a 5' cap structure which then undergo processing in the nucleus and the cytoplasm which results in the formation of a mature microRNA. The genomic locus of microRNAs, illustrated

in Figure 15, can differ: microRNA genes may exist in an independent transcriptional unit with a promoter. Similarly several microRNA genes can be transcribed together producing a single primary microRNA but can be subsequently cropped to form the individual mature microRNAs; these are known as microRNA clusters. MicroRNAs that are controlled by their own promoter are usually found in intergenic regions. Some microRNA genes are located in intragenic regions and are regulated by the promoters of the protein coding host gene within which they lie and therefore require splicing following transcription. Some intronic microRNAs have been found to be regulated by their own promoters which also lie upstream in the intergenic region. Mirtrons are microRNAs that are generated from short introns which make use of the spliceosome machinery and followed by debranching to ensure the correct pre-microRNA boundaries and in some cases mirtrons can still possess a tail of ribonucleotides which are subsequently trimmed by the exosome to form functional pri-microRNA [186].

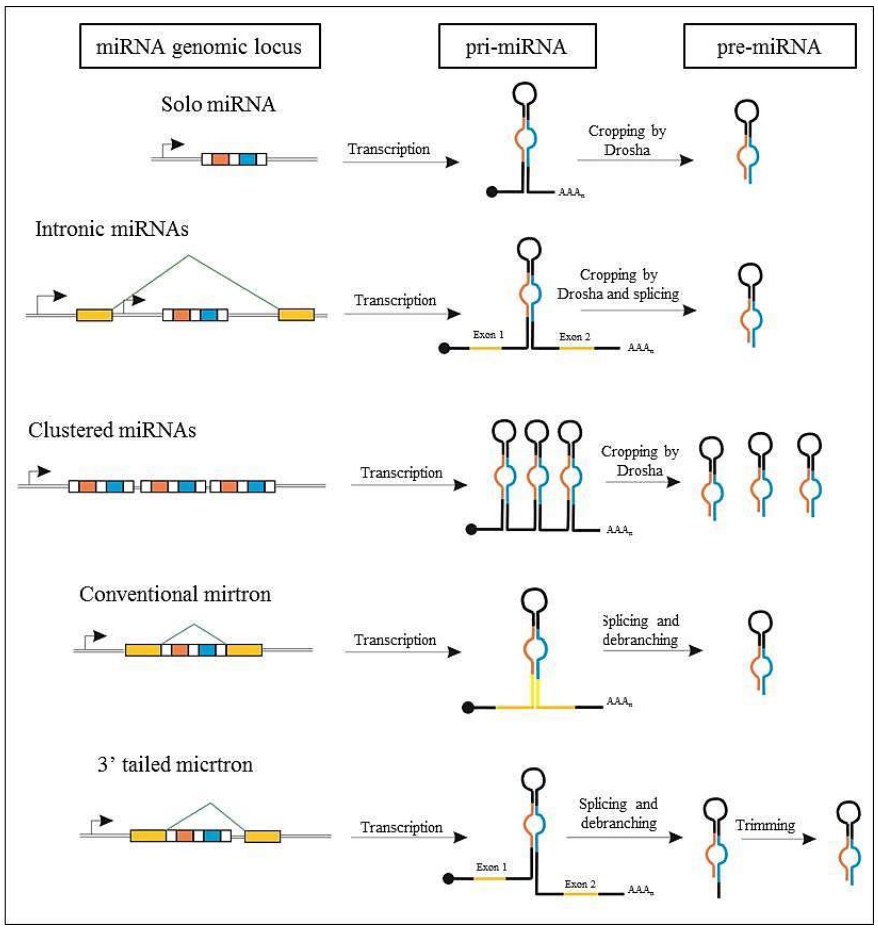

Figure 15. MicroRNA genomic locus. A single microRNA or a cluster of microRNAs can be transcribed from a microRNA gene which has a promoter. Intronic microRNAs are generally under the control of a host gene promoter and require splicing following transcription. The primary microRNA (pri-miRNA) undergoes processing in the nucleus to form the precursor microRNA (pre-microRNA) which is exported to the cytoplasm to undergo processing by Dicer. (Figure adapted from Berezikov, Evolution of microRNA diversity and regulation in animals, nature reviews genetics, doi10.1038/nrg3079).

Regardless of where the microRNA gene is located, the most distinctive feature of microRNA biogenesis is the ability of the intermediary transcripts to fold into hairpin structures which allows for their recognition and subsequent processing by the microRNA biogenesis machinery. Figure 16 illustrates the microRNA biogenesis process. With exception to mirtrons which do not make use of a Drosha–DGCR8 (Pasha) complex, following transcription all other microRNA genes are cleaved into a 60-75 nucleotide hairpin precursor by the RNase III endonuclease Drosha in the nucleus. The hairpin precursors also known as pre-miRNAs are exported to the cytoplasm by the protein Exportin 5. In the cytoplasm pre-miRNA is cleaved by the RNase Dicer which cleaves the loop at the end of the hairpin by recognizing the end of the pre-miRNA hairpin and calculating approximately 20 base pairs in distance from the end of the hairpin [180]. Helicase activity induces separation of the small double stranded RNA; the microRNA-microRNA* duplex to form the mature single-stranded microRNA and single stranded microRNA* which is generally degraded but in certain cases can also be loaded in the mRISC. The single stranded mature microRNA is loaded into a RNA-induced silencing (RISC)/Argonaute complex, where it can direct the regulation of target messenger RNA which contains complimentary sequences in their 3' untranslated region (UTR) to the miRNA sequence. Sequence complimentary between miRNA and its target mRNA determines whether or not the miRNA induces posttranscriptional repression of the mRNA and therefore determines protein translation. Degradation of the target mRNA is as a result of complete complimentary of target mRNA and miRNA. Translational inhibition or exonucleolytic mRNA decay of the target mRNA is as a result of incomplete complimentary between the target mRNA and miRNA, due to the existence of central bulges between nucleotides 9-12 and/or G-U wobbles [181] [187].

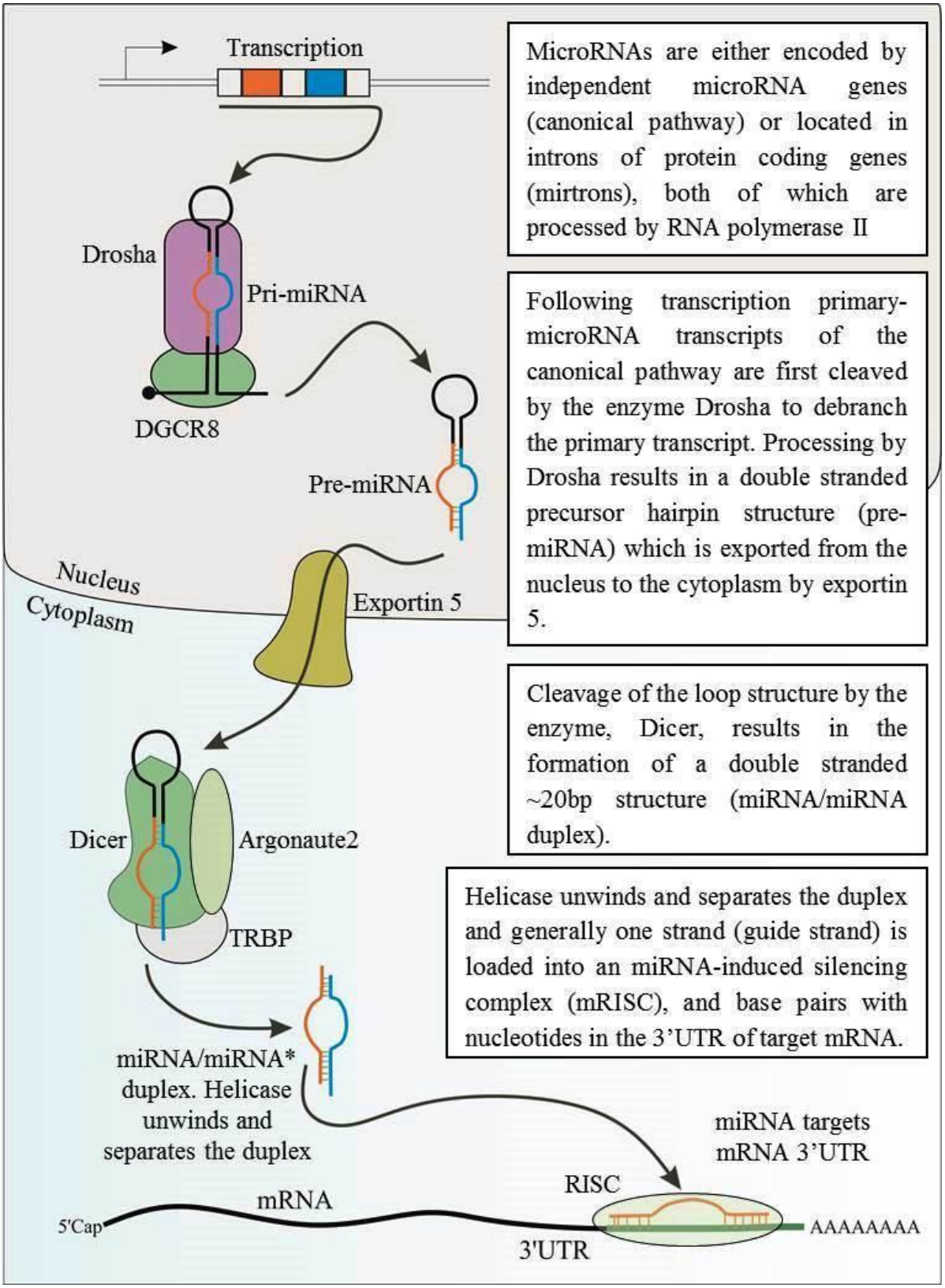

Figure 16. MicroRNA biogenesis. The process by which microRNAs are processed from their primary transcripts to mature microRNA which targets mRNA at the mRISC, which includes processing by the microprocessor complex (Drosha and DGCR8) in the nucleus and cleavage by Dicer in the cytoplasm. (Figure adapted from Krol *et al*, The widespread regulation of microRNA biogenesis, function and decay, doi:10.1038/nrg2843).

Identifying targets of microRNAs elucidates the potential role of the microRNA in question and reveals more about the regulatory pathway in which the specific microRNA is involved. Commonly, it was believed that nucleotides 2-7 of the 5' end of mature animal microRNA, the microRNA seed, was the most important factor in microRNA targeting. It is the microRNA seed which complimentary base pairs to ribonucleotides in the 3'UTR of target mRNA (Figure 17) which is the basis for identifying target mRNAs experimentally due to the ability to predict likely targets of microRNA especially with the utilisation of current target prediction programs. However target prediction can fail to identify targets known as false negatives and despite perfect Watson-crick base pairing between the nucleotides 2-7 of the seed and target mRNA, the mRNA may also not be a true target which is known as a false positive. Other target pairing configurations have been identified such as centred pairing and 3' end pairing to the 5'UTR of mRNA which do not follow the seed matching rule, which can make experimental identification of mRNA targets difficult. Brodersen and Voinnet comprehensively review the principles of microRNA target recognition, revising the mechanisms that microRNAs employ to select their target and the mechanisms of regulation used by microRNAs [187].

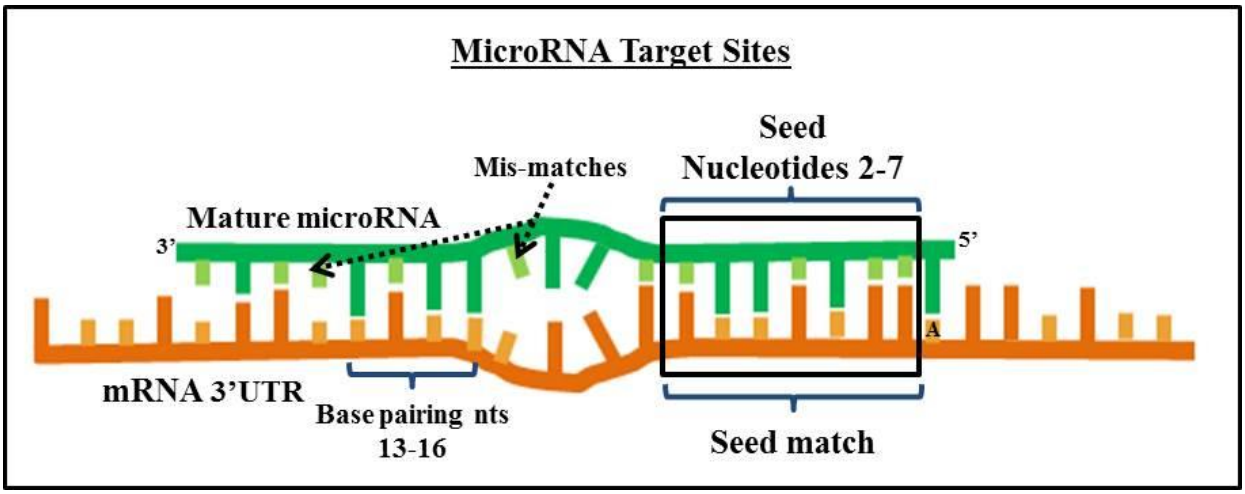

Figure 17. Mature microRNA binding to mRNA 3'UTR showing typical seed matching at nucleotides 2-7 of the 5' end of mature miRNA. (Figure adapted from Filipowicz *et al*, Mechanisms of post-transcriptional regulation by microRNAs: are the answers in sight?, Nature Reviews Genetics 9, 102-114 (February 2008) | doi:10.1038/nrg2290).

1.2.2 MicroRNA expression in Osteoarthritis and importance of microRNA identification

1.2.2.1 MicroRNA expression in Osteoarthritis

MicroRNA expression signatures have been associated with distinct pathological features and disease. The functions of certain microRNAs in biological processes have been elucidated and therefore it is possible to investigate the role of microRNAs in OA disease progression. As described in chapter 1.1, the homeostatic balance must be maintained in articular cartilage and it is apparent that up-regulation of catabolic factors induces cartilage degradation. MicroRNAs may have functions in maintaining the anabolic-catabolic balance in articular chondrocytes, aberrant signaling may have an impact upon microRNA expression which may induce changes in expression of genes involved with maintaining the anabolic-catabolic balance [188]. Iliopoulos *et al* investigated the expression of microRNAs from OA cartilage compared to normal cartilage and identified 16 microRNAs which were differentially expressed [189]. In a slightly different approach Diaz-Prado *et al* isolated chondrocytes from OA and normal cartilage and investigated microRNA expression and found that 7 microRNAs were differentially expressed between OA and normal chondrocytes [190]. Despite identification of differential expression of certain microRNAs in OA cartilage, elucidation of the function of some of the identified microRNAs has not been investigated. Some research groups have identified microRNA expression in OA chondrocytes and defined the function of the microRNA with respect to OA pathology.

Many of the microRNAs which have been shown to exhibit aberrant expression are listed in table 2. An example of microRNA dysregulated expression in OA and the impact upon articular cartilage is miR-140. The expression of miR-140 has been found to be significantly down-regulated in OA cartilage compared to normal cartilage [191], [192]. Miyaki *et al* identified a down-regulation of miR-140 following treatment of chondrocytes with IL-1β and treatment of chondrocytes also induced *ADAMTS5* expression up-regulation. Transfection of chondrocytes with miR-140 was able to suppress IL-1β induced *ADAMTS5* expression and up-regulate *aggrecan* expression, which suggests that miR-140 either directly or indirectly targets the aggrecanase *ADAMTS5* [191]. OA pathogenesis is associated with an increase in catabolic associated mediators. ADAMTS5, also known as aggrecanase 2, cleaves aggrecan [193] and in a murine model of OA, deletion of the catalytic domain of Adamts5 resulted in a reduction to cartilage destruction severity due to the inability of Adamts5 to mediate aggrecan degradation [194]. The reduced expression of miR-140 in OA therefore enables de-repression of *ADAMTS5* expression which is able to cleave aggrecan and mediate articular cartilage degradation. Following on from the initial study, Miyaki *et al* later created miR-140 deficient mice and cartilage specific miR-140 transgenic mice. Mice which were deficient of miR-140 exhibited age related OA associated changes, including loss of proteoglycans and articular cartilage fibrillation and also increased protein levels of Adamts-5 in articular cartilage. Transgenic mice which overexpressed

miR-140 in cartilage were found to be resistant to adjuvant induced arthritis and chondrocytes exhibited decreased *Adamts-5* expression. Luciferase assays also clarified *Adamts-5* as a direct target of miR-140 [195]. Given the down-regulated expression of miR-140 observed in OA and the overexpression of miR-140 in chondrocytes mediating protection from adjuvant induced arthritis, one function of miR-140 in articular cartilage is to regulate levels of ADAMTS5 or aggrecanase 2, down-regulation of miR-140 induces up-regulation of aggrecanase 2 which contributes to aggrecan degradation. The administration of exogenous miR-140 to areas of articular cartilage injury and OA joints may therefore prevent and/or slow the break-down of aggrecan through miR-140 targeted down-regulation of *ADAMTS5*. Figure 18 illustrates a proposed model for miR-140-5p function in normal and OA articular cartilage.

MiR-140 was shown to target *ADAMTS-5* which encodes ADAMTS5, a major aggrecanase in articular cartilage. MicroRNAs which regulate articular cartilage ECM components may therefore have a role in the underlying pathology of OA. MicroRNAs which function in inflammation, modulating anabolic factors, modulating catabolic factors, regulating articular chondrocyte apoptosis and modulating proteolytic enzymes may all have differing roles in maintaining articular cartilage homeostasis. Dysregulation in microRNA expression may induce changes to any of these processes and may therefore contribute to articular chondrocyte and cartilage degeneration.

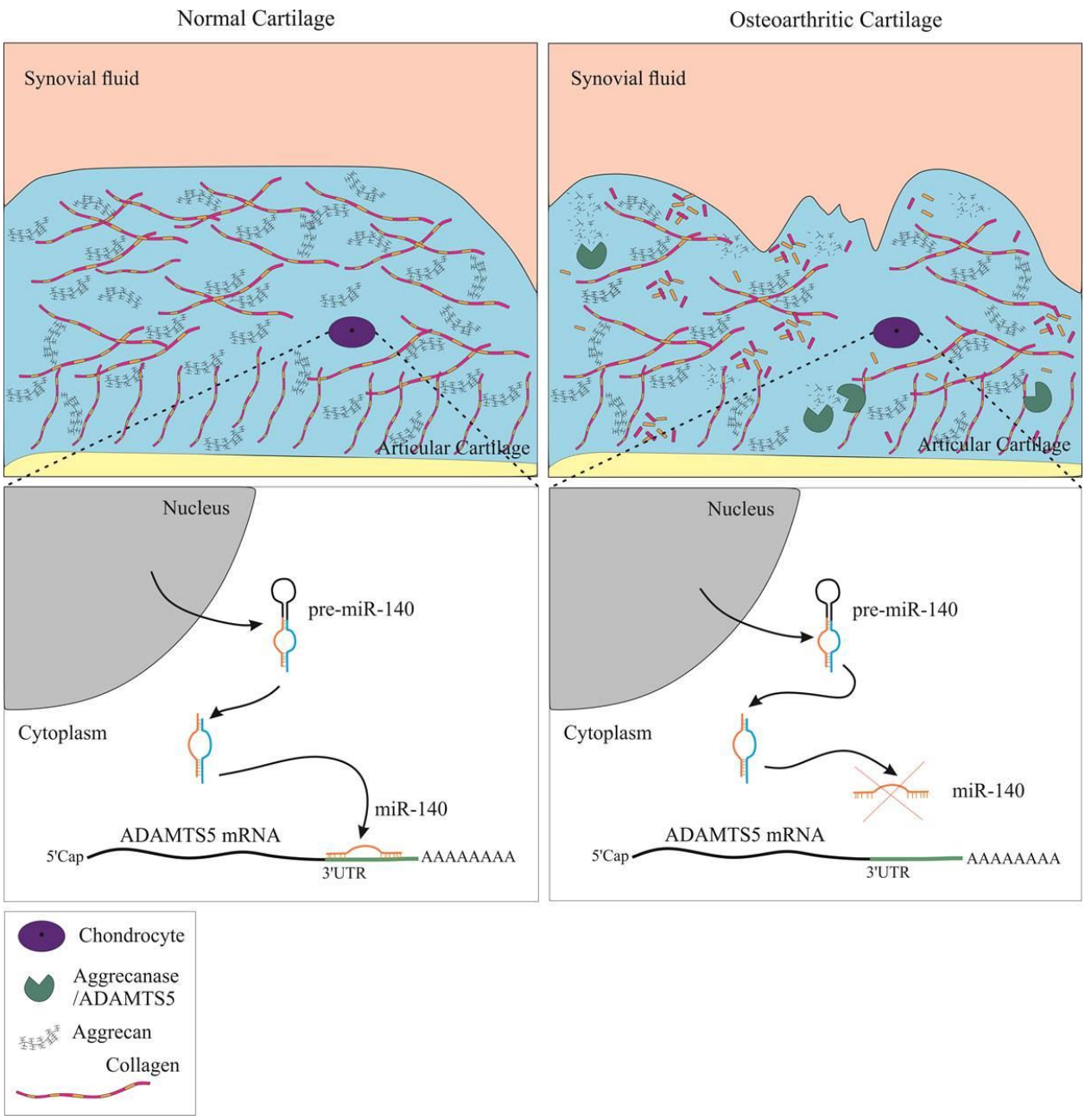

Figure 18. Proposed schematic model for miR-140-5p function in normal and OA articular cartilage. In normal cartilage, miR-140 targets *ADAMTS-5* mRNA 3'UTR, which results in the down-regulation of ADAMTS-5, which prevents ADAMTS-5 from degrading native aggrecan present in the articular cartilage. In OA, miR-140 is down-regulated which enables ADMATS-5 expression de-repression, which is likely to contribute to increased aggrecan degradation.

1.2.2.2 MicroRNAs as biomarkers of Osteoarthritis

Biomarkers are indicators of a biological state which can be measured to give an indication of biological process. Biomarkers can therefore be used to identify pathogenic processes that may be taking place within the body and used to diagnose disease. Given that some microRNAs are tissue specific, stable and are likely to be differentially expressed in disease state they make ideal candidates as biomarkers [196]. Osteoarthritis may be as a result of defective genes encoding microRNAs leading to either the over or under expression of certain genes due to the inability of specific microRNAs to induce normal regulatory function which helps to control articular cartilage tissue homeostasis. It may also be possible that the signaling pathways which control microRNA gene expression are defective which may also result in OA. Abnormal microRNA expression in OA indicates the expression of specific microRNAs aberrantly expressed for diagnosis of disease state. Table 2 lists and describes many of the functions of dysregulated microRNAs identified in OA cartilage and/or chondrocytes, dysregulated microRNAs could therefore serve as biomarkers for identification and diagnosis and potential severity of OA.

1.2.2.3 MicroRNAs as therapeutic targets in Osteoarthritis

MicroRNAs for use in therapeutic application may be advantageous over other therapies. Two strategies can be interpreted when referring to the potential application of microRNAs for therapeutic application. One strategy is the concept of inhibiting microRNA activity through use of microRNA antagonists which induces endogenous microRNA degradation and original target gene expression up-regulation and resultant gain of function. The second strategy is miRNA replacement with miRNA mimics which induce target gene expression repression and resultant loss of function. MicroRNAs need to be tightly regulated so as to either inducing repression of microRNAs or inducing the expression of optimistic microRNAs to appropriate levels to induce the correct effects upon target gene and protein expression.

The small size of microRNAs offer an advantage over larger sized protein therapeutics and the known and conserved sequence also offers an advantage from a therapeutic development standpoint. MicroRNA mimics have the same sequences as the naturally occurring microRNAs which enable the microRNA mimic to target and regulate mRNAs which are regulated by the endogenous microRNA. Additionally microRNAs generally target many mRNAs which can all be involved in similar cellular mechanisms or pathways, therefore modulation of a single microRNA may result in the simultaneous down-regulation of a broad set of targets which may have a far greater impact.

Osteoarthritis as a result of microRNA down-regulation which may allow for de-repression of negative regulators of articular chondrocyte and cartilage homeostasis which induce a catabolic effect could potentially be treated through the administration of exogenous microRNAs. Osteoarthritis as a result of overexpression of microRNAs which target positive regulators of articular chondrocyte and cartilage homeostasis could be potentially treated by the administration of exogenous anti-miRs which

block the action of microRNAs. Various *in vivo* studies have made use of exogenous microRNA modulation to investigate therapeutic effect upon diseased state. As described previously, the expression of miR-140 has been found to down-regulated in human chondrocytes isolated from cartilage from patients with OA, implicating miR-140 is involved with OA pathogenesis [197]. MiR-140 deficient mice have been shown to exhibit age-related OA changes such as fibrillation of the articular cartilage and loss of proteoglycan. Overexpression of miR-140 in the cartilage of transgenic mice has also shown cartilage to be protected from adjuvant induced arthritis [195]. The exogenous administration of miR-140 may therefore provide a suitable therapy for OA conferring a chondro-protective role. In addition to miR-140, several microRNAs have been identified as exhibiting dysregulated expression in OA, as listed in table 2. The application of microRNA inhibitors or mimics to regulate specific microRNA expression in diseased cartilage may help to control OA progression.

MicroRNA expression in Osteoarthritis

MicroRNA	MicroRNA expression in OA chondrocytes or cartilage compared to normal	Target gene	Outcome of dysregulated microRNA expression in OA chondrocytes or cartilage	Potential therapeutic intervention in OA
miR-140	Down-regulated in miR-140-/- mice [191] and in human OA chondrocytes [192].	**ADAMTS-5** The 3'UTR of *ADAMTS-5* was identified as a target of miR-140 **[191].** ADAMTS5 cleaves aggrecan [193] and in a murine model of OA deletion of the catalytic domain of Adamts5 resulted in a reduction to cartilage destruction severity due to the inability of Adamts5 to mediate aggrecan degradation [194].	Down-regulation of miR-140 allows for *ADAMTS-5* expression de-repression	miR-140 mimic to down-regulate ADAMTS-5 expression
miR-320c	Down-regulated in human cartilage with increasing age [198].	**ADAMTS-5** ADAMTS-5 expression was found to be down-regulated which correlated with increasing miR-320xc expression **[198].**	Down-regulation of miR-320c induces *ADAMTS5* de-repression, which can therefore mediate aggrecan cleavage.	miR-320c mimic to down-regulate ADAMTS-5 expression.
miR-125b	Down-regulated in chondrocytes from human OA knee cartilage [199].	**ADAMTS-4** miR-125b was found to directly target the 3'UTR of *ADAMTS-4* [199]. ADAMTS-4 or aggrecanase 1 cleaves aggrecan, which has been found to be expressed in human OA cartilage [200].	Down-regulation of miR-125b observed in OA cartilage induces *ADAMTS-4* de-repression, which can therefore mediate aggrecan cleavage [199].	miR-125b mimic to down-regulated ADAMTS-4 expression.
miR-27b	Down-regulated in IL-1β treated human chondrocytes [201].	**MMP-13 [201].** miR-27b was found to target 3'UTR of *MMP13* [201]. Comparison of OA articular cartilage and normal articular cartilage has identified that MMP-1 and MMP-13 exhibited the strongest up-regulation in OA articular cartilage, especially in late stage OA specimens. The study by Bau *et al* suggests MMP13 as the most critical collagenase in OA cartilage [57]. MMPs or collagenases initiate matrix degradation which are secreted in latent form and activated through pro-peptide cleavage. Type II collagen is the preferred substrate of MMP-13, a zinc dependent collagenase, which recognises a specific site through its Hpx and catalytic domains within the tropocollagen molecule and induces disruption to the triple helix which enables enzymatic cleavage [59]. Aberrant up-regulation of pro-inflammatory IL-1β in OA induces the upregulation of MMPs which induce articular cartilage degradation through the cleavage of critical ECM proteoglycans, observed as fissuring and fibrillation of articular cartilage.	Down-regulation of miR-27b observed in OA cartilage induces *MMP-13* de-repression, which can therefore mediate collagen cleavage [201].	miR-27b mimic to down-regulate MMP-13 expression.

miR-411	Down-regulated in OA human cartilage [202].	**MMP13** miR-411 was found to directly target the 3'UTR of *MMP13* [202].	Down-regulation of miR-411 observed in OA cartilage enable to the de-repression of *MMP-13* expression which mediates degradative changes in the ECM.	miR-411 mimic to down-regulate MMP-13 expression.
miR-210	Down-regulated in OA chondrocytes [203]	**HIF3A** miR-210 was found to directly target the 3'UTR of *HIF3A* [203]. *HIF3A* encodes HIF-3alpha, a hypoxia inducible transcription factor. Previous examination of cartilaginous tissues at various levels of differentiation revealed that the expression of *HIF3A* correlates with the human articular chondrocyte phenotype. *HIF3A* expression was diminished in cells which express high levels of hypertrophic markers such as *COLXA1* and *MMP13* expression, such as OA chondrocytes. The study revealed that *HIF3A* has an inverse correlation with expression of hypertrophic markers, suggesting that up-regulation of *HIF3A* down-regulates hypertrophy [204].	The overexpression of miR-210 which showed down-regulated expression of *HIF3A, COLXA1* and *MMP13* implies that *HIF3A* regulates the hypertrophy genes, which is the opposite finding to the study by Markway *et al* which showed that an up-regulated expression of *COLXA1* and *MMP13* was observed with down-regulated *HIF3A* expression. To ascertain the function of miR-210 in OA and in articular chondrocytes with regard to *HIF3A* regulation, further research into the function of *HIF3A* expression in articular chondrocytes is required.	
miR-105	Down-regulated in OA cartilage [205]	**RUNX2** MiR-105 was found to directly target the 3'UTR of *RUNX2* [205]. Runx2 deficient mice have been shown to lack hypertrophic chondrocytes, implying a role for Runx2 in hypertrophic chondrocyte differentiation [206]. Runx2 expression has been shown to be increased in fibrillated OA cartilage and believed to induce *MMP-13* expression [207]. Runx2 has been shown to bind to a *Colxa1* promoter and is required for *Colxa1* expression and terminal differentiation of chondrocytes in mice and likely to contribute to OA phenotype [208].	Ji *et al* suggest the pathological involvement of FGF2 signaling in OA which induces miR-105 down-regulation and enables RUNX2 expression de-repression, which up-regulates aggrecanases which can mediate collagen and aggrecan degradation in the articular cartilage ECM [205].	miR-105 mimic to down-regulate RUNX2 expression.

miR-222	Down-regulated in chondrocytes from human OA cartilage [209].	**HDAC4** [209] miR-222 was found to directly target the 3'UTR of *HADC4* [209] Use of HDAC inhibitors to suppress induction of *MMP-1* and *MMP-13* expression by pro-inflammatory cytokines in chondrocytes and inhibit cartilage degradation in an *ex vivo* model has previously been shown, implicating the action of HDACs in cartilage degradation [210]. Use of an HDAC inhibitor has also been shown to induce SOX9 induced *Col2a1* expression [211].	down-regulation of miR-222 induces *HDAC4* de-repression which induces *MMP-13* expression which then ultimately induces cartilage degradation [209].	miR-222 mimic to down-regulate HDAC4 expression.
miR-675	Down-regulated in chondrocytes cultured under catabolic conditions, through treatment with IL-1β and TNF-α [212].	Unknown target	Steck *et al* showed that *H19, COL2A1* and miR-675 were up-regulated in chondrocytes cultured under anabolic conditions, which consisted of culturing chondrocytes with deferoxamine (DFO) to inhibit hydroxylating enzymes which mediate HIF1α degradation; thereby inducing hypoxic signaling which was verified through *MMP13* expression down-regulation [212].	miR-675 mimic to down-regulate potential negative regulators of anabolic signaling in chondrocytes.
miR-181b	Up-regulated in chondrocytes isolated from human OA cartilage [213].	Unknown target	No target of miR-181b has been validated, but given the negative effect upon *COL2A1* expression and positive effect upon *MMP-13* expression, a likely target candidate is a negative regulator of *MMP-13* expression. Up-regulation of miR181b may induce down-regulation of an inhibitor of *MMP-13* expression, which would induce *MMP-13* expression up-regulation. MiR-181b may also target a positive regulator of	miR-181b inhibitor to allow inhibition on MMP13 expression and prevent Col2a1 expression down-regulation.

			COL2A1 expression [213]	
miR-199a-3p	Up-regulated with age indicating the involvement of miR-199a-3p upon the aging process of articular chondrocytes and a possible role in chondrocyte senescence [198].	Unknown target	The down-regulation of genes encoding critical ECM components implies the negative effect of miR-199a-3p upon articular cartilage ECM and the potential negative role in articular cartilage degradation [198].	miR-199a-3p inhibitor to prevent down-regulation of articular cartilage ECM genes.
miR-193	Up-regulated with increased age of human articular cartilage [198].	Unknown target	The down-regulation of genes encoding critical ECM components implies the negative effect of miR-193 upon articular cartilage ECM and the potential negative role in articular cartilage degradation with age [198].	miR-193 inhibitor to prevent down-regulation of cartilage ECM genes.
miR-455	Up-regulated in human OA cartilage [214].	**ACVR2B** The type-IIB activin receptor has been shown to be expressed in cultured chondrocytes [215]. **SMAD2** SMAD2 has been shown to be an essential intracellular component of the TGF-β signaling pathway. SMAD2 interacts with the TGF-β receptor and undergoes phosphorylation [216]. **CHRDL1** Chorin-like 1 is a secreted protein which acts as a BMP inhibitor and has been shown to be expressed in chondrocytes [217]. Chordin-like 1 was found to be enriched in juvenile chondrocytes compared to adult chondrocytes with a suggested role in proliferation and survival of human bone marrow derived MSCs [218].	miR-445 up-regulation may down-regulate TGF-β signaling and disrupt maintenance to articular cartilage inducing OA-like changes [214].	miR-455 inhibitor to prevent down-regulation of TGF-β signaling.
miR-194	Up-regulated in human chondrocytes treated with IL-β [219].	**SOX5** Han *et al* have shown that the action of the 'sox trio' inclusive of SOX5, SOX6 and SOX9 is required for aggrecan expression. SOX9 binds to the *Agc1* enhancer only in the presence of SOX5 and SOX6 [165].	miR-194 may indirectly modulate articular cartilage ECM production through regulating expression of *SOX5*. Up-regulation of miR-194 may therefore	miR-194 inhibitor to prevent potential down-regulation of SOX5 expression.

			induce down-regulation of anabolic associated *SOX5* expression which may contribute to OA-like articular cartilage degenerative changes [219].	
miR-101	Up-regulated in rat chondrocytes treated with IL-β [220].	**SOX9** miR-101 was found to directly target the 3'UTR of *Sox9* [220] SOX9 is required for aggrecan expression [165], Col2a1 expression [221], Col9a1 expression [222] and Col11a2 expression[223] and has been shown to bind to chondrocyte specific enhancer elements in all of these genes.	In articular chondrocytes miR-101 targeted inhibition of *Sox9* could induce articular cartilage ECM degradation through the down-regulation of a critical anabolic transcription factor required for ECM maintenance [220].	miR-101 inhibitor to prevent down-regulation of SOX9 expression.
miR-30a	Up-regulated in chondrocytes from OA cartilage [224].	**SOX9** miR-30a was found to directly target the 3'UTR of *SOX9* [224].	miR-30a up-regulation suppresses *SOX9* expression which induces ECM degradation through modulating downstream effectors critical for cartilage function [224].	miR-30a inhibitor to prevent down-regulation of SOX9 expression.
miR-22	Up-regulated in human OA cartilage [225].	**PPAR** The peroxisome proliferator-activated receptor alpha (PPAR-alpha) was previously identified to have a role in acute inflammation. Inflammatory models of PPAR-alpha knockout in mice have been shown to induce an augmentation in inflammatory symptoms as well as an increase in TNF-α and IL-1β expression [226]. **BMP7** BMP7 has been shown to regulate aggrecan synthesis through interaction with a responsive element in the aggrecan promoter [227].	**miR-22 inhibitor** miR-22 is able to indirectly induce articular cartilage ECM degradation through targeted repression of *BMP7* which mediates aggrecan expression and also through inflammatory IL-1β up-regulated expression through PPARA regulation [225]	miR-22 inhibitor to prevent done-regulation of PPAR-alpha and BMP7.
miR-146a	Up-regulated in cartilage of patients with low grade OA [228].	**IRAK1** Binding of IL-1 to type I IL-1 receptor results in the activation of NF-κB. Intracellular IRAK1 associates with IL-1RI and undergoes phosphorylation upon IL-1 binding at the cell surface [231], which in turn up-regulates catabolic associated factors, cytokines and inflammatory mediators inducing articular cartilage degradation. **TRAF6**	It was postulated that miR-146a increased in expression may be to attenuate the inflammatory response by targeting components of the	miR-146a mimic to down-regulate IRAK1 and TRAF6 expression to suppress inflammation

	Up-regulated in OA rat model [229]. Up-regulated in mechanically injured human chondrocytes [230]	TRAF6 has been shown to activate NF-κB during IL-1 signaling by associating with IRAK1 [232]. **SMAD4** The intracellular common SMAD4 is required for TGF-β and activin signaling [233]. Mutant mice with chondrocytes which lacked responsiveness to the TGF-β signalling pathway resulted in terminal hypertrophic differentiation with an osteoarthritis phenotype [27].	inflammatory cascade including *IRAK1* and *TRAF6* mRNA [228]. miR-146a targets the TGF-β signaling pathway, by targeting *SMAD4*, which results in the activation of articular cartilage ECM degradation.	miR-146a inhibitor to prevent down-regulation of SMAD4 expression.
miR-199a*	Down-regulated in chondrocytes isolated from human OA cartilage [234].	**COX-2** miR-199a* was found to directly target the 3'UTR of *COX-2* [234]. COX-2 has been found to be up-regulated in inflamed joints and responsible for the augmentation in prostaglandin E2 production from arachidonic acid, and is likely to be induced by pro-inflammatory cytokines such as IL-1β and TNF-α [235]. Prostaglandin E2 has been shown to exert catabolic effects. Culture of cartilage explants with prostaglandin E2 inhibited proteoglycan synthesis, induced collagen degradation and augmented MMP-13 secretion [236]. Microsomal prostaglandin E synthase 1 (mPGES1) has been shown to be up-regulated in the presence of IL-1β and is up-regulated during COX-2 dependent prostaglandin E2 production [237].	Down-regulation of miR-199* in articular chondrocytes may contribute to OA development through the de-repression of *COX-2* expression which can induce prostaglandin E2 synthesis and mediate articular cartilage degeneration [234]	miR-199* mimic to down-regulate COX-2 expression.
miR-502-5p	Down-regulated in human OA articular tissues [238].	**TRAF2** miR-502-5p was found to directly target 3'UTR of *TRAF2* [238]. IL-1β has been suggested to up-regulate TNF-α [239] and TRAF2 is a critical adaptor mediator of TNF-α induced signaling of the NF-κB pathway [240]. TNF-α is a key inflammatory cytokine which is involved with the underlying pathophysiology of OA.	Down-regulated expression of miR-502-5p in chondrocytes may therefore induce *TRAF2* de-repression expression which can function as part of the IL-1β induced TNF-α, NF-κB specific pathway to up-regulate pro-inflammatory mediators and induce cartilage degradation.	miR-502-5p mimic to down-regulate TRAF2 expression and suppress inflammation.
miR-26a-5p	Down-regulated in human OA damaged cartilage samples compared to smooth cartilage samples [241].	**iNOS** miR-26a-5p was found to directly target 3'UTR of *iNOS* [241]. IL-1β induced NF-κB signaling up-regulates the expression of iNOS which functions to catalyse nitric oxide (NO) production [242]. NO has been shown to mediate the expression of pro-inflammatory cytokines, suppress collagen and proteoglycan synthesis and induce apoptosis [243].	Down-regulation of miR-26a-5p may induce *iNOS* expression de-repression which may induce NO production and mediate degradative and inflammatory effects	miR-26a-5p mimic to down-regulate iNOS expression.

			in chondrocytes contributing to OA progression [241].	
miR-588	Down-regulated in human articular chondrocytes [244]	**COX-2** MiR-588 found to directly target 3'UTR of *COX-2* [244].	Down-regulation of miR-558 in articular chondrocytes may contribute to OA development through the de-repression of *COX-2* expression which can induce prostaglandin E2 synthesis and mediate articular cartilage degeneration [244].	miR-588 mimic to down-regulate COX-2 expression.
miR-34a	Up-regulated in rat chondrocytes treated with IL-1β [245]	Unknown target	The inhibition of miR-34a was shown to inhibit IL-1β induced down-regulation of *Col2a1*, *iNOS* and reduce the number of TUNEL-positive cells. Inhibition of miR-34a was suggested to reduce IL-1β induced chondrocyte apoptosis [245].	miR-34a inhibitor acts to potentially prevent down-regulation of Col2a1 and iNOS expression and prevent apoptosis.
miR-29	MiR-29 family were found to be up-regulated in human OA articular cartilage [246].	Several WNT-related genes were identified as direct targets of miR-29 including FZD3, FZD5, DVL3, FRAT2 and CK2A2. The miR-29 family also negatively regulated NF-κB, SMAD in addition to WNT signalling pathway	The up-regulation of miR-29 is likely to induce suppression of critical signalling pathways which maintain cartilage homeostasis which may contribute to OA onset and disease progression.	miR-29 family inhibitors to prevent down-regulation of chondrocyte signaling pathways.
miR-30b	Up-regulated in human OA articular cartilage [247].	**ERG** The transcription factor ETS–related gene (ERG) 3'UTR was identified as a direct target of miR-30b. The transcription factor ERG has been speculated to play role in the maintenance of the articular chondrocyte phenotype and function throughout life. Overexpression of ERG chondrocytes exhibit immature articular phenotypes, expression of cartilage matrix components inclusive of aggrecan and tenascin-C [33]	The overexpression of miR-30b may induce ERG expression inhibition which mediates ECM composition change.	miR-30b inhibitor to prevent down-regulation of ERG expression.

miR-16-5p	Up-regulated in human OA cartilage	**SMAD3** directly target the 3'UTR of *SMAD3* SMAD3 is a down-stream mediator of TGF-β signalling. Mutant Smad3 mice with chondrocytes which lacked responsiveness to the TGF-β signalling pathway resulted in terminal hypertrophic differentiation with an osteoarthritis phenotype. TGF-β signalling was believed to be responsible for the inhibition of terminal hypertrophic differentiation in chondrocytes and therefore responsible in maintaining articular cartilage integrity [27].	Up-regulation of miR-16-5p therefore negatively regulates chondrocyte homeostasis, down-regulating TGF-β signalling resulting in potential degradative changes to the ECM and onset of OA.	miR-16-5p inhibitor to prevent down-regulation of SMAD3 expression.
miR-139	Up-regulated in damaged areas of OA cartilage [248].	**MCPIP1** MiR-139 was found to directly interact with the 3'UTR of *MCPIP1* MCPIP1 can destabilize inflammatory cytokines through binding to the cytokine mRNA 3'UTR. MCPIP1 has previously been shown to directly bind to IL-6 mRNA and modulation of MCPIP1 has been shown to regulate IL-6 expression in human cartilage and chondrocytes [249].	Up-regulation of miR-139 in chondrocytes may therefore induce MCIPI1 expression which enables de-repression expression of IL-6, which can mediate pro-inflammatory and degradative changes to articular cartilage ECM.	miR-139 inhibitor to prevent down-regulation of MCPIP1 expression.

Table 2. MicroRNAs identified in OA and target genes and potential therapeutic intervention.

The importance of identifying dysregulated microRNAs and their function in OA may enable application of microRNA modulation in a clinical setting to treat or alleviate OA symptoms. Treatment of specific diseases through modulating microRNA expression would require exogenous administration of either microRNA mimics or microRNA antagomiRs. The use of microRNAs in a clinical setting is of much interest and microRNA therapeutic companies have focused on pre-clinical animal model studies in the hope to advance to human clinical trials [250]. Recently the first microRNA mimic was entered into a Phase I clinical trial in humans. MRX34 is a liposomal formulated double stranded mimic of miR-34 which has been found to be down-regulated in various haematological tumors. MiR-34 has been found function as a tumor suppressor and regulates the expression of cancer related genes including CDK4/6, SIRT1, WNT1/3, HDAC1, BCL2, AXL, FOXP1 and MEK1. The multicenter phase 1 clinical trial involves MRX34 administration to patients with hepatocellular carcinoma, metastatic cancer with liver involvement, hematologic malignancies or selected solid tumors. The objectives of the phase 1 clinical trial are to identify the maximum tolerated dose of MRX34 and recommended phase 2 dose with focus on assessing tumor uptake of the miR-34 mimic along with down-regulation of target gene expression [251]. Preliminary results of the multicenter Phase 1 clinical trial in solid tumor patients were presented at the American Association for Cancer Research in November 2015, which showed that MRX34 has a safety profile manageable with standard interventions and tests used by oncologists. Clinical responses were achieved in two patients with stage IV cancer following MRX34 treatment: one patient with acral lentiginous

melanoma with metastasis to the lymph nodes and in one patient with hepatocellular carcinoma with metastasis to the lung, more than 30% tumor shrinkage was observed [252].

Regulus Therapeutics (www.regulusrx.com) have developed anti-miRs to block endogenous microRNA function. Currently an anti-miR-21, RG-012, is being tested in a human phase 1 clinical trial for investigating the effect of miR-21 knockdown on fibrosis in patients with Alport syndrome. Alport syndrome is an inherited kidney disease caused by mutations to the type IV collagen genes which disrupts the integrity and functioning of the glomerular basement membrane. MiR-21 has been found to be up-regulated in Alport syndrome. The anti-miR-21, RG-012, is currently being tested for its ability to reduce renal fibrosis

The relatively novel field of microRNA research has progressed and expanded quickly, with the identification of the first microRNA only discovered in 1993 [182] and yet microRNA based therapeutic research has already progressed to human clinical trials. There is real promise for synthetic microRNA mimics and microRNA inhibitors to serve as potential therapeutics in treating OA or reducing articular cartilage degradation in the future. Table 2 lists some of the identified dysregulated microRNAs in OA to date and the potential therapeutic use of exogenous microRNA in treating or alleviating OA.

1.2.3 MicroRNAs target components involved in deciding stem cell fate

MicroRNAs are involved with regulating stem cell differentiation and self-renewal through targeting different components which are involved with deciding stem cell fate [179]. Several early experiments show the importance of microRNA in stem cell differentiation. The very first evidence that miRNAs played a vital role in development came from the studies on lin-4 miRNA and let-7 miRNA in *Caenorhabditis elegans* [182]. The work by Lee *et al* paved the way forward for the investigation into the regulatory function of let-7 microRNA which was found to act upon a later stage in development in *C.elegans*; controlling the transition between L4 and adult stages in development. It was identified that let-7 microRNA controlled this stage in development through the interaction with the 3'UTR region of several genes encoding transcription factors at the larval 4 to adult transition stage [253].

The initial work on lin-4 and let-7 showed that miRNAs have vital roles in development; the initial findings showed that miRNAs have a key function in preventing the production of protein from messenger RNAs existent from an earlier stage in differentiation and can therefore help to determine cell fate through their regulatory function. The importance of miRNAs in stem cell development is shown by Dicer deficient studies. Bernstein *et al* have shown that the RNase protein; Dicer required for miRNA processing is essential for early development through the creation of a mouse strain with a chromosomal lesion in *Dicer 1* by use of a PGK-neomycin-resistant cassette which disrupted the first RNase III domain. The mutant *Dicer 1* allele was used to create chimeric mice; 62 mice were born from heterozygous intercrosses of which none were homozygous mutants indicating that *Dicer 1* deficient mice were not viable. Additionally, it was also investigated as to which stage of development that Dicer is required; Berstein *et al* conducted timed heterozygous matings and collected embryos on different days and found that embryos were either necrotic or normal which correlated with *Dicer 1* deficient or normal. The earliest stage of development was day 7.5 whereby *Dicer 1* deficient embryos appeared small and morphologically abnormal in comparison to wild type embryos. The development of *Dicer 1* mutants was arrested prior to the configuration of the body plan during gastrulation which shows that the Dicer protein is an essential requirement to development. In this study the loss of Dicer affected the pluripotent stem cell pools that were present in the early embryo, showing the importance of the Dicer protein in miRNA processing. Bernstein *et al* went on to show that the transcription factor Oct-4, which is a key regulator of embryonic stem cell maintenance and proliferation, was reduced in *Dicer 1* deficients, indicating that the absence of the Dicer protein prevents the processing of miRNAs which either function directly or indirectly to regulate Oct-4 [254].

Another dicer deficient study by Wienholds *et al* also showed the importance of miRNAs in stem cell development through loss of Dicer 1 in zebrafish whereby homozygous and trans-heterozygous dicer deficient embryos exhibited debilitating behavior and developmental growth arrest after 8 days; which

as with the study by Bernstein *et al* show that the deficiency of Dicer 1 resulted in the loss of stem cell populations and embryonic lethality [255]. Argonaute 2 is another protein essential for miRNA processing and function in mammals; Liu *et al* showed that creation of mutations in the cryptic ribonuclease domain in Argonaute 2 rendered the RNA induced silencing complex inactive. Similar to the *Dicer 1* deficient studies, intercrosses of Ago2 heterozygotes produced an embryonic lethal phenotype and also exhibited developmental abnormalities during gestation, reinforcing the idea that anything that causes disruption to the processing of microRNAs will cause developmental defects due to the requirement of microRNAs in development [256].

The studies discussed above, all examine the loss of proteins involved with the processing of microRNA and the correlation to stem cell viability. Dicer 1 is essential for the formation of miRNAs and therefore essential in vertebrate development as is Argonaute 2. Studying the loss of Dicer 1 and Argonaute 2, however, does not identify which specific microRNA/s may be responsible for the loss of stem cell populations and induction of differentiation and if regulation of target gene expression by microRNA is direct or indirect. Other studies have shown how a specific microRNA is important in development. Detection of microRNAs is the first hurdle in identifying the microRNAs that may be present in a specific tissue at a certain developmental time point.

Recent research has shown that microRNAs play important roles in chondrogenic differentiation. MicroRNAs carry out their role by interacting with different components involved in deciding skeletal stem cell fate, either by targeting key components associated with different signaling pathways involved in chondrogenesis, such as key transcription factors or by regulating the production of matrix vital for cells to exist within their defined niche. There are several microRNAs documented to be involved in chondrogenesis and it is anticipated that there are many more to be discovered. MicroRNAs that have been identified to date typically regulate cartilage formation; negatively by targeting positive regulators of chondrogenesis or positively by targeting negative regulators of chondrogenesis. Identifying which genes particular miRNAs target will give an insight as to which stage of chondrogenic differentiation microRNAs regulate.

MicroRNAs exert their function by repressing posttranscriptional translation, some microRNAs act as negative regulators of chondrogenic differentiation by targeting genes associated with inducing chondrogenesis therefore having an inhibitory role. Other microRNAs can act as positive regulators by targeting negative regulators of chondrogenesis and therefore have a stimulatory role on chondrogenic differentiation. To understand the regulatory network controlling chondrogenesis it is also important to comprehend factors that may up-regulate or down-regulate specific microRNAs such as transcription factors. Figure 19 outlines the mechanisms which may govern microRNA expression and consequently microRNA mediated target gene expression.

MicroRNA activation mechanism and effect on chondrogenesis

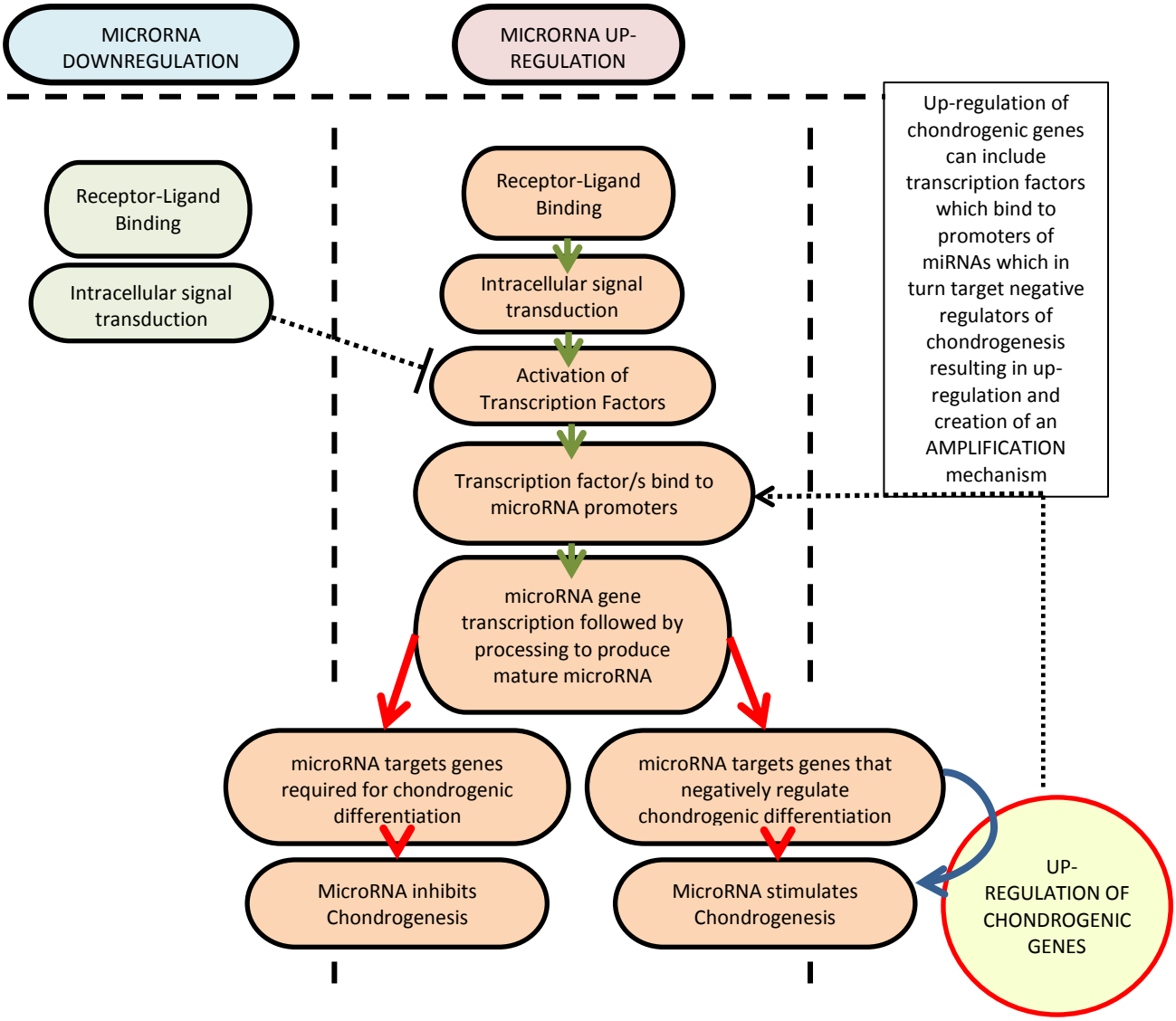

Figure 19. MicroRNA activation. How microRNAs themselves are regulated by signalling pathways which may up-regulate or down-regulate microRNA expression which subsequently determines if they are transcribed, which in turns allows for microRNAs depending on their function, to either inhibit or promote/stimulate chondrogenesis.

1.2.4 MicroRNAs in Chondrogenesis and significance of identification

In vitro models of stem cell chondrogenic differentiation have allowed for the analysis of microRNAs which may be involved with post transcriptional regulation of chondrocyte and cartilage development; microRNAs which directly or indirectly are responsible for gene activation or suppression during the process of articular cartilage formation. Many of the different microRNAs and their targets studied to date in chondrogenic differentiation of stem cells are listed in table 3. A specific microRNA may be found to target a positive regulator of chondrogenesis and therefore be assumed to be an inhibitor of chondrogenic differentiation, but some of these inhibitory microRNAs may ensure optimal levels of regulatory molecules for example transcription factors ensuring that levels do not become excessive. The balance between proliferation and differentiation must be maintained given that for differentiation to proceed, proliferation must take place and the proliferation pool must not be depleted; microRNAs play a huge role in maintaining this balance.

MicroRNA expression in Chondrogenic Differentiation of Stem Cells

MicroRNA	Expression during chondrogenesis	Gene Target	Potential use of microRNA in inducing chondrogenesis
miR-145	miR-145 was found to be down-regulated during chondrogenesis of bone marrow derived murine MSCs [257].	*Sox9* was found to be a direct target of miR-145 [257]. SOX9 is required for aggrecan expression [165], Col2a1 expression [221], Col9a1 expression [222] and Col11a2 expression[223] and has been shown to bind to chondrocyte specific enhancer elements in all of these genes.	Further suppress miR-145 expression with miR-145 inhibitor
miR-194	miR-194 was found to be down-regulated during chondrogenesis of human adipose derived stem cells [219].	*SOX5* was fund to be a target of miR-194 [219]. SOX5 and SOX6 were found to be co-expressed with SOX9 during chondrogenic differentiation to enhance *Col2a1* expression [162]. Murine *Sox5/Sox6* double null fetuses died *in utero* and an absence of cartilage was observed [163]. Han *et al* have shown that the action of the 'sox trio' inclusive of SOX5, SOX6 and SOX9 is required for aggrecan expression. SOX9 binds to the *Agc1* enhancer only in the presence of SOX5 and SOX6 [165].	Further suppress miR-194 expression with miR-194 inhibitor
miR-140-5p	Chondrogenic differentiation of human mesenchymal stem cells resulted in the up-regulated expression of miR-140 [191]. miR-140 was found to be up-regulated during chondrogenic	miR-140 found to target the chemokine (CXC motif) ligand 12 (CXCL12) and ADAMTS-5 [258]. *CXCL12* encodes CXCL12: Stromal derived factor 1, a chemokine which binds to the CXCR4 G-coupled protein receptor. CXCL12 regulates stem cell and precursor cell migration through chemotaxis. CXCL12 has been shown to be down-regulated in chondrogenesis [260] and has also been shown to have a role in actin organisation in chondrogenic differentiation [261]. ADAMTS-5: A disintegrin and metalloproteinase with thrombospondin motifs 5 or aggrecanase-2 functions to proteolytically cleave the ECM protein aggrecan within its	Collectively the studies outlined indicate the up-regulated expression of miR-140 in chondrogenic differentiation. Pais *et al* indicate

	differentiation of equine cord blood derived mesenchymal stromal cells [258]. miR-140-5p exhibited up-regulated expression in chondrogenic differentiation of human bone marrow derived MSCs [259].	interglobular domain [262]. Expression of *ADAMTS-5* has been shown to be down-regulated during chondrogenic differentiation [263] Following overexpression of miR-140 and inhibition of miR-140 in murine C3H10T1/2 cells, mRNA array was conducted to identify differences in mRNA expression as a result of either miR-140 inhibition or miR-140 overexpression. Further examination of targets of miR-140 which were regulated solely at the protein level, identified Smad3 as a direct target of miR-140 [264]. It may be possible that TGF-β signalling can up-regulate miR-140 which in turn functions to regulate TGF-β signalling through targeted repression of Smad3, perhaps a mechanism to regulate TGF-β signalling threshold. MiR-140-5p was shown to directly target the 3'UTR of *RALA* [259]. *RALA* encodes Ras-related protein Ral-A (RALA), a small GTPase which functions to bind and hydrolyse guanosine triphosphate. In mammalian cells RALA has been found to be involved with regulating actin cytoskeletal remodelling and vesicle transport. The exocyst complex functions to direct vesicles following export from the Golgi to specific plasma membrane locations. RALA has been shown to interact with the exocyst complex in mediating cytoskeletal and secretory pathways [265]. RALA has been shown to be involved in TGF-β signalling through internalisation of membrane receptor activin type II [266] and also may be involved with the trafficking and secretion of glycosaminoglycans [267].	miR-140 as a negative regulator of TGF-β signalling, while Karlson *et al* imply that miR-140 is a positive regulator of chondrogenic differentiation. Given the significance of miR-140 expression during chondrogenesis, perhaps miR-140 functions to induce chondrogenic differentiation homeostasis. Up-regulation of miR-140-5p in several cell studies indicates the use of miR-140-5p mimic to induce further miR-140-5p expression.
miR-140-3p	miR-140-3p exhibited up-regulated expression in chondrogenic differentiation of human bone marrow derived MSCs [259].	Along with miR-140-5p, miR-140-3p was found to be the most up-regulated during chondrogenic differentiation of MSCs. Both miR-140-3p and miR-140-5p were shown to be the most highly expressed microRNAs in differentiated MSCs and uncultured articular chondrocytes [259]. Gene targets of miR-140-3p remain unknown.	Up-regulation of miR-140-3p indicates the use of miR-140-3p mimic to induce further miR-140-3p expression
miR-199a*	miR-199a* was found to be down-regulated during early chondrogenesis in murine C3H10T1/2 cells [268]	miR-199a* was found to directly target *Smad1* [268]. Smad1 is an intracellular transducer of BMP-2 signalling, a receptor mediated Smad which is phosphorylated upon BMP binding to the cell surface BMP type II membrane receptor. *Smad1* and *Smad5* ablation in mice has been shown to induce chondrodysplasia [269].	Further suppress miR-199a* expression using miR-199* inhibitor
miR-337	miR-337 was found to be down-regulated during femoral head cartilage development in rats [270].	miR-337 was found to directly target *Tgfbr2* [270]. TGFBR2 forms a heteromeric complex with TGFBR1. Binding of TGF-β to the receptor complex induces intracellular TGF-β-SMAD signalling. Transgenic mice exhibiting overexpression of dominant negative *Tgfbr2* resulted in an OA phenotype [79]. *Tgfbr2* knockout in mice limbs resulted in failure of joint interzone development [271].	Further suppress miR-337 expression using miR-337 inhibitor
miR-495	miR-495 was found to be down-regulated	miR-495 was found to directly target *SOX9* [272]. SOX9 is required for aggrecan expression [165], Col2a1 expression	Further suppress miR-495

	during chondrogenesis of human MSCs [272].	[221], Col9a1 expression [222] and Col11a2 expression [223] and has been shown to bind to chondrocyte specific enhancer elements in all of these genes.	expression using miR-495 inhibitor
miR-29a	miR-29a was found to be down-regulated during chondrogenesis in human MSCs [273], [274].	SOX9 was found to down-regulate miR-29a expression likely through binding to the miR-29a promoter region [273]. miR-29a was found to directly target *FOXO3A* [274]. The expression of transcription factor *FOXO3A* was found to be up-regulated during chondrogenesis and modulation of *FOXO3A* expression was found to regulate *SOX9*, *AGCAN* and *COL2A1* expression, FOXO3A binding sites were also identified within the genomic sequences of these genes [274].	Further suppress miR-29a expression using miR-29a inhibitor
miR-547-3p	miR-574-3p was found to be up-regulated during chondrogenesis in human MSCs [275].	miR-574-3p was found to be up-regulated by SOX9 binding to miR-574-3p promoter. miR-574-3p was found to directly target *RXRA* [275]. *RXRA* encodes retinoid X receptor alpha, a nuclear receptor which can form homodimers or heterodimers and act as transcriptional repressors in the absence of ligand binding. Retinoids bind to RXRs and retinoid acid receptors (RARs) and induce dissociation from co-repressors and bind co-activators [276]. AP-1 binding sites are located within the TGF-β1 promoter. RXRα has been shown to antagonise AP-1 transcription factor which was suggested to down-regulate the TGF-β1 promoter [277]. Guerit *et al* suggest that altered balance between RXR and RAR may affect RXRα signalling in MSCs [275], based on previous findings that RXR homodimerisation induced p21 up-regulation and apoptosis and the presence of RAR interfered with RXR mediated p21 induction [278]. RXRα is suggested to play a role in MSC multipotency and stem cells state and down-regulation induces differentiation [275]	Further up-regulation of miR-574-3p expression using miR-574-3p mimic
miR-335-5p	miR-335-5p was found to be up-regulated during chondrogenesis in murine MSCs [279]	miR-355-5p was found to directly target *ROCK1* and *DAAM1* [279]. Inhibition of ROCK signalling has been shown to induce glycosaminoglycan synthesis and up-regulate expression of *SOX9* [280]. Daam1 has been shown to bind to Dishevelled and Rho [281], Rho then activates Rho-associated kinase ROCK1 [280]. Inhibition of both ROCK1 and Damm1 up-regulates *SOX9* expression and downstream targets [279].	Further up-regulation of miR-29a expression using miR-29a mimic
miR-30a	miR-30a was found to be up-regulated during chondrogenesis of rat bone marrow derived MSCs [282].	miR-30a was found to directly target *Dll4*, which encodes Delta like 4 [282]. DLL4 is transmembrane ligand which can interact with Notch receptors [283]. Examination of Notch signalling in cartilage development *in vivo* has shown that overexpression of Notch signalling resulted in decreased cartilage precursor proliferation and sclerotome differentiation. Expression of *Dll4* was shown to be expressed through *in situ* hybridisation in rats overexpressing Notch1 [284]. Activation of Notch signalling in mice limb bud mesenchymal progenitor cells has also been shown to inhibit chondrogenic differentiation [285]. miR-30a may therefore supress Notch signalling through targeted inhibition of *Dll4* expression to prevent inhibitory effects of Notch signalling upon chondrogenesis.	Further up-regulation of miR-30a expression using miR-30a mimic.
miR-455-3p	miR-455-3p was	miR-455-3p was found to directly target *Runx2* [286]. Runx2	Further up-

	found upregulated during chondrogenic differentiation of ATDC5 murine cells [214] [286].	deficient mice have been shown to lack hypertrophic chondrocytes, implying a role for Runx2 in hypertrophic chondrocyte differentiation [206]. Joint formation failure and permanent cartilage formation failure was observed in *Runx2* overexpressing transgenic mice , indicating a requirement for Runx2 down-regulating during early chondrogenesis [287].	regulation of miR-455-3p expression using miR-455-3p mimic.
miR-675	miR-675 was found to be down-regulated with serial passage of human articular cartilage isolated chondrocytes, suggesting dedifferentiation of articular chondrocytes [288].	miR-675 was down-regulated with dedifferentiation with correlated down-regulation of *COL2A1*. Overexpression of miR-675 was shown to up-regulate COL2A1 mRNA and protein levels and could induce up-regulation of COL2A1 protein expression in *SOX9* depleted chondrocytes. miR-675 was suggested to target a negative regulator of *COL2A1* and be a potential downstream target of SOX9 [288].	Further up-regulation of miR-675 expression using miR-675 mimic.
miR-193b	miR-193b was found to be up-regulated during TGF-β3 induced chondrogenic differentiation of human adipose derived stem cells [289], [290]and ATDC5 cells [290]	miR-193b was found to directly target *Tgfbr2* and *Tgfbr3* [290]. TGFβR2 complexes with TGFβRI at the cell surface membrane upon TGF-β binding inducing TGF-β intracellular signalling [291]. Deletion of *Tgfbr2* has been shown to prevent interzone development and affect joint formation, limiting chondrogenic differentiation [271], [292].	Down-regulation of miR-193b expression using miR-193b inhibitor
miR-221	miR-221 was found to be up-regulated during JNK inhibitor induced chondrogenic differentiation inhibition in chick limb bud mesenchymal cells [293].	miR-221 was found to directly target *mdm2* [293]. Mdm2 has been shown to form a complex with p53 and Slug which mediates Slug degradation [294]. Slug overexpression was suggested to induce apoptosis. Slug overexpression was thought to be exhibited as a result of miR-221 mediated *Mdm2* expression inhibition which could not target Slug for degradation [293]. Down-regulation of miR-221 or Slug was shown to induce chondrogenic markers in human mesenchymal stem cells [295]	Down-regulation of miR-221 expression using miR-221 inhibitor
miR-34a	miR-34a was found to be up-regulated during JNK inhibitor induced chondrogenic differentiation inhibition in chick limb bud mesenchymal cells [296].	miR-34a was found to directly target *Rac1* [296]. Rac1 has been shown to promote chondrogenesis. Inhibition of Rac1 has been shown to reduce the size and number of cellular condensations and a down-regulation of N-cadherin expression and chondrogenic marker gene expression [297]. Kim *et al* propose that opposing activity of Rac1 and RhoA is essential for cell dynamics and morphology. In JNK inhibitor treated cells, intensified stress fibers were observed suggested to be as a result of suppression of miR-434a targeted Rac1 expression, suggesting miR-34a in modulating Rac1/RhoA and regulation of actin cytoskeleton reorganisation essential for chondrocyte specific morphological changes [296]	Down-regulation of miR-34a expression using miR-34a inhibitor

Table 3. MicroRNAs identified in chondrogenic differentiation of stem cells and target genes and potential use of identified microRNAs to enhance chondrogenic differentiation.

1.2.5 Importance of identifying the roles of differing microRNAs in Chondrogenesis

Comprehension of miRNA expression profiles and the role that microRNAs play in regulation of gene expression during the chondrogenic differentiation of skeletal stem cells allows for a better understanding of molecular mechanisms which regulate the process, which will also allow for the possibility of using miRNAs in tissue engineering strategies. A possibility is using microRNAs for improvement of skeletal stem cell transplantation. There are differing ideas surrounding the use of microRNAs for improving skeletal stem cell transplantation. One idea is the transfection of anti-apoptotic microRNAs into skeletal stem cells prior to transplantation therefore potentially increasing the probability of effective engraftment of the skeletal stem cells at defective sites. Another idea is that skeletal stem cells could be also used as a source for tissue regeneration in combination with microRNAs which induce and enhance differentiation. Table 3 lists some of the microRNAs identified in chondrogenesis to date, given the identified function of specific microRNAs, use of exogenous microRNA mimics or inhibitors could be used to enhance chondrogenic differentiation.

Use of microRNAs for improving engraftment and function in skeletal stem cells transplantation is a possibility. It has previously been shown that the use of a cocktail of microRNAs including miR-21, miR-24 and miR-221 have been used to improve the engraftment of transplanted cardiac progenitor cells (CPC) into the myocardium of mice which had suffered ischemic heart disease. Shijun *et al* transduced cardiac progenitor cells with lentiviruses which carried the miR-21, miR-24 and miR-221 precursors. Transduced CPCs were administered to the mice by intra-myocardial injection and were found to increase functional recovery of the infarct area. CPCs that had been transduced with the cocktail of microRNAs survived for a significantly longer period of time compared to CPCs that had not been transduced with the cocktail of microRNAs. In addition it was shown that the apoptotic activator Bim was a target of the microRNA cocktail therefore indicating that the microRNA cocktail was able to improve the survival of transplanted CPCs by suppression of apoptosis [298]. Shijun *et al* therefore proposed a concept whereby stem cells are preconditioned prior to engraftment to enhance their survival capacity following transplant. This same concept could also be applied to improve the engraftment of transplanted skeletal stem cells in articular cartilage defect sites or articular cartilage deteriorated through OA.

Another possibility is using microRNAs to induce successful stem cell differentiation *in vivo*. Properties of skeletal stem cells including the ability of skeletal stem cells to undergo chondrogenic differentiation and immuno-modulatory properties make them a viable and promising cell source to help regenerate articular cartilage. The other advantage to the potential of using skeletal stem cells in articular cartilage reparation is that these cells can be sourced from the individual themselves, allowing for an autologous transplant procedure. Skeletal stem cells have been shown to be regulated in part by microRNAs which regulate different genes involved with the differentiation process post-transcriptionally. The use of skeletal stem cells in combination with microRNA modulation could

provide a new approach to articular cartilage regeneration. Cui *et al* have shown that the overexpression of seven microRNAs miR-1246, miR-148a, miR-1290, miR-30a, miR-424, miR-122 and miR-542-5 in combination can induce the differentiation of human MSCs into mature induced hepatocytes (iHEP) *in vitro*. Transplantation of the iHEP cells into mice with CCL4 induced acute liver injury, in which hepatocytes exhibited ballooning degeneration and necrosis, was able to increase the serum albumin level and decrease alanine transaminase and aspartate aminotransferase; levels of which are both usually increased as a result of liver damage. MicroRNA induced cells were able to repair the injured site by 2 weeks post cell transplantation. It was claimed that MSCs transfected with the combination of microRNAs promoted hepatogenesis more quickly compared to hepatic differentiation by conventional method of using growth factors and additionally the cell morphology changed from fibroblast to epithelial which was not observed in the conventional induction group. This study shows that not only how microRNAs can be used in combination to induce differentiation and reparation of liver tissue, but also that the use of microRNAs as inducers of hepatic differentiation is a faster method compared to conventional use of growth factors to induce differentiation *in vitro* and also compared to using just MSC alone *in vivo* [299].

The study by Hu *et al* previously discussed; which used a cocktail of microRNAs including miR-21, miR-24 and miR-221 which showed improved engraftment of transplanted cardiac progenitor cells (CPC) in the myocardium of mice which had suffered ischemic heart disease [298]. Hu *et al* therefore propose a concept whereby stem cells are preconditioned prior to engraftment to enhance their survival capacity following transplant, Similarly, another murine model of myocardial infarction; miR-126 transfected MSCs were injected into infarct zones and after 6 weeks found to improve angiogenesis and cardiac function believed to be due to miR-126 targeting the negative VEGF regulators; *Spred1* and *Pik3r2*. VEGF promotes angiogenesis indicating that engraftment of miR-126 preconditioned MSCs resulted in successful angiomyogenesis [300].

Chen *et al* have looked to study the effect microRNA transfected MSCs in heterotopic bone formation. The modulation of miR-34a *in vivo* by transfecting isolated human MSCs with either pre-miR-34a or anti-miR-34a and loading onto hydroxyapatite/ tricalcium phosphate based ceramic beads scaffold followed by subcutaneous implantation in SCID/NOD mice for a total of 8 weeks was carried out. Overexpression of miR-34a resulted in reduction of bone formation and inhibition of miR-34a in MSCs resulted in a significant increase in bone formation [301]. Similarly, Eskildsen *et al* carried out transfection of either pre-miR-138 or anti-miR-138 into human MSCs loaded onto hydroxyapatite/tricalcium phosphate (HA/TCP) ceramic powder and subcutaneously implanted into NOD/SCID mice, which allowed for examination of miR-138 function *in vivo*. MiR-138 overexpression showed a reduction of ectopic bone formation and inhibition of miR-138 showed that bone formation was enhanced by 60% [302]. Implantation of pre-conditioned isolated stem cells provides an alternative approach to therapy and also implies that targeting of miR-138 to enhance bone formation.

Currently following cartilage injury there are limited surgical procedures that can be carried out, all which have limitations. Two potential concepts could be utilised; direct injection of pro-chondrogenic microRNAs to stimulate chondrocytes *in situ* to maintain their phenotype. The use of autologous isolated bone marrow derived skeletal stem cells treated with exogenous microRNA could be transplanted to the defect area, inducing more efficient chondrogenic differentiation and enhancing the formation of articular cartilage.

1.2.6 MicroRNAs in Osteoarthritis and Chondrogenesis Project Hypotheses and Objectives

Project overview

Comprehension of the functioning of microRNAs in osteoarthritis and chondrogenesis allows for research into the application of microRNAs as potential therapy. MicroRNAs could be directly administered to articular cartilage, having direct effect upon resident articular chondrocytes, as a potential form of treatment in cartilage injury and OA. Additionally exogenous microRNAs could be used in combination with isolated skeletal stem cells and transplanted to defective articular sites to induce regeneration. Elucidation of the microRNA regulatory network which governs chondrogenic differentiation may help in the development of novel strategies to enhance cartilage formation. Before microRNAs can be used in potential tissue engineering strategies the discovery and role of functional microRNAs involved with OA and chondrogenesis is required.

Project hypotheses

1) Specific microRNAs are dysregulated in OA

- The expression of miR-146b in human osteoarthritic articular chondrocytes is dysregulated compared to the expression of miR-146b in control human chondrocytes.
- Treatment of chondrocytes with OA associated catabolic cytokine IL-1β induces miR-146b up-regulation and treatment of chondrocytes with anabolic TGF-β3 induces miR-146b down-regulation and TGF-β3 can subdue the effects of IL-1β.

2) Specific skeletal populations can be derived using specific microRNAs, to selectively direct cell differentiation and function along the chondrogenic lineage.

- MicroRNA-34a targets specific genes in human fetal femur-derived cells which regulate the ability of the fetal femur-derived cells to undergo chondrogenic differentiation.
- MicroRNA-146b targets specific genes in human bone marrow derived skeletal stem cells which regulate the ability of human bone marrow derived skeletal stem cells to undergo chondrogenic differentiation.

Project aims and objectives

- To identify if miR-146b displays dysregulated expression in human OA articular chondrocytes.
- To identify the expression of miR-146b following treatment of chondrocytes with either: IL-1β, TGF-β3 and IL-1β and TGF-β3 combined treatment.
- To identify miR-34a expression and function during chondrogenic differentiation of fetal femur-derived stem cells and to modulate chondrogenic differentiation in human fetal femur-derived stem cells using miR-34a inhibitor and miR-34a mimic *in vitro.*
- To identify miR-146b expression and function during chondrogenic differentiation of human bone marrow derived skeletal stem cells and to modulate chondrogenic differentiation in human bone marrow derived skeletal stem cells using miR-146b inhibitor and miR-146b mimic *in vitro.*

Chapter 2
Materials and Methods

2.1 Cell sources and cell culture methodology

2.1.1 Isolation and culture of human articular chondrocytes

With consent, the femoral heads obtained from patients having undergone femoral head ostectomy at Southampton General Hospital were used for isolation of articular chondrocytes from the articular cartilage with approval of Southampton and South West Hampshire Research Ethics Committee (194/99/1 & 210/01). Articular cartilage was cut away from the femoral head and cut into small pieces. Cartilage pieces were incubated in 2.5ml 10% trypsin (v/v) (Sigma Aldrich Cat.No.T4174) for 30 minutes at 37°C and shook every 10 minutes. Trypsin was then removed from the cartilage pieces followed by washing with PBS (Lonza Cat.No.BE17-516F). Cartilage pieces were then incubated in 2.5ml of 0.1% hyaluronidase (w/v) (Sigma Aldrich Cat.No.H3506) for 15 minutes and shook at 7.5 minutes. Following removal of hyaluronidase, cartilage pieces were washed in PBS (Lonza Cat.No.BE17-516F) and incubated in 2.5ml of 1% collagenase B (w/v) (Roche Diagnostics Cat.No.11088815001) in a shaking incubator at 37°C for no longer than 15 hours. 5ml of α-MEM (Lonza Cat.No.LZBE02-002F) was added to the digested suspension of articular chondrocytes and filtered through a 70μm filter. The filtered cell suspension was then centrifuged at 1800rpm for 5 minutes. The supernatant was decanted and either isolated chondrocytes were re-suspended in appropriate media and plated in tissue culture flasks or lysis buffer was applied for RNA extraction.

2.1.2 Isolation and culture of human fetal femur-derived cells

With informed and written consent human fetal tissue was obtained from women having undergone a termination of pregnancy procedure agreeing to the guidelines ensued by the Polkinghorn Report. Ethical approval was obtained from the Southampton and South West Hampshire Local Research Ethics Committee (LREC 296100). Fetal age was determined by measurement of the foot length and expressed as weeks post conception; as displayed in table 4. All experiments were carried using fetal femurs between the ages of 53 and 61 days post conception. Femurs were isolated from the surrounding skeletal muscle and connective tissue, followed by digestion with α-MEM (Lonza Cat.No.LZBE02-002F) containing Collagenase B (Roche Diagnostics Cat.No.11088815001) overnight. Cells were collected after passing through a 70μm filter and cultured in α-MEM (Lonza Cat.No.LZBE02-002F) containing 10% (v/v) fetal calf serum (FCS) (Life Technologies Cat.No.10270106) and 1% (v/v) penicillin/streptomycin (Sigma Aldrich Cat.No.P4333). Cells were expanded in monolayer culture until sub-confluency was reached.

Fetal foot length (mm)	Days Post conception	Weeks post conception
4.0	53	7.5
4.5	54	7.5
5.0	55	7.5
5.5	56	8.0
6.0	59	8.5
6.5	61	8.5

Table 4. Age of human fetus in days and weeks post conception as determined by the fetus foot length in millimetres

2.1.3 Isolation and culture of human bone marrow derived skeletal stem cells

2.1.3.1 Cell Isolation

Skeletal stem cells derived from human bone marrow were obtained from the bone marrow of patients undergoing total hip replacement surgery at Southampton General Hospital with full ethical consent and approval from the local hospital ethics committee (LREC 194/99/w, 27/10/10). Cells were isolated from human bone marrow by washing bone marrow samples repeatedly with α-MEM (Lonza Cat.No.LZBE02-002F) with the resultant solution isolated and passed through a 70μm cell filter strainer to remove debris. The resultant solution was then made up to 10ml with α-MEM (Lonza Cat.No.LZBE02-002F) and centrifuged for 5 minutes at 1200rpm at room temperature. Following centrifugation the supernatant was decanted and resulting cell pellet washed with 10ml of α-MEM (Lonza Cat. No. LZBE02-002F) a further 2 times.

2.1.3.2 Lymphoprep for isolation of bone marrow mononuclear cells

The washed cell pellet was re-suspended in 25ml of α-MEM (Lonza Cat. No LZBE02-002F) and layered over 20ml lymphoprep solution (Scientific Laboratory supplies Cat. No. 17-829e), which was then spun at 2200rpm for 40 minutes at room temperature with the centrifuge brake off. Mononuclear cells from the interphase were then removed with a pastette and suspended in 25ml of fresh α-MEM (Lonza Cat. No LZBE02-002F) and centrifuged for 5minutes at 1200rpm at room temperature. Following removal of the supernatant, the resulting cell pellet was re-suspended in 10ml of α-MEM (Lonza Cat. No LZBE02-002F) to wash the cells followed by centrifugation for 5 minutes at 1200rpm. The supernatant was decanted leaving a cell pellet of human bone marrow derived mononuclear cells.

2.1.3.3 Stro-1 antibody hybridoma supernatant production

Stro-1 hybridoma was derived from a donation provided by Dr. Jon N. Beresford, University of Bath. Cells were cultured in Dulbecco's modified eagle's medium (DMEM) (Lonza) and 20% FCS (Sigma) Following initial proliferation of cells FCS concentration was reduced to 5%. Cells were transferred

into a cell bioreactor (CELLine, Integra). Cells were harvested each week and the supernatant containing the Stro-1 antibody was collected following centrifugation at 1,400 rpm.

2.1.3.4 MACS – Magnetic activated cell sorting of Stro-1 positive skeletal stem cells

Isolated bone marrow mononuclear cells were re-suspended in 2ml MACS blocking buffer for 30 minutes at 4°C. MACS blocking buffer was previously made up to contain: 17ml α-MEM (Lonza Cat.No.LZBE02-002F), 2ml of AB human serum (Sigma Aldrich Cat.No.H4522), 0.2g BSA (Fischer Scientific Cat.No.12737119) and 1ml FCS (Life Technologies Cat.No.10270106) mixed and filter sterilised. Following incubation of cells in MACS blocking buffer cells were washed with 10ml of MACS buffer (containing 5g BSA (Fischer Scientific Cat.No.12737119) and 0.74448g EDTA (Fischer Scientific Cat.No.10716481) dissolved in 1L PBS, previously made up and filter sterilised) by re-suspension in MACS buffer followed by centrifugation for 5 minutes at 1200rpm. The supernatant was removed and the resulting cell pellet was re-suspended in 1ml of Stro-1 antibody (undiluted supernatant harvested from the Stro-1 hybridoma made in-house) for 30 minutes at 4°C. Cells were then washed 3 times with 10ml of MACs buffer followed by centrifugation at 1200rpm for 5 minutes. The resulting cell pellet was re-suspended in secondary antibody solution made up of 800µl MACs buffer and 200µl rat anti-mouse IgM microbeads (Miltenyi Biotec Cat.No.130047301) and incubated for 30 minutes at 4°C. 10ml MACs buffer was then added and cell suspension centrifuged at 1200rpm for 5 minutes at room temperature followed by two further washes with MACS buffer. 5ml of MACs buffer was then added to the cell pellet. MACS separation columns (Miltenyi Biotec Cat.No.130-042-201) were then placed into the magnetic field of the VarioMACs and 3ml of MACs buffer added to the column to wash the columns through. The 5ml cell suspension was then added to the column followed by washing the column three times with 3ml MACs buffer. The column was then removed from the VarioMACs assembly to release magnetically attached cells within the column and a fresh collection tube placed underneath the column. 5ml fresh MACs buffer was added to the column and a plunger used to flush out the Stro-1 positive fraction of cells. Cells were then suspended in 10ml MACs buffer and centrifuged at 1200rpm for 5 minutes at room temperature. The resulting cell pellet was re-suspended in α-MEM (Lonza Cat. No LZBE02-002F) containing 10% (v/v) FCS (Life Technologies Cat.No.10270106) and 1% P/S (v/v) (Sigma Aldrich Cat.No.P4333) and placed into tissue culture flasks for adhesion and expansion.

2.2 Cell treatment assays

2.2.1 Treatment of articular chondrocytes with IL-1β and/or TGF-β3

Human articular chondrocytes isolated from articular cartilage were expanded in monolayer culture in α-MEM (Lonza Cat. No LZBE02-002F) containing 5% (v/v) FCS (Life Technologies Cat.No.10270106) and 1% (v/v) penicillin/streptomycin (Sigma Aldrich Cat.No.P4333) and were cultured in T175 tissue culture flasks until confluent. Cells were then trypsinised and seeded at a cell density of 1 x 10^5 per 10µl in central spots of individual wells of a 24 well plate and cultured in high

density micromass culture. Initially the spot containing the high density cells were left in the incubator for 2 hours, after which time 500µl of α-MEM (Lonza Cat. No LZBE02-002F) containing 5% (v/v) FCS (Life Technologies Cat.No.10270106) and 1% (v/v) P/S (Sigma Aldrich Cat.No.P4333) was carefully added to each well and left overnight. Four treatment groups were investigated which involved four different types of culture media included media containing TGF-β3, media containing IL-1β, media containing both TGF-β3 and IL-1β and control media containing no TGF-β3 or no IL-1β. Following the initial culture of cells overnight in basal media, the basal media was removed from the wells and replaced with 500µl of one of the types of culture media. Media which contained: 10ng/ml TGF-β3 (Peprotech Cat. No. 100-36E), 100µM ascorbate-2-phosphate (Sigma Aldrich Cat.No.A8960), 10nM dexamethasone (Sigma Aldrich Cat.No.D4902) and 10% (v/v) ITS solution (Sigma Aldrich Cat.No.I3146) in α-MEM (Lonza Cat.No.LZBE02-002F) containing 1% (v/v) P/S (Sigma Aldrich Cat.No.P4333). Media which contained IL-1β was made up of 2.5ng/ml IL-1β (Sigma Aldrich Cat.No.SRP3083), 2.5ng/ml oncostatin M (Sigma Aldrich Cat.No.O9635) and 10µl/ml ITS solution (Sigma Aldrich Cat.No.I3146) in α-MEM (Lonza Cat.NoLZBE02-002F) containing 1% P/S (Sigma Aldrich Cat.No.P4333). Media which contained both TGF-β3 and IL-1β was made up of 10ng/ml TGF-β3 (Peprotech Cat.No.100-36E), 100µM ascorbate-2-phosphate (Sigma Aldrich Cat.No.A8960), 10nM dexamethasone (Sigma Aldrich Cat.No.D4902), 2.5ng/ml IL-1β (Sigma Aldrich Cat.No.SRP3083), 2.5ng/ml oncostatin M (Sigma Aldrich Cat.No.O9635) and 10µl/ml ITS solution (Sigma Aldrich Cat.No.I3146) in α-MEM containing 1% (v/v) P/S (Sigma Aldrich Cat.No.P4333). Control media which contained no TGF-β3 or IL-1β was made up of 10% 10µl/ml ITS solution (Sigma Aldrich Cat.No.I3146) in α-MEM (Lonza Cat.NoLZBE02-002F) containing 1% (v/v) P/S (Sigma Aldrich Cat.No.P4333). For each cell culture media condition, media was changed every 42 hours and cells cultured for up to 21 days.

2.2.2 Adipogenic differentiation assay in human bone marrow derived skeletal stem cells

Cells previously isolated from human bone marrow following the MACS procedure were trypsinised and re-seeded at a density of 1 x 10^4 cells per ml in two 6 welled plates and allowed to grow to approximately 80% confluence in basal medium (α-MEM) (Lonza Cat.NoLZBE02-002F) supplemented with 10% FSC (Life Technologies Cat.No.10270106) and 1% penicillin/streptomycin (Sigma Aldrich Cat.No.P4333)) followed by substitution with adipogenic medium containing α-MEM (Lonza Cat.NoLZBE02-002F), 10% FCS (Life Technologies Cat.No.10270106), 1% penicillin/streptomycin (Sigma Aldrich Cat.No.P4333), 100nM dexamethasone (Sigma Aldrich Cat.No.D4902), 0.5mM 3-isobutyl-1-methylxanthine (IBMX) (Sigma Aldrich Cat.No.I7018), 1µM rosiglitazone (Sigma Aldrich Cat.NoR2408) and 3µg/ml of Insulin-Transferrin-Selenium (ITS) solution (Sigma Aldrich Cat.No. I3146) or control basal medium containing no growth factors. Medium was changed every 3 days and cultures grown for 7 and 14 days at which point cells were either fixed for histological analysis or lysed for alkaline phosphatase (ALP) activity assay.

2.2.3 Osteogenic differentiation assay in human bone marrow derived skeletal stem cells

Cells previously isolated from human bone marrow following the MACS procedure were trypsinised and re-seeded at a density of 1 x 10^4 cells per ml in two 6 welled plates and allowed to grow to approximately 80% confluence in basal medium (α-MEM) (Lonza Cat.NoLZBE02-002F) supplemented with 10% FSC (Life Technologies Cat.No.10270106) and 1% penicillin/streptomycin (Sigma Aldrich Cat.No.P4333)) followed by substitution osteogenic medium containing α-MEM (Lonza Cat.NoLZBE02-002F) supplemented with 10% FCS (Life Technologies Cat.No.10270106), 1% Penicillin/Streptomycin (Sigma Aldrich Cat.No.P4333), 100μM ascorbate-2-phosphate (Sigma Aldrich Cat.No. A8960) and 10nM dexamethasone (Sigma Aldrich Cat.No.D4902) or control basal medium containing no growth factors. Medium was changed every 3 days and cultures grown for 7 and 14 days at which point cells were either fixed for histological analysis or lysed for ALP protein assay.

2.2.4 Chondrogenic micromass differentiation assay in human bone marrow derived skeletal stem cells and human fetal femur-derived cells

Human bone marrow derived Stro-1 enriched skeletal stem cells or human fetal femur- derived cells which had been previously isolated and expanded in monolayer culture in α-MEM (Lonza Cat.No.LZBE02-002F) containing 10% (v/v) FCS (Life Technologies Cat.No.10270106) and 1% (v/v) P/S (Sigma Aldrich Cat.No.P4333) and expanded in T175 culture flasks until confluent were then trypsinised and seeded at a cell density of 1 x 10^5 per 10μl in central spots of individual wells of a 24 well plate. Initially the spot containing the high density cells were left in the incubator for 2 hours, after which time 500μl of α-MEM (Lonza Cat.No.LZBE02-002F) containing 5% (v/v) FCS (Life Technologies Cat.No.10270106) and 1% (v/v) P/S (Sigma Aldrich Cat.No.P4333) was carefully added to each well and left overnight. The following day the basal media was removed from the wells and replaced with 500μl of either chondrogenic differentiation inducing media containing 100μM ascorbate-2-phosphate (Sigma Aldrich Cat. No. A8960), 10nM dexamethasone (Sigma Aldrich Cat.No.D4902), 10μl/ml ITS solution (Sigma Aldrich Cat.No.I3146) and 10ng/ml TGF-β3 (Peprotech Cat.No.100-36E) or control media containing α-MEM (Lonza Cat.No.LZBE02-002F) with no FCS 10μl/ml ITS solution (Sigma Aldrich Cat.No.I3146). Both chondrogenic differentiation media and control media containing was replenished every 42 hours and cells cultured in the micromass system for up to 21 days.

2.2.5 Alkaline Phosphatase activity in differentiated human bone marrow derived skeletal stem cells

Cells which had been subject to basal, adipogenic and osteogenic culture conditions for 7 and 14 days were fixed with 90% ethanol (Fischer Scientific Cat.No.12468750) for 15 minutes. 600μl of 0.05% of Triton-X-100 (Sigma Aldrich Cat.No.X100) was then added to each well. A cell scraper was used to remove cells from the bottom of the plate followed by storage of the plates at -20°C for 30 minutes,

followed by thawing at 37°C for 30 minutes and scraping again, the freeze/thaw process was repeated twice more. To conduct the alkaline phosphatase assay a substrate consisting of distilled water containing 33% 1.5M alkaline buffer solution (Sigma Aldrich Cat.No.A9226) and 0.0013g of phosphatase substrate (Sigma Aldrich Cat.No.P4744) per ml was made up and 90µl added to 10µl of cell lysate. Standards were also made up using assay buffer consisting of distilled water containing 33% 1.5M alkaline buffer solution (Sigma Aldrich Cat.No.A9226) and 2µl/ml of Igepal CA-630 (Sigma I3021), the assay buffer was added to set amounts of AP Standard p-nitrophenol 10µmol/ml (Sigma Aldrich Cat.No.N7660) to make up standard concentrations. 100µl of standards and 100µl of lysate/substrate were added to 96 well plates. Plates were then incubated at 37°C for samples to allow change of colour in samples to yellow. The time for colour change was recorded and 100µl of NaOH was added to all wells to terminate the reaction. The plate was then transferred to a colorimetric plate reader (BioTel ELx-800) and absorbance at 410nm measured.

2.3 Histological Techniques

2.3.1 Oil red O staining

After 14 days cells cultured in basal, osteogenic and adipogenic media were fixed with bakers formal calcium containing 1% calcium chloride (w/v) (Sigma Aldrich Cat.No.1016) and 4% (v/v) formaldehyde (Sigma Aldrich Cat.No.15587) followed by washing cultures with 60% isopropanol (Sigma Aldrich Cat.No.I9516). 1ml of oil red O solution (Sigma Aldrich Cat.No.O0625) was then added to each well and incubated at room temperature for 15 minutes after which time cultures were washed 3 times with distilled water. Cultures were then imaged using a Carl Zeiss AxioVert 200 microscope with AxioCam HR and AxioCam MR3 digital cameras using AxioVision version 4.7 software (Carl Zeiss Ltd, Cambridge, UK).

2.3.2 Alkaline phosphatase staining

To examine cultures for alkaline phosphatase activity, after 14 days cells cultured in basal, osteogenic and adipogenic media were fixed in 90% ethanol (Fischer Scientific Cat.No.12468750) following two PBS washes for 10 minutes. The alkaline phosphatase staining solution was prepared by adding 0.024% (w/v) Fast Violet B salt (Sigma Aldrich Cat.No.F1631) and 4% (v/v) Napthol AS-MX phosphate (Sigma Aldrich Cat.No.855) to water which was added to monolayer cultures for up to 45 minutes. The reaction was terminated by washing cells with distilled water followed by visualisation and imaging with a Carl Zeiss AxioVert 200 microscope with AxioCam HR and AxioCam MR3 digital cameras using AxioVision version 4.7 software (Carl Zeiss Ltd, Cambridge, UK).

2.3.3 Alcian blue and sirus red staining of the human fetal femur

Following isolation of the fetal femur, the fetal femur was submerged in 4% (v/v) PFA in PBS (AffymetrixCat.No.19943) overnight for fixation. The fetal femur was then washed in PBS (Lonza Cat.No.BE17-516F) and dehydrated through ascending ethanol concentrations and histoclear (HD

supplies Cat.No.CC500) cultures were left in 50% (v/v) ethanol (Fischer Scientific Cat.No.12468750) for 1 hour followed by submersion in 90% (v/v) ethanol (Fischer Scientific Cat.No.12468750) for 1 hour, 100% ethanol (Fischer Scientific Cat.No.12468750) for 1 hour followed by fresh 100% ethanol (Fischer Scientific Cat.No.12468750) for another 1 hour, 100% histoclear (HD supplies Cat.No.CC500) for 1 hour and finally another 100% histoclear (HD supplies Cat.No.CC500) for 1 hour. Femurs were then left in molten wax for 1 hour, the wax was then removed and femur submerged in fresh molten wax for a further 1 hour to ensure all histoclear had been removed. Femurs were then embedded in paraffin wax by filling the embedding tray containing the samples with wax and allowing to cool and set. Samples were then removed from the embedding trays, embedded in paraffin wax blocks which were then sectioned at 7μm on a microtome and sections collected on slides and allowed to air dry. Slides were then deparaffinised and rehydrated through submerging slides in histoclear (HD supplies Cat.No.CC500) twice for 7 minutes each and then submerging slides in descending methanol concentration; 100% methanol for 2 minutes repeated twice, 90% (v/v) methanol for 2 minutes followed by 50% (v/v) methanol for 2 minutes, followed by a wash in distilled water. Equal volumes of Weigert's haematoxylin A (Sigma Aldrich Cat.No.HT107) and B solution (Sigma Aldrich Cat.No.HT109) were then made up and applied to slides for 10minutes. Slides were then washed and dipped 3 times in acid/alcohol (1% (v/v) hydrochloric acid in 70% (v/v) ethanol (Fischer Scientific Cat.No.12468750)) followed by further washing in water. Slides were then submerged in alcian blue stain (Fischer Scientific Cat.No.10786953) for 10 minutes followed by washing in water and then stained in molybdophosphoric acid (Sigma Aldrich Cat.No.221856) for 10 minutes. Slides were then washed and then submerged in sirus red stain (Sigma Aldrich Cat.No.365548) for 40 minutes. Slides were then washed in water and then samples rehydrated by submerging slides in 50% ethanol (Fischer Scientific Cat.No.12468750) for 30 seconds followed by 90% ethanol (Fischer Scientific Cat.No.12468750) for seconds, 100% ethanol (Fischer Scientific Cat.No.12468750) for 30 seconds followed by 100% ethanol (Fischer Scientific Cat.No.12468750) for a further 30 seconds and histoclear (HD supplies Cat.No.CC500) for 30 seconds followed by mounting slides in DPX (Fischer Scientific Cat.No.10050080) overnight ready for visualisation with an Olympus BX-51/22 dotSlide digital virtual microscope using OlyVIA 2.1 software (Olympus Soft Imaging Solutions, GmBH, UK).

2.3.4 Stro-1 immunohistochemistry of the human fetal femur

Fetal femurs which had previously undergone fixation, embedding, processing were subject to Stro-1 immunostaining and counterstained with alcian blue. Slides were subject to 3% hydrogen peroxide (Sigma Aldrich Cat.No.H1009) for 5 minutes followed by washing. Samples were blocked with 1% (w/v) BSA (Fischer Scientific Cat.No.12737119) in PBS (Lonza Cat.No.BE17-516F) for 5 minutes, followed by incubation with Stro-1 antibody (diluted supernatant harvested from the Stro-1 hybridoma made in-house) at 4°C overnight and was used at 1/50. Samples were then washed 3 times in 20% PBS tween-20 (Sigma Aldrich Cat.No.20274348) followed by incubation with a biotinylated

goat-anti-mouse secondary antibody (Sigma Aldrich Cat.No.B9265) 1/100 for 1 hour. Following washing 3 times with 20% PBS tween-20 (Sigma Aldrich Cat.No.20274348), extravidin peroxidase (Sigma Aldrich Cat.No.E2886) was applied to samples for 30 minutes followed again by washing 3 times in 20% PBS tween-20 (Sigma Aldrich Cat.No.20274348) 3 amino-9-ethyl-carbazole (Sigma Aldrich Cat.No.A5754) was filtered onto samples for 10 minutes followed by termination of reaction by washing in water. Finally samples were counterstained with alcian blue by immersing samples in alcian blue stain (Fischer Scientific Cat.No.10786953) for 45 seconds. Following washing samples were mounted in hydromount (Fischer Scientific Cat.No.1294910) and imaged using an Olympus BX-51/22 dotSlide digital virtual microscope using OlyVIA 2.1 software (Olympus Soft Imaging Solutions, GmBH, UK).

2.3.5 Stro-1 immunohistochemistry of human bone marrow derived Stro-1 enriched skeletal stem cells and human follicular dendritic (HK) cells

To ensure that cells isolated by the MACs procedure were the cells required for experimentation and therefore exhibited the Stro-1 antigen upon their cell surfaces, Stro-1 immunocytochemistry was conducted. Additionally Stro-1 antigen positive bearing cells, human follicular dendritic (HK) cells, was utilised as a positive control for Stro-1 immunocytochemistry. Human bone marrow derived mononuclear cells which had been isolated through MACS and expanded in basal medium (α-MEM (Lonza Cat.NoLZBE02-002F) supplemented with 10% (v/v) FSC (Life Technologies Cat.No.10270106) and 1% (v/v) penicillin/streptomycin (Sigma Aldrich Cat.No.P4333)) were used for Stro-1 staining. HK cells (human follicular dendritic cells) were cultured in Iscoves Modified Dulbeccos Media (IMDM) (Lonza) supplemented with 10% (v/v) FCS, 1% 64 sodium pyruvate (Life Technologies), 1% non-essential amino acids solution (Life Technologies) and 1% penicillin/streptomycin. Both human bone marrow derived mononuclear cells isolated through Stro-1 MACS isolation and Stro-1 positive HK cells were fixed in 4% (v/v) paraformaldehyde in PBS for 5 minutes followed by 3 rinses in 0.5% PBS Tween-20. Cultures were then incubated in blocking buffer (1 X PBS containing 0.3% triton X-100 (Sigma Aldrich Cat.No.X100) and 5% serum) for 60 minutes at room temperature. The primary antibody; anti-Stro-1 antibody (supernatant harvested from the Stro-1 hybridoma made in-house) was diluted in antibody dilution buffer (1 X PBS containing 1% bovine serum albumin (Fischer Scientific Cat.No.12737119) and 0.3% (v/v) triton X-100 (Sigma Aldrich Cat.No.X100)) to a concentration of 1:50. The diluted antibody was applied to cultures and left to incubate at 4°C overnight. Cultures were then washed 3 times with PBS tween-20 and the diluted secondary antibody; AlexaFluor 488 conjugated goat-anti-mouse (Life Technologies Cat.No.A10667) applied at a concentration of 1:200 and left to incubate for 60 minutes at room temperature in the dark. Cultures were then washed 3 times in PBS tween and Alexa Fluor 568 Phalloidin stain (Life Technologies Cat.No.A12380) added at a concentration of 1:30 for 20 minutes followed by three washes in PBS tween-20 and finally followed by a DAPI nuclear counterstain (Life Technologies Cat.No.D3571) applied for 10 minutes at a concentration of 1:200 followed by 3 washes

in PBS tween-20 ready for visualisation and imaging. A Carl Zeiss AxioVert 200 microscope with AxioCam HR and AxioCam MR3 digital cameras using AxioVision version 4.7 software (Carl Zeiss Ltd, Cambridge, UK) was used for fluorescence imaging.

2.3.6 Processing and Embedding of micromass cultures

To examine cultures histologically for chondrogenesis, micromass cultures composed of either human fetal femur cells or human bone marrow derived skeletal stem cells having undergone chondrogenesis required processing and embedding in paraffin wax. Both micromass cultures which had formed 3D masses and cells cultured in control media which did not maintain 3D masses were fixed in 4% (v/v) PFA (Affymetrix Cat. No.19943) for 30 minutes followed by washing with PBS (Lonza Cat.No.BE17-516F). Micromass cultures were removed from the base of the welled plate to ensure PFA penetration of the entire culture mass. Micromass cultures were then dehydrated through ascending ethanol concentrations and histoclear; cultures were left in 50% (v/v) ethanol (Fischer Scientific Cat.No.12468750) for 30 minutes followed by submersion in 90% (v/v) ethanol (Fischer Scientific Cat.No.12468750) for 30 minutes, 100% ethanol (Fischer Scientific Cat.No.12468750) for 30 minutes followed by fresh 100% ethanol (Fischer Scientific Cat.No.12468750) for another 30 minutes, 100% histoclear (HD supplies Cat.No. CC500) for 30 minutes and finally another 100% histoclear (HD supplies Cat.No.CC500) for 30 minutes. Micromass cultures were then left in molten wax for 30 minutes, the wax was then pipetted off and cultures submerged in fresh molten wax for another 30 minutes to ensure all histoclear had been removed. The micromass cultures were then embedded in paraffin wax by filling the embedding tray containing the samples with wax and allowing to cool and set. Samples were then removed from the embedding trays, embedded in paraffin wax blocks which were then sectioned at 7μm on the microtome and sections collected on slides and allowed to air dry.

2.3.7 Type II Collagen immunostaining of micromass cultures

Chondrogenic micromass cultures which had previously undergone processing and embedding, sectioned micromass cultures was then deparaffinised and rehydrated through submerging slides in histoclear (HD supplies Cat.No.CC500) twice for 7 minutes each and then submerging slides in descending methanol concentration; 100% methanol for 2 minutes repeated, 90% methanol for 2 minutes followed by 50% (v/v) methanol for 2 minutes, followed by a wash in distilled water. To examine cultures for chondrogenesis both sectioned micromass samples and cells in monolayer culture were subject to type II collagen immunostaining. Following rehydration slides and monolayer control cultures were subject to antigen retrieval by addition of 0.01M citrate buffer (Sigma Aldrich Cat.No. P4809) and incubated at 70°C for 20 minutes, after washing, 3% (v/v) hydrogen peroxide (Sigma Aldrich Cat.No.H1009) was added for 5 minutes followed by washing and incubation with 520U/ml hyaluronidase (Sigma Aldrich Cat.No.H3506) for 20 minutes at 37°C followed by washing with water. Samples were blocked with 1% BSA (Fischer Scientific Cat.No.12737119) in PBS (Lonza

Cat.No.BE17-516F) for 1 hour followed by incubation with primary antibody at 4°C overnight, collagen type II polyclonal rabbit antibody (Calbiochem Cat.No.234187) was used at 1/500. Samples were then washed 3 times in 20% PBS tween-20 (Sigma Aldrich Cat.No.20274348) followed by incubation with a biotinylated goat anti-rabbit secondary antibody (Sigma Aldrich Cat.No.B8895) at 1/100 for 1 hour. Following washing 3 times with 20% PBS tween-20 (Sigma Aldrich Cat.No.20274348), extravidin peroxidase (Sigma Aldrich Cat.No.E2886) was applied to samples for 30 minutes followed again by washing 3 times in 20% PBS tween-20 (Sigma Aldrich Cat.No.20274348). 3 amino-9-ethyl-carbazole (Sigma Aldrich Cat.No. A5754) was filtered onto samples for 10 minutes followed by termination of reaction by washing in water. Finally samples were counterstained with haematoxylin (Sigma Aldrich Cat.No.HT107/HT109) and slides mounted in DPX (Fischer Scientific Cat.No.10050080). Slides were visualised with an Olympus BX-51/22 dotSlide digital virtual microscope using OlyVIA 2.1 software (Olympus Soft Imaging Solutions, GmBH, UK) and monolayer cultures in welled plates were visualised with a Carl Zeiss AxioVert 200 microscope with AxioCam HR and AxioCam MR3 digital cameras using AxioVision version 4.7 software (Carl Zeiss Ltd, Cambridge, UK).

2.3.8 Alcian Blue staining of micromass cultures

To examine for chondrogenesis, sectioned micromass cultures and wells containing fixed cells were stained with alcian blue and counterstained with haematoxylin. Cells from the welled plates were fixed in 4% (v/v) PFA (Affymetrix Cat. No.19943) and sections of micromass cultures having undergone sectioning and embedding were dehydrated. Both samples; cells cultured in control media which developed into monolayer cultures and sectioned micromass cultures were washed twice in PBS (Lonza Cat.No.BE17-516F) and haematoxylin stain (Sigma Aldrich Cat.No.HT107/HT109) applied for 10 minutes followed by a rinse in acid alcohol and then washed with water. Samples were then stained in alcian blue (Fischer Scientific Cat.No.10786953) for 10 minutes followed by washing in water and then stained in molybdophosphoric acid (Sigma Aldrich Cat.No.221856) for 10 minutes. Slides were then washed and slides were dehydrated by submerging slides in 50% ethanol (Fischer Scientific Cat.No.12468750) for 30 seconds followed by 90% (v/v) ethanol (Fischer Scientific Cat.No.12468750) for seconds, 100% ethanol (Fischer Scientific Cat.No.12468750) for 30 seconds followed by 100% ethanol (Fischer Scientific Cat.No.12468750) for a further 30 seconds and histoclear (HD supplies Cat.No. CC500) for 30 seconds followed by mounting slides in DPX (Fischer Scientific Cat.No.10050080) overnight and PBS (Lonza Cat.No.BE17-516F) applied to cells fixed and stained in welled plates ready for visualisation. Slides were visualised with an Olympus BX-51/22 dotSlide digital virtual microscope using OlyVIA 2.1 software (Olympus Soft Imaging Solutions, GmBH, UK) and monolayer cultures in welled plates were visualised with a Carl Zeiss AxioVert 200 microscope with AxioCam HR and AxioCam MR3 digital cameras using AxioVision version 4.7 software (Carl Zeiss Ltd, Cambridge, UK).

2.3.9 Safranin O staining of micromass cultures

To examine for chondrogenesis, sectioned micromass cultures and wells containing fixed cells were stained with safranin O (Sigma Aldrich Cat.No.S2255) and counterstained with haematoxylin. Cells from the welled plates were fixed in 4% (v/v) PFA (Affymetrix Cat. No.19943) and sectioned micromasses, having undergone sectioning and embedding, were dehydrated. Samples were first stained with haematoxylin (Sigma Aldrich Cat.No.HT107/HT109) for 10 minutes followed by washing. Acid/alcohol was applied 3 times followed by washing with water. Samples were rinsed with 1% acetic acid (Fischer Scientific Cat.No.10304980) and then safranin O (Sigma Aldrich Cat.No.S2255) was applied for 5 minutes followed by washing in water and sectioned samples were dehydrated by submerging slides in 50% ethanol (Fischer Scientific Cat.No.12468750) for 30 seconds followed by 90% (v/v) ethanol (Fischer Scientific Cat.No.12468750) for 30 seconds, 100% ethanol (Fischer Scientific Cat.No.12468750) for 30 seconds followed by 100% ethanol (Fischer Scientific Cat.No.12468750) for a further 30 seconds and histoclear (HD supplies Cat.No.CC500) for 30 seconds followed by mounting slides in DPX (Fischer Scientific Cat.No.10050080) overnight and PBS (Lonza Cat.No.BE17-516F) applied to cells fixed and stained in welled plates ready for visualisation. Slides were visualised with an Olympus BX-51/22 dotSlide digital virtual microscope using OlyVIA 2.1 software (Olympus Soft Imaging Solutions, GmBH, UK) and monolayer cultures in welled plates were visualised with a Carl Zeiss AxioVert 200 microscope with AxioCam HR and AxioCam MR3 digital cameras using AxioVision version 4.7 software (Carl Zeiss Ltd, Cambridge, UK).

2.4 Molecular Techniques

2.4.1 RNA extraction

RNA was extracted using mirVana™ RNA Isolation System Kit (Life Technologies Cat.No.AM1561) in accordance with the manufacturer's protocol or Qiagen AllPrep DNA/RNA Mini kit (Qiagen Cat.No.80204). In brief in all experiments requiring molecular analysis, samples were washed twice with PBS (Lonza Cat.No.BE17-516F). 600µl of lysis buffer was then added to allow for cell membrane lysis and release of RNA. MicroRNA homogenizing agent at 10% of the volume of lysis buffer (60µl) was then added followed by addition and mixing of 600µl acid phenol-chloroform (Life Technologies Cat.No.AM9722) to carry out phase separation. The aqueous phase was transferred and added to ethanol (Fischer Scientific Cat.No.12468750) followed by spin column based ribonucleic acid purification with use of supplied buffers for washing followed by elution of RNA with RNase free water. RNA quantity and purity was determined using 1µl of RNA with a Thermo Scientific NanoDrop ND-1000 spectrophotometer and accompanying software.

2.4.2 cDNA synthesis of mRNA and qPCR

Following RNA extraction and quantification, RNA was diluted with appropriate volumes of water to give the same concentration of RNA in all samples. For cDNA synthesis of mRNA in samples, SuperScript® VILO cDNA Synthesis kit (Life Technologies Cat.No.11754250) was used. In brief RNA was combined with 2µl 5X VILO™ reaction mix and 1µl 10X SuperScript® enzyme and incubated for 10 minutes at 25°C followed by incubation at 42°C for 2 hours and 85°C for a further 5 minutes. Following synthesis of cDNA, the samples were diluted with the same amount of water to give RNA concentrations not exceeding 10ng/µl. cDNA samples. Quantitative or real time PCR was performed using 5µl of SYBR-Green master mix (Life Technologies Cat.No.4368708), 2.5µl of upH_2O and 1µl of reverse primer and 1µl of forward primer for the gene of interest (primers used are summarised in table 5 and were either designed by myself or members of the Bone and Joint research group using primer blast and Thermo Scientific multiple primer analyser followed by primer efficiency testing, melt curve analysis and post-PCR testing) and 0.5µl of cDNA sample. The final mixture of 10µl was then added to a 96 well-plate and subsequently analysed with Applied Biosystems, 7500 Real Time PCR system and data produced was analysed with Applied Biosystems 7500 System SDS software, version 2.0.5 program. β-actin, an endogenous housekeeping gene was used to normalise Ct (cross-over threshold) values for each sample in experiments involving human bone marrow derive skeletal stem cells or human fetal femur derived cells and GAPDH was used as an endogenous housekeeping gene to normalise Ct (cross-over threshold) values in experiments which involved human articular chondrocytes. The delta-delta Ct method was used to calculate fold expression levels for each target gene. All reactions were performed in triplicate and included a negative control lacking cDNA.

Gene	Primer Sequences	Amplicon size
Human *ACTB*	F: 5'ggcatcctcaccctgaagta 3' R: 5'aggtgtggtgccagattttc 3'	82bp
Human *GAPDH*	F: 5' ccaggtggtctcctctgacttc 3' R: 5' tcataccaggaaatgagcttgaca 3'	108bp
Human *SOX9*	F: 5' cccttcaacctcccacacta 3' R: 5' tggtggtcggtgtagtcgta 3'	74bp
Human *COL2A1*	F: 5'cctggtccccctggtcttgg 3' R: 5' catcaaatcctccagccatc 3'	58bp
Human *ACGAN*	F: 5'gacggcttccaccagtgt 3' R: 5'gtctccatagcagccttcc 3'	90bp
Human *COL9A1*	F: 5' cctggtgctcttggtttga 3' R: 5' cacgctcccccttttctc 3'	58bp
Human *MMP13*	F: 5' ttaaggagcatggcgacttct 3' R: 5' cccaggaggaaaagcatgag 3'	71bp
Human *SMAD4*	F: 5'ccaggatcagtaggtggaatagc 3' R: 5'tctttgatgctctgtcttgggta 3'	146bp
Human *SOX5*	F: 5' tagctagtccttcagccagagtt 3' R: 5'ccttcatttgccgagcttctt 3'	93bp
Human *TGIF2*	F: 5' ccaacctgtcagtgctgcaa 3' R: 5' cggcgggaaatggtaaactg 3'	115bp

Table 5. Primer sequences for genes examined in different experiments and the amplicon size.

2.4.3 MicroRNA expression analysis

Following RNA extraction and dilution of samples with water to the same concentration of RNA across all samples, samples were analysed for microRNA expression analysis using TaqMan® MicroRNA Assays (Applied Biosystem, Life Technologies, listed below). Each individual assay contains two primers; one primer for cDNA synthesis and one primer for TaqMan q-PCR. The assays used in the experiments are listed in table 6.

MicroRNA	TaqMan MicroRNA Assay Name	Assay ID number
Mamm U6 – U6 spliceosome RNA	U6 snRNA	001973
miR-140-5p	mmu-miR-140-5p	001187
miR-140-3p	has-miR-140-3p	002234
miR-145-5p	has-miR-145-5p	002278
miR-146a-5p	has-miR-146a	00468
miR-146b-5p	has-miR-146b	001097
miR-34a-5p	has-miR-34a	000426

Table 6. TaqMan® MicroRNA Assays used for microRNA expression analysis from Applied Biosystems, Life Technologies.

TaqMan® MicroRNA Reverse Transcription Kit (Life Technologies Cat.No.4366597) was used to generate cDNA specific to each assay specific microRNA from total RNA following a modified manufacturer's protocol. In brief, a reaction mixture was made up of 3.58µl upH_2O, 0.75µ 10X Buffer, 0.094µl of RNase inhibitor, 1.5µl of reverse transcription (RT) primer, 0.075µl of dNTPs, 0.5µl MultiScribe™ Reverse Transcriptase (MSRT) and 10ng of total RNA and incubated for 30 minutes at 16°C followed by 42°C for 30minutes and 85°C for 5 minutes. For qPCR, 5µl of TaqMan® Universal PCR Master Mix with No AmpErase® UNG (Life Technologies Cat.No.4324018) was used in a reaction mix also containing 3.335µl of upH_2O, 0.5µl of TM primer and 0.8µl of cDNA. This mix was then transferred to a 96 well-plate and analysed with Applied Biosystems, 7500 Real Time PCR system and data produced was analysed with Applied Biosystems 7500 System SDS software, version 2.0.5 program. MammU6, an endogenous RNA housekeeping control (Mamm-U6) for microRNA was used to normalise Ct (cross-over threshold) values for each sample and the delta-delta Ct methods was used to calculate fold expression levels for each target gene. All reactions were performed in duplicate and also included a negative control which lacked cDNA.

2.5 Protein Techniques

2.5.1 Protein extraction from cultured cells

Following three washes with PBS (Lonza Cat.No.BE17-516F) cells were lysed with approximately 30µl RIPA buffer (made up of 0.079g Tris base (Sigma Aldrich Cat.No.T1503) and 0.9g NaCl (Sigma Aldrich Cat.No.S3014) in 7.5ml of distilled water adjusted to pH 7.5 with HCl and followed by addition of 1ml 10% IGEPAL® CA-630 (Sigma Aldrich Cat.No.18896), 500µl 10% Na-deoxy-cho1ate (Sigma Aldrich Cat.No.D6750), 100µl 100mM EDTA (Fischer Scientific Cat.No.10716481) and 100µl 10% SDS (Sigma Aldrich Cat.No.L4509) with added protease inhibitors (Roche Cat.No.11836153001). Cell lysates were then incubated on ice for 20 minutes followed by centrifugation at 13,000 rpm for 20 minutes at 4°C after which time the supernatant was collected for protein determination.

2.5.2 Protein determination

The protein concentration of samples was determined using Pierce BCA protein assay kit (Thermo scientific Cat.No.23227). Standard samples were made up using BSA supplied with the BCA protein assay kit and RIPA buffer as a dilutent to create a range of protein concentrations from 0-2000µg/ml and was used to determine protein concentration in experimental samples. For each sample or standard 8µl of reagent A was mixed with 2µl of reagent B from the Pierce BCA protein assay kit and 2µl of sample or standard was added and combined in an eppendorf and incubated for 30 minutes at 37°C. Following incubation samples were placed on ice while standard samples were first measured to create a standard curve using a Thermo Scientific NanoDrop ND-1000 spectrophotometer and accompanying software, followed by protein concentration determination. Following protein concentration determination, samples were adjusted to contain the same amount of protein in each sample by addition of appropriate volumes of RIPA buffer. In a 1:1 ratio – (sample:DTT and loading dye) samples were treated with 90% loading dye and 10% DTT reducing agent (New England Biolabs: Blue loading Buffer Pack Cat.No.B7703S) and incubated at 95°C for 5 minutes followed by incubation on ice.

2.5.3 Western blotting

2.5.3.1 Gel Electrophoresis - SDS-PAGE

Gels were prepared as follows using reagents from National Diagnostics for SDS gel electrophoresis: glass plates were clamped together and filled with 10% resolving gel which consisted of 1.65ml Protogel (National Diagnostics Cat.No.EC-890), 1.3ml 4 X Protogel resolving buffer (National Diagnostics Cat.No.EC-892), 1.95ml distilled water, 5µl TEMED (National Diagnostics Cat.No.EC-503) and 25µl of 10% APS (National Diagnostics Cat.No.EC-504). The resolving gel was pipetted into the space between the glass plates with a layer of isopropanol (Sigma Aldrich Cat.No.I9516) placed over the top and left to set for 30 minutes. Stacking gel was prepared as follows: 0.65ml of

Protogel (National Diagnostics Cat.No.EC-890), 1.25ml Protogel stacking buffer (National Diagnostics Cat.No EC-893), 3.05ml of distilled water, 5µl of TEMED (National Diagnostics Cat.No.EC-503) and 25µl 10% APS (National Diagnostics Cat.No.EC-504) were combined. The isopropanol was removed from the top of the resolving gel by inverting the apparatus holding the glass plates and the stacking buffer was pipetted on top of the resolving buffer. A comb was inserted into the top of the glass plates into the stacking gel and left to set for 20 minutes. Following setting of the stacking gel, combs were carefully removed and the glass plates containing the set gels loaded into an electrophoresis tank. The tanks were filled with 1 X running buffer which comprised of 100ml of 10 X running buffer with 900ml of water. 10 x running buffer was made up of 30.39g of Tris (Sigma Aldrich Cat.No.T1503), 144g glycine (Sigma Aldrich Cat.NoG7126) and 10g SDS (Sigma Aldrich Cat.No.L4509) in 1L of distilled water. Gel wells were filled with the same amount of protein for each sample which had previously been combined and heated with DDT reducing agent and sample loading buffer. Gel electrophoresis was run initially at 70V for samples to move through the stacking gel and reach the resolving gel and then at 150V until samples had reached the bottom of the resolving gel.

2.5.3.2 Transfer

While the SDS-PAGE was running, sponges and filter paper were incubated at 4°C in transfer buffer. Polyvinylidene fluoride (PVDF) membrane was incubated in methanol for 5 minutes followed by incubation in transfer buffer at 4°C. Transfer buffer comprised of 80ml of 10 X running buffer and 200ml methanol and 720ml of distilled water. Following SDS-PAGE glass plates were opened and gel removed and the stacking gel cut off from the top of the gel. In a tray containing transfer buffer a cassette was set-up to contain in order: a wet sponge previously incubated in transfer buffer, followed by soaked filter paper, the gel, PVDF membrane, another soaked filter paper followed by another wet sponge. The cassette was closed and placed into a tank containing an ice pack and filled with transfer buffer. Transfer was run at 100V for 1hour and 30 minutes at 4°C.

2.5.3.3 Antibody staining

Following completion of transfer of protein samples from the gel onto polyvinylidene fluoride (PVDF) membrane, PVDF membrane was removed from the cassette and incubated in blocking buffer containing 1 x PBS, 0.5% tween-20 (Sigma Aldrich Cat.No. 20274348) with 5% non-fat dry milk for one hour at room temperature followed by incubation with either rabbit polyclonal anti-SMAD4 antibody (Abcam Cat.No.ab182637) (1:375) or rabbit polyclonal anti-SOX5 antibody (Abcam Cat.No.ab157003) (1:750) or rabbit polyclonal anti-TGF beta induced factor 2 antibody (Abcam Cat.No.ab190152) overnight at 4°C. Immunoblots were then washed five times for 5 minutes in 1 x PBS, 0.5% tween-20 (Sigma Aldrich Cat.No.20274348) followed by incubation with Horseradish peroxidase (HRP) conjugated goat anti-rabbit IgG secondary antibody (Abcam Cat.No.ab6721) (1:3000) for one hour at room temperature followed by five, 5 minute washes in 1 x PBS, 0.5%

tween-20 (Sigma Aldrich Cat.No.20274348). The immunoblot was then incubated in enhanced chemiluminescence (ECL) substrate (Millipore Cat.No.WBKL0100) for 5 minutes followed by chemiluminescent detection with BioRad® Versadoc™ imaging system and analysed with BioRad® Quantity One® imaging software. Following visualisation of the desired protein on the immunoblots, the PVDF membrane was washed and incubated in rabbit polyclonal anti-β-actin antibody (Abcam Cat.No.ab75186) (1:500) for 1 hour at room temperature. Immunoblots were then washed five times for 5 minutes in 1 x PBS, 0.5% tween-20 (Sigma Aldrich Cat.No.20274348) followed by incubation with Horseradish peroxidase (HRP) conjugated goat anti-rabbit IgG secondary antibody (Abcam Cat.No.ab6721) (1:3000) for one hour at room temperature followed by five, 5 minute washes in 1 x PBS, 0.5% tween-20 (Sigma Aldrich Cat.No.20274348). The immunoblot was then incubated in enhanced chemiluminescence (ECL) substrate (Millipore Cat.No.WBKL0100) for 5 minutes followed by chemiluminescent detection with BioRad® Versadoc™ imaging system and analysed with BioRad® Quantity One® imaging software.

2.6 MicroRNA inhibition and overexpression

2.6.1 Identifying potential microRNA targets

Computational algorithm programmes including the webserver TargetScanHuman release 6.2, Diana webserverv5.0 interface, PicTar, PITA – Segal lab of computational biology and microRNA.org (August 2010 release) were all used to predict biological mRNA targets of miR-34a in human fetal femur-derived cells and biological mRNA targets of miR-146b in human bone marrow derived skeletal stem cells.

2.6.2 Transfection optimisation

2.6.2.1 DharmaFECT®1 concentration optimisation

Cells were cultured in 6 welled plates in α-MEM containing 10% FCS (Life Technologies Cat.No.10270106) and 1% P/S (Sigma Aldrich Cat.No.P4333) until sub-confluency at which stage cells were washed 3 times with PBS. Cells were then transfected with the 4 different concentrations of DharmaFECT®1; 0.25%, 0.5%, 0.75% or 1% of the total media volume (GE Healthcare Dharmacon Cat.No.T-2001) and also a no DharmaFECT®1 control and also 4 differing concentrations of either microRNA inhibitor or microRNA mimic. After 24 hours of transfection, AlamarBlue reagent (Life technologies Cat.No.DAL1025) was added at 10% of the media volume to each well and incubated for 4 hours, after which time the media was pipetted off the wells of a 24 welled plate and re-plated to an opaque 96-well plate for fluorescent spectrophotometric analysis at wavelength 530-560nm and emission wavelength of 590nm. Cells transfected with differing percentages of DharmaFECT®1 were visualised by light field microscopy and photographs taken with a Canon G10 digital Camera (Canon Europe Ltd., Uxbridge, UK).

2.6.2.2 MicroRNA mimic and microRNA inhibitor concentration optimisation

Cells were cultured in 6 welled plates in α-MEM containing 10% FCS (Life Technologies Cat.No.10270106) and 1% P/S (Sigma Aldrich Cat.No.P4333) until sub-confluency at which stage cells were washed 3 times with PBS. Cells were then transfected with DharmaFECT®1 (GE Healthcare Dharmacon Cat.No.T-2001) in combination with either microRNA mimic positive control, microRNA hairpin inhibitor positive control, non-targeting negative control microRNA hairpin inhibitor or non-targeting negative control microRNA mimic (GE healthcare, Dharmacon) in α-MEM containing 10% FCS (Life Technologies Cat.No.10270106) and no P/S. MicroRNA mimic positive control targeting *GAPDH* mRNA was used at 4 different concentrations in combination with 4 different concentrations of DharmaFECT®1 and a microRNA hairpin inhibitor positive control targeted to inhibit miR-16 was used at 4 different concentrations in combination with 4 different concentrations of DharmaFECT®1. The volume of DharmaFECT®1 was used at 0.25%, 0.5%, 0.75% and 1.0% of the total media volume in combination with microRNA mimic or microRNA hairpin inhibitor at either: 25nM, 50nM, 75nM and 100nM final concentration in total media. Following culture of cells in differing concentrations of final microRNA mimic or microRNA hairpin inhibitor and differing concentrations of DharmaFECT®1, media was removed and cells washed with PBS. RNA and microRNA was extracted using extracted using mirVana™ RNA Isolation System Kit (Life Technologies Cat.No.AM1561) in accordance with the manufacturer's protocol followed by either cDNA synthesis using SuperScript® VILO cDNA Synthesis kit (Life Technologies Cat.No.11754250) or TaqMan® MicroRNA Reverse Transcription Kit (Life Technologies Cat.No.4366597) and TaqMan® MicroRNA assay miR-16 (Applied Biosystems, Life Technologies assay ID#00391) and Mamm U6 (Applied Biosystems, Life Technologies assay ID#001973).The expression of *GADPH* mRNA was analysed in cells which had been transfected with microRNA mimic positive control targeting *GAPDH* mRNA and in cells which had been transfected with microRNA mimic negative, non-targeting control (a non-targeting mimic negative control based on the C.elegans cel-miR-67 mature sequence UCACAACCUCCUAGAAAGAGUAGA). The expression of miR-16 was analysed in cells which had been transfected with microRNA hairpin inhibitor positive control inhibiting miR-16 and in cells transfected with microRNA hairpin inhibitor negative, non-targeting control. Table 7 lists the positive and negative microRNA mimic and inhibitor controls used in the transfection optimisation experiments.

MicroRNA mimic positive control or inhibitor positive control used	MicroRNA control non-targeting mimic or non-targeting inhibitor used	Effect of microRNA mimic of inhibitor positive controls tested by
miRIDIAN microRNA mimic positive control #2 (GAPDH) (Cat.No.CP-001000-02) targets the endogenous housekeeping gene *GAPDH*	miRIDIAN MicroRNA mimic negative control #1 (cat.no. CN-001000-01)	*GAPDH* mRNA expression
microRNA hairpin inhibitor positive control (Cat.No.IP-004000-01) inhibits miR-16	miRIDIAN MicroRNA hairpin inhibitor negative control #1 (cat.no. IN-001005-01)	miR-16 expression

Table 7. Optimisation of microRNA mimic and microRNA inhibitor concentration using defined synthetic microRNA mimic positive and microRNA inhibitor positive controls from Dharmacon, GE healthcare.

2.6.2.3 Transfection optimisation using microRNA mimic control with Dy547 and microRNA hairpin inhibitor control with Dy547

Cells were cultured in 6 welled plates in α-MEM containing 10% FCS (Life Technologies Cat.No.10270106) and 1% P/S (Sigma Aldrich Cat.No.P4333) until sub-confluency at which stage cells were washed 3 times with PBS. Cells were then transfected for 48 hours with either microRNA mimic control with Dy547 (GE Healthcare, Dharmacon Cat.No.CP-004500-01) or microRNA hairpin inhibitor control with Dy547 (GE Healthcare, Dharmacon Cat.No.IP-004500-01). Cells were then washed with PBS and imaged with a Carl Zeiss AxioVert 200 microscope with AxioCam HR and AxioCam MR3 digital cameras using AxioVision version 4.7 software (Carl Zeiss Ltd, Cambridge, UK).

2.6.3 MicroRNA Transfection Assay in human fetal femur-derived cells and human bone marrow derived skeletal stem cells

The functional relevance of specific mature microRNAs was investigated in human fetal femur-derived cells and human bone marrow derived skeletal stem cells. To investigate the effect of specific microRNA upon target gene and protein expression cells were cultured in 6 welled plates in α-MEM containing 10% FCS (Life Technologies Cat.No.10270106) and 1% P/S (Sigma Aldrich Cat.No.P4333) until sub-confluency at which stage they were washed 3 times with PBS. Cells were then transfected with 0.5% DharmaFECT®1 (GE Healthcare Dharmacon Cat.No.T-2001) in combination with either microRNA mimic, microRNA hairpin inhibitor, non-targeting negative control microRNA hairpin inhibitor or non-targeting negative control microRNA mimic (GE

healthcare, Dharmacon) at final concentrations of 100nM in α-MEM containing 10% FCS (Life Technologies Cat.No.10270106) and no P/S. Table lists 8 the microRNA mimics and microRNA inhibitors used in the experiments. For RNA extraction cells were cultured in transfection media for 48 hours only and for protein extraction cells were cultured in transfection media for 72 hours. All microRNA mimic and hairpin inhibitors were purchased from Dharmacon, GE Healthcare. For molecular and protein analysis the expression of specific mRNA and protein was examined in cells cultured with either the transfected microRNA mimic or inhibitor with respect to the expression of specific mRNA and protein in cells transfected with the respective relevant negative control mimic or negative control hairpin inhibitor.

Desired Effect	MicroRNA mimic or inhibitor used	Control non-targeting mimic or inhibitor used
Fetal femur cell transfection assay		
miR-34a overexpression	meridian hsa-miR-34a-5p mimic ID - MIMAT0000255 (cat.no. C-300551-07)	miRIDIAN MicroRNA mimic negative control #1 (cat.no. CN-001000-01)
miR-34a inhibition	miRIDIAN hsa-miR-34a-5p inhibitor ID - MIMAT0000255 (cat.no. IH-300551-08)	miRIDIAN MicroRNA Hairpin inhibitor negative control #1 (cat.no. IN-001005-01)
Bone marrow derived skeletal stem cells transfection assay		
miR-146b overexpression	miRIDIAN hsa-miR-146b-5p mimic ID – MIMAT0002809 (cat.no. C-300754-03)	miRIDIAN MicroRNA mimic negative control #1 (cat.no. CN-001000-01)
miR-146b inhibition	miRIDIAN hsa-miR-146b-5p inhibitor ID - MIMAT0002809 (cat.no. IH-300754-05)	miRIDIAN MicroRNA hairpin inhibitor negative control #1 (cat.no. IN-001005-01)

Table 8. Overexpression and inhibition of microRNA expression through use of synthetic microRNA reagents from Dharmacon, GE healthcare.

2.7 *SOX5* 3'UTR and miR-146b plasmid construction for luciferase reporter assay

2.7.1 Polymerase chain reaction

Human DNA was amplified using the conventional polymerase chain reaction. 50ng of human DNA was used for the reaction with a total reaction volume of 20µl using the GoTaq® Hot Start Polymerase kit (Promega Cat.No.M5005) with the following components; 100µM of forward and reverse primers found in table 9 (sigma), 4µl buffer, 0.5µl DMSO, 0.4µl Taq polymerase, 2µl $MgCl_2$ and the appropriate volume of DNA to make 50ng and water to adjust to the final volume of 20µl for

the total reaction. Cycling conditions were as follows; initial activation time of 2 minutes at 95°C, denaturation time of 30 seconds at 95°C, annealing temperatures of 65°C for amplification of SOX5-3'UTR sequence and 66°C for the amplification of miR-146b sequence for 30 seconds, extension time of seconds at 72°C with 35 cycles and a final extension time of 5 minutes at 72°C followed by 4°C to complete the reaction. Following PCR completion the reaction was tested for yield quality and the presence of primer dimerization with agarose gel electrophoresis and UV imaging. Primers and sequences were annotated using the programme SnapGeneViewer.

Primer	Enzyme attached	Sequence	Product size
For examining miR-146b-SOX5 mRNA 3'UTR interaction			
SOX5 3'UTR forward	XbaI	TCTAGA GCACACCACACTACATCTTTGAGC	380bp
SOX5 3'UTR reverse	NotI	GCGGCCGC ACCAGTCACTTGGGAGGATGTGGG	
miR-146b forward	XbaI	TCTAGA ACCCATCCTGGGCCTCAACT	263bp
miR-146b reverse	HindIII	AAGCTT GCCAGTGGGCAAGATGTGGG	

Table 9. Primers used for amplifying target sequences required for cloning

2.7.2 TOPO cloning

Following PCR, the amplified product was subject to TOPO sub-cloning using a TOPO® TA cloning kit (Invitrogen™ Cat.No.450641). 0.5µl of linearized and topoisomerase I-activated pCR®2.1-TOPO® Vector was combined with 0.5µl salt solution (1.2M NaCl and 0.06M $MgCl_2$) and 1.5µl of the original PCR product and incubated at room temperature for 30 minutes. Competent bacteria – 5-aplha *E.coli* cells (New England Biolabs Cat.No.C2987H) were thawed on ice for 15 minutes after which time the 2.5µl of TOPO vector mix was added to the 50µl vial of competent *E.coli* cells and gently mixed by pipetting followed by incubation on ice for 30 minutes. The vial containing the *E.coli* cells was then heat shocked at 42°C for 30 seconds and then incubated on ice for a further 2 minutes followed by mixing with 250µl of SOC medium and incubating at 37°C for 1 hour at 9,000rpm. The cells were then plated on agar containing ampicillin overnight. Following overnight incubation colonies were picked with pipette tips and left to incubate overnight in 4ml of liquid broth containing ampicillin. On the final day the liquid broth containing transformed bacteria was spun down to form a bacterial pellet which was then subject to plasmid DNA isolation using a QIAprep Spin Mini plasmid preparation kit (Qiagen Cat.No.27104). Following plasmid isolation 5µl of sample was subject to digestion with 0.5µl restriction enzyme EcoRI in a total volume of 20µl also containing 2µl CutSmart buffer (New England Biolabs Cat.No.B72045) and 12.5µl water, incubated for 1 hour at 37°C, followed by agarose gel electrophoresis and UV imaging to identify the presence of the original insert

into the plasmid. On identification of insert positive samples, the DNA plasmids using M13 primer were sequenced using SUPREMERUN^{TM} sequencing (GATC Biotech) to analyse non-mutated insert sequences. DNA sequences were visualised using Chromas Lite 2.1.1 and CLC Sequence Viewer version 6.8.1.

2.7.3 pRL-TK cloning and pcDNA3.1(-) cloning

Following DNA sequencing and successful sub-cloning of the SOX5 3'UTR sequence or miR-146b sequence, SOX5-3'UTR sequence were subject to pRL-TK cloning and miR-146b sequence was subject to pcDNA3.1(-) cloning. The process involved the isolation of the DNA sequences from the pCR®2.1-TOPO®-SOX-3'UTR plasmids or pCR®2.1-TOPO®-miR-146b plasmids and ligation of the sequence into an empty pRL-TK plasmid or empty pcDNA3.1(-) plasmid and transformation of competent *E.cloi* cells. 25µl pCR®2.1-TOPO® plasmid containing the SOX5-3'UTR sequence (pCR®2.1-TOPO®-SOX-3'UTR) and 25µl of an empty pRL-TK plasmid were independently combined with 2 µl NotI restriction enzyme (NEB Cat.No.R0189S), 2µl XbaI restriction enzyme (NEB Cat.No.R0145S), 4µl NEBuffer 3.1 (NEB Cat.No.B7230S) and 7µl water and incubated for 3 hours at 37°C followed by agarose gel electrophoresis which separated the TOPO linearised plasmid from the SOX5-3'UTR insert sequence. 25µl pCR®2.1-TOPO® plasmid containing the miR-146b sequence (pCR®2.1-TOPO-miR-146b) and 25µl of an empty pRL-TK plasmid were independently combined with 2 µl HindIII restriction enzyme (NEB Cat.No.R0189S), 2µl XbaI restriction enzyme (NEB Cat.No.R0145S), 4µl NEBuffer 3.1 (NEB Cat.No.B7230S) and 7µl water and incubated for 3 hours at 37°C followed by agarose gel electrophoresis which separated the TOPO linearised plasmid from the miR-146b insert sequence. The gel was imaged under UV light and the SOX5-3'UTR sequence band, empty pRLTK plasmid band, miR-146b sequence band and pcDNA3.1(-) plasmid band were cut from the gel and DNA extracted from the differing gel sections using QIAquick gel extraction kit (Qiagen Cat.No.28704). Samples were then quantified using a NanoDrop and a centrifugal evaporator was used to concentrate samples. The original insert sequence and target plasmid: SOX5-3'UTR sequence and pRLTK, and miR-146b and pcDNA3.1(-) were then ligated using 2µl ligation buffer, 2µl T4 DNA ligase and 3 times the amount of insert to target plasmid, made to a final volume of 20µl with water and incubated at 16°C overnight. Following overnight ligation the ligated plasmids were then transformed into bacteria by adding 5µl of the ligated plasmid to competent 5-aplha *E.coli* cells (NEB Cat.No.C2987H). *E.coli* cells were first thawed on ice for 15 minutes after which time the 5µ of pRL-TK-SOX5-3'UTR plasmid or pcDNA3.1(-)-miR-146b was added to the 50µl vial of competent *E.coli* cells and gently mixed by pipetting followed by incubation on ice for 30 minutes. The vial containing the *E.coli* cells was then heat shocked at 42°C for 30 seconds and then incubated on ice for a further 2 minutes followed by mixing with 250µl of SOC medium and incubating at 37°C for 1 hour at 9,000rpm. The cells were then plated on agar containing ampicillin overnight. Following overnight incubation, bacterial colonies were picked with pipette tips and left to incubate overnight in 4ml of liquid broth containing ampicillin. On the final day the liquid

broth containing transformed bacteria was spun down to form a bacterial pellet which was then subject to plasmid DNA isolation from the bacteria using QIAprep Spin Mini plasmid preparation kit (Qiagen Cat.No.27104). The pRLTK-SOX5-3'UTR plasmids using a pre-designed primer (5' GAAGATGCACCTGATGAAATGGG) and pcDNA3.1(-)-miR-146b plasmids using T7 primer were sequenced using SUPREMERUN^{TM} (GATC Biotech) to analyse insert sequences for mutations. DNA sequences were visualised using Chromas Lite 2.1.1 and CLC Sequence Viewer version 6.8.1. All samples containing the correct insert sequence were then subject to large scale colony growth and plasmid DNA isolated using QIAGEN plasmid Maxi kit (Qiagen Cat.No.12163).

2.7.4 Site directed Mutagenesis

Substitution mutations at the miR-146b binding site in the seed region of SOX5-3'UTR sequence in pRL-TK-SOX5-3'UTR plasmids were generated by conversion of bases to create XhoI restriction enzyme recognition sites using QuickChange II Site-Directed Mutagenesis Kit (Agilent Technologies Cat.No.200523). Primers for mutagenesis were designed using PrimerX programme (www.bioinformatice.org/primerx/) (Table 10). Primers were designed to substitute GTTC for CGAG in the seed sequence of *SOX5* 3'UTR

Primer	Sequence
For examining miR-146b-SOX5 mRNA 3'UTR interaction	
SOX5 3'UTR seed region mutagenesis forward	5' GGAAACTGTAGGTGCTcgagTCAGGTGAAAAGAGAG 3'
SOX5 3'UTR seed region mutagenesis reverse	5' CTCTCTTTTCACCTGActcgAGCACCTACAGTTTCC 3'

Table 10. Primers designed used in site directed mutagenesis of miR-146b binding site in SOX5-3'UTR sequence in pRL-TK-SOX5-3'UTR plasmids. Lowercase letters indicate mutated bases.

Site directed mutagenesis was carried out using QuickChange II Site-Directed Mutagenesis Kit (Agilent Technologies Cat.No.200523) to create vector constructs containing mutated microRNA target sequences. In brief 25ng of plasmid construct containing the appropriate specific microRNA target sequence – pRL-TK-SOX5-3'UTR was combined with 5µl Reaction buffer, 125ng mutagenesis forward primer, 125ng mutagenesis reverse primer, 1µl dNTPs, 1µl pfuTurbo DNA polymerase and made up to 50µl with upH_2O. pRL-TK-SOX5-3'UTR plasmid mutagenesis reaction mixture were incubated in a thermocycler initially at 98°C for 10 seconds followed 12 cycles of 95°C for 30 seconds, 76°C for 1 minute and 68°C for 4.5 minutes, following cycling the sample was cooled to 37°C. 1µl DpnI was then added to the amplified reaction followed by incubation at 37°C for 1 hour. 1µl of DpnI treated sample was then transformed into 5-aplha *E.coli* cells (NEB Cat.No.C2987H) as described previously and cells were then plated on agar containing ampicillin overnight. Following

overnight incubation bacterial colonies were picked with pipette tips and left to incubate overnight in 4ml of liquid broth containing ampicillin. On the final day the liquid broth containing transformed bacteria was spun down to form a bacterial pellet which was then subject to plasmid DNA isolation from the bacteria using QIAprep Spin Mini plasmid preparation kit (Qiagen Cat.No.27104). Following plasmid isolation 5µl of sample was subject to digestion with 0.5µl XhoI restriction enzyme, 2µl CutSmart buffer (NEB Cat.No.B72045) made up with upH_2O to a total volume of 20µl and incubated for 1 hour at 37°C. Following by agarose gel electrophoresis and UV imaging, samples were sequenced using SUPREMERUN^{TM} (GATC Biotech) to analyse insert sequences for mutations. DNA sequences were visualised using Chromas Lite 2.1.1 and CLC Sequence Viewer version 6.8.1.

2.8 Statistical Methods and graphical representation of data

2.8.1 Statistical analysis of gene expression data

Relative quantification for qPCR was used in all experiments involving mRNA expression investigation and microRNA expression investigation, changes in mRNA or microRNA expression were analysed in a given sample relative to the expression of mRNA or microRNA in another reference sample which was either the untreated control sample or Day 0 time point. The comparative Ct method was employed for relative quantification. The comparative or ΔΔCt method of qPCR data analysis involved obtaining two or more different experimental RNA samples (control/untreated and treated RNA sample/s) which were directly normalised to a housekeeping gene prior to comparison. The ΔΔCt value determined was calculated by identifying the difference in ΔCt values between the control sample and experimental/treated samples. The fold-change in expression of the mRNA was then calculated using 2^(-ΔΔCt). All mRNA expression graphs produced from qPCR data show data as relative expression level in the experimental/treated sample as a fold change in expression compared to the control sample which was set to 1.

Statistical analysis was then performed on the fold change in mRNA or microRNA relative expression, with all data presented in graphical form as values from biological repeats, the median value and interquartile range of fold change. Statistical analysis was performed on the fold change relative expression data and not raw Ct values because the Ct is determined through a log-linear plot of the PCR fluorescence signal against cycle number, Ct values are therefore exponentials as previously described by Livak and Schmittgen [303]. The p-value was set to 0.05 and following statistical analysis, experimental samples which were identified to display significant difference in relative expression fold change relative to the control sample, $p \leq 0.05$ was considered statistically significant as indicated by the presence of an asterisk displayed on graphs (*). The appropriate statistical test was chosen depending on the type of samples and the numbers of conditions that were tested. The GraphPad Prism software, version 6.0 was used to input all data and carry out all statistical tests. All statistical tests used to analyse relative expression fold change data were non-parametric tests.

Non-parametric tests were selected because primary cells were used in all studies. There is high variability amongst primary cells from differing patient samples which may impact upon the mRNA and microRNA relative expression in the control and experimental samples and therefore a non-parametric test is suitable as it does not make assumptions with regard to normal distribution. Use of non-parametric tests follow that the data may not be normally distributed, the median therefore would be a better measure of central tendency. Additionally the interquartile range is a more appropriate measure of spread of data, a measure which indicates the extent to which the central 50% of values within the dataset are dispersed. The interquartile range is unaffected by extreme ranges which exists within non-normally distributed datasets. A small number of biological repeats were carried out for different experiments, small sample sizes do not allow for an observation of the distribution of the data and therefore the most appropriate statistical tests are non-parametric.

For analysing mRNA and microRNA significance in relative expression, fold change between two unpaired groups the non-parametric Mann Whitney test was employed. The Mann Whitney test was employed to investigate difference in relative expression fold change in different patient samples of osteoarthritic articular chondrocytes compared control non-osteoarthritic chondrocytes from different patient samples. For analysing mRNA and microRNA significance in relative expression fold change between two paired groups the non-parametric Wilcoxon signed rank test was employed. The Wilcoxon signed rank test was employed to investigate difference in mRNA and microRNA relative expression fold change in human fetal femur-derived cells from 4 individual patient samples treated with TGF-β3 compared to control non-TGF-β3 treated cells. The Wilcoxon signed rank test was also employed to investigate difference in mRNA and microRNA relative expression fold change in human bone marrow derived skeletal stem cells from 6 individual patient samples treated with TGF-β3 compared to control non-TGF-β3 treated cells. The Wilcoxon signed rank test was also employed to investigate difference in mRNA and microRNA relative expression fold change in fetal femur cells from 4 individual patient samples treated with miR-34a mimic or miR-34a inhibitor compared to control non-targeting mimic or control non targeting hairpin inhibitor treated samples. The Wilcoxon signed rank test was also employed to investigate difference in mRNA and microRNA relative expression fold change in human bone marrow derived skeletal stem cells from 6 individual patient samples treated with miR-146b mimic or miR-146b hairpin inhibitor compared to control non-targeting mimic or control non-targeting hairpin inhibitor treated samples.

For analysing mRNA and microRNA relative expression fold change amongst several test conditions the Friedman test with Dunn's multiple comparison post-test was employed. Friedman test with Dunn's multiple comparison post-test was used to investigate differences in mRNA and microRNA relative expression fold change in articular chondrocytes which had been subject to 4 different conditions; treatment with TGF-β3, treatment with IL-1β, treatment with a combination of TGF-β3 and IL-1β and a non-treatment control. Friedman test with Dunn's multiple comparison post-test was used to investigate differences in mRNA and microRNA relative expression fold change in fetal

femur-derived cells which had been subject chondrogenic differentiation for 4 differential time points; treatment with TGF-β3 for 7 days, treatment with TGF-β3 for 14 days, treatment with TGF-β3 for 21 days and a non-treatment day 0 control.

2.8.2 Statistical analysis of protein expression data

Changes in protein expression were analysed by comparing the protein expression in the experimental sample relative to the expression of protein in the untreated control sample. Immunoblots were examined using BioRad® Quantity One® imaging software to extrapolate the densitometry data corresponding to protein expression observed upon immunoblots. Densitometry values were measured for both the protein of interest and β-actin for each sample tested, both experimental samples and control samples. β-actin was chosen as a loading control to normalise the protein of interest in all samples. Following normalisation, values were subject to fold change calculation compared to the control sample by dividing the normalised experimental sample value by the normalised control sample value. All protein expression graphs show data as protein expression level in the experimental or treated sample as a fold change in expression compared to the control sample which was set to 1. The fold-change of protein expression was used for statistical analysis. The p-value was set to 0.05 and following statistical analysis, experimental samples which were identified to display significant difference in protein expression fold change relative to the control sample, $p \leq 0.05$ was considered statistically significant as indicated by the presence of an asterisk displayed upon graphs (*).The GraphPad Prism software, version 6.0 was used to input all data and carry out all statistical tests. The nonparametric Wilcoxon signed rank test was used to identify significant differences in specific protein expression between control cells treated with a non-targeting mimic or non-targeting hairpin inhibitor and cells treated with either specific microRNA mimic or microRNA hairpin inhibitor. Data is presented as individual biological repeats with the median value and interquartile range.

Chapter 3
Results: Expression of microRNA 146b in human osteoarthritic articular chondrocytes & in cytokine and growth factor treated chondrocytes

3.1 Introduction

The loss of chondrocytes and the diminishment of the accompanying specialised extracellular matrix in the joints as a result of articular cartilage injury can result in an osteoarthritic phenotype. The aetiology of OA still remains unknown, however, it is clear that various components are involved inclusive of environmental factors and genetic predisposition [304]. Endogenous regeneration is limited and therefore articular cartilage is not sufficiently replaced; there are complex signalling networks involved in chondrocyte differentiation, chondrocyte apoptosis and extracellular matrix maintenance. Gene expression dysregulation in any of these molecular systems is likely to be attributable to disease pathogenesis.

Cui *et al* conducted microarray studies in an attempt to create an in-depth gene expression analysis of OA pathogenesis [305] identifying 52 up-regulated genes and 89 down-regulated genes between OA and control samples, concluding that many of the dysregulated genes related to extracellular matrix interaction, and cell death are likely to function via multiple signalling pathways, playing critical roles in the manifestation of OA [305]. What has become apparent is that the regulatory mechanisms which govern the expression of normally expressed genes in chondrocytes, which under normal conditions tissue homeostasis ensues, become perturbed in OA. One subset of gene expression regulators; microRNAs, have been identified to play a role in chondrogenesis and cartilage homeostasis. Critically, microRNAs which govern gene expression in cartilage have also been shown to be differentially expressed in OA cartilage compared to normal cartilage [306].

Of particular interest, the sequence of the mature form of miR-146b, which is located on chromosome 10, only differs by two nucleotides from the sequence of mature miR-146a which is located on chromosome 5 [307], miR-146a and miR-146b have closely related sequences (Figure 20). MicroRNAs function to regulate cell processes by targeting related proteins. MicroRNAs with the same seed repertoire generally target the same genes and therefore possess similar cellular function [308]. The homology in the seed sequences of miR-146a and miR-146b mean that these related microRNAs target the same mRNAs and therefore may work co-operatively to enhance efficiency of target repression. If miR-146a and miR-146b work co-operatively they may not only target the same mRNA but also be induced by the same stimuli.

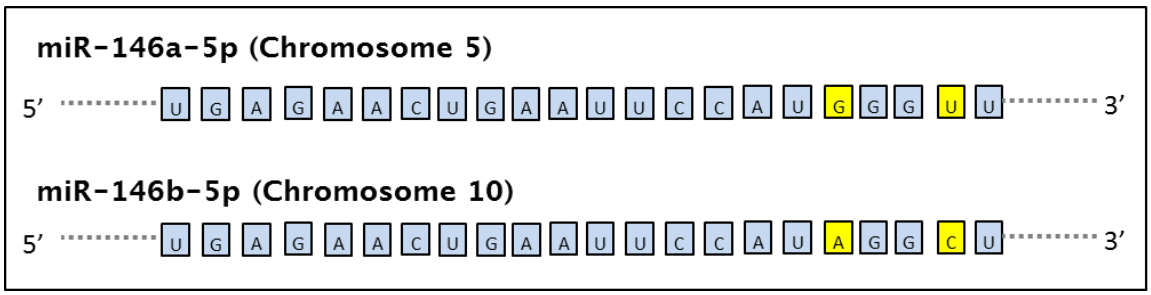

Figure 20. miR-146a-5p and miR-146b-5p mature sequences. Both sequences are the same with exception to the two nucleotides from each sequence highlighted in yellow.

MiR-146a has previously been identified as exhibiting an up-regulated expression in osteoarthritic cartilaginous tissue [228]. The expression of miR-146a was expressed at a greater level in OA cartilage compared to normal cartilage. Critically, the study identified that miR-146a was not expressed in normal chondrocytes but initiation of miR-146a expression occurred when chondrocytes were beginning to undergo degenerative changes. IL-1β, a prominent cytokine in OA pathogenesis, increased the expression of miR-146a in normal chondrocytes indicating that miR-146a expression is induced in OA pathogenesis [228]. MiR-146a was also found to be up-regulated in an OA rat model, targeting *Smad4* mRNA, [309] and miR-146a has also been shown to be up-regulated in human mechanically injured human chondrocytes [230]. Both miR-146a and miR-146b have been described as key molecules in inflammatory response which have been found to be up-regulated in human pathologies associated with inflammatory response activation [307], [310], [311], [312], [313], [314], [315], [316], [317], [318], [319], [320].

Taganov *et al* first described the up-regulated expression of miR-146a and miR-146b in a monocyte cell line following stimulation with lipopolysaccharide. Promoter analysis identified the pro-inflammatory associated NF-κB was required for miR-146a expression by lipopolysaccharide, IL-1β or TNFα stimulation. Taganov *et al* postulated that both miR-146a and miR-146b targeted downstream toll-like receptor and cytokine receptor signalling through targeting TRAF6 and IRAK1; indicating that the up-regulated expression of miR-146a and miR-146b may be to attenuate the inflammatory response by targeting components of the inflammatory cascade [307]. The up-regulation of miR-146a in OA cartilaginous tissue has been previously documented [228] and given the closely related sequence of miR-146a to miR-146b and the up-regulated expression of miR-146b in inflammatory response activation studies [307], [313], [318], [319], it can be hypothesized that miR-146b may also be up-regulated during osteoarthritis.

If miR-146b is up-regulated in OA chondrocytes, the underlying inducer of miR-146b expression may be the same as the inducer of miR-146a expression in OA chondrocytes. Previous studies listed in table 11 have observed the concurrent up-regulation in miR-146a and miR-146b expression following

treatment of cells with IL-1β. The pro-inflammatory cytokine, IL-1β, present in OA may induce miR-146b expression as well as miR-146a expression in OA chondrocytes.

Study	Reference
An increase in miR-146a and miR-146b expression was observed following treatment of THP-1 monocytic cells with IL-1β.	[307]
An increase in miR-146a and miR-146b expression was observed following treatment of human alveolar A549 lung epithelial cells with IL-1β.	[311]
An increase in miR-146a and miR-146b expression was observed following treatment of human umbilical vein endothelial cells with IL-1β.	[321]
The expression of miR-146a and miR-146b was increased upon monocyte differentiation into immature dendritic cells and mature dendritic cells. The differentiation medium contained IL-1β and the expression of miR-146a and miR-146b decreased when IL-1β was not added to the differentiation maturation cocktail medium. Restriction of other differentiation maturation cocktail factors to the medium did not affect miR-146a or miR-146b expression indicating IL-1β as the predominant factor which induced miR-146a and miR-146b expression.	[322]

Table 11. Studies which have all observed an increase in both miR-146a and miR-146b expression following treatment of cells with IL-1β.

IL-1β has been shown to be an important cytokine in the pathogenesis of OA, inducing inflammatory responses and a catabolic effect within the joint space [40]. IL-1β is released by sentinel cells including macrophages and monocytes and other cell types inclusive of endothelial, epithelial and fibroblast cells in response to damage or danger associated molecular (DAMPs) which are released from damaged cells [323]. IL-1β can be secreted systemically or in a paracrine manner and induce the expression of many genes inclusive of itself; which is regulated by a positive feedback system, resulting in amplification of the IL-1β response [323]. IL-1β binds to the type I IL-1 receptor (IL-1R1), which along with the co-receptor, IL-1 receptor accessory protein (IL-1RAcP), induces signal transduction which ultimately induces NF-κB and AP-1 dependent expression of pro-inflammatory cytokines and chemokines. Proteoglycan depletion and cytotoxicity is the result of elevated IL-1β levels in the synovial fluid and the joint tissues during osteoarthritis. Mononuclear cells, activated synoviocytes and cartilage tissue can all release IL-1β which in turn can activate other pro-inflammatory cytokines and matrix metalloproteases [324]. IL-1β is a major catabolic component in the pathophysiology of osteoarthritis, which also decreases the anabolic activity in OA joints. Transgenic mice bearing inducible IL-1β expression in the temporomandibular joints were found to exhibit pathological joint changes including fibrillations and cartilage remodelling, joint dysfunction and related pain, all classical features of osteoarthritis [50]. Intra articular injection of IL-1β in mice

was found to reduce proteoglycan synthesis and an enhanced breakdown of proteoglycan. Furthermore, repeated IL-1β administration resulted in highly inflamed joints [325].

Epiphyseal chondrocyte differentiation in an *in vitro* model has shown that use of exogenous TGF-β1 prevents epiphyseal chondrocytes from undergoing terminal differentiation into hypertrophic chondrocytes [78]. Overexpression of a dominant negative TGF-β type II receptor in the skeletal tissues of mice resulted in the joints with the resemblance of human OA [79]. Mutant Smad3 mice with chondrocytes which lacked responsiveness to the TGF-β signalling pathway resulted in terminal hypertrophic differentiation with an osteoarthritis phenotype. TGF-β signalling was believed to be responsible for the inhibition of terminal hypertrophic differentiation in chondrocytes and therefore responsible in maintaining articular cartilage integrity [27]. The two studies of aberrant TGF-β signalling in mice indicate the need of TGF-β to prevent hypertrophic chondrocyte terminal differentiation and in the prevention of OA development. In epidemiological studies a polymorphism in asporin, which exhibited increased inhibition of the TGF-β signalling pathway and suppression of cartilage ECM components compared to the common asporin, was found at a higher frequency in patients with OA [81], [82]. SMAD3 is a key intracellular molecule of the TGF-β signalling pathway and a single nucleotide polymorphism mapped to intron 1 of *SMAD3* has been found at high frequency in knee and hip OA in a European cohort [83]. Mutations in *SMAD3* have been identified in patients with aneurysm-osteoarthritis syndrome whereby osteoarthritis manifests early [84]. Osteoarthritis is also a clinical feature in some individuals of the connective tissue disorder, Loeys-Dietz syndrome which is caused by mutations in any of *TGFβR1, TGFβR2, TGFβ2* and *SMAD3* genes [85]. The studies indicate that supressed TGF-β signalling as a result of either direct TGF-β de-regulation or a component of TGF-β intracellular signalling is positively related to the development of OA. Despite the studies which all indicate that supressed TGF-β signalling relate to the development of OA, overexpression of TGF-β signalling has also been shown to have adverse effects and TGF-β aberrant overexpression may also be involved with the development of OA [326], [327], [328], [329].

Treatment of chondrocytes with TGF-β1 in combination with IL-1β has been shown to reduce protease activity and exhibit a reversal towards a more normal ECM, in contrast to chondrocytes treated with IL-1β alone which induced protease activity and failure of proteoglycan incorporation in the ECM [330]. TGF-β1 has also previously been shown to reduce the effects of IL-1β on matrix metabolism and to also down-regulate IL-1β receptor expression in chondrocytes [331]. A study which examined TGF-β modulation of IL-1β on proteoglycan synthesis and degradation found that intra-articular injections of TGF-β counteracted the inhibition of proteoglycan synthesis induced by IL-1β treatment [329]. Smith *et al* have shown that adenoviruses containing TGFβ-1 gene which were transduced into chondrocytes and then chondrocytes treated with IL-1β, resulted in chondrocytes with a maintained proteoglycan synthesis compared to chondrocytes transduced with an adenovirus containing a control *lac* Z gene. The overexpression of TGF-β1 gene in transduced chondrocytes prevented the degradative effects of IL-1β [332]. These studies all indicate that TGF-β can inhibit and

at least partially supress the catabolic effects of IL-1β in articular chondrocytes, postulating a potential role for the use of exogenous TGF-β or modulation of the TGF-β signalling pathway in OA treatment.

MiR-146a has previously been shown to be up-regulated in OA chondrocytes [228] and has also been shown to exhibit up-regulation in chondrocytes treated with IL-1β [229]. The sequence of mature miR-146b only differs by two nucleotides from the sequence of mature miR-146a with both microRNAs possessing the same seed sequences which bind to microRNA response elements within the 3'UTR of target mRNA (Figure 20). Therefore miR-146b may function in a similar manner to miR-146a and is likely to target the same genes. Given that miR-146a has been found to be up-regulated in OA cartilage it is possible that miR-146b may also be up-regulated in OA cartilage. If both miR-146a and miR-146b possess similar cellular function, it may also be possible that both microRNAs are up-regulated by the same stimuli. The expression miR-146a has been shown to be up-regulated by IL-1β signalling in chondrocytes and therefore it is possible that chondrocytes treated with IL-1β in culture may also exhibit miR-146b up-regulation. TGF-β has also been shown to counteract IL-1β effects upon cartilage destruction [330], [331], [329], [332], miR-146a and miR-146b expression may therefore be differentially regulated by these two proposed antagonistic mediators.

3.2 Hypothesis and Aims

3.2.1 Hypothesis

The expression of miR-146b in human osteoarthritic articular chondrocytes is dysregulated compared to the expression of miR-146b in control human chondrocytes, the pro-inflammatory, catabolic cytokine IL-1β can induce miR-146b expression in human chondrocytes and anabolic associated TGF-β3 can subdue the effects of IL-1β on miR-146b expression.

3.2.2 Aims and Objectives

1. To analyse the expression of genes associated with osteoarthritis in human OA articular chondrocytes isolated from the articular cartilage from OA patient donors compared to the gene expression in chondrocytes isolated from osteoporotic (OP)/fracture neck of femur (NoF) patients.

2. To analyse the expression of previously identified miR-146a, miR-140-3p and miR-140-5p in human OA articular chondrocytes isolated from the articular cartilage from OA patient donors compared to the microRNA expression in chondrocytes isolated from osteoporotic (OP)/fracture neck of femur (NoF) patients.

3. To analyse the expression of miR-146b in human OA articular chondrocytes isolated from the articular cartilage from OA patient donors compared to miR-146b expression in chondrocytes isolated from osteoporotic (OP)/fracture neck of femur (NoF) patients.

4. To analyse the expression of genes associated with osteoarthritis with IL-1β, TGF-β3 and IL-1β and TGF-β3 in combination across 21 days.

5. To analyse the expression of miR-146b, miR-146a, miR-140-3p and miR-140-5p in human chondrocytes treated with IL-1β, TGF-β3 and IL-1β and TGF-β3 in combination across 21 days.

6. To collate all studies which have previously observed the expression of miR-146a and/or miR-146b in inflammation.

3.3 Gene expression in human osteoarthritic articular chondrocytes

Chondrocytes isolated from the articular cartilage of femoral heads from osteoarthritic patients and the cartilage of femoral heads from patients as a consequence of breakage at the neck of femur (NOF) and deemed non-osteoarthritic by visual examination (control) were examined for the presence of genes which have previously exhibited dysregulation. Analysis of genes by qPCR showed that the expression of *MMP13* (Figure 21A) and *COL2A1* (Figure 21B) were significantly up-regulated in OA chondrocytes compared to control chondrocytes, with median fold changes of 390 and 30 respectively. The expression of *AGCAN* (Figure 21C) was significantly down-regulated in OA chondrocytes, with a median fold change of 0.45 and the expression of *COL9A1* (Figure 21D) showed up-regulation in OA chondrocytes, but with no significant differences in expression.

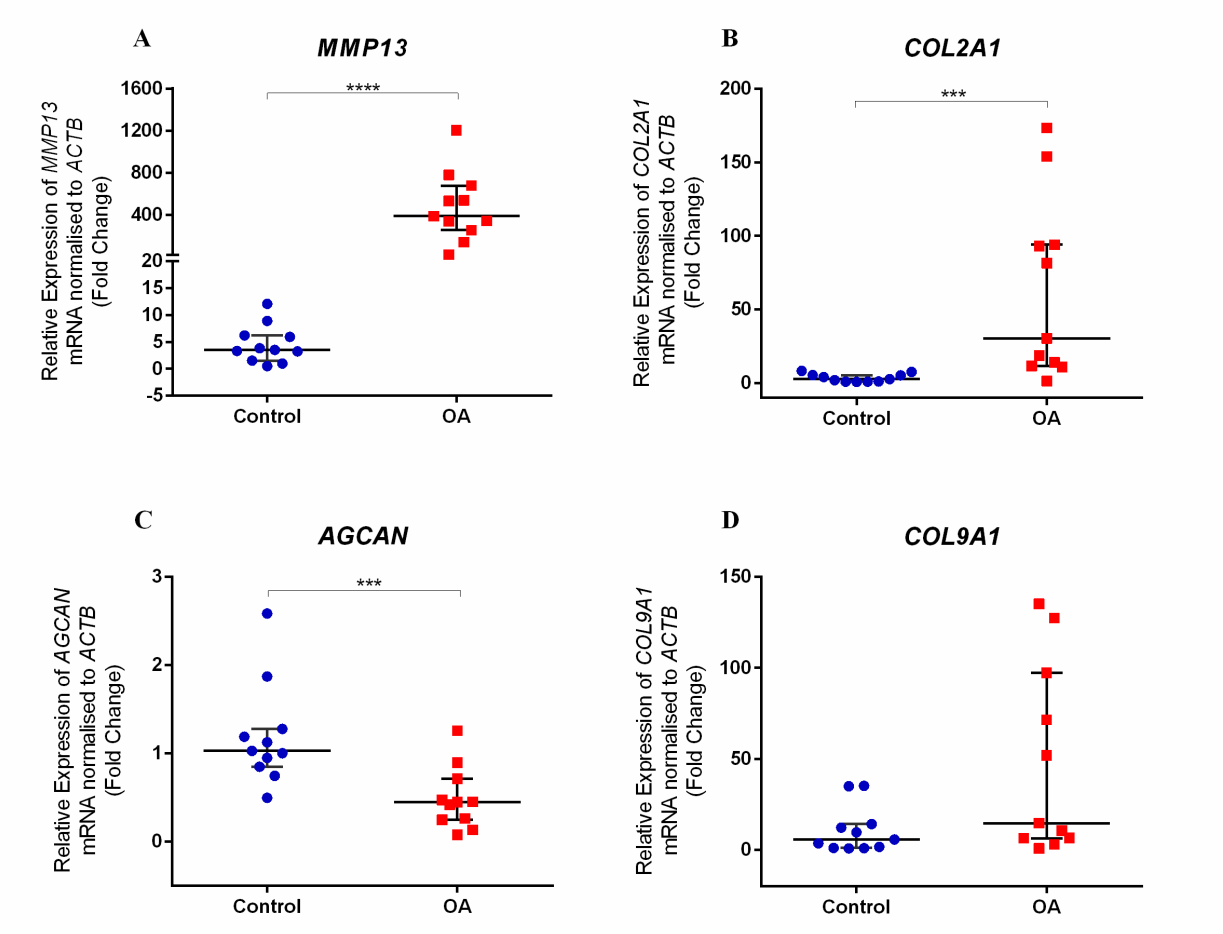

Figure 21. Differences in mRNA expression between OA articular chondrocytes and control chondrocytes. Data is presented as the median and interquartile range of the fold change in *MMP13* (A), *COL2A1* (B), *AGCAN* (C) and *COL9A1* (D) mRNA expression in OA articular chondrocytes relative to control chondrocytes from samples deemed non-OA. Values are presented as individual biological replicates n=11, *** p <0.001, **** p <0.0001, Mann Whitney test.

3.4 MicroRNA expression in human osteoarthritic articular chondrocytes

Chondrocytes isolated from the articular cartilage of femoral heads from osteoarthritic patients and the cartilage of femoral heads from patients donated due to breakage at the neck of femur (NOF) and deemed non-osteoarthritic by visual examination (control) were examined for the presence of microRNAs which have previously exhibited dysregulation. Analysis of microRNA expression by qPCR showed that the expression of miR-140-3p (Figure 22A) was significantly down-regulated in OA chondrocytes compared to the control chondrocytes, with a median fold change of 0.15. The expression of miR-140-5p (Figure 22B) showed no significant difference in expression. The expression of miR-146a (Figure 22C) was significantly up-regulated in OA chondrocytes, with a median fold change of 33. The expression of miR-146b (Figure 22D) was found to be significantly up-regulated with a median fold change of ~123 in OA chondrocytes compared to miR-146b expression in control chondrocytes.

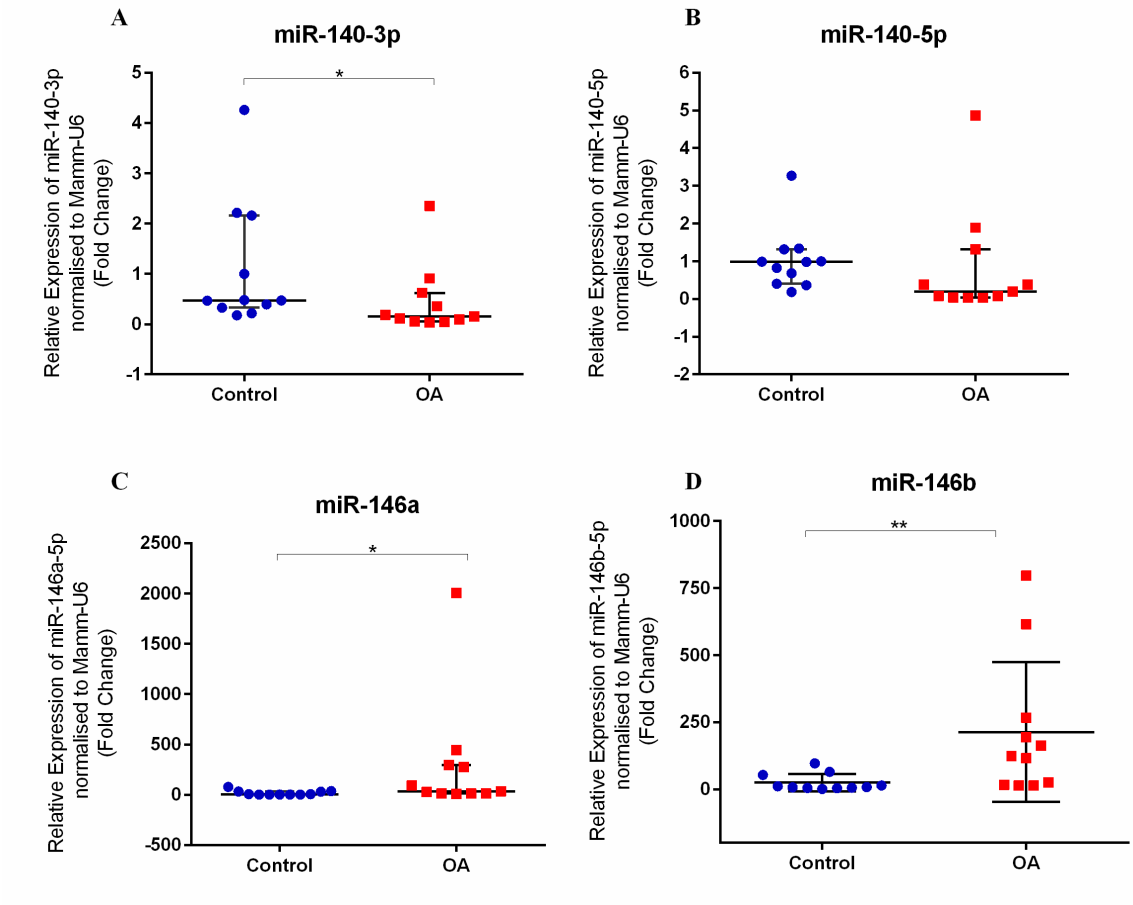

Figure 22. Differences in miRNA expression between OA articular chondrocytes and control chondrocytes. Data is presented as the median and interquartile range of the fold change in miR-140-3p (A), miR-140-5p (B) miR-146a (C) and miR-146b (D) expression in OA articular chondrocytes relative to control chondrocytes from samples deemed non-OA. Values are presented as individual biological replicates n=11, * $p < 0.05$, ** $p < 0.01$, Mann Whitney test.

3.5 Gene expression in human chondrocytes following treatment with IL-1β, TGF-β3 or IL-1β and TGF-β3 in combination up to 21 days

Chondrocytes isolated from the articular cartilage of femoral heads from osteoarthritic patients were cultured in the presence of either: IL-1β, TGF-β3 or a combination of IL-1β and TGF-β3 and expression of *MMP13, COL2A1,* and *AGCAN* mRNA was examined at days 7, 14 and 21 compared to expression in untreated chondrocytes at day 7. All mRNA expression results have been plotted collectively for each mRNA examined and the data for individual patient samples has also been plotted on individual graphs. Chondrocytes isolated from different patient samples have a high degree of variability and therefore results can be misinterpreted and trends overlooked, representing mRNA expression data as individual patient samples enables for trends to clearly interpreted.

3.5.1 *MMP13* expression

Analysis of three patient samples has shown that the expression of *MMP13* was not significantly different in chondrocytes cultured in the presence of any of the treatment groups compared to control chondrocytes at any of the time points examined. No significant differences in *MMP13* expression were observed between chondrocytes cultured in the presence of IL-1β, in the presence of TGF-β3 or in the presence of both IL-1β and TGF-β3 at 7, 14 and 21 days compared to control untreated chondrocytes (Figure 23A). Analysis of the collective samples has shown no significant differences in *MMP13* expression, however, examination of *MMP13* expression for the individual patient samples (Figure 23BCD) has shown that in all three patient samples the expression of *MMP13* was up-regulated in chondrocytes treated with IL-1β at 7, 14 and 21 days compared to control untreated chondrocytes (Figure 23BCD). Examination of *MMP13* expression for the individual samples has also shown that in all three patient samples the expression of *MMP13* was up-regulated in chondrocytes treated with IL-1β and TGF-β3 at 7, 14 and 21 days compared to control untreated chondrocytes, but not to the level which was observed in chondrocytes which were treated with IL-1β alone, with exception of patient 3 at day 14 (Figure 23BCD). Examination of *MMP13* expression for the individual samples has also shown that in all three patient samples the expression of *MMP13* was down-regulated in chondrocytes treated with TGF-β3 at 7, 14 and 21 days compared to control untreated chondrocytes, with exception to patient 1 and 3 at day 21 (Figure 23BCD).

3.5.2 *COL2A1* expression

Analysis of three patient samples has shown that the expression of *COL2A1* was not significantly different in chondrocytes cultured in the presence of any of the treatment groups compared to control chondrocytes at any of the time points examined. No significant differences in *COL2A1* expression were observed between chondrocytes cultured in the presence of IL-1β, in the presence of TGF-β3 or in the presence of both IL-1β and TGF-β3 at 7, 14 and 21 days compared to control untreated chondrocytes (Figure 24A). Analysis of the collective samples has shown no significant differences in *COL2A1* expression, however, examination of *COL2A1* expression has shown that in all three patient

samples individually the expression of *COL2A1* was up-regulated in chondrocytes treated with TGF-β3 at 7, 14 and 21 days compared to control untreated chondrocytes, with exception to patient 1 at day 7 (Figure 24BCD). Examination of *COL2A1* expression has also shown that in all three patient samples the expression of *COL2A1* (Figure 24BCD) was down-regulated in chondrocytes treated with both IL-1β and TGF-β3 and also down-regulated in chondrocytes treated with IL-1β alone at 7, 14 and 21 days compared to control untreated chondrocytes (Figure 24BCD).

3.5.3 *AGCAN* expression

Analysis of three patient samples has shown that the expression of *AGCAN* was not significantly different in chondrocytes cultured in the presence of any of the treatment groups compared to control chondrocytes at any of the time points examined. No significant differences in *AGCAN* expression were observed between chondrocytes cultured in the presence of IL-1β, in the presence of TGF-β3 or in the presence of both IL-1β and TGF-β3 at 7, 14 and 21 days compared to control untreated chondrocytes (Figure 25A). Analysis of the collective samples has shown no significant differences in *AGCAN* expression, however, examination of *AGCAN* expression for the individual patient samples (Figure 25BCD) has shown that in all three patient samples the expression of *AGCAN* was up-regulated in chondrocytes treated with TGF-β3 at 7, 14 and 21 days compared to control untreated chondrocytes, with exception to patients 2 and 3 at day 21 (Figure 25BCD). Examination of *AGCAN* expression for the individual samples has also shown that in all three patient samples the expression of *AGCAN* was down-regulated in chondrocytes treated with IL-1β at days 7, 14 and 21 compared to control untreated chondrocytes (Figure 25BCD). Examination of *AGCAN* expression for the individual samples has also shown that in all three patient samples the expression of *AGCAN* was down-regulated in chondrocytes treated with IL-1β and TGF-β3 at 7, 14 and 21 days compared to control untreated chondrocytes, but not to the level which was observed in chondrocytes which were treated with IL-1β alone and with exception to patient 1 and 2 at day 14 (Figure 25BCD).

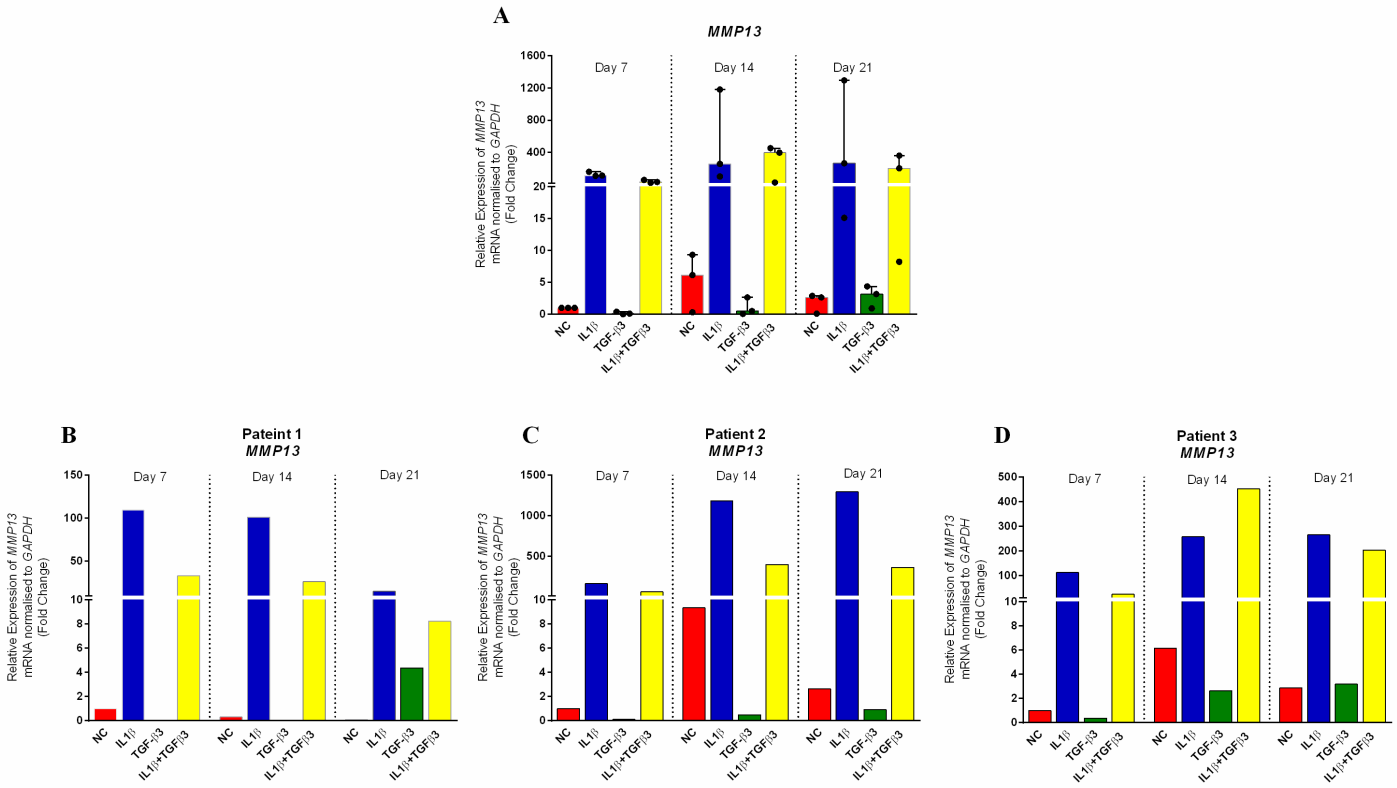

Figure 23. Effect of IL-1β, TGF-β3 and IL-1β and TGF-β3 treatment for up to 21 days in human articular chondrocytes on *MMP13* mRNA expression. Data is presented by different graphical representation. The same collective sample data from three patients is presented in graph A upon which statistical analysis was performed. The data is presented as the median and upper quartile range of the fold change in *MMP13* mRNA expression in human articular chondrocytes relative to untreated control chondrocytes at day 7 (NC). n=3, Freidman test with Dunn's post-test (A). Data is presented as individual patient samples: patient 1 (B), patient 2 (C), patient 3 (D).

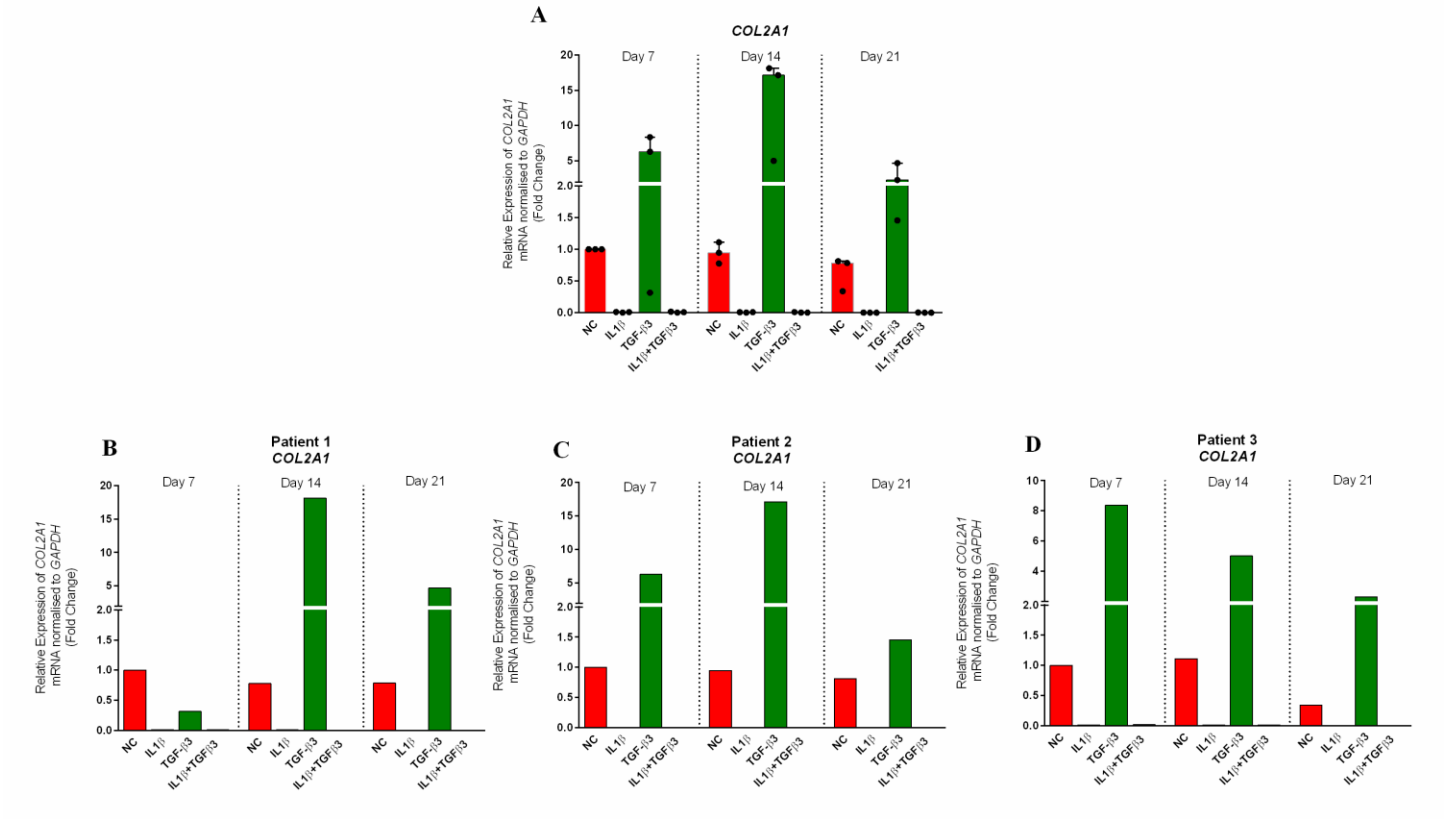

Figure 24. Effect of IL-1β, TGF-β3 and IL-1β and TGF-β3 treatment for up to 21 days in human articular chondrocytes on *COL2A1* mRNA expression. Data is presented by different graphical representation. The same collective sample data from three patients is presented in graph A upon which statistical analysis was performed. The data is presented as the median and upper quartile range of the fold change in *COL2A1* mRNA expression in human articular chondrocytes relative to untreated control chondrocytes at day 7 (NC). n=3, Freidman test with Dunn's post-test (A). Data is presented as individual patient samples: patient 1 (B), patient 2 (C), patient 3 (D).

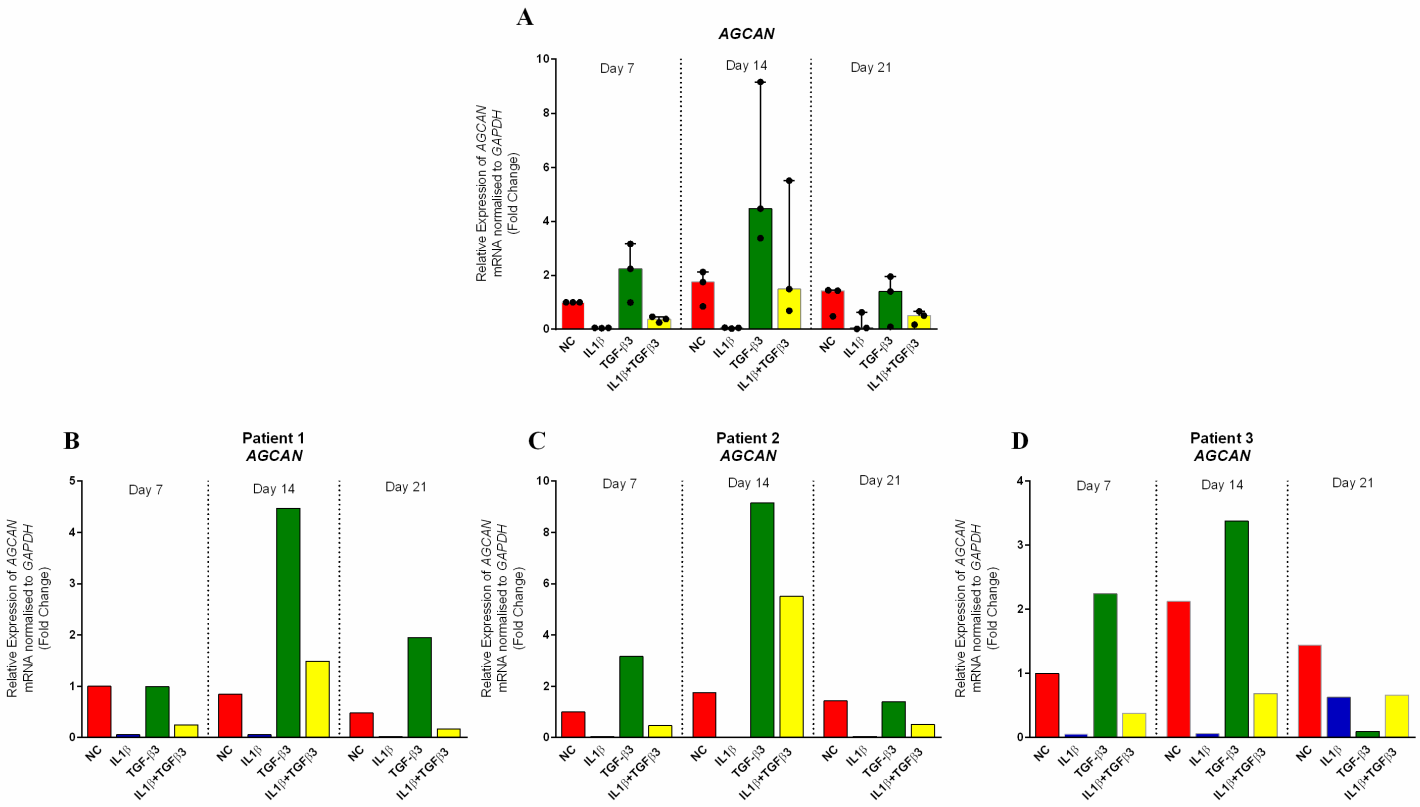

Figure 25. Effect of IL-1β, TGF-β3 and IL-1β and TGF-β3 treatment for up to 21 days in human articular chondrocytes on *AGCAN* mRNA expression. Data is presented by different graphical representation. The same collective sample data from three patients is presented in graph A upon which statistical analysis was performed. The data is presented as the median and upper quartile range of the fold change in *AGCAN* mRNA expression in human articular chondrocytes relative to untreated control chondrocytes at day 7 (NC). n=3, Freidman test with Dunn's post-test (A). Data is presented as individual patient samples: patient 1 (B), patient 2 (C), patient 3 (D).

3.6 MicroRNA expression in human chondrocytes following treatment with IL-1β, TGF-β3 or IL-1β and TGF-β3 in combination up to 21 days

Chondrocytes isolated from the articular cartilage of femoral heads from osteoarthritic patients were cultured in the presence of either IL-1β, TGF-β3 or a combination of IL-1β and TGF-β3 and expression of miR-145, miR-140-3p, miR-140-5p, miR-146a and miR-146b was examined at days 7, 14 and 21 compared to expression in untreated chondrocytes at day 7. All microRNA expression results for all patient samples have been plotted collectively for each microRNA examined and the data for individual patient samples has also been plotted on individual graphs. Chondrocytes isolated from different patient samples have a high degree of variability and therefore results can be misinterpreted and trends overlooked, representing microRNA expression data as individual patient samples enables for trends to be clearly interpreted.

3.6.1 miR-145 expression

Analysis of three patient samples has shown that the expression of miR-145 was not significantly different in chondrocytes cultured in the presence of any of the treatment groups compared to control chondrocytes at any of the time points examined. No significant differences in miR-145 expression were observed between chondrocytes cultured in the presence of IL-1β, in the presence of TGF-β3 or in the presence of both IL-1β and TGF-β3 at 7, 14 and 21 days compared to control untreated chondrocytes (Figure 26A). Analysis of the collective samples has shown no significant differences in miR-145 expression, however, examination of miR-145 expression for the individual patient samples (Figure 26BCD) has shown that in all three patient samples the expression of miR-145 was up-regulated in chondrocytes treated with TGF-β3 at 7, 14 and 21 days compared to control untreated chondrocytes (Figure 26BCD). Examination of miR-145 expression in chondrocytes treated with IL-1β alone has also shown differential expression amongst the three patient samples. The expression of miR-145 was down-regulated in chondrocytes treated with IL-1β in patients 1 and 2 at days 7, 14 and 21 with exception to patient 2 at day 14, while the expression of miR-145 was found to be up-regulated in chondrocytes treated with IL-1β across all time points in patient 3 (Figure 26BCD). The expression of miR-145 for the individual samples has also shown that in all three patient samples the expression of miR-145 was up-regulated in chondrocytes treated with both TGF-β3 and IL-1β at days 7, 14 and 21 compared to control untreated chondrocytes. The levels of miR-145 expression up-regulation are mixed amongst the individual samples following treatment with both IL-1β and TGF-β3. In patient 3 miR-145 up-regulation observed was not to the same level observed in chondrocytes treated with TGF-β3, however, in patients 1 at days 14 and 21 and patient 2 at day 21 miR-145 expression is more up-regulated in chondrocytes treated with both IL-1β and TGF-β3 than in chondrocytes treated with TGF-β3 alone (Figure 26BCD).

3.6.2 miR-140-3p expression

Analysis of three patient samples has shown that the expression of miR-140-3p was not significantly different in chondrocytes cultured in the presence of any of the treatment groups compared to control chondrocytes at any of the time points examined. No significant differences in miR-140-3p expression were observed between chondrocytes cultured in the presence of IL-1β, in the presence of TGF-β3 or in the presence of both IL-1β and TGF-β3 at 7, 14 and 21 days compared to control untreated chondrocytes (Figure 27A). Analysis of the collective samples has shown no significant differences in miR-140-3p expression, however, examination of miR-140-3p expression for the individual patient samples (Figure 27BCD) has shown that in two of the three patient samples the expression of miR-140-3p was up-regulated in chondrocytes treated with TGF-β3 at 7, 14 and 21 days compared to control untreated chondrocytes (Figure 27BCD). Examination of miR-140-3p expression in chondrocytes treated with IL-1β alone has also shown differential expression amongst the three patient samples. The expression of miR-140-3p was down-regulated in chondrocytes treated with IL-1β in patients 1 and 2 at days 7, 14 and 21 and patient 3 at day 21 but miR-140-3p was found to be up-regulated in patient 3 at days 14 and 21(Figure 27BCD). The expression of miR-140-3p for the individual samples has also shown that in all three patient samples the expression of miR-140-3p was down-regulated in chondrocytes treated with both TGF-β3 and IL-1β at days 7, 14 and 21 compared to control untreated chondrocytes, with exception to patient 2 at day 21 and patient 3 at day 7 (Figure 27BCD).

3.6.3 miR-140-5p expression

Analysis of three patient samples has shown that the expression of miR-140-5p was not significantly different in chondrocytes cultured in the presence of any of the treatment groups compared to control chondrocytes at any of the time points examined. No significant differences in miR-140-5p expression were observed between chondrocytes cultured in the presence of IL-1β, in the presence of TGF-β3 or in the presence of both IL-1β and TGF-β3 at 7, 14 and 21 days compared to control untreated chondrocytes (Figure 28A). Analysis of the collective samples has shown no significant differences in miR-140-5p expression, however, examination of miR-140-5p expression for the individual patient samples (Figure 28BCD) has shown mixed results for the different treatment groups between the three patients. Treatment of chondrocytes with TGF-β3 resulted in the up-regulation of miR-140-5p only at day 14 in patient 1, at days 7 and 14 in patient 2 and at all three times points, days 7, 14 and 21, in patient 3 (Figure 28BCD). Treatment of chondrocytes with IL-1β resulted in the down-regulation of miR-140-5p at all three time points in both patients 2 and 3 and at days 7 and 14 in patient 3. Combination treatment of both IL-1β and TGF-β3 resulted in the down-regulation of miR-140-5p in patient 1 at days 7 and 14, in patient 2 at days 7 and 14 and at day 21 in patient 3 (Figure 28BCD).

3.6.4 miR-146a expression

Analysis of three patient samples has shown that the expression of miR-146a was not significantly different in chondrocytes cultured in the presence of any of the treatment groups compared to control chondrocytes at any of the time points examined. No significant differences in miR-146a expression were observed between chondrocytes cultured in the presence of IL-1β, in the presence of TGF-β3 or in the presence of both IL-1β and TGF-β3 at 7, 14 and 21 days compared to control untreated chondrocytes (Figure 29A). Analysis of the collective samples has shown no significant differences in miR-146a expression, however, examination of miR-146a expression for the individual patient samples (Figure 29BCD) has shown that in all three patient samples the expression of miR-146a was down-regulated in chondrocytes treated with TGF-β3 at all three time points, 7, 14 and 21 days, compared to control untreated chondrocytes (Figure 29BCD). Treatment of chondrocytes with IL-1β resulted in the up-regulation of miR-146a at all three time points in all three patients (Figure 29BCD). Combination treatment of both IL-1β and TGF-β3 resulted in the up-regulation of miR-146a in at all 3 time points in all three patients (Figure 29BCD). The level of miR-146a expression was found to be higher in chondrocytes treated with both IL-β and TGF-β3 compared to the level of miR-146a expression in chondrocytes treated with IL-1β alone at all three time points in patients 1 and 2 and at day 7 in patient 3.

3.6.5 miR-146b expression

Analysis of three patient samples has shown that the expression of miR-146b was not significantly different in chondrocytes cultured in the presence of any of the treatment groups compared to control chondrocytes at any of the time points examined. No significant differences in miR-146b expression were observed between chondrocytes cultured in the presence of IL-1β, in the presence of TGF-β3 or in the presence of both IL-1β and TGF-β3 at 7, 14 and 21 days compared to control untreated chondrocytes (Figure 30A). Examination of miR-146b expression for the individual patient samples (Figure 30BCD) has shown that treatment of chondrocytes with TGF-β3 resulted in the down-regulation of miR-146b at all three time points in patients 1 and 3, but an up-regulation in miR-146b expression was observed at all three time points in patient 2 (Figure 30BCD). Treatment of chondrocytes with IL-1β resulted in the down-regulation of miR-146b at all three time points in patients 1 and 2 (Figure 30BCD). Combination treatment of both IL-1β and TGF-β3 resulted in the up-regulation of miR-144b in patient 1 at all three time points and at day 21 in patient 3, and a down-regulation of miR-146b was observed at all three time points in patient 2 and at days 7 and 14 in patient 3 (Figure 30BCD).

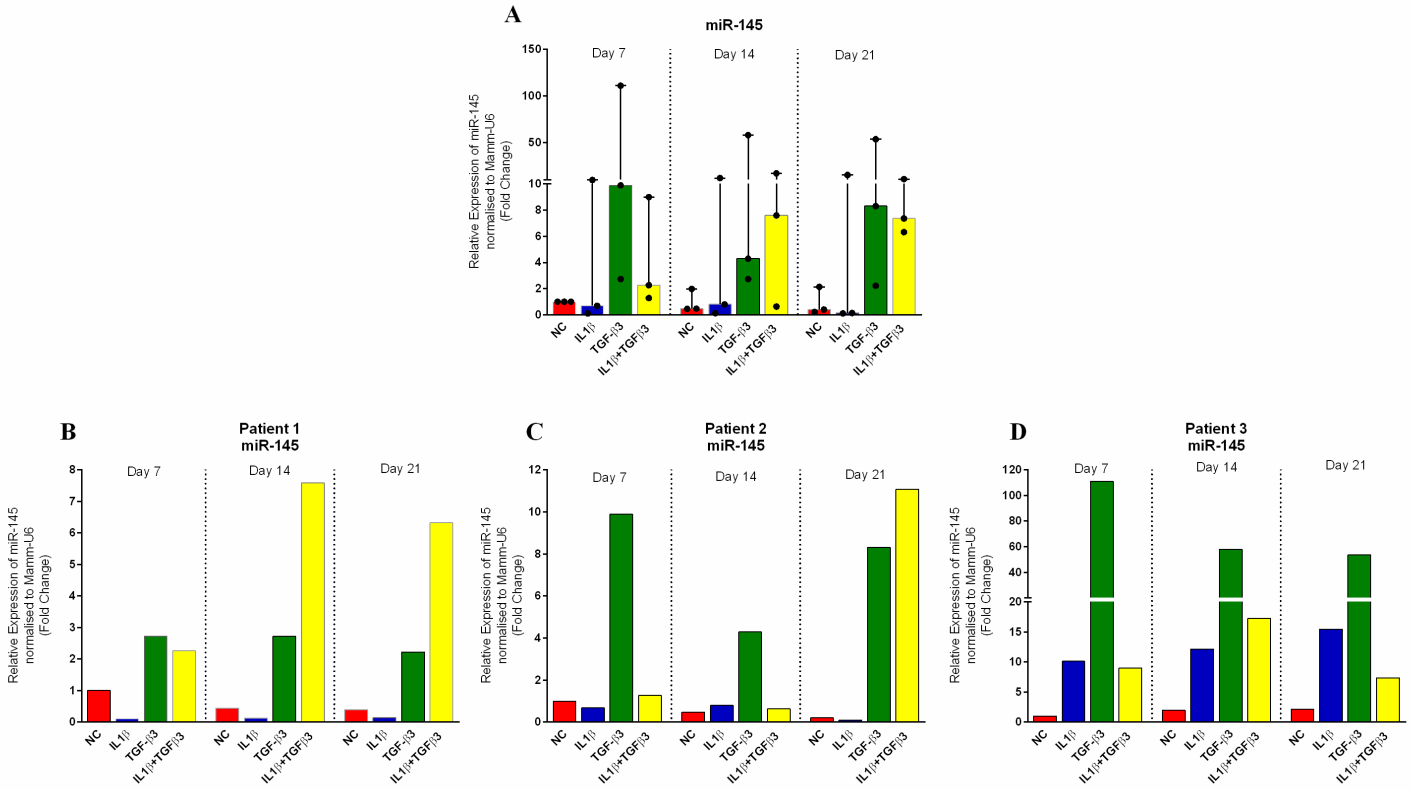

Figure 26. Effect of IL-1β, TGF-β3 and IL-1β and TGF-β3 treatment for up to 21 days in human articular chondrocytes on miR-145 expression. Data is presented by different graphical representation. The same collective sample data from three patients is presented in graph A upon which statistical analysis was performed. The data is presented as the median and upper quartile range of the fold change in miR-145 expression in human articular chondrocytes relative to untreated control chondrocytes at day 7 (NC). n=3, Freidman test with Dunn's post-test (A). Data is presented as individual patient samples: patient 1 (B), patient 2 (C), patient 3 (D).

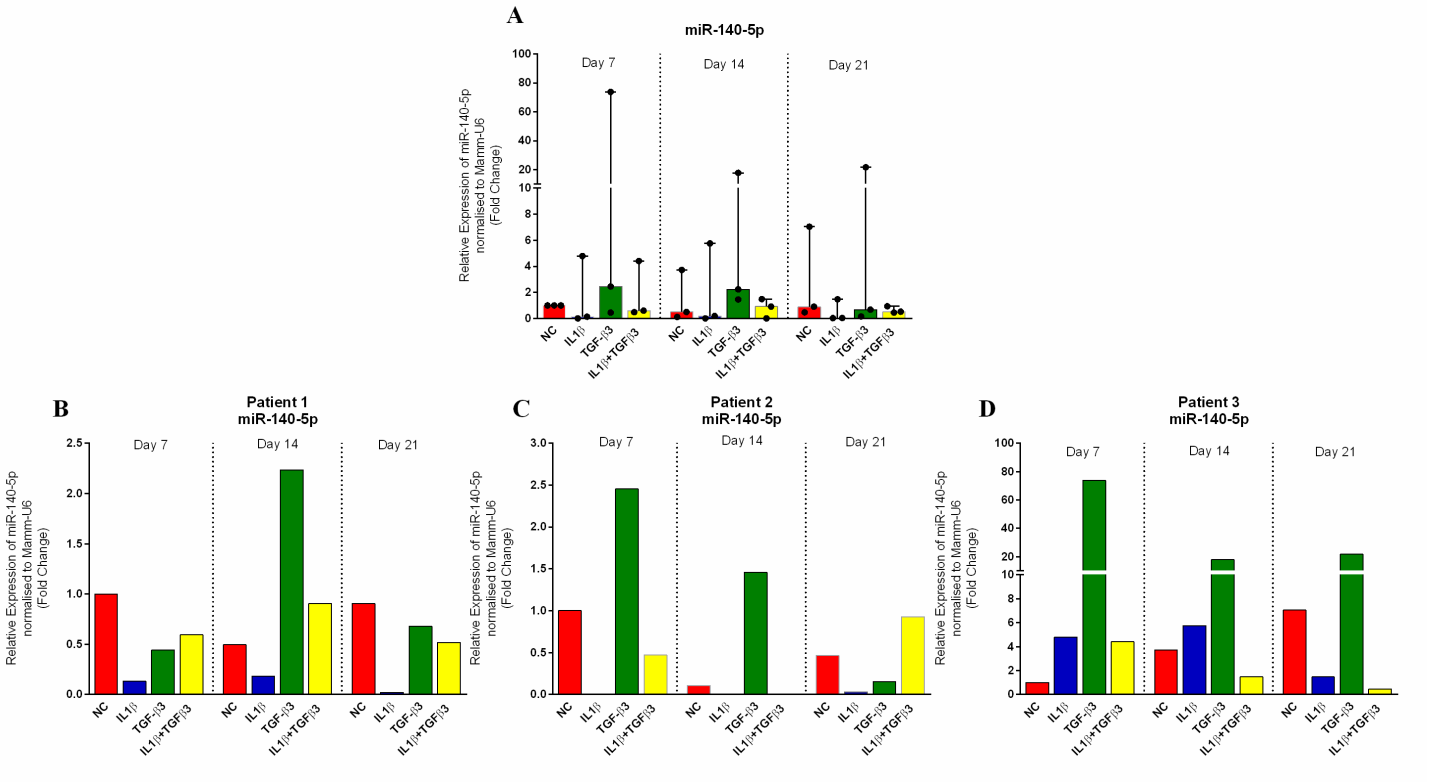

Figure 27. Effect of IL-1β, TGF-β3 and IL-1β and TGF-β3 treatment for up to 21 days in human articular chondrocytes on miR-140-5p expression. Data is presented by different graphical representation. The same collective sample data from three patients is presented in graph A upon which statistical analysis was performed. The data is presented as the median and upper quartile range of the fold change in miR-140-5p expression in human articular chondrocytes relative to untreated control chondrocytes at day 7 (NC). n=3, Freidman test with Dunn's post-test (A). Data is presented as individual patient samples: patient 1 (B), patient 2 (C), patient 3 (D).

.

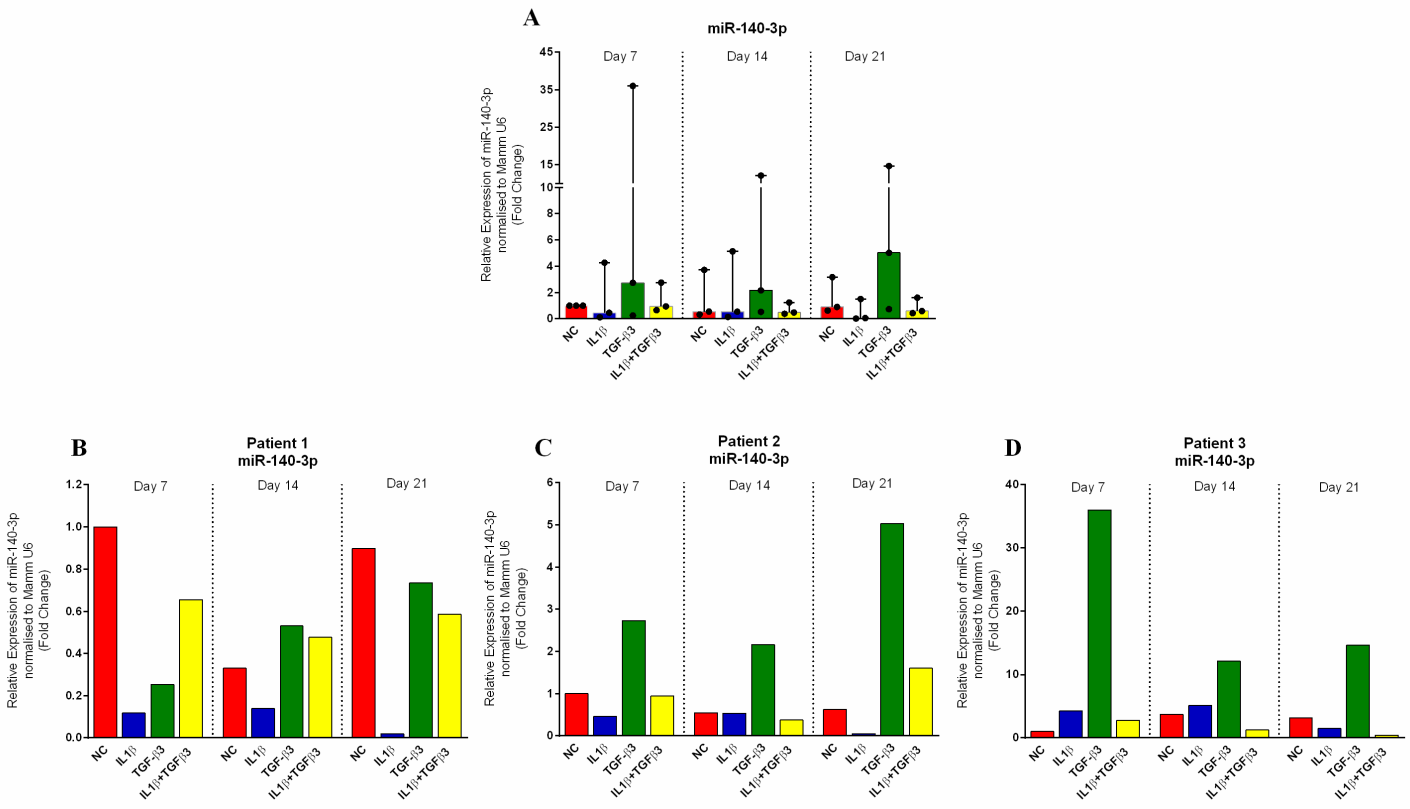

Figure 28. Effect of IL-1β, TGF-β3 and IL-1β and TGF-β3 treatment for up to 21 days in human articular chondrocytes on miR-140-5p expression. Data is presented by different graphical representation. The same collective sample data from three patients is presented in graph A upon which statistical analysis was performed. The data is presented as the median and upper quartile range of the fold change in miR-140-5p expression in human articular chondrocytes relative to untreated control chondrocytes at day 7 (NC). n=3, Freidman test with Dunn's post-test (A). Data is presented as individual patient samples: patient 1 (B), patient 2 (C), patient 3 (D).

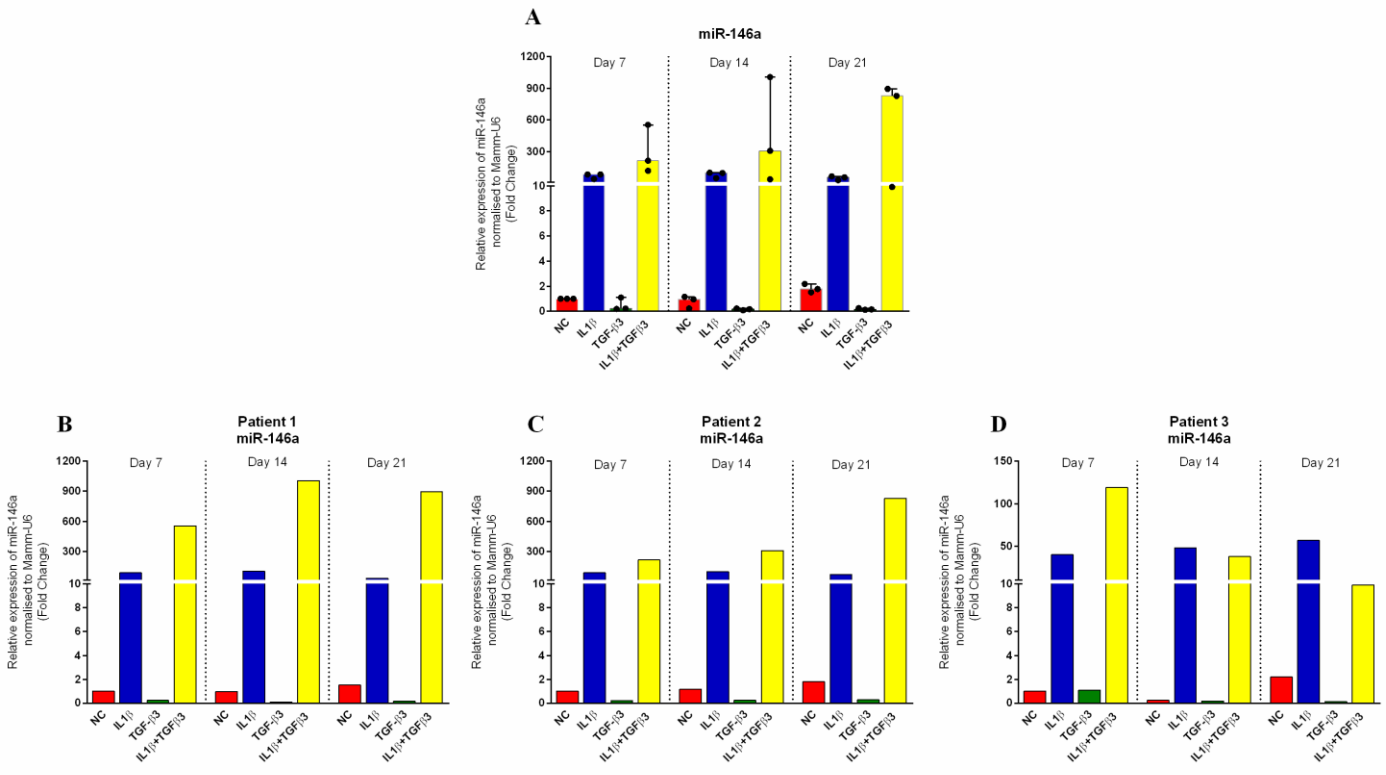

Figure 29. Effect of IL-1β, TGF-β3 and IL-1β and TGF-β3 treatment for up to 21 days in human articular chondrocytes on miR-146a expression. Data is presented by different graphical representation. The same collective sample data from three patients is presented in graph A upon which statistical analysis was performed. The data is presented as the median and upper quartile range of the fold change in miR-146a expression in human articular chondrocytes relative to untreated control chondrocytes at day 7 (NC). n=3, Freidman test with Dunn's post-test (A). Data is presented as individual patient samples: patient 1 (B), patient 2 (C), patient 3 (D).

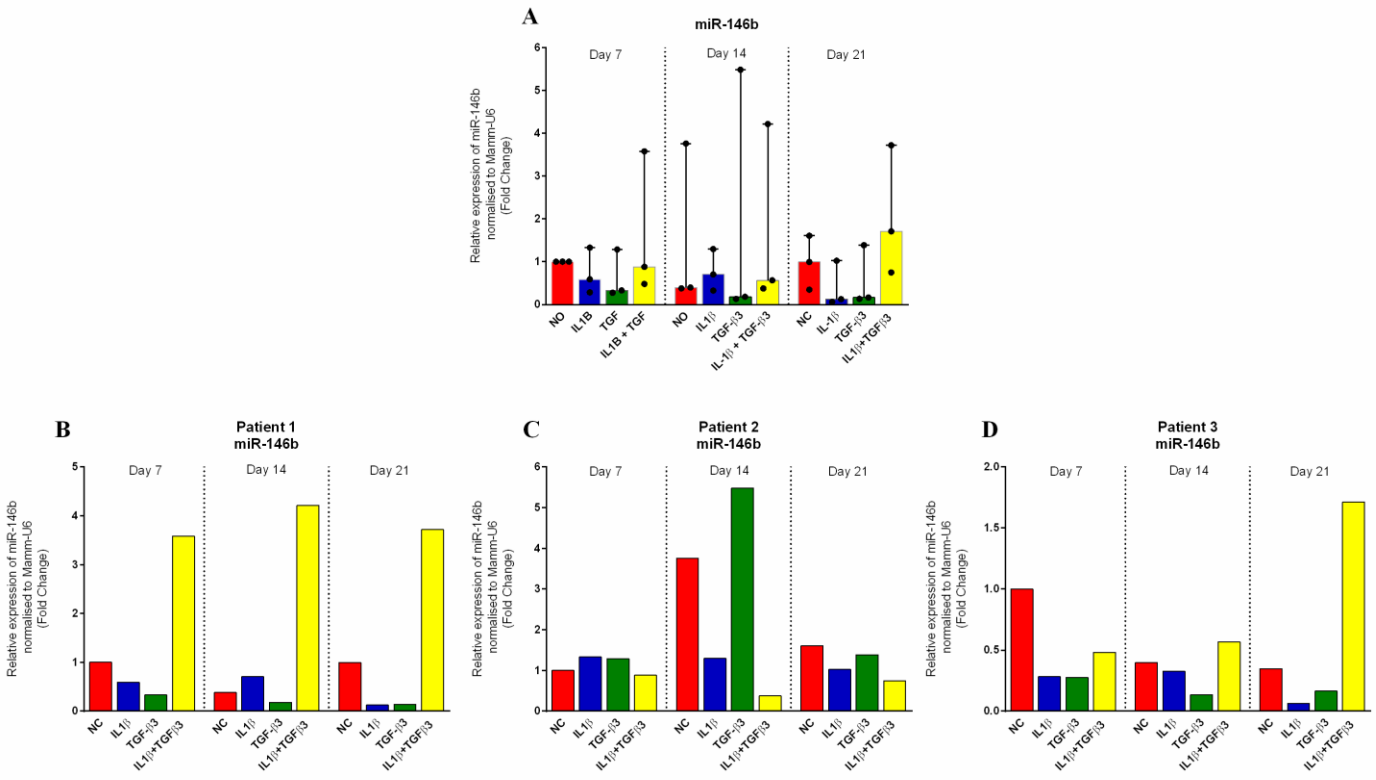

Figure 30. Effect of IL-1β, TGF-β3 and IL-1β and TGF-β3 treatment for up to 21 days in human articular chondrocytes on miR-146b expression. Data is presented by different graphical representation. The same collective sample data from three patients is presented in graph A upon which statistical analysis was performed. The data is presented as the median and upper quartile range of the fold change in miR-146b expression in human articular chondrocytes relative to untreated control chondrocytes at day 7 (NC). n=3, Freidman test with Dunn's post-test (A). Data is presented as individual patient samples: patient 1 (B), patient 2 (C), patient 3 (D).

3.7 Literature search – validated and potential inflammatory associated targets of miR-146a and miR-146b

An in depth literature search was conducted to identify all studies to date which identify inflammatory targets which are targeted by miR-146a and/or miR-146b. All of the studies all propose miR-146a and/or miR-146b as anti-inflammatory microRNAs which function to down-regulate an inflammatory associated targets. Of all of the studies identified, five of the studies show up-regulation of both miR-146a and miR-146b in inflammation as indicated by the highlighted blue surrounding text in table. Of the five studies, which all show the up-regulated expression of both miR-146a and miR-146b, *IRAK1*, *TRAF6* and *CCL5* (highlighted in yellow in table) were suggested to be targets of both miR-146a and miR-146b. All of the inflammatory studies identified and listed in table 12 all validated experimentally or suggested the function of miR-146a and/or miR-146b as anti-inflammatory mediators which target the proposed inflammatory associated targets listed.

A search of TargetScanHuman also found numerous inflammatory associated targets which are predicted to be targeted by both miR-146a and miR-146b. Some of the targets listed in TargetScanHuman have been verified experimentally and are listed in table12. Table 13 lists the remaining inflammatory associated targets predicted to be targeted by miR-146a and miR-146b which to date have not been validated experimentally and have not been reported in the literature

Following the literature search and identification of studies which validate inflammatory targets of miR-146a and/or miR-146b and the search of TargetScanHuman to identify inflammatory associated targets of miR-146a and/or miR-146b not yet validated and reported, a diagram to illustrate some of the validated and predicted inflammatory targets was created. The diagram shows that many of the validated and predicted targets or miR-146a and/or miR-146b have roles associated with inflammatory signalling pathways (Figure 31).

.

MiR-146a/b Target	Target Function	Inflammatory study
TRAF6	TNF receptor associated factor 6 (TRAF6) mediates signal transduction of the NF-κB pathway [232]. TRAF6 is a critical mediator of IL-1R and TLR signalling in addition to mediating signal transduction of pathogenic proteins [333].	MiR-146a and miR-146b exhibited up-regulation after stimulation with either LPS, TNF-α or IL-1β. Promoter analysis identified a NF-κB binding site in the promoter of miR-146a. miR-146a and miR-146b were predicted to target TRAF6 [307]. Monocytes stimulated with LPS have been shown to up-regulate miR-146b expression. Mir-146b was proposed to modulate the TLR4 pathway by direct targeting of TRAF6 amongst other components. Monocytes stimulated with IL-10 also showed recruitment of STAT3 to a predicted STAT3 binding site in the miR-146b promoter. MiR-146b was shown to be an IL-10 responsive microRNA with an anti-inflammatory role through targeting of components of the TLR4 signalling pathway [334]. Both miR-146a and miR-146b have been shown to be up-regulated during human monocyte differentiation into immature and mature dendritic cells (DC). Both miR-146a and miR-146b have been shown to promote DC apoptosis by targeting TRAF6, inhibiting NF-κB signalling [322].
IRAK1	Interleukin 1 receptor-associated kinase 1 is phosphorylated following IL-1 binding to IL-1R which ultimately results in the activation of NF-κB [231].	An *in vivo* murine study of immune tolerance shows prevention of bacteria induced intestinal epithelial damage during the transition from fetal to neonatal to adult life by miR-146a expression. miR-146a expression induced down-regulation of IRAK1 which induced immune tolerance to intestinal epithelial in neonates which was therefore then protected from damage from ingested bacteria [335]. MiR-146a and miR-146b exhibited up-regulation after stimulation with either LPS, TNF-α or IL-1β. Promoter analysis identified a NF-κB binding site in the promoter of miR-146a. miR-146a and miR-146b were predicted to target IRAK1 [307]. Monocytes stimulated with LPS have been shown to up-regulate miR-146b expression. Mir-146b was proposed to modulate the TLR4 pathway by direct targeting of IRAK1 amongst other components. Monocytes stimulated with IL-10 also showed recruitment of STAT3 to a predicted STAT3 binding site in the miR-146b promoter. MiR-146b was shown to be an IL-10 responsive microRNA with an anti-inflammatory role through targeting of components of the TLR4 signalling pathway [334]. Both miR-146a and miR-146b have been shown to be up-regulated during human monocyte differentiation into immature and mature dendritic cells (DC). Both miR-146a and miR-146b have been shown to promote DC apoptosis by targeting IRAK1, inhibiting NF-κB signalling [322].
TANK	TRAF family member-associated NF-κB activator (TANK) is activated by TRAF6 and involved with mediating activating NF-κB [336].	MiR-146a was found to be up-regulated in prion-infected mice brain tissues, with miR-146a showing up-regulation in microglia. TANK was found to up-regulated following miR-146a knockdown, suggesting that miR-146a targets TANK in the prion model. miR-146a was speculated to have an anti-inflammatory role in microglia in prion induced neurodegeneration [337].
TLR4	Toll-like receptor 4 activates NF-κB and up-regulation of inflammatory cytokines in response to recognition of pathogen associated molecular patterns, in particular microbial lipopolysaccharide [338].	Monocytes stimulated with LPS have been shown to up-regulate miR-146b expression. Mir-146b was proposed to modulate the TLR4 pathway by direct targeting of TLR4 amongst other components. Monocytes stimulated with IL-10 also showed recruitment of STAT3 to a predicted STAT3 binding site in the miR-146b promoter. MiR-146b was shown to be an IL-10 responsive microRNA with an anti-

		inflammatory role through targeting of components of the TLR4 signalling pathway [334].
TIRAP	Toll-interleukin 1 receptor (TIR) domain containing adaptor protein mediates downstream signalling of TLR2 and TLR4, activating NF-κB, ERK1/2 and JNK1 [339].	In 5q syndrome a subtype of myelodysplastic syndrome it has been speculated that loss of miR-146a results in inappropriate activation of immune signalling. Elevated expression of TIRAP in haematopoietic stem/progenitor cells (HSPCs) was as a result of miR-146a knockdown. Inappropriate immune signalling in HSPCs was shown to result in the same clinical features which manifest in 5q syndrome [340].
CCL5	Chemokine CC motif ligand 5 also known as RANTES can induce and recruit inflammatory cells upon binding and activation of G protein coupled receptors. Other cell types inclusive of epithelial and fibroblast cells produce CCL5 [341].	Stimulation of human lung alveolar epithelial cells with IL-1β resulted in the up-regulated expression of both miR-146a and miR-146b. MiR-146a was found to target RANTES [311]. The expression of miR-146a and miR-146b was found to be up-regulated in human retinal pigment epithelial cells following treatment with IL-1β, TNF-α and IFN-γ, which was associated with an up-regulation of CCL5 [318]
IRF5	Interferon regulatory factor 5 is a transcription factor which mediates interferon induced signalling pathways including regulating type I interferon expression and cytokine up-regulation in response to pathogen recognition by TLRs [342].	MiR-146a was found to exhibit down-regulated expression in peripheral blood leukocytes from patients with systemic lupus erythematosus (SLE). MiR-146a was found to target IRF5, therefore regulating the IFN pathway. Introduction of miR-146a into PBMCs was able to alleviate activation of IFN signalling. Under-expression of miR-146a is likely to contribute to changes in IFN signalling in SLE [343].
FAF1	FAS-associated factor 1 binds to the apoptotic transducing receptor Fas/APO-1 and caspase 8 intracellularly, exhibiting a similar function to Fas-associated death domain (FADD) which enhances Fas-mediated apoptosis [344].	Increased expression of miR-146a was identified in $CD4^+$T cells patients with rheumatoid arthritis. FAF1 was identified as a target of miR-146a and shown to modulate apoptosis. The increased expression of miR-146a was able to supress T cell apoptosis by regulation of FAF1 [345].
CD80	Cluster of differentiation 80 (CD80) or B7-1 is a cell surface protein located on activate monocytes and B cells. CD80 binds to CD28 on T-cells surfaces and is required as a co-stimulatory signal for T-cell activation and survival [346].	MiR-146a was found to be up-regulated in a murine model of the autoimmune condition Sjögren's syndrome (SjS) and in peripheral blood mononuclear cells from SjS patients. CD80 was identified and validated as a direct target of miR-146a. Reduced CD80 protein levels in salivary gland epithelial cells negatively correlated with increased miR-146a expression [347].
PTGS1	Prostaglandin-endoperoxide synthase 1 or cyclooxygenase 1 is an enzyme required for prostanoid biosynthesis from arachidonic acid during inflammation [348].	Expression of miR-146a in human trabecular meshwork (HTM) cells was shown to target and down-regulate PTGS1. Up-regulated expression of miR-146a in replicative senescence of HTM cells may function to prevent the production of inflammatory mediators in senescent cells and inhibit the damaging effects upon surrounding tissue [349]
PTGS2	Prostaglandin-endoperoxide synthase 2 or cyclooxygenase 2 is an enzyme required for prostanoid biosynthesis from arachidonic acid during inflammation [348].	MiR-146a expression was found to not be as up-regulated in fibroblasts from patients with chronic obstructive pulmonary disease (COPD) compared to fibroblasts from patients with no COPD. COPD fibroblasts were found to produce more Prostaglandin E_2 (PGE_2). COX-2 is required for PGE_2 production, which was found to be increased in COPD fibroblasts. miR-146a was found to target PTGS2 (COX-2). The down-regulated expression of miR-146a in COPD fibroblasts was speculated to result in higher expression of inflammatory COX-2 which may result in the abnormal inflammation associated with COPD [350]. The expression of miR-146a and miR-146b was found to be up-regulated in human airway smooth muscle cells (hASMCs) after treatment with a combination of pro-inflammatory cytokines to mimic inflammatory state in late stage inflammation in asthmatic airways. MiR-146a was found to target PTGS2 (COX-2) in hASMCs following treatment with pro-inflammatory cytokines [351].

CARD10	Caspase recruitment domain-containing protein 10 interacts with BCL10 and activates NF-κB and is involved with apoptotic signalling [352].	MiR-146a was found to be up-regulated in a murine model of gastric cancer and in human adenocarcinomas. CARD10 was identified as a direct target of miR-146a. CARD10 is part of the G protein-coupled receptor (GPCR) mediated signalling which activates NF-κB. MiR-146a was speculated to be up-regulated to inhibit the GPCR mediated activation of NF-κB and therefore act as a tumour suppressor and down-regulate cytokine expression inclusive of CCL5 [353]. The lung tissue of mice that was examined after exposure to allergen. MiR-146b was found to be significantly up-regulated after 1, 5 and 10 weeks exposure. It was speculated that miR-146b may be correlated with mRNA related to apoptotic processes via the NF-κB pathway. CARD10 which is a upstream mediator of NF-κB signalling was found to be targeted by miR-146b [354].

Table 12. Inflammatory associated mRNA targets which have either been validated experimentally or suggested to be targeted by miR-146a and/or miR-146b and reported in the literature.

miR-146a and miR-146b potential inflammatory associated targets listed by TargetScanHuman version 7 with no studies reported in the literature	
MiR-146a/b target	**Target Function**
IRAK4	Interleukin 1 receptor-associated kinase 4 mediates signal transduction from IL-1R and TLR family members [355].
TIFA	Traf-interacting protein with forkhead-associated domain binds to Traf2 [356], Irak1 and Traf6 [357]. Shown to induce polymerisation and polyubiquitination of TRAF6, activating TAK1 and IKK activating NF-κB [358].
TLR8	Toll-like receptor 8 recognises pathogen associated molecular patterns and mediate production of cytokines in response to viral or bacterial ssRNA [359].
IFNAR1	Interferon-alpha/beta receptor chain is a cell surface receptor to which interferon alpha (IFN-α) and interferon beta (IFN-β) bind [360].
IRF6	Interferon regulatory factor 6 (IRF6) is a transcription factor which has been shown to be activated by TLR2 signalling in epithelial cells. The chemokine CCL5 was found to be up-regulated by TLR2 induced IRF6 activation [361].
CASP10	Cysteine-aspartic acid protease (caspase) 10 mediates cell apoptosis [362]
CASP9	Caspase 9 is the initiator caspase in intrinsic or mitochondrial apoptosis. Cellular stresses, inclusive of DNA damage, cytoskeletal disruption, hypoxia, growth factor deprivation and accumulation of unfolded proteins activates intrinsic apoptosis. Caspase 9 is activated by cytochrome C release from the mitochondria and apoptosome formation proceeds [362].
CASP7	Caspase 7 is an executioner caspase. Excessive caspase 1 activation can induce pyroptosis through activation of caspase 7. Pyroptosis is a programmed cell death which causes cell membrane swelling and rupture with release of all intracellular pro-inflammatory cytokines [362].
CASP2	Caspase 2 is induced in response to metabolic perturbation, DNA damage, heat shock and cytoskeletal disruption [362].
ADAM17	ADAM metallopeptidase 17 also known as TACE (Tumour necrosis factor-α-converting enzyme) processes TNF-α at the cell surface. ADAM17 cleaves and releases pro-TNF-α to its mature soluble form, a process known as 'shedding' [65]
CD28	Cluster of differentiation 28 (CD28) is a receptor expressed on T-cell surface membrane and is required for T-cell activation and survival. CD28 receptor can bind to CD80 or CD86. TCR which bind with MHC-antigen complex in the absence of CD28:CD80 interaction renders the T-cell anergic [346].
CD86	Cluster of differentiation 86 (CD86) or B7-2 is a cell surface protein expressed on antigen presenting cells. Like CD80, CD86 binds to CD28 on T-cells surfaces and can activate T-cells. CD80 and CD86 have been shown to be able to substitute for one another in the activation of T cells [363].
CARD11	Caspase recruitment domain-containing protein 11 (CARD11) has been shown to interact with BCL10, which mediates NK-κB activation and can regulate apoptosis. CARD11 phosphorylates BCL10 [352].
MALT1	Mucosa-associated lymphoid tissue 1 (MALT1) interacts with BCL10 and is required for activation of NF-κB [364].
CD40	Cluster of differentiation 40 (CD40) is a co-stimulatory protein located on the surface of antigen presenting cells. Binding of CD40L on T helper cells to CD40 on antigen presenting cells activates antigen presenting cells [365].
GPR75	G-protein-coupled receptor 75 upon interaction with chemokine CCL5 mediates intracellular signalling [366].
PRG2	Proteoglycan 2 or eosinophil granule major basic protein is a protein enzyme which makes up eosinophil granules. Eosinophils release granule stored proteins inclusive of MBP/proteoglycan 2, upon interaction with helminthic parasites, through piecemeal degranulation or cytolysis [367]. Eosinophils are also associated with allergic disease. Degranulation results in localized immune responses and MBP is cytotoxic and results in tissue damage [368].
CARD8	Caspase recruitment domain-containing protein 8 (CARD8) is involved with pathways resulting in the activation of NF-κB [369].

Table 13. Inflammatory associated mRNA listed in TargetScanHuman as predicted targets of both miR-146a and miR-146b which have not been validated experimentally or reported in the literature

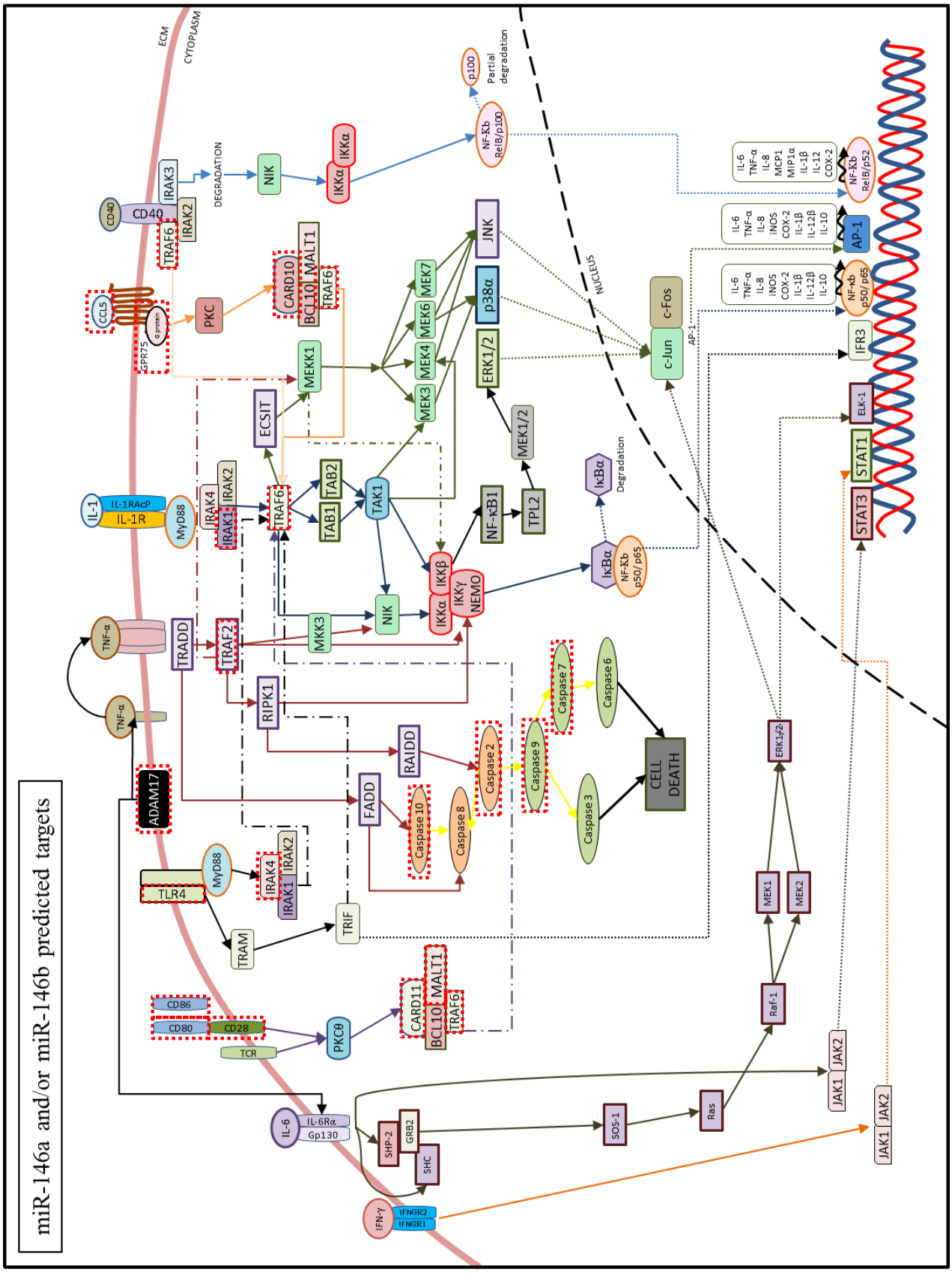

Figure 31. Predicted targets of miR-146a and/or miR-146b in inflammation. Predicted targets of miR-146a and/or miR-146b which have roles in inflammation are highlighted in red. The roles of the inflammatory targets have either previously been experimentally verified in inflammatory studies as targets of miR-146a and/or miR-146b listed in table 12 or are predicted targets of miR-146a and/or miR-146b listed in TargetScanHuman and listed in table 13.

3.8 Discussion

The expression of miR-146a has been shown to be up-regulated in OA cartilaginous tissues [228]. The nucleotide sequence of miR-146b, with exception to two nucleotides, is the same as the nucleotide sequence of miR-146a (Figure 20). The seed sequences of both miR-146b and miR-146a, required for the binding of miR-146a and miR-146b to the microRNA response elements within the 3'UTR of target mRNAs, are exactly the same. MicroRNAs with the same seed repertoire usually target the same genes and therefore possess similar cellular function [308]. Given the sequence homology of miR-146a and miR-146b, both microRNAs may work co-operatively to enhance target gene repression in chondrocytes and may also be regulated by the same stimuli and miR-146b was hypothesised to exhibit a similar up-regulated expression in OA chondrocytes. The current study, demonstrates for the first time, that expression of miRNA-146b was found to be up-regulated in chondrocytes isolated from human osteoarthritic articular cartilage compared to the expression of miR-146b in chondrocytes which were isolated from cartilage deemed non-osteoarthritic (Figure 22D). Samples were also examined for the presence of microRNA and mRNA which have previously exhibited dysregulation. Analysis of microRNA by TaqMan qPCR showed that miR-146a was up-regulated in OA chondrocytes and miR-140-3p was down-regulated (Figure 22C&A). Analysis of genes by qPCR showed that the expression of *MMP13* and *COL2A1* were significantly up-regulated in OA chondrocytes compared to the control chondrocytes (Figure 21A&B). The expression of *AGCAN* was significantly down-regulated (Figure 21D).

COL2A1 encodes the pro-alpha1(II) chain of type two collagen and three pro-alpha1(II) chains comprise a triple helix, cross linking induces the formation of collagen fibrils and ultimately the formation of type II collagen fibers. Type II collagen, produced by chondrocytes represents 90% to 95% of all collagen in the extracellular matrix of articular cartilage [4] and type II collagen fibrils are damaged in OA and there is a resultant loss of type II collagen. Despite the loss of type II collagen observed in OA there is an increase in the synthesis of type II collagen [370] and therefore an up-regulation in *COL2A1* expression. Overexpression of *Col2a1* in mice results in the generation of thick abnormal collagen fibrils and is believed that this disrupts the mechanism which governs the growth of cartilage fibrils [371]. The up-regulation of *COL2A1* expression in OA chondrocytes in this current study (Figure 21B) confirms that samples selected for analysis are of OA origin.

MMP13, found to be significantly up-regulated in OA chondrocytes in this study, encodes matrix metalloproteinase 13, also known as collagenase 3 which degrades type II collagen, found to be up-regulated in osteoarthritic cartilage [372], [373]. Antibody-induced arthritis in *MMP13* null mice exhibited a decreased severity of arthritis showing that *MMP13* expression plays a role in OA [374]. Several inflammatory associated ligands including IL-1β and TNF-α are involved with the activation of signalling pathways which induce the expression of *MMP* genes [375]. The up-regulation of

MMP13 expression in OA chondrocytes in this current study (Figure 21A) confirms that samples selected for analysis are of OA origin.

AGCAN, found to be significantly down-regulated in OA chondrocytes in this study, encodes the extracellular matrix protein aggrecan. The major proteoglycan of cartilage interacts with link protein and hyaluronic acid providing a hydrated gel structure [8]. Previously treatment of OA chondrocytes with the OA associated cytokine; IL-1β, has been found to down-regulate the expression of *AGCAN* [376], [52]. The down-regulation of *AGCAN* expression in OA chondrocytes in this current study (Figure 21C) confirms that samples selected for analysis are of OA origin.

Miyaki *et al* identified that miR-140 was down-regulated in cartilage tissue from human knee articular cartilage compared to the expression in cartilage tissue from normal knee joints [197] and the expression of miR-140 was found to be down-regulated in chondrocytes from OA cartilage compared to chondrocytes from normal cartilage [192]. Despite the studies by Miyaki *et al* and Tardif *et al*, in contrast Swingler *at al* observed an up-regulation of miR-140-5p in OA cartilage compared to control cartilage [214]. This current study showed no differences in expression of miR-140-5p between chondrocytes isolated from OA cartilage compared to chondrocytes isolated from control cartilage (Figure 22B). However, miR-140-3p was found to exhibit significant down-regulated expression (Figure 22A), indicating that miR-140-3p, originating from the same precursor microRNA as miR-140-5p (pre-miR-140) may play an important role in OA pathogenesis. The down-regulation of miR-140-3p observed is reinforced by the earlier finding that miR-140-3p exhibited down-regulated expression in human OA chondrocytes [377]. Both miR-140-3p and miR-140-5p are transcribed from pre-miR-140 but contain differing seed sequences and therefore have been predicted to target different genes which may provide reasoning for the differences in expression observed.

The current study demonstrated that miR-146a is significantly up-regulated in chondrocytes isolated from OA articular cartilage compared to the expression in control chondrocytes (Figure 22C). It was expected that miR-146a expression would be up-regulated due to previous studies which state the involvement of miR-146a in osteoarthritis [228], [378], [229]. Yamasaki *et al* first identified that miR-146a was up-regulated in osteoarthritic cartilage tissue samples compared to the expression observed in normal tissue samples [228].

For the first time, the expression of miR-146b was identified as being significantly up-regulated in chondrocytes isolated from OA cartilage compared to the expression of miR-146b in chondrocytes isolated from control cartilage (Figure 22D). The high sequence homology that miR-146b shares with miR-146a makes it likely that miR-146b plays a role similar to that of miR-146a. The dysregulated association that miR-146a has with OA pathogenesis [228] indicated that miR-146b may well also be dysregulated in osteoarthritis. Taganov *et al* first described the up-regulated expression of miR-146a and miR-146b in a monocyte cell line following stimulation with lipopolysaccharide and postulated that both miR-146a and miR-146b targeted downstream toll-like receptor and cytokine receptor

signalling through targeting TRAF6 and IRAK1 [307]. Having identified that miR-146b is up-regulated in osteoarthritis in these studies and the previous inflammatory response studies which identify up-regulation of miR-146b [307], [313], [318], [319], it is possible that miR-146b functions as an anti-inflammatory mediator of OA, acting to attenuate the inflammatory response.

The expression of miR-146a has previously been shown to be up-regulated in chondrocytes cultured in the presence of IL-1β, a prominent cytokine involved in OA pathogenesis [228]. Given that miR-146a and miR-146b both possess the same seed sequences and target many of the same targets, miR-146a and miR-146b are likely to have similar cellular functions in chondrocytes. Given the up-regulation of miR-146a in chondrocytes following IL-1β treatment, chondrocytes were cultured in the presence of IL-β to identify if the catabolic, pro-inflammatory cytokine was also an inducer of miR-146b expression in chondrocytes. This current study demonstrated that while IL-β up-regulated the expression of miR-146a in chondrocytes, IL-1β did not have the same effect on the expression of miR-146b.

Previous studies have indicated that suppression of TGF-β signalling is associated with the development of OA [78], [27], [81], [82], [83], [84], [79] and use of anabolic associated TGF-β3 has been shown to counteract the effects of catabolic IL-1β in chondrocytes [330], [331], [329], [332]. This study utilised catabolic IL-1β and anabolic TGF-β3 to investigate if the two antagonistic mediators resulted in the differential expression of miR-146a and miR-146b in chondrocytes. Demonstrated for the first time, the expression trend of miR-146a was found to be more up-regulated in chondrocytes treated with both IL-1β and TGF-β3 than in chondrocytes treated with just IL-1β and chondrocytes treated with TGF-β3 resulted in the down-regulation of miR-146a. Similar expression patterns were not replicated with miR-146b (Figure 30) suggesting that despite miR-146a and miR-146b having identical seed sequences and potentially having similar functional roles in chondrocytes, while IL-1β is a positive stimulator of miR-146a expression, IL-1β does not induce the expression of miR-146b in chondrocytes. Critically, the study has identified that TGF-β3 and IL-1β individually do have opposite effects on miR-146a expression, however, while TGF-β3 treatment resulted in the down-regulation of miR-146a and IL-1β treatment resulted in the up-regulation of miR-146a, combined treatment of TGF-β3 and IL-1β resulted in the up-regulation of miR-146a, suggesting for the first time that together, TGF-β3 and IL-1β, have a synergistic role on miR-146a expression in chondrocytes (Figure 29).

An up-regulated trend in *MMP13* expression was observed in human chondrocytes from all three patient samples which were cultured in the presence of IL-1β compared to untreated chondrocytes, consistent with the previous study conducted by Fan *et al* [56]. Chondrocytes cultured in the presence of TGF-β3 exhibited a down-regulation of *MMP13* (Figure 23), consistent with previous findings that TGF-β signalling represses *MMP13* expression [379], [380] via SMAD3 to repress Runx2-inducible *MMP13* expression. TGF-β signalling via SMAD3 is one regulatory mechanism that has been shown to prevent *MMP13* mediated degeneration of cartilage, playing an essential role in the prevention of

osteoarthritis [380]. Despite a down-regulated trend in expression of *MMP13* in chondrocytes cultured in the presence of TGF-β3, the combined treatment of IL-1β and TGF-β3 resulted in up-regulation of *MMP13* expression in chondrocytes. The repressive effect of TGF-β signalling on *MMP13* expression could only partially counteract the inductive effect of IL-1β signalling, shown by previous studies which indicate TGF-β signalling to attenuate IL-1β signalling in chondrocytes [330], [331], [329], [332], [86].

Given the up-regulated trend in expression of *COL2A1* in TGF-β3 treated chondrocytes and the down-regulated trend in *COL2A1* expression exhibited in both IL-1β treated and combinational treatment of IL-1β and TGF-β3 chondrocytes, the presence of TGF-β3 was not able to counteract the action of IL-1β (Figure 24). The expression trend of *AGCAN* was up-regulated in TGF-β3 treated chondrocytes and down-regulated in TGF-β3 and IL-1β treated chondrocytes, but not to the extent observed in chondrocytes treated with IL-1β alone (Figure 25). The results suggest that in this instance, TGF-β3 was able to partially counteract the action of IL-1β on *AGCAN* expression but not *COL2A1* expression.

Previously, Yang *et al* have shown that treatment of chondrocytes with IL-1β resulted in the up-regulation of miR-145 in both normal and OA chondrocytes [381] and therefore miR-145 was selected for investigation to serve as a positive control for treatment of chondrocytes with IL-1β. In this current study no expression trend of miR-145 could be interpreted following treatment of chondrocytes with IL-1β given that the expression of miR-145 differed between chondrocytes isolated from the three different patient samples. Stimulation of chondrocytes with TGF-β3 resulted in an up-regulated trend of miR-145 expression in chondrocytes isolated from all three patient samples. An up-regulated trend in miR-145 expression was observed in chondrocytes treated with IL-1β and TGF-β3 together in chondrocytes isolated from three patient samples, but not to the extent observed with TGF-β3 treatment (Figure 26). It is impossible to comment on the effect of TGF-β3 on IL-1β signalling in chondrocytes as no trend could be identified given the variability in miR-145 expression results in patients treated with IL-1β.

To date no study has looked at the expression of miR-145 in chondrocytes following treatment with TGF-β, however Martinez-Sanchez *et al* have previously shown the up-regulation of miR-145 during human articular chondrocytic de-differentiation [382]. The previous findings by Martinez-Sanchez *et al*, which showed the up-regulation of miR-145 in chondrocytes having undergone serial passage and thus implied dedifferentiation also exhibited down-regulated expression of *SOX9*, *COL2A1* and *AGCAN* and up-regulation of *MMP13* [382]. In this current study, treatment of chondrocytes with TGF-β3 resulted in the down-regulation of *MMP13* and up-regulation of critical cartilage components *COL2A1* and *AGCAN* suggesting de-differentiation processes were not involved in the up-regulation of miR-145 observed in this study. In this current study anabolic TGF-β3 stimulus up-regulated miR-145 expression and in chondrocytes treated with both IL-1β and TGF-β3. However, the concept that TGF-β3 may be acting to counteract IL-1β cannot be concluded as the expression of miR-145 was found to exhibit both up-regulated expression following treatment with IL-1β in chondrocytes from

one patient and down-regulated expression in chondrocytes from two patients and also in patient one the combined treatment of IL-1β and TGF-β3 resulted in a more up-regulated expression of miR-145 in chondrocytes from patient 1. The novel finding from the current study is that miR-145 exhibits an up-regulated trend following treatment of chondrocytes with TGF-β3. Previously, TGF-β signalling has been found to activate both the SMAD pathway and p38MAPK pathway which ultimately were shown to converge at a CArG box and a sterol binding element in the upstream region of miR-145, which directly mediated the transcription of miR-145 in human coronary artery smooth muscle cells [383]. Perhaps the up-regulation of miR-145 observed in chondrocytes by TGF-β signalling activates the same pathways.

Previously, Miyaki *et al* have shown that treatment of chondrocytes with IL-1β resulted in the down-regulation of miR-140 [191] and therefore both miR-140-3p and miR-140-5p were selected for investigation to serve as a positive controls for treatment of chondrocytes with IL-1β. In this current study no expression trend of miR-140-3p or miR-140-5p could be interpreted following treatment of chondrocytes with IL-1β or TGF-β3 or both TGF-β3 and IL-1β given that the expression of miR-140-3p and miR-140-5p differed between chondrocytes isolated from the three different patient samples (Figures 27 & 28).

Previously, Yamasaki *et al* have shown that treatment of chondrocytes with IL-1β resulted in the up-regulation of miR-146a [228] and therefore miR-146a was selected for investigation to serve as a positive control for the treatment of chondrocytes with IL-1β. The expression trend of miR-146a was found to be up-regulated in chondrocytes from all three patients following treatment with IL-1β, consistent with the finding by Yamasaki *et al* [228]. The expression trend of miR-146a was found to be consistently down-regulated in chondrocytes from all three patients following treatment with TGF-β3 (Figure 29). Individual treatment of either IL-1β or TGF-β3 resulted in the opposite effect upon miR-146a expression, indicating antagonistic roles on miR-146a expression. However, combined treatment of IL-1β and TGF-β3 on chondrocytes resulted in the up-regulation of miR-146a and was found to be at a higher level than in IL-1β treated chondrocytes in two patients, indicating a potential synergistic role of TGF-β3 and IL-1β, when used in combination, on miR-146a expression.

Previously co-stimulation with TGF-β and IL-1β has resulted in the up-regulated secretion of MCP-1 or CCL2 [384], [385]. It is possible that IL-1β and TGF-β use similar intracellular mechanisms to enhance specific inflammatory responses. The synergistic up-regulation of miR-146a expression observed may be as a result of up-regulation of certain inflammatory mediators. MiR-146a has been proposed as an anti-inflammatory regulator and therefore miR-146a up-regulation may be in place to try and down-regulate specific mediators of inflammation inclusive of chemokines. Given the previous evidence in the literature that combination stimulation with TGF-β and IL-1β results in the up-regulation of the chemokine CCL2, it can be speculated that miR-146a is up-regulated by the co-stimulation to target the chemokine CCL5 in human chondrocytes. Studies have previously shown that miR-146a targets CCL5 under inflammatory conditions [311], [386]. CCL5 has been shown to

induce the expression of IL-6 [63], Kuppner *et al* have shown that the combined treatment of TGF-β1 and IL-1β in retinal pigment epithelial (RPE) cells lead to the induction of IL-6 [387]. The up-regulated expression of miR-146a observed with combinational treatment of TGF-β and IL-1β may function to target CCL5; which may potentially be up-regulated itself by the co-stimulatory treatment to induce IL-6, further studies would need to be conducted.

The expression of miR-146a has previously been shown to be up-regulated in chondrocytes cultured in the presence of IL-1β [228]. Given the close homology in sequences between miR-146a and miR-146b, miR-146b was hypothesised to exhibit up-regulated expression following treatment with Il-1β. In this current study miR-146b expression trends could not be interpreted in chondrocytes from any of the patient samples following treatment with IL-1β. MiR-146b expression trends could not be interpreted in chondrocytes treated with TGF-β3 or in chondrocytes treated with both IL-1β and TGF-β3. Li *et al* have previously shown the activation pathway of miR-146a following IL-1β treatment [229]. Given the sequence homology of miR-146b with miR-146a, it was hypothesised that miR-146b may also be activated by IL-1β signalling. Given the variation in miR-146b expression in chondrocytes it cannot be clarified if miR-146b is activated by IL-1β signalling. Both miR-146a and miR-146b have been observed to exhibit up-regulated expression in OA chondrocytes, despite this, treatment with IL-1β does not cause both miR-146a and miR-146a to exhibit similar expression patterns. The treatment of chondrocytes with IL-1β suggest that miR-146a is under the regulation of IL-1β signalling, which has been previously shown [229], whereas miR-146b is likely to be under the control of another catabolic mediator/s in OA.

Despite initial hypotheses the co-stimulation of chondrocytes with TGF-β3 and IL-1β, TGF-β was unable to salvage the negative effects of IL-1β in some of the genes and microRNAs investigated. The microRNA and gene expression results attained from this study suggest a connection between IL-1β and TGF-β signalling in chondrocytes. Whilst TGF-β signalling has been shown to counteract IL-1β signalling and IL-1β signalling shown to abrogate TGF-β signalling, current results imply that IL-1β signalling and TGF-β signalling may have synergistic effects as well as counteractive effects depending on the target gene or microRNA. Long term treatment of chondrocytes with anabolic factor TGF-β3 induced a down-regulated trend of *MMP13* and the up-regulation of *COL2A1* and *AGCAN*, suggesting a potential role for TGF-β3 in the treatment of OA. However, the inhibitory effect IL-1β has on TGF-β signalling should also be considered. Knowledge of the down-stream effects of TGF-β and in combination with IL-1β signalling and also other immuno-modulatory molecules will help in the development of novel therapies to help in the treatment of OA.

Given that miR-146a and miR-146b both possess the same seed sequences and target many of the same targets, miR-146a and miR-146b are likely to have similar cellular functions in chondrocytes. Despite the observation that only miR-146a up-regulation resulted following treatment of chondrocytes with IL-1β and no observable up-regulation of miR-146b, these two similar microRNAs

may still have similar functions in chondrocytes despite not exhibiting similar expression pattern to the same pro-inflammatory stimuli. The literature search conducted (Table 12) and search of TargetScanHuman (Table 13) identified many inflammatory associated mRNAs which have been either validated or predicted to be targeted by both miR-146a and miR-146b which suggests that miR-146a and miR-146b act as anti-inflammatory mediators in OA and may explain the up-regulation of both miR-146a and miR-146b in human chondrocytes isolated from OA articular cartilage. Taganov *et al* have suggested that miR-146a and miR-146b are negative regulators of inflammation, functioning in negative feedback loops to dampen inflammatory response [307].

Chapter 4
Results: MicroRNA 34a expression in human fetal femur-derived cells during chondrogenic differentiation

4.1 Introduction

Human fetal femur-derived skeletal stem cells have been shown to differentiate down differing mesenchymal lineages including the adipogenic, osteogenic and chondrogenic lineages [388]. Fetal-derived stem cells have also been shown to possess enhanced proliferation, plasticity and expansion potential compared to mesenchymal stem cells derived from adult sources [389]. Additionally fetal derived stem cells have been found to display lower HLA class I expression compared with adult derived stem cells and also lack HLA class II expression, indicating an immunological inert role of fetal tissue derived stem cells [390]. Given these characteristics fetal femur-derived stem cells provide, potentially, an alternative cell source for tissue engineering applications with the potential to be used in cartilage reparation.

The properties of skeletal stem cells make them a promising cell source for cartilage repair. Skeletal stem cells have been shown to be regulated in part by microRNAs and have been shown to be involved in chondrogenic differentiation. The use of skeletal stem cells in combination with microRNA modulation could provide a new approach to cartilage tissue reparation. Modulation of microRNAs may therefore provide a method for enhancing the chondrogenic potential of skeletal stem cells pre- and post-implantation in cartilage lesions and also OA joints. However, to exploit the use of microRNAs for their potential in regulating differentiation, understanding the expression patterns and the role of microRNAs in chondrogenesis is essential.

The majority of studies in the literature induce chondrogenesis by incubating cells in defined media containing dexamethasone, ascorbic acid and TGF-β in combination with a three-dimensional culture system. A three-dimensional culture system is different to the conventional monolayer, two-dimensional culture system in that such an approach is thought to convey *in vivo* conditions. There are indications that skeletal stem cells cultured *in vitro* as two-dimensional monolayers on tissue culture plastic may lose cell specific properties. Two-dimensional differentiated chondrocytes have been shown to display a predisposition to dedifferentiate [117]. Three-dimensional culture of skeletal stem cells may therefore retain cell properties and provide a better method for differentiating mesenchymal stem cells toward the chondrogenic lineage *in vitro.* A 3D culture system allows for greater cell-cell contact and enhanced cell-ECM interaction which may have influences on cell signalling and also mimics a more consistent cellular environment comparable to the *in vivo* environment in terms of mimicking mesenchymal condensation.

Previously miR-34a has been identified as being a negative regulator of chondrogenesis in chick limb mesenchymal cells and was found to be up-regulated after inhibition of JNK induced chondrogenesis [391], [296]. The function that miR-34a played in inhibiting chondrogenesis was thought to be through targeting Rac1; required for the actin cytoskeleton organization in establishing chondrocyte morphology [296]. MiR-34a has also been found to be was found to be up-regulated in cells from the diaphyseal region of the fetal femur compared to cells from the epiphyseal; indicating a potential role for miR-34a during early fetal limb development and therefore a potential role in chondrogenic differentiation [392]. Given the identification of differentially expressed miR-34a previously, miR-34a may be differentially expressed during chondrogenic differentiation of human fetal femur-derived cells.

4.2 Hypothesis and Aims

4.2.1 Hypothesis

MicroRNA 34a targets specific genes in human fetal femur-derived cells which regulate the ability of the fetal femur-derived cells to undergo chondrogenic differentiation.

4.2.2 Aims and Objectives

1. To identify the expression of miR-34a during TGF-β3 induced chondrogenesis. The expression of miR-34a will be assessed following culture of fetal femur-derived cells for 21 days in a 3D micromass culture system containing TGF-β3 compared to cells cultured in in a 3D micromass system containing no TGF-β3.
2. To identify the expression pattern of miR-34a in TGF-β3 induced chondrogenesis across 21 days by examining the expression at 7 day intervals.
3. To select from putative targets, genes which are relevant to chondrogenesis using bioinformatic analysis.
4. To validate potential gene targets of miR-34a examined by carrying out miR-34a overexpression or inhibition assays to identify the effects upon target genes *in vitro*.

4.3 Cell source for chondrogenesis

4.3.1 Fetal femur-derived cells

Cells derived from the human fetal femur comprise of a mixed population of cells. Femurs used in this work ranged in age from 54-59 days post conception. The development of the fetal femur proceeds by mesenchymal stem cells undergoing the endochondral ossification process to ultimately produce adult femur as discussed in chapter 1.1, section 1.1.1.2. Fetal femurs provide a mixed population of cells including stem cells, developing chondrocytes and potentially osteoblasts dependent upon the age of the fetal femur. Alcian blue and sirus red staining of the fetal femur clearly shows differences in matrix deposition (Figure 32). The predominant alcian blue staining of the fetal femur shows the proteoglycan anlage with proliferating chondrocytes located at the epiphyseal regions of the fetal femur. The diaphysis exhibits sirus red staining indicating collagen deposition at the location of bone collar formation and microscopic analysis also clearly shows the hypertrophic state of alcian blue stained chondrocytes located in the diaphysis **(**Figure 32**).** Despite the epiphyses and diaphysis being structurally different following Stro-1 immunostaining, both the epiphyses and diaphysis clearly show positive staining for Stro-1 indicating the presence of skeletal progenitor cells in both regions (Figure 33).

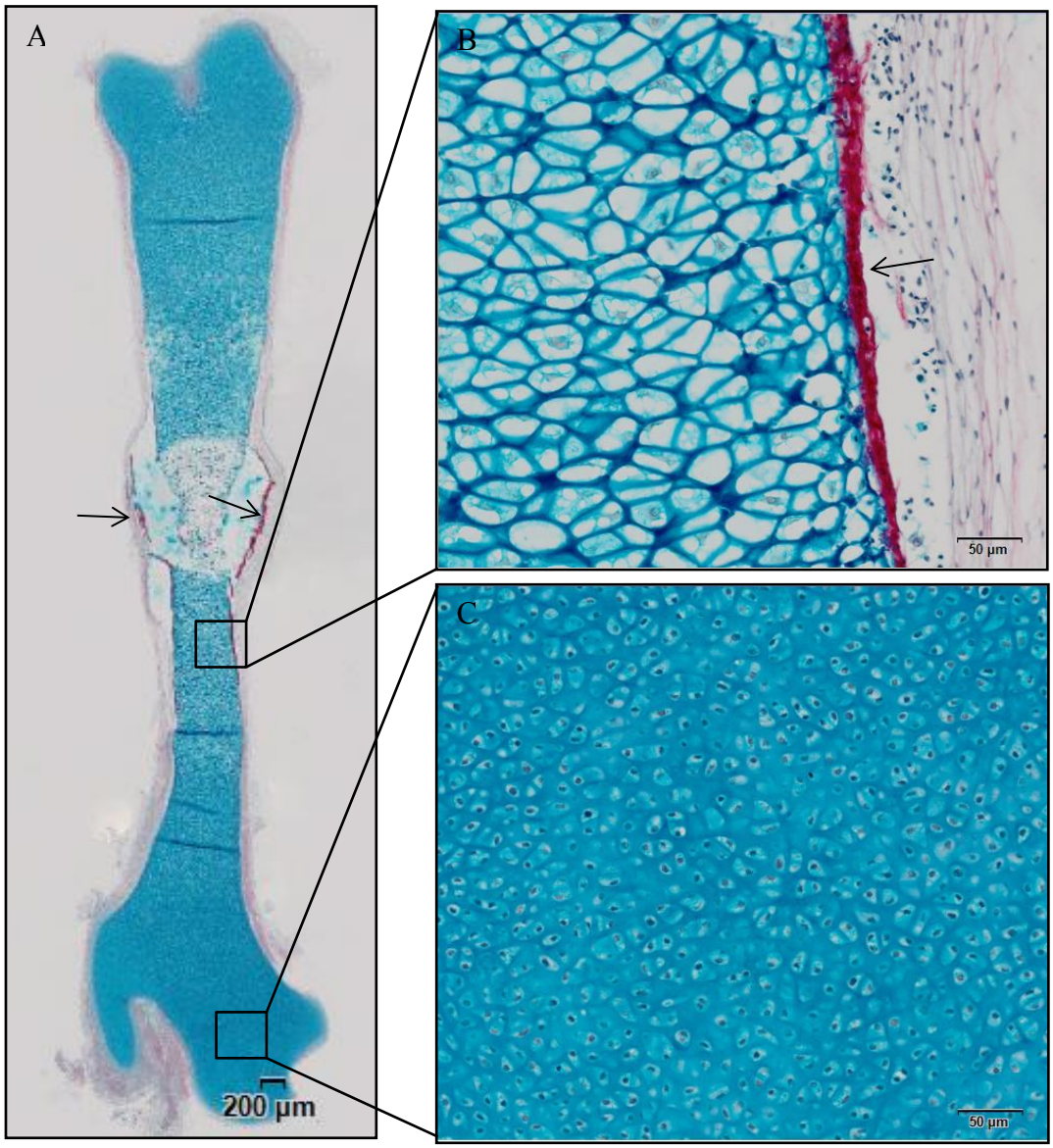

Figure 32. Alcian blue and sirus red staining of the fetal femur aged 59 days (A). Fetal femur is made up of a proteoglycan anlage as indicated by alcian blue staining, predominantly in epiphyseal regions; located at the ends of the fetal femur home to proliferating chondrocytes (C) and the diaphysis; the middle section of the femur which contains hypertrophic chondrocytes and developing bone collar as indicated by sirus red staining (C). Scale bar = 200µm A and 50µm B & C. Arrows indicate the location of the developing bone collar.

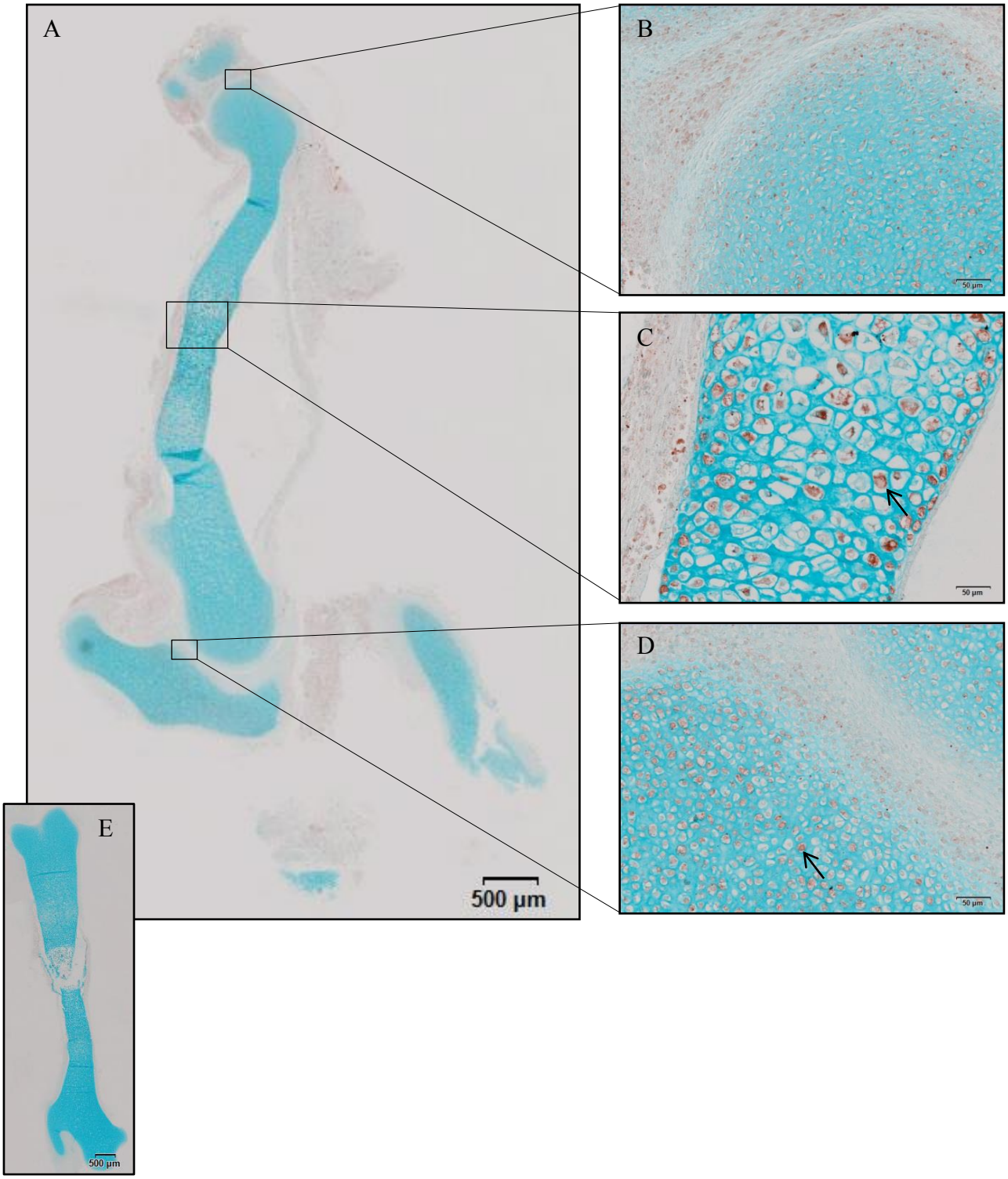

Figure 33. Alcian blue and Stro-1 immunostaining in human fetal femur aged 55 days (A) with Stro-1 staining present in the epiphyses (B & D) and also the middle section; the diaphysis (C). Stro-1 immunostaining was absent in the negative control sample (E). Scale bars = 500µm A and E, 50µm B, C & D.

4.4 Positive cues for chondrogenesis: chondrogenic marker gene expression, chondrogenic histological analysis and microRNA expression.

4.4.1 Chondrogenic marker gene analysis following chondrogenic differentiation assay in fetal femur-derived cells

Cells derived from the fetal femur were expanded for 2 passages to yield a sufficient number of cells for high density micromass culture set-up. Fetal femur derived cells were cultured for 21 days in media containing either TGF-β3 or no TGF-β-3 in a micromass culture system. After 21 days, examination of chondrogenic marker genes by qPCR showed that *SOX9* (median fold change of ~2.4) (Figure 34A), *ACGAN* (median fold change of ~ 4.4) (Figure 34B) and *COL2A1* (median fold change of ~71.3) (Figure 34C) were up-regulated in cells cultured in TGF-β3 compared to cells grown in cultures containing no TGF-β3, confirming that in the presence of TGF-β3, cells differentiate down the chondrogenic lineage (Figure 34).

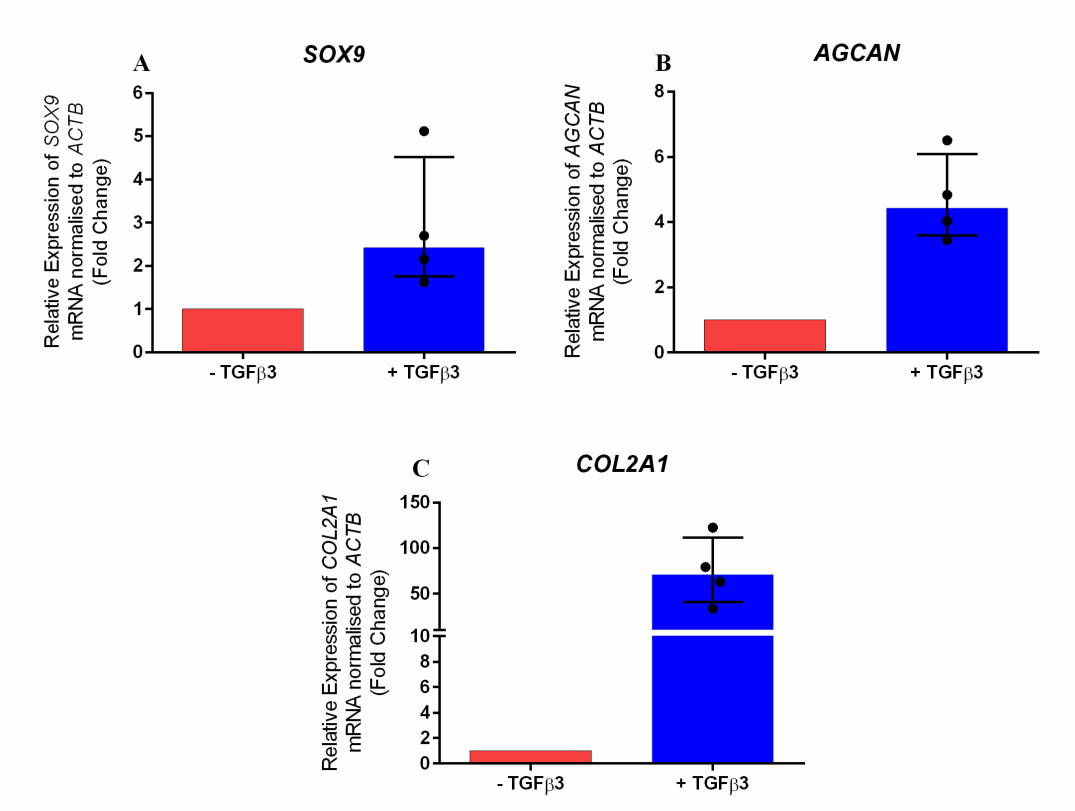

Figure 34. Effect of TGF-β3 treatment for 21 days in human fetal femur-derived cells on mRNA expression. Data is presented as the median and interquartile quartile range of the fold change in *SOX9* (A), *AGCAN* (B) and *COL2A1* (C) mRNA expression in human fetal femur-derived cells cultured in the presence of TGF-β3 for 21 days relative to control untreated fetal femur-derived cells cultured in the absence of TGF-β3 (NC) for 21 days. n=4, Wilcoxon signed rank test.

4.4.2 Histological analysis of chondrogenic differentiation

Micromass cultures processed for histological analysis after 21 days showed that cells cultured in TGF-β3 condensed to form 3D cultures, whereas cells cultured in the absence of TGF-β3 failed to condense and the cells spread out on the tissue culture plastic and grew as a 2D monolayer, indicating TGF-β3 is required for appropriate chondrogenic induction and formation of a 3D culture system. Histological analysis has shown that efficient chondrogenesis occurs in cultures containing TGF-β3 evidenced by the presence of alcian blue (Figure 35) and safranin O staining (Figure 36) compared to the absence of alcian blue and safranin O staining in cells cultured in the absence of TGF-β3. Micromass cultures also showed positive staining for type II collagen (Figure 37) in the presence of TGF-β3 but not in the absence of TGF-β3. Histological analysis indicated that cells cultured in the presence of TGF-β3 successfully differentiated down the chondrogenic lineage.

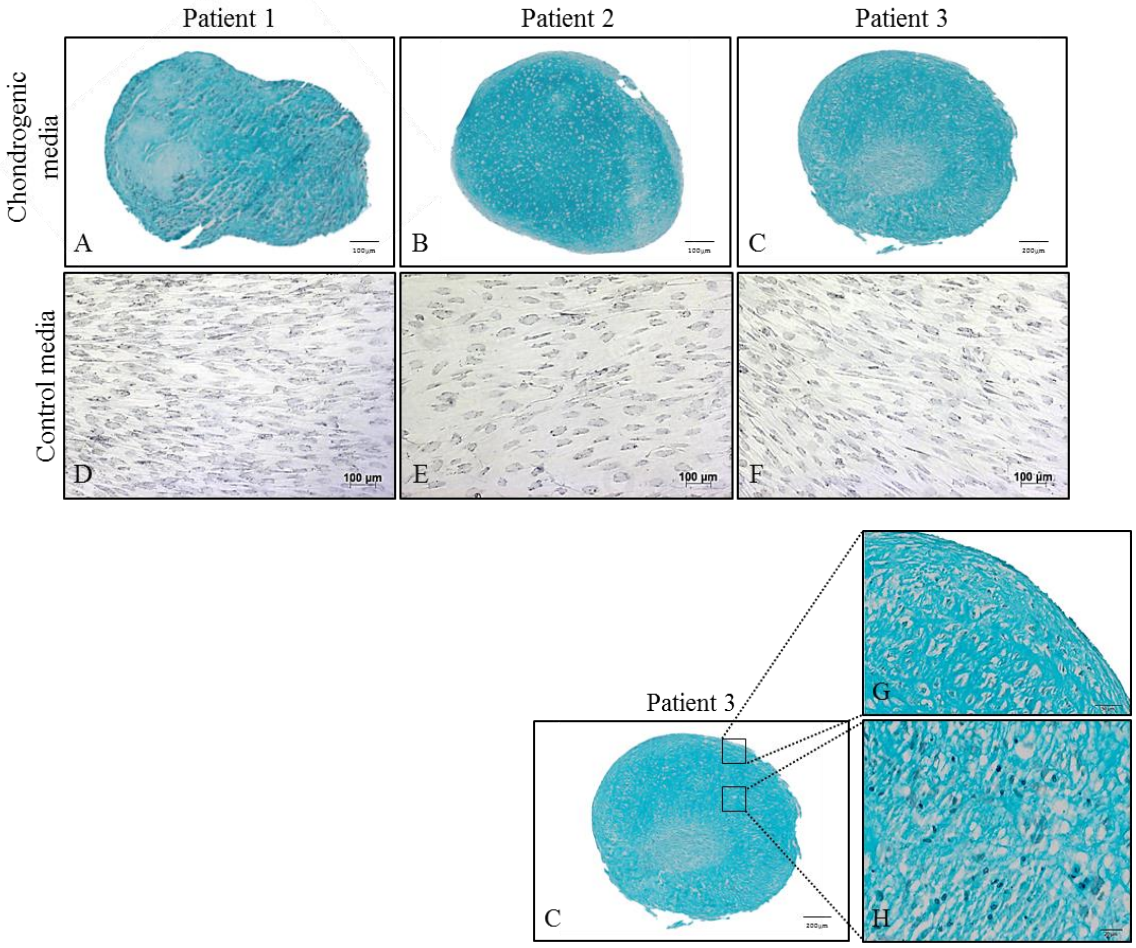

Figure 35. Alcian blue and haematoxylin counterstain in fetal femur-derived micromass cultures after 21 days in the presence of TGF-β3 (A, B, C, G & H) and absence of TGF-β3 (D, E and F) of TGF-β3. Scale bar = 100µm (D, E & F) 200µm (A, B & C) 50µm (G) 20µm (H).

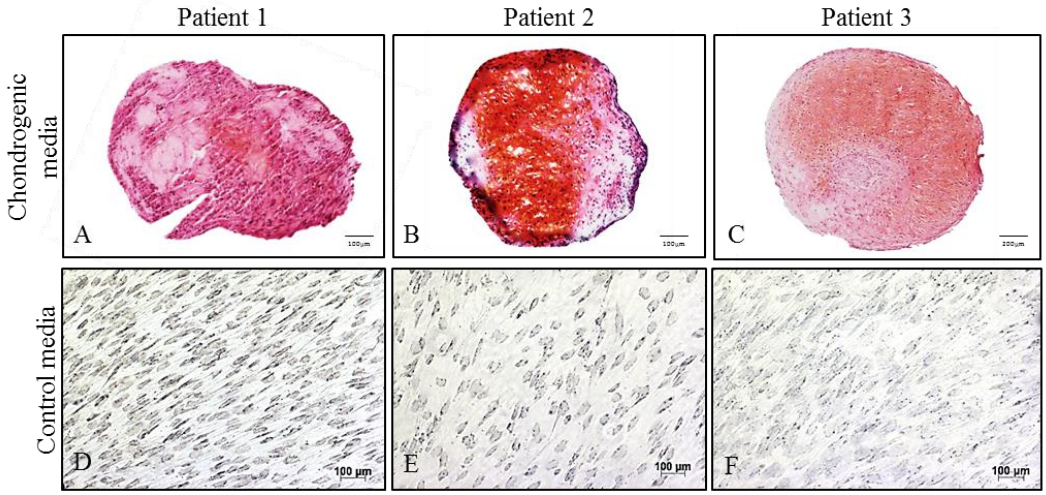

Figure 36. Safranin O and haematoxylin counterstain in fetal femur-derived micromass cultures after 21 days in the presence of TGF-β3 (A, B, C, G & H) and absence of TGF-β3 (D, E and F) of TGF-β3. Scale bar = 100µm (D, E & F) 200µm (A, B & C) 50µm (G & H).

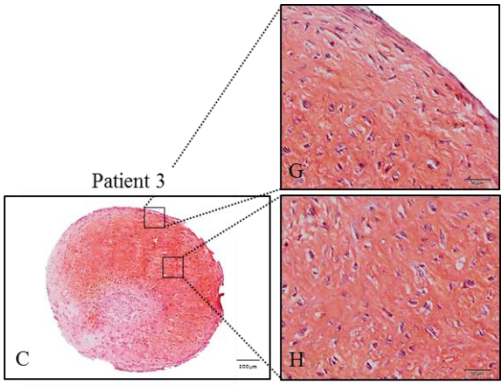

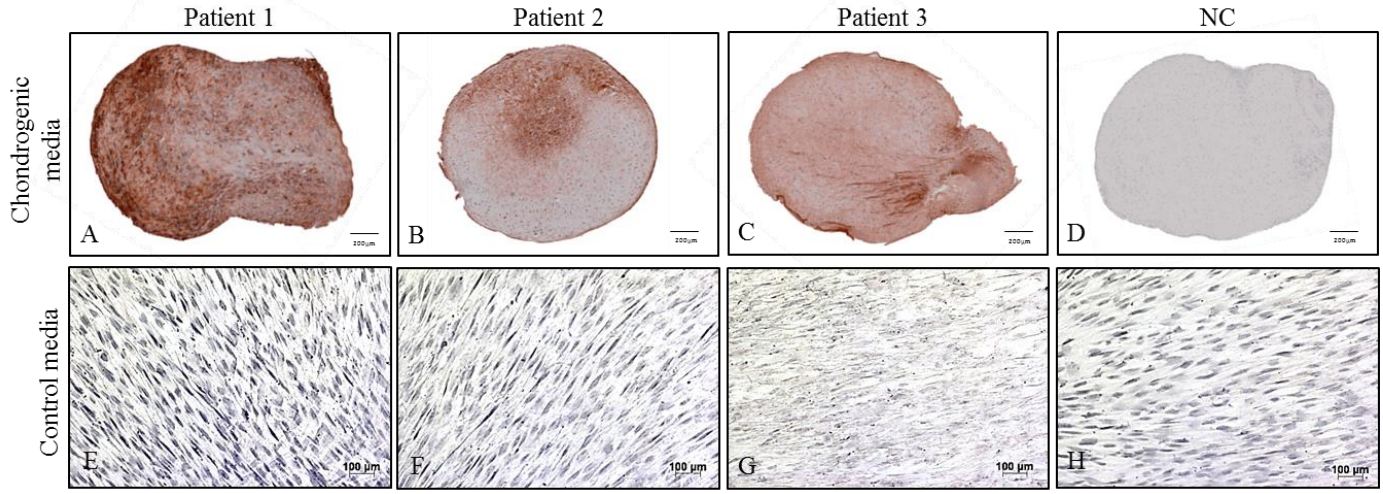

Figure 37. Type II Collagen immunostaining and haematoxylin counterstaining in fetal femur-derived micromass cultures cultured for 21 days in the presence of TGF-β3 (A, B & C) and absence of TGF-β3 (E, F & G) and the absence of type II collagen immunostaining from primary antibody negative control samples (D & H) Scale bars = 200µm (A, B, C & D) 100µm (E, F, G & H) 50µm (I & J).

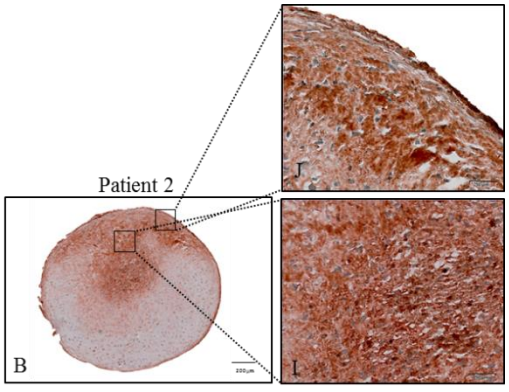

4.4.3 MicroRNA expression following chondrogenic differentiation assay in fetal femur derived cells

Examination of previously identified chondrogenic associated microRNAs by TaqMan qPCR showed that miR-140-3p (median fold change of ~12.4) (Figure 38A), miR-140-5p (median fold change of ~16.4) (Figure 38B) and miR-145 (median fold change of ~3) (Figure 38C) were up-regulated in cells cultured in the presence of TGF-β3 compared to those cells cultured in the absence of TGF-β3 (Figure 38). Examination of expression of miR-34a by TaqMan qPCR showed that miR-34a was up-regulated in cells cultured in the presence of TGF-β3 compared to cells cultured in the absence of TGF-β3, with a median fold change of ~4.4 (Figure 38D).

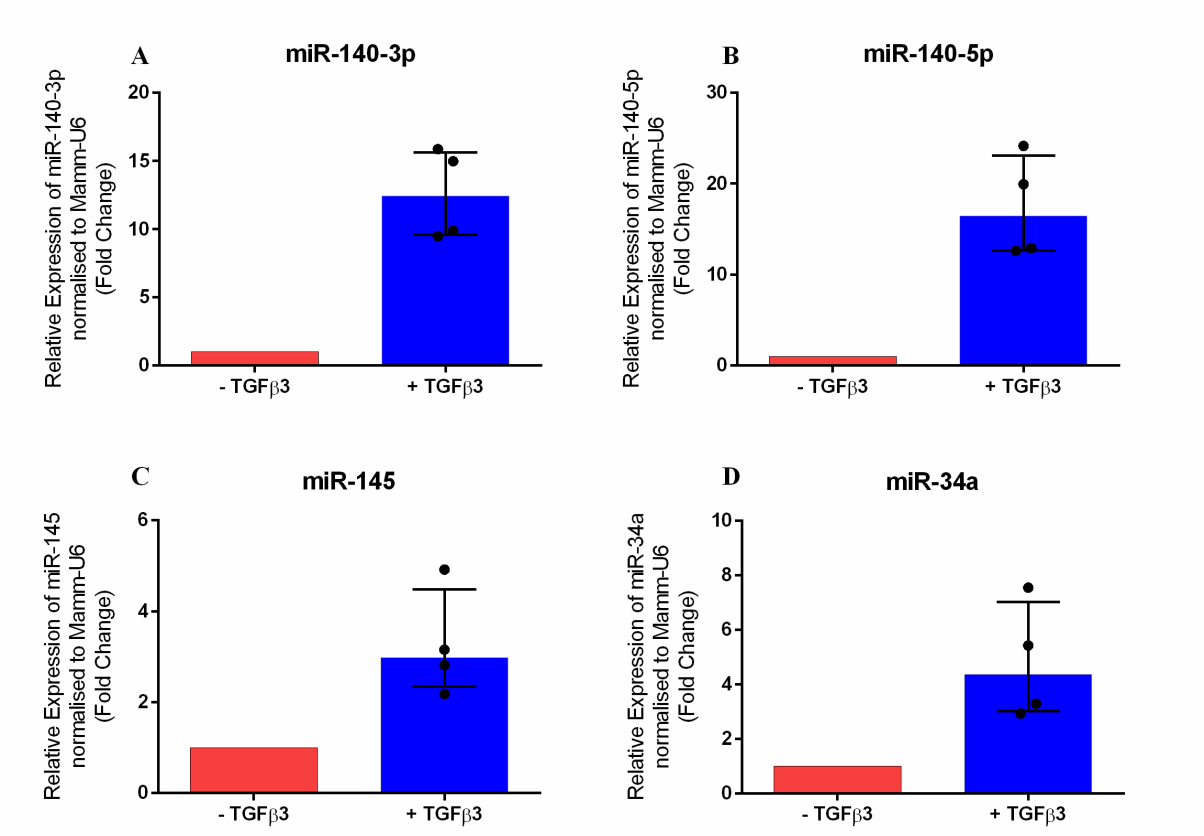

Figure 38. Effect of TGF-β3 treatment for 21 days in human fetal femur-derived cells on miRNA expression. Data is presented as the median and interquartile quartile range of the fold change in miR-140-3p (A), miR-140-5p (B) miR-145 (C) and miR-34a (D) expression in human fetal femur-derived cells cultured in the presence of TGF-β3 for 21 days relative to control untreated fetal femur-derived cells cultured in the absence of TGF-β3 for 21 days (NC). n=4, Wilcoxon signed rank test.

4.5 Time course chondrogenic differentiation assay in fetal femur-derived cells

4.5.1 Chondrogenic marker gene expression across 21 days

Fetal femur derived cells were subject to micromass culture in the presence of TGF-β3 and examined for chondrogenic differentiation potential over 21 days at 7 day timed intervals (day 0, day 7, day 14 and day 21). Examination by qPCR showed that the chondrogenic marker genes; transcription factor *SOX9* (Figure 39A), extracellular matrix product *AGCAN* (Figure 39B) and *COL2A1* (Figure 39C) increase in expression over 21 days in the presence of TGF-β3, with *AGCAN* expression exhibiting significant upregulation at day 14 (median fold change of ~3.3) and day 21 (median fold change of ~3.9) compared to expression at day 0 and *COL2A1* expression showing significant up-regulation at day 21 compared to expression at day 0 (median fold change of ~20,208) (Figure 39).

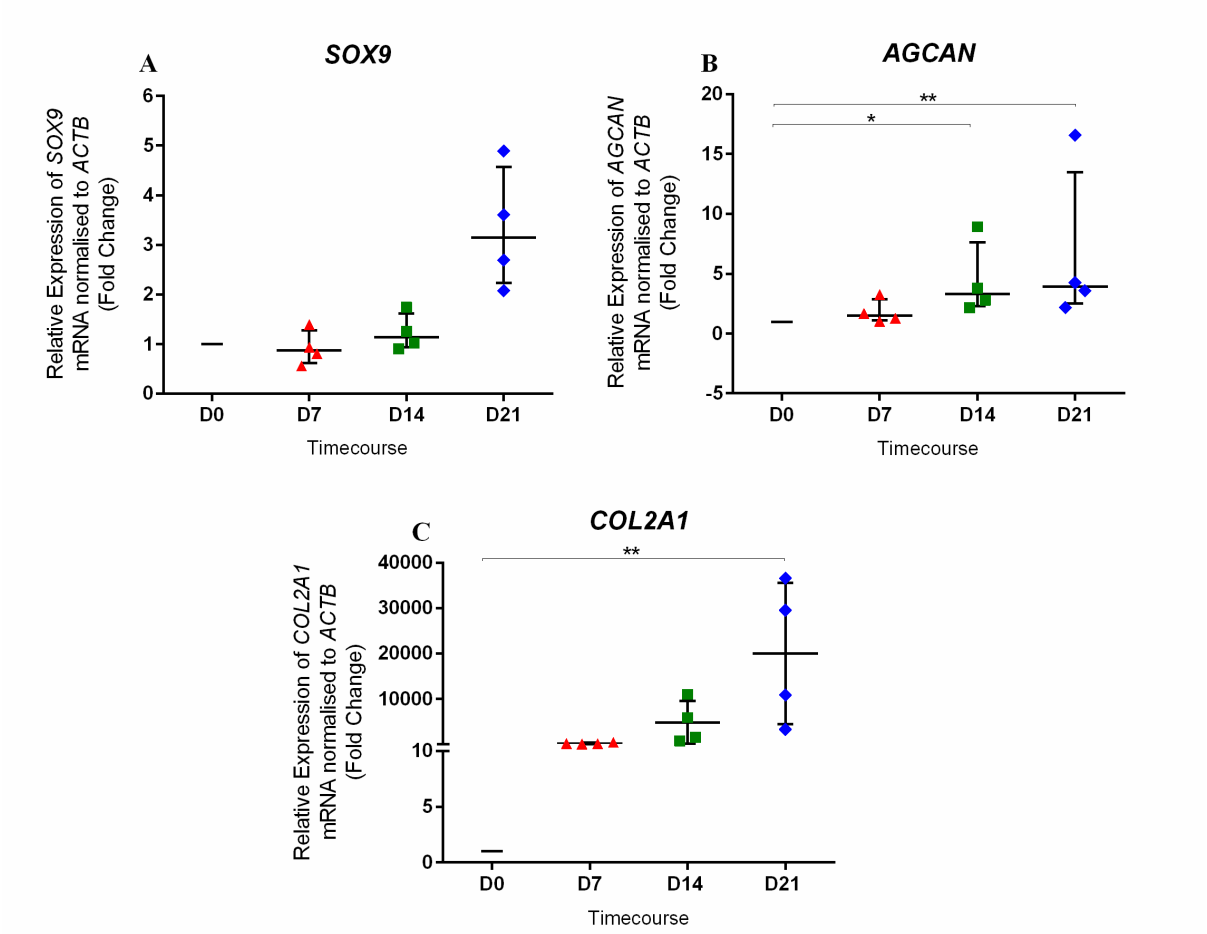

Figure 39. Effect of TGF-β3 treatment for up to 21 days in human fetal femur-derived cells on mRNA expression. Data is presented as the median and interquartile quartile range of the fold change in *SOX9* (A), *AGCAN* (B) and *COL2A1* (C) mRNA expression in human fetal femur-derived cells cultured in the presence of TGF-β3 for up to 21 days relative to control untreated fetal femur-derived cells at day 0 (NC). n=4, * $p < 0.05$, ** $p < 0.01$.Friedman test with Dunn's post-test.

4.5.2 MicroRNA expression across 21 days

The expression of previously identified chondrogenic associated microRNAs; miR-140-3p and miR-140-5p increased in expression across 21 days with miR-145 exhibiting a staggered up-regulated expression (Figure 40ABC). A significant up-regulation in miR-140-3p and miR-140-5p expression was observed at day 21 compared to the expression at day 0 (median fold changes of ~19.2 and ~14.4 respectively). Examination of miR-34a by TaqMan qPCR showed miR-34a was up-regulated across 21 days in cells cultured in the presence of TGF-β3, with a significant difference in miR-34a expression observed at day 21 compared to the expression at day 0 (median fold change of ~2.5) (Figure 40D).

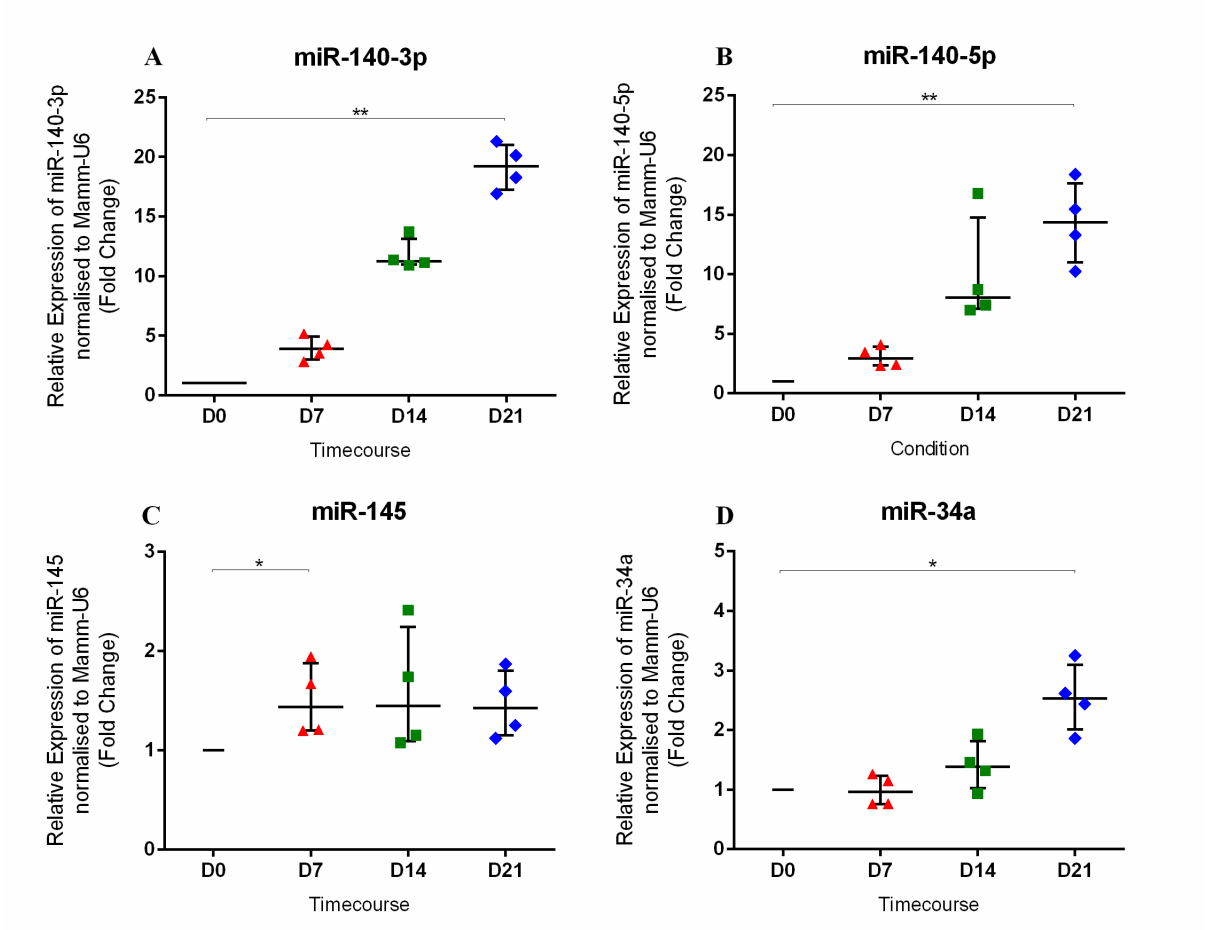

Figure 40. Effect of TGF-β3 treatment for up to 21 days in human fetal femur-derived cells on miRNA expression. Data is presented as the median and interquartile quartile range of the fold change in miR-140-3p (A), miR-140-5p (B) miR-145 (C) and miR-34a (D) expression in human fetal femur-derived cells cultured in the presence of TGF-β3 for up to 21 days relative to control untreated fetal femur-derived cells at day 0 (NC). n=4, * $p < 0.05$, ** $p < 0.01$.Friedman test with Dunn's post-test.

4.6 Bioinformatic analysis of miR-34a

The webserver Target prediction programme, TargetScanHuman was initially used to search for predicted targets of miR-34a. Table 14 lists all of the predicted targets of miR-34a which have been predicted to possess 3'UTR binding sites which complimentary base pair with miR-34a and the predicted number of miR-34a binding sites located within the 3'UTR. From the list of predicted miR-34a mRNA targets, TGF-β-induced factor homeobox 2 (TGIF2) was selected as a target for further experimental validation because *TGIF2* encodes the protein TGIF2; a DNA binding homeobox and translation repressor protein; repressing TGF-β mediated translation [393]. TGIF2 represses TGF-β induced Smad mediated transcription by interacting with TGF-β activated Smad 3 protein and has been shown to interact with DNA via its homeodomain and also interact with HDAC1 [394]. A study employing *in situ* hybridisation has shown the expression pattern of *tgif2* during mouse embryogenesis; exhibiting high expression in Meckel's cartilages and moderate expression in primordial cartilage of the ribs and vertebrate. *TGIF2* expression has been found to increase in response to TGF-β1 treatment hypothesising the action of this TGF-β mediated transcriptional repressor to work via a negative feedback mechanism [395].

The expression of miR-34a was found to be up-regulated during chondrogenic differentiation of fetal femur derived stem cells (Figure 40D) which indicates that miR-34a may be up-regulated to target a negative regulator of chondrogenesis. Searching through the list of predicted targets in table 14, *TGIF2* was selected due to its function as a repressor protein, which inhibits TGF-β mediated transcription and therefore playing a potential negative role in the TGF-β3 induced chondrogenesis. Additionally previous studies in other cell types, listed in table 15, have validated TGIF2 as a target of miR-34a.

In addition to TargetScanHuman, other bioinformatic based target prediction programmes were searched to identify if *TGIF2* mRNA was also predicted to be a potential target of miR-34a. Table 16 lists the microRNA target prediction databases searched and the predicted *TGIF2* mRNA 3'UTR position where miR-34a is predicted to bind. All 5 target prediction programmes all returned a positive match for miR-34a predicted binding to *TGIF2* mRNA also all 5 predicted miR-34a to bind at position 90-97 of *TGIF2* mRNA (Table 16). Figure 41 depicts the structure of mature miR-34a and the structure of miR-34a which is predicted to target *TGIF2*. TagetScanHuman, version 6.2 predicts that *TGIF2* 3'UTR contains only 1 conserved site where miR-34a is predicted to bind. The location of the seed match region whereby miR-34a base pairs at a location within the *TGIF2* 3' UTR is predicted to be located at position 90-97 of *TGIF2* 3'UTR (Figure 41).

TargetScanHuman list of predicted miR-34a mRNA targets

Ortholog of target gene	Representative transcript	Gene name	Conserved sites total	Poorly conserved sites total
MDM4	ENST00000391947.2	Mdm4 p53 binding protein homolog (mouse)	4	3
HCN3	ENST00000368358.3	hyperpolarization activated cyclic nucleotide-gated potassium channel 3	4	2
FAM76A	ENST00000373954.6	family with sequence similarity 76, member A	3	0
SCN2B	ENST00000278947.5	sodium channel, voltage-gated, type II, beta subunit	3	1
SYT1	ENST00000457153.2	synaptotagmin I	4	0
FAM167A	ENST00000284486.4	family with sequence similarity 167, member A	1	3
RRAS	ENST00000246792.3	related RAS viral (r-ras) oncogene homolog	1	1
FUT9	ENST00000302103.5	fucosyltransferase 9 (alpha (1,3) fucosyltransferase)	3	3
MYCN	ENST00000281043.3	v-myc avian myelocytomatosis viral oncogene neuroblastoma derived homolog	2	0
VAMP2	ENST00000316509.6	vesicle-associated membrane protein 2 (synaptobrevin 2)	3	0
SLC23A3	ENST00000396775.3	solute carrier family 23, member 3	1	3
ANK3	ENST00000280772.2	ankyrin 3, node of Ranvier (ankyrin G)	2	1
SAMD12	ENST00000409003.4	sterile alpha motif domain containing 12	1	5
FOSL1	ENST00000448083.2	FOS-like antigen 1	1	1
FKBP1B	ENST00000380991.4	FK506 binding protein 1B, 12.6 kDa	1	1
DLL1	ENST00000366756.3	delta-like 1 (Drosophila)	3	0
PVRL1	ENST00000264025.3	poliovirus receptor-related 1 (herpesvirus entry mediator C)	3	4
FLOT2	ENST00000394906.2	flotillin 2	2	1
CDIP1	ENST00000564828.1	cell death-inducing p53 target 1	1	1
E2F5	ENST00000418930.2	E2F transcription factor 5, p130-binding	1	1
TBCK	ENST00000273980.5	TBC1 domain containing kinase	2	2
TPD52	ENST00000379096.5	tumor protein D52	1	1
TGIF2	ENST00000373874.2	TGFB-induced factor homeobox 2	1	1
KCNK3	ENST00000302909.3	potassium channel, subfamily K, member 3	2	2
TMED8	ENST00000216468.7	transmembrane emp24 protein transport domain containing 8	2	1
LRRC55	ENST00000497933.1	leucine rich repeat containing 55	1	2
PER2	ENST00000254658.3	period circadian clock 2	1	5
CPLX2	ENST00000359546.4	complexin 2	2	1
PNOC	ENST00000301908.3	prepronociceptin	1	0
SMIM15	ENST00000339020.3	small integral membrane protein 15	1	0
IGSF1	ENST00000370900.1	immunoglobulin superfamily, member 1	1	1
CUEDC1	ENST00000577830.1	CUE domain containing 1	2	0
ELMOD1	ENST00000265840.7	ELMO/CED-12 domain containing 1	1	1
DGKH	ENST00000261491.5	diacylglycerol kinase, eta	1	6
ATG4B	ENST00000404914.3	autophagy related 4B, cysteine peptidase	1	0
AREGB	ENST00000380846.3	amphiregulin B	1	0
GABRA3	ENST00000370314.4	gamma-aminobutyric acid (GABA) A receptor, alpha 3	1	1
LMBR1L	ENST00000267102.8	limb development membrane protein 1-like	1	0
NUMBL	ENST00000252891.4	numb homolog (Drosophila)-like	2	0
NAV3	ENST00000228327.6	neuron navigator 3	3	0
FXYD2	ENST00000528014.1	FXYD domain containing ion transport regulator 2	1	0

MARCH8	ENST00000453424.2	membrane-associated ring finger (C3HC4) 8, E3 ubiquitin protein ligase	1	1
SATB2	ENST00000417098.1	SATB homeobox 2	2	0
ALDOA	ENST00000569798.1	aldolase A, fructose-bisphosphate	1	0
DPYSL4	ENST00000338492.4	dihydropyrimidinase-like 4	2	0
SGSM2	ENST00000426855.2	small G protein signaling modulator 2	2	2
GMNC	ENST00000442080.1	geminin coiled-coil domain containing	1	0
LGR4	ENST00000379214.4	leucine-rich repeat containing G protein-coupled receptor 4	1	1
HOXA13	ENST00000222753.4	homeobox A13	1	1
PREB	ENST00000260643.2	prolactin regulatory element binding	1	1
BRINP1	ENST00000265922.3	bone morphogenetic protein/retinoic acid inducible neural-specific 1	1	0
AREG	ENST00000395748.3	amphiregulin	1	0
TMEM200B	ENST00000521452.1	transmembrane protein 200B	2	0
SURF4	ENST00000545297.1	surfeit 4	1	1
ERGIC1	ENST00000393784.3	endoplasmic reticulum-golgi intermediate compartment (ERGIC) 1	2	0
MET	ENST00000397752.3	met proto-oncogene	2	0
XYLT1	ENST00000261381.6	xylosyltransferase I	1	4
ANKRD52	ENST00000267116.7	ankyrin repeat domain 52	2	3
PEG10	ENST00000482108.1	paternally expressed 10	3	0
MPP2	ENST00000377184.3	membrane protein, palmitoylated 2 (MAGUK p55 subfamily member 2)	2	1
LEF1	ENST00000265165.1	lymphoid enhancer-binding factor 1	1	0
VPS4A	ENST00000254950.11	vacuolar protein sorting 4 homolog A (S. cerevisiae)	1	3
FAM175B	ENST00000298492.5	family with sequence similarity 175, member B	1	0
ZDHHC16	ENST00000345745.5	zinc finger, DHHC-type containing 16	1	0
FGD6	ENST00000343958.4	FYVE, RhoGEF and PH domain containing 6	1	1
SPRN	ENST00000414069.2	shadow of prion protein homolog (zebrafish)	1	1
LRRC40	ENST00000370952.3	leucine rich repeat containing 40	1	0
NRIP3	ENST00000309166.3	nuclear receptor interacting protein 3	1	0
CCNE2	ENST00000520509.1	cyclin E2	1	0
GAS1	ENST00000298743.7	growth arrest-specific 1	1	0
EVI5L	ENST00000270530.4	ecotropic viral integration site 5-like	2	0
NAV1	ENST00000295624.6	neuron navigator 1	3	1
TMEM246	ENST00000374847.1	transmembrane protein 246	2	0
ORAI3	ENST00000318663.4	ORAI calcium release-activated calcium modulator 3	2	0
RAB43	ENST00000476465.1	RAB43, member RAS oncogene family	1	3
LIMD2	ENST00000259006.3	LIM domain containing 2	1	1
HSPA1B	ENST00000375650.3	heat shock 70kDa protein 1B	1	0
GNAO1	ENST00000262493.6	guanine nucleotide binding protein (G protein), alpha activating activity polypeptide O	1	0
CALCR	ENST00000359558.2	calcitonin receptor	2	0
FUT8	ENST00000360689.5	fucosyltransferase 8 (alpha (1,6) fucosyltransferase)	1	0
RCAN1	ENST00000482533.1	regulator of calcineurin 1	1	1
PPP2R3A	ENST00000264977.3	protein phosphatase 2, regulatory subunit B", alpha	1	1
RPS6KL1	ENST00000555647.1	ribosomal protein S6 kinase-like 1	2	0
DNAH10OS	ENST00000514254.2	dynein, axonemal, heavy chain 10 opposite strand	1	2
FAM117B	ENST00000392238.2	family with sequence similarity 117, member B	1	1
SLC30A3	ENST00000233535.4	solute carrier family 30 (zinc transporter), member 3	1	0

STX1A	ENST00000395156.3	syntaxin 1A (brain)	1	1
TMEM184B	ENST00000361906.3	transmembrane protein 184B	1	2
ZNF281	ENST00000294740.3	zinc finger protein 281	1	0
TMUB2	ENST00000590235.1	transmembrane and ubiquitin-like domain containing 2	1	0
TSPAN18	ENST00000340160.3	tetraspanin 18	1	1
KLF4	ENST00000374672.4	Kruppel-like factor 4 (gut)	1	0
VPS37B	ENST00000267202.2	vacuolar protein sorting 37 homolog B (S. cerevisiae)	1	2
AMER1	ENST00000330258.3	APC membrane recruitment protein 1	1	3
PDGFRA	ENST00000257290.5	platelet-derived growth factor receptor, alpha polypeptide	2	0
TTC19	ENST00000261647.5	tetratricopeptide repeat domain 19	1	0
SERPINF2	ENST00000382061.4	serpin peptidase inhibitor, clade F (alpha-2 antiplasmin, pigment epithelium derived factor), member 2	1	0
CA7	ENST00000394069.3	carbonic anhydrase VII	1	0
GRIN2B	ENST00000609686.1	glutamate receptor, ionotropic, N-methyl D-aspartate 2B	1	1
HTR2C	ENST00000371950.3	5-hydroxytryptamine (serotonin) receptor 2C, G protein-coupled	1	0
MYADM	ENST00000391770.4	myeloid-associated differentiation marker	1	1
LZTS3	ENST00000329152.3	Homo sapiens leucine zipper, putative tumor suppressor family member 3 (LZTS3), transcript variant 2, mRNA.	1	2
JAKMIP1	ENST00000282924.5	janus kinase and microtubule interacting protein 1	1	0
ESYT3	ENST00000389567.4	extended synaptotagmin-like protein 3	1	2
RTN4RL1	ENST00000331238.6	reticulon 4 receptor-like 1	1	0
AXL	ENST00000301178.4	AXL receptor tyrosine kinase	1	0
ASIC2	ENST00000225823.2	acid-sensing (proton-gated) ion channel 2	1	0
BMP3	ENST00000282701.2	bone morphogenetic protein 3	1	1
DGKZ	ENST00000343674.6	diacylglycerol kinase, zeta	1	0
C9orf69	ENST00000561457.1	chromosome 9 open reading frame 69	1	1
NOTCH1	ENST00000277541.6	notch 1	1	1
HNF4A	ENST00000316099.4	hepatocyte nuclear factor 4, alpha	2	1
SGPP1	ENST00000247225.6	sphingosine-1-phosphate phosphatase 1	1	0
PLAG1	ENST00000316981.3	pleiomorphic adenoma gene 1	1	0
TUSC5	ENST00000333813.3	tumor suppressor candidate 5	1	1
ZNF282	ENST00000479907.1	zinc finger protein 282	1	1
RSPO4	ENST00000217260.4	R-spondin 4	1	1
MAP2K1	ENST00000307102.5	mitogen-activated protein kinase kinase 1	1	0
GCH1	ENST00000491895.2	GTP cyclohydrolase 1	1	1
ZCCHC17	ENST00000344147.5	zinc finger, CCHC domain containing 17	1	1
VAT1	ENST00000355653.3	vesicle amine transport 1	1	0
RALGPS2	ENST00000367635.3	Ral GEF with PH domain and SH3 binding motif 2	2	0
DMWD	ENST00000377735.3	dystrophia myotonica, WD repeat containing	1	0
TSN	ENST00000536142.1	translin	1	1
CAPN6	ENST00000324068.1	calpain 6	1	1
ARHGAP19-SLIT1	ENST00000453547.2	ARHGAP19-SLIT1 readthrough (NMD candidate)	3	3
DHRS13	ENST00000378895.4	dehydrogenase/reductase (SDR family) member 13	1	0
PEA15	ENST00000360472.4	phosphoprotein enriched in astrocytes 15	1	0
FOXJ2	ENST00000162391.3	forkhead box J2	1	1
ZNF304	ENST00000391705.3	zinc finger protein 304	1	1
GALNT7	ENST00000265000.4	UDP-N-acetyl-alpha-D-galactosamine:polypeptide N-acetylgalactosaminyltransferase 7 (GalNAc-T7)	1	1

TMEM126B	ENST00000534341.1	transmembrane protein 126B	1	0
ISY1-RAB43	ENST00000418265.1	ISY1-RAB43 readthrough	1	3
SHISA7	ENST00000376325.4	shisa family member 7	2	1
KCND3	ENST00000369697.1	potassium voltage-gated channel, Shal-related subfamily, member 3	1	2
DDX17	ENST00000396821.3	DEAD (Asp-Glu-Ala-Asp) box helicase 17	1	0
DNAJC24	ENST00000465995.1	DnaJ (Hsp40) homolog, subfamily C, member 24	1	0
SNTB2	ENST00000336278.4	syntrophin, beta 2 (dystrophin-associated protein A1, 59kDa, basic component 2)	1	1
RAP1GDS1	ENST00000408927.3	RAP1, GTP-GDP dissociation stimulator 1	1	1
LINC00998	ENST00000397764.3	long intergenic non-protein coding RNA 998	1	1
LDHA	ENST00000227157.4	lactate dehydrogenase A	1	0
LPAR2	ENST00000586703.1	lysophosphatidic acid receptor 2	1	3
ZDHHC17	ENST00000426126.2	zinc finger, DHHC-type containing 17	1	0
ROCK1	ENST00000399799.2	Rho-associated, coiled-coil containing protein kinase 1	1	2
E2F3	ENST00000346618.3	E2F transcription factor 3	1	0
GREM2	ENST00000318160.4	gremlin 2, DAN family BMP antagonist	1	0
DIXDC1	ENST00000440460.2	DIX domain containing 1	1	0
NETO1	ENST00000327305.6	neuropilin (NRP) and tolloid (TLL)-like 1	1	0
RDH11	ENST00000381346.4	retinol dehydrogenase 11 (all-trans/9-cis/11-cis)	1	1
CORO1C	ENST00000261401.3	coronin, actin binding protein, 1C	1	0
MAPT	ENST00000344290.5	microtubule-associated protein tau	1	2
INA	ENST00000369849.4	internexin neuronal intermediate filament protein, alpha	1	0
STRN3	ENST00000355683.5	striatin, calmodulin binding protein 3	1	0
NOS1AP	ENST00000361897.5	nitric oxide synthase 1 (neuronal) adaptor protein	1	2
OSGIN2	ENST00000451899.2	oxidative stress induced growth inhibitor family member 2	1	0
PEAK1	ENST00000312493.4	pseudopodium-enriched atypical kinase 1	1	2
POGZ	ENST00000392723.1	pogo transposable element with ZNF domain	1	0
CALN1	ENST00000329008.5	calneuron 1	1	1
DCP1A	ENST00000607628.1	decapping mRNA 1A	1	1
ONECUT2	ENST00000491143.2	one cut homeobox 2	1	3
GNAQ	ENST00000286548.4	guanine nucleotide binding protein (G protein), q polypeptide	1	1
UBP1	ENST00000283629.3	upstream binding protein 1 (LBP-1a)	1	1
PRRG3	ENST00000370353.3	proline rich Gla (G-carboxyglutamic acid) 3 (transmembrane)	1	1
ACBD3	ENST00000366812.5	acyl-CoA binding domain containing 3	1	0
NDST1	ENST00000261797.6	N-deacetylase/N-sulfotransferase (heparan glucosaminyl) 1	3	2
CR2	ENST00000367058.3	complement component (3d/Epstein Barr virus) receptor 2	1	0
DNAJC16	ENST00000375847.3	DnaJ (Hsp40) homolog, subfamily C, member 16	1	1
RGS17	ENST00000367225.2	regulator of G-protein signaling 17	1	0
FOXP1	ENST00000318789.4	forkhead box P1	2	0
C3orf58	ENST00000441925.2	chromosome 3 open reading frame 58	1	0
SEPT3	ENST00000396425.3	septin 3	1	2
BNC2	ENST00000380672.4	basonuclin 2	2	1
ADAM10	ENST00000260408.3	ADAM metallopeptidase domain 10	1	1
VTI1B	ENST00000554659.1	vesicle transport through interaction with t-SNAREs 1B	1	2
HNRNPA1	ENST00000546500.1	heterogeneous nuclear ribonucleoprotein A1	1	0
SIDT1	ENST00000264852.4	SID1 transmembrane family, member 1	1	0

CTDSPL	ENST00000443503.2	CTD (carboxy-terminal domain, RNA polymerase II, polypeptide A) small phosphatase-like	1	1
CACNB3	ENST00000301050.2	calcium channel, voltage-dependent, beta 3 subunit	1	0
NCEH1	ENST00000475381.1	neutral cholesterol ester hydrolase 1	1	0
PHF15	ENST00000395003.1	PHD finger protein 15	1	2
ARHGAP1	ENST00000311956.4	Rho GTPase activating protein 1	1	0
WASF1	ENST00000392587.2	WAS protein family, member 1	1	0
AP3S2	ENST00000336418.4	adaptor-related protein complex 3, sigma 2 subunit	1	2
RIC8B	ENST00000392837.4	RIC8 guanine nucleotide exchange factor B	1	0
CTNND2	ENST00000304623.8	catenin (cadherin-associated protein), delta 2	1	0
TRANK1	ENST00000428977.2	tetratricopeptide repeat and ankyrin repeat containing 1	1	0
RRAGC	ENST00000373001.3	Ras-related GTP binding C	1	0
CHST12	ENST00000258711.6	carbohydrate (chondroitin 4) sulfotransferase 12	1	1
STK38L	ENST00000389032.3	serine/threonine kinase 38 like	1	1*
KIAA1217	ENST00000396445.1	KIAA1217	1	0
SNX15	ENST00000377244.3	sorting nexin 15	1	0
BCL2L13	ENST00000355028.3	BCL2-like 13 (apoptosis facilitator)	1	0
EML5	ENST00000554922.1	echinoderm microtubule associated protein like 5	1	0
LIN54	ENST00000395282.2	lin-54 homolog (C. elegans)	1	1
KIAA1210	ENST00000402510.2	KIAA1210	1	1
AL117190.3	ENST00000599197.1	Esophagus cancer-related gene-2 interaction susceptibility protein; Uncharacterized protein	1	1
ARHGAP26	ENST00000378004.3	Rho GTPase activating protein 26	1	0
SLC25A27	ENST00000371347.5	solute carrier family 25, member 27	1	1
ARHGAP36	ENST00000370922.1	Rho GTPase activating protein 36	1	0
CDK6	ENST00000265734.4	cyclin-dependent kinase 6	1	2
SDK2	ENST00000392650.3	sidekick cell adhesion molecule 2	1	4
GPR22	ENST00000304402.4	G protein-coupled receptor 22	1	0
CBFA2T3	ENST00000327483.5	core-binding factor, runt domain, alpha subunit 2; translocated to, 3	1	0
NOTCH2	ENST00000256646.2	notch 2	1	0
ATP5S	ENST00000245448.6	ATP synthase, H+ transporting, mitochondrial Fo complex, subunit s (factor B)	1	0
PACS1	ENST00000320580.4	phosphofurin acidic cluster sorting protein 1	2	0
ATMIN	ENST00000299575.4	ATM interactor	1	0
RPS6KA4	ENST00000528057.1	ribosomal protein S6 kinase, 90kDa, polypeptide 4	1	1
KIAA1462	ENST00000375377.1	KIAA1462	1	0
ORMDL3	ENST00000304046.2	ORM1-like 3 (S. cerevisiae)	1	0
SPRY1	ENST00000394339.2	sprouty homolog 1, antagonist of FGF signaling (Drosophila)	1	1
CCDC135	ENST00000394337.4	coiled-coil domain containing 135	1	0
LMAN2L	ENST00000264963.4	lectin, mannose-binding 2-like	1	0
FRK	ENST00000606080.1	fyn-related kinase	1	1
TMEM251	ENST00000415050.2	transmembrane protein 251	1	1
YY1	ENST00000262238.4	YY1 transcription factor	1	1
TMCC3	ENST00000261226.4	transmembrane and coiled-coil domain family 3	1	1
ADO	ENST00000373783.1	2-aminoethanethiol (cysteamine) dioxygenase	1	0
TMEM25	ENST00000411589.2	transmembrane protein 25	1	0
IL6R	ENST00000344086.4	interleukin 6 receptor	1	1
MYRIP	ENST00000302541.6	myosin VIIA and Rab interacting protein	2	0

CADM4	ENST00000222374.2	cell adhesion molecule 4	1	0
ITSN1	ENST00000379960.5	intersectin 1 (SH3 domain protein)	1	0
RAE1	ENST00000395841.2	ribonucleic acid export 1	1	0
PALLD	ENST00000261509.6	palladin, cytoskeletal associated protein	1	0
PPP1R11	ENST00000376773.1	protein phosphatase 1, regulatory (inhibitor) subunit 11	2	0
RAB21	ENST00000261263.3	RAB21, member RAS oncogene family	1	1
CERS6	ENST00000305747.6	ceramide synthase 6	1	0
PGM1	ENST00000371084.3	phosphoglucomutase 1	1	0
PEX5L	ENST00000467460.1	peroxisomal biogenesis factor 5-like	1	1
BTBD11	ENST00000280758.5	BTB (POZ) domain containing 11	1	1
SVIP	ENST00000354193.4	small VCP/p97-interacting protein	1	0
MTMR9	ENST00000221086.3	myotubularin related protein 9	2	0
LMAN1	ENST00000251047.5	lectin, mannose-binding, 1	1	0
AMER2	ENST00000357816.2	APC membrane recruitment protein 2	1	0
RANBP10	ENST00000317506.3	RAN binding protein 10	1	2
GK5	ENST00000392993.2	glycerol kinase 5 (putative)	1	0
LYPLAL1	ENST00000366928.5	lysophospholipase-like 1	1	0
FOXN2	ENST00000340553.3	forkhead box N2	2	0
ZMYM4	ENST00000314607.6	zinc finger, MYM-type 4	1	0
GPR158	ENST00000376351.3	G protein-coupled receptor 158	1	0
TOM1	ENST00000447733.1	target of myb1 (chicken)	1	1
B3GAT1	ENST00000392580.1	beta-1,3-glucuronyltransferase 1 (glucuronosyltransferase P)	1	1
MAP1A	ENST00000382031.1	microtubule-associated protein 1A	1	1
C1QL3	ENST00000298943.3	complement component 1, q subcomponent-like 3	1	0
LCMT2	ENST00000567039.1	leucine carboxyl methyltransferase 2	1	1
SGTA	ENST00000221566.2	small glutamine-rich tetratricopeptide repeat (TPR)-containing, alpha	1	0
ADK	ENST00000372734.3	adenosine kinase	1	0
LGI1	ENST00000542308.1	leucine-rich, glioma inactivated 1	1	0
GPR85	ENST00000297146.3	G protein-coupled receptor 85	1	1
ELL2	ENST00000237853.4	elongation factor, RNA polymerase II, 2	1	1
SLC6A1	ENST00000287766.4	solute carrier family 6 (neurotransmitter transporter), member 1	1	1
PPARGC1B	ENST00000309241.5	peroxisome proliferator-activated receptor gamma, coactivator 1 beta	2	0
C8orf37	ENST00000286688.5	chromosome 8 open reading frame 37	1	0
PLEKHH2	ENST00000282406.4	pleckstrin homology domain containing, family H (with MyTH4 domain) member 2	1	0
CREB3L1	ENST00000529193.1	cAMP responsive element binding protein 3-like 1	1	0
METAP1	ENST00000296411.6	methionyl aminopeptidase 1	1	0
NDC1	ENST00000540001.1	NDC1 transmembrane nucleoporin	1	0
GRM7	ENST00000486284.1	glutamate receptor, metabotropic 7	1	0
APH1A	ENST00000360244.4	APH1A gamma secretase subunit	1	0
ATXN7L3B	ENST00000519948.2	ataxin 7-like 3B	1	1
PKIA	ENST00000396418.2	protein kinase (cAMP-dependent, catalytic) inhibitor alpha	1	0
NR4A2	ENST00000339562.4	nuclear receptor subfamily 4, group A, member 2	1	0
CAMK4	ENST00000282356.4	calcium/calmodulin-dependent protein kinase IV	1	1
ZNF275	ENST00000370251.3	zinc finger protein 275	1	2
UHRF2	ENST00000276893.5	ubiquitin-like with PHD and ring finger domains 2, E3 ubiquitin protein ligase	1	0

FAM46A	ENST00000369754.3	family with sequence similarity 46, member A	1	1
TMEM52B	ENST00000298530.3	transmembrane protein 52B	1	0
THSD4	ENST00000355327.3	thrombospondin, type I, domain containing 4	1	2
DCX	ENST00000356915.2	doublecortin	1	0
PRKD1	ENST00000331968.5	protein kinase D1	1	1
PPP4R2	ENST00000356692.5	protein phosphatase 4, regulatory subunit 2	1	0
USF1	ENST00000368020.1	upstream transcription factor 1	1	0
SIDT2	ENST00000324225.4	SID1 transmembrane family, member 2	2	0
CCDC85A	ENST00000407595.2	coiled-coil domain containing 85A	1	0
CASP2	ENST00000310447.5	caspase 2, apoptosis-related cysteine peptidase	1	0
RALGDS	ENST00000372050.3	ral guanine nucleotide dissociation stimulator	1	0
PAX5	ENST00000358127.4	paired box 5	1	1
VPS37A	ENST00000324849.4	vacuolar protein sorting 37 homolog A (S. cerevisiae)	1	0
MTA2	ENST00000278823.2	metastasis associated 1 family, member 2	1	0
PROX1	ENST00000366958.4	prospero homeobox 1	1	0
CSF1R	ENST00000286301.3	colony stimulating factor 1 receptor	1	0
CELF3	ENST00000290585.4	CUGBP, Elav-like family member 3	2	0
FUT11	ENST00000394790.1	fucosyltransferase 11 (alpha (1,3) fucosyltransferase)	1	0
POMGNT1	ENST00000396420.3	protein O-linked mannose N-acetylglucosaminyltransferase 1 (beta 1,2-)	1	0
SRPR	ENST00000332118.6	signal recognition particle receptor (docking protein)	1	0
BCL2	ENST00000398117.1	B-cell CLL/lymphoma 2	1	0
BRPF3	ENST00000357641.6	bromodomain and PHD finger containing, 3	1	0
CNTN2	ENST00000331830.4	contactin 2 (axonal)	1	1
LIN28A	ENST00000326279.6	lin-28 homolog A (C. elegans)	1	0
ADD2	ENST00000264436.4	adducin 2 (beta)	1	1
LRRTM2	ENST00000274711.6	leucine rich repeat transmembrane neuronal 2	1	1
FBXO10	ENST00000432825.2	F-box protein 10	1	1
NRXN2	ENST00000301894.2	neurexin 2	1	0
IKZF1	ENST00000331340.3	IKAROS family zinc finger 1 (Ikaros)	1	0
GPR12	ENST00000405846.3	G protein-coupled receptor 12	1	0
TMEM109	ENST00000227525.3	transmembrane protein 109	1	0
MCFD2	ENST00000444761.2	multiple coagulation factor deficiency 2	1	1
ZC3H12B	ENST00000338957.4	zinc finger CCCH-type containing 12B	1	0
DAAM1	ENST00000395125.1	dishevelled associated activator of morphogenesis 1	1	0
TRIM41	ENST00000315073.5	tripartite motif containing 41	1	0
PARD6B	ENST00000371610.2	par-6 family cell polarity regulator beta	1	0
ANK2	ENST00000357077.4	ankyrin 2, neuronal	1	0
MPPED2	ENST00000358117.5	metallophosphoesterase domain containing 2	1	0
SOX4	ENST00000244745.1	SRY (sex determining region Y)-box 4	1	0
FBXO30	ENST00000237281.4	F-box protein 30	1	0
CES4A	ENST00000540947.2	carboxylesterase 4A	1	1
AAGAB	ENST00000261880.5	alpha- and gamma-adaptin binding protein	1	0
C15orf38-AP3S2	ENST00000398333.3	C15orf38-AP3S2 readthrough	1	2
ZNF641	ENST00000301042.3	zinc finger protein 641	1	2
ATP1A2	ENST00000361216.3	ATPase, Na+/K+ transporting, alpha 2 polypeptide	1	0

PLA2G15	ENST00000219345.5	phospholipase A2, group XV	1	0
MLLT3	ENST00000380338.4	myeloid/lymphoid or mixed-lineage leukemia (trithorax homolog, Drosophila); translocated to, 3	2	0
CRTC1	ENST00000338797.6	CREB regulated transcription coactivator 1	1	0
AGTRAP	ENST00000376627.2	angiotensin II receptor-associated protein	1	1
UNC13C	ENST00000545554.1	unc-13 homolog C (C. elegans)	1	0
HDAC1	ENST00000373548.3	histone deacetylase 1	1	0
CACNA1E	ENST00000526775.1	calcium channel, voltage-dependent, R type, alpha 1E subunit	2	2
AGO4	ENST00000373210.3	argonaute RISC catalytic component 4	1	0
MAGT1	ENST00000358075.6	magnesium transporter 1	1	1
CNTNAP2	ENST00000361727.3	contactin associated protein-like 2	1	0
RASGRP4	ENST00000586305.1	RAS guanyl releasing protein 4	1	0
F2RL2	ENST00000296641.4	coagulation factor II (thrombin) receptor-like 2	1	0
SLC44A2	ENST00000335757.5	solute carrier family 44 (choline transporter), member 2	1	0
PIP5K1A	ENST00000368890.4	phosphatidylinositol-4-phosphate 5-kinase, type I, alpha	1	0
GOLPH3L	ENST00000271732.3	golgi phosphoprotein 3-like	1	0
KIAA1045	ENST00000242315.3	KIAA1045	1	0
C12orf73	ENST00000547975.1	chromosome 12 open reading frame 73	1	0
ADIPOR2	ENST00000357103.4	adiponectin receptor 2	1	0
SVOP	ENST00000299134.5	SV2 related protein homolog (rat)	1	0
PPP1R10	ENST00000376511.2	protein phosphatase 1, regulatory subunit 10	1	0
TANC2	ENST00000424789.2	tetratricopeptide repeat, ankyrin repeat and coiled-coil containing 2	1	0
MYOCD	ENST00000425538.1	myocardin	1	0
POU2F1	ENST00000367866.2	POU class 2 homeobox 1	1	1
ITGB8	ENST00000222573.4	integrin, beta 8	1	0
TOX	ENST00000361421.1	thymocyte selection-associated high mobility group box	1	0
B4GALT2	ENST00000434555.2	UDP-Gal:betaGlcNAc beta 1,4- galactosyltransferase, polypeptide 2	1	0
TMEM164	ENST00000372073.1	transmembrane protein 164	1	1
TOB2	ENST00000327492.3	transducer of ERBB2, 2	1	2
LRRC7	ENST00000310961.5	leucine rich repeat containing 7	1	0
NFE2L1	ENST00000585291.1	nuclear factor, erythroid 2-like 1	1	1
RNF44	ENST00000274811.4	ring finger protein 44	1	1
TAF4B	ENST00000269142.5	TAF4b RNA polymerase II, TATA box binding protein (TBP)-associated factor, 105kDa	1	0
STX17	ENST00000259400.6	syntaxin 17	2	0
AP1B1	ENST00000357586.2	adaptor-related protein complex 1, beta 1 subunit	1	1
RALY	ENST00000375114.3	RALY heterogeneous nuclear ribonucleoprotein	1	2
CHD1	ENST00000284049.3	chromodomain helicase DNA binding protein 1	1	0
SEMA4B	ENST00000411539.2	sema domain, immunoglobulin domain (Ig), transmembrane domain (TM) and short cytoplasmic domain, (semaphorin) 4B	1	0
SLCO3A1	ENST00000318445.6	solute carrier organic anion transporter family, member 3A1	1	0
ARSJ	ENST00000315366.7	arylsulfatase family, member J	1	0
MSANTD3-TMEFF1	ENST00000502978.1	MSANTD3-TMEFF1 readthrough	1	0
DNAJB1	ENST00000254322.2	DnaJ (Hsp40) homolog, subfamily B, member 1	1	0
SMTNL2	ENST00000338859.4	smoothelin-like 2	1	2
ALCAM	ENST00000306107.5	activated leukocyte cell adhesion molecule	1	0
NAA50	ENST00000240922.3	N(alpha)-acetyltransferase 50, NatE catalytic subunit	1	2
CTDSP2	ENST00000398073.2	CTD (carboxy-terminal domain, RNA polymerase II, polypeptide A) small phosphatase 2	1	0

MGAT5B	ENST00000428789.2	mannosyl (alpha-1,6-)-glycoprotein beta-1,6-N-acetyl-glucosaminyltransferase, isozyme B	1	0
MBD6	ENST00000355673.3	methyl-CpG binding domain protein 6	1	0
SIPA1	ENST00000534313.1	signal-induced proliferation-associated 1	1	1
TMEFF1	ENST00000374879.4	transmembrane protein with EGF-like and two follistatin-like domains 1	1	0
TMOD2	ENST00000249700.4	tropomodulin 2 (neuronal)	1	1
C3orf70	ENST00000335012.2	chromosome 3 open reading frame 70	1	1
CNTNAP1	ENST00000264638.4	contactin associated protein 1	1	0
SNX12	ENST00000374274.3	sorting nexin 12	1	0
OXSR1	ENST00000311806.3	oxidative stress responsive 1	1	0
HNF4G	ENST00000396423.2	hepatocyte nuclear factor 4, gamma	1	0
VWA5B2	ENST00000426955.2	von Willebrand factor A domain containing 5B2	1	0
JHDM1D	ENST00000397560.2	jumonji C domain containing histone demethylase 1 homolog D (S. cerevisiae)	1	0
MCIDAS	ENST00000513312.1	multiciliate differentiation and DNA synthesis associated cell cycle protein	1	0
PTPRM	ENST00000332175.8	protein tyrosine phosphatase, receptor type, M	1	0
PPP1R16B	ENST00000299824.1	protein phosphatase 1, regulatory subunit 16B	1	1
FKBP9	ENST00000242209.4	FK506 binding protein 9, 63 kDa	1	0
TRAFD1	ENST00000257604.5	TRAF-type zinc finger domain containing 1	1	1
ELMSAN1	ENST00000394071.2	ELM2 and Myb/SANT-like domain containing 1	1	0
ZDHHC23	ENST00000330212.3	zinc finger, DHHC-type containing 23	1	0
SIX3	ENST00000260653.3	SIX homeobox 3	1	0
SHANK3	ENST00000414786.2	SH3 and multiple ankyrin repeat domains 3	1	1
FRMD4A	ENST00000358621.4	FERM domain containing 4A	1	0
FAT3	ENST00000298047.6	FAT atypical cadherin 3	1	2
FNDC8	ENST00000158009.5	fibronectin type III domain containing 8	1	0
DAGLA	ENST00000257215.5	diacylglycerol lipase, alpha	1	1
PPM1L	ENST00000498165.1	protein phosphatase, Mg2+/Mn2+ dependent, 1L	1	1
JAG1	ENST00000254958.5	jagged 1	1	0
TSPAN14	ENST00000429989.3	tetraspanin 14	1	2
SPCS2	ENST00000263672.6	signal peptidase complex subunit 2 homolog (S. cerevisiae)	1	0
TM9SF3	ENST00000371142.4	transmembrane 9 superfamily member 3	1	0
IGFBP3	ENST00000381086.5	insulin-like growth factor binding protein 3	1	0
SUPT6H	ENST00000314616.6	suppressor of Ty 6 homolog (S. cerevisiae)	1	1
CDKN1C	ENST00000414822.3	cyclin-dependent kinase inhibitor 1C (p57, Kip2)	1	0
FAM73B	ENST00000358369.4	family with sequence similarity 73, member B	1	0
SEMA4F	ENST00000357877.2	sema domain, immunoglobulin domain (Ig), transmembrane domain (TM) and short cytoplasmic domain, (semaphorin) 4F	2	1
PPM1A	ENST00000395076.4	protein phosphatase, Mg2+/Mn2+ dependent, 1A	1	3
RTF1	ENST00000389629.4	Rtf1, Paf1/RNA polymerase II complex component, homolog (S. cerevisiae)	1	0
FOSB	ENST00000586615.1	FBJ murine osteosarcoma viral oncogene homolog B	1	0
TRIM67	ENST00000444294.3	tripartite motif containing 67	1	1
ARID4A	ENST00000431317.2	AT rich interactive domain 4A (RBP1-like)	1	0
SYT9	ENST00000318881.6	synaptotagmin IX	1	0
ANP32B	ENST00000339399.4	acidic (leucine-rich) nuclear phosphoprotein 32 family, member B	1	1
INPP5K	ENST00000421807.2	inositol polyphosphate-5-phosphatase K	1	0
PRKACB	ENST00000370689.2	protein kinase, cAMP-dependent, catalytic, beta	1	0

ANKS1A	ENST00000360359.3	ankyrin repeat and sterile alpha motif domain containing 1A	1	2
SLC6A17	ENST00000331565.4	solute carrier family 6 (neutral amino acid transporter), member 17	1	0
PKP4	ENST00000389757.3	plakophilin 4	1	0
STAC2	ENST00000333461.5	SH3 and cysteine rich domain 2	1	0
SLC4A7	ENST00000295736.5	solute carrier family 4, sodium bicarbonate cotransporter, member 7	1	0
PDE7A	ENST00000401827.3	phosphodiesterase 7A	1	0
PLOD1	ENST00000196061.4	procollagen-lysine, 2-oxoglutarate 5-dioxygenase 1	1	0
PTPN4	ENST00000263708.2	protein tyrosine phosphatase, non-receptor type 4 (megakaryocyte)	1	1
WDR91	ENST00000344400.5	WD repeat domain 91	1	0
SLC27A4	ENST00000300456.4	solute carrier family 27 (fatty acid transporter), member 4	1	2
PAG1	ENST00000220597.4	phosphoprotein associated with glycosphingolipid microdomains 1	1	0
KCNH7	ENST00000332142.5	potassium voltage-gated channel, subfamily H (eag-related), member 7	1	0
ARHGAP44	ENST00000340825.3	Rho GTPase activating protein 44	1	0
WSCD2	ENST00000332082.4	WSC domain containing 2	1	0
SHOC2	ENST00000369452.4	soc-2 suppressor of clear homolog (C. elegans)	1	0
MTUS1	ENST00000381869.3	microtubule associated tumor suppressor 1	1	0
MCTP1	ENST00000515393.1	multiple C2 domains, transmembrane 1	1	0
GHDC	ENST00000414034.3	GH3 domain containing	1	0
TAF5	ENST00000369839.3	TAF5 RNA polymerase II, TATA box binding protein (TBP)-associated factor, 100kDa	1	0
ACSL1	ENST00000454703.2	acyl-CoA synthetase long-chain family member 1	1	0
ZBTB46	ENST00000245663.4	zinc finger and BTB domain containing 46	1	1
SLC5A3	ENST00000608209.1	sodium/myo-inositol cotransporter	1	0
SLC5A3	ENST00000381151.3	solute carrier family 5 (sodium/myo-inositol cotransporter), member 3	1	0
RELN	ENST00000428762.1	reelin	1	0
PAN3	ENST00000282391.5	PAN3 poly(A) specific ribonuclease subunit homolog (S. cerevisiae)	1	0
FAM133A	ENST00000538690.1	family with sequence similarity 133, member A	1	0
FAM131B	ENST00000443739.2	family with sequence similarity 131, member B	1	2
PHF19	ENST00000373896.3	PHD finger protein 19	1	2
ZNF579	ENST00000325421.4	zinc finger protein 579	1	1
BMP8B	ENST00000372827.3	bone morphogenetic protein 8b	1	0
ESRRA	ENST00000405666.1	estrogen-related receptor alpha	1	0
PDE4B	ENST00000371045.5	phosphodiesterase 4B, cAMP-specific	1	0
ST8SIA3	ENST00000324000.3	ST8 alpha-N-acetyl-neuraminide alpha-2,8-sialyltransferase 3	1	0
KMT2D	ENST00000301067.7	lysine (K)-specific methyltransferase 2D	1	0
CDH4	ENST00000360469.5	cadherin 4, type 1, R-cadherin (retinal)	1	0
PARP15	ENST00000483793.1	poly (ADP-ribose) polymerase family, member 15	1	0
TNRC18	ENST00000399537.4	trinucleotide repeat containing 18	1	0
MYH9	ENST00000216181.5	myosin, heavy chain 9, non-muscle	1	0
SLC4A5	ENST00000423644.1	solute carrier family 4 (sodium bicarbonate cotransporter), member 5	1	0
CTTNBP2NL	ENST00000271277.6	CTTNBP2 N-terminal like	1	0
ZIC5	ENST00000267294.4	Zic family member 5	1	0
TNKS	ENST00000310430.6	tankyrase, TRF1-interacting ankyrin-related ADP-ribose polymerase	1	2
UNC45A	ENST00000394275.2	unc-45 homolog A (C. elegans)	1	0
AGAP2	ENST00000257897.3	ArfGAP with GTPase domain, ankyrin repeat and PH domain 2	1	0
HK1	ENST00000359426.6	hexokinase 1	1	1

LONRF3	ENST00000304778.7	LON peptidase N-terminal domain and ring finger 3	1	1
FOXG1	ENST00000382535.3	forkhead box G1	1	0
MLLT1	ENST00000252674.7	myeloid/lymphoid or mixed-lineage leukemia (trithorax homolog, Drosophila); translocated to, 1	1	1
OTUD3	ENST00000375120.3	OTU domain containing 3	1	1
PDCD4	ENST00000280154.7	programmed cell death 4 (neoplastic transformation inhibitor)	1	1
CNOT6L	ENST00000504123.1	CCR4-NOT transcription complex, subunit 6-like	1	1
RET	ENST00000355710.3	ret proto-oncogene	1	0
SEMA5B	ENST00000195173.4	sema domain, seven thrombospondin repeats (type 1 and type 1-like), transmembrane domain (TM) and short cytoplasmic domain, (semaphorin) 5B	1	0
RNF34	ENST00000361234.5	ring finger protein 34, E3 ubiquitin protein ligase	1	0
TBC1D13	ENST00000372648.5	TBC1 domain family, member 13	1	1
FOXP2	ENST00000408937.3	forkhead box P2	1	0
TMEM104	ENST00000335464.5	transmembrane protein 104	1	1
SCML2	ENST00000251900.4	sex comb on midleg-like 2 (Drosophila)	1	0
PRPF38B	ENST00000370025.4	pre-mRNA processing factor 38B	1	0
SRR	ENST00000344595.5	serine racemase	1	0
PURB	ENST00000395699.2	purine-rich element binding protein B	1	2
GORASP2	ENST00000234160.4	golgi reassembly stacking protein 2, 55kDa	1	0
SCN1A	ENST00000423058.2	sodium channel, voltage-gated, type I, alpha subunit	1	0
LHX9	ENST00000367390.3	LIM homeobox 9	1	0
CDC25A	ENST00000302506.3	cell division cycle 25A	1	0
RAP1GAP	ENST00000290101.4	RAP1 GTPase activating protein	1	0
SEMA4C	ENST00000305476.5	sema domain, immunoglobulin domain (Ig), transmembrane domain (TM) and short cytoplasmic domain, (semaphorin) 4C	1	1
CAPN5	ENST00000278559.3	calpain 5	1	0
TP73	ENST00000378280.1	tumor protein p73	1	1
ZC3H4	ENST00000253048.5	zinc finger CCCH-type containing 4	1	0
TANGO2	ENST00000434570.2	transport and golgi organization 2 homolog (Drosophila)	1	1
GPR64	ENST00000379873.2	G protein-coupled receptor 64	1	1*
ATG9A	ENST00000396761.2	autophagy related 9A	1	0
SP2	ENST00000376741.4	Sp2 transcription factor	1	1
KCNQ3	ENST00000388996.4	potassium voltage-gated channel, KQT-like subfamily, member 3	1	1
GABBR2	ENST00000259455.2	gamma-aminobutyric acid (GABA) B receptor, 2	1	0
LHX2	ENST00000373615.4	LIM homeobox 2	1	0
COPS7B	ENST00000373608.3	COP9 signalosome subunit 7B	1	0
PGRMC2	ENST00000296425.5	progesterone receptor membrane component 2	1	0
PPP3R1	ENST00000234310.3	protein phosphatase 3, regulatory subunit B, alpha	1	1
GLRA3	ENST00000274093.3	glycine receptor, alpha 3	1	0
NMT2	ENST00000378165.4	N-myristoyltransferase 2	1	0
FAM81A	ENST00000288228.5	family with sequence similarity 81, member A	1	0
CDC37	ENST00000222005.2	cell division cycle 37	1	0
KCNN3	ENST00000271915.4	potassium intermediate/small conductance calcium-activated channel, subfamily N, member 3	1	1
CREB5	ENST00000357727.2	cAMP responsive element binding protein 5	1	1
SLC12A2	ENST00000262461.2	solute carrier family 12 (sodium/potassium/chloride transporter), member 2	1	0
KLF7	ENST00000309446.6	Kruppel-like factor 7 (ubiquitous)	1	0
POU3F3	ENST00000361360.2	POU class 3 homeobox 3	1	0

NCOA1	ENST00000405141.1	nuclear receptor coactivator 1	1	0
CAMSAP1	ENST00000389532.4	calmodulin regulated spectrin-associated protein 1	1	0
CCDC88A	ENST00000336838.6	coiled-coil domain containing 88A	1	0
NPNT	ENST00000379987.2	nephronectin	1	0
BAZ2A	ENST00000379441.3	bromodomain adjacent to zinc finger domain, 2A	1	1
CHMP7	ENST00000313219.7	charged multivesicular body protein 7	1	0
INHBB	ENST00000295228.3	inhibin, beta B	1	0
SOGA2	ENST00000359865.3	SOGA family member 2	1	0
CBFB	ENST00000290858.6	core-binding factor, beta subunit	1	0
JMJD1C	ENST00000399251.1	jumonji domain containing 1C	1	0
SPRY3	ENST00000302805.2	sprouty homolog 3 (Drosophila)	1	0
C22orf23	ENST00000403305.1	chromosome 22 open reading frame 23	1	0
KITLG	ENST00000228280.5	KIT ligand	1	1
MGAT4A	ENST00000264968.3	mannosyl (alpha-1,3-)-glycoprotein beta-1,4-N-acetylglucosaminyltransferase, isozyme A	2	0
NAPEPLD	ENST00000417955.1	N-acyl phosphatidylethanolamine phospholipase D	1	1
CCND1	ENST00000227507.2	cyclin D1	1	0
ZNF207	ENST00000394670.4	zinc finger protein 207	1	0
CLOCK	ENST00000309964.4	clock circadian regulator	1	1
SATB1	ENST00000338745.6	SATB homeobox 1	1	0
GPC6	ENST00000377047.4	glypican 6	1	0
MRAS	ENST00000289104.4	muscle RAS oncogene homolog	1	0
RORA	ENST00000335670.6	RAR-related orphan receptor A	1	0
DBNL	ENST00000494774.1	drebrin-like	1	2
SNX30	ENST00000374232.3	sorting nexin family member 30	1	0
PGF	ENST00000555567.1	placental growth factor	1	0
SNAP25	ENST00000254976.2	synaptosomal-associated protein, 25kDa	1	3
ERN1	ENST00000433197.3	endoplasmic reticulum to nucleus signaling 1	1	0
CACNB1	ENST00000394303.3	calcium channel, voltage-dependent, beta 1 subunit	1	0
RARB	ENST00000437042.2	retinoic acid receptor, beta	1	0
PODXL	ENST00000541194.1	podocalyxin-like	1	0
PGAP2	ENST00000396993.4	post-GPI attachment to proteins 2	1	0
TCF12	ENST00000267811.5	transcription factor 12	1	0
RFX3	ENST00000382004.3	regulatory factor X, 3 (influences HLA class II expression)	1	0
KLC2	ENST00000316924.5	kinesin light chain 2	1	0
WTAP	ENST00000358372.4	Wilms tumor 1 associated protein	1	0
AL163636.6	ENST00000553909.1	Homo sapiens ribonuclease, RNase A family, 4 (RNASE4), transcript variant 4, mRNA.	1	0
FAM126B	ENST00000418596.3	family with sequence similarity 126, member B	1	0
AFF4	ENST00000265343.5	AF4/FMR2 family, member 4	1	0
ARID4B	ENST00000349213.3	AT rich interactive domain 4B (RBP1-like)	1	0
DCAF7	ENST00000310827.4	DDB1 and CUL4 associated factor 7	1	0
NRN1	ENST00000244766.2	neuritin 1	1	0
C2CD4A	ENST00000355522.5	C2 calcium-dependent domain containing 4A	1	0
CACNA2D1	ENST00000356860.3	calcium channel, voltage-dependent, alpha 2/delta subunit 1	1	0
SDHC	ENST00000367975.2	succinate dehydrogenase complex, subunit C, integral membrane protein, 15kDa	1	0
ACSL4	ENST00000469796.2	acyl-CoA synthetase long-chain family member 4	1	0

UBE2G1	ENST00000396981.2	ubiquitin-conjugating enzyme E2G 1	1	0
PSD3	ENST00000327040.8	pleckstrin and Sec7 domain containing 3	1	0
HECW2	ENST00000260983.3	HECT, C2 and WW domain containing E3 ubiquitin protein ligase 2	1	0
RHOV	ENST00000220507.4	ras homolog family member V	1	0
EVX2	ENST00000308618.4	even-skipped homeobox 2	1	0
CSMD1	ENST00000400186.3	CUB and Sushi multiple domains 1	1	0
ATXN7	ENST00000295900.6	ataxin 7	1	0
ASB1	ENST00000264607.4	ankyrin repeat and SOCS box containing 1	1	2
GNAI2	ENST00000313601.6	guanine nucleotide binding protein (G protein), alpha inhibiting activity polypeptide 2	1	0
TGFBRAP1	ENST00000393359.2	transforming growth factor, beta receptor associated protein 1	1	0
CTRC	ENST00000375943.2	chymotrypsin C (caldecrin)	1	0
PCDH1	ENST00000503492.1	protocadherin 1	1	1
UBN2	ENST00000473989.3	ubinuclein 2	2	1
YTHDC1	ENST00000344157.4	YTH domain containing 1	1	0
SPEN	ENST00000375759.3	spen homolog, transcriptional regulator (Drosophila)	1	0
THRA	ENST00000450525.2	thyroid hormone receptor, alpha	1	1
ACTR1A	ENST00000487599.1	ARP1 actin-related protein 1 homolog A, centractin alpha (yeast)	1	0
INO80	ENST00000361937.3	INO80 complex subunit	1	3
ADCY5	ENST00000462833.1	adenylate cyclase 5	1	1
BCL11B	ENST00000357195.3	B-cell CLL/lymphoma 11B (zinc finger protein)	2	0
CNOT6	ENST00000393356.1	CCR4-NOT transcription complex, subunit 6	1	0
CTNND1	ENST00000524630.1	catenin (cadherin-associated protein), delta 1	1	0
C15orf53	ENST00000318792.1	chromosome 15 open reading frame 53	1	0
SYVN1	ENST00000294256.8	synovial apoptosis inhibitor 1, synoviolin	1	0
SBK1	ENST00000341901.4	SH3 domain binding kinase 1	1	1
ZFHX4	ENST00000521891.2	zinc finger homeobox 4	1	0
GRHL2	ENST00000251808.3	grainyhead-like 2 (Drosophila)	1	1
IQGAP3	ENST00000361170.2	IQ motif containing GTPase activating protein 3	1	0
GAB1	ENST00000262995.4	GRB2-associated binding protein 1	1	0
C9orf114	ENST00000361256.5	chromosome 9 open reading frame 114	1	0
TFCP2L1	ENST00000263707.5	transcription factor CP2-like 1	1	3
ADAM22	ENST00000398204.4	ADAM metallopeptidase domain 22	1	3
HMGB1	ENST00000399489.1	high mobility group box 1	1	1
ARPC4-TTLL3	ENST00000397256.1	ARPC4-TTLL3 readthrough	1	0
CPEB2	ENST00000538197.1	cytoplasmic polyadenylation element binding protein 2	1	0
POFUT1	ENST00000375749.3	protein O-fucosyltransferase 1	1	0
GMFB	ENST00000358056.3	glia maturation factor, beta	1	0
TBC1D25	ENST00000376771.4	TBC1 domain family, member 25	1	0
CRHR1	ENST00000398285.3	corticotropin releasing hormone receptor 1	1	0
DOK6	ENST00000382713.5	docking protein 6	1	0
PPP4R1L	ENST00000334187.8	protein phosphatase 4, regulatory subunit 1-like	1	0
OTUD7A	ENST00000307050.4	OTU domain containing 7A	1	0
TFDP2	ENST00000499676.2	transcription factor Dp-2 (E2F dimerization partner 2)	1	0
RGMB	ENST00000308234.7	RGM domain family, member B	1	0
SHE	ENST00000304760.2	Src homology 2 domain containing E	1	0

CPD	ENST00000225719.4	carboxypeptidase D	1	0
GATAD2B	ENST00000368655.4	GATA zinc finger domain containing 2B	1	2
WDR37	ENST00000358220.1	WD repeat domain 37	1	2
RWDD1	ENST00000466444.2	RWD domain containing 1	1	0
CD47	ENST00000361309.5	CD47 molecule	1	2
RRAGD	ENST00000369415.4	Ras-related GTP binding D	2	1
SZRD1	ENST00000401089.3	SUZ RNA binding domain containing 1	1	1
RALGPS1	ENST00000259351.5	Ral GEF with PH domain and SH3 binding motif 1	1	1
TNPO3	ENST00000393245.1	transportin 3	1	0
FAT2	ENST00000261800.5	FAT atypical cadherin 2	1	0
VCL	ENST00000372755.3	vinculin	1	0
C2orf49	ENST00000258457.2	chromosome 2 open reading frame 49	1	0
ADAM11	ENST00000200557.6	ADAM metallopeptidase domain 11	1	1
KREMEN1	ENST00000400335.4	kringle containing transmembrane protein 1	1	1
ABR	ENST00000302538.5	active BCR-related	1	0
EEA1	ENST00000322349.8	early endosome antigen 1	1	0
RNF152	ENST00000312828.3	ring finger protein 152	1	0
ZER1	ENST00000291900.2	zyg-11 related, cell cycle regulator	1	1
JPH3	ENST00000284262.2	junctophilin 3	1	0
LMTK3	ENST00000600059.1	lemur tyrosine kinase 3	1	0
GPX8	ENST00000296734.6	glutathione peroxidase 8 (putative)	1	0
AFF3	ENST00000409236.2	AF4/FMR2 family, member 3	1	0
DAB2IP	ENST00000408936.3	DAB2 interacting protein	1	0
GIGYF1	ENST00000275732.5	GRB10 interacting GYF protein 1	1	0
ATXN7L3	ENST00000454077.2	ataxin 7-like 3	1	2
HCFC2	ENST00000229330.4	host cell factor C2	1	0
PLCG1	ENST00000244007.3	phospholipase C, gamma 1	1	3
SPTBN2	ENST00000529997.1	spectrin, beta, non-erythrocytic 2	1	0
FAT4	ENST00000394329.3	FAT atypical cadherin 4	1	0
SOCS4	ENST00000395472.2	suppressor of cytokine signaling 4	1	0
PARP8	ENST00000503750.2	poly (ADP-ribose) polymerase family, member 8	1	0
PPP6C	ENST00000373547.4	protein phosphatase 6, catalytic subunit	1	0
ATXN7L1	ENST00000419735.3	ataxin 7-like 1	1	0
HS2ST1	ENST00000370550.5	heparan sulfate 2-O-sulfotransferase 1	1	0
SYNJ1	ENST00000357345.3	synaptojanin 1	1	0
HOOK3	ENST00000307602.4	hook microtubule-tethering protein 3	1	1
GLCE	ENST00000559420.2	glucuronic acid epimerase	1	1
SEC16A	ENST00000313050.7	SEC16 homolog A (S. cerevisiae)	1	1
CREBRF	ENST00000540014.1	CREB3 regulatory factor	1	1
TMEM55A	ENST00000285419.3	transmembrane protein 55A	1	0
MAZ	ENST00000219782.6	MYC-associated zinc finger protein (purine-binding transcription factor)	1	0
RNF213	ENST00000582970.1	ring finger protein 213	1	2
ERC1	ENST00000355446.5	ELKS/RAB6-interacting/CAST family member 1	1	1
DSEL	ENST00000310045.7	dermatan sulfate epimerase-like	1	0
GATS	ENST00000436886.2	GATS, stromal antigen 3 opposite strand	1	0

RIMS3	ENST00000372684.3	regulating synaptic membrane exocytosis 3	1	2
PTCHD1	ENST00000379361.4	patched domain containing 1	1	2
CSNK1G1	ENST00000303052.7	casein kinase 1, gamma 1	1	0
ARPP19	ENST00000566423.1	cAMP-regulated phosphoprotein, 19kDa	1	0
PDK3	ENST00000441463.2	pyruvate dehydrogenase kinase, isozyme 3	1	0
FNDC3B	ENST00000336824.4	fibronectin type III domain containing 3B	1	0
DCAF11	ENST00000446197.3	DDB1 and CUL4 associated factor 11	1	0
IRF2BP2	ENST00000366610.3	interferon regulatory factor 2 binding protein 2	1	0
GRAP2	ENST00000344138.4	GRB2-related adaptor protein 2	1	2
KIAA1024	ENST00000305428.3	KIAA1024	1	0
FRMD5	ENST00000484674.1	FERM domain containing 5	1	0
ATOH1	ENST00000306011.3	atonal homolog 1 (Drosophila)	1	0
TBC1D30	ENST00000542120.1	TBC1 domain family, member 30	1	0
ZSCAN29	ENST00000396976.2	zinc finger and SCAN domain containing 29	1	1
NEK9	ENST00000238616.5	NIMA-related kinase 9	1	0
EHD4	ENST00000220325.4	EH-domain containing 4	1	0
THTPA	ENST00000288014.6	thiamine triphosphatase	1	0
EMX1	ENST00000258106.6	empty spiracles homeobox 1	1	0
PTPRD	ENST00000381196.4	protein tyrosine phosphatase, receptor type, D	1	0
SLC7A2	ENST00000494857.1	solute carrier family 7 (cationic amino acid transporter, y+ system), member 2	1	0
POLR3H	ENST00000396504.2	polymerase (RNA) III (DNA directed) polypeptide H (22.9kD)	1	2
XPO5	ENST00000265351.7	exportin 5	1	0
CYB561D1	ENST00000496961.1	cytochrome b561 family, member D1	1	0
GPR26	ENST00000284674.1	G protein-coupled receptor 26	2	0
SEH1L	ENST00000262124.11	SEH1-like (S. cerevisiae)	1	0
KCTD16	ENST00000507359.3	potassium channel tetramerization domain containing 16	1	0
ACOT11	ENST00000343744.2	acyl-CoA thioesterase 11	1	0
KIAA0753	ENST00000361413.3	KIAA0753	1	0
ACVR2B	ENST00000352511.4	activin A receptor, type IIB	1	3
LPHN1	ENST00000340736.6	latrophilin 1	1	0
EPN2	ENST00000314728.5	epsin 2	1	0
LMNB2	ENST00000325327.3	lamin B2	1	0
MAP4K4	ENST00000413150.2	mitogen-activated protein kinase kinase kinase kinase 4	1	0
ACVRL1	ENST00000550683.1	activin A receptor type II-like 1	1	0
TRPM3	ENST00000377111.2	transient receptor potential cation channel, subfamily M, member 3	1	0
SMAD4	ENST00000398417.2	SMAD family member 4	1	0
TM7SF3	ENST00000343028.4	transmembrane 7 superfamily member 3	1	0
DOCK3	ENST00000266037.9	dedicator of cytokinesis 3	1	1
NEDD4L	ENST00000256832.7	neural precursor cell expressed, developmentally down-regulated 4-like, E3 ubiquitin protein ligase	1	1
TBL1XR1	ENST00000430069.1	transducin (beta)-like 1 X-linked receptor 1	1	1
RAB4A	ENST00000366690.4	RAB4A, member RAS oncogene family	1	0
MYO18A	ENST00000354329.4	myosin XVIIIA	1	0
GSG1	ENST00000396302.3	germ cell associated 1	1	0
FOXN3	ENST00000345097.4	forkhead box N3	1	1
C6orf120	ENST00000332290.2	chromosome 6 open reading frame 120	1	0

NSD1	ENST00000439151.2	nuclear receptor binding SET domain protein 1	2	0
RAB11FIP4	ENST00000325874.8	RAB11 family interacting protein 4 (class II)	1	0
PDXK	ENST00000468090.1	pyridoxal (pyridoxine, vitamin B6) kinase	1	3
SERPINE1	ENST00000223095.4	serpin peptidase inhibitor, clade E (nexin, plasminogen activator inhibitor type 1), member 1	1	1
MLEC	ENST00000228506.3	malectin	1	0
CACNA2D2	ENST00000423994.2	calcium channel, voltage-dependent, alpha 2/delta subunit 2	1	0
AHCYL2	ENST00000325006.3	adenosylhomocysteinase-like 2	1	0
SNAP29	ENST00000215730.7	synaptosomal-associated protein, 29kDa	1	0
TNRC6B	ENST00000335727.9	trinucleotide repeat containing 6B	1	3
PITPNM2	ENST00000280562.5	phosphatidylinositol transfer protein, membrane-associated 2	1	1
FBXO41	ENST00000295133.5	F-box protein 41	1	2
BCL9L	ENST00000334801.3	B-cell CLL/lymphoma 9-like	1	1
DNAH3	ENST00000415178.1	dynein, axonemal, heavy chain 3	1	2
COL12A1	ENST00000322507.8	collagen, type XII, alpha 1	1	0
PAOX	ENST00000368539.4	polyamine oxidase (exo-N4-amino)	1	0
GALNT10	ENST00000297107.6	UDP-N-acetyl-alpha-D-galactosamine:polypeptide N-acetylgalactosaminyltransferase 10 (GalNAc-T10)	1	0
TMEM255A	ENST00000309720.5	transmembrane protein 255A	1	0
USP31	ENST00000219689.7	ubiquitin specific peptidase 31	1	2
PDE7B	ENST00000308191.6	phosphodiesterase 7B	1	0
DGKI	ENST00000453654.2	diacylglycerol kinase, iota	1	0
WAC	ENST00000375664.4	WW domain containing adaptor with coiled-coil	1	1
UCK2	ENST00000367879.4	uridine-cytidine kinase 2	1	0
SLC7A6	ENST00000219343.6	solute carrier family 7 (amino acid transporter light chain, y+L system), member 6	1	0
IPO11	ENST00000409534.1	importin 11	1	0
PDE3A	ENST00000359062.3	phosphodiesterase 3A, cGMP-inhibited	1	0
MFSD6	ENST00000392328.1	major facilitator superfamily domain containing 6	1	1
THAP1	ENST00000345117.2	THAP domain containing, apoptosis associated protein 1	1	0
SPRED1	ENST00000299084.4	sprouty-related, EVH1 domain containing 1	1	0
ASPHD2	ENST00000215906.5	aspartate beta-hydroxylase domain containing 2	2	0
MSL2	ENST00000309993.2	male-specific lethal 2 homolog (Drosophila)	1	0
PCNX	ENST00000304743.2	pecanex homolog (Drosophila)	1	0
C9orf64	ENST00000376344.3	chromosome 9 open reading frame 64	1	2
ZNF644	ENST00000370440.1	zinc finger protein 644	1	0
ADAT2	ENST00000606514.1	adenosine deaminase, tRNA-specific 2	1	1
GDAP1L1	ENST00000342560.5	ganglioside induced differentiation associated protein 1-like 1	1	0
CLCN3	ENST00000513761.1	chloride channel, voltage-sensitive 3	1	1
LOXL3	ENST00000264094.3	lysyl oxidase-like 3	1	0
SLC8A1	ENST00000406785.2	solute carrier family 8 (sodium/calcium exchanger), member 1	1	2
CDS2	ENST00000460006.1	CDP-diacylglycerol synthase (phosphatidate cytidylyltransferase) 2	1	3
SAR1A	ENST00000373242.2	SAR1 homolog A (S. cerevisiae)	1	0
HPX	ENST00000265983.3	hemopexin	1	2
G3BP1	ENST00000394123.3	GTPase activating protein (SH3 domain) binding protein 1	1	0
GRID1	ENST00000327946.7	glutamate receptor, ionotropic, delta 1	1	0
C14orf28	ENST00000325192.3	chromosome 14 open reading frame 28	1	0
PITPNC1	ENST00000335257.6	phosphatidylinositol transfer protein, cytoplasmic 1	2	0

NABP1	ENST00000410026.2	nucleic acid binding protein 1	1	2
GFRA1	ENST00000439649.3	GDNF family receptor alpha 1	1	0
MMAB	ENST00000545712.2	methylmalonic aciduria (cobalamin deficiency) cblB type	1	2
EMC3	ENST00000245046.2	ER membrane protein complex subunit 3	1	0
MON2	ENST00000546600.1	MON2 homolog (S. cerevisiae)	1	1
AIDA	ENST00000340020.6	axin interactor, dorsalization associated	1	0
CERS4	ENST00000559336.1	ceramide synthase 4	1	0
HSBP1	ENST00000433866.2	heat shock factor binding protein 1	1	0
FAM208A	ENST00000493960.2	family with sequence similarity 208, member A	1	0
TRIM13	ENST00000378182.3	tripartite motif containing 13	1	0
USP24	ENST00000294383.6	ubiquitin specific peptidase 24	1	0
PPFIA1	ENST00000253925.7	protein tyrosine phosphatase, receptor type, f polypeptide (PTPRF), interacting protein (liprin), alpha 1	1	0
GRHPR	ENST00000318158.6	glyoxylate reductase/hydroxypyruvate reductase	1	0
ZNF423	ENST00000561648.1	zinc finger protein 423	1	0
SHKBP1	ENST00000291842.5	SH3KBP1 binding protein 1	1	0
AHSA2	ENST00000394457.3	AHA1, activator of heat shock 90kDa protein ATPase homolog 2 (yeast)	1	0
ERP44	ENST00000262455.6	endoplasmic reticulum protein 44	1	0
TMEM216	ENST00000334888.5	transmembrane protein 216	1	0
MRPL3	ENST00000264995.3	mitochondrial ribosomal protein L3	1	0
G6PC3	ENST00000269097.4	glucose 6 phosphatase, catalytic, 3	1	1
MRPL52	ENST00000397505.2	mitochondrial ribosomal protein L52	1	0
SLC2A4RG	ENST00000266077.2	SLC2A4 regulator	1	0
WHAMM	ENST00000286760.4	WAS protein homolog associated with actin, golgi membranes and microtubules	2	0
TMEM134	ENST00000393877.3	transmembrane protein 134	1	0
GABRB1	ENST00000295454.3	gamma-aminobutyric acid (GABA) A receptor, beta 1	2	2
ZNF593	ENST00000270812.5	zinc finger protein 593	1	2
ZBTB20	ENST00000462705.1	zinc finger and BTB domain containing 20	2	1
TMEM97	ENST00000226230.6	transmembrane protein 97	1	0
GATSL2	ENST00000426327.3	GATS protein-like 2	2	1
CACNG2	ENST00000300105.6	calcium channel, voltage-dependent, gamma subunit 2	1	0
WNT1	ENST00000293549.3	wingless-type MMTV integration site family, member 1	1	0
RBCK1	ENST00000356286.5	RanBP-type and C3HC4-type zinc finger containing 1	1	1
NEUROD2	ENST00000302584.4	neuronal differentiation 2	1	0
RGS7BP	ENST00000334025.2	regulator of G-protein signaling 7 binding protein	1	0
CNTD1	ENST00000588408.1	cyclin N-terminal domain containing 1	1	0
KLHDC8A	ENST00000367155.3	kelch domain containing 8A	1	0
TRIM44	ENST00000299413.5	tripartite motif containing 44	1	1

Table 14. TargetScanHuman list of predicted miR-34a mRNA targets and predicted number of conserved and poorly conserved binding sites within the 3'UTR. mRNA highlighted in yellow were selected for experimental validation.

Study	Cell type	Reference
MiR-34a was shown to be down-regulated during the process of in vitro osteoclast differentiation and Tgif2 expression was increased during osteoclastogenesis. Tgif2 was found to be down-regulated upon miR-34a overexpression and up-regulated upon miR-34a inhibition in human and mouse osteoclast cultures	Osteoclasts	[396]
MiR-34a was identified to be down-regulated in gastric cancer tissues compared to matched non-tumour tissues and that TGIF2 was up-regulated in gastric cancer tissues compared to matched non-tumour tissues indicating the function of miR-34a as a tumour suppressor. Gastric cancer cells transiently transfected with miR-34a mimic exhibited significant TGIF2 expression down-regulation.	Gastric cancer cells	[397]

Table 15. Previous studies which have validated *TGIF2* as a target of miR-34a

Database	***TGIF2* putative target of miR-34a**	**Predicted position 90-97 of *TGIF2* 3'UTR**
TargetScanHuman release 6.2	Yes	Yes
Diana web server v5.0 interface	Yes	Yes
PicTar	Yes	Yes
PITA – Segal Lab of computational biology	Yes	Yes
microRNA.org (Aug 2010 release)	Yes	Yes

Table 16. Target prediction programmes that predict *TGIF2* mRNA as a positive target of miR-34a and the predicted location of miR-34a binding in the *TGIF2* mRNA 3'UTR.

MicroRNA-34a structure

A) Primary miR-34a structure

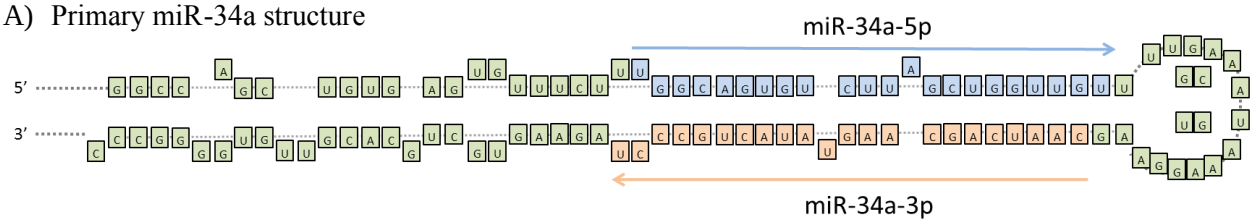

B) Mature miR-34a-5p structure

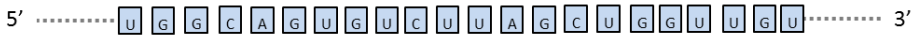

C) miR-34a-5p seed match base pairing at position 90-97 of *TGFI2* mRNA 3' UTR

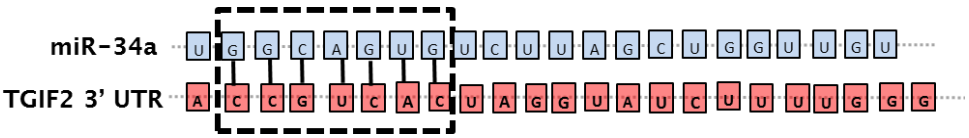

TGIF2 3'UTR 5' …GGGUUUUCUAUGGAUCACUGCCA…3'

miR-34a 3' UGUUGGUCGAUUCUGUGACGGU 5'

Figure 41. MicroRNA-34a structure. The structure and sequence of primary miR-34a (A). The sequence of mature miR-34a-5p (B). The seed match base pairing of mature miR-34a seed region to the designated sequence within *TGIF2* 3'UTR transcript.

4.7 Transient inhibition and overexpression of miR-34a in fetal femur-derived cells

4.7.1 Transfection optimisation

Transfection is the deliberate introduction of nucleic acids into cells; the change in cell properties as a result of newly introduced nucleic acids. A transfection reagent is used to transport the desired nucleic acids into the cell. DharmaFECT®1 contains cationic and non-ionic lipids which form liposome complexes with negative charged nucleic acids. These liposomes which have a positive overall charge are able to fuse with the negative charges cell membrane allowing complexes to enter the cell by endocytosis. Liposomes enter cells via endocytosis but have to avoid endosomes which trigger intracellular degradation. Despite many transfection reagents being able to penetrate the plasma membrane, this often elicits a cytotoxic response. A balance therefore needs to be sought; between efficient gene delivery and minimising cellular toxicity. Cellular toxicity is dependent on transfection reagent and cell type. The concentration of both the transfection reagent and nucleic acids to be transfected are critical to maximize transfection efficiency and minimising cellular toxicity. Both the transfection reagent DharmaFECT®1 and microRNA mimics and microRNA inhibitors were titrated to identify optimum volumes for use in future transfection experiments.

4.7.1.1 Optimal DharmaFECT®1 Concentration

To identify the optimal concentration of DharmaFECT®1 transfection reagent, DharmaFECT®1 was titrated to determine the optimal percentage with minimal cell cytotoxicity and maximum transfer of nucleic acid. Four concentrations of DharmaFECT®1 and also a no DharmaFECT®1 control and also four differing concentrations of either microRNA inhibitor or microRNA mimic were investigated. According to the manufacturer protocol, concentrations of DharmaFECT®1 which result in cell viability above 80% is deemed as having a low toxic effect on cell viability and deemed suitable for use. For the microRNA mimic experiment, DharmaFECT®1 which was used at 0.25%, 0.5% and 0.75% of the total cell media volume used resulted with more than 80% of cells exhibiting cell viability (Figure 42). For the microRNA inhibitor experiment, DharmaFECT®1 which was used at 0.25% and 0.5% of the total cell media volume used resulted with more than 80% of cells exhibiting cell viability (Figure 44). Additionally bright field microscopy showed higher cell viability in cell cultures treated with lower percentages of DharmaFECT®1 (Figures 43 & 45).

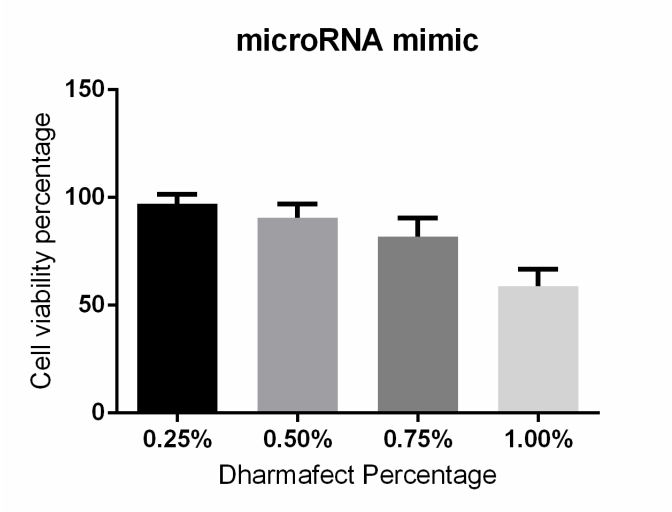

Figure 42. Cell viability percentage of cells following transfection with different percentages of DharmaFECT®1 in total culture media using AlamarBlue assay.

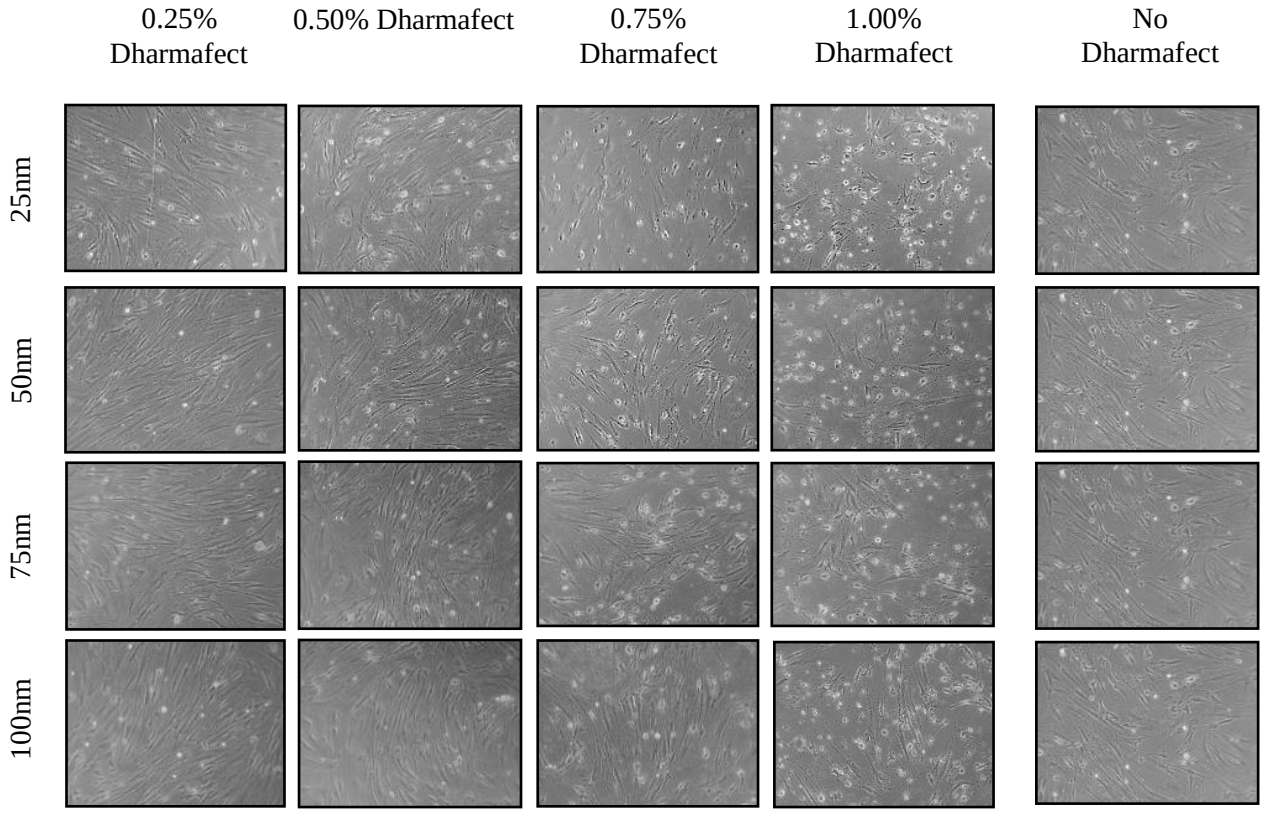

Figure 43. Light field microscopy images showing cells cultured in differing percentages of DharmaFECT®1 in total culture media in combination with differing concentrations of microRNA mimic positive control.

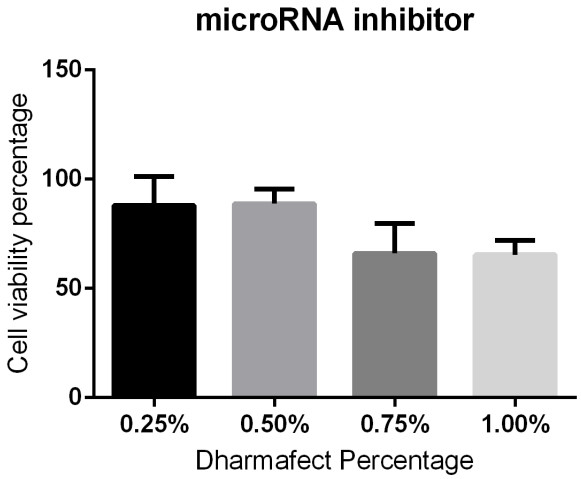

Figure 44. Cell viability percentage of cells following transfection with different percentages of DharmaFECT®1 in total culture media using AlamarBlue assay.

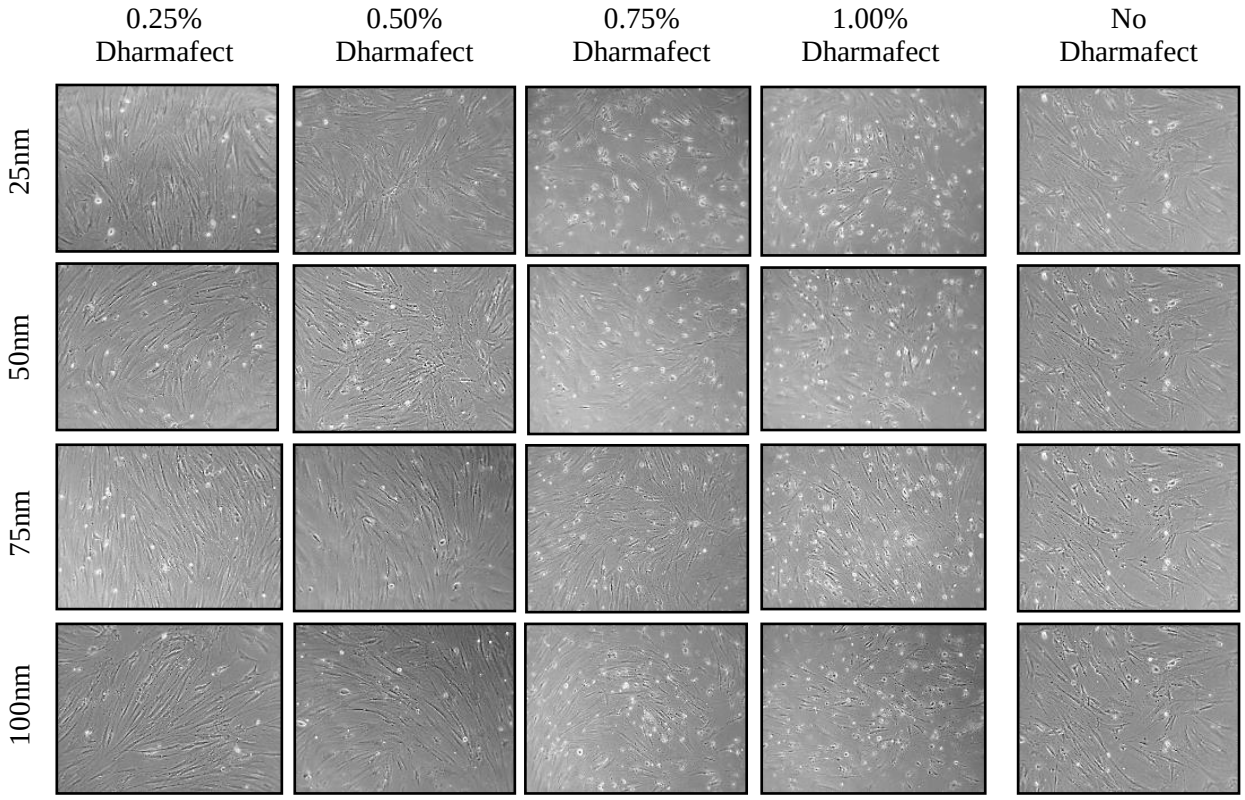

Figure 45. Light field microscopy images showing cells cultured in differing percentages of DharmaFECT®1 in total culture media in combination with differing concentrations of microRNA mimic positive control.

A

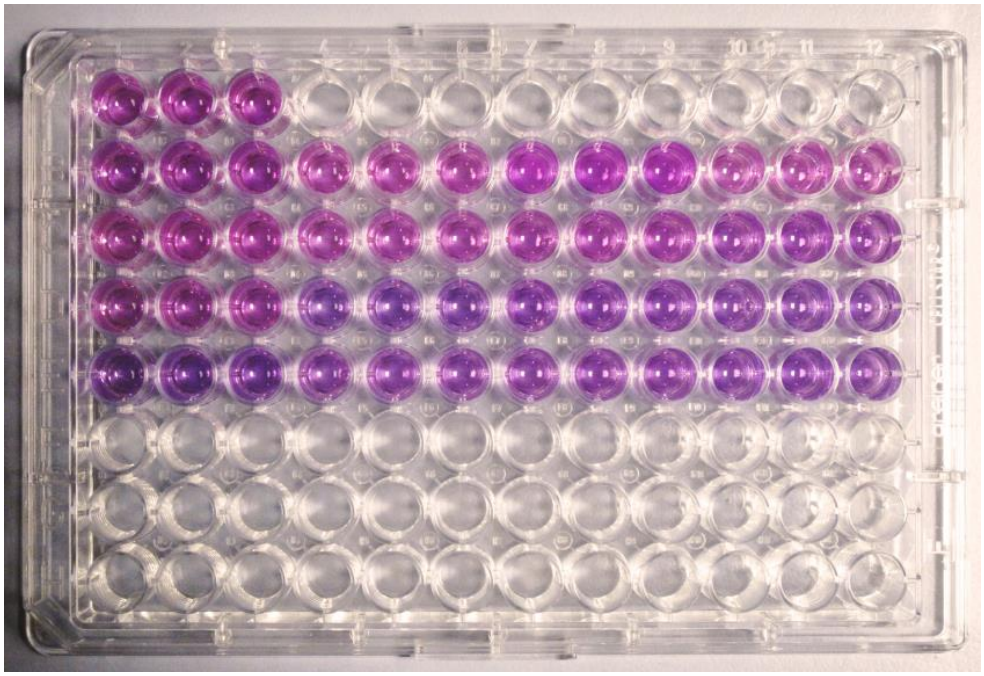

B

	1	2	3	4	5	6	7	8	9	10	11	12
A	0% D	0% D	0% D									
B	0.25% D 25nM	0.25% D 25nM	0.25% D 25nM	0.25% D 50nM	0.25% D 50nM	0.25% D 50nM	0.25% D 75nM	0.25% D 75nM	0.25% D 75nM	0.25% D 100nM	0.25% D 100nM	0.25% D 100nM
C	0.50% D 25nM	0.50% D 25nM	0.50% D 25nM	0.50% D 50nM	0.50% D 50nM	0.50% D 50nM	0.50% D 75nM	0.50% D 75nM	0.50% D 75nM	0.50% D 100nM	0.50% D 100nM	0.50% D 100nM
D	0.75% D 25nM	0.75% D 25nM	0.75% D 25nM	0.75% D 50nM	0.75% D 50nM	0.75% D 50nM	0.75% D 75nM	0.75% D 75nM	0.75% D 75nM	0.75% D 100nM	0.75% D 100nM	0.75% D 100nM
E	1% D 25nM	1% D 25nM	1% D 25nM	1% D 50nM	1% D 50nM	1% D 50nM	1% D 75nM	1% D 75nM	1% D 75nM	1% D 100nM	1% D 100nM	1% D 100nM
F	MOC	MOC	MOC									
G												
H												

D – Dharmafect concentration
MOC – Media only control

Figure 46. 96 well plate showing the media colour change in the presence of 10% AlamarBlue reagent in media after 4 hours incubation with different concentrations of DharmaFECT®1 and different concentrations of microRNA mimic (A) and the layout of the plate corresponding to A (B).

4.7.1.2 Optimal concentration of microRNA mimic or microRNA inhibitor

In addition to the optimisation of DharmaFECT®1 concentration which should allow for efficient transfection and minimal toxic side effects, the concentration of microRNA mimic and microRNA inhibitor was optimised. The use of a microRNA mimic positive control and a microRNA hairpin inhibitor positive control was used to assess the optimal amount of mimic or inhibitor required for successful target gene knockdown or overexpression.

- miRIDIAN microRNA mimic positive control (GE healthcare, Dharmacon Cat.No.CP-001000-02) targets the endogenous housekeeping gene *GAPDH*, therefore after transfection with the microRNA mimic positive control it was expected that a decrease in *GAPDH* mRNA expression should be observed compared to the negative control; which is a non-targeting mimic negative control based on the C.elegans cel-miR-67 mature sequence UCACAACCUCCUAGAAAGAGUAGA.
- miRIDIAN microRNA hairpin inhibitor positive control (GE healthcare, Dharmacon Cat.No.IP-004000-01) inhibits miR-16, therefore after transfection with the microRNA hairpin inhibitor positive control it was expected that a decrease in miR-16 expression should be observed compared to the negative control; which is a non-targeting hairpin inhibitor negative control based on the C.elegans cel-miR-67 mature sequence UCACAACCUCCUAGAAAGAGUAGA.

For optimisation of microRNA mimic concentration and microRNA hairpin inhibitor concentration, a microRNA mimic positive control was used at four different concentrations in combination with four different concentrations of DharmaFECT®1 and a microRNA hairpin inhibitor positive control was used at four different concentrations in combination with 4 different concentrations of DharmaFECT®1. The volume of DharmaFECT®1 was used at 0.25%, 0.5%, 0.75% and 1.0% of the total media volume in combination with microRNA mimic or microRNA hairpin inhibitor at either 25nM, 50nM, 75nM and 100nM final concentration in total media. RNA and microRNA was extracted and the expression of *GADPH* mRNA was analysed in cells which had been transfected with microRNA mimic positive control and in cells which had been transfected with microRNA mimic negative control. The expression of miR-16 was analysed in cells which had been transfected with microRNA hairpin inhibitor positive control and in cells transfected with microRNA hairpin inhibitor negative control.

Cells transfected with the microRNA mimic positive control targeting *GAPDH* mRNA were found to exhibit down-regulated expression of *GAPDH* mRNA in all concentrations of microRNA mimic positive control used compared to expression in cells transfected with respective concentrations of microRNA mimic negative non-targeting control (Figure 47). Cells transfected with the microRNA hairpin inhibitor positive control did not exhibit down-regulation of miR-16 expression compared to cells transfected with the respective concentrations of microRNA hairpin inhibitor negative, non-

targeting control (Figure 48). The result of insufficient inhibition of miR-16 may be as a result of using primary cells, as cell line usage was recommended in the manufacturer's protocol.

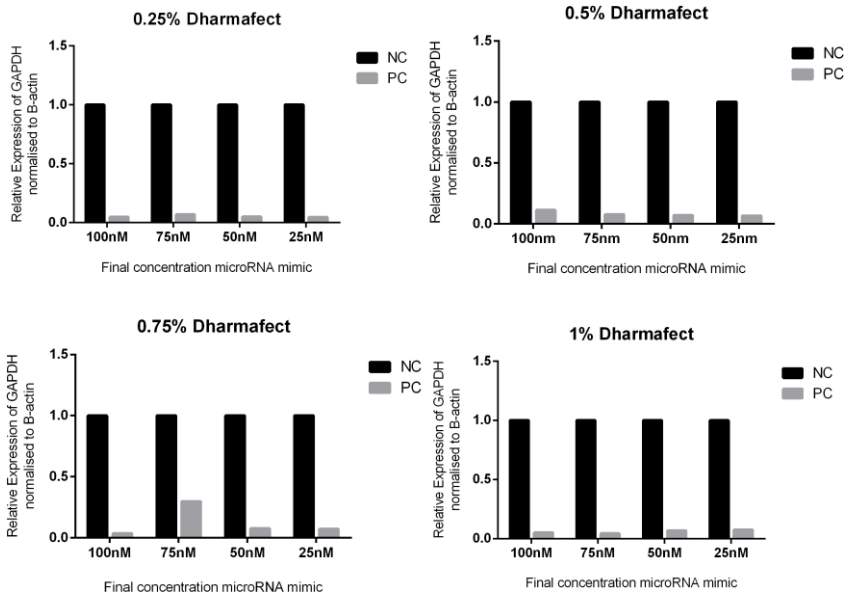

Figure 47. Relative expression of *GAPDH* mRNA in cells transfected with differing concentrations of microRNA mimic positive control (PC) targeting *GAPDH* mRNA in combination with differing concentration of DharmaFECT®1 compared to the expression of *GAPDH* mRNA in cells transfected with non-targeting microRNA mimic negative control (NC).

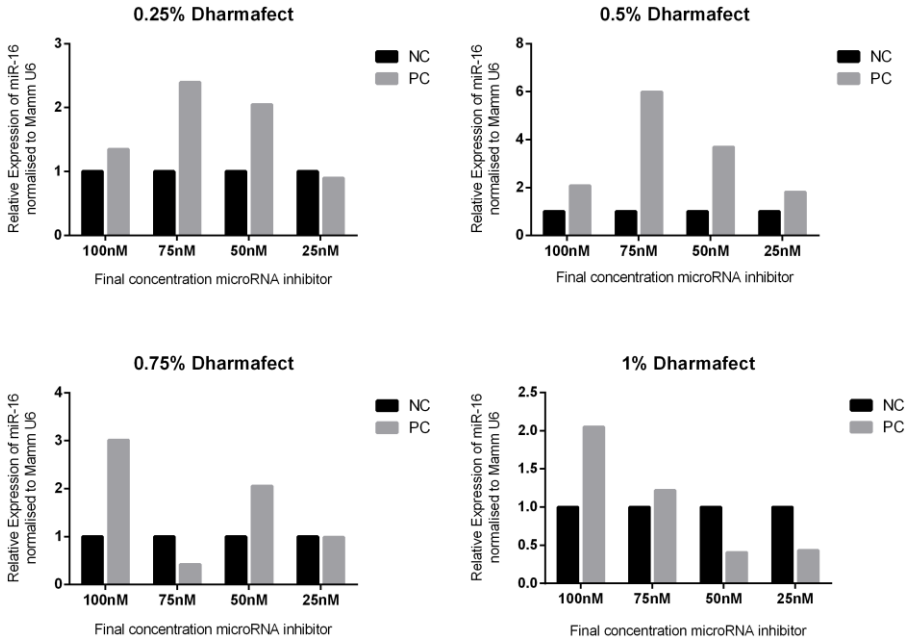

Figure 48. Relative expression of miR-16 in cells transfected with differing concentrations of microRNA inhibitor positive control (PC) targeting miR-16 in combination with differing concentrations of DharmaFECT®1 compared to the relative expression of miR-16 in cells transfected with non-targeting microRNA inhibitor negative control (NC).

4.7.1.3 Transfection optimisation using microRNA mimic control with Dy547or microRNA hairpin inhibitor control with Dy547

The miRIDIAN microRNA mimic transfection control is a Dy547 labelled microRNA mimic which is based on the C.elegans microRNA cel-miR67. The miRIDIAN microRNA hairpin inhibitor transfection control is a Dy547 labelled microRNA hairpin inhibitor which is also based on the C.elegans microRNA cel-miR67. Both the Dy547 labelled microRNA mimic and Dy547 labelled microRNA hairpin inhibitor are non-targeting and therefore can be used to assess solely transfection efficiency in cells. Figures 49 and 50 show the presence of the Dy547 microRNA mimic control and Dy457 microRNA hairpin inhibitor control, however, it is difficult to determine if microRNA mimic and microRNA hairpin inhibitor staining observed was intracellular.

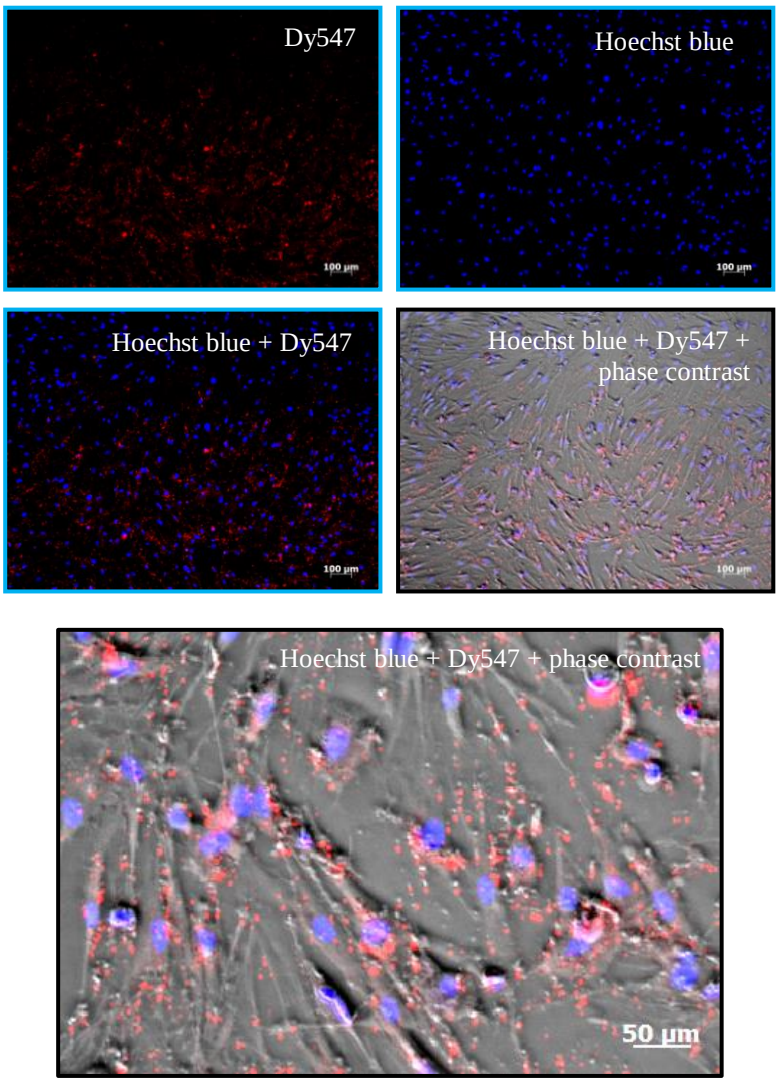

Figure 49. Cells transfected with 75nm fluorescent Dy547 microRNA mimic positive control and 0.5% DharmaFECT®1 and counterstained with Hoechst blue. (Scale bars = 100µm and 50µm).

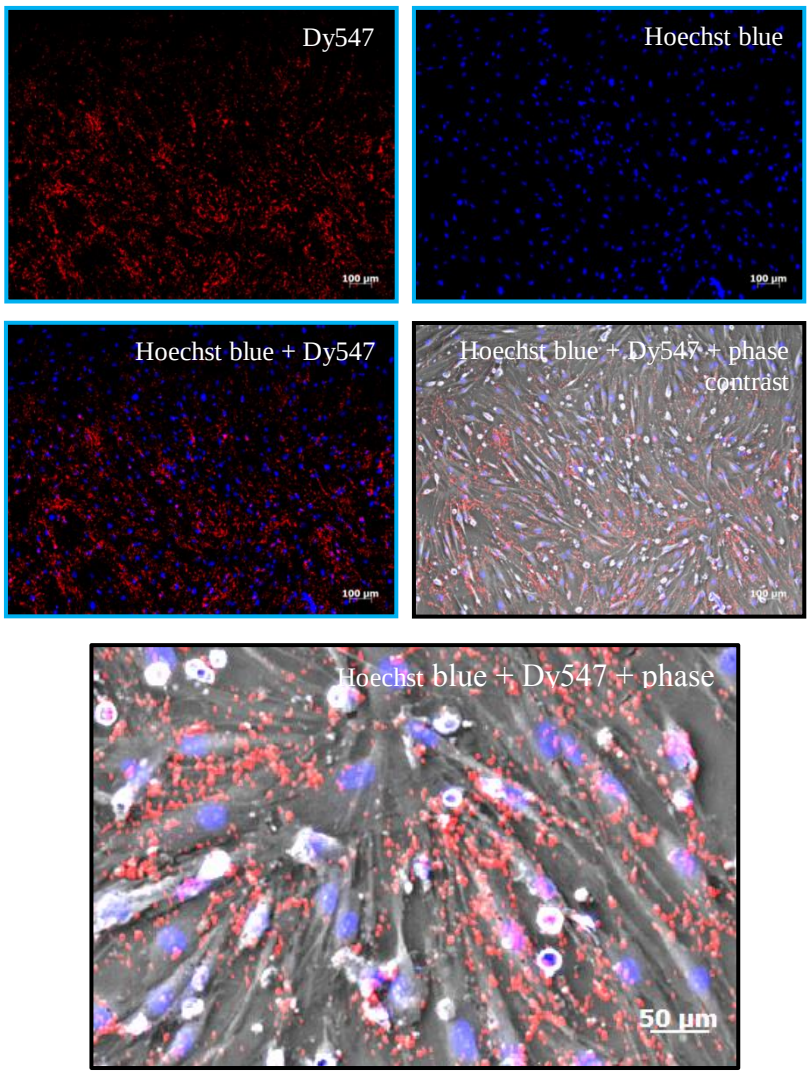

Figure 50. Cells transfected with 75nm fluorescent Dy547 microRNA hairpin inhibitor positive control and 0.5% DharmaFECT®1 and counterstained with Hoechst blue. (Scale bars = 100µm and 50µm).

4.7.2 miR-34a expression, *TGIF2* expression and chondrogenic marker gene expression following transient transfection with miR-34a inhibitor or mimic

Following transient transfection of fetal femur-derived cells with miR-34a inhibitor, miR-34a was found to be down-regulated compared to the expression of miR-34a in cells treated with the negative control inhibitor (median fold change of ~0.11) (Figure 51A). The identified potential mRNA target of miR-34a; *TGFI2* showed no difference in expression after treatment with miR-34a inhibitor compared to the cells treated with the negative control inhibitor (Figure 51C). Fetal femur derived cells treated with miR-34a mimic exhibited up-regulation of miR-34a (median fold change of ~3759) (Figure 51B) and the potential mRNA target; *TGIF2* was found to be downregulated following miR-34a overexpression with miR-34a mimic (median fold change ~0.7) (Figure 51D). Chondrogenic marker genes; *SOX9, AGCAN* and *COL2A1* mRNA exhibited no significant changes in expression following transfection in cells with miR-34a mimic or miR-34a inhibitor (Figure 52).

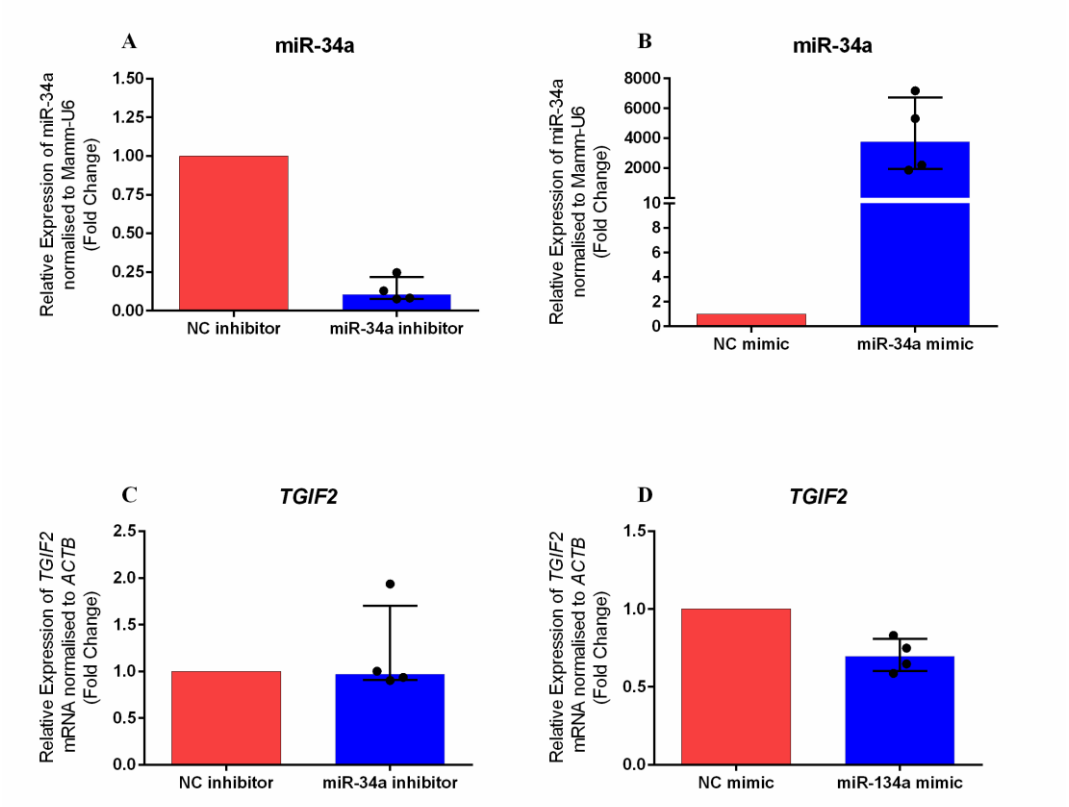

Figure 51. Effect of miR-34a inhibition and overexpression on miR-34a expression and *TGIF2* mRNA expression in human fetal femur-derived cells. Data is presented as the median and interquartile quartile range of the fold change in miR-34a (A & B) and *TGIF2* mRNA (C & D) expression in human fetal femur-derived cells cultured in the presence of either miR-34a inhibitor relative to control cells treated with non-targeting hairpin inhibitor (NC) (A & C) or miR-34a mimic relative to the control cells treated with non-targeting mimic (B & D). n=4, * p <0.05, Wilcoxon signed rank test.

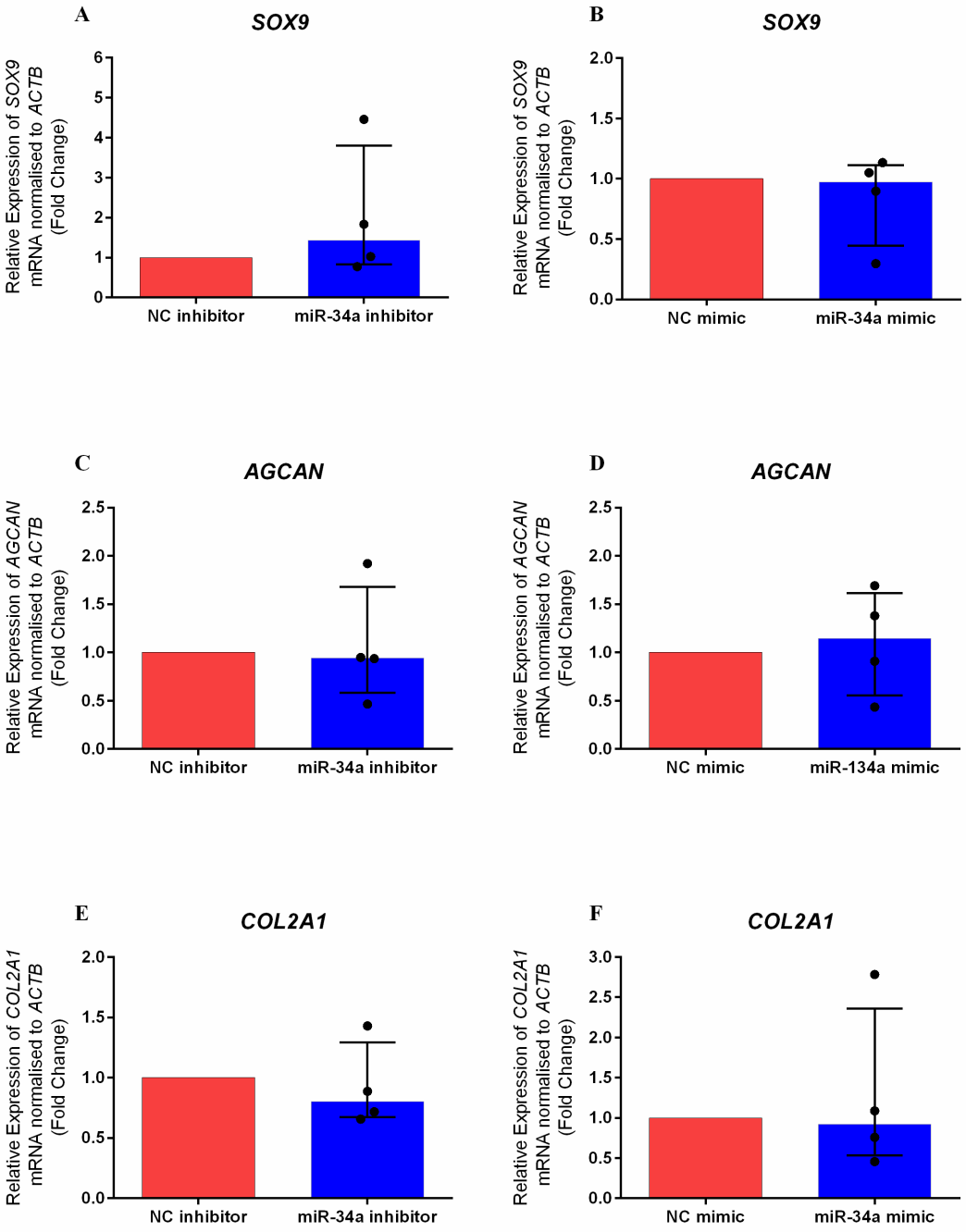

Figure 52. Effect of miR-34a inhibition and overexpression on mRNA expression in human fetal femur-derived cells. Data is presented as the median and interquartile quartile range of the fold change in *SOX9* (A & B), *AGCAN* (C & D) and *COL2A1*(E & F) mRNA expression in human fetal femur-derived cells cultured in the presence of either miR-34a inhibitor relative to control cells treated with non-targeting hairpin inhibitor (NC) (A, C & E) or miR-34a mimic relative to the control cells treated with non-targeting mimic (B, D & F). n=4, Wilcoxon signed rank test.

4.7.3 TGIF2 protein expression in fetal femur-derived cells following transient transfection with miR-34a inhibitor or mimic

Following transient transfection of fetal femur derived cells for 48 hours with either: miR-34a inhibitor, non-targeting inhibitor oligonucleotide (NC), miR-34a mimic or non-targeting mimic control (NC) cells were lysed and protein extracted and quantified. Western blotting and densitometry analysis was employed to determine the effect of transient transfection upon TGIF2 protein expression, with β-actin protein expression which served as an internal control. Cells transfected with either miR-34a inhibitor or non-targeting inhibitor oligonucleotide (NC) were compared for the expression of TGFIF2 and densitometry analysis of the immunoblots showed that there was no significant differences in TGIF2 expression between the two treatment groups (Figure 54A). Cells transfected with either miR-34a mimic or non-targeting mimic oligonucleotide (NC) were compared for the expression of TGIF2 and densitometry analysis of the immunoblots showed that there was no significant difference in TGIF2 expression between the two treatment groups, however, despite this result all samples were down-regulated to some degree (Figure 54B). Immunoblots displayed below from the western blot (Figure 53) were used for densitometry analysis.

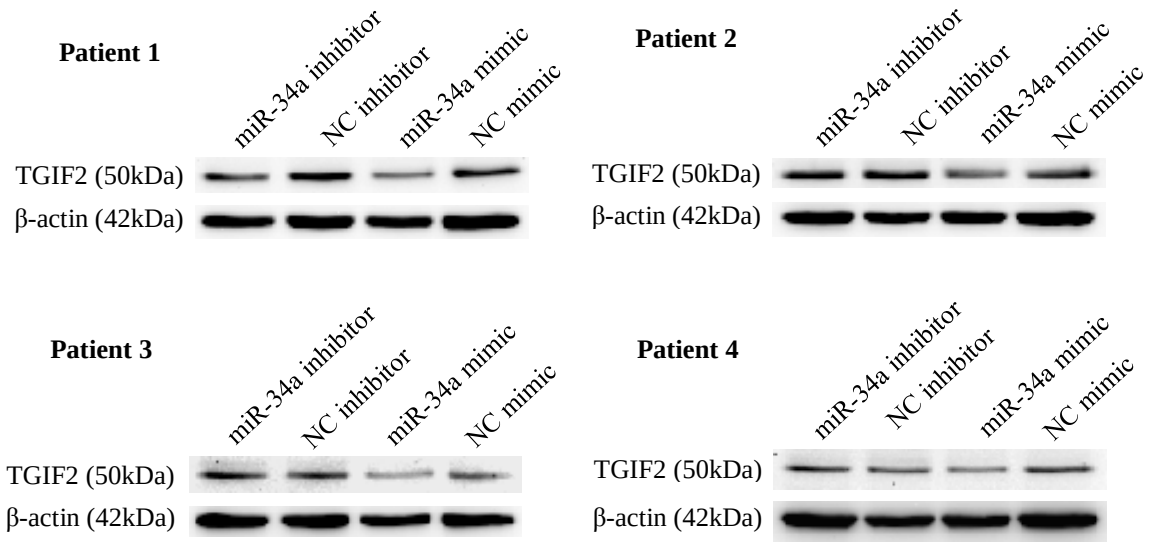

Figure 53. Western blotting immunoblots showing protein expression of TGIF2 and internal normalising control β-actin, following transient transfection of fetal femur derived cells with miR-34a mimic, mimic non-targeting oligonucleotide, miR-34a inhibitor or inhibitor non-targeting oligoneucletide in 4 individual patient samples,

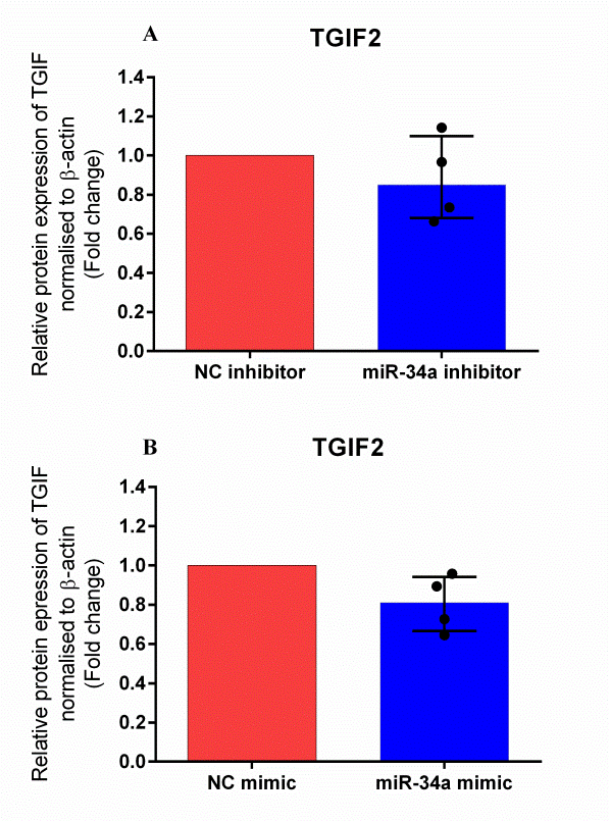

Figure 54. Effect of miR-34a inhibition and overexpression on TGIF2 protein expression in human fetal femur-derived cells. Data is presented as the median and interquartile quartile range of the fold change in TGIF2 expression in human fetal femur-derived cells cultured in the presence of either miR-34a inhibitor relative to control cells treated with non-targeting hairpin inhibitor (NC) (A) or miR-34a mimic relative to the control cells treated with non-targeting mimic (B). n=4, Wilcoxon signed rank test.

4.8 Discussion

This current study identified that a mixed population of human fetal femur-derived cells, including Stro-1 enriched skeletal stem cells, upon TGF-β3 induced chondrogenesis resulted in the up-regulation of miR-34a. Bioinformatic analysis identified *TGIF2* mRNA as a putative target of miR-34a. However, inhibition and overexpression studies of miR-34a had no effect upon the expression of *TGIF2* mRNA or TGIF2 protein expression in fetal femur-derived cells. *TGIF2* mRNA 3'UTR may therefore not be targeted by miR-34a during chondrogenesis. However, factors should be taken into consideration to explain the results attained, for example alternative polyadenylation; one possible cellular mechanism which may control miR-34a mediated *TGIF2* expression. This current study also identified that miR-145 was up-regulated during chondrogenesis of fetal femur-derived cells, which opposes previous studies which recognise miR-145 as exhibiting a down-regulated expression during chondrogenesis.

The developing human fetal femur contains a mixed population of cells, including Stro-1 positive skeletal stem cells; as shown by positive anti-Stro-1 immunohistochemistry which was present throughout the whole fetal femur (Figure 33). Stro-1 positive staining was present in the epiphyses and the diaphysis of the fetal femur and both proliferating and hypertrophic chondrocytes exhibited positive Stro-1 staining (Figure 33). Despite Stro-1 being a positive marker with enrichment specificity for adult skeletal stem cells, the positive Stro-1 staining of proliferating and hypertrophic chondrocytes of the fetal femur indicates a novel observation. Previously Gothard *et al* have shown the expression of Stro-1 during the development of the human fetal femora with Stro-1 expression observed in both the epiphyses and diaphysis, which was indicated to be due to the presence of a shared skeletal stem cell sub-population and Stro-1 immuno-selected populations isolated from the fetal femur were shown to undergo multi-lineage differentiation [398]. Use of fetal femur-derived cells for differentiation assays provided a good source for experimental investigation of chondrogenesis. Fetal femur-derived cells cultured in chondrogenic media proceeded down the chondrogenic lineage and are more chondrogenic than cells cultured in control media containing no TGF-β3, evidenced by chondrogenic marker gene expression results of *COL2A1*, *SOX9* and *AGCAN* (Figures 34 & 39) and positive alcian blue, safranin O and type II collagen immunostaining (Figures 35, 36 & 37). Cells cultured in chondrogenic media aggregated and condensed and maintained their three dimensional shape compared to cells cultured in control media containing no chondrogenic inductive factor TGF-β3, which do not retain the three dimensional shape. TGF-β3 was essential for cells to differentiate down the chondrogenic lineage and resulted in the production of cartilaginous extra cellular matrix helping to retain the 3D micromass structure.

Previously microRNAs have been identified as having differing roles in chondrogenesis. MicroRNA-140 has been extensively covered in the literature [399], [400], [264], [401], [402], [403], [195]. MicroRNA-140 has been found to be up-regulated throughout chondrogenesis [258] and therefore was selected as positive control for positive induction of cells down the chondrogenic lineage. Fetal

femur-derived cells cultured in the presence of TGF-β3 exhibited significant up-regulated expression of both miR-140-3p and miR-140-5p after 21 days in culture compared to expression at day 0 (Figure 40AB). This finding in addition to the chondrogenic marker gene expression observations indicates the ability of the fetal femur-derived cells to undergo chondrogenesis.

MicroRNA-145 has also been identified as having a role in chondrogenic differentiation [257] and served also as a positive control, anticipating that the expression of miR-145 would decrease when fetal femur-derived cells were cultured in chondrogenic media [257]. MiR-145 did not decrease in expression and actually showed a significant increase in expression after 7 days of culture in chondrogenic media (Figure 40C). The chondrogenic marker gene expression results indicate that the fetal femur-derived cells proceeded down the chondrogenic differentiation pathway. The unexpected up-regulation of miR-145 could be due to several reasons. The study conducted by Yang *et al* delineated miR-145 as anti-chondrogenic and identified *Sox9* as a direct target. It was proposed that miR-145 was attenuated during TGF-β3 induced chondrogenesis promoting chondrogenic differentiation through the positive regulation of *Sox9* [257]. The difference in miR-145 expression observed in TGF-β3 induced chondrogenesis may be attributable to the different cell types studied; Yang *et al* investigated miR-145 expression in murine embryonic mesenchymal C3H10T1/2 cells from a cell line and the current study investigated the expression of miR-145 in primary fetal femur-derived cells.

The interaction of miR-145 with target *SOX9* mRNA 3'UTR may be attributable for the differences in miR-145 expression which was observed between the study conducted in murine mesenchymal cells by Yang *et al* and the current study in human fetal femur-derived cells. TargetScanHuman identified that miR-145 have identical sequences in human and mouse. Even if miR-145 is predicted to target the same gene transcripts in both mouse and human cells, it should be considered that the gene transcript itself may possess different properties between mice and human which enable it to alter its interaction with the microRNA and ultimately alter *SOX9* expression level. For example the presence of alternative polyadenylation sites in the 3'UTR [404]. Additionally in different species the length of the 3'UTR may differ and also the presence of multiple microRNA binding sites which can also influence the strength of target repression and resultant target output [405].

In support of the observed up-regulation of miR-145, a number of other studies show the up-regulation of miR-145 in response to TGF-β signalling. Mayorga and Penn show that miR-145 is up-regulated in mesenchymal stem cells derived from rat bone marrow in response to TGF-β1 stimulation [406]. MiR-145 expression is up-regulated in response to TGF-β1 stimulation in human coronary artery smooth muscle cells [383], human pulmonary artery smooth muscle cells [407] and in regulating myofibroblast differentiation in human pulmonary fibroblasts in response to TGF-β1 [408]. Given the studies which identify miR-145 as exhibiting up-regulated expression in response to TGF-β treatment, having also identified miR-145 expression as being up-regulated during TGF-β3 induced chondrogenesis in fetal femur derived cells, perhaps the suggested down-regulation of miR-145

proposed by Yang *et al* [257] should not be considered as a positive control for investigating the effect of TGF-β induced chondrogenesis in human cells.

MiR-34a showed differential expression between fetal femur-derived cells cultured in the presence of TGF-β3 compared to cells cultured in the absence of TGF-β3 with a median of differences in fold change relative expression of 3.4 (Figure 38D). The expression of miR-34a was found to be significantly up-regulated in cells cultured in the chondrogenic media after 21 days in culture compared to cells which had not been submitted to the chondrogenic differentiation assay at day 0 (Figure 40D). This finding indicates that miR-34a is up-regulated during chondrogenesis, specifically TGF-β signalling induced chondrogenesis. In support of the up-regulation of miR-34a expression observed, Zhou *et al* also identify the same finding of miR-34a upregulation in response to TGF-β1 treatment in a rat renal fibroblast cell line (NRK-49F) study [409].

Previously miR-34a had been identified as being a negative regulator of chondrogenesis in chick limb mesenchymal cells and found to be up-regulated after inhibition of JNK induced chondrogenesis [391], [296]. The studies by Kim *et al* found that miR-34a was up-regulated during inhibition of chondrogenesis while this current study found that miR-34a was up-regulated in cells after induction of chondrogenesis. Differences in the expression of miR-34a between this previous study by Kim *et al* and the current study may be due to differences in cell origin; the study by Kim *et al* was conducted in chick derived MSCs. Additionally the current study used TGF-β3 to induce chondrogenesis while Kim *et al* investigated chondrogenesis through modulating the JNK signalling pathway which has been implicated in chondrogenesis [410]. Inhibition of chondrogenesis through inhibition of JNK signalling showed miR-34a up-regulation indicating miR34a as a negative regulator of chondrogenesis through targeting Rac1; required for the actin cytoskeleton organization in establishing chondrocyte morphology [296]. Given that the role of JNK in chondrogenesis remains uncertain as shown by evidence to suggest that JNK supresses chondrogenesis [411] and other studies which depict JNK signalling as inductive in chondrogenesis [412], [410] , the indicated role of miR-34a as anti-chondrogenic suggested by Kim *et al* is thus debateable and should not serve as a comparison to the results identified in the current study.

Bioinformatic *in silico* analysis identified *TGIF2* as a potential target of miR-34a. Five different microRNA target prediction programmes all listed *TGIF2* mRNA as a target of miR-34a and all five programmes all listed the same predicted miR-34a binding site at location 90-97 within the 3'UTR of *TGIF2* mRNA (Table 16). *TGIF2* mRNA was selected as a target for experimental validation because of the potential negative role *TGIF2* may have in chondrogenesis and also the previous studies which have shown *TGIF2* as a target of miR-34a in osteoclasts [396] and gastric cancer cells [397]. *TGIF2* encodes the protein TGIF2; a DNA binding homeobox and translation repressor protein; repressing TGF-β mediated translation [393]. TGIF2 represses TGF-β induced Smad mediated

transcription by interacting with TGF-β activated Smad 3 protein and has been shown to interact with DNA via its homeodomain and also interact with HDAC1 [394]. A study employing *in situ* hybridisation has shown the expression pattern of *tgif2* during mouse embryogenesis; exhibiting high expression in Meckel's cartilages and moderate expression in primordial cartilage of the ribs and vertebrate. *TGIF2* expression has been found to increase in response to TGF-β1 treatment hypothesising the action of this TGF-β mediated transcriptional repressor to work via a negative feedback mechanism. *TGIF2* up-regulation was also observed when HDAC4 was silenced, indicating the role of HDAC4 in regulating *TGIF2* [395].

In support of *TGIF2* as a putative target of miR-34a, *Tgif2* has been shown to be a target of miR-34a in a study conducted by Krzeszinski *et al* [396]. MiR-34a was shown to be down-regulated during the process of *in vitro* osteoclast differentiation and *Tgif2* expression was increased during osteoclastogenesis. *Tgif2* was found to be down-regulated upon miR-34a overexpression and up-regulated upon miR-34a inhibition in human and mouse osteoclast cultures [396]. Hu *et al* also identified *TGIF2* as a target of miR-34a in human gastric cancer cells. MiR-34a was identified to be down-regulated in gastric cancer tissues compared to matched non-tumour tissues and that *TGIF2* was up-regulated in gastric cancer tissues compared to matched non-tumour tissues indicating the function of miR-34a as a tumour suppressor. Gastric cancer cells transiently transfected with miR-34a mimic exhibited significant *TGIF2* expression down-regulation [397].

It can be hypothesised that miR-34a is up-regulated because miR-34a targets *TGIF2*. *TGIF2* encodes the protein TGIF2; a DNA binding homeobox and translation repressor protein; repressing TGF-β mediated translation [393]. In this study cells underwent chondrogenic differentiation in a 3D micromass system in the presence of TGF-β3 which activated the TGF-β-SMAD pathway inducing chondrogenesis. It could be hypothesised therefore that any repressor of this pathway is inhibitory to the process and requires regulation to ensure successful chondrogenesis is not perturbed by any negative regulators. Given that TGIF2 is a repressor of the TGF-β-SMAD pathway it is likely to be a negative regulator of chondrogenesis and needs to be regulated to prevent its negative effect on TGF-β signalling. MiR-34a may therefore be up-regulated during chondrogenesis, targeting TGIF2; inhibiting its negative effect upon chondrogenic differentiation. As previously discussed it has been identified that *TGIF2* is up-regulated in response to TGF-β1 treatment and therefore *TGIF2* expression is potentially up-regulated in response to TGF-β3 treatment, acting as a negative feedback effector to finely regulate TGF-β3 activity. MiR-34a targeting *TGIF2* in turn acts to regulate *TGIF2* activity, acting to fine tune the TGF-β3 induced signalling in fetal femur-derived cells during chondrogenesis.

Despite the putative target prediction and previous studies indicating potential miR-34a function in chondrogenesis by targeting *TGIF2*, transient transfection of miR-34a inhibitor in fetal femur-

derived cells showed no effect upon *TGIF2* mRNA expression (Figure 51) or TGIF2 protein expression (Figure 54). However, transient transfection of miR-34a mimic showed a slight down-regulation of *TGIF2* mRNA expression levels in all samples and TGIF2 protein expression levels were also down-regulated by varying amounts but no significant difference in TGIF2 down-regulated expression was observed (Figures 51D & 54B). Inhibition and overexpression of miR-34a had no effect on the expression of chondrogenic genes, with no significant differences in *SOX9* mRNA, *AGCAN* mRNA or *COL2A1* mRNA following treatment of cells with either miR-34a inhibitor or miR-34a mimic (Figure 52). If miR-34a had successfully targeted and repressed TGIF2 it would be expected that the expression of down-stream genes would also be affected. Given that miR-34a was found to be up-regulated during chondrogenesis, it is likely to play a role, however, the results suggest that miR-34a does not target *TGIF2* mRNA 3'UTR. It may be possible that miR-34a targets and represses a different target during chondrogenesis, which were not investigated. However, other mechanisms of gene and protein regulation may be accountable for the outcome observed. The presence of alternative polyadenylation sites within the 3'UTR [404] of *TGIF2* would enable this target to avoid targeted down-regulation by miR-34a. If alternative polyadenylation is responsible for the finding that miR-34a inhibition and overexpression had no effect on *TGIF2* expression or no effect on chondrogenic gene expression, this could explain why miR-34a was shown to exhibit up-regulated expression during chondrogenesis. Future steps to investigate the different isoforms of *TGIF2* and the presence and location of the microRNA response elements in the 3'UTR and their position in relation to any predicted polyadenylation sites would potentially identify if alterative polyadenylation sites are responsible for the results observed in this study.

Chapter 5

Results: MicroRNA 146b expression in human bone marrow derived skeletal stem cells during chondrogenic differentiation

5.1 Introduction

The use of cell based therapies to repair articular cartilage defects with the aim to allow a fully functional joint surface which is capable of tolerating the stresses and strains induced in joint loading is a promising ideal for the regeneration of cartilaginous tissue. Endogenous repair of cartilage does not occur spontaneously resulting in the loss of chondrocytes and diminishment of the surrounding specialised extracellular matrix. The use of autologous skeletal stem cells for cartilage repair is one proposed method for cartilaginous tissue reparation. In chapter 4, fetal femur-derived stem cells were utilised as a source for chondrogenic differentiation and microRNA expression analysis, however, the unavailability of human fetal femurs following the initial studies in chapter 4 made it necessary to utilise human bone marrow derived skeletal stem cells as an alternative source for investigating microRNA expression during chondrogenesis. Previous studies have reported the therapeutic effect of stem cell administration in patients; Nejadnik *et al* found that patients administered with bone marrow stem cells into chondral lesions were found to have better physical chondrocyte implantation [172]. Kasemkijwattana *et al* found that patients who were administered autologous bone marrow mesenchymal stem cells exhibited significant improvement in knee function with good defect filling [174]. Davatchi *et al* found that patients with moderate to severe osteoarthritis who were administered autologous mesenchymal stem cells showed a reduction in pain [175]. A young male athlete had an articular cartilage defect in the medial femoral condyle and was treated with autologous bone marrow stromal cells. Seven months post-surgery, histological analysis showed the defect was filled with hyaline like cartilage. One year after surgery, the patient was able to return to his previous sporting activity and experienced no pain, with significant improvement in clinical symptoms [176].

Skeletal stem cells isolated from bone marrow possess several properties which make them a promising candidate for tissue regeneration. Skeletal stem cells have been found to accumulate and home to the site of injury and inflammation most likely due to the paracrine properties skeletal stem cells possess. Skeletal stem cells have been reported to secrete growth factors, chemokines and cytokines and these factors it is proposed enables skeletal stem cells to mediate anti-apoptotic, anti-inflammatory, mitogenic and angiogenic properties [413]. Skeletal stem cells are reported to be hypo-immunogenic and to have a low level expression of HLA class I antigens and possess no cell surface HLA class II antigens. Co-culture of allogeneic mesenchymal stem cells with peripheral blood lymphocytes (PBL) had been shown to elicit no proliferative response in the lymphocytes. In addition, no effect was observed when MSCs had been pre-treated with IFN-γ to induce the expression of HLA class II alloantigen or when MSCs were differentiated down osteogenic, adipogenic or the

chondrogenic lineage prior to co-culture [414]. Skeletal stem cells also lack the cell surface receptors CD80, CD86, CD40 and CD40L which are implicated in T lymphocyte activation. Mixed lymphocyte reaction studies show that skeletal stem cells do not elicit T lymphocyte proliferation likely due to suppressive mechanisms [415], [416].

Brittberg *et al* first described the method of autologous chondrocyte implantation (ACI) in 1994 for the repair of chondral knee lesions [417]. The use of skeletal stem cells for cartilage repair compared to the technique of ACI has a number of advantages; bone marrow biopsy is less invasive than arthroscopy which is required to remove healthy cartilage to expand chondrocytes in culture for transplantation into the defect site in ACI. Chondrocytes also have a predisposition to de-differentiate in culture whereas skeletal stem cells can be isolated, cultured and expanded *in vitro* and then differentiated down the chondrogenic lineage [418] [419].

The properties of skeletal stem cells make them a promising cell source for cartilage repair. Skeletal stem cells have been shown to be regulated in part by microRNAs and have been shown to be involved in chondrogenic differentiation, regulating different genes involved with the differentiation process post-transcriptionally [420]. The use of skeletal stem cells in combination with microRNA modulation could provide a new approach to cartilage tissue reparation. MicroRNAs may therefore pave one way to enhancing the chondrogenic potential of these cells pre- and post-implantation in cartilage lesions and also OA joints. However, to exploit the use of microRNAs for their potential in regulating differentiation, understanding the expression patterns and the role of microRNAs in chondrogenesis is essential.

Previously, miR-146b has been found to be up-regulated in epiphyseal cells isolated from the human fetal femur compared to cells isolated from the diaphyseal region, indicating a potential role for miR-146b in chondrogenic differentiation in human fetal femur-derived cells [392]. McAlinden *et al* also identified that miR-146b was expressed at higher levels in precursor chondrocytes compared to miR-146b expression in differentiated chondrocytes in fetal limb tissue [421]. Given the identification of differential expression of miR-146b associated with chondrogenesis and chondrocyte maturation, miR-146b may have a potential role during chondrogenic differentiation of human bone marrow derived skeletal stem cells.

5.2 Hypothesis and Aims

5.2.1 Hypothesis

MicroRNA 146b targets specific genes in human bone marrow derived skeletal stem cells which regulate the ability of human bone marrow derived skeletal stem cells to undergo chondrogenic differentiation.

5.2.2 Aims and Objectives

1. To identify the expression of mR-146b during TGF-β3 induced chondrogenesis. The expression of miR-146b will be assessed following culture of human bone marrow derived skeletal stem cells for 21 days in a 3D micromass culture system containing TGF-β3 compared to cells cultured in in a 3D micromass system containing no TGF-β3.
2. To identify the expression pattern of miR-146b in TGF-β3 induced chondrogenesis across 21 days by examining the expression at 7 day intervals
3. To select from putative targets, genes which are relevant to chondrogenesis using bioinformatic analysis.
4. To validate potential gene targets of miR-146b examined, by carrying out miR-146b overexpression or inhibition assays to identify the effects upon target genes *in vitro*.

5.3 Cell source for chondrogenesis

Human bone marrow derived skeletal stem cells can be isolated through Stro-1 positive selection with use of magnetic activated cell sorting (MACS) which makes use of magnetic nanoparticles conjugated to secondary antibodies which in turn bind to primary antibodies which select for the Stro-1 antigen present on the cell surface of human bone marrow derived skeletal stem cells. Human bone marrow samples were processed and sorted using anti-Stro-1 antibody labelling and magnetic activated cells sorting (MACS) to produce an enriched Stro-1 antigen bearing sample of bone mononuclear cells containing skeletal stem cells. Following culture of isolated Stro-1 enriched bone marrow mononuclear cells, these adult skeletal stem cells which were cultured in basal media were immune-stained with anti-Stro-1 (Figure 55). Following isolation and expansion of Stro-1 enriched human bone marrow derived skeletal stem cells, culturing skeletal stem cells in defined media containing different growth factors allows them to differentiate down differing lineages including the adipogenic, osteogenic and chondrogenic lineages.

Oil red O staining of Stro-1 enriched human bone marrow derived skeletal stem cells showed positive staining in cells cultured in adipogenic media for 14 days and negative oil red O staining in cells cultured in basal control media and osteogenic media for 14 days (Figure 56). Histological analysis has shown that efficient adipogenesis occurs in cultures containing adipogenic media evidenced by the presence of oil red O staining (Figure 56). Alkaline phosphatase staining of Stro-1 enriched human bone marrow derived skeletal stem cells showed positive staining in cells cultured in osteogenic media and negligible alkaline phosphatase staining in cells cultured in basal control media and adipogenic media for 14 days (Figure 57). These results show that Stro-1 enriched human bone marrow derived skeletal stem cells can undergo successful osteogenic differentiation in the presence of osteogenic media. Alkaline phosphatase activity was greatest in cells cultured in osteogenic media for 14 days (Figure 57). Alcian blue, safranin O staining and type II collagen immunostaining of Stro-1 enriched human bone marrow derived skeletal stem cells showed positive staining in cells cultured in chondrogenic media and negative staining in cells cultured in the absence of chondrogenic inducing TGF-β3 (Figures 59, 60 & 61). The culture of Stro-1 enriched skeletal stem cells in defined differentiation media followed by histological analysis shows the ability of human bone marrow derived Stro-1 enriched skeletal stem cells to undergo multi-lineage differentiation.

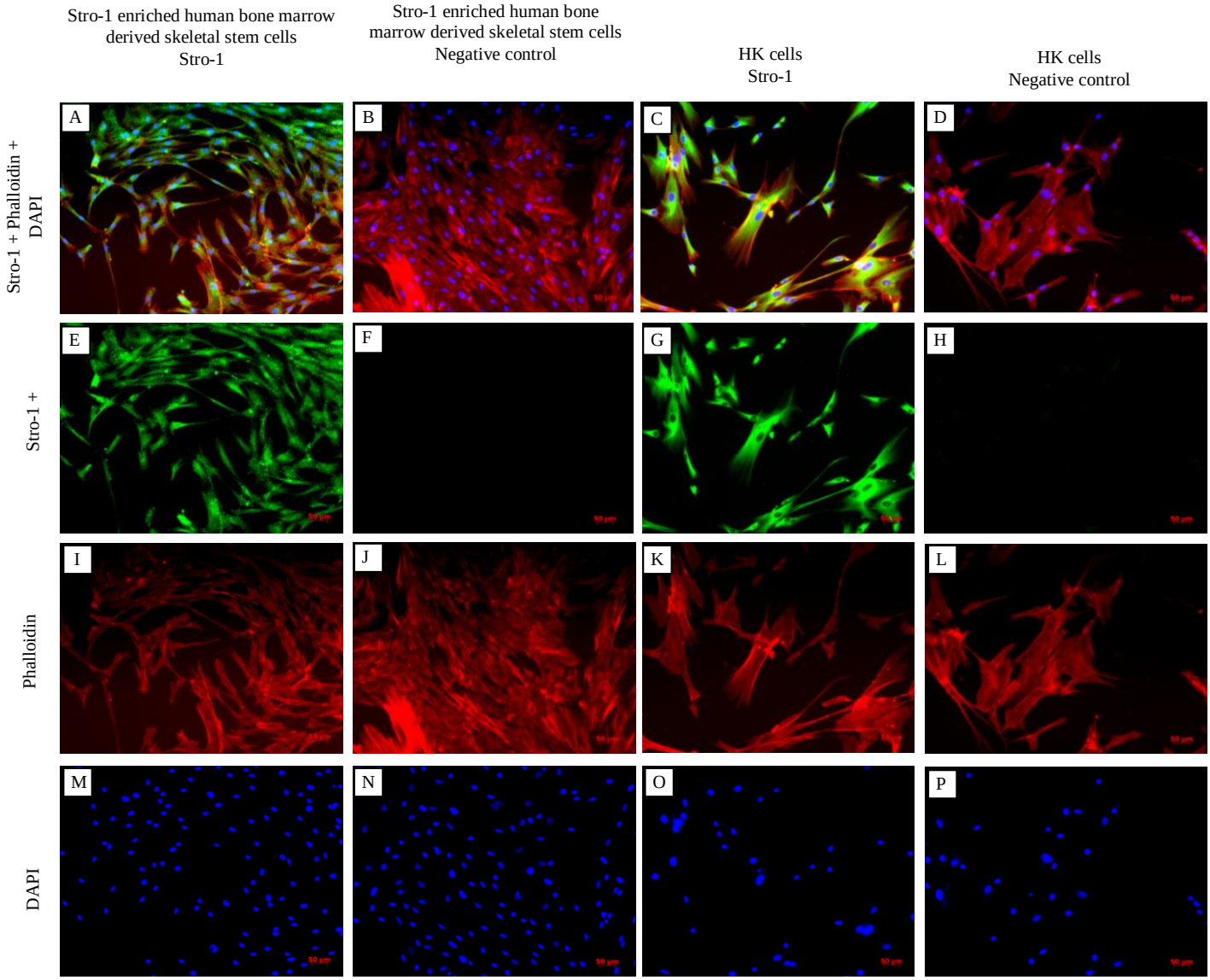

Figure 55. Stro-1 immunostaining of human bone marrow derived skeletal stem cells. Human skeletal stem cells (A, E, I & M); Stro-1 positive immunostaining (A & E), phalloidin cytoskeletal staining (A & I) and DAPI nuclear staining (A & M). Human skeletal stem cells primary antibody negative control (B, F, J, N); Stro-1 immunostaining (B & F), phalloidin cytoskeletal staining (B & J) and DAPI nuclear staining (B & N). HK cells (positive control for Stro-1 staining) (C, G, K & O); Stro-1 immunostaining (C & G), phalloidin cytoskeletal staining (C & K) and DAPI nuclear staining (C & O). Primary antibody negative control staining in HK cells (D, H, L & P); Stro-1 immunostaining (D & H), phalloidin cytoskeletal staining (D & L) and DAPI nuclear staining (D & P) Scale bars = 50µM

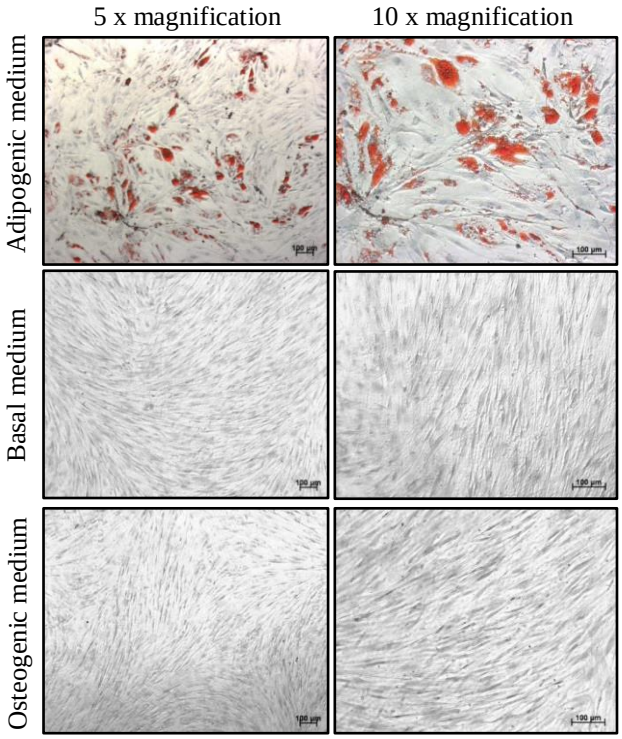

Figure 56. Oil Red O Staining. Stro-1 enriched skeletal stem cells cultured for 14 days in either adipogenic, basal or osteogenic media followed by lysochromal oil red O staining to identify for the presence of lipid droplets resultant of adipogenesis (scale bars 100 μm).

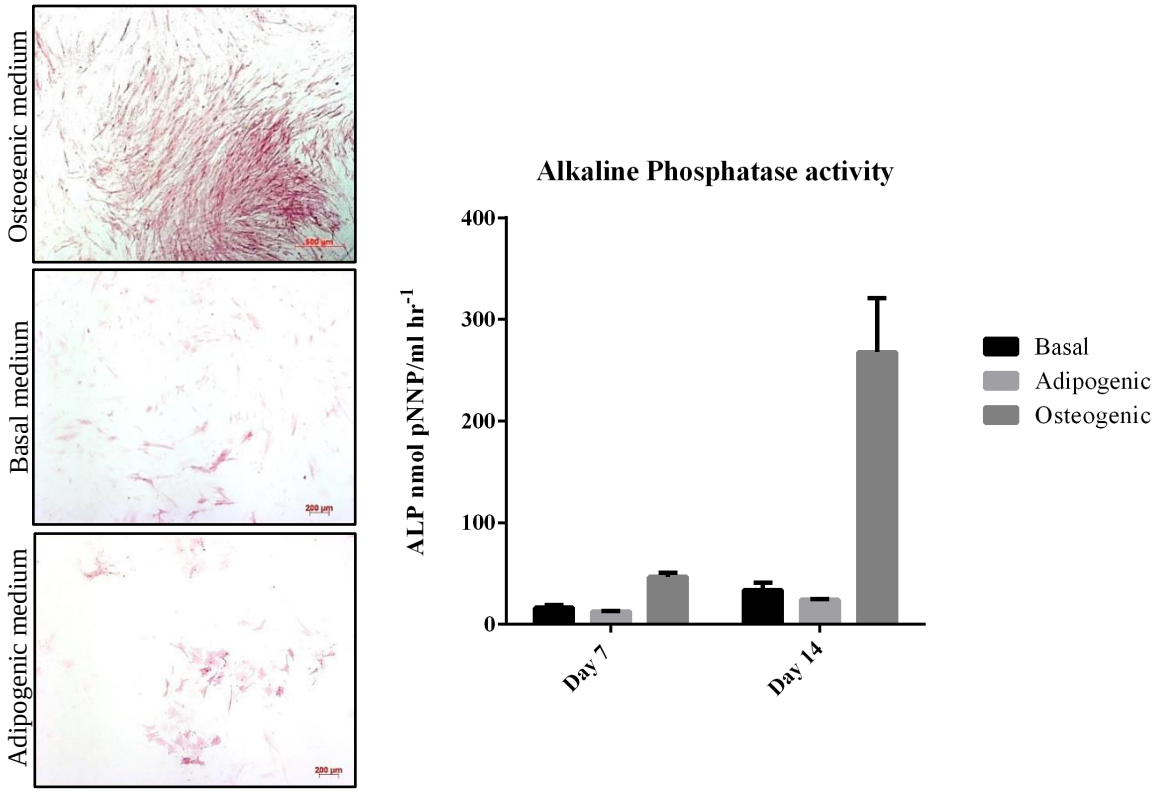

Figure 57. Alkaline phosphatase staining and activity. Stro-1 enriched human bone marrow derived skeletal stem cells cultured for 14 days in either adipogenic, basal or osteogenic media followed by alkaline phosphatase staining (scale bars 200 μm and 500 μm). Cells cultured for 7 and 14 days in either adipogenic, basal or osteogenic media followed by alkaline phosphatase activity assay.

5.4 Chondrogenic analysis: chondrogenic marker gene expression, chondrogenic histological analysis and microRNA expression.

5.4.1 Chondrogenesis marker gene analysis following chondrogenic differentiation assay in human bone marrow derived skeletal stem cells

Human bone marrow derived skeletal stem cells were expanded for 2 passages to yield a sufficient number of cells for high density micromass culture set-up. Cells were cultured for 21 days in media containing either TGF-β3 or no TGF-β-3 in a micromass culture system. After 21 days, examination of chondrogenic marker genes by qPCR showed that *SOX9* (median fold change of ~5.8) (Figure 58A), *ACGAN* (median fold change of approximately ~15.9) (Figure 58B), *COL2A1* (median fold change of ~30,443) (Figure 58C), *COL9A1* (median fold change of ~60,828) (Figure 58D) and *COLXA1* (Figure 58E) (median fold change of ~968) mRNA were all significantly up-regulated in cells cultured in TGF-β3 compared to cells grown in the absence of TGF-β3. Results show that in the presence of TGF-β3, cells differentiate down the chondrogenic lineage (Figure 58).

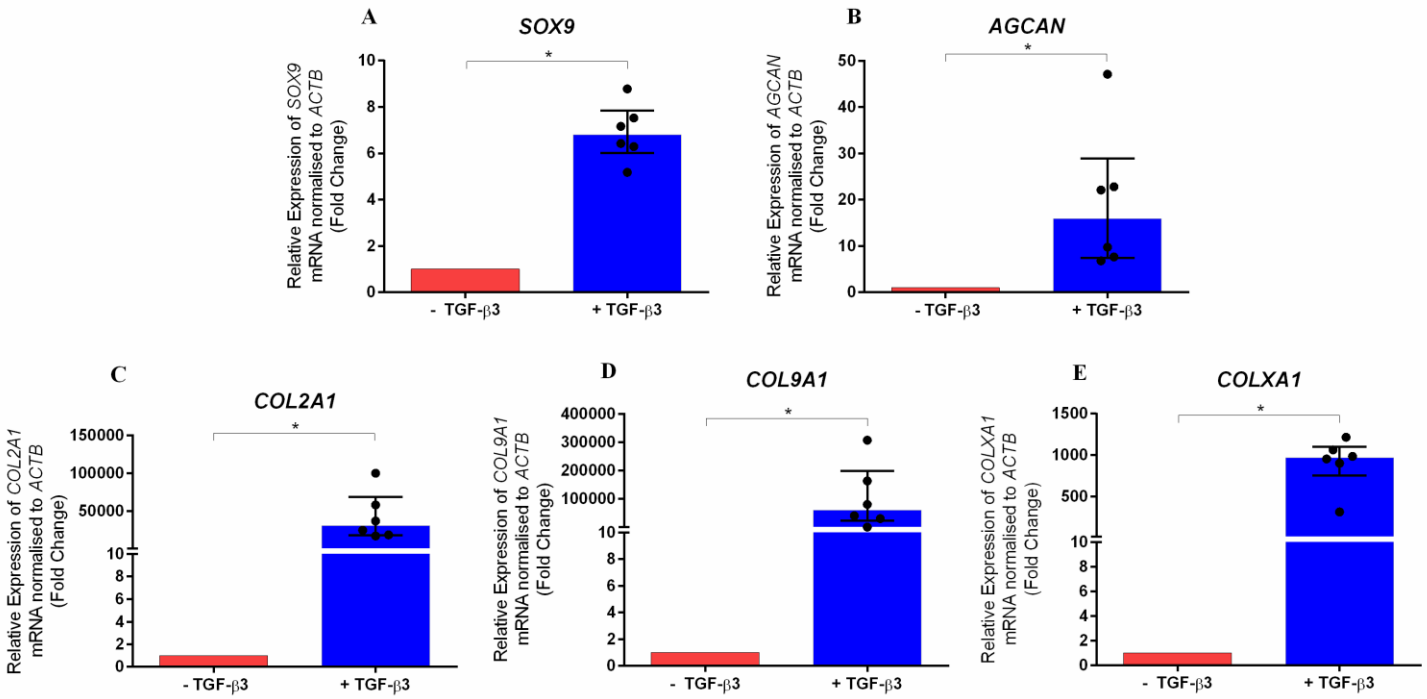

Figure 58. Effect of TGF-β3 treatment for 21 days in human bone marrow derived skeletal stem cells on mRNA expression. Data is presented as the median and interquartile quartile range of the fold change in *SOX9* (A), *AGCAN* (B) *COL2A1* (C) *COL9A1* (D) and *COLXA1* (E) mRNA expression in human bone marrow derived skeletal stem cells cultured in the presence of TGF-β3 for 21 days relative to untreated control bone marrow derived skeletal stem cell cultured in the absence of TGF-β3 (NC) for 21 days. n=6, * p <0.05, Wilcoxon signed rank test.

5.4.2 Histological analysis of chondrogenic differentiation

Micromass cultures processed for histological analysis after 21 days showed that human bone marrow derived skeletal stem cells cultured in TGF-β3 condensed to form 3D cultures, whereas cells cultured in the absence of TGF-β3 failed to condense and the cells were observed to be spread out on the tissue culture plastic and grew as a 2D monolayer. These results suggest that TGF-β3 is required for appropriate chondrogenic induction and formation of a 3D culture system. Histological analysis has shown that efficient chondrogenesis occurs in cultures containing TGF-β3 evidenced by the presence of alcian blue (Figure 59) and safranin O staining (Figure 60) compared to the absence of alcian blue and safranin O staining in cells cultured in the absence of TGF-β3. Micromass cultures also showed positive staining for collagen type II (Figure 61) in the presence of TGF-β3 but not in the absence of TGF-β3. Histological analysis showed that cells cultured in the presence of TGF-β3 differentiated down the chondrogenic lineage.

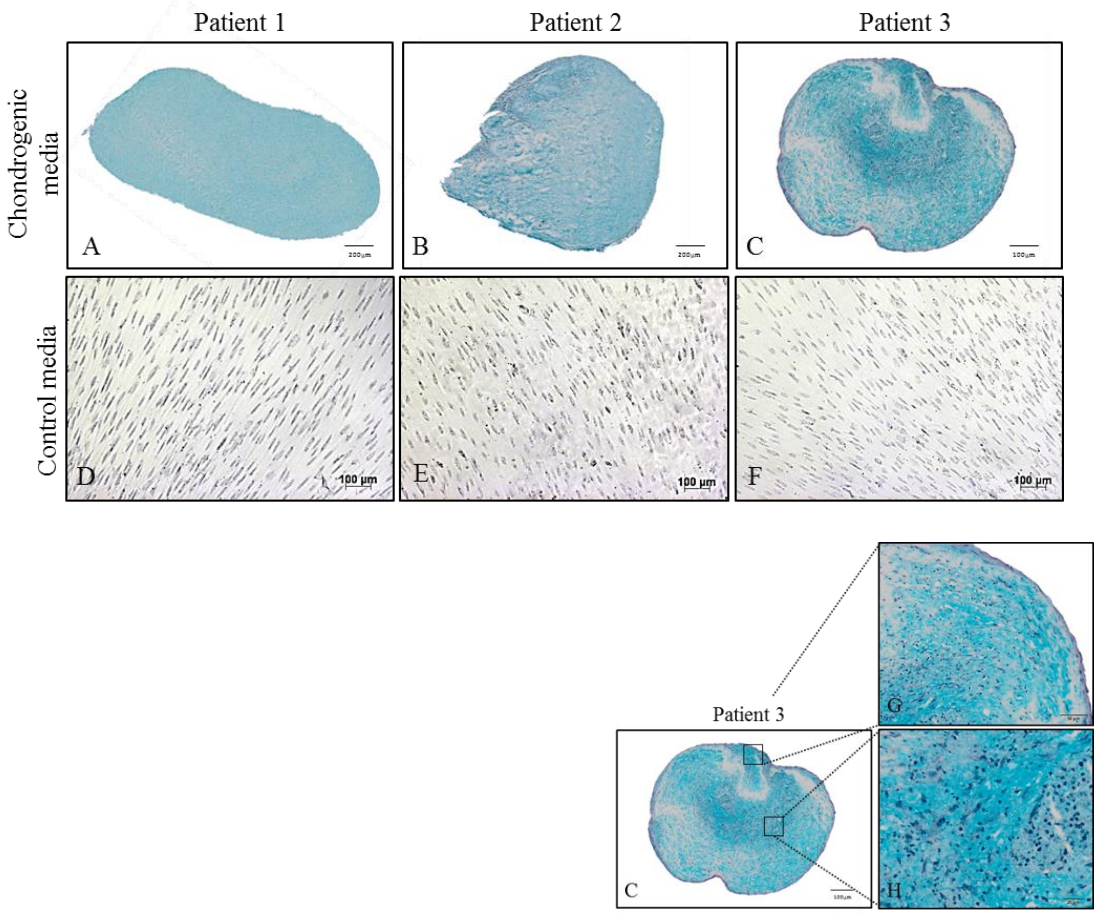

Figure 59. Alcian blue and haematoxylin counterstain in human bone marrow derived skeletal stem cells after 21 days in micromass culture the presence of TGF-β3 (A, B &C) and absence of TGF-β3 (D, E and F). Scale bar = 100µm (D, E & F), 200µm (A, B & C), 50µm (G) and 20µm (H).

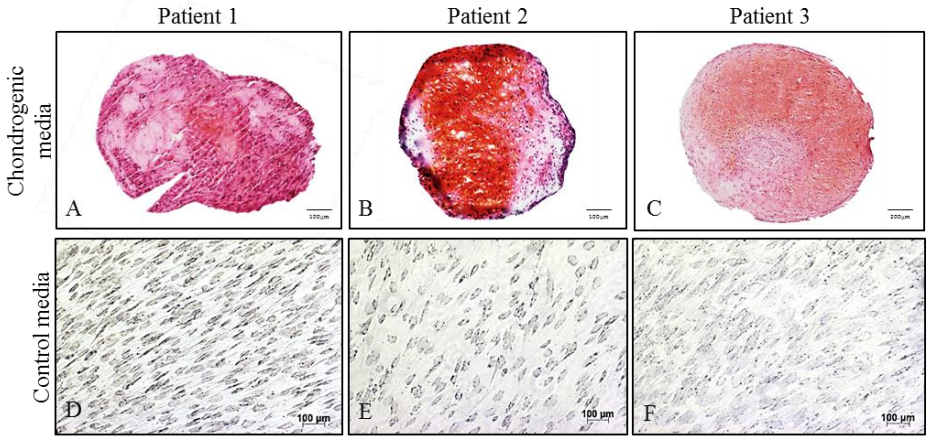

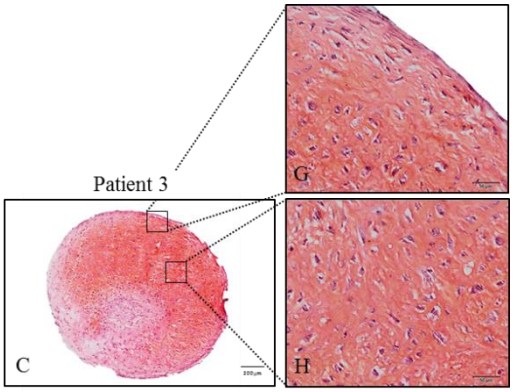

Figure 60. Safranin O and haematoxylin counterstain in human bone marrow derived skeletal stem cells cultured for 21 days in micromass culture in the presence of TGF-β3 (A, B & C) and absence of TGF-β3 (D, E and F). Scale bar = 100µm (D, E & F), 200µm (A, B & C) and 50µm (G & H)

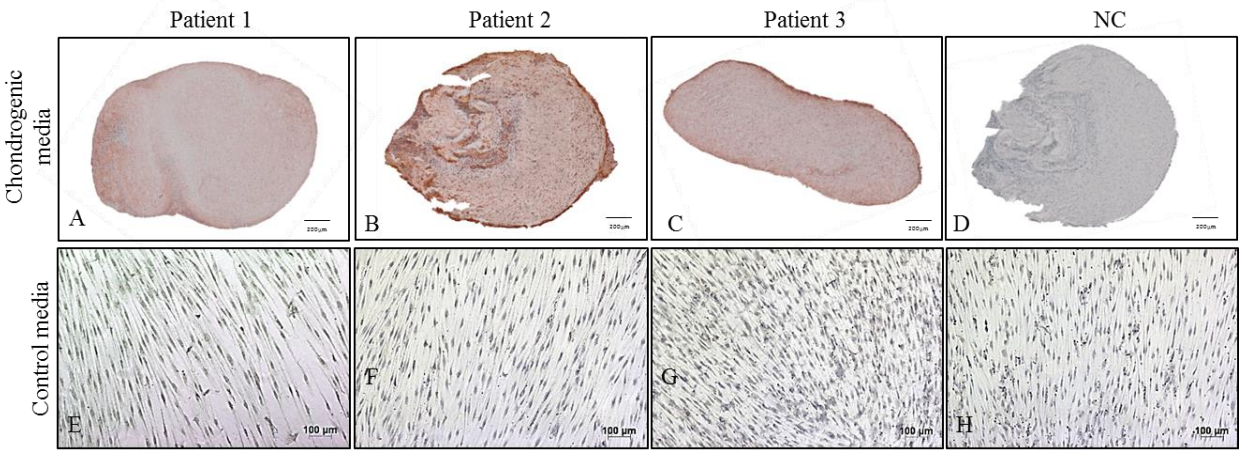

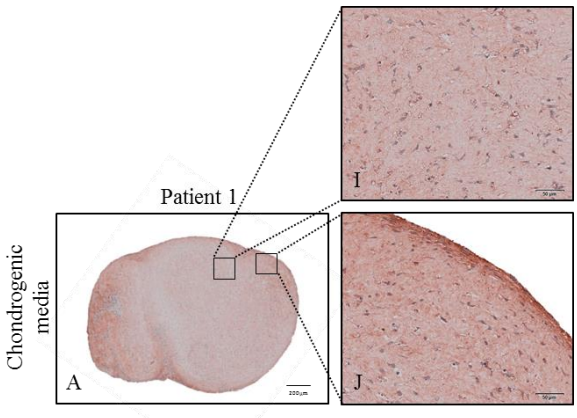

Figure 61. Collagen type II immunostaining and haematoxylin counterstain in human bone marrow derived skeletal stem cells cultured for 21 days in micromass culture in the presence of TGF-β3 (A, B & C) and absence of TGF-β3 (D, E & F). Scale bar = 200µm (A, B, C & D), 100µm (E, F, G & H) and 50µm (I & J).

5.4.3 MicroRNA expression in human bone marrow derived skeletal stem cells following chondrogenic differentiation.

Examination of previously identified chondrogenic associated microRNAs by TaqMan qPCR showed that miR-140-3p (median fold change of ~21.2) (Figure 62A), miR-140-5p (median fold change of ~25.8) (Figure 62B) and miR-145 (median fold change of ~4.6) (Figure 62C) were all significantly up-regulated in human bone marrow derived skeletal stem cells cultured in the presence of TGF-β3 compared to those cells cultured in the absence of TGF-β3. Examination of expression of miR-146b by TaqMan qPCR showed that miR-146b was significantly down-regulated in cells cultured in the presence of TGF-β3 compared to cells cultured in the absence of TGF-β3 (median fold change of ~0.28) (Figure 62D).

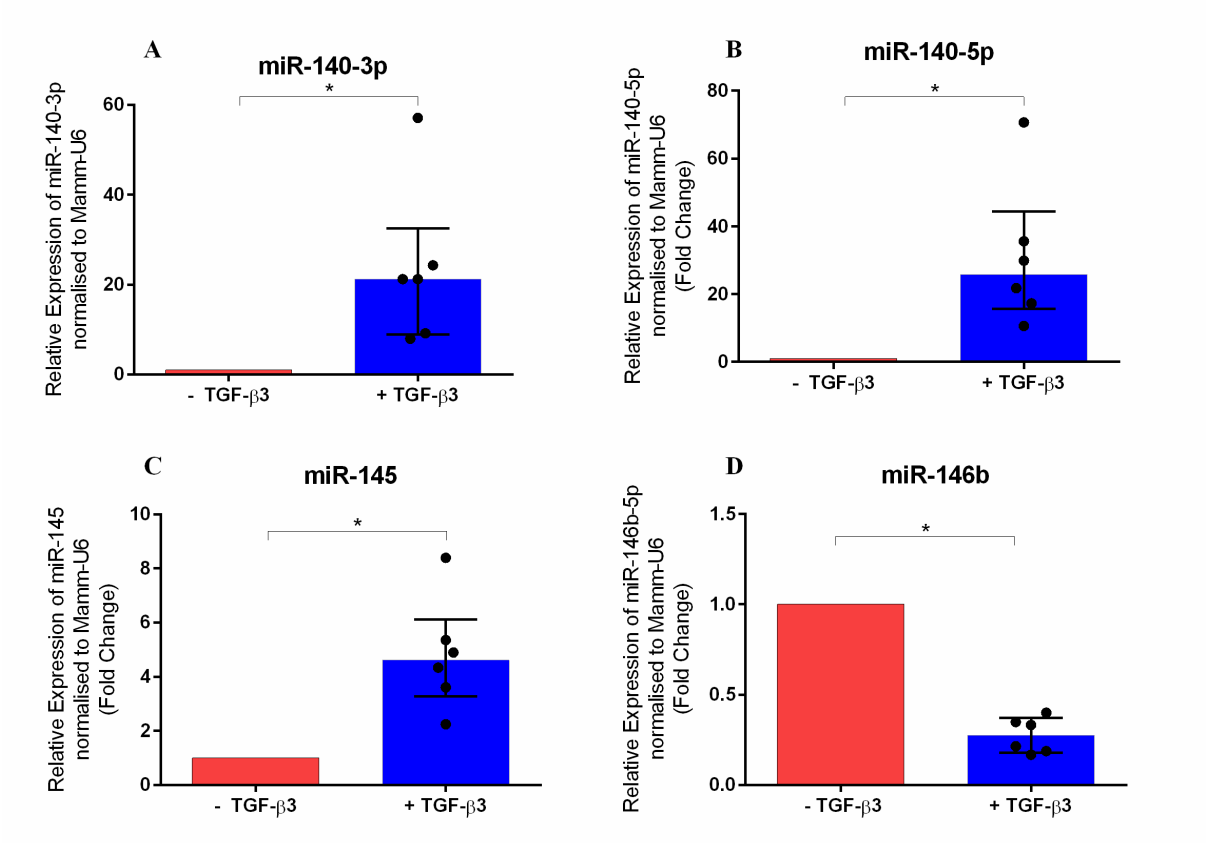

Figure 62. Effect of TGF-β3 treatment for 21 days in human bone marrow derived skeletal stem cells on miRNA expression. Data is presented as the median and interquartile quartile range of the fold change in miR-140-3p (A), miR-140-5p (B) and miR-145 (C) expression in human bone marrow derived skeletal stem cells cultured in the presence of TGF-β3 for 21 days relative to untreated control human bone marrow derived skeletal stem cells cultured in the absence of TGF-β3 for 21 days (NC). n=6, * $p < 0.05$, Wilcoxon signed rank test.

5.5 Time course chondrogenic differentiation assay in human bone marrow derived skeletal stem cells

5.5.1 Chondrogenic marker gene expression across 21 days

Human bone marrow derived skeletal stem cells were subject to micromass culture in the presence of TGF-β3 and examined for chondrogenic differentiation potential over the 21 days at 7 day timed intervals (day 0, day 7, day 14 and day 21). Examination by qPCR showed that the chondrogenic marker genes; *SOX9* (Figure 63A), *AGCAN* (Figure 63B), *COL2A1* (Figure 63C), *COL9A1* (Figure 63D) and *COLXA1* (Figure 63E) increased in expression over 21 days in the presence of TGF-β3. *SOX9*, *AGCAN*, *COL2A1* and *COLXA1* mRNA all exhibited significant upregulation in expression at day 14 and day 21 compared to expression at day 0. *COL9A1* expression was significantly up-regulated at day 21 compared to the expression at day 0 (Figure 63).

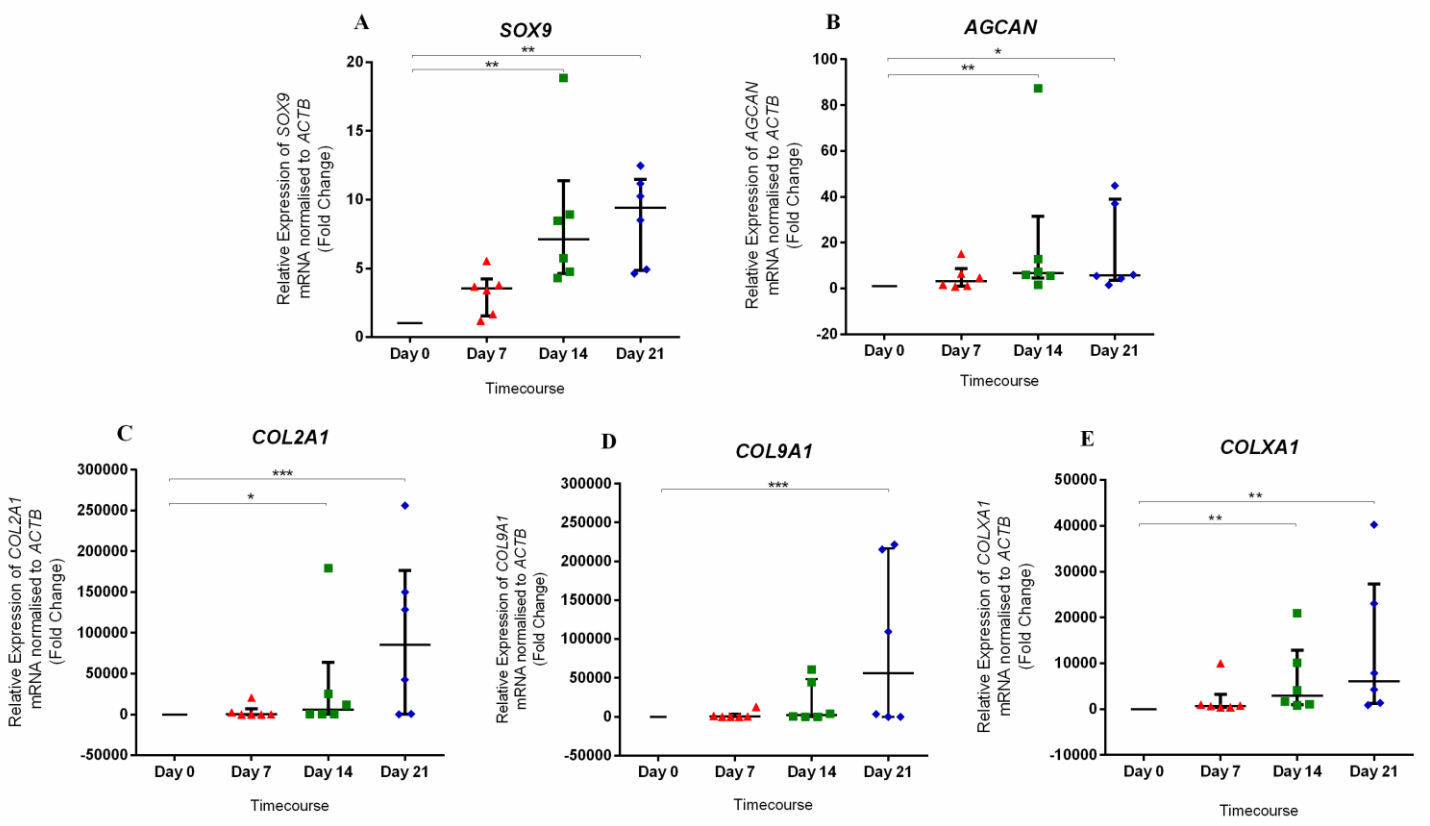

Figure 63. Effect of TGF-β3 treatment for up to 21 days in human bone marrow derived skeletal stem cells on mRNA expression. Data is presented as the median and interquartile quartile range of the fold change in *SOX9* (A), *AGCAN* (B) *COL2A1* (C) *COL9A1* (D) and *COLXA1* (E) mRNA expression in human bone marrow derived skeletal stem cells cultured in the presence of TGF-β3 for up to 21 days relative to untreated control human bone marrow derived skeletal stem cells at day 0 (NC). n=6, * $p < 0.05$, ** $p < 0.01$, *** $p < 0.001$, Friedman test with Dunn's post-test.

5.5.2 MicroRNA expression across 21 days

The expression of previously identified chondrogenic associated microRNAs; miR-140-3p and miR-140-5p increased in expression across 21 days with miR-145 exhibiting an up-regulated staggered expression (Figure 64). Cells exhibited significant upregulation in expression of miR-140-3p (Figure 64A), miR-140-5p (Figure 64B) and miR-145 (Figure 64C) at day 14 and day 21 compared to the expression at day 0. Examination of miR-146b by TaqMan qPCR showed that the expression of miR-146b was down-regulated across 21 days, with a significant difference in miR-146b expression observed at day 14 and day 21 compared to the expression at day 0 (Figure 64D).

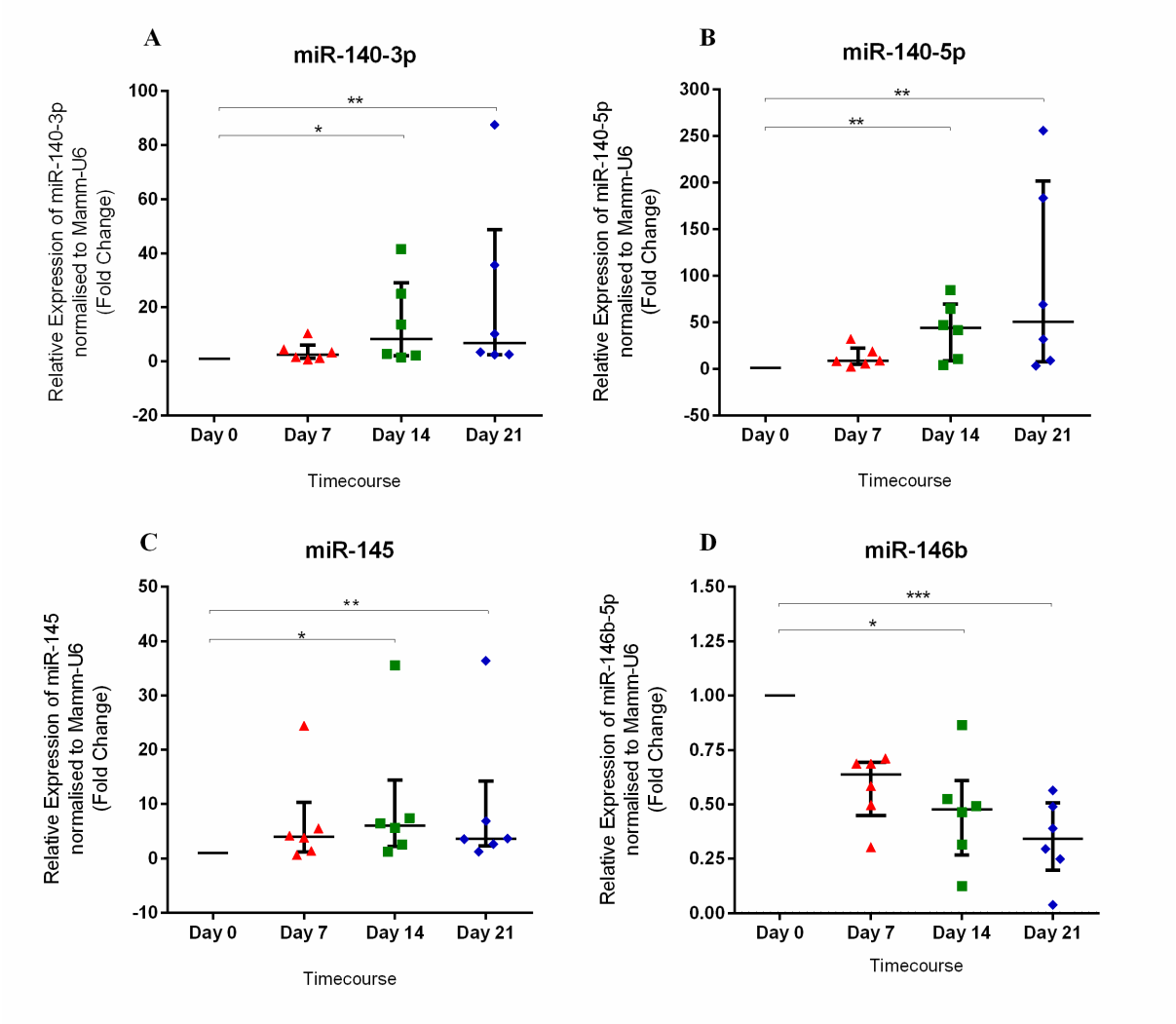

Figure 64. Effect of TGF-β3 treatment for up to 21 days in human bone marrow derived skeletal stem cells on miRNA expression. Data is presented as the median and interquartile quartile range of the fold change in miR-140-3p (A), miR-140-5p (B) and miR-145 (C) expression in human bone marrow derived skeletal stem cells cultured in the presence of TGF-β3 for up to 21 days relative to untreated control human bone derived skeletal stem cells at day 0 (NC). n=6, * $p < 0.05$, ** $p < 0.01$, *** $p < 0.001$.Friedman test with Dunn's post-test.

5.6 Bioinformatic analysis of miR-146b

The webserver Target prediction programme, TargetScanHuman was initially used to search for predicted targets of miR-146b. Table 17 lists all of the predicted targets of miR-146b which have been predicted to possess 3'UTR binding sites which complimentary base pair with miR-146b and the predicted number of miR-146b binding sites located within the 3'UTR. From the list of predicted miR-146b mRNA targets, *SMAD4* and *SOX5* were selected as targets for further experimental validation because:

- *SMAD4* encodes the SMAD4 protein which modulates TGF-β signalling by acting as an intermediate of signal transduction between the cell membrane and the nucleus. Upon TGF-β3 binding at the cell membrane to the TGF-β receptor, the receptor regulated SMADS; SMAD2 and SMAD3 are activated which in turn bind to SMAD4 forming a complex which translocates to the nucleus and binds DNA to up-regulate chondrogenic gene expression. In chondrogenesis *SMAD4* is essential as shown by previous studies; deletion of *Smad4* in chondrocytes in mice resulted in reduced proliferation with premature hypertrophic differentiation resulting in growth plate disorganisation [422].
- In chondrogenesis the transcription factor SOX5 has been identified as being co-expressed with Sox9 and Sox6. It is thought that Sox5 and Sox6 form homo and heterodimers which co-operate with Sox9 to enhance chondrogenic associated gene up-regulation such as the up-regulation of *COL2A1* [423].

The expression of miR-146b was found to be down-regulated in human bone marrow derived skeletal stem cells cultured in the presence of TGF-β3 (Figures 62D & 64D) which indicates that miR-146b is down-regulated throughout TGF-β3 induced chondrogenic differentiation because it plays a role as a negative regulator. If miR-146b is a negative regulator in the chondrogenic differentiation of human bone marrow derived skeletal stem cells, miR-146b is likely to target a positive regulator of chondrogenesis. Searching through the list of predicted miR-146b mRNA targets, both *SMAD4* and *SOX5* are listed which are both positive regulators involved in chondrogenic differentiation.

In addition to TargetScanHuman, other bioinformatic based target prediction programmes were searched to identify if *SMAD4* mRNA and *SOX5* mRNA were also predicted to be potential targets of miR-146b. Table 18 lists the microRNA target prediction databases searched and the predicted *SMAD4* mRNA 3'UTR position where miR-146b is predicted to bind. Table 19 lists the microRNA target prediction databases searched and the predicted *SOX5* mRNA 3'UTR position where miR-146b is predicted to bind. All 5 target prediction programmes all returned a positive match for miR-146b predicted binding to *SMAD4* mRNA and with all 5 target prediction programmes predicted miR-146b to bind at position 390-397 of *SMAD4* mRNA. All 5 target prediction programmes all returned a positive match for miR-146b predicted binding to *SOX5* mRNA and with all 5 target prediction programmes predicted miR-146b to bind at position 883-889 of *SOX5* mRNA 3'UTR. Figure 65 depicts the structure of mature miR-146b and the structure of miR-146b which is predicted to target

SMAD4 and *SOX5*. TagetScanHuman, version 6.2 predicts that *SMAD4* 3'UTR contains only 1 conserved site where miR-146b is predicted to bind. The location of the seed match region where miR-146b base pairs at a location within the *SMAD4* 3' UTR is predicted to be located at position 390-397 of *SMAD4* 3'UTR (Figure 65). TagetScanHuman, version 6.2 predicts that *SOX5* 3'UTR contains only 1 conserved site where miR-146b is predicted to bind. The location of the seed match region where miR-146b base pairs at a location within the *SOX5* 3' UTR is predicted to be located at position 883-889 of *SOX5* 3'UTR (Figure 65).

TargetScanHuman list of predicted miR-146b mRNA targets

Ortholog of target gene	Representative transcript	Gene name	Conserved sites total	Poorly conserved sites total
IGSF1	ENST00000370900.1	immunoglobulin superfamily, member 1	1	1
KBTBD4	ENST00000450908.1	HCG1992246; KBTBD4 protein; Uncharacterized protein	1	0
PSMA4	ENST00000558094.1	proteasome (prosome, macropain) subunit, alpha type, 4	1	0
CDKN2AIP	ENST00000302350.4	CDKN2A interacting protein	2	0
ZBTB2	ENST00000325144.4	zinc finger and BTB domain containing 2	1	1
IRAK1	ENST00000369980.3	interleukin-1 receptor-associated kinase 1	2	0
SLC10A3	ENST00000369649.4	solute carrier family 10, member 3	1	0
HNRNPD	ENST00000313899.7	heterogeneous nuclear ribonucleoprotein D (AU-rich element RNA binding protein 1, 37kDa)	1	0
ZDHHC13	ENST00000446113.2	zinc finger, DHHC-type containing 13	1	0
NOVA1	ENST00000465357.2	neuro-oncological ventral antigen 1	2	0
TRAF6	ENST00000526995.1	TNF receptor-associated factor 6, E3 ubiquitin protein ligase	3	3
TDRKH	ENST00000368825.3	tudor and KH domain containing	1	0
AC012215.1	ENST00000437887.1	Uncharacterized protein	1	1
TMEM120B	ENST00000449592.2	transmembrane protein 120B	1	1
RARB	ENST00000437042.2	retinoic acid receptor, beta	1	0
LFNG	ENST00000402045.1	LFNG O-fucosylpeptide 3-beta-N-acetylglucosaminyltransferase	1	0
CD80	ENST00000264246.3	CD80 molecule	1	0
NUMB	ENST00000554546.1	numb homolog (Drosophila)	1	0
NUDT17	ENST00000334513.5	nudix (nucleoside diphosphate linked moiety X)-type motif 17	1	0
NRAS	ENST00000369535.4	neuroblastoma RAS viral (v-ras) oncogene homolog	1	0
EIF4G2	ENST00000526148.1	eukaryotic translation initiation factor 4 gamma, 2	1	0
USP3	ENST00000380324.3	ubiquitin specific peptidase 3	1	0
AFAP1L2	ENST00000304129.4	actin filament associated protein 1-like 2	1	1
TMEM194A	ENST00000379391.3	transmembrane protein 194A	1	0
ERLEC1	ENST00000185150.4	endoplasmic reticulum lectin 1	1	0
FAM169A	ENST00000380515.3	family with sequence similarity 169, member A	1	0
FAM26E	ENST00000368599.3	family with sequence similarity 26, member E	1	4
WWC2	ENST00000403733.3	WW and C2 domain containing 2	1	2
ZBTB26	ENST00000373656.3	zinc finger and BTB domain containing 26	1	0
FBXO28	ENST00000424254.2	F-box protein 28	1	2
ACER3	ENST00000532485.1	alkaline ceramidase 3	1	1
CARD10	ENST00000403299.1	caspase recruitment domain family, member 10	1	1
STRBP	ENST00000447404.2	spermatid perinuclear RNA binding protein	1	0

ZNF532	ENST00000336078.4	zinc finger protein 532	1	1
SLC19A3	ENST00000258403.3	solute carrier family 19 (thiamine transporter), member 3	1	1
KLF7	ENST00000309446.6	Kruppel-like factor 7 (ubiquitous)	2	2
SCN3B	ENST00000392770.2	sodium channel, voltage-gated, type III, beta subunit	1	1
VASN	ENST00000304735.3	vasorin	1	0
DNPEP	ENST00000273075.4	aspartyl aminopeptidase	1	0
C21orf33	ENST00000291577.6	chromosome 21 open reading frame 33	1	0
DCAF12	ENST00000361264.4	DDB1 and CUL4 associated factor 12	1	0
FAM210A	ENST00000322247.3	family with sequence similarity 210, member A	1	1
PTPRA	ENST00000216877.6	protein tyrosine phosphatase, receptor type, A	1	0
OSTN	ENST00000445281.1	osteocrin	1	0
FBXW2	ENST00000608872.1	F-box and WD repeat domain containing 2	1	0
STRA13	ENST00000580435.1	stimulated by retinoic acid 13	1	0
GABPA	ENST00000354828.3	GA binding protein transcription factor, alpha subunit 60kDa	1	1
ZNRF2	ENST00000323037.4	zinc and ring finger 2	1	2
GOSR1	ENST00000225724.5	golgi SNAP receptor complex member 1	1	1
NF2	ENST00000347330.5	neurofibromin 2 (merlin)	1	0
BCORL1	ENST00000540052.1	BCL6 corepressor-like 1	1	1
ESYT2	ENST00000251527.5	extended synaptotagmin-like protein 2	1	1
CDC14A	ENST00000370125.2	cell division cycle 14A	1	1
C17orf78	ENST00000300618.4	chromosome 17 open reading frame 78	1	0
SH3GL2	ENST00000380607.4	SH3-domain GRB2-like 2	1	0
ZNF148	ENST00000360647.4	zinc finger protein 148	1	1
GDNF	ENST00000326524.2	glial cell derived neurotrophic factor	1	0
PRR26	ENST00000381489.5	proline rich 26	1	0
SMAD4	ENST00000398417.2	SMAD family member 4	1	0
BAG1	ENST00000472232.3	BCL2-associated athanogene	1	0
SBSPON	ENST00000297354.6	somatomedin B and thrombospondin, type 1 domain containing	1	0
APPL1	ENST00000288266.3	adaptor protein, phosphotyrosine interaction, PH domain and leucine zipper containing 1	1	0
VPS52	ENST00000482399.1	vacuolar protein sorting 52 homolog (S. cerevisiae)	2	0
ZNF652	ENST00000362063.2	zinc finger protein 652	1	2
SEC23IP	ENST00000369075.3	SEC23 interacting protein	1	3*
MARCH6	ENST00000274140.5	membrane-associated ring finger (C3HC4) 6, E3 ubiquitin protein ligase	1	1
C16orf72	ENST00000327827.7	chromosome 16 open reading frame 72	1	0
SIAH2	ENST00000312960.3	siah E3 ubiquitin protein ligase 2	1	0
RCAN1	ENST00000482533.1	regulator of calcineurin 1	1	1
PGK1	ENST00000373316.4	phosphoglycerate kinase 1	1	0
SORT1	ENST00000256637.6	sortilin 1	1	2
CASK	ENST00000421587.2	calcium/calmodulin-dependent serine protein kinase (MAGUK family)	1	1
VTI1B	ENST00000554659.1	vesicle transport through interaction with t-SNAREs 1B	1	2
LCOR	ENST00000371103.3	ligand dependent nuclear receptor corepressor	1	1
STC1	ENST00000290271.2	stanniocalcin 1	1	0
ACKR2	ENST00000442925.1	atypical chemokine receptor 2	1	0
FMO2	ENST00000441535.1	flavin containing monooxygenase 2 (non-functional)	1	0
ZNRF3	ENST00000544604.2	zinc and ring finger 3	2	0
MMP16	ENST00000286614.6	matrix metallopeptidase 16 (membrane-inserted)	1	2

SLC2A3	ENST00000075120.7	solute carrier family 2 (facilitated glucose transporter), member 3	1	0
POU3F2	ENST00000328345.5	POU class 3 homeobox 2	1	0
CELF3	ENST00000290585.4	CUGBP, Elav-like family member 3	1	0
GALNT10	ENST00000297107.6	UDP-N-acetyl-alpha-D-galactosamine:polypeptide N-acetylgalactosaminyltransferase 10 (GalNAc-T10)	1	0
CRB3	ENST00000598494.1	crumbs homolog 3 (Drosophila)	1	0
TMEM216	ENST00000334888.5	transmembrane protein 216	1	1
SYT1	ENST00000457153.2	synaptotagmin I	1	0
PIK3CB	ENST00000477593.1	phosphatidylinositol-4,5-bisphosphate 3-kinase, catalytic subunit beta	1	0
TBC1D20	ENST00000354200.4	TBC1 domain family, member 20	1	0
UBE2W	ENST00000517608.1	ubiquitin-conjugating enzyme E2W (putative)	1	0
CLCN6	ENST00000312413.6	chloride channel, voltage-sensitive 6	1	0
RP11-156E8.1	ENST00000607453.1		1	1
MYBL1	ENST00000522677.3	v-myb avian myeloblastosis viral oncogene homolog-like 1	1	0
BTG2	ENST00000290551.4	BTG family, member 2	1	0
ZNF367	ENST00000375256.4	zinc finger protein 367	1	0
LCP2	ENST00000046794.5	lymphocyte cytosolic protein 2 (SH2 domain containing leukocyte protein of 76kDa)	1	0
VAT1	ENST00000355653.3	vesicle amine transport 1	1	1
ERI2	ENST00000569729.1	ERI1 exoribonuclease family member 2	1	0
PDE7A	ENST00000401827.3	phosphodiesterase 7A	1	0
PNKP	ENST00000600910.1	polynucleotide kinase 3'-phosphatase	1	0
RPA3	ENST00000223129.4	replication protein A3, 14kDa	1	0
PRKAA2	ENST00000371244.4	protein kinase, AMP-activated, alpha 2 catalytic subunit	1	1
GPR75	ENST00000394705.2	G protein-coupled receptor 75	1	0
SLC39A1	ENST00000356205.4	solute carrier family 39 (zinc transporter), member 1	1	0
ST5	ENST00000526757.1	suppression of tumorigenicity 5	3	0
NRP2	ENST00000360409.3	neuropilin 2	1	1
SNX22	ENST00000325881.4	sorting nexin 22	1	0
CDS1	ENST00000295887.5	CDP-diacylglycerol synthase (phosphatidate cytidylyltransferase) 1	1	1
FAM83F	ENST00000333407.6	family with sequence similarity 83, member F	1	2
RFTN2	ENST00000295049.4	raftlin family member 2	1	0
FLOT2	ENST00000394906.2	flotillin 2	1	0
C16orf52	ENST00000542527.2	chromosome 16 open reading frame 52	1	0
EHF	ENST00000257831.3	ets homologous factor	1	2*
ROBO1	ENST00000436010.2	roundabout, axon guidance receptor, homolog 1 (Drosophila)	1	0
HIPK3	ENST00000303296.4	homeodomain interacting protein kinase 3	1	0
KIF26B	ENST00000366518.4	kinesin family member 26B	1	1
IST1	ENST00000329908.8	increased sodium tolerance 1 homolog (yeast)	1	0
PM20D2	ENST00000275072.4	peptidase M20 domain containing 2	1	0
PPP1R11	ENST00000376773.1	protein phosphatase 1, regulatory (inhibitor) subunit 11	1	1
LRRC15	ENST00000347624.3	leucine rich repeat containing 15	2	2
SMARCA5	ENST00000283131.3	SWI/SNF related, matrix associated, actin dependent regulator of chromatin, subfamily a, member 5	1	0
KCTD15	ENST00000284006.6	potassium channel tetramerization domain containing 15	1	0
LRRC8B	ENST00000330947.2	leucine rich repeat containing 8 family, member B	1	0
REL	ENST00000295025.8	v-rel avian reticuloendotheliosis viral oncogene homolog	1	0
RNASEL	ENST00000367559.3	ribonuclease L (2',5'-oligoisoadenylate synthetase-dependent)	1	0
DGKG	ENST00000265022.3	diacylglycerol kinase, gamma 90kDa	1	1

TANC2	ENST00000424789.2	tetratricopeptide repeat, ankyrin repeat and coiled-coil containing 2	1	0
RABGAP1	ENST00000373647.4	RAB GTPase activating protein 1	1	0
KIF24	ENST00000402558.2	kinesin family member 24	1	0
TM9SF2	ENST00000376387.4	transmembrane 9 superfamily member 2	1	0
RUNX1T1	ENST00000523629.1	runt-related transcription factor 1; translocated to, 1 (cyclin D-related)	1	0
PRX	ENST00000291825.7	periaxin	2	1
MED1	ENST00000300651.6	mediator complex subunit 1	2	0
SLCO3A1	ENST00000318445.6	solute carrier organic anion transporter family, member 3A1	1	1
PRCP	ENST00000313010.3	prolylcarboxypeptidase (angiotensinase C)	1	1
RFX7	ENST00000423270.1	regulatory factor X, 7	1	0
ZBTB8B	ENST00000609129.1	zinc finger and BTB domain containing 8B	1	3
SYT13	ENST00000020926.3	synaptotagmin XIII	1	1
WASF3	ENST00000335327.5	WAS protein family, member 3	1	0
RCSD1	ENST00000367854.3	RCSD domain containing 1	1	0
POLH	ENST00000372226.1	polymerase (DNA directed), eta	1	1
KDM2B	ENST00000536437.1	lysine (K)-specific demethylase 2B	1	1
FZD1	ENST00000287934.2	frizzled family receptor 1	1	0
MARK1	ENST00000366918.4	MAP/microtubule affinity-regulating kinase 1	1	0
PHOX2B	ENST00000226382.2	paired-like homeobox 2b	1	0
LSM11	ENST00000286307.5	LSM11, U7 small nuclear RNA associated	1	0
DYNLL2	ENST00000579991.2	dynein, light chain, LC8-type 2	1	0
BRD4	ENST00000263377.2	bromodomain containing 4	1	0
SLITRK3	ENST00000475390.1	SLIT and NTRK-like family, member 3	1	0
FAM208A	ENST00000493960.2	family with sequence similarity 208, member A	1	0
ZC3H6	ENST00000343936.4	zinc finger CCCH-type containing 6	1	0
SAMD8	ENST00000372687.4	sterile alpha motif domain containing 8	1	0
DLGAP2	ENST00000421627.2	discs, large (Drosophila) homolog-associated protein 2	1	3
STXBP6	ENST00000396700.1	syntaxin binding protein 6 (amisyn)	1	1
RNF4	ENST00000511859.1	ring finger protein 4	1	0
AAK1	ENST00000409085.4	AP2 associated kinase 1	1	0
UNC5D	ENST00000287272.2	unc-5 homolog D (C. elegans)	1	1
IMPA2	ENST00000269159.3	inositol(myo)-1(or 4)-monophosphatase 2	1	0
DDHD1	ENST00000323669.5	DDHD domain containing 1	1	3
ZNF512B	ENST00000369888.1	zinc finger protein 512B	1	1
KPNA6	ENST00000373625.3	karyopherin alpha 6 (importin alpha 7)	1	1
MYT1	ENST00000328439.1	myelin transcription factor 1	1	0
DNAJB14	ENST00000442697.2	DnaJ (Hsp40) homolog, subfamily B, member 14	1	0
RNF32	ENST00000311822.8	ring finger protein 32	1	0
JAZF1	ENST00000283928.5	JAZF zinc finger 1	1	0
XKR4	ENST00000327381.6	XK, Kell blood group complex subunit-related family, member 4	1	3
TMEM200C	ENST00000581347.2	transmembrane protein 200C	1	0
CCNJ	ENST00000265992.5	cyclin J	1	0
ADAM19	ENST00000257527.4	ADAM metallopeptidase domain 19	1	0
SP8	ENST00000418710.2	Sp8 transcription factor	1	0
C10orf76	ENST00000370033.4	chromosome 10 open reading frame 76	1	0
BMPR1A	ENST00000372037.3	bone morphogenetic protein receptor, type IA	1	0

CAMSAP1	ENST00000389532.4	calmodulin regulated spectrin-associated protein 1	1	0
LTB	ENST00000446745.2	lymphotoxin beta (TNF superfamily, member 3)	1	0
STK40	ENST00000359297.2	serine/threonine kinase 40	1	1
TNIK	ENST00000436636.2	TRAF2 and NCK interacting kinase	1	1
FRYL	ENST00000503238.1	FRY-like	1	0
DUSP16	ENST00000298573.4	dual specificity phosphatase 16	1	1
LAYN	ENST00000525126.1	layilin	1	0
MYLK3	ENST00000394809.4	myosin light chain kinase 3	1	1
MAN1C1	ENST00000374332.4	mannosidase, alpha, class 1C, member 1	1	1
POLR3H	ENST00000396504.2	polymerase (RNA) III (DNA directed) polypeptide H (22.9kD)	1	0
XIAP	ENST00000371199.3	X-linked inhibitor of apoptosis	1	0
EDNRB	ENST00000377211.4	endothelin receptor type B	1	0
ZFYVE1	ENST00000318876.5	zinc finger, FYVE domain containing 1	1	0
ERBB4	ENST00000342788.4	v-erb-b2 avian erythroblastic leukemia viral oncogene homolog 4	1	2
HEYL	ENST00000372852.3	hairy/enhancer-of-split related with YRPW motif-like	1	0
PRELID2	ENST00000334744.4	PRELI domain containing 2	1	1
SLC2A14	ENST00000340749.5	solute carrier family 2 (facilitated glucose transporter), member 14	1	0
SRSF12	ENST00000452027.2	serine/arginine-rich splicing factor 12	1	0
WASF2	ENST00000536657.1	WAS protein family, member 2	1	0
NUCKS1	ENST00000367142.4	nuclear casein kinase and cyclin-dependent kinase substrate 1	1	0
USP44	ENST00000552440.1	ubiquitin specific peptidase 44	1	0
ABL2	ENST00000502732.1	c-abl oncogene 2, non-receptor tyrosine kinase	1	2
CCDC6	ENST00000263102.6	coiled-coil domain containing 6	1	1
GMPS	ENST00000496455.2	guanine monphosphate synthase	1	1
GRSF1	ENST00000254799.6	G-rich RNA sequence binding factor 1	1	1
NAIF1	ENST00000373078.4	nuclear apoptosis inducing factor 1	1	0
TAF9B	ENST00000341864.5	TAF9B RNA polymerase II, TATA box binding protein (TBP)-associated factor, 31kDa	1	0
LIN28A	ENST00000326279.6	lin-28 homolog A (C. elegans)	1	0
QKI	ENST00000392127.2	QKI, KH domain containing, RNA binding	1	1
PPP1R3B	ENST00000310455.3	protein phosphatase 1, regulatory subunit 3B	1	0
MYO6	ENST00000369981.3	myosin VI	1	0
AMN	ENST00000299155.5	amnion associated transmembrane protein	1	0
SCN1A	ENST00000423058.2	sodium channel, voltage-gated, type I, alpha subunit	1	0
NFATC2	ENST00000371564.3	nuclear factor of activated T-cells, cytoplasmic, calcineurin-dependent 2	1	1
MAPT	ENST00000344290.5	microtubule-associated protein tau	1	0
SRRM4	ENST00000267260.4	serine/arginine repetitive matrix 4	1	0
TMEM33	ENST00000504986.1	transmembrane protein 33	1	0
GNL1	ENST00000376621.3	guanine nucleotide binding protein-like 1	1	1
PTCD1	ENST00000292478.4	pentatricopeptide repeat domain 1	1	0
TLCD2	ENST00000330676.6	TLC domain containing 2	1	0
CELF1	ENST00000395290.2	CUGBP, Elav-like family member 1	1	0
CNTFR	ENST00000351266.4	ciliary neurotrophic factor receptor	1	0
BNC1	ENST00000345382.2	basonuclin 1	1	0
ZNF37A	ENST00000361085.5	zinc finger protein 37A	1	0
BEND4	ENST00000504360.1	BEN domain containing 4	1	0
ARMC8	ENST00000469044.1	armadillo repeat containing 8	1	0

HSPA4L	ENST00000296464.4	heat shock 70kDa protein 4-like	1	0
RIMS2	ENST00000507740.1	regulating synaptic membrane exocytosis 2	1	1
PTGFRN	ENST00000393203.2	prostaglandin F2 receptor inhibitor	1	0
USP47	ENST00000339865.5	ubiquitin specific peptidase 47	1	1
GGA2	ENST00000309859.4	golgi-associated, gamma adaptin ear containing, ARF binding protein 2	1	1
FAM65B	ENST00000259698.4	family with sequence similarity 65, member B	1	0
MYO5A	ENST00000399231.3	myosin VA (heavy chain 12, myoxin)	2	1
SPRY3	ENST00000302805.2	sprouty homolog 3 (Drosophila)	1	0
DNAL1	ENST00000553645.2	dynein, axonemal, light chain 1	1	1
STRN	ENST00000263918.4	striatin, calmodulin binding protein	1	2
WDR12	ENST00000261015.4	WD repeat domain 12	1	0
MFHAS1	ENST00000276282.6	malignant fibrous histiocytoma amplified sequence 1	1	0
KCND3	ENST00000369697.1	potassium voltage-gated channel, Shal-related subfamily, member 3	1	0
NPAS4	ENST00000311034.2	neuronal PAS domain protein 4	1	0
PQLC1	ENST00000590381.1	PQ loop repeat containing 1	1	0
PDZD8	ENST00000334464.5	PDZ domain containing 8	1	1
KMT2D	ENST00000301067.7	lysine (K)-specific methyltransferase 2D	1	0
CDON	ENST00000392693.3	cell adhesion associated, oncogene regulated	1	0
CRNKL1	ENST00000377327.4	crooked neck pre-mRNA splicing factor 1	1	1
TCF21	ENST00000367882.4	transcription factor 21	1	1
SEMA3G	ENST00000231721.2	sema domain, immunoglobulin domain (Ig), short basic domain, secreted, (semaphorin) 3G	1	0
GRID1	ENST00000327946.7	glutamate receptor, ionotropic, delta 1	1	1
SETD9	ENST00000285947.2	SET domain containing 9	1	2
NSD1	ENST00000439151.2	nuclear receptor binding SET domain protein 1	1	1
PIP5K1B	ENST00000265382.3	phosphatidylinositol-4-phosphate 5-kinase, type I, beta	1	0
TTL	ENST00000233336.6	tubulin tyrosine ligase	1	1
KCMF1	ENST00000409785.4	potassium channel modulatory factor 1	1	2
IGF2R	ENST00000356956.1	insulin-like growth factor 2 receptor	1	0
PER1	ENST00000317276.4	period circadian clock 1	1	0
SOX5	ENST00000546136.1	SRY (sex determining region Y)-box 5	1	0
EIF5A2	ENST00000474096.1	eukaryotic translation initiation factor 5A2	1	0
SRRD	ENST00000215917.7	SRR1 domain containing	1	0
IKZF3	ENST00000346872.3	IKAROS family zinc finger 3 (Aiolos)	1	0
GINM1	ENST00000367419.5	glycoprotein integral membrane 1	1	0
PBX2	ENST00000375050.4	pre-B-cell leukemia homeobox 2	1	0
UBA6	ENST00000322244.5	ubiquitin-like modifier activating enzyme 6	1	0
MTDH	ENST00000336273.3	metadherin	1	0
TMEM136	ENST00000529187.1	transmembrane protein 136	1	0
HIC2	ENST00000407464.2	hypermethylated in cancer 2	1	0
STAU2	ENST00000522695.1	staufen double-stranded RNA binding protein 2	1	0
RRAGD	ENST00000369415.4	Ras-related GTP binding D	1	1
GPBP1	ENST00000424459.3	GC-rich promoter binding protein 1	1	0
RPAP2	ENST00000610020.1	RNA polymerase II associated protein 2	1	3*
C17orf75	ENST00000577809.1	chromosome 17 open reading frame 75	1	0
ATG7	ENST00000354449.3	autophagy related 7	2	0
DNAJC14	ENST00000357606.3	DnaJ (Hsp40) homolog, subfamily C, member 14	1	0

SGIP1	ENST00000371036.3	SH3-domain GRB2-like (endophilin) interacting protein 1	1	0
GLYATL3	ENST00000371197.4	glycine-N-acyltransferase-like 3	1	0
KCNK10	ENST00000340700.5	potassium channel, subfamily K, member 10	1	2
GRK5	ENST00000392870.2	G protein-coupled receptor kinase 5	1	0
GATA6	ENST00000269216.3	GATA binding protein 6	1	0
PDF	ENST00000288022.1	peptide deformylase (mitochondrial)	1	0
RP11-343C2.12	ENST00000562949.1	Conserved oligomeric Golgi complex subunit 8	1	0
CD3D	ENST00000300692.4	CD3d molecule, delta (CD3-TCR complex)	1	0
PDHB	ENST00000474765.1	pyruvate dehydrogenase (lipoamide) beta	1	0
ATP5J2-PTCD1	ENST00000413834.1	ATP5J2-PTCD1 readthrough	1	0
C4orf3	ENST00000399075.4	chromosome 4 open reading frame 3	1	1
SMTNL2	ENST00000338859.4	smoothelin-like 2	1	0

Table 17. TarrgetScanHuman list of predicted miR-146b mRNA targets and predicted number of conserved and poorly conserved binding sites within the 3'UTR. mRNA targets selected for validation are highlighted in yellow.

Database	***SMAD4* putative target of miR-146b**	**Predicted position 390-397 of *SMAD4* 3'UTR**
TargetScanHuman release 6.2	Yes	Yes
Diana web server v5.0 interface	Yes	Yes
PicTar	Yes	Yes
PITA – Segal Lab of computational biology	Yes	Yes
microRNA.org (Aug 2010 release)	Yes	Yes

Table 18. Target prediction programmes that identify *SMAD4* as a predicted target of miR-146b

Database	***SOX5* putative target of miR-146b**	**Predicted position 883-889 of *SOX5* 3'UTR**
TargetScanHuman release 6.2	Yes	Yes
Diana web server v5.0 interface	Yes	Yes
PicTar	Yes	Yes
PITA – Segal Lab of computational biology	Yes	Yes
microRNA.org (Aug 2010 release)	Yes	Yes

Table 19. Target prediction programmes that identify *SOX5*as a predicted target of miR-146b

MicroRNA-146b structure

A) Primary miR-146b structure

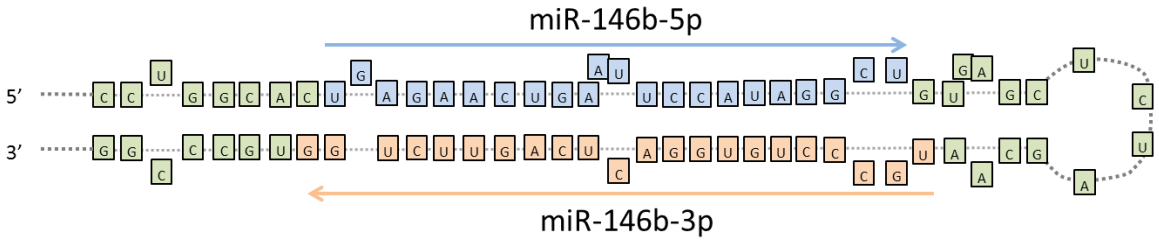

B) Mature miR-146b-5p structure

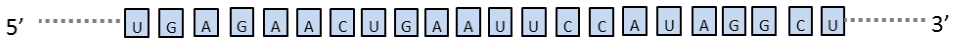

C) miR-146b-5p seed match base pairing at position 390-397 of *SMAD* 4 mRNA 3' UTR

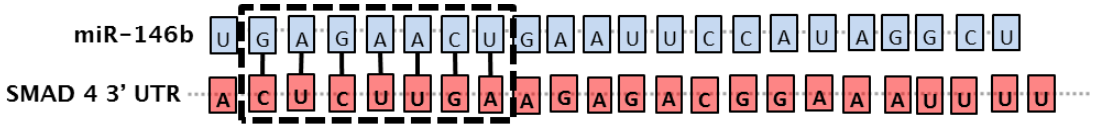

SMAD4 3'UTR 5' …UUUUAAAGGCAGAGAAGUUCUCA…3'

miR-146b 3' UCGGAUUCCUUAAGUCAAGAGU 5'

D) miR-146b-5p seed match base pairing at position 883-889 of *SOX5* mRNA 3'UTR

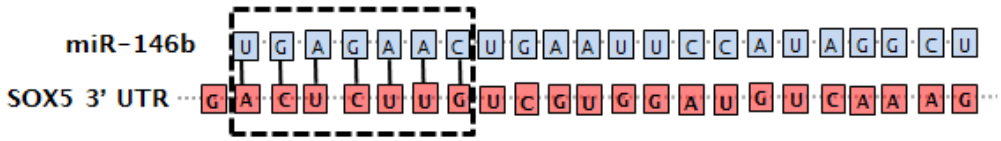

SOX5 3'UTR 5' …GAAACUGUAGGUGCUGUUCUCAG…3'

miR-146b 3' UCGGAUACCUUAAGUCAAGAGU

Figure 65. MicroRNA-146b structure. The structure and sequence of primary miR-146b (A). The sequence of mature miR-146b-5p (B). The seed match base pairing of mature miR-146b seed region to the designated sequence within SMAD4 3'UTR (C). The seed match base pairing of mature miR-146b seed region to the designated sequence within SOX5 3'UTR (D). (Information regarding microRNA sequences and targets were interpreted from TargetScanHuman, version 6.0).

5.7 Transient inhibition and overexpression of miR-146b in human bone marrow derived skeletal stem cells

5.7.1 miR-146b, *SMAD4*, *SOX5* and chondrogenic associated gene expression following transient transfection with miR-146b inhibitor or miR-146b mimic

Following transient transfection of human bone marrow derived skeletal stem cells with miR-146b inhibitor for 48 hours, miR-146b was found to be significantly down-regulated compared to the expression of miR-146b in cells treated with the negative control oligonucleotide (median fold change of ~0.29) (Figure 66A). The identified potential mRNA targets of miR-146b; *SMAD4* and *SOX5* showed no significant differences in expression after treatment with miR-146b inhibitor compared to the cells treated with the negative control inhibitor (Figure 66 C & E). Cells treated with miR-146b mimic exhibited up-regulation of miR-146b (median fold change of ~56754) (Figure 66B) and the potential mRNA targets; *SMAD4* and *SOX5* exhibited no differences in expression following miR-146b overexpression through transfection with miR-146b mimic (Figure 66 D & F). Chondrogenic marker genes; *SOX9*, *AGCAN* and *COL2A1* exhibited no significant differences in expression following transfection in cells with miR-146b mimic or miR-146b inhibitor (Figure 67).

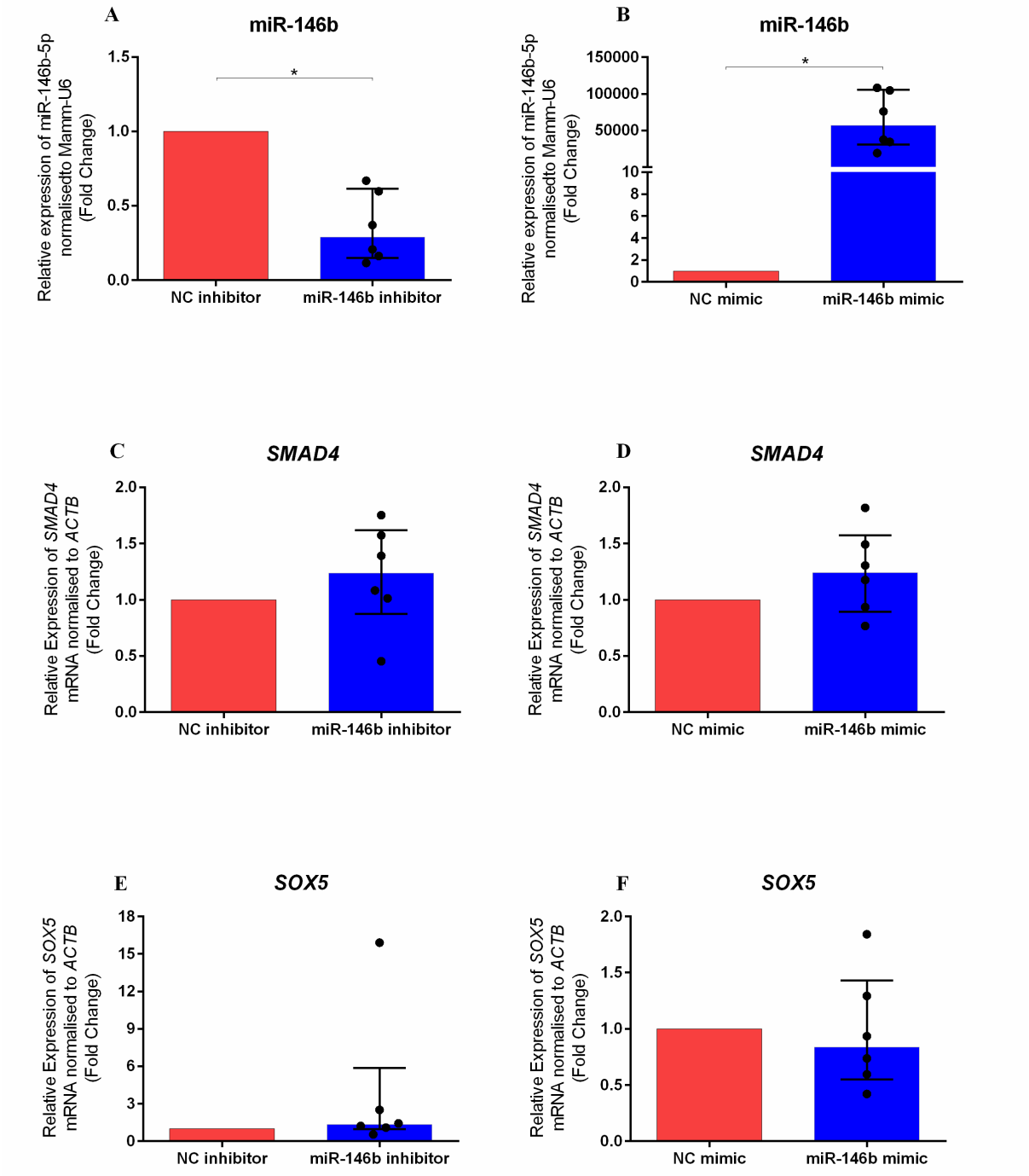

Figure 66. Effect of miR-146b inhibition and overexpression on miR-146b expression and *SMAD4* and *SOX5* mRNA expression in human bone marrow derived skeletal stem cells. Data is presented as the median and interquartile quartile range of the fold change in miR-34a (A & B), *SMAD2* mRNA (C & D) and *SOX5* mRNA expression in human bone marrow derived skeletal stem cells cultured in the presence of either miR-34a inhibitor relative to control cells treated with non-targeting hairpin inhibitor (NC) (A, C & E) or miR-34a mimic relative to the control cells treated with non-targeting mimic (B, D & F). n=6, * $p < 0.05$, Wilcoxon signed rank test.

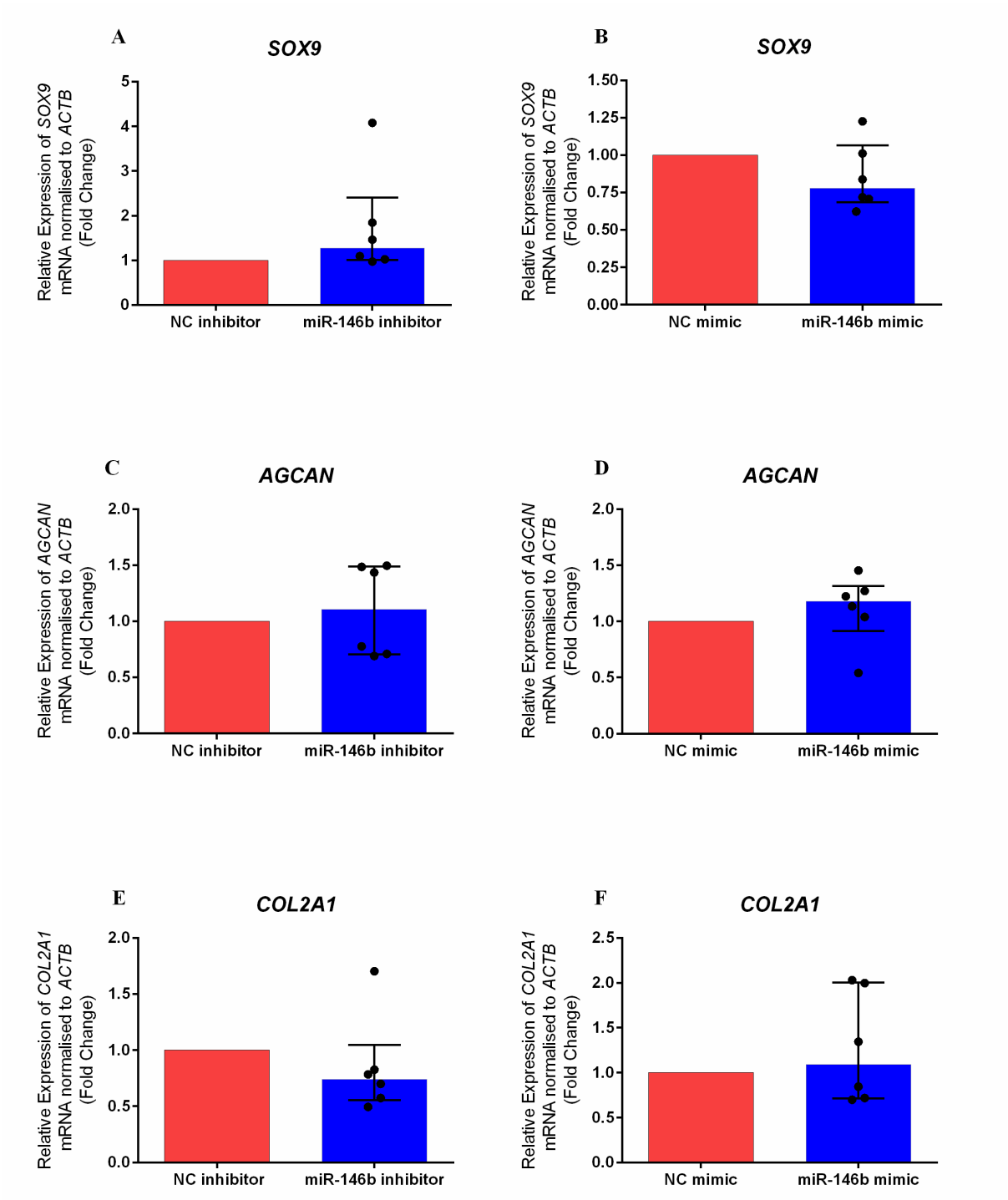

Figure 67. Effect of miR-146b inhibition and overexpression on mRNA expression in human bone marrow derived skeletal stem cells. Data is presented as the median and interquartile quartile range of the fold change in *SOX9* (A & B), *AGCAN* (C & D) and *COL2A1* (E & F) mRNA expression in human bone marrow derived skeletal stem cells cultured in the presence of either miR-146b inhibitor relative to control cells treated with non-targeting hairpin inhibitor (NC) (A, C & E) or miR-146b mimic relative to the control cells treated with non-targeting mimic (B, D & F). n=6, Wilcoxon signed rank test.

5.7.2 SMAD4 protein expression in human bone marrow derived skeletal stem cells following transient transfection with miR-146b inhibitor or miR-146b mimic

Following transient transfection of human bone marrow derived skeletal stem cells for 72 hours with either: miR-146b inhibitor, non-targeting inhibitor oligonucleotide (NC), miR-146b mimic or non-targeting mimic control (NC) cells were lysed and protein extracted and quantified. Western blotting and densitometry analysis was employed to determine the effect of transient transfection upon SMAD4 protein expression, β-actin protein expression served as an internal control. Cells transfected with either miR-146b inhibitor or non-targeting inhibitor oligonucleotide (NC) were compared for the expression of SMAD4 and densitometry analysis of the immunoblots showed that there was no significant differences in SMAD4 expression between the two treatment groups, indicating that miR-146b has no effect upon SMAD4 expression (Figure 69A). Cells transfected with either miR-146b mimic or non-targeting mimic oligonucleotide (NC) were compared for the expression of SMAD4 and densitometry analysis of the immunoblots showed that there was no significant difference in SMAD4 expression between the two treatment groups, however, despite this result all samples were up-regulated to some degree (Figure 69B). Immunoblots displayed in Figure 68 from the western blot were used for densitometry analysis.

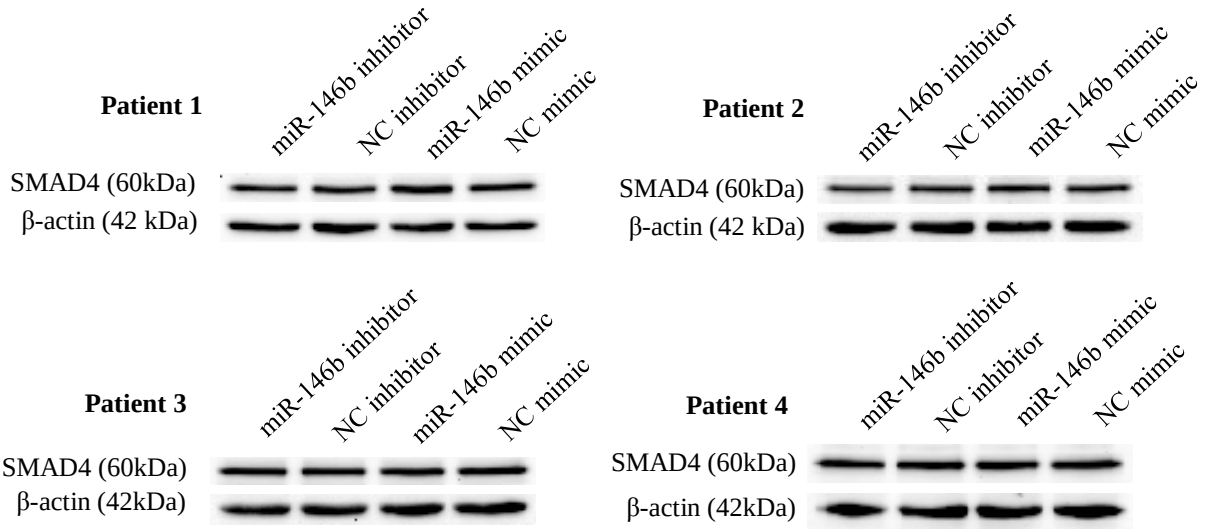

Figure 68. Western blotting immunoblots. Protein expression of SMAD4 and internal normalising control β-actin, following transient transfection of human bone marrow derived skeletal stem cells with miR-146b inhibitor, non-targeting hairpin inhibitor, miR-146b mimic and non-targeting mimic in 4 individual patient samples.

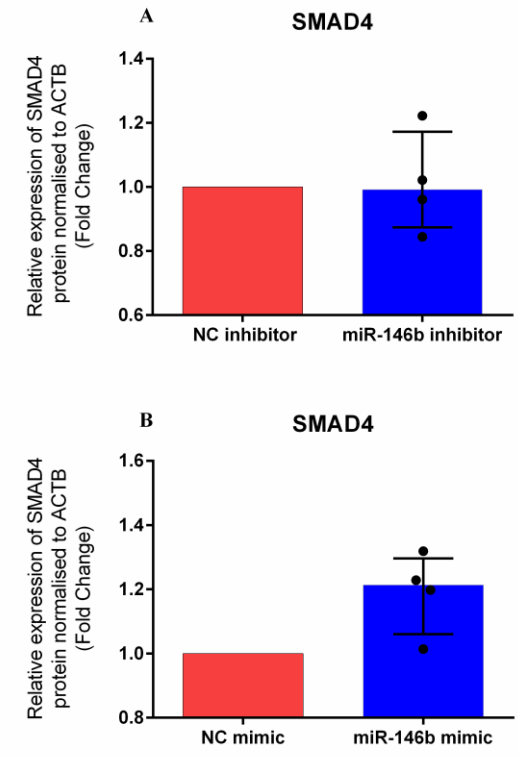

Figure 69. Effect of miR-146b inhibition and overexpression on SMAD4 protein expression in human bone marrow derived skeletal stem cells. Data is presented as the median and interquartile quartile range of the fold change in SMAD4 expression in human bone marrow derived skeletal stem cells cultured in the presence of either miR-146b inhibitor relative to control cells treated with non-targeting hairpin inhibitor (NC) (A) or miR-146b mimic relative to the control cells treated with non-targeting mimic (B). n=4, Wilcoxon signed rank test.

5.7.3 SOX5 protein expression in human bone marrow derived skeletal stem cells following transient transfection with miR-146b inhibitor or miR-146b mimic

Following transient transfection of human bone marrow derived skeletal stem cells for 72 hours with either: miR-146b inhibitor, non-targeting inhibitor oligonucleotide (NC), miR-146b mimic or non-targeting mimic control (NC) cells were lysed and protein extracted and quantified. Western blotting and densitometry analysis was employed to determine the effect of transient transfection upon SOX5 protein expression, β-actin protein expression which served as an internal control. Cells transfected with either miR-146b inhibitor or non-targeting inhibitor oligonucleotide (NC) were compared for the expression of SOX5, densitometry analysis of the immunoblots showed that there was no significant difference in SOX5 expression between the two treatment groups (Figure 71A). Cells transfected with either miR-146b mimic or non-targeting mimic oligonucleotide (NC) were compared for the expression of SOX5 and densitometry analysis of the immunoblots showed that protein expression level of SOX5 was significantly reduced in cells which were transfected with miR-146b mimic (median fold change of ~0.67) (Figure 71B). Immunoblots displayed in Figure 70 from the western blot were used for densitometry analysis.

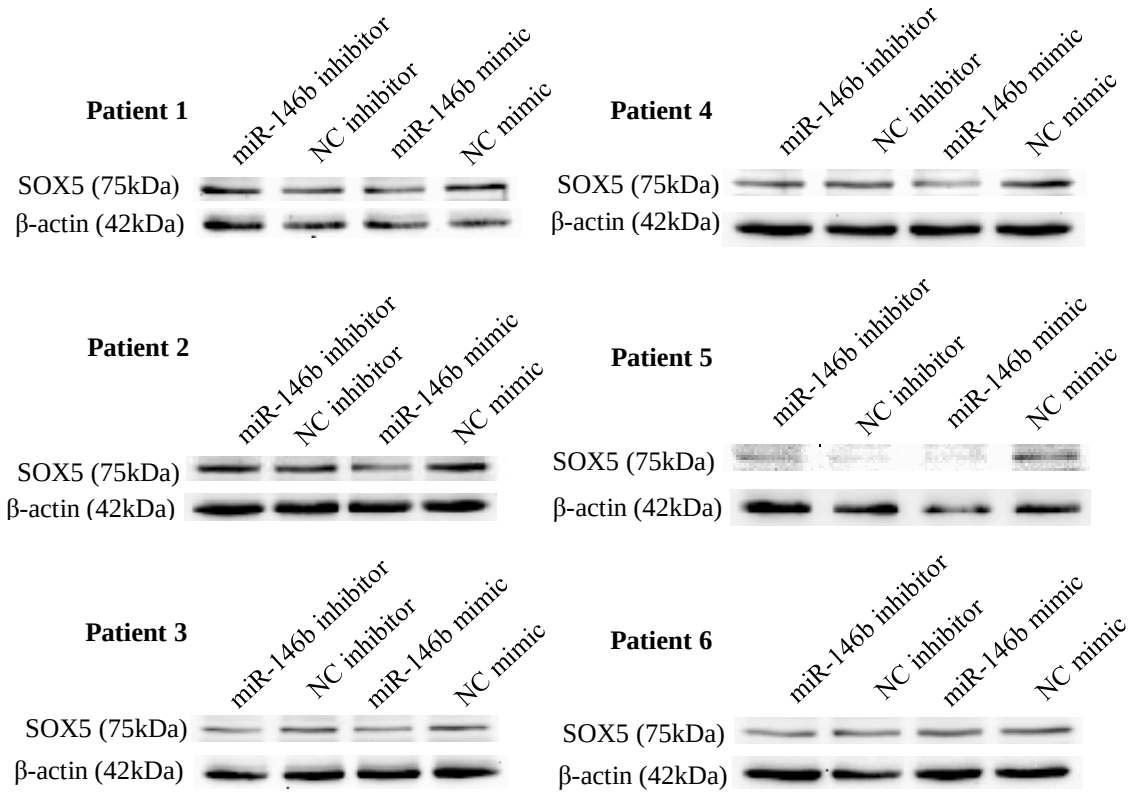

Figure 70. Western blotting immunoblots. Protein expression of SOX5 and internal normalising control β-actin, following transient transfection of human bone marrow derived skeletal stem cells with miR-146b mimic, mimic non-targeting oligonucleotide, miR-146b inhibitor or inhibitor non-targeting oligoneucletide in 6 individual patient samples,

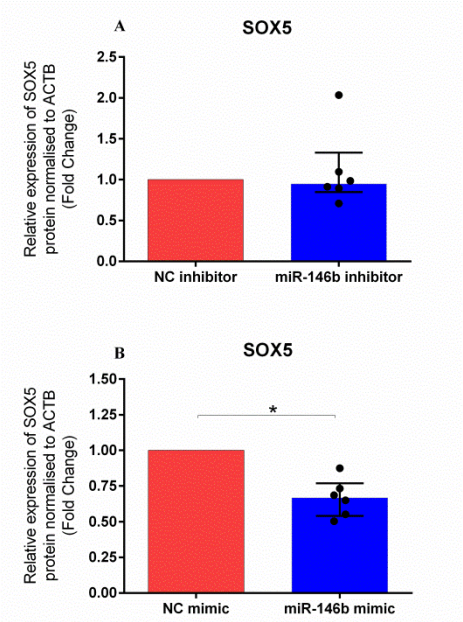

Figure 71. Effect of miR-146b inhibition and overexpression on SOX5 protein expression in human bone marrow derived skeletal stem cells. Data is presented as the median and interquartile quartile range of the fold change in SOX5 expression in human bone marrow derived skeletal stem cells cultured in the presence of either miR-146b inhibitor relative to control cells treated with non-targeting hairpin inhibitor (NC) (A) or miR-146b mimic relative to the control cells treated with non-targeting mimic (B). n=6, * $p < 0.05$, Wilcoxon signed rank test.

5.8 Validating miR-146b interaction with *SOX5* mRNA 3'UTR – Plasmid construction in preparation for luciferase reporter assay

A luciferase reporter assay can be used to test the effect of microRNA mediated regulation on predicted target gene/s. The experimental method of validating the interaction between microRNA and its targeting sites within the 3'UTR of target mRNA requires the construction of appropriate vectors which carry either the microRNA sequence or the target mRNA 3'UTR sequence. The microRNA-mRNA 3'UTR interaction can be quantified by the construction of a luciferase gene construct which contains the microRNA targeted sequence from the target gene which is generally located within the 3'UTR. The luciferase gene construct containing the target gene and a separate construct containing the microRNA sequence can be co-transfected into cells and a dual luciferase reporter assay system can be employed to quantify luciferase activity. A luciferase reporter assay can test the interaction between target mRNA and microRNA; microRNA which binds to its target mRNA prevents protein translation, if the construct containing the target mRNA interacts with the microRNA the mRNA will not undergo protein translation and nor will the attached luciferase mRNA and therefore luciferase protein expression is down-regulated and the reaction producing light does not occur, this can be compared to a luciferase gene construct containing the target gene which has been purposefully mutated therefore preventing microRNA-mRNA interaction, target mRNA and luciferase mRNA can successfully undergo protein translation, emitting light during the luciferase assay which can be quantified. In human bone marrow derived skeletal stem cells levels of miR-146b were increased through transfection of a miR-146b mimic, which was found to down-regulate SOX5 protein expression (Figures 70 & 71 B).

A series of experimental techniques were conducted to create a vector construct containing the targeted SOX5 3'UTR sequence and also to try and create a vector construct containing miR-146b sequence and a vector construct containing a mutated SOX5 3'UTR sequence. Figure 72 illustrates the vectors and enzymes used in attempting to create all vectors required for a future luciferase reporter assay to validate the interaction of miR-146b at the miR-146b binding site located at position 883-889 within the *SOX5* mRNA 3'UTR. Initially the SOX5 mRNA 3'UTR sequence containing the miR-146b binding site was cloned into a TOPO plasmid followed by isolation and ligation into a pRLTK plasmid. Initially the miR-146b sequence was cloned into a TOPO plasmid followed by isolation and attempted ligation into a pcDNA3.1(-) plasmid. Following successful creation of the pRLTK-SOX5-3'UTR plasmid, site directed mutagenesis was conducted to attempt to induce a mutation within the miR-146b binding site within the SOX5'3'UTR sequence of some of the pRLTK-SOX5-3'UTR plasmids.

Despite repeated tries to create the appropriate plasmid vectors required for luciferase reporter assay validation of miR-146b-*SOX5* mRNA 3'UTR interaction, the creation of the miR-146b-pcDNA3.1(-) and the site directed mutagenesis of pRLTK-SOX5-3'UTR was unsuccessful. However, the following

laboratory techniques outlined below were employed for the attempted creation of appropriate vector constructs required for luciferase reporter assay to test miR-146b-*SOX5* mRNA 3'UTR interaction.

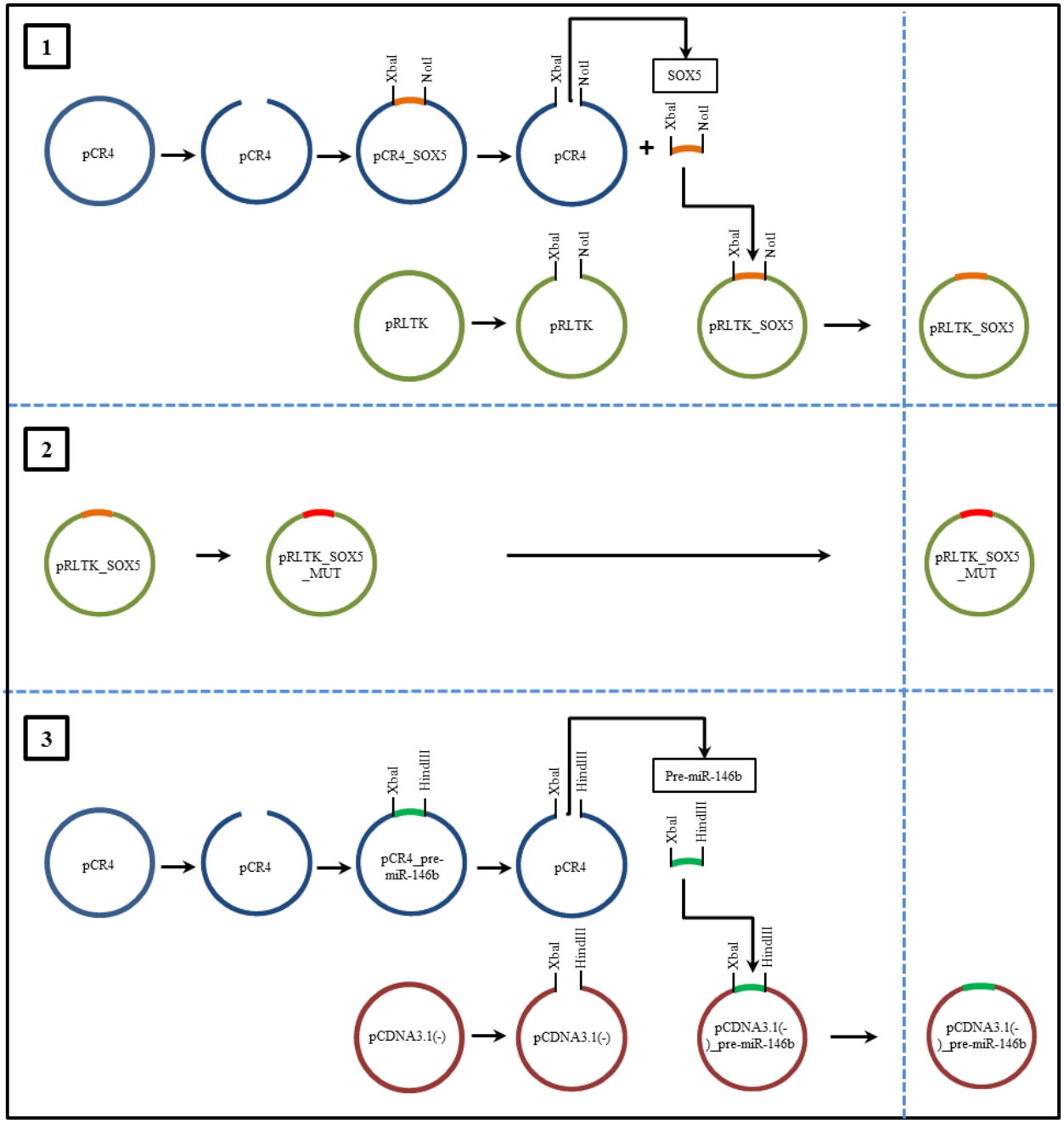

Figure 72. Vector construction methods required for future luciferase reporter assay to assess miR-146b interaction with *SOX5* mRNA 3'UTR. 1) The genomic region encompassing SOX5 3'UTR sequence containing the miR-146b target site was cloned into pCR4 TOPO vector followed by digestion with XbaI and NotI restriction enzymes. The excised fragment was cloned into pRLTK to produce a vector construct containing the SOX5 genomic sequence (pRLTK_SOX5). 2) Site directed mutagenesis of pRLTK_SOX5 to deliberately introduce a mutation to the miR-146b target region (the seed site) was attempted to create a vector containing SOX5 genomic sequence with mutated seed (pRLTK_SOX5_MUT). 3) The genomic region encompassing miR-146b precursor sequence containing the miR-146b mature sequence was cloned into pCR4 TOPO vector, followed by digestion with XbaI and HindII restriction enzymes. An attempt was made to clone the excised fragment into pcDNA3.1(-) to produce a vector construct containing precursor miR-146b genomic sequence (pcDNA3.1(-)_pre-miR-146b) .

5.8.1 Primer selection for polymerase chain reaction of *SOX5* mRNA 3'UTR sequence and miR-146b sequence

The first step in the construction process was TOPO cloning; the process in which the target DNA was cloned into specific plasmid vectors without DNA ligases and using Taq polymerase, which has non-template-dependent terminal transferase activity, which results in the addition of a single deoxyadenosine residue to the 3' end of PCR products.

Design of primers located within the 3'UTR of *SOX5* allowed for amplification of the 3'UTR of SOX5 containing the miR-146b binding sequence. Design of primers located around the primary sequence of miR-146b allowed for amplification of the full miR-146b sequence. Only mature miR-146b-5p of miR-146b was required to assess interaction with SOX5 3'UTR, however, the whole primary sequence of miR-146b was required so that the mature form can be produced from the pre-cursor miR-146b once transfected within cells in the final luciferase reporter assay experiment.

As described previously in section 5.6 of this chapter, miR-146b is predicted to bind to only one site within the 3'UTR of *SOX5* mRNA. The base pair interaction according to TargetScanHuman predicts that the residues GUUCUCA located at position 883-889 of the SOX5 3'UTR base pair with residues CAAGAG of mature miR-146b-5p as shown below.

SOX5 3'UTR 5'…GAAACUGUAGGUGCUGUUCUCAG…3'
miR-146b 3' UCGGAUACCUUAAGUCAAGAGU 5'

The primers for both SOX5 3'UTR sequence and miR-146b sequence were designed with restriction enzyme sequences at the appropriate ends of the primer sequences to allow for incorporation at the ends of the PCR product sequences by overlap extension PCR (Table 20). Incorporation of the restriction enzyme sequences at the ends of the PCR product sequences allowed for the PCR product sequences to be ligated into plasmids containing the same restriction enzyme sequences during pRL-TK and pcDNA3.1(-) cloning . Figure 73 illustrates the primer locations and sequences of SOX5 3'UTR and miR-146b

Primer	Restriction enzyme sequence attached	Sequence	Product size
For examining miR-146b-SOX5 mRNA 3'UTR interaction			
SOX5 3'UTR forward	XbaI	TCTAGA GCACACCACACTACATCTTTGAGC	380bp
SOX5 3'UTR reverse	NotI	GCGGCCGC ACCAGTCACTTGGGAGGATGTGGG	
miR-146b forward	XbaI	TCTAGA ACCCATCCTGGGCCTCAACT	263bp
miR-146b reverse	HindIII	AAGCTT GCCAGTGGGCAAGATGTGGG	

Table 20. Primers used for amplifying target sequences required for cloning

1. SOX5 mRNA 3'UTR sequence

2. miR-146b sequence

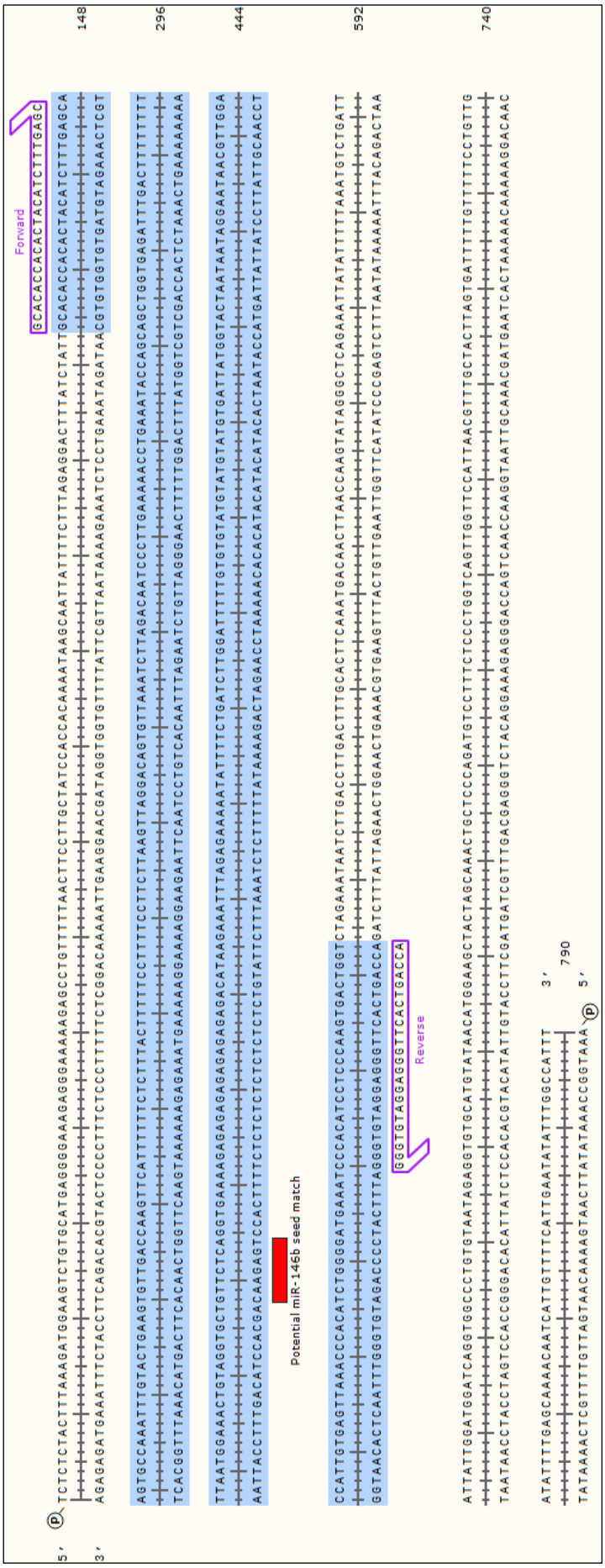

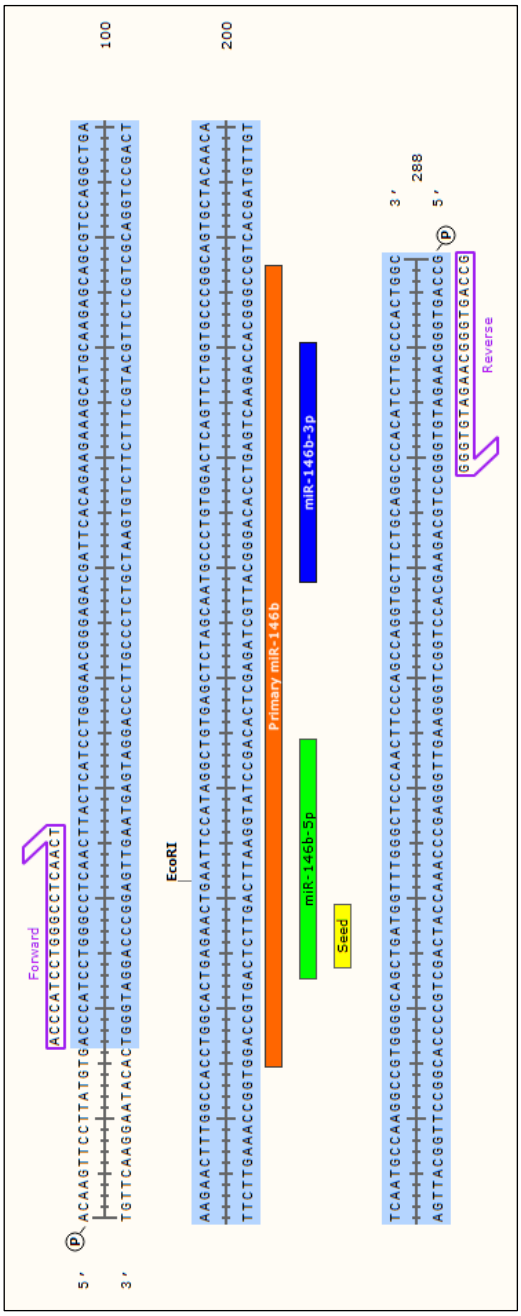

Figure 73. Sequences of SOX5 3'UTR with predicted miR-146b binding site highlighted in red (1) and sequence of precursor miR-146b which contains the mature miR-146b-5p sequence highlighted in green and the seed region highlighted in yellow predicted to target *SOX5* mRNA 3'UTR at position 883-889 (2). Diagrams created using SnapGene Viewer

Human DNA previously isolated was amplified using the conventional polymerase chain reaction. Different reactions using the appropriate forward and reverse primers were carried out for the amplification of the *SOX5* 3'UTR sequence and the miR-146b sequence (Table 20). After PCR completion the samples were tested for yield quality and the presence of primer dimer formation with agarose gel electrophoresis and UV imaging. Different annealing temperatures were tested to identify the appropriate temperature which yielded the greatest product amount and negative control reactions were tested to identify for primer dimer formation. Figure 74 shows the UV image of agarose gel electrophoresis following PCR of SOX5 3'UTR sequence with differing annealing temperatures and reactions which contained DNA in columns 1, 3, 5, 7, 9 and 11 and reactions without DNA (negative controls) in columns 2, 4, 6, 8, 10 and 12. Annealing temperatures of 55°C-64°C resulted in more visible primer dimer formation and less visible primer dimer formation was observed with annealing temperatures of 65°C-66°C. 65°C was selected as the appropriate annealing temperature for PCR of SOX5 3'UTR sequence. The UV image also clearly showed that the correct PCR product size of 380bp was amplified (Figure 74). Figure 75 shows the UV image of agarose gel electrophoresis following PCR of miR-146b sequence with differing annealing temperatures and reactions which contained DNA in columns 1, 3, 5, 7, 9 and 11 and reactions without DNA (negative controls) in columns 2, 4, 6, 8, 10 and 12. Annealing temperatures across 58°C-68°C all showed good product yield with low primer dimer formation. 66°C was selected as the appropriate annealing temperature for PCR of miR-146b sequence. The UV image also clearly showed that the correct product size of 273bp was amplified (Figure 75).

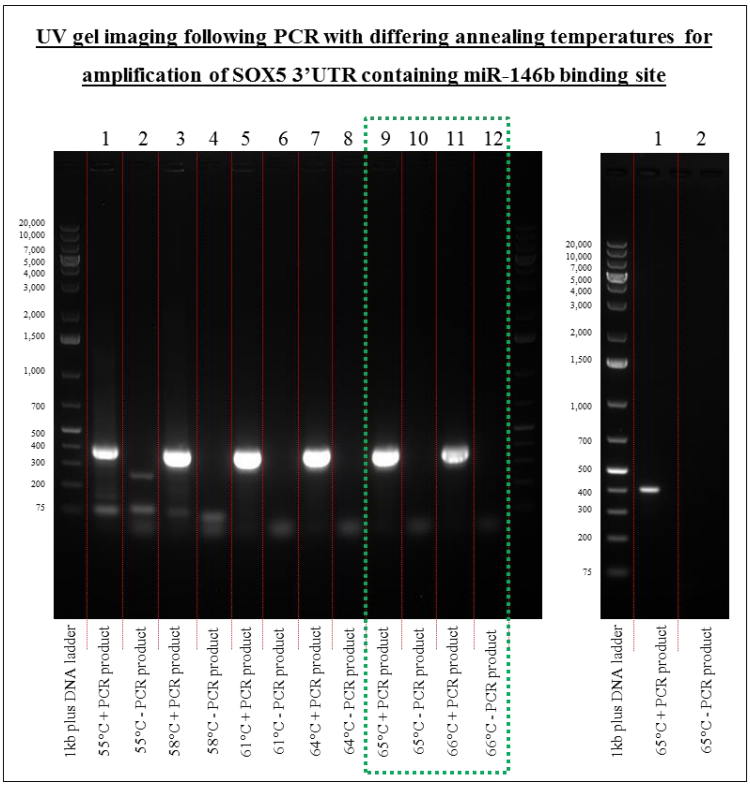

Figure 74. Agarose gel electrophoresis and UV imaging of expected SOX5 3'UTR sequence PCR product (380bp) created using differing annealing temperatures. Columns 1, 3, 5, 7, 9 and 11 all contained DNA during the PCR reaction and columns 2, 4, 6, 8, 10 and 12 all contained no DNA during the PCR reaction (negative controls). The green box indicates the most appropriate annealing temperature which was used for amplification of *SOX5* 3'UTR sequence.

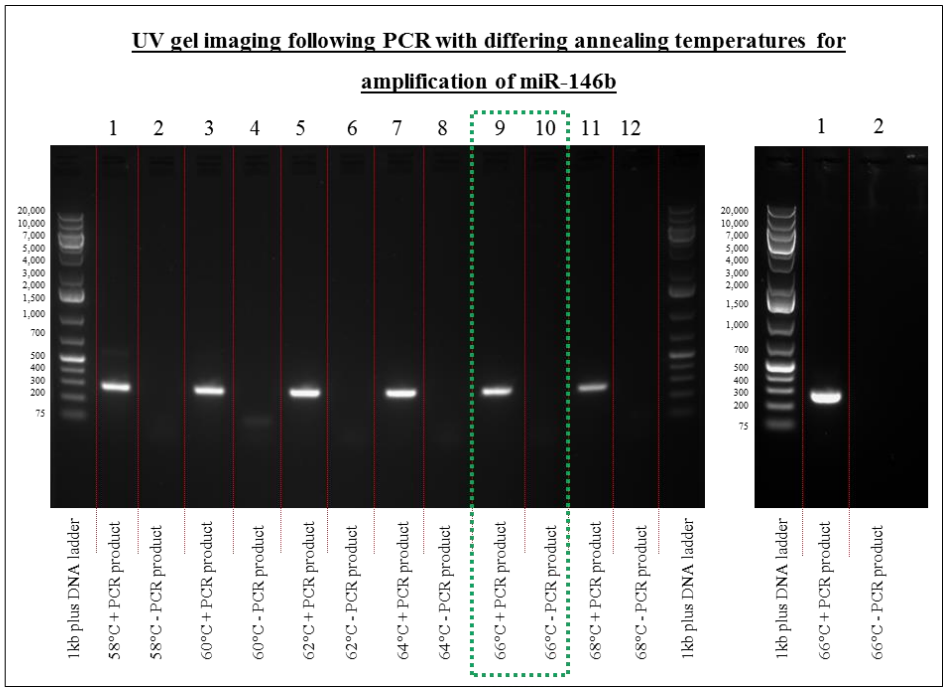

Figure 75. Agarose gel electrophoresis and UV imaging of expected miR-146b sequence PCR product (273bp) created using differing annealing temperatures. Columns 1, 3, 5, 7, 9 and 11 all contained DNA during the PCR reaction and columns 2, 4, 6, 8, 10 and 12 all contained no DNA during the PCR reaction (negative controls). The green box indicates the most appropriate annealing temperature which was used for amplification of miR-146b sequence.

5.8.2 TOPO cloning of SOX5 3'UTR sequence and miR-146b sequence, bacterial transformation, plasmid isolation and digestion

Following PCR, the amplified product was subject to TOPO cloning. Following bacterial transformation, plasmid isolation and digestion, agarose gel electrophoresis and UV imaging was conducted to identify the presence of the original insert into the TOPO vector. Figure 76 shows the UV image of 9 different clones selected from the agar plate. The 9 DNA plasmid clones were sequenced using SUPREMERUN^{TM} sequencing (GATC Biotech) and M13 primer. DNA sequencing data revealed that only clone 5 contained a sequence identical to native *SOX5* mRNA 3'UTR, all other clones contained mutations within the sequence. Figure 77 shows the native SOX5 mRNA 3'UTR sequence compared against the DNA isolated from the TOPO vector of clone 5, 100% conservation was observed. Clone 5 was then used for sub-cloning into pRL-TK plasmid vector. Figure 78 shows the UV image of 10 different clones selected from the agar plate. Of the 10 clones selected which had been subject to vector isolation and digestion, only clone 2 contained an insert. DNA sequencing data revealed that clone 2 contained a sequence identical to native miR-146b. Figure 79 shows the native miR-146b sequence compared against the DNA isolated from the TOPO vector of clone 2, 100% conservation was observed. Clone 2 was then used for sub-cloning into pcDNA3.1(-) plasmid vector.

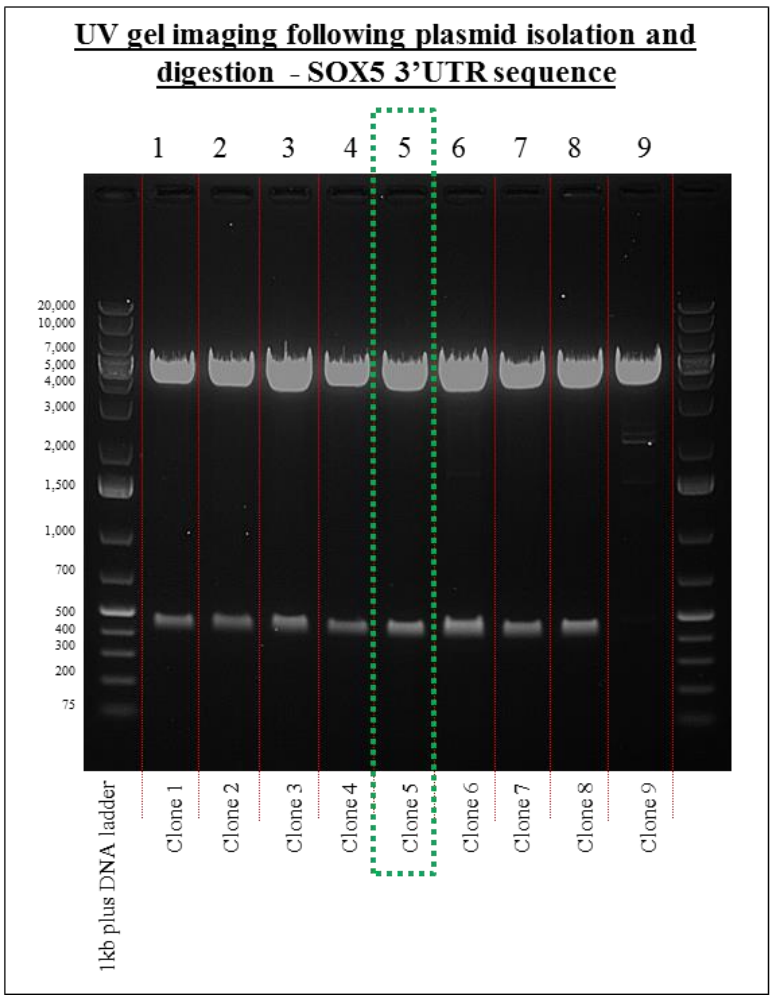

Figure 76. Agarose gel electrophoresis and UV imaging of EcoR1 restriction enzyme digested TOPO-SOX5 3'UTR plasmids, isolated from 9 different bacterial colonies. The green box indicates the only clone which following DNA sequencing was found to contain no mutations and have 100% conserved sequence to SOX5 mRNA 3'UTR sequence.

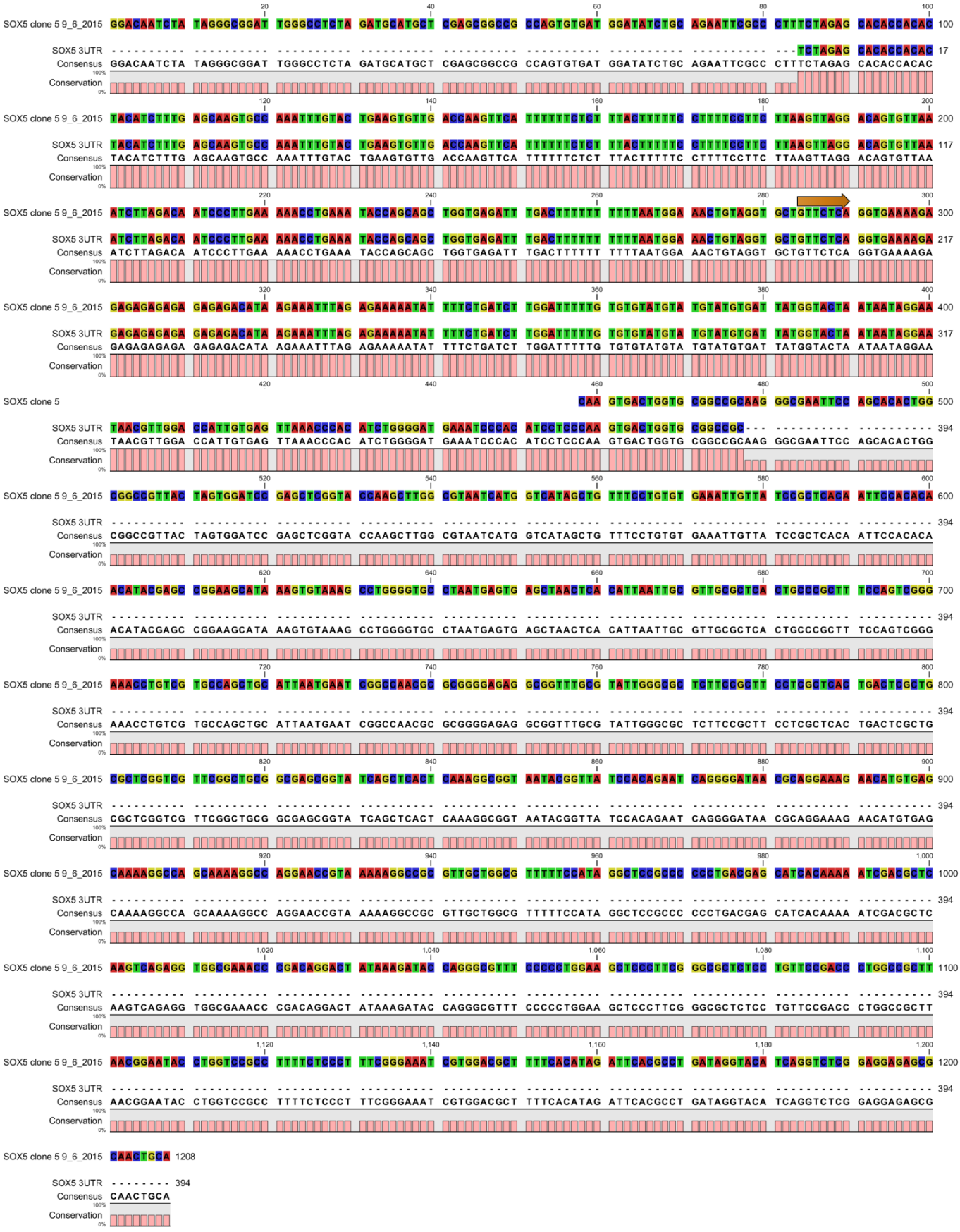

Figure 77. Diagram illustrates the sequencing data for TOPO-SOX5-3'UTR clone 5 and the native SOX5-3'UTR sequence. A sequence within the TOPO-SOX5-3'UTR plasmid displays a completely conserved match to the native SOX5-3'UTR sequence. The arrow identifies the location within the SOX5 3'UTR sequence which is predicted to contain the miR-146b binding site. Diagram created using CLC sequence viewer.

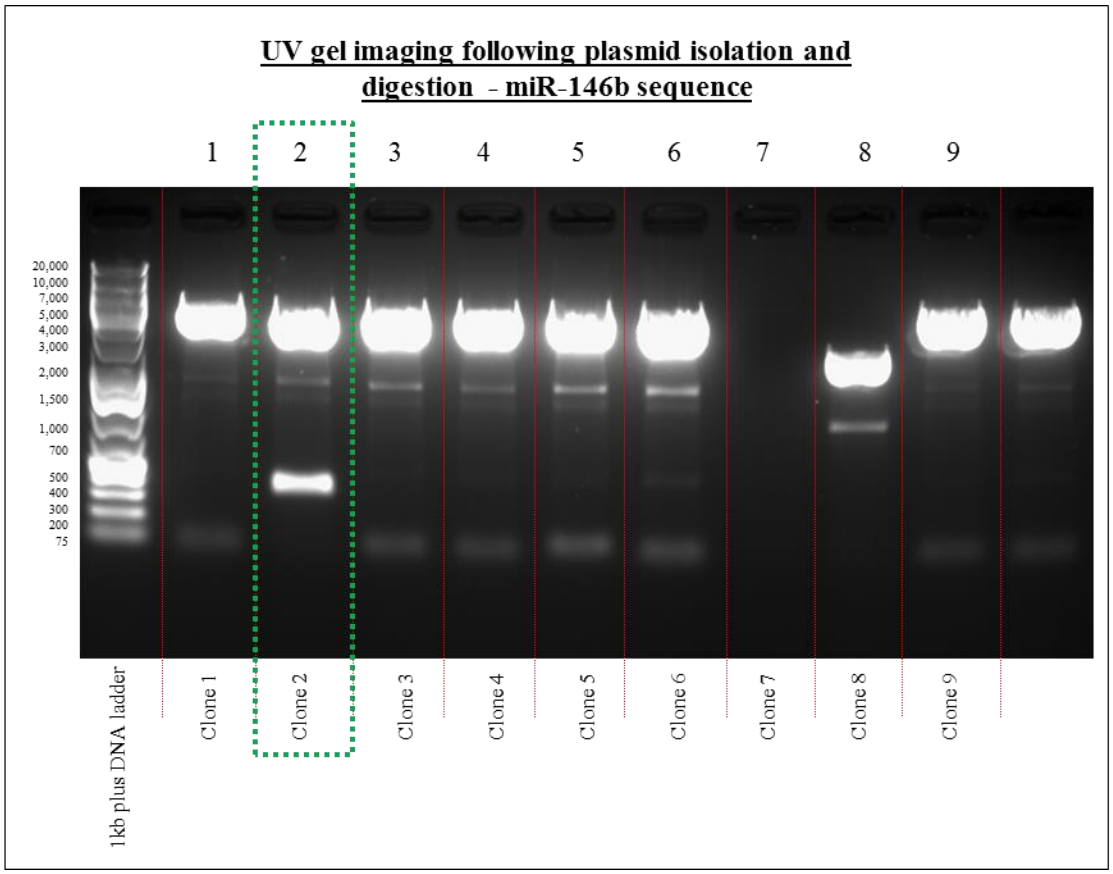

Figure 78. Agarose gel electrophoresis and UV imaging of EcoRI digested TOPO-miR-146b plasmids, isolated from 10 different bacterial colonies. The green box indicates the only clone which following DNA sequencing was found to contain no mutations and have 100% conserved sequence to miR-146b sequence.

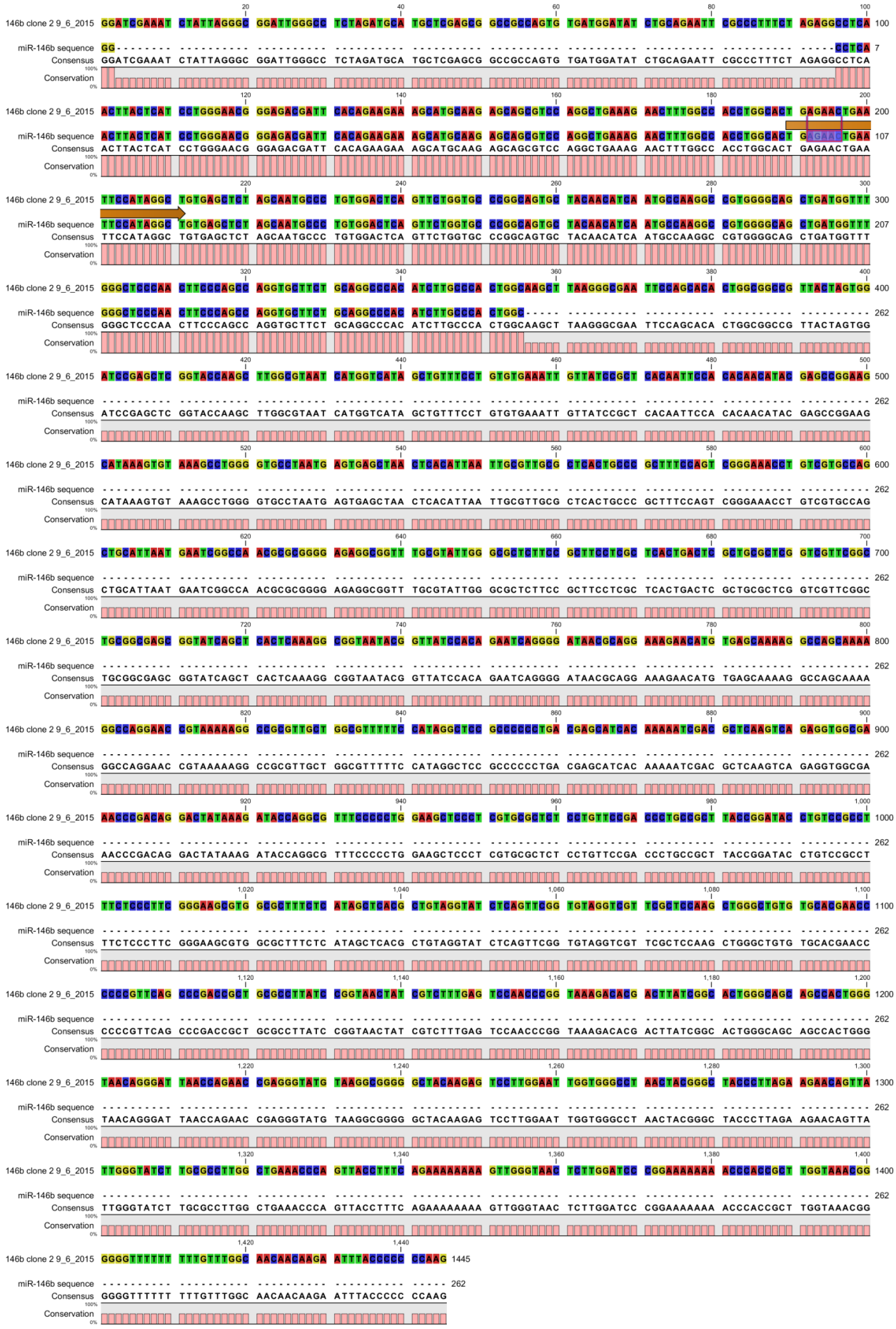

Figure 79. Diagram illustrates the sequencing data for TOPO-miR-146b clone 2 and the native miR-146b sequence. A sequence within the TOPO-miR-146b plasmid displays a completely conserved match to the native miR-146b sequence. The arrow identifies the location of mature miR-146b sequence. Diagram created using CLC sequence viewer.

5.8.3 Sub-cloning of SOX5 3'UTR sequence into pRL-TK vector and sub-cloning of miR-146b sequence into pcDNA3.1(-) vector

Following successful cloning of SOX5 3'UTR sequence into TOPO plasmid vector and miR-146b sequence into TOPO plasmid vector, SOX5 3'UTR sequence was subject to pRLTK sub-cloning and miR-146b sequence was subject to pcDNA3.1(-) sub-cloning. The process involved the isolation of SOX5 3'UTR and miR-146b sequences from the either clone 5 TOPO-SOX5 3'UTR plasmid vector or clone 2 TOPO-miR-146b plasmid vector followed by ligation of isolated SOX5 3'UTR sequence with pRL-TK plasmid and ligation of isolated miR-146b sequence with pcDNA3.1(-) plasmid vector followed by transformation of competent *E.cloi* cells. Initially, following isolation and digestion of TOPO-SOX5 3'UTR and TOPO-miR-146b plasmid vectors from bacteria, agarose gel electrophoresis enabled the separation of the digested linearised TOPO plasmid vectors from the either the SOX5 3'UTR or miR-146b sequence inserts. Cutting the original DNA insert from the gel and the target plasmid vectors enabled them to be cleaned and ligated. Figure 80 shows the UV image which was taken following electrophoresis of XbaI and NotI digested empty pRLTK plasmid vector, XbaI and NotI digested TOPO-SOX5-3'UTR plasmid vector, XbaI and HindIII empty pcDNA3.1(-) plasmid vector and XbaI and HindIII digested TOPO-miR-146b plasmid vector. The isolated SOX5 3'UTR DNA insert sequence was cut from the agarose gel from column 4 (Figure 80) along with the pRLTK plasmid from column 2 followed by a gel extraction technique and overnight ligation followed by bacterial transformation of the ligated pRLTK-SOX5-3'UTR plasmid vector. The isolated miR-146b DNA insert sequence was cut from the agarose gel from column 10 (Figure 80) along with the pcDNA3.1(-) plasmid from column 8 followed by a gel extraction technique and overnight ligation followed by bacterial transformation of the ligated pcNDA3.1(-)-miR-146b plasmid vector.

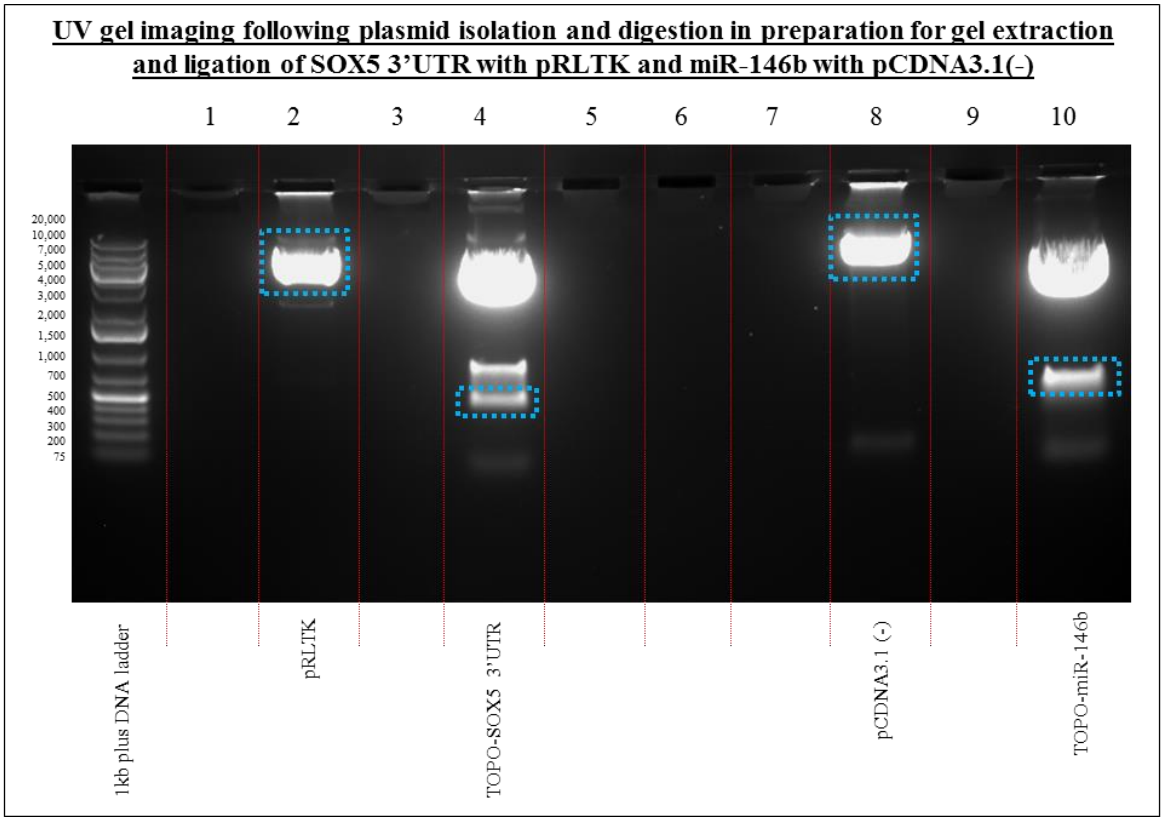

Figure 80. Agarose gel electrophoresis and UV imaging of digested linearised plasmids; XbaI and NotI digested empty pRLTK plasmid (column 2), XbaI and NotI digested TOPO-SOX5 3'UTR plasmid (column 4), XbaI and HindIII digested empty pcDNA3.1(-) plasmid (column 8) and XbaI and HindII digested TOPO-miR-146b plasmid (column10). The blue dots indicate the areas of the gel which were cut and subject to DNA extraction from gel followed by ligation and bacterial transformation.

Following bacterial transformation of either the ligated pRLTK-SOX5-3'UTR plasmid vector or pcDNA3.1(-)-miR-146b plasmid vector, plasmids were isolated from bacteria and digested and subject to agarose gel electrophoresis and UV imaging enabling identification of the original SOX5 3'UTR sequence insert or the original miR-146b sequence insert. Figure 81 shows the UV image taken following electrophoresis of the digested pRLTK-SOX5-3'UTR, the image clearly shows the presence of 10 different clones. The 10 clones were sent for sequencing and clone 2 was the only clone to return 100% conservation with native *SOX5* mRNA 3'UTR sequence and contained no mutations. Figure 82 shows the data from the sequencing results of pRLTK-SOX-3'UTR plasmid vector compared against the native *SOX5* mRNA 3'UTR sequence. Figure 83 shows the UV image taken following electrophoresis of the digested pcDNA3.1(-)-miR-146b plasmid, the image clearly shows the presence of 10 clones. The 10 clones were sent for sequencing, all 10 clones were found to display no conservation with the native miR-146b sequence. The process of miR-146b ligation with pcDNA3.1(-) was carried out many times followed by bacterial transformation and bacterial colony picking following by DNA sequencing, however, a conserved non-mutated clone of miR-146b was never identified.

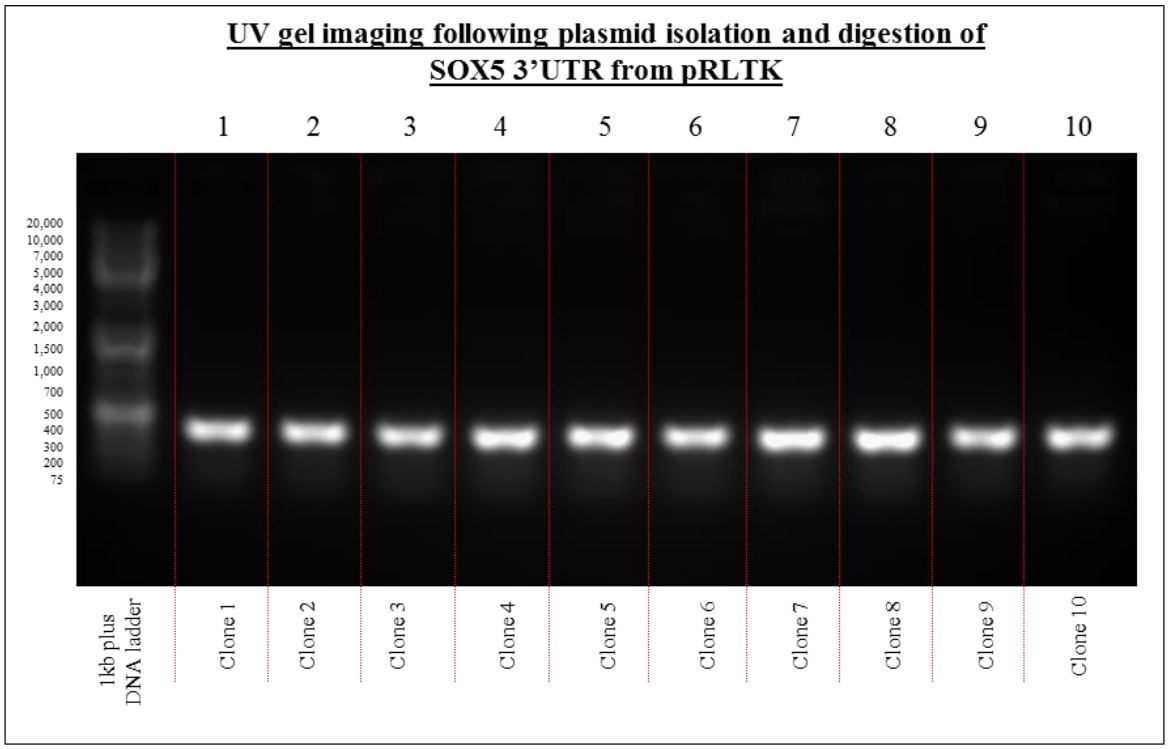

Figure 81. Agarose gel electrophoresis and UV imaging showing separated SOX5-3'UTR sequence insert from pRLTK vector following digestion, isolated from 10 different bacterial colonies. Clone 2 returned a 100% conserved matched to native *SOX5* mRNA 3'UTR sequence following sequencing.

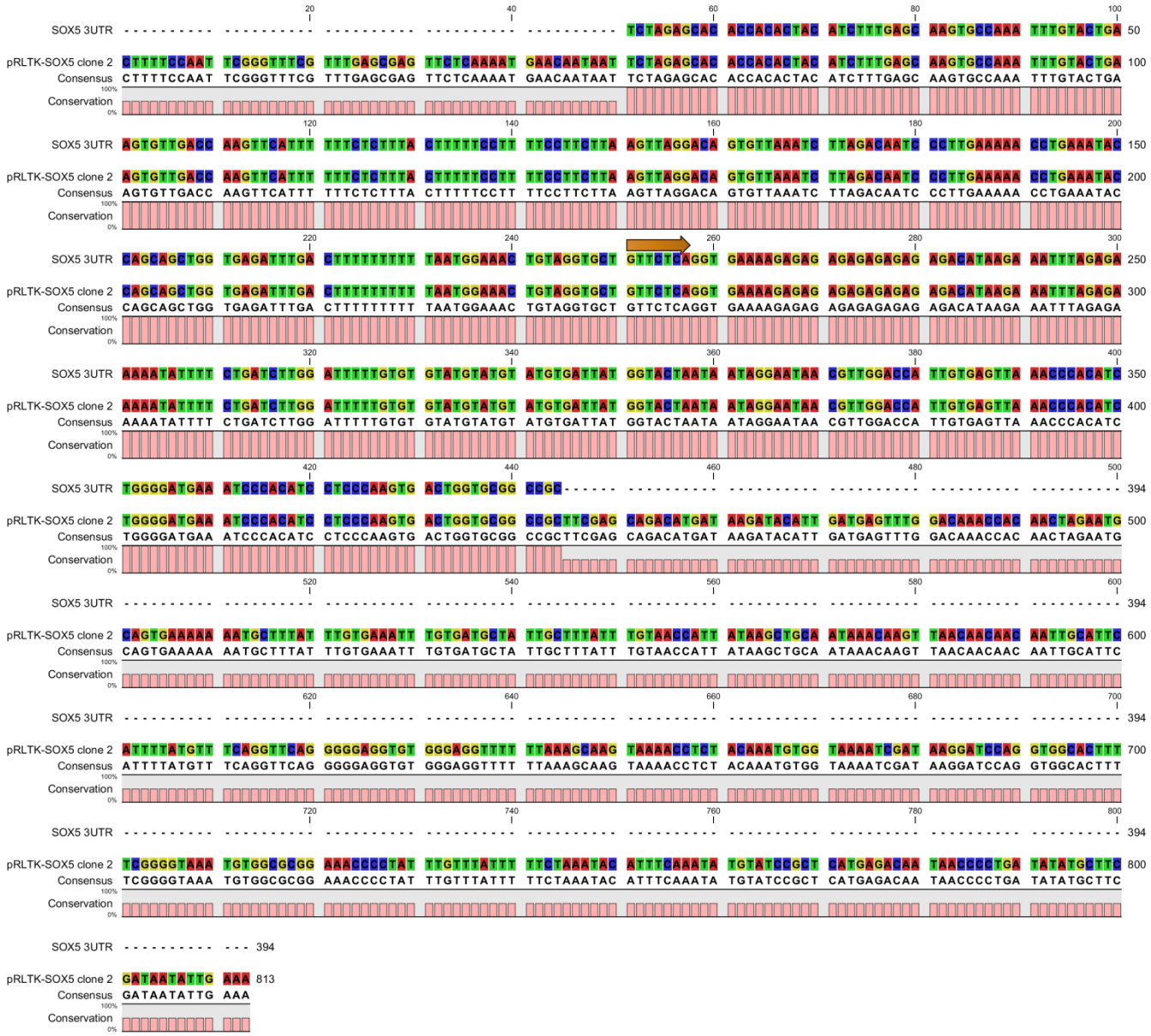

Figure 82. Diagram illustrates the sequencing data for pRLTK-SOX5-3'UTR clone 2 and the native SOX5-3'UTR sequence. A sequence within the pRLTK-SOX5-3'UTR plasmid displays a complete match to the native SOX5-3'UTR sequence. The arrow identifies the location within the SOX5 3'UTR sequence which is predicted to contain the miR-146b binding site. Diagram created using CLC sequence viewer.

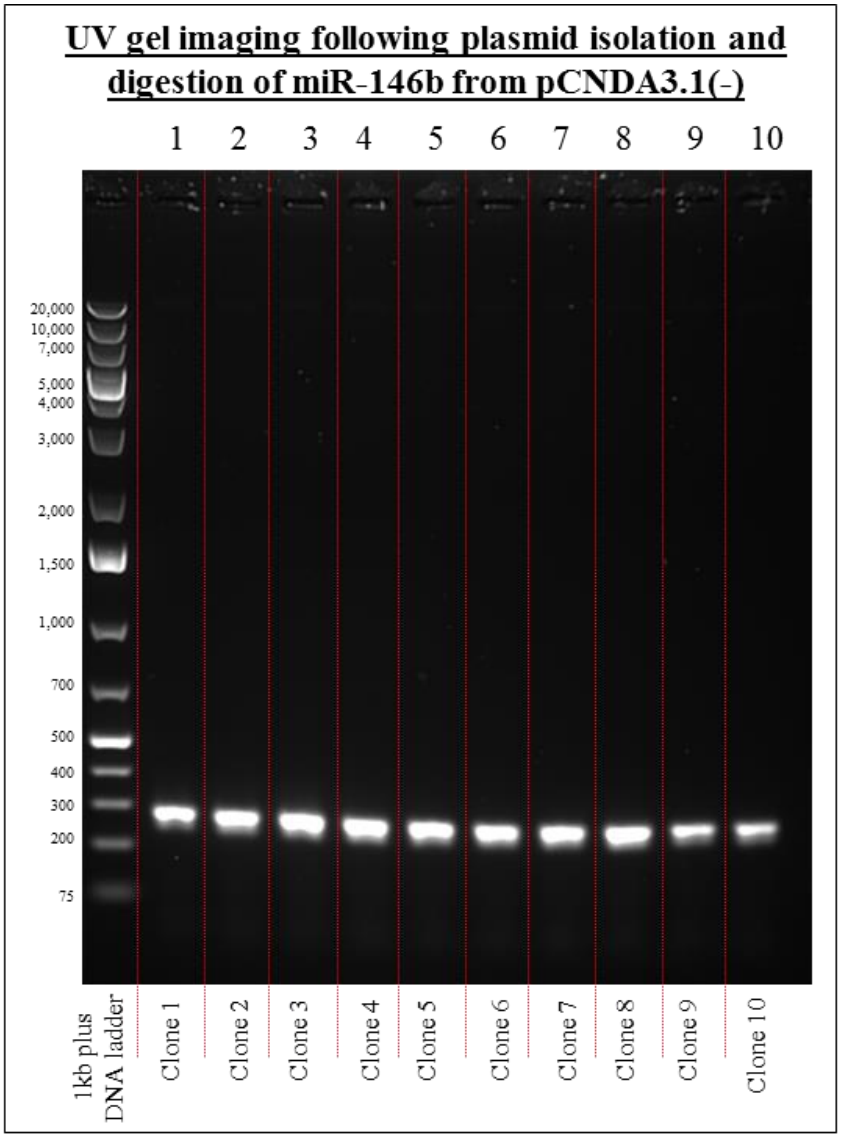

Figure 83. Agarose gel electrophoresis and UV imaging showing the separated miR-146b sequence insert from pcDNA3.1(-) plasmid, isolated from 10 different bacterial colonies. All clones were sent for DNA sequencing.

5.8.4 Site directed mutagenesis

To assess the interaction miR-146b with the target mRNA *SOX5* mRNA 3'UTR, site directed mutagenesis of SOX5 3'UTR target sequence was required. Site directed mutagenesis of the miR-146b binding site within the SOX5 3'UTR sequence should prevent miR-146b from binding. If miR-146b binds to the 3'UTR of *SOX5* mRNA, site directed mutagenesis of the miR-146b target site within SOX5 3'UTR would enable the translation of SOX5 which would also enable translation of the luciferase mRNA resulting in the production of luciferase protein required for production of luciferin, which can be quantified.

Substitution mutations the miR-146b binding site in the seed region of SOX5 3'UTR was generated by conversion of bases to create XhoI restriction enzyme recognition sites using a site directed mutagenesis kit (Agilent Technologies Cat.No.200523). Primers for mutagenesis were designed using PrimerX programme (www.bioinformatice.org/primerx/) (Table 21).

Primers designed contained the same mutation and were between the required 25-45 nucleotides in length (36 nucleotides for forward and reverse SOX5 primers). Primer melting temperature (Tm) was calculated with the following equation: Tm = 81.5 + 0.41(%GC)-675/N - % mismatch where "%GC" is the percentage of guanosine+cytosines in the primer and "N" is number of nucleotides in the primer. Additional parameters included: primer GC content was at least 40%, primers terminated in G or C bases and the desired mutation was located within the middle of the primer with 10-15 nucleotides surrounding the mutation.

Primers were designed to substitute GTTC for CGAG in the seed sequence of SOX5 3'UTR

SOX5 3'UTR seed region sequence: CTGTTCTC

SOX5 3'UTR mutated seed region sequence: CTCGAGTC

Substitution of GTTC to CGAG creates a XhoI restriction enzyme recognition site (CTCGAG) which can be exploited following bacterial transformation as a quick method to establish if site directed mutagenesis is successful with XhoI restriction enzyme digestion.

miR-146b binding site within the 3'UTR of SOX5 mRNA sequence used for plasmid creation.

TTCTTAAGTTAGGACAGTGTTAAATCTTAGACAATCCCTTGAAAAACCTGAAATACCAGCAGCTGGTG
AGATTTGACTTTTTTTTTTAATGGAAACTGTAGGTGCTGTTCTCAGGTGAAAAGAGAGAGAGAGAGAG
AGACATAAGAAATTTAGAGAAAAATATTTTCTGATCTTGGATTT

Site directed mutagenesis results in the introduction of a XhoI restriction enzyme recognition site (CTCGAG) within the miR-146b binding site region of the SOX5 3'UTR sequence.

TTCTTAAGTTAGGACAGTGTTAAATCTTAGACAATCCCTTGAAAAACCTGAAATACCAGCAGCTGGTG
AGATTTGACTTTTTTTTTTAATGGAAACTGTAGGTG**CTCGAG**TCAGGTGAAAAGAGAGAGAGAGAGAG
AGACATAAGAAATTTAGAGAAAAATATTTTCTGATCTTGGATTT

Primer	Sequence
For examining miR-146b-SOX5 mRNA 3'UTR interaction	
SOX5 3'UTR seed region mutagenesis forward	5' GGAAACTGTAGGTGCTcgagTCAGGTGAAAAGAGAG 3'
SOX5 3'UTR seed region mutagenesis reverse	5' CTCTCTTTTCACCTGActcgAGCACCTACAGTTTCC 3'

Table 21. Primers designed used in site directed mutagenesis of specific miR-146b target sequence within the 3'UTR of SOX5. Lowercase letters indicate mutated bases.

Following the site directed mutagenesis procedure mutated vectors were then transformed into competent *E.coli* cells and overnight incubation on agar. Following plasmid isolation from bacteria, clones were sent for DNA sequencing. Figure 84 illustrates the predicted result of sequencing following mutagenesis resulting in the substitution of 4 bases at the miR-146b binding site which would result in incomplete conservation with a mutated SOX5 3'UT sequence. Site directed mutagenesis was conducted many times but sequencing resulted in failure to identify any clones with substituted bases at the miR-146b binding site within SOX5 3'UTR sequence. Figure 85 shows illustrated sequencing data of one of the many clones which was picked which had been subject to site directed mutagenesis, which shows that the targeted site failed to undergo base substation and displayed complete conservation with native *SOX5* mRNA 3'UTR.

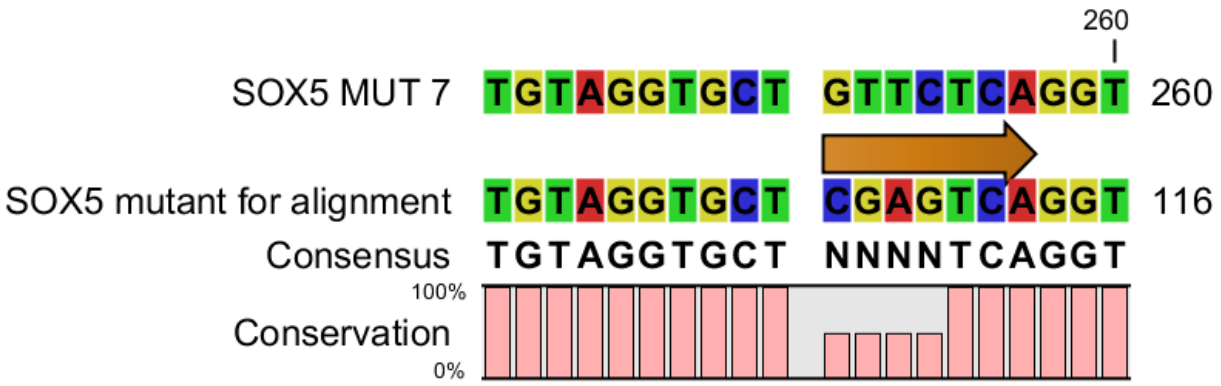

Figure 84. Diagram illustrates predicted sequencing result following site directed mutagenesis at the miR-146b binding site within the 3'UTR of SOX5. The arrow indicates the predicted miR-146b binding site. Diagram created using CLC sequence viewer.

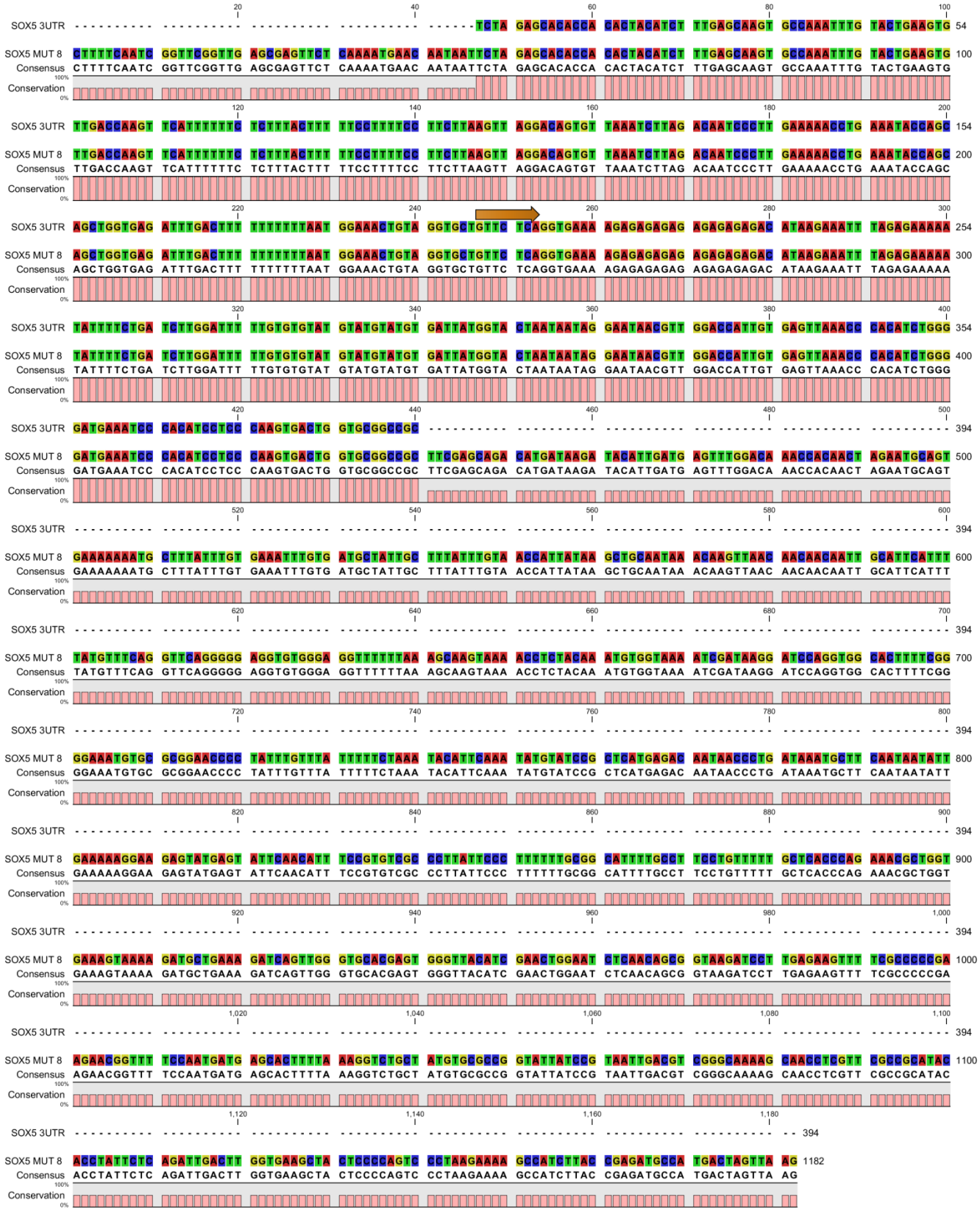

Figure 85. Diagram illustrates the sequencing data for a pRLTK-SOX5-3'UTR clone which was subject to site directed mutagenesis and the native SOX5-3'UTR sequence. A sequence within the pRLTK-SOX5-3'UTR plasmid contained a completely conserved match to the native SOX5-3'UTR sequence which showed that the site directed mutagenesis was not successful. The arrow identifies the location within the SOX5 3'UTR sequence which is predicted to contain the miR-146b binding site. Diagram created using CLC sequence viewer.

5.9 Discussion

Articular cartilage lacks the ability to undergo endogenous regeneration, making it an appealing target for tissue engineering. The ability of stem cells isolated from human bone marrow to undergo chondrogenic differentiation makes them a potential source for reparation of cartilage lesions. Chondrogenic differentiation can be induced in skeletal stem cells isolated from bone marrow through addition of TGF-β3 to a three dimensional micromass culture system [147], [418]. This current study identified that human bone marrow skeletal stem cells, positive for the Stro-1 antigen, upon TGF-β3 treatment induced chondrogenesis resulted in significant down-regulation of miR-146b. Bioinformatic analysis identified both *SMAD4* mRNA and *SOX5* mRNA as putative targets of miR-146b. However, overexpression studies of miR-146b resulted in the significant down-regulation of only SOX5 expression. MiR-146b could therefore be used as a potential therapeutic therapy in skeletal stem cells to induce chondrogenesis. This current study also identified that miR-145 was up-regulated during chondrogenic differentiation of human bone marrow derived skeletal stem cells, which opposes previous studies which recognise miR-145 as exhibiting a down-regulated expression during chondrogenesis.

Human bone marrow derived skeletal stem cells were sorted by anti-Stro-1 antigen selection and exhibited positive Stro-1 immunohistochemistry (Figure 55). Human bone marrow derived Stro-1 enriched skeletal stem cells have the ability to undergo multi-lineage differentiation, evidenced by positive oil red O staining in cells cultured in adipogenic media (Figure 56), alkaline phosphatase staining and activity in cells cultured in osteogenic media (Figure 57) and alcian blue staining (Figure 59) and safranin O staining (Figure 60) in cells cultured in chondrogenic media. Human bone marrow Stro-1 enriched skeletal stem cells cultured in chondrogenic media proceeded down the chondrogenic lineage and were found to be more chondrogenic than cells cultured in control media containing no TGF-β3 evidenced by chondrogenic marker gene expression results of *COL2A1*, *SOX9* and *AGCAN* (Figure 58) and positive alcian blue, safranin O and type II collagen immunostaining (Figures 59, 60 & 61). Cells cultured in chondrogenic media aggregated and condensed and maintained their three dimensional shape compared to cells cultured in control media containing no chondrogenic inductive factor TGF-β3 which do not retain the three dimensional shape. TGF-β3 was essential for cells to differentiate down the chondrogenic lineage and resulted in the production of cartilaginous extra cellular matrix which helped cultures to retain the 3D micromass structure.

Human bone marrow derived Stro-1 enriched skeletal stem cells were selected as a cell source for investigation following the unavailability of human fetal femurs and therefore a lack of human fetal femur-derived cells in order to conduct the experiment. Despite exhibiting positive chondrogenic gene expression markers and chondrogenic histological staining, following culture in the presence of TGF-β3, the expression of *COLXA1* mRNA expression was also significantly up-regulated in human bone marrow derived cells (Figures 58 E & 63 E). *COLXA1* encodes collagen X alpha 1 (COLXA1) chain which forms a homotrimer with two additional COLXA1 chains to form Collagen type X [424] and is

up-regulated during chondrocyte hypertrophy which is more typical of endochondral ossification [425]. While hyaline cartilage specific markers including *COL2A1* and *AGCAN* were up-regulated during chondrogenesis so was the expression of *COLXA1*. Other than in the thin layer of calcified cartilage, collagen type X is absent from articular cartilage [426] and expression of COLXA1 in articular cartilage has been linked to osteoarthritis [427]. The use of human bone marrow derived skeletal stem cells cultured in the presence of TGF-β3 to replicate articular cartilage development, despite providing a model of *in vitro* chondrogenesis enabling the examination of microRNA expression, is limited by the observed up-regulation in *COLXA1* mRNA expression. However, to date there has not been a better approach defined which eliminates the up-regulation of *COLXA1* expression observed during *in vitro* chondrogenesis of stem cells.

Previously microRNAs have been identified to have differing roles in chondrogenesis. MicroRNA-140 has been extensively covered in the literature and observed to be up-regulated throughout chondrogenesis [399], [400], [264], [401], [402], [403], [258] and therefore was selected as positive control for positive induction of cells down the chondrogenic lineage. Bone marrow derived skeletal stem cells cultured in the presence of TGF-β3 exhibited significant up-regulated expression of both miR-140-3p and miR-140-5p after 21 days in culture compared to expression at day 0 (Figures 62 & 64). This finding in addition to the chondrogenic marker gene expression observations indicates the ability of the human bone marrow derived skeletal stem cells to undergo chondrogenesis.

Bioinformatic *in silico* analysis identified *SMAD4* as a potential target of miR-146b. Five different microRNA target prediction programmes all listed *SMAD4* mRNA as a target of miR-146b and all five programmes all listed the same predicted miR-146b binding site at location 390-397 within the 3'UTR of *SMAD4* mRNA (Table 18). *SMAD4* mRNA was selected as a target for experimental validation because in chondrogenesis *SMAD4* encodes the SMAD4 protein which modulates TGF-β signalling by acting as an intermediate of signal transduction between the cell membrane and the nucleus. Upon TGF-β3 binding at the cell membrane to the TGF-β receptor, the receptor regulated SMADS; SMAD2 and SMAD3 are activated which in turn bind to SMAD4 forming a complex which translocates to the nucleus and binds DNA to up-regulate chondrogenic gene expression. In chondrogenesis *SMAD4* is essential as shown by previous studies; deletion of *Smad4* in chondrocytes in mice resulted in reduced proliferation with premature hypertrophic differentiation resulting in growth plate disorganisation [422]. Inactivation of *Smad4* in mice limb bud mesenchyme resulted in disruption to aggregation and condensation of mesenchymal progenitors to form cartilage with failure to deposit collagen type II in the ECM and loss of SOX9 [428]. *SMAD4* was selected for investigation given the study conducted by Geraldo *et al*, which previously had shown that miR-146b-5p was overexpressed in papillary thyroid carcinoma (PTC) and *SMAD4* was shown to be a direct target. Geraldo *et al* suggested that miR-146b-5p overexpression disrupted the TGF-β pathway by targeting and decreasing SMAD4 levels [429]. Additionally Khanna *et al* have shown that miR-146b was up-regulated in myoblast differentiation in inverse correlation with decreasing levels of expression of SMAD4. Inhibition of miR-146b prevented the down-regulation of SMAD4 during myogenesis,

revealing that *SMAD4* was a direct target of miR-146b [430]. The miR-146b studies outlined above ascertain that *SMAD4* is a bona fide target of miR-146b in the studied cell types and along with the *in silico* analysis that was conducted in the current study indicate that *SMAD4* could be a target of miR-146b during chondrogenic differentiation in skeletal stem cells isolated from human bone marrow. However, transient overexpression and inhibition of miR-146b in skeletal stem cells showed no effect on *SMAD4* transcript expression (Figure 66C&D) or SMAD4 protein expression (Figure 69A&B) which leads to the conclusion that miR-146b modulation had no effect upon *SMAD4* in bone marrow derived stem cells.

Additionally bioinformatic *in silico* analysis also identified that miR-146b potentially targets *SOX5*; a gene which encodes the transcription factor SOX5. Five different microRNA target prediction programmes all listed *SOX5* mRNA as a target of miR-146b and all five programmes all listed the same predicted miR-146b binding site at location 883-889 within the 3'UTR of *SOX5* mRNA (Table 19). *SOX5* mRNA was selected as a target for experimental validation because in chondrogenesis SOX5 has been identified as being co-expressed with Sox9 and Sox6. It is thought that Sox5 and Sox6 form homo and heterodimers which co-operate with Sox9 to enhance chondrogenic associated gene up-regulation such as the up-regulation of *COL2A1* [423]. SOX5 along with SOX6 and SOX9 has been shown to bind to the enhancer region of *COL2A1* and the co-expression of all SOX proteins was shown to induce higher expression of *COL2A1* [162]. Successful chondrogenic differentiation has been demonstrated in cells only in the presence of the 'SOX trio': SOX5, SOX6 and SOX9 in combination, compared to the action of each SOX transcription factor individually [164]. Han *et al* have shown that both SOX5 and SOX6 are required for the binding of SOX9 to the *AGC1*, *COL2A1* and *COL11A1* enhancers [165]. Given the positive role that *SOX5* has during chondrogenesis, the levels must be regulated to ensure its proper functioning, miR-146b acts as a negative regulator of *SOX5*.

This current study has shown that overexpression of miR-146b reduces SOX5 expression (Figure 71 B) and the down-regulation of miR-146b expression observed during chondrogenesis is to prevent the negative effect miR-146b has upon SOX5 expression. Despite identifying a significant decrease in SOX5 protein expression following an increase in miR-146b expression following transfection, the expression of *SOX5* mRNA did not change (Figure 66F). mRNA and protein have a non-linear relationship, in which only weak correlations exist between mRNA and protein abundancies [431]. Approximately 40% of protein levels can be predicted from mRNA measurements [432] and many factors have been proposed to influence mRNA and protein correlation such as regulatory proteins, RNA secondary structure, small RNAs, Shine Dalgarno sequence differences, ribosome occupancy, codon bias, translation initiation, mRNA half-life and protein half-life [431]. A decrease in SOX5 protein but not *SOX5* mRNA expression is also likely to be as a result of miR-146b mediated *SOX5* mRNA inhibition, whereby the *SOX5* mRNA is inhibited from undergoing translation as a result of miR-146b binding to the 3'UTR, but is not degraded. Which would result in a decrease in SOX5 protein levels as less *SOX5* mRNA is actively involved in translation but would not alter *SOX5*

mRNA levels. MicroRNA targeted mRNA have been shown to accumulate in P-bodies [433] and Bhattachatyya *et al* have shown that P-bodies act as storage sites for microRNA inhibited mRNA [434].

A significant decrease in SOX5 expression was observed following transfection of cells with miR-146b mimic (Figure 71B), however, no difference in SOX5 expression was observed following inhibition of miR-146b (Figure 71A), this result is likely to be due to other microRNAs which may also target *SOX5*. Genes which are predicted to be highly regulated by multiple microRNAs are less likely to respond to microRNA inhibitor treatment against a single microRNA and the coordinated action of several microRNAs, termed microRNA co-regulation, is a dominant feature of microRNA regulatory networks [435]. *SOX5* 3'UTR is likely to contain numerous microRNA response elements/binding sites for many endogenous microRNAs and therefore inhibition of miR-146b is likely to result in either non-detectable or modest de-repression of SOX5 expression [250]. The use of several different microRNA inhibitors in combination, which all have been identified to target SOX5, in addition to the use of miR-146b inhibitor, would potentially result in an up-regulation of SOX5.

Increased levels of miR-146b with use of the miR-146b mimic resulted in the significant decrease in SOX5 expression (Figure 71B). An effect was observed with the miR-146b mimic but not the miR-146b inhibitor because both of the synthetic oligonucleotides function in a different manner. MiR-146b mimic is a double stranded oligonucleotide which undergoes processing within transfected cells and mocks endogenous miR-146b activity and miR-146b inhibitor is a chemically modified antisense oligonucleotide which binds to miR-146b and competes with target mRNA. Given the different function of the synthetic oligonucleotides used in miR-146b overexpression and inhibition studies, miR-146b mimic and miR-146b inhibitor cannot and should not be compared when interpreting why increasing levels of miR-146b resulted in the significant down-regulation of SOX5 expression but inhibition of miR-146b resulted in no change in SOX5 expression.

Increasing the levels of miR-146b through transient transfection of miR-146b mimic resulted in the down-regulation of SOX5 expression, which indicates that SOX5 is down-regulated because miR-146b seed sequence complementary base pairs with a sequence located within the 3'UTR of *SOX5* mRNA. Base pairing between a microRNA response element in the 3'UTR of *SOX5* mRNA and miR-146b seed sequence would result in the inhibition of SOX5 translation. However, despite the *in silico* analysis which predicts a miR-146b binding site within *SOX5* mRNA 3'UTR, at location 883-889 (Figure 65D) and the experimental results which show the down-regulation of SOX5 following miR-146b overexpression, the binding between miR-146b and *SOX5* mRNA 3'UTR can only be inferred. The binding of miR-146b seed sequence and *SOX5* mRNA 3'UTR at location 883-889 was not validated experimentally with use of a luciferase reporter assay. The inability to create the appropriate miR-146b vector and inability to carry out site directed mutagenesis of SOX5 3'UTR miR-146b response element/binding site prevented the luciferase assay from being conducted. To validate *SOX5* as a direct target of miR-146b, the luciferase reporter assay which would assess the interaction

between the *SOX5* mRNA 3'UTR miR-146b binding element and the miR-146b seed sequence, needs to be conducted. The results from this study only infer *SOX5* as a direct target of miR-146b. The overexpression of miR-146b does have an effect on the expression of SOX5, however, due to the lack of validation evidence from a luciferase reporter assay, *SOX5* cannot be defined truly as a direct target of miR-146b, as *SOX5* may well function as an indirect target of miR-146b.

MiR-145 was used as a positive control for chondrogenesis given that previously miR-145 down-regulated expression had been observed during chondrogenesis of murine embryonic mesenchymal C3H10T1/2 cells [257]. However, miR-145 expression was up-regulated as a result of TGF-β3 induced chondrogenesis in human bone marrow derived skeletal stem cells used in this study (Figures 62C & 64C) , opposite to the down-regulated expression observed in the study conducted by Yang *et al*. The chondrogenic associated gene expression results validate that the human skeletal stem cells proceeded down the chondrogenic differentiation pathway (Figures 58 & 63). This unexpected up-regulation of miR-145 could be due a number of factors. The study conducted by Yang *et al,* delineate miR-145 as anti-chondrogenic and identify *Sox9* as a direct target. miR-145 expression was speculated to be attenuated during TGF-β3 induced chondrogenesis promoting chondrogenic differentiation through the positive regulation of *Sox9* [257]. The difference in miR-145 expression observed in TGF-β3 induced chondrogenesis may be attributable to the different cell types studied: Yang *et al* investigated miR-145 expression in murine embryonic mesenchymal C3H10T1/2 cells from a cell line and the current study examined the expression of miR-145 in primary skeletal stem cells isolated from human bone marrow.

The interaction of miR-145 with the *SOX9* mRNA 3'UTR may be accountable for the differences in expression of miR-145 which have been observed between the current study conducted in human bone marrow derived skeletal stem cells and the expression of miR-145 in murine embryonic mesenchymal C3H10T1/2 cells conducted by Yang *et al*. TargetScanHuman identified that miR-145 have identical sequences in human and mouse. Even if miR-145 is predicted to target the same gene transcripts in both mouse and human cells, the gene transcript itself may contain different sequences which enable it to alter gene transcript interaction with the microRNA. The presence of alternative polyadenylation sites can induce the formation of gene transcript isoforms which alter length at the 3'UTR and can therefore enable the gene transcript to bypass interaction with microRNA [404]. The presence of several microRNA binding sites located within the 3'UTR of a target gene transcript can also influence the strength of target repression and resultant target output [405]. Other studies have shown the up-regulation of miR-145 as a result of TGF-β signalling [406], [383], [407], [408]. Given the evidence in the literature which identifies miR-145 as exhibiting up-regulated expression in response to TGF-β treatment and having identified miR-145 expression as being up-regulated during TGF-β3 induced chondrogenesis in human bone marrow derived skeletal stem cells, the down-regulated expression of miR-145 during chondrogenesis identified by Yang *et al* [257] should not necessarily be used as a positive control for investigating the effect of TGF-β signalling in stem cells.

Together, the data indicate that TGF-β3 induced chondrogenesis in a three dimensional micromass culture system induces the down-regulation of miR-146b. Through direct targeting of transcription factor *SOX5*, miR-146b can modulate chondrogenic differentiation. During chondrogenic differentiation miR-146b has been shown to be down-regulated which enabled de-repression of SOX5; which is crucial to early chondrogenic differentiation. Anti-chondrogenic miR-146b is likely to be regulated by TGF-β signalling, either by direct or indirect SMAD modulation upon the miR-146b promoter region. Understanding the key biological processes within stem cell differentiation will enable the exploitation of microRNAs to be potentially used as therapeutic intervention; further down-regulation of anti-chondrogenic miR-146b could potentially induce chondrogenesis to occur more efficiently. Future steps are required to examine the effect of stable miR-146b knockdown and overexpression with use of lentiviral transfection on chondrogenic differentiation of human bone marrow derived skeletal stem cells. Additionally, use of an articular cartilage defect model and transplantation of pre-conditioned miR-146b inhibiting or miR-146b overexpressing human bone marrow derived skeletal stem cells to the defect site, would access the ability of miR-146b to enhance chondrogenic differentiation *in vivo*.

Chapter 6
Discussion

Comprehension of the functioning of microRNAs in osteoarthritis and chondrogenesis allows for research into the application of microRNAs as potential therapy. MicroRNAs might be dysregulated in osteoarthritis which can therefore enable the microRNA to serve as a biomarker of OA and also the potential use of the microRNA as a direct therapy. In addition, understanding the role of microRNAs in chondrogenesis may also improve chondrogenic differentiation capacity of skeletal stem cells following transplantation. MicroRNAs could be directly administered to articular cartilage, having direct effect upon resident articular chondrocytes, as a form of treatment in cartilage injury and OA. Additionally exogenous microRNAs could be used in combination with isolated skeletal stem cells and transplanted to defective articular sites to induce regeneration. Prior to making use of microRNAs in cell and tissue engineering strategies, the discovery and role of functional microRNAs involved with OA and chondrogenesis is required. The work in this thesis has sought to identify if miR-146b is differentially expressed in OA chondrocytes and if miR-146b expression is regulated by IL-1β. The work in this thesis has also sought to identify if miR-34a is expressed during the chondrogenic differentiation of human fetal femur-derived stem cells and to identify the functional role of miR-34a. Unavailability of human fetal femurs resulted in a finite source of fetal femur-derived cells to conduct experiments upon and therefore an alternative cell source was sought. Human bone marrow derived skeletal stem cells were used to identify if miR-146b is expressed during chondrogenic differentiation and to identify the functional role of miR-146b during chondrogenesis.

6.1 The expression of miR-146b in human articular OA chondrocytes

6.1.1 The expression of miR-146b is up-regulated in human OA articular chondrocytes

MiR-146b was hypothesised to be up-regulated in OA chondrocytes due to the close homology miR-146b shares with miR-146a. MicroRNAs with the same seed repertoire generally target the same genes and therefore possess similar cellular function [308]. The homology in the seed sequences of miR-146a and miR-146b mean that they are likely to target the same mRNAs and therefore may work co-operatively to enhance efficiency of target repression. MiR-146a has previously been identified in osteoarthritis [228], [378], [229] and has been shown to exhibit up-regulation in OA chondrocytes and therefore miR-146b was predicted to be up-regulated in OA chondrocytes. In addition to the close homology that miR-146b shares with miR-146a, miR-146b has been shown to exhibit up-regulation in inflammatory studies in other disease models [307], [313], [318], [319]. Critically, for the first time, the work conducted in chapter 3 has shown that miR-146b is up-regulated in OA articular chondrocytes compared to chondrocytes isolated from the articular cartilage from osteoporotic bone which served as a control.

6.1.2 The expression of miR-146b is not induced by long term treatment of human chondrocytes with IL-1β

If miR-146a and miR-146b work co-operatively they may not only target the same mRNA, be expressed in the same tissue but also may be induced by the same stimuli. If miR-146b is up-regulated in OA chondrocytes, the underlying inducer of miR-146b expression may be the same as the inducer of miR-146a expression in OA chondrocytes. The concurrent up-regulation in miR-146a and miR-146b expression following treatment of cells with IL-1β has previously been observed in other cell types [307], [311], [321], [322]. The pro-inflammatory cytokine, IL-1β, present in OA was hypothesised to induce miR-146b expression as well as miR-146a expression in OA chondrocytes. Despite the highly up-regulated expression trend of miR-146a in response to IL-1β treatment in chondrocytes, the expression trend of miR-146b was not replicated.

Taganov *et al* have previously shown that promoter analysis identified that the pro-inflammatory associated NF-κβ was required for miR-146a expression by IL-1β in monocytes [307]. The up-regulation of miR-146a observed in chondrocytes indicates that miR-146a may be up-regulated by IL-1β induced NF-κB signalling. Despite the up-regulated expression of both miR-146a and miR-146b in OA chondrocytes, described in chapter 3, the pro-inflammatory cytokine IL-1β was only able to induce up-regulated expression of miR-146a. While miR-146b expression was not shown to be induced by IL-1β, it is highly likely that miR-146b is activated by another inflammatory mediator in chondrocytes. MiR-146a and miR-146b are both up-regulated in OA chondrocytes but are not induced by the same stimuli as predicted.

Kutty *et al* have shown that both miR-146a and miR-146b are highly induced in response to pro-inflammatory cytokines in human retinal epithelial (RPE) cells. The expression of miR-146a in RPE cells was found to be dependent upon IL-1β treatment, whereas the expression of miR-146b was found to be dependent upon IFN-γ treatment. Promoter analysis of miR-146a and miR-146b showed that IL-1β is critical for pro-inflammatory cytokine regulation of the miR-146a promoter and that treatment with IFN-γ induced increased activity of the miR-146b promoter in comparison to treatment with IL-1β or TNF-α. While miR-146a was activated by IL-1β most likely through NF-κB signaling, JAK inhibitor 1; an inhibitor of the IFN-γ signaling via the JAK/STAT pathway could block miR-146b promoter activity but not miR-146a promoter activity, indicating up-regulation of miR-146b via the JAK/STAT pathway of IFN-γ signaling [318]. Kutty *et al* have identified and have shown that both miR-146a and miR-146b are up-regulated by pro-inflammatory cytokines, however, miR-146a is predominantly up-regulated by IL-1β and miR-146b is predominantly upregulated by IFN-γ. The distinct differences in activation of miR-146a and miR-146b suggest that miR-146a and miR-146b up-regulation in OA articular chondrocytes may be due to the presence of differing cytokines. While miR-146a is definitely indicated to be up-regulated by IL-1β as evidenced by treatment of articular chondrocytes with IL-1β in chapter 3, miR-146b expression was not shown to be induced by IL-1β leading to the assumption that miR-146b is up-regulated by another inflammatory mediator in OA,

potentially IFN-γ. IFN-γ has been shown to induce IL-6 and IL-1R in normal chondrocytes [436] and has been sown to reduce the synthesis of type II collagen in articular chondrocytes [437]. Further investigation as to the expression of miR-146b in IFN-γ treated human articular chondrocytes would identify if miR-146b is regulated by pro-inflammatory cytokine IFN-γ.

6.1.3 The combinational treatment of human chondrocytes with IL-1β and TGF-β3 may result in a synergistic effect upon miR-146a expression

Differing studies have shown the effect of the combined treatment of IL-1β and TGF-β3 in chondrocytes, suggesting that TGF-β3 has a potential anabolic effect and is able to counteract the catabolic effect of IL-1β. MiR-146b was predicted to be up-regulated by IL-1β due to the sequence homology that miR-146b shares with miR-146a and the studies that have shown the up-regulation of both miR-146a and miR-146b following IL-1β treatment. If both miR-146a and miR-146b could be up-regulated by anabolic IL-1β, it was hypothesised that anabolic TGF-β3 may have the opposite effect on both miR-146a and miR-146b expression given the proposed anabolic role of TGF-β signalling in chondrocytes.

A down-regulated expression trend of miR-146a was observed in chondrocytes cultured in the presence of TGF-β3 and an up-regulated expression trend of miR-146a was observed in chondrocytes cultured in the presence of IL-1β. As discussed previously (6.1.2) the expression trend of miR-146b was not up-regulated following treatment of chondrocytes with IL-1β and no miR-146b expression trend was observed following treatment of chondrocytes in TGF-β3. While no effect upon miR-146b expression was observed in TGF-β3, IL1β or TGF-β3 and IL-1β treated chondrocytes, indicating that miR-146b is not induced or suppressed by the catabolic and anabolic mediators, the expression trend of miR-146a suggests that IL-1β is able to induce miR-146a expression and TGF-β3 is able to suppress miR-146a expression.

The opposite expression of miR-146a resulted following culture of chondrocytes with anabolic TGF-β3 and culture of chondrocytes with catabolic IL-1β and therefore combinational treatment of chondrocytes with IL1-β and TGF-β3 was predicted to result in miR-146a expression falling midway between levels observed with independent IL-1β or TGF-β3 treatment, suggesting a counteractive effect of TGF-β3 on IL-1β signalling. However, in chapter 3 the expression of miR-146a in human articular chondrocytes treated with IL-1β and TGF-β3 in combination was found to be more up-regulated than the expression of miR-146a in articular chondrocytes treated with just IL-1β. The miR-146a expression results observed suggests a cross-talk between TGF-β signalling and IL-1β signalling. Co-stimulation with TGF-β and IL-1β has previously been shown to induce the up-regulated secretion of the chemokines MCP-1 or CCL2 in intestinal epithelial cells [384], [385]. It is possible that IL-1β and TGF-β may use similar intracellular mechanisms to TGF-β and IL-1β co-stimulation in intestinal epithelial cells, to up-regulate chemokines in chondrocytes. The synergistic up-regulation of miR-146a expression observed may be as a result of up-regulation of certain inflammatory mediators. MiR-146a has been proposed as an anti-inflammatory regulator and

therefore its up-regulation may be to down-regulate specific mediators of inflammation inclusive of chemokines.

The synergistic relationship between IL-1β and TGF-β has been documented in previous studies. Kuppner *et al* have shown that combined treatment of both IL-1β and TGF-β induced the up-regulation of IL-6 in RPE cells [387]. An Intestinal epithelial cell line cultured in the presence of both IL-1β and TGF-β resulted in the synergistic enhancement of IL-6 secretion [438]. Chondrocytes from both normal and osteoarthritic joints have been shown to produce IL-6, with an increase in IL-6 following stimulation with IL-1, TNF-α and IFN-γ. Chondrocytes can produce IL-6 in response to pro-inflammatory stimuli [60], [439]. Gurene *et al* showed that TGF-β was able to significantly induce IL-6 synthesis in human articular chondrocytes [60]. Despite the association that TGF-β has with anabolism in OA, given the previous studies in the literature which indicate IL-1β and TGF-β synergism, co-stimulation of chondrocytes with IL-1β and TGF-β may act synergistically to induce the expression of IL-6 in chondrocytes. MiR-146a has been shown to be up-regulated in senescing human fibroblasts with suppressive effects upon pro-inflammatory IL-6 [313]. The down-regulated expression of miR-146a in patients with sepsis was hypothesised to be responsible for the increase in IL-6 expression [440]. LPS induced inflammation in macrophage cells induced the expression of miR-146a. Overexpression of miR-146a was found to suppress the production of LPS-induced IL-6 [441]. The up-regulated expression of miR-146a in response to treatment with both IL-1β and TGF-β3 in human articular chondrocytes, in chapter 3, could be in response to induction of IL-6 synthesis. If IL-1β and TGF-β3 act in synergy to induce IL-6 in chondrocytes, perhaps the up-regulated expression of miR-146a is to control the expression of IL-6 and act to potentially down-regulate this pro-inflammatory cytokine. Future studies to observe the expression of IL-6 following TGF-β3 and IL-1β treatment in articular chondrocytes would need to be conducted primarily and a potential link between IL-6 induction and miR-146a up-regulation to be verified experimentally.

A genome wide gene expression study conducted by Takahashi *et al* in a murine chondrocytic cell line in response to IL-1 and TGF-β treatment alone and in combination found that antagonism was the dominant mode of interaction between TGF-β and IL-1β. Antagonism was the dominant mode of action between IL-1β and TGF-β upon pro-inflammatory genes but an additive effect was observed on cell cycle regulators including vascular endothelial growth factor (*VEGF*), vascular endothelial growth factor C (*VEGFC*), connective tissue growth factor (*CTGF*) and tissue inhibitor of metalloproteinase (*TIMP*) [86]. Perhaps miR-146a up-regulation in chondrocytes, observed in chapter 4, as a result of IL-1β and TGF-β3 co-stimulation, could therefore be due to a non-inflammatory function such as cell cycle regulation. Future studies to investigate genome wide gene expression in response to IL-1β and TGF-β3 may help identify other potential targets of miR-146a and also help in identifying the function of miR-146a in IL-1β and TGF-β3 treated chondrocytes. Despite ideas as to the up-regulation of miR-146a, primarily investigating the synergistic effects of IL-1β and TGF-β3 in chondrocytes upon gene expression may give more of an insight as to why miR-146a is up-regulated.

6.1.4 The treatment of human chondrocytes with TGF-β3 results in the up-regulation of miR-145

MiR-145 was selected for investigation to serve as a positive control for treatment of chondrocytes with IL-1β given the previous finding that miR-145 was found to be up-regulated in chondrocytes cultured in the presence of IL-1β [381]. In this current study no expression trend of miR-145 could be interpreted following treatment of chondrocytes with IL-1β given that the expression of miR-145 differed between chondrocytes isolated from the three different patient samples. Given the assumption that miR-145 would exhibit up-regulated expression following IL-1β treatment, it was predicted that miR-145 may exhibit down-regulated expression following treatment with anabolic TGF-β3. Stimulation of chondrocytes with TGF-β3 resulted in an up-regulated trend of miR-145 expression in chondrocytes isolated from all three patient samples. TGF-β signalling has been generally deemed as an anabolic mediator in chondrocyte homeostasis. TGF-β signalling has been found to activate both the SMAD-dependent and SMAD-independent pathways [442]. The SMAD-dependent pathway involves the interaction of phosphorylated receptor SMADS; SMAD2 and SMAD3 to common SMAD4. The heteromeric SMAD complex then translocates to the nucleus where it binds to Smad-binding elements (SBE) of DNA [442]. Long *et al* have previously shown that TGF-β1 activation of the SMAD-dependent pathway was shown to culminate at a sterol binding element (SBE) in the upstream region of miR-145, which directly mediated the transcription of miR-145 in human coronary artery smooth muscle cells [383]. Given the up-regulation of miR-145 observed following TGF-β3 treatment of human articular chondrocytes, it is possible that TGF-β3 directly up-regulates miR-145 also through the SMAD-dependent pathway; through stimulation of a miR-145 enhancer.

The up-regulation of miR-145 in response to anabolic TGF-β3 treatment in chondrocytes could signify a role for miR-145 as a potential therapy in the treatment of OA. Given that miR-145 is a downstream target of TGF-β3 signalling in articular chondrocytes, miR-145 has the potential to mediate the positive anabolic effects of TGF-β3. However, studies to elucidate the role of miR-145 in human articular chondrocytes are required. Elucidation and validation of potential targets of miR-145 are required to identify the exact function of miR-145 in human articular chondrocytes.

6.1.5 Limitations and Future Perspectives

Despite having identified that miR-146b is significantly up-regulated in human chondrocytes isolated from human OA articular cartilage and reaffirmed the up-regulated expression of miR-146a in OA articular chondrocytes, the functional relevance of miR-146b up-regulation in OA articular chondrocytes was not established. An extensive literature search identified that miR-146b is up-regulated in numerous inflammatory studies and that miR-146b has been shown to target inflammatory associated targets in differing cell types, but from the search miR-146b can only be assumed to have a similar anti-inflammatory function in OA articular chondrocytes. Primarily, inflammatory mRNA targets of miR-146b need to be investigated to identify the effect that miR-146b has upon predicted inflammatory targets in chondrocytes. Future work to investigate the effect of

potential anti-inflammatory effects of miR-146a and miR-146b on chondrocyte and cartilage health would need to be conducted. An *in vivo* model of miR-146a and miR-146b exogenous administration to an OA joint would identify if miR-146a and miR-146b serve as anti-inflammatory mediators in OA and also identify the possibility of miR-146a and miR-146b use as a therapeutic treatment for OA.

Given the sequence homology that miR-146a shares with miR-146b it is likely that both microRNAs have similar cellular function. However, despite both miR-146a and miR-146b exhibiting up-regulation in human OA articular chondrocytes, IL-1β, which has previously been shown to induce miR-146a expression in chondrocytes, could not induce up-regulation of miR-146b. The results indicate that miR-146a is stimulated by IL-1β and miR-146b is not, but the limiting factor may be that the expression of miR-146a and miR-146b was assessed over a long time period. Previously, the expression of miR-146b has been shown to be up-regulated by IL-1β but at a much shorter time duration, in which the expression of both miR-146a and miR-146b were examined at 3 hour time intervals for up to 24 hours following treatment with IL-1β. MiR-146b was found to reach a plateau after 6 hours with a steady decline in expression after [311]. Future studies would need to assess the expression of miR-146a and miR-146b in chondrocytes following IL-1β at shorter time points. Another possibility is that the up-regulated expression of both miR-146a and miR-146b in OA chondrocytes may be regulated by different stimuli present within the OA joint. Use of differing pro-inflammatory cytokines such as IFN-γ and TNF-α may establish which inflammatory mediator is responsible for the up-regulation of miR-146b in OA chondrocytes. MiR-146b promoter analysis would identify the intracellular cell signalling pathway responsible for activating miR-146b in chondrocytes. Future experiments combined would enable a more in depth understanding of what stimulates miR-146b expression, the intracellular mechanisms which govern the up-regulation process and the functional role of miR-146b in OA chondrocytes.

Generally IL-1β and TGF-β3 have opposite functions, with catabolic IL-1β being associated with pro-inflammation and anabolic TGF-β3 being associated with anti-inflammation. The synergism between IL-1β and TGF-β3 identified in up-regulating miR-146a in chondrocytes suggests a cross talk between these two inflammatory mediators, in which case TGF-β3 may act with IL-1β in a pro-inflammatory manner. Therefore microRNAs such as miR-146a and probably miR-146b function to down-regulate the inflammatory response and prevent the autocrine amplification of chronic inflammation in OA. Future studies need to look to investigate the potential synergistic effect that miR-146a may have upon mRNA expression in chondrocytes. A gene expression microarray may also identify potential mRNA targets of synergistic up-regulated miR-146a by IL-1β and TGF-β3 in chondrocytes.

6.2 The expression of specific microRNAs and their functional role during chondrogenesis

6.2.1 MiR-34a is up-regulated during the chondrogenic differentiation of fetal femur-derived cells but has no effect on the predicted target *TGIF2*

The expression of miR-34a in human fetal femur-derived cells was found to be up-regulated during chondrogenesis. Despite the differences in miR-34a expression observed, the putative target chosen for validation, *TGIF2* was found not to differ in expression following miR-34a inhibition and overexpression experiments. *TGIF2* may not be a true target of miR-34a but other cell regulatory mechanisms should not be discounted and may control miR-34a mediated *TGIF2* mRNA expression which may enable *TGIF2* mRNA expression de-repression.

The potential presence of RNA binding proteins, natural antisense transcripts and multiple polyadenylation sites within the 3'UTR *TGIF2* mRNA may allow for *TGIF2* to escape miR-34a mediated down-regulation. Polyadenylation is the addition of multiple adenosine monophosphates, known as the poly(A) tail, to pre-messenger RNA [443]. When the 3'UTR contains multiple polyadenylation signal sequences, known as alternative polyadenylation (APA), several gene isoforms which maintain the same coding region but differ in the length of the 3'UTR can result. Like microRNAs, alternative polyadenylation is a post-transcriptional mechanism of gene expression regulation. mRNA with different lengths of 3'UTR, as a result of alternative polyadenylation, can therefore be differentially regulated by microRNAs [444] (Figure 86). It has been indicated that over 50% of human genes possess alternative polyadenylation (APA) sites [445]. APA can produce mRNA isoforms and short isoforms may avoid microRNA targeted inhibition, while longer isoforms may contain seed sequences enabling microRNA binding and therefore down-regulation of gene expression [446], [447].

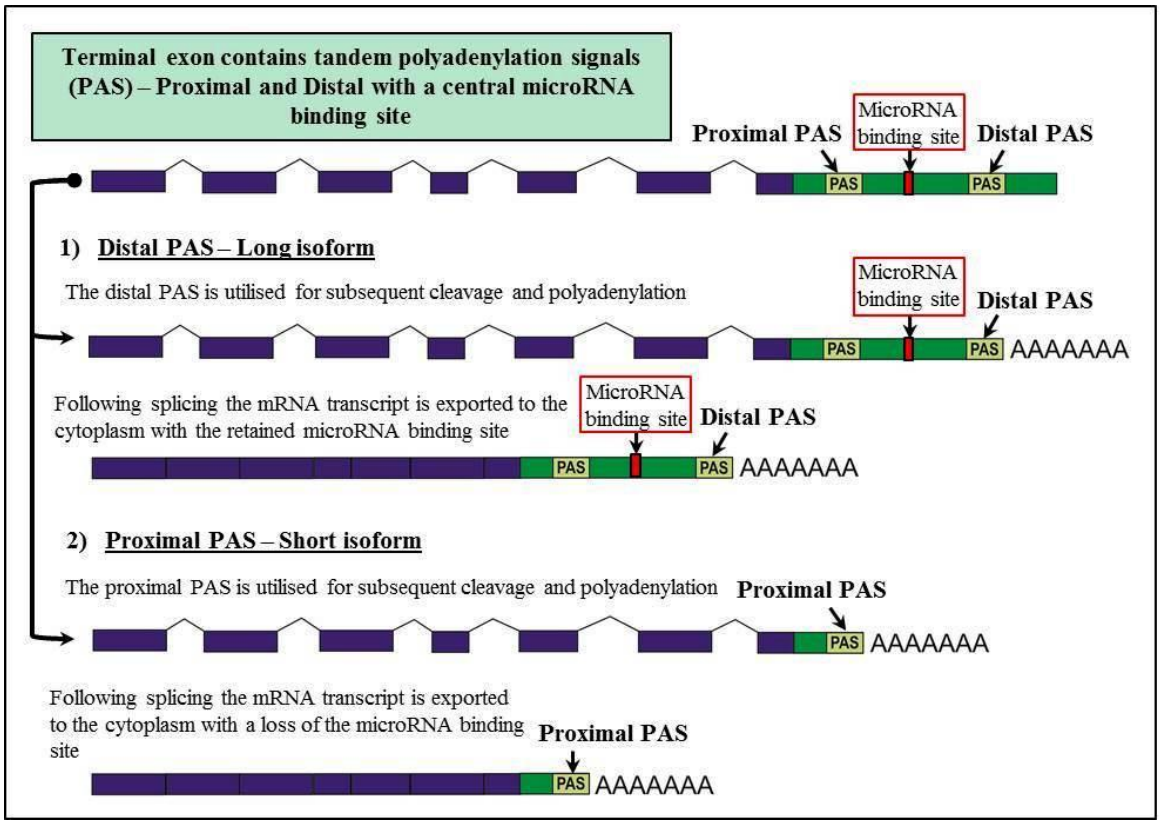

Figure 86. Tandem Alternative Polyadenylation. The presence of tandem polyadenylation signals in the 3'UTR can result in the transcription of coding genes with variable 3'UTR lengths. The presence of a proximal and distal polyadenylation signal (PAS) can result in the formation of a long and short isoform differing only by the length of the 3'UTR. Shorter 3'UTRs may escape microRNA mediated targeting, due to the absence of the microRNA target sequence, resulting in target gene expression de-repression. (Figure adapted from Elkon *et al*, Alternative cleavage and polyadenylation: extent, regulation and function, Nature Reviews Genetics 14,496–506 (2013) doi:10.1038/nrg3482).

The most recent transcriptomic research indicates the presence of natural antisense transcripts (NATs) which can bind to non-coding RNAs (ncRNAs) and also coding mRNAs [448]. Faghihi *et al* have identified the presence of a noncoding antisense transcript for the gene *BACE1*; a gene encoding beta-secretase-1. The noncoding antisense transcript was named *BACE1*-antisense transcript (BACE1-AS) [449]. BACE1-AS was later shown to prevent miR-485-5p induced translational expression of BACE1 mRNA by masking of the miR-485-5p binding site [450]. RNA-binding proteins (RBPs) can function to stabilise and destabilise a target gene transcript [451]. The presence of RBPs can inhibit miRNA action either through competition for the same binding motif/site or through the RBP induced restructuring of RNA which may render the binding site inaccessible to miRNA [452] Genome-wide analyses has shown that the same 3'UTR motifs can be recognised by both RBPs and miRNAs [453]. The RBP, Human antigen R (HuR), has been shown to bind to and stabilise cationic acid transporter 1 (CAT1) mRNA in competition with miR-122 during stress related conditions [454]. The potential presence of

alternative polyadenylation sites within the 3'UTR of *TGIF,* or the potential presence of natural antisense transcripts which mask the miR-34 *TGIF2* binding site, or the potential presence of RBPs which may compete with miR-34a to stabilise *TGIF2* mRNA, could all prevent miR-34a from inhibiting the expression of *TGIF2* mRNA, all explanations for the observation that no difference in *TGIF2* expression resulted following miR-34a inhibition and overexpression.

6.2.2 MiR-146b is down-regulated during the chondrogenic differentiation of human bone derived skeletal stem cells and induces down-regulation of predicted target SOX5 but not SMAD4

In chapter 5, chondrogenic differentiation of human bone marrow derived skeletal stem cells resulted in the significant down-regulation of miR-146b. Bioinformatic analysis identified *SMAD4* mRNA and *SOX5* mRNA 3'UTRs as containing a putative binding site/s for miR-146b. Overexpression or inhibition of miR-146b resulted in no differences in *SMAD4* mRNA or SMAD4 protein expression. *SMAD4* mRNA may not be a true target of miR-146b or the potential presence of RNA binding proteins, natural antisense transcripts and multiple polyadenylation sites within the 3'UTR *SMAD4* mRNA may allow for *SMAD4* to escape miR-146b mediated down-regulation.

Overexpression analysis of miR-146b resulted in the significant down-regulation of SOX5 protein. In chondrogenesis SOX5 has been identified as being co-expressed with Sox9 and Sox6. It is thought that Sox5 and Sox6 form homo and heterodimers which co-operate with Sox9 to enhance chondrogenic associated gene up-regulation such as the up-regulation of *COL2A1* [423]. Chondrogenic differentiation was only found to be successful when Sox5, Sox6 and Sox9 were co-expressed when investigated in differing cell types compared to the action of each Sox gene individually [164]. Han *et al* have shown that the action of the 'sox trio' inclusive of SOX5, SOX6 and SOX9, binds to the *Agc1* enhancer only in the presence of SOX5 and SOX6 [165]. Given the positive role in chondrogenesis that *SOX5* plays, the levels must be regulated to ensure its proper functioning, miR-146b acts as a negative regulator of *SOX5*. Examination of the role of miR-146b has shown that overexpression of miR-146b reduces SOX5 expression and the down-regulation of miR-146b expression observed during chondrogenesis is to therefore prevent the negative effect miR-146b has upon SOX5 expression.

6.2.3 MiR-145 is up-regulated in during the chondrogenic differentiation of both fetal femur-derived cells and human bone marrow derived stem cells

In chapters 4 and 5, miR-145 alongside miR-140-3p and miR-140-5p was selected as a positive control for indication of chondrogenic differentiation in both fetal femur derived-cells and human bone marrow derived skeletal stem cells. MiR-145 was selected as a positive control for chondrogenesis given that previously miR-145 down-regulated expression has been observed during chondrogenesis of murine embryonic mesenchymal C3H10T1/2 cells [257]. Yang *et al* define miR-145 as anti-chondrogenic and identify *Sox9* as a direct target. It is proposed that miR-145 is attenuated

during TGF-β3 induced chondrogenesis promoting chondrogenic differentiation through the positive regulation of *Sox9* [257]. Despite previous observations, the expression of miR-145 was significantly up-regulated as a result of TGF-β3 induced chondrogenesis in both human bone marrow derived skeletal stem cells and human fetal femur-derived cells.

The difference in miR-145 expression observed in TGF-β3 induced chondrogenesis may be attributable to the different cell types studied; Yang *et al* investigate miR-145 expression in murine embryonic mesenchymal C3H10T1/2 cells from a cell line and the current study investigates the expression of miR-145 in primary skeletal stem cells isolated from human bone marrow and primary fetal femur-derived cells. Differences in the cell origin may have an impact upon differences of miR-145 expression observed. Different species may contain differences in target gene structure which may enable or disallow the target gene to interact with miR-145. For example if the 3'UTR sequence of SOX9 differs between chick and human cells this may affect miR-145 binding to SOX9 and therefore ultimately affect the expression of SOX9. In support of the observed up-regulation of miR-145 a number of other studies show the up-regulation of miR-145 in response to TGF-β signalling. Mayorga and Penn show that miR-145 is up-regulated in mesenchymal stem cells derived from rat bone marrow in response to TGF-β1 stimulation [406]. MiR-145 expression is up-regulated in response to TGF-β1 stimulation in human coronary artery smooth muscle cells [383], human pulmonary artery smooth muscle cells [407] and in regulating myofibroblast differentiation in human pulmonary fibroblasts in response to TGF-β1 [408].

6.2.4 Limitations and Future Perspectives

Future studies to investigate the presence of RBPs, NATs and alternative polyadenylation sites would identify if the regulatory mechanisms may control miR-34a mediated *TGIF2* expression. The overexpression and inhibition miR-34a studies were conducted in undifferentiated cells. Previously, examination of genes involved in embryonic development found that mouse genes with longer 3'UTRs are more expressed as development progresses. Additionally an *in vitro* model of C2C12 myogenesis indicated that 3'UTR lengthening during myoblast differentiation correlated with down-regulated expression of pre-mRNA 3' processing genes, inclusive of genes associated with polyadenylation, indicating diminishment of mRNA polyadenylation activity which ultimately enables post-transcriptional control of gene expression by microRNAs as a result [455]. A positive correlation has been reported between the length of the 3'UTR and progression of differentiation [456], [457]. It may therefore be possible that miR-34a does target *TGIF2* mRNA but at a later stage of chondrogenic differentiation, once the 3'UTR has lengthened to reveal the miR-34a binding site. *TGIF2* mRNA may have been a short isoform which would have enabled *TGIF2* mRNA to escape binding and subsequent regulation by the miR-34a. Future research could look into the possible lengthening of the *TGIF2* mRNA 3'UTR during fetal femur-derived stem cell chondrogenic differentiation and the potential existence of alternative polyadenylation sites within the 3'UTR or *TGIF2* mRNA.

Unavailability of human fetal femurs during the study meant there was only a finite source of human fetal femur-derived stem cells and therefore human bone marrow derived skeletal stem cells were selected as an alternative source to continue work. The limitation with utilising human bone marrow derived skeletal stem cells for chondrogenic differentiation is the ability of cells to express *COLXA1* indicating hypertrophic differentiation of cells. Given that the ultimate aim for future work would be to use cells for articular cartilage repair, hypertrophic differentiation would not enable the regeneration of native articular cartilage. Future studies need to look to utilising an *in vitro* cell model of chondrogenesis which does not undergo hypertrophic changes. The use of growth factors such as GDF-5 and parathyroid hormone related peptide in chondrogenic medium may induce a more articular cartilage differentiation process and possibly reduce hypertrophic changes.

To investigate the effect of miR-146b upon target gene expression, the method of transient transfection was employed. Transient transfection is a chemical based transfection method which follows the concept of positively charged nucleic acid which is attracted to the negatively charged cell membrane which induces endocytosis, the nucleic acid is then unloaded in the cytoplasm. In microRNA research for overexpression analysis; synthetic miRNA can be transiently transfected and for inhibition analysis; modified antisense oligonucleotides, which are able to bind to the endogenous mature microRNAs, are transiently transfected. The limitation to transient transfection is that nucleic acid introduced into the cell is not integrated into the nuclear genome. The novel nucleic acid is only present in the cells which were present during transfection, therefore when cells undergo mitosis the nucleic acid will not be retained in the daughter cells; the transfected nucleic acid is therefore only present for a finite amount of time. In order to assess the effect of microRNAs over a longer period of time such as during differentiation, transfection of the synthetic microRNA or modified antisense oligonucleotide needs to be retained within the cells, including during mitosis which can be accomplished through stable transfection. Retroviruses and lentiviruses can infect and integrate into the host cell genome as a provirus. Specific microRNA precursors can be cloned into lentiviral vectors. Lentiviral transfection of host cells allows for the overexpression of a microRNA transgene. Transfection of human bone marrow derived stem cells with a lentivirus containing miR-146b sequence would assess the effect of long term stable expression of miR-146b.

To further investigate the effect of inhibiting miR-146b expression on modulation of chondrogenic differentiation, a long term miR-146b loss of function study needs to be performed. Stable repression of miR-146b function could be achieved via methods such as genetic knockout, sponges [458] or tough decoy (TuD) RNAs [459]. Complete deletion of the gene encoding miR-146b would ensure the complete loss of miR-146b function. Additionally creation of a transgene producing sponge or TuD RNA to sequester miR-146b could also be a possibility.

In addition to *in vitro* long term miR-146b enhanced loss of function study, ultimately an *in vivo* study would reveal the effects of enhanced down-regulation of miR-146b on chondrogenic differentiation in a true articular cartilage lesion. The definitive aim is to utilise skeletal stems as a source for cartilage regeneration in combination with microRNA modulated treated. Skeletal stem cells would need to be isolated from human bone marrow and expanded in culture. Use of a miR-146b sponge or TuD RNA targeting miR-146b would potentially induce further miR-146b expression down-regulation in skeletal stem cells. The treated skeletal stem cells would then be inserted into an articular cartilage defect model such as a SCID mouse harbouring an articular cartilage lesion. Lolli *et al* have conducted the first *in vivo* study which combined microRNA modulation with transplanted stem cells to an osteochondral defect. Inhibition of an anti-chondrogenic regulator, miR-221, was able to induce hMSCs to repair an osteoochondral defect [460]. Given the previous study showing successful repair of an osteochondral defect using microRNA modulation in combination with stem cell treatment, inhibition of anti-chondrogenic miR-146b in isolated human bone marrow derived stem cells could be transplanted to cartilage defect sites and investigated for the ability to repair articular cartilage.

Despite having identified that SOX5 expression was down-regulated following miR-146b overexpression by increasing the levels of miR-146b within human bone marrow derived skeletal stem cells using a miR-146b mimic, *SOX5* mRNA 3'UTR could not be distinguished as a direct target of miR-146b from an indirect target of miR-146b. The down-regulation of SOX5 may be a downstream effect from the down-regulation of a different target. Both the bioinformatic analysis and the effect of overexpression of miR-146b on SOX5 expression imply *SOX5* mRNA as a direct target of miR-146b. To validate *SOX5* mRNA as a direct target of miR-146b, the binding interaction between miR-146b and the miR-146b binding site within the 3'UTR of *SOX5* needs to be validated. Interaction between miR-146b and the miR-146b response element within the 3'UTR of *SOX5* mRNA can be assessed with a luciferase reporter assay. Techniques were carried out to construct the vectors required for a luciferase reporter assay. However, a succession of failed attempts to create the appropriate vectors meant that the endpoint luciferase reporter assay could not be carried out. A luciferase reporter assay needs to be conducted to validate miR-146b binding to the 3'UTR of *SOX5* mRNA. The methods used to construct the vectors could be optimised to attempt to create the vectors for the luciferase reporter assay. The mutagenesis method employed to induce base substitution within the miR-146b binding site of the *SOX5* mRNA 3'UTR requires optimisation. Optimisation to the temperatures used for thermal cycling, reducing the number of bases to be substituted at the potential mutation site and using an alternative polymerase are some of the factors which require investigation.

Increased levels of miR-146b induced the down-regulation of SOX5 expression but no changes in *SMAD4* mRNA or SMAD protein expression were observed. Similar to the concept discussed in 6.2.1, the presence of RBPs, NATs and alternative polyadenylation sites may be responsible

for the outcome. *SMAD4* mRNA may avoid miR-146b targeted down-regulation due to other regulatory mechanisms which override miR-146b *SMAD4* mRNA targeted inhibition. The result may also indicate that *SMAD4* mRNA is not a target of miR-146b. Future studies to investigate the presence of potential RBPs, NATS and alternative polyadenylation sites within the 3'UTR of *SMAD4* mRNA would need to be carried out.

6.3 Conclusion

The expression of miR-146b in human OA articular chondrocytes is dysregulated compared to the expression of miR-146b in control human chondrocytes. This hypothesis is true. For the first time the up-regulation of miR-146b was observed in human chondrocytes isolated from OA articular cartilage. Given inflammatory environment associated with OA, the up-regulated expression of miR-146b is likely to function to dampen chronic inflammatory response. Further work is required to validate the anti-inflammatory role of miR-146b in OA and the stimulus responsible for miR-146b up-regulation. The close sequence homology that miR-146b shares with miR-146a suggests that both miR-146a and miR-146b may have roles in inflammation in OA. If miR-146b is an anti-inflammatory mediator acting to attenuate inflammatory response in OA, miR-146b could be used as a potential anti-inflammatory therapy in the future for alleviating the symptoms of OA. The pro-inflammatory, catabolic cytokine IL-1β could not induce miR-146b expression in human chondrocytes and consequently anabolic associated TGF-β3 had no effect of IL-1β induced miR-146b expression and therefore the initial hypothesis is false. Future work to identify other potential catabolic pro-inflammatory inducers of miR-146b expression may establish the mediator responsible for miR-146b up-regulation observed in human OA articular chondrocytes.

The hypothesis that skeletal populations can be derived using specific microRNAs, to selectively direct cell differentiation and function along the chondrogenic lineage is true. While modulation of miR-34a was found not to have an effect on predicted target *TGIF2*, indicating that miR-34a does not play a role in the chondrogenic differentiation of fetal femur-derived stem cells, this may be due to cell regulatory mechanisms in place to fine tune gene expression such as alternative polyadenylation. Modulation of miR-146b had an effect on SOX5 expression and miR-146b was found to be down-regulated during the chondrogenic differentiation of bone marrow derived skeletal stem cells due to the negative effect upon SOX5 expression. Identification of the down-regulated expression pattern of miR-146b during the chondrogenic differentiation of human bone marrow derived skeletal stem cells and identification of miR-146b function may enable the use of exogenous miR-146b modulation in combination with stem cell therapy for treating articular cartilage defects in the future.

References

1. Hall, B.K., *Bones and Cartilage: Developmental and Evolutionary Skeletal Biology*. 2005: Elsevier Science.
2. Athanasiou, K.A., E.M. Darling, and J.C. Hu, *Articular Cartilage Tissue Engineering*. 2009: Morgan & Claypool Publishers.
3. Williams, R.J., L. Peterson, and B.J. Cole, *Cartilage Repair Strategies*. 2008: Humana Press.
4. Sophia Fox, A.J., A. Bedi, and S.A. Rodeo, *The basic science of articular cartilage: structure, composition, and function.* Sports Health, 2009. **1**(6): p. 461-8.
5. Comper, W.D., *Extracellular Matrix: Molecular components and interactions*. 1996: Harwood Academic Publishers.
6. Luo, Z.P., et al., *Single molecule mechanical properties of type II collagen and hyaluronan measured by optical tweezers.* Biorheology, 2004. **41**(3-4): p. 247-54.
7. Seibel, M.J., S.P. Robins, and J.P. Bilezikian, *Dynamics of Bone and Cartilage Metabolism: Principles and Clinical Applications*. 2006: Elsevier Science.
8. Kiani, C., et al., *Structure and function of aggrecan.* Cell Res, 2002. **12**(1): p. 19-32.
9. Yang, Y., *Skeletal morphogenesis during embryonic development.* Crit Rev Eukaryot Gene Expr, 2009. **19**(3): p. 197-218.
10. Olsen, B.R., A.M. Reginato, and W. Wang, *Bone development.* Annu Rev Cell Dev Biol, 2000. **16**: p. 191-220.
11. Pocock, G., C.D. Richards, and D.A. Richards, *Human Physiology*. 2013: OUP Oxford.
12. Arai, F., et al., *Mesenchymal stem cells in perichondrium express activated leukocyte cell adhesion molecule and participate in bone marrow formation.* J Exp Med, 2002. **195**(12): p. 1549-63.
13. Kronenberg, H.M., *How PTHrP controls growth plate chondrocytes.* BonekEy-Osteovision, 2005. **2**(11): p. 7-15.
14. Decker, R.S., E. Koyama, and M. Pacifici, *Genesis and morphogenesis of limb synovial joints and articular cartilage.* Matrix Biology, 2014. **39**: p. 5-10.
15. Pacifici, M., E. Koyama, and M. Iwamoto, *Mechanisms of synovial joint and articular cartilage formation: recent advances, but many lingering mysteries.* Birth Defects Res C Embryo Today, 2005. **75**(3): p. 237-48.
16. Holder, N., *An experimental investigation into the early development of the chick elbow joint.* J Embryol Exp Morphol, 1977. **39**: p. 115-27.
17. Karsenty, G. and E.F. Wagner, *Reaching a Genetic and Molecular Understanding of Skeletal Development.* Developmental Cell, 2002. **2**(4): p. 389-406.
18. Brunet, L.J., et al., *Noggin, cartilage morphogenesis, and joint formation in the mammalian skeleton.* Science, 1998. **280**(5368): p. 1455-7.

19. Francis-West, H.P., et al., *BMP/GDF-signalling interactions during synovial joint development.* Cell and Tissue Research. **296**(1): p. 111-119.
20. Hartmann, C. and C.J. Tabin, *Wnt-14 Plays a Pivotal Role in Inducing Synovial Joint Formation in the Developing Appendicular Skeleton.* Cell. **104**(3): p. 341-351.
21. Storm, E.E., et al., *Limb alterations in brachypodism mice due to mutations in a new member of the TGF beta-superfamily.* Nature, 1994. **368**(6472): p. 639-43.
22. Koyama, E., et al., *A distinct cohort of progenitor cells participates in synovial joint and articular cartilage formation during mouse limb skeletogenesis.* Dev Biol, 2008. **316**(1): p. 62-73.
23. Coleman, C.M. and R.S. Tuan, *Functional role of growth/differentiation factor 5 in chondrogenesis of limb mesenchymal cells.* Mechanisms of Development, 2003. **120**(7): p. 823-836.
24. Hyde, G., et al., *Lineage tracing using matrilin-1 gene expression reveals that articular chondrocytes exist as the joint interzone forms.* Dev Biol, 2007. **304**(2): p. 825-33.
25. Aszodi, A., et al., *Normal skeletal development of mice lacking matrilin 1: redundant function of matrilins in cartilage?* Mol Cell Biol, 1999. **19**(11): p. 7841-5.
26. Huang, X., D.E. Birk, and P.F. Goetinck, *Mice lacking matrilin-1 (cartilage matrix protein) have alterations in type II collagen fibrillogenesis and fibril organization.* Dev Dyn, 1999. **216**(4-5): p. 434-41.
27. Yang, X., et al., *TGF-beta/Smad3 signals repress chondrocyte hypertrophic differentiation and are required for maintaining articular cartilage.* J Cell Biol, 2001. **153**(1): p. 35-46.
28. Eames, B.F., L. de la Fuente, and J.A. Helms, *Molecular ontogeny of the skeleton.* Birth Defects Res C Embryo Today, 2003. **69**(2): p. 93-101.
29. Dy, P., et al., *Synovial joint morphogenesis requires the chondrogenic action of Sox5 and Sox6 in growth plate and articular cartilage.* Dev Biol, 2010. **341**(2): p. 346-59.
30. Akiyama, H., et al., *The transcription factor Sox9 has essential roles in successive steps of the chondrocyte differentiation pathway and is required for expression of Sox5 and Sox6.* Genes & Development, 2002. **16**(21): p. 2813-2828.
31. Osborne, A.C., et al., *Short-term rigid and flaccid paralyses diminish growth of embryonic chick limbs and abrogate joint cavity formation but differentially preserve pre-cavitated joints.* J Musculoskelet Neuronal Interact, 2002. **2**(5): p. 448-56.
32. Lamb, K.J., et al., *Defining boundaries during joint cavity formation: going out on a limb.* International Journal of Experimental Pathology, 2003. **84**(2): p. 55-67.
33. Pacifici, M., et al., *Cellular and Molecular Mechanisms of Synovial Joint and Articular Cartilage Formation.* Annals of the New York Academy of Sciences, 2006. **1068**: p. 74-86.
34. Mathers, D.S.C.a.B.P., *Global burden of osteoarthritis in the year 2000.*

.

35. Seo, S.-S., C.-W. Kim, and D.-W. Jung, *Management of Focal Chondral Lesion in the Knee Joint.* Knee Surgery & Related Research, 2011. **23**(4): p. 185-196.
36. McGonagle, D., et al., *Heberden's nodes and what Heberden could not see: the pivotal role of ligaments in the pathogenesis of early nodal osteoarthritis and beyond.* Rheumatology (Oxford), 2008. **47**(9): p. 1278-85.
37. Benjamin, M., et al., *The "enthesis organ" concept: Why enthesopathies may not present as focal insertional disorders.* Arthritis & Rheumatism, 2004. **50**(10): p. 3306-3313.
38. Binks, D.A., et al., *Potential role of the posterior cruciate ligament synovio-entheseal complex in joint effusion in early osteoarthritis: a magnetic resonance imaging and histological evaluation of cadaveric tissue and data from the Osteoarthritis Initiative.* Osteoarthritis and Cartilage, 2014. **22**(9): p. 1310-1317.
39. Benjamin, M. and D. McGonagle, *Histopathologic changes at "synovio-entheseal complexes" suggesting a novel mechanism for synovitis in osteoarthritis and spondylarthritis.* Arthritis Rheum, 2007. **56**(11): p. 3601-9.
40. Wojdasiewicz, P., et al., *The Role of Inflammatory and Anti-Inflammatory Cytokines in the Pathogenesis of Osteoarthritis.* Mediators of Inflammation, 2014. **2014**: p. 19.
41. Melchiorri, C., et al., *Enhanced and coordinated in vivo expression of inflammatory cytokines and nitric oxide synthase by chondrocytes from patients with osteoarthritis.* Arthritis Rheum, 1998. **41**(12): p. 2165-74.
42. Farahat, M.N., et al., *Cytokine expression in synovial membranes of patients with rheumatoid arthritis and osteoarthritis.* Annals of the rheumatic diseases, 1993. **52**(12): p. 870-875.
43. Sohn, D.H., et al., *Plasma proteins present in osteoarthritic synovial fluid can stimulate cytokine production via Toll-like receptor 4.* Arthritis Res Ther, 2012. **14**(1): p. R7.
44. Smith, M.D., et al., *Synovial membrane inflammation and cytokine production in patients with early osteoarthritis.* J Rheumatol, 1997. **24**(2): p. 365-71.
45. Kubota, E., et al., *Interleukin 1 beta and stromelysin (MMP3) activity of synovial fluid as possible markers of osteoarthritis in the temporomandibular joint.* J Oral Maxillofac Surg, 1997. **55**(1): p. 20-7; discussion 27-8.
46. Saha, N., et al., *Interleukin-1beta-converting enzyme/caspase-1 in human osteoarthritic tissues: localization and role in the maturation of interleukin-1beta and interleukin-18.* Arthritis Rheum, 1999. **42**(8): p. 1577-87.
47. Martel-Pelletier, J., et al., *The interleukin-1 receptor in normal and osteoarthritic human articular chondrocytes. Identification as the type I receptor and analysis of binding kinetics and biologic function.* Arthritis Rheum, 1992. **35**(5): p. 530-40.
48. Tiku, K., et al., *Articular chondrocytes secrete IL-1, express membrane IL-1, and have IL-1 inhibitory activity.* Cell Immunol, 1992. **140**(1): p. 1-20.

49. Shlopov, B.V., M.L. Gumanovskaya, and K.A. Hasty, *Autocrine regulation of collagenase 3 (matrix metalloproteinase 13) during osteoarthritis.* Arthritis & Rheumatism, 2000. **43**(1): p. 195-205.
50. Lai, Y.C., et al., *Intraarticular induction of interleukin-1beta expression in the adult mouse, with resultant temporomandibular joint pathologic changes, dysfunction, and pain.* Arthritis Rheum, 2006. **54**(4): p. 1184-97.
51. Wheaton, A.J., et al., *Detection of changes in articular cartilage proteoglycan by T(1)(ρ) magnetic resonance imaging.* Journal of orthopaedic research : official publication of the Orthopaedic Research Society, 2005. **23**(1): p. 102-108.
52. Richardson, D.W. and G.R. Dodge, *Effects of interleukin-1beta and tumor necrosis factor-alpha on expression of matrix-related genes by cultured equine articular chondrocytes.* Am J Vet Res, 2000. **61**(6): p. 624-30.
53. Loo, A.A.J., et al., *Direct effect of murine rIL-1 on cartilage metabolismin vivo.* Agents and Actions. **26**(1): p. 153-155.
54. Daheshia, M. and J.Q. Yao, *The interleukin 1beta pathway in the pathogenesis of osteoarthritis.* J Rheumatol, 2008. **35**(12): p. 2306-12.
55. Cortial, D., et al., *Activation by IL-1 of bovine articular chondrocytes in culture within a 3D collagen-based scaffold. An in vitro model to address the effect of compounds with therapeutic potential in osteoarthritis.* Osteoarthritis Cartilage, 2006. **14**(7): p. 631-40.
56. Fan, Z., et al., *Freshly isolated osteoarthritic chondrocytes are catabolically more active than normal chondrocytes, but less responsive to catabolic stimulation with interleukin-1β.* Arthritis & Rheumatism, 2005. **52**(1): p. 136-143.
57. Bau, B., et al., *Relative messenger RNA expression profiling of collagenases and aggrecanases in human articular chondrocytes in vivo and in vitro.* Arthritis & Rheumatism, 2002. **46**(10): p. 2648-2657.
58. Kobayashi, M., et al., *Role of interleukin-1 and tumor necrosis factor α in matrix degradation of human osteoarthritic cartilage.* Arthritis & Rheumatism, 2005. **52**(1): p. 128-135.
59. Howes, J.M., et al., *The recognition of collagen and triple-helical toolkit peptides by MMP-13: sequence specificity for binding and cleavage.* J Biol Chem, 2014. **289**(35): p. 24091-101.
60. Guerne, P.A., D.A. Carson, and M. Lotz, *IL-6 production by human articular chondrocytes. Modulation of its synthesis by cytokines, growth factors, and hormones in vitro.* J Immunol, 1990. **144**(2): p. 499-505.
61. Aigner, T., et al., *Gene expression profiling of serum- and interleukin-1β-stimulated primary human adult articular chondrocytes – A molecular analysis based on chondrocytes isolated from one donor.* Cytokine, 2005. **31**(3): p. 227-240.
62. Lotz, M., R. Terkeltaub, and P.M. Villiger, *Cartilage and joint inflammation. Regulation of IL-8 expression by human articular chondrocytes.* J Immunol, 1992. **148**(2): p. 466-73.

63. Alaaeddine, N., et al., *Production of the chemokine RANTES by articular chondrocytes and role in cartilage degradation.* Arthritis Rheum, 2001. **44**(7): p. 1633-43.
64. Pulsatelli, L., et al., *Chemokine production by human chondrocytes.* J Rheumatol, 1999. **26**(9): p. 1992-2001.
65. Black, R.A., *Tumor necrosis factor-alpha converting enzyme.* Int J Biochem Cell Biol, 2002. **34**(1): p. 1-5.
66. Henderson, B. and E.R. Pettipher, *Arthritogenic actions of recombinant IL-1 and tumour necrosis factor alpha in the rabbit: evidence for synergistic interactions between cytokines in vivo.* Clinical and Experimental Immunology, 1989. **75**(2): p. 306-310.
67. Keffer, J., et al., *Transgenic mice expressing human tumour necrosis factor: a predictive genetic model of arthritis.* The EMBO Journal, 1991. **10**(13): p. 4025-4031.
68. Kammermann, J.R., et al., *Tumor necrosis factor-alpha (TNF-alpha) in canine osteoarthritis: Immunolocalization of TNF-alpha, stromelysin and TNF receptors in canine osteoarthritic cartilage.* Osteoarthritis Cartilage, 1996. **4**(1): p. 23-34.
69. Grunke, M. and H. Schulze‐Koops, *Successful treatment of inflammatory knee osteoarthritis with tumour necrosis factor blockade.* Annals of the Rheumatic Diseases, 2006. **65**(4): p. 555-556.
70. Saklatvala, J., *Tumour necrosis factor [alpha] stimulates resorption and inhibits synthesis of proteoglycan in cartilage.* Nature, 1986. **322**(6079): p. 547-549.
71. Tetlow, L.C., D.J. Adlam, and D.E. Woolley, *Matrix metalloproteinase and proinflammatory cytokine production by chondrocytes of human osteoarthritic cartilage: Associations with degenerative changes.* Arthritis & Rheumatism, 2001. **44**(3): p. 585-594.
72. Xue, J., et al., *Tumor necrosis factor-alpha induces ADAMTS-4 expression in human osteoarthritis chondrocytes.* Mol Med Rep, 2013. **8**(6): p. 1755-60.
73. Shuler, F.D., et al., *Increased matrix synthesis following adenoviral transfer of a transforming growth factor β1 gene into articular chondrocytes.* Journal of Orthopaedic Research, 2000. **18**(4): p. 585-592.
74. Galéra, P., et al., *Transforming growth factor-β1 (TGF-β1) up-regulation of collagen type II in primary cultures of rabbit articular chondrocytes (RAC) involves increased mRNA levels without affecting mRNA stability and procollagen processing.* Journal of Cellular Physiology, 1992. **153**(3): p. 596-606.
75. Gunther, M., et al., *Transforming growth factor beta 1 regulates tissue inhibitor of metalloproteinases-1 expression in differentiated human articular chondrocytes.* Arthritis Rheum, 1994. **37**(3): p. 395-405.
76. Su, S., F. Dehnade, and M. Zafarullah, *Regulation of tissue inhibitor of metalloproteinases-3 gene expression by transforming growth factor-beta and dexamethasone in bovine and human articular chondrocytes.* DNA Cell Biol, 1996. **15**(12): p. 1039-48.

77. Qureshi, H.Y., et al., *TGF-beta-induced expression of tissue inhibitor of metalloproteinases-3 gene in chondrocytes is mediated by extracellular signal-regulated kinase pathway and Sp1 transcription factor.* J Cell Physiol, 2005. **203**(2): p. 345-52.
78. Ballock, R.T., et al., *TGF-beta 1 prevents hypertrophy of epiphyseal chondrocytes: regulation of gene expression for cartilage matrix proteins and metalloproteases.* Dev Biol, 1993. **158**(2): p. 414-29.
79. Serra, R., et al., *Expression of a truncated, kinase-defective TGF-beta type II receptor in mouse skeletal tissue promotes terminal chondrocyte differentiation and osteoarthritis.* J Cell Biol, 1997. **139**(2): p. 541-52.
80. Blaney Davidson, E., et al., *Reduced transforming growth factor-beta signaling in cartilage of old mice: role in impaired repair capacity.* Arthritis Research & Therapy, 2005. **7**(6): p. 1-10.
81. Kizawa, H., et al., *An aspartic acid repeat polymorphism in asporin inhibits chondrogenesis and increases susceptibility to osteoarthritis.* Nat Genet, 2005. **37**(2): p. 138-144.
82. Ikegawa, S., *[Asporin, a susceptibility gene for osteoarthritis].* Clin Calcium, 2006. **16**(9): p. 1548-52.
83. Valdes, A.M., et al., *Genetic variation in the SMAD3 gene is associated with hip and knee osteoarthritis.* Arthritis Rheum, 2010. **62**(8): p. 2347-52.
84. van de Laar, I.M.B.H., et al., *Mutations in SMAD3 cause a syndromic form of aortic aneurysms and dissections with early-onset osteoarthritis.* Nat Genet, 2011. **43**(2): p. 121-126.
85. Loeys, B.L. and H.C. Dietz, *Loeys-Dietz Syndrome*, in *GeneReviews(R)*, R.A. Pagon, et al., Editors. 1993, University of Washington, Seattle: Seattle WA.
86. Takahashi, N., et al., *Elucidation of IL-1/TGF-β interactions in mouse chondrocyte cell line by genome-wide gene expression.* Osteoarthritis and Cartilage, 2005. **13**(5): p. 426-438.
87. Bauge, C., et al., *Interleukin-1beta impairment of transforming growth factor beta1 signaling by down-regulation of transforming growth factor beta receptor type II and up-regulation of Smad7 in human articular chondrocytes.* Arthritis Rheum, 2007. **56**(9): p. 3020-32.
88. Bitzer, M., et al., *A mechanism of suppression of TGF-beta/SMAD signaling by NF-kappa B/RelA.* Genes Dev, 2000. **14**(2): p. 187-97.
89. Hayashi, H., et al., *The MAD-related protein Smad7 associates with the TGFbeta receptor and functions as an antagonist of TGFbeta signaling.* Cell, 1997. **89**(7): p. 1165-73.
90. Kavsak, P., et al., *Smad7 Binds to Smurf2 to Form an E3 Ubiquitin Ligase that Targets the TGFβ Receptor for Degradation.* Molecular Cell. **6**(6): p. 1365-1375.
91. Ebisawa, T., et al., *Smurf1 interacts with transforming growth factor-beta type I receptor through Smad7 and induces receptor degradation.* J Biol Chem, 2001. **276**(16): p. 12477-80.
92. Suzuki, C., et al., *Smurf1 regulates the inhibitory activity of Smad7 by targeting Smad7 to the plasma membrane.* J Biol Chem, 2002. **277**(42): p. 39919-25.

93. Zhang, S., et al., *Smad7 antagonizes transforming growth factor beta signaling in the nucleus by interfering with functional Smad-DNA complex formation.* Mol Cell Biol, 2007. **27**(12): p. 4488-99.
94. Yan, X., et al., *Yin Yang 1 (YY1) synergizes with Smad7 to inhibit TGF-beta signaling in the nucleus.* Sci China Life Sci, 2014. **57**(1): p. 128-36.
95. Stattin, E.L., et al., *A missense mutation in the aggrecan C-type lectin domain disrupts extracellular matrix interactions and causes dominant familial osteochondritis dissecans.* Am J Hum Genet, 2010. **86**(2): p. 126-37.
96. Williams, C.J., et al., *Spondyloepiphyseal dysplasia and precocious osteoarthritis in a family with an Arg75-->Cys mutation in the procollagen type II gene (COL2A1).* Hum Genet, 1993. **92**(5): p. 499-505.
97. Hoornaert, K.P., et al., *Czech dysplasia metatarsal type: another type II collagen disorder.* Eur J Hum Genet, 2007. **15**(12): p. 1269-1275.
98. Ala-Kokko, L., et al., *Single base mutation in the type II procollagen gene (COL2A1) as a cause of primary osteoarthritis associated with a mild chondrodysplasia.* Proc Natl Acad Sci U S A, 1990. **87**(17): p. 6565-8.
99. Holderbaum, D., et al., *Human Cartilage from Late Stage Familial Osteoarthritis Transcribes Type II Collagen mRNA Encoding a Cysteine in Position 519.* Biochemical and Biophysical Research Communications, 1993. **192**(3): p. 1169-1174.
100. Williams, C.J., et al., *Three new point mutations in type II procollagen (COL2A1) and identification of a fourth family with the COL2A1 Arg519-->Cys base substitution using conformation sensitive gel electrophoresis.* Hum Mol Genet, 1995. **4**(2): p. 309-12.
101. Miyamoto, Y., et al., *A type II collagen mutation also results in oto-spondylo-megaepiphyseal dysplasia.* Human Genetics, 2005. **118**(2): p. 175-178.
102. Regalado, E.S., et al., *Exome sequencing identifies SMAD3 mutations as a cause of familial thoracic aortic aneurysm and dissection with intracranial and other arterial aneurysms.* Circ Res, 2011. **109**(6): p. 680-6.
103. van de Laar, I.M., et al., *Phenotypic spectrum of the SMAD3-related aneurysms-osteoarthritis syndrome.* J Med Genet, 2012. **49**(1): p. 47-57.
104. Wang, T., et al., *Single Nucleotide Polymorphisms and Osteoarthritis: An Overview and a Meta-Analysis.* Medicine, 2016. **95**(7): p. e2811.
105. UK, A.R., *Arthritis in the UK - Key facts. 2008.*
106. Life, P.H., *Reducing risks, Promoting Healthy Life. 2002.*
107. Scott, D.L., et al., *The clinical management of rheumatoid arthritis and osteoarthritis: strategies for improving clinical effectiveness.* Br J Rheumatol, 1998. **37**(5): p. 546-54.
108. Jackson, R.A., V. Nurcombe, and S.M. Cool, *Coordinated fibroblast growth factor and heparan sulfate regulation of osteogenesis.* Gene, 2006. **379**: p. 79-91.

109. pensions, D.f.w.a., *Analysis of New Claims for Disability Living Allowance and Attendance Allowance by Main Disabling Condition: 2011/2012*. 2012.
110. Holroyd, C., C. Cooper, and E. Dennison, *Epidemiology of osteoporosis.* Best Pract Res Clin Endocrinol Metab, 2008. **22**(5): p. 671-85.
111. Falah, M., et al., *Treatment of articular cartilage lesions of the knee.* International Orthopaedics, 2010. **34**(5): p. 621-630.
112. Messner, K. and W. Maletius, *The long-term prognosis for severe damage to weight-bearing cartilage in the knee: a 14-year clinical and radiographic follow-up in 28 young athletes.* Acta Orthop Scand, 1996. **67**(2): p. 165-8.
113. Browne, J.E. and T.P. Branch, *Surgical alternatives for treatment of articular cartilage lesions.* J Am Acad Orthop Surg, 2000. **8**(3): p. 180-9.
114. Ahmed, T.A. and M.T. Hincke, *Strategies for articular cartilage lesion repair and functional restoration.* Tissue Eng Part B Rev, 2010. **16**(3): p. 305-29.
115. Robb, C.A., et al., *Survival of autologous osteochondral grafts in the knee and factors influencing outcome.* Acta Orthop Belg, 2012. **78**(5): p. 643-51.
116. Panagopoulos, A., L. van Niekerk, and I. Triantafillopoulos, *Autologous chondrocyte implantation for knee cartilage injuries: moderate functional outcome and performance in patients with high-impact activities.* Orthopedics, 2012. **35**(1): p. e6-14.
117. Schnabel, M., et al., *Dedifferentiation-associated changes in morphology and gene expression in primary human articular chondrocytes in cell culture.* Osteoarthritis Cartilage, 2002. **10**(1): p. 62-70.
118. McGee, M.A., et al., *Implant retrieval studies of the wear and loosening of prosthetic joints: a review.* Wear, 2000. **241**(2): p. 158-165.
119. Duynstee, M.L., et al., *The dual role of perichondrium in cartilage wound healing.* Plast Reconstr Surg, 2002. **110**(4): p. 1073-9.
120. Schofield, R., *The relationship between the spleen colony-forming cell and the haemopoietic stem cell.* Blood Cells, 1978. **4**(1-2): p. 7-25.
121. Li, L. and T. Xie, *Stem cell niche: structure and function.* Annu Rev Cell Dev Biol, 2005. **21**: p. 605-31.
122. Karlsson, C., et al., *Identification of a stem cell niche in the zone of Ranvier within the knee joint.* Journal of Anatomy, 2009. **215**(3): p. 355-363.
123. Candela, M.E., et al., *Resident mesenchymal progenitors of articular cartilage.* Matrix Biol, 2014. **39**: p. 44-9.
124. Dowthwaite, G.P., et al., *The surface of articular cartilage contains a progenitor cell population.* Journal of Cell Science, 2004. **117**(6): p. 889-897.
125. Hattori, S., C. Oxford, and A.H. Reddi, *Identification of superficial zone articular chondrocyte stem/progenitor cells.* Biochemical and biophysical research communications, 2007. **358**(1): p. 99-103.

126. Yasuhara, R., et al., *Roles of β-catenin signaling in phenotypic expression and proliferation of articular cartilage superficial zone cells.* Laboratory investigation; a journal of technical methods and pathology, 2011. **91**(12): p. 1739-1752.
127. Scharenberg, C.W., M.A. Harkey, and B. Torok-Storb, *The ABCG2 transporter is an efficient Hoechst 33342 efflux pump and is preferentially expressed by immature human hematopoietic progenitors.* Blood, 2002. **99**(2): p. 507-512.
128. Grogan, S.P., et al., *Mesenchymal progenitor cell markers in human articular cartilage: normal distribution and changes in osteoarthritis.* Arthritis Research & Therapy, 2009. **11**(3): p. R85-R85.
129. Alsalameh, S., et al., *Identification of mesenchymal progenitor cells in normal and osteoarthritic human articular cartilage.* Arthritis & Rheumatism, 2004. **50**(5): p. 1522-1532.
130. Seol, D., et al., *Chondrogenic progenitor cells respond to cartilage injury.* Arthritis & Rheumatism, 2012. **64**(11): p. 3626-3637.
131. Wickham, M.Q., et al., *Multipotent stromal cells derived from the infrapatellar fat pad of the knee.* Clin Orthop Relat Res, 2003(412): p. 196-212.
132. Jones, E.A., et al., *Synovial fluid mesenchymal stem cells in health and early osteoarthritis: detection and functional evaluation at the single-cell level.* Arthritis Rheum, 2008. **58**(6): p. 1731-40.
133. De Bari, C., et al., *Multipotent mesenchymal stem cells from adult human synovial membrane.* Arthritis & Rheumatism, 2001. **44**(8): p. 1928-1942.
134. Kurth, T.B., et al., *Functional mesenchymal stem cell niches in adult mouse knee joint synovium in vivo.* Arthritis & Rheumatism, 2011. **63**(5): p. 1289-1300.
135. Weiner, L., *Definitions and Criteria for Stem Cells*, in *Neural Stem Cells*, L. Weiner, Editor. 2008, Humana Press. p. 3-8.
136. Tare, R.S., et al., *Skeletal stem cells and bone regeneration: translational strategies from bench to clinic.* Proc Inst Mech Eng H, 2010. **224**(12): p. 1455-70.
137. Boris, V.A., E. Elena, and R.Z. Axel, *, A.J. Friedenstein, founder of the mesenchymal stem cell concept,.* Hamburg University Medical Center, St.Petersburg State Medical I.Pavlov University., 2009.
138. Augello, A. and C. De Bari, *The regulation of differentiation in mesenchymal stem cells.* Hum Gene Ther, 2010. **21**(10): p. 1226-38.
139. Mirmalek-Sani, S.-H., et al., *Characterization and Multipotentiality of Human Fetal Femur–Derived Cells: Implications for Skeletal Tissue Regeneration.* STEM CELLS, 2006. **24**(4): p. 1042-1053.
140. Hwang, N.S., et al., *Mesenchymal stem cell differentiation and roles in regenerative medicine.* Wiley Interdiscip Rev Syst Biol Med, 2009. **1**(1): p. 97-106.
141. Pittenger, M.F., et al., *Multilineage potential of adult human mesenchymal stem cells.* Science, 1999. **284**(5411): p. 143-7.

142. Chen, X., M.A. Armstrong, and G. Li, *Mesenchymal stem cells in immunoregulation.* Immunol Cell Biol, 2006. **84**(5): p. 413-421.
143. Chen, P.-M., et al., *Immunomodulatory properties of human adult and fetal multipotent mesenchymal stem cells.* Journal of Biomedical Science, 2011. **18**(1): p. 49.
144. Murray, I.R. and B. Péault, *Q&A: Mesenchymal stem cells — where do they come from and is it important?* BMC Biology, 2015. **13**: p. 99.
145. Sordi, V., et al., *Bone marrow mesenchymal stem cells express a restricted set of functionally active chemokine receptors capable of promoting migration to pancreatic islets.* Blood, 2005. **106**(2): p. 419-427.
146. Bhattacharyya, S., A. Kumar, and K. Lal Khanduja, *The voyage of stem cell toward terminal differentiation: a brief overview.* Acta Biochim Biophys Sin (Shanghai), 2012. **44**(6): p. 463-75.
147. Mackay, A.M., et al., *Chondrogenic differentiation of cultured human mesenchymal stem cells from marrow.* Tissue Eng, 1998. **4**(4): p. 415-28.
148. Sekiya, I., et al., *In vitro cartilage formation by human adult stem cells from bone marrow stroma defines the sequence of cellular and molecular events during chondrogenesis.* Proc Natl Acad Sci U S A, 2002. **99**(7): p. 4397-402.
149. Djouad, F., et al., *Microenvironmental changes during differentiation of mesenchymal stem cells towards chondrocytes.* Arthritis Research & Therapy, 2007. **9**(2): p. R33-R33.
150. Yoo, J.U., et al., *The Chondrogenic Potential of Human Bone-Marrow-Derived Mesenchymal Progenitor Cells*.* J Bone Joint Surg Am, 1998. **80**(12): p. 1745-57.
151. Frith, J. and P. Genever, *Transcriptional control of mesenchymal stem cell differentiation.* Transfus Med Hemother, 2008. **35**(3): p. 216-27.
152. Yu, D.-A., J. Han, and B.-S. Kim, *Stimulation of Chondrogenic Differentiation of Mesenchymal Stem Cells.* International Journal of Stem Cells, 2012. **5**(1): p. 16-22.
153. Kawakami, Y., J. Rodriguez-León, and J.C.I. Belmonte, *The role of TGFβs and Sox9 during limb chondrogenesis.* Current Opinion in Cell Biology, 2006. **18**(6): p. 723-729.
154. Barry, F., et al., *Chondrogenic Differentiation of Mesenchymal Stem Cells from Bone Marrow: Differentiation-Dependent Gene Expression of Matrix Components.* Experimental Cell Research, 2001. **268**(2): p. 189-200.
155. Weber, M., et al., *Formation of cartilage matrix proteins by BMP-transfected murine mesenchymal stem cells encapsulated in a novel class of alginates.* Biomaterials, 2002. **23**(9): p. 2003-13.
156. Noël, D., et al., *Short-Term BMP-2 Expression Is Sufficient for In Vivo Osteochondral Differentiation of Mesenchymal Stem Cells.* STEM CELLS, 2004. **22**(1): p. 74-85.
157. Tang, T.T., et al., *Ectopic bone formation of human bone morphogenetic protein-2 gene transfected goat bone marrow-derived mesenchymal stem cells in nude mice.* Chin J Traumatol, 2005. **8**(1): p. 3-7.

158. Danišovič, Ľ., I. Varga, and Š. Polák, *Growth factors and chondrogenic differentiation of mesenchymal stem cells.* Tissue and Cell, 2012. **44**(2): p. 69-73.
159. Bi, W., et al., *Haploinsufficiency of Sox9 results in defective cartilage primordia and premature skeletal mineralization.* Proceedings of the National Academy of Sciences, 2001. **98**(12): p. 6698-6703.
160. Huang, W., et al., *The chondrogenic transcription factor Sox9 is a target of signaling by the parathyroid hormone-related peptide in the growth plate of endochondral bones.* Proceedings of the National Academy of Sciences, 2001. **98**(1): p. 160-165.
161. Tsuda, M., et al., *Transcriptional co-activators CREB-binding protein and p300 regulate chondrocyte-specific gene expression via association with Sox9.* J Biol Chem, 2003. **278**(29): p. 27224-9.
162. Lefebvre, V., P. Li, and B. de Crombrugghe, *A new long form of Sox5 (L‐Sox5), Sox6 and Sox9 are coexpressed in chondrogenesis and cooperatively activate the type II collagen gene.* The EMBO Journal, 1998. **17**(19): p. 5718-5733.
163. Smits, P., et al., *The transcription factors L-Sox5 and Sox6 are essential for cartilage formation.* Dev Cell, 2001. **1**(2): p. 277-90.
164. Ikeda, T., et al., *The combination of SOX5, SOX6, and SOX9 (the SOX trio) provides signals sufficient for induction of permanent cartilage.* Arthritis Rheum, 2004. **50**(11): p. 3561-73.
165. Han, Y. and V. Lefebvre, *L-Sox5 and Sox6 drive expression of the aggrecan gene in cartilage by securing binding of Sox9 to a far-upstream enhancer.* Mol Cell Biol, 2008. **28**(16): p. 4999-5013.
166. Im, G.I., et al., *Repair of cartilage defect in the rabbit with cultured mesenchymal stem cells from bone marrow.* J Bone Joint Surg Br, 2001. **83**(2): p. 289-94.
167. Murphy, J.M., et al., *Stem cell therapy in a caprine model of osteoarthritis.* Arthritis & Rheumatism, 2003. **48**(12): p. 3464-3474.
168. Al Faqeh, H., et al., *The potential of intra-articular injection of chondrogenic-induced bone marrow stem cells to retard the progression of osteoarthritis in a sheep model.* Exp Gerontol, 2012. **47**(6): p. 458-64.
169. Wakitani, S., et al., *Mesenchymal cell-based repair of large, full-thickness defects of articular cartilage.* J Bone Joint Surg Am, 1994. **76**(4): p. 579-92.
170. Berninger, M.T., et al., *Treatment of Osteochondral Defects in the Rabbit's Knee Joint by Implantation of Allogeneic Mesenchymal Stem Cells in Fibrin Clots.* Journal of Visualized Experiments : JoVE, 2013(75): p. 4423.
171. Grigolo, B., et al., *Osteoarthritis treated with mesenchymal stem cells on hyaluronan-based scaffold in rabbit.* Tissue Eng Part C Methods, 2009. **15**(4): p. 647-58.
172. Nejadnik, H., et al., *Autologous bone marrow-derived mesenchymal stem cells versus autologous chondrocyte implantation: an observational cohort study.* Am J Sports Med, 2010. **38**(6): p. 1110-6.

173. Haleem, A.M., et al., *The Clinical Use of Human Culture–Expanded Autologous Bone Marrow Mesenchymal Stem Cells Transplanted on Platelet-Rich Fibrin Glue in the Treatment of Articular Cartilage Defects: A Pilot Study and Preliminary Results.* Cartilage, 2010. **1**(4): p. 253-261.

174. Kasemkijwattana, C., et al., *Autologous bone marrow mesenchymal stem cells implantation for cartilage defects: two cases report.* J Med Assoc Thai, 2011. **94**(3): p. 395-400.

175. Davatchi, F., et al., *Mesenchymal stem cell therapy for knee osteoarthritis. Preliminary report of four patients.* Int J Rheum Dis, 2011. **14**(2): p. 211-5.

176. Kuroda, R., et al., *Treatment of a full-thickness articular cartilage defect in the femoral condyle of an athlete with autologous bone-marrow stromal cells.* Osteoarthritis Cartilage, 2007. **15**(2): p. 226-31.

177. Cheng, L.C., M. Tavazoie, and F. Doetsch, *Stem cells: from epigenetics to microRNAs.* Neuron, 2005. **46**(3): p. 363-7.

178. Barter, M.J., C. Bui, and D.A. Young, *Epigenetic mechanisms in cartilage and osteoarthritis: DNA methylation, histone modifications and microRNAs.* Osteoarthritis Cartilage, 2012. **20**(5): p. 339-49.

179. Yu, Z., et al., *miRNAs regulate stem cell self-renewal and differentiation.* Front Genet, 2012. **3**: p. 191.

180. Jaskiewicz, L. and W. Filipowicz, *Role of Dicer in Posttranscriptional RNA Silencing*, in *RNA Interference*, P. Paddison and P. Vogt, Editors. 2008, Springer Berlin Heidelberg. p. 77-97.

181. Pasquinelli, A.E., S. Hunter, and J. Bracht, *MicroRNAs: a developing story.* Curr Opin Genet Dev, 2005. **15**(2): p. 200-5.

182. Lee, R.C., R.L. Feinbaum, and V. Ambros, *The C. elegans heterochronic gene lin-4 encodes small RNAs with antisense complementarity to lin-14.* Cell, 1993. **75**(5): p. 843-54.

183. Ambros, V. and H.R. Horvitz, *The lin-14 locus of Caenorhabditis elegans controls the time of expression of specific postembryonic developmental events.* Genes Dev, 1987. **1**(4): p. 398-414.

184. Lagos-Quintana, M., et al., *Identification of novel genes coding for small expressed RNAs.* Science, 2001. **294**(5543): p. 853-8.

185. Calin, G.A., et al., *Frequent deletions and down-regulation of micro- RNA genes miR15 and miR16 at 13q14 in chronic lymphocytic leukemia.* Proceedings of the National Academy of Sciences of the United States of America, 2002. **99**(24): p. 15524-15529.

186. Berezikov, E., *Evolution of microRNA diversity and regulation in animals.* Nat Rev Genet, 2011. **12**(12): p. 846-60.

187. Brodersen, P. and O. Voinnet, *Revisiting the principles of microRNA target recognition and mode of action.* Nat Rev Mol Cell Biol, 2009. **10**(2): p. 141-8.

188. Yu, C., W.P. Chen, and X.H. Wang, *MicroRNA in osteoarthritis.* J Int Med Res, 2011. **39**(1): p. 1-9.

189. Iliopoulos, D., et al., *Integrative MicroRNA and Proteomic Approaches Identify Novel Osteoarthritis Genes and Their Collaborative Metabolic and Inflammatory Networks.* PLoS ONE, 2008. **3**(11): p. e3740.

190. Díaz-Prado, S., et al., *Characterization of microRNA expression profiles in normal and osteoarthritic human chondrocytes.* BMC Musculoskeletal Disorders, 2012. **13**(1): p. 1-14.

191. Miyaki, S., et al., *MicroRNA-140 is expressed in differentiated human articular chondrocytes and modulates interleukin-1 responses.* Arthritis & Rheumatism, 2009. **60**(9): p. 2723-2730.

192. Tardif, G., et al., *Regulation of the IGFBP-5 and MMP-13 genes by the microRNAs miR-140 and miR-27a in human osteoarthritic chondrocytes.* BMC Musculoskeletal Disorders, 2009. **10**(1): p. 148.

193. Abbaszade, I., et al., *Cloning and characterization of ADAMTS11, an aggrecanase from the ADAMTS family.* J Biol Chem, 1999. **274**(33): p. 23443-50.

194. Glasson, S.S., et al., *Deletion of active ADAMTS5 prevents cartilage degradation in a murine model of osteoarthritis.* Nature, 2005. **434**(7033): p. 644-8.

195. Miyaki, S., et al., *MicroRNA-140 plays dual roles in both cartilage development and homeostasis.* Genes Dev, 2010. **24**(11): p. 1173-85.

196. Velu, V.K., R. Ramesh, and A.R. Srinivasan, *Circulating MicroRNAs as Biomarkers in Health and Disease.* J Clin Diagn Res, 2012. **6**(10): p. 1791-5.

197. Miyaki, S., et al., *MicroRNA-140 is expressed in differentiated human articular chondrocytes and modulates interleukin-1 responses.* Arthritis Rheum, 2009. **60**(9): p. 2723-30.

198. Ukai, T., et al., *MicroRNA-199a-3p, microRNA-193b, and microRNA-320c are correlated to aging and regulate human cartilage metabolism.* Journal of Orthopaedic Research, 2012. **30**(12): p. 1915-1922.

199. Matsukawa, T., et al., *MicroRNA-125b regulates the expression of aggrecanase-1 (ADAMTS-4) in human osteoarthritic chondrocytes.* Arthritis Research & Therapy, 2013. **15**(1): p. R28-R28.

200. Naito, S., et al., *Expression of ADAMTS4 (aggrecanase-1) in human osteoarthritic cartilage.* Pathology International, 2007. **57**(11): p. 703-711.

201. Akhtar, N., et al., *MicroRNA-27b regulates the expression of matrix metalloproteinase 13 in human osteoarthritis chondrocytes.* Arthritis Rheum, 2010. **62**.

202. Wang, G., et al., *MicroRNA-411 inhibited matrix metalloproteinase 13 expression in human chondrocytes.* Am J Transl Res, 2015. **7**(10): p. 2000-6.

203. Li, Z., et al., *Overexpression of microRNA210 promotes chondrocyte proliferation and extracellular matrix deposition by targeting HIF3alpha in osteoarthritis.* Mol Med Rep, 2016.

204. Markway, B.D., et al., *Hypoxia-inducible factor 3-alpha expression is associated with the stable chondrocyte phenotype.* Journal of Orthopaedic Research, 2015. **33**(11): p. 1561-1570.

205. Ji, Q., et al., *miR-105/Runx2 axis mediates FGF2-induced ADAMTS expression in osteoarthritis cartilage.* J Mol Med (Berl), 2016.
206. Takeda, S., et al., *Continuous expression of Cbfa1 in nonhypertrophic chondrocytes uncovers its ability to induce hypertrophic chondrocyte differentiation and partially rescues Cbfa1-deficient mice.* Genes Dev, 2001. **15**(4): p. 467-81.
207. Wang, X., et al., *Regulation of MMP-13 expression by RUNX2 and FGF2 in osteoarthritic cartilage.* Osteoarthritis Cartilage, 2004. **12**(12): p. 963-73.
208. Higashikawa, A., et al., *Identification of the core element responsive to runt-related transcription factor 2 in the promoter of human type X collagen gene.* Arthritis Rheum, 2009. **60**(1): p. 166-78.
209. Song, J., et al., *MicroRNA-222 regulates MMP-13 via targeting HDAC-4 during osteoarthritis pathogenesis.* BBA Clinical, 2015. **3**: p. 79-89.
210. Young, D.A., et al., *Histone deacetylase inhibitors modulate metalloproteinase gene expression in chondrocytes and block cartilage resorption.* Arthritis Research & Therapy, 2005. **7**(3): p. R503-R512.
211. Furumatsu, T., et al., *Sox9 and p300 cooperatively regulate chromatin-mediated transcription.* J Biol Chem, 2005. **280**(42): p. 35203-8.
212. Steck, E., et al., *Regulation of H19 and its encoded microRNA-675 in osteoarthritis and under anabolic and catabolic in vitro conditions.* J Mol Med (Berl), 2012. **90**(10): p. 1185-95.
213. Song, J., et al., *MicroRNA-181b regulates articular chondrocytes differentiation and cartilage integrity.* Biochemical and Biophysical Research Communications, 2013. **431**(2): p. 210-214.
214. Swingler, T.E., et al., *The expression and function of microRNAs in chondrogenesis and osteoarthritis.* Arthritis Rheum, 2012. **64**(6): p. 1909-19.
215. Funaba, M., K. Ogawa, and M. Abe, *Expression and localization of activin receptors during endochondral bone development.* Eur J Endocrinol, 2001. **144**(1): p. 63-71.
216. Macías-Silva, M., et al., *MADR2 Is a Substrate of the TGFβ Receptor and Its Phosphorylation Is Required for Nuclear Accumulation and Signaling.* Cell, 1996. **87**(7): p. 1215-1224.
217. Nakayama, N., et al., *A novel chordin-like protein inhibitor for bone morphogenetic proteins expressed preferentially in mesenchymal cell lineages.* Dev Biol, 2001. **232**(2): p. 372-87.
218. Taylor, S.E., et al., *Identification of human juvenile chondrocyte-specific factors that stimulate stem cell growth.* Tissue Eng Part A, 2016.
219. Xu, J., et al., *MiR-194 Regulates Chondrogenic Differentiation of Human Adipose-Derived Stem Cells by Targeting Sox5.* PLoS ONE, 2012. **7**(3): p. e31861.
220. Dai, L., et al., *Silencing of microRNA-101 prevents IL-1β-induced extracellular matrix degradation in chondrocytes.* Arthritis Research & Therapy, 2012. **14**(6): p. R268-R268.
221. Bell, D.M., et al., *SOX9 directly regulates the type-II collagen gene.* Nat Genet, 1997. **16**(2): p. 174-8.

222. Zhang, P., S.A. Jimenez, and D.G. Stokes, *Regulation of human COL9A1 gene expression. Activation of the proximal promoter region by SOX9.* J Biol Chem, 2003. **278**(1): p. 117-23.

223. Liu, Y., et al., *Identification of an enhancer sequence within the first intron required for cartilage-specific transcription of the alpha2(XI) collagen gene.* J Biol Chem, 2000. **275**(17): p. 12712-8.

224. Chang, T., et al., *MicroRNA-30a promotes extracellular matrix degradation in articular cartilage via downregulation of Sox9.* Cell Proliferation, 2016: p. n/a-n/a.

225. Iliopoulos, D., et al., *Integrative microRNA and proteomic approaches identify novel osteoarthritis genes and their collaborative metabolic and inflammatory networks.* PLoS ONE, 2008. **3**: p. e3740.

226. Cuzzocrea, S., et al., *The role of the peroxisome proliferator-activated receptor-alpha (PPAR-alpha) in the regulation of acute inflammation.* J Leukoc Biol, 2006. **79**(5): p. 999-1010.

227. Yeh, L.-C.C. and J.C. Lee, *Identification of an osteogenic protein-1 responsive element in the aggrecan promoter*. Biochemical and Biophysical Research Communications, 2004. **323**(1): p. 223-228.

228. Yamasaki, K., et al., *Expression of MicroRNA-146a in osteoarthritis cartilage.* Arthritis Rheum, 2009. **60**(4): p. 1035-41.

229. Li, J., et al., *miR-146a, an IL-1beta responsive miRNA, induces vascular endothelial growth factor and chondrocyte apoptosis by targeting Smad4.* Arthritis Res Ther, 2012. **14**(2): p. R75.

230. Jin, L., et al., *Role of miR-146a in human chondrocyte apoptosis in response to mechanical pressure injury in vitro.* Int J Mol Med, 2014. **34**(2): p. 451-63.

231. Cao, Z., W.J. Henzel, and X. Gao, *IRAK: a kinase associated with the interleukin-1 receptor.* Science, 1996. **271**(5252): p. 1128-31.

232. Cao, Z., et al., *TRAF6 is a signal transducer for interleukin-1*. Nature, 1996. **383**(6599): p. 443-6.

233. Zhou, S., et al., *Targeted deletion of Smad4 shows it is required for transforming growth factor β and activin signaling in colorectal cancer cells.* Proceedings of the National Academy of Sciences, 1998. **95**(5): p. 2412-2416.

234. Akhtar, N. and T.M. Haqqi, *MicroRNA-199a* regulates the expression of cyclooxygenase-2 in human chondrocytes.* Annals of the rheumatic diseases, 2012. **71**(6): p. 1073-1080.

235. Martel-Pelletier, J., J.-P. Pelletier, and H. Fahmi, *Cyclooxygenase-2 and prostaglandins in articular tissues.* Seminars in Arthritis and Rheumatism, 2003. **33**(3): p. 155-167.

236. Attur, M., et al., *Prostaglandin E2 exerts catabolic effects in osteoarthritis cartilage: evidence for signaling via the EP4 receptor.* J Immunol, 2008. **181**(7): p. 5082-8.

237. Claveau, D., et al., *Microsomal prostaglandin E synthase-1 is a major terminal synthase that is selectively up-regulated during cyclooxygenase-2-dependent prostaglandin E2 production in the rat adjuvant-induced arthritis model.* J Immunol, 2003. **170**(9): p. 4738-44.

238. Zhang, G., et al., *MiR-502-5p inhibits IL-1beta-induced chondrocyte injury by targeting TRAF2.* Cell Immunol, 2016. **302**: p. 50-7.
239. Saperstein, S., et al., *IL-1beta augments TNF-alpha-mediated inflammatory responses from lung epithelial cells.* J Interferon Cytokine Res, 2009. **29**(5): p. 273-84.
240. Pomerantz, J.L. and D. Baltimore, *NF-kappaB activation by a signaling complex containing TRAF2, TANK and TBK1, a novel IKK-related kinase.* The EMBO Journal, 1999. **18**(23): p. 6694-6704.
241. Rasheed, Z., et al., *MicroRNA-26a-5p regulates the expression of inducible nitric oxide synthase via activation of NF-κB pathway in human osteoarthritis chondrocytes.* Archives of Biochemistry and Biophysics, 2016. **594**: p. 61-67.
242. Aktan, F., *iNOS-mediated nitric oxide production and its regulation.* Life Sciences, 2004. **75**(6): p. 639-653.
243. Abramson, S.B., *Osteoarthritis and nitric oxide.* Osteoarthritis and Cartilage. **16**: p. S15-S20.
244. Park, S.J., E.J. Cheon, and H.A. Kim, *MicroRNA-558 regulates the expression of cyclooxygenase-2 and IL-1beta-induced catabolic effects in human articular chondrocytes.* Osteoarthritis Cartilage, 2013. **21**(7): p. 981-9.
245. Abouheif, M.M., et al., *Silencing microRNA-34a inhibits chondrocyte apoptosis in a rat osteoarthritis model in vitro.* Rheumatology (Oxford), 2010. **49**.
246. Le, L.T., et al., *The microRNA-29 family in cartilage homeostasis and osteoarthritis.* J Mol Med (Berl), 2015.
247. Li, L., et al., *Elevated expression of microRNA-30b in osteoarthritis and its role in ERG regulation of chondrocyte.* Biomed Pharmacother, 2015. **76**: p. 94-9.
248. Makki, M.S. and T.M. Haqqi, *miR-139 modulates MCPIP1/IL-6 expression and induces apoptosis in human OA chondrocytes.* Exp Mol Med, 2015. **47**: p. e189.
249. Makki, M.S., A. Haseeb, and T.M. Haqqi, *MCPIP1 regulates the expression of interleukin-6 in human osteoarthritis chondrocytes.* Osteoarthritis and Cartilage. **22**: p. S166.
250. Hydbring, P. and G. Badalian-Very, *Clinical applications of microRNAs.* F1000Research, 2013. **2**: p. 136.
251. Beg, M.S., et al., *Abstract CT327: Multicenter phase I study of MRX34, a first-in-class microRNA miR-34 mimic liposomal injection.* Cancer Research, 2014. **74**(19 Supplement): p. CT327-CT327.
252. Beg, M.S., et al., *Abstract C43: Safety, tolerability, and clinical activity of MRX34, the first-in-class liposomal miR-34 mimic, in patients with advanced solid tumors.* Molecular Cancer Therapeutics, 2015. **14**(12 Supplement 2): p. C43-C43.
253. Grosshans, H., et al., *The temporal patterning microRNA let-7 regulates several transcription factors at the larval to adult transition in C. elegans.* Dev Cell, 2005. **8**(3): p. 321-30.
254. Bernstein, E., et al., *Dicer is essential for mouse development.* Nat Genet, 2003. **35**(3): p. 215-7.

255. Wienholds, E., et al., *The microRNA-producing enzyme Dicer1 is essential for zebrafish development.* Nat Genet, 2003. **35**(3): p. 217-8.

256. Liu, J., et al., *Argonaute2 is the catalytic engine of mammalian RNAi.* Science, 2004. **305**(5689): p. 1437-41.

257. Yang, B., et al., *MicroRNA-145 Regulates Chondrogenic Differentiation of Mesenchymal Stem Cells by Targeting Sox9.* PLoS ONE, 2011. **6**(7): p. e21679.

258. Buechli, M.E., J. LaMarre, and T.G. Koch, *MicroRNA-140 expression during chondrogenic differentiation of equine cord blood-derived mesenchymal stromal cells.* Stem cells and development, 2012. **22**(8): p. 1288-1296.

259. Karlsen, T.A., et al., *microRNA-140 targets RALA and regulates chondrogenic differentiation of human mesenchymal stem cells by translational enhancement of SOX9 and ACAN.* Stem Cells Dev, 2014. **23**(3): p. 290-304.

260. Cristino, S., et al., *Expression of CXC chemokines and their receptors is modulated during chondrogenic differentiation of human mesenchymal stem cells grown in three-dimensional scaffold: evidence in native cartilage.* Tissue Eng Part A, 2008. **14**(1): p. 97-105.

261. Murata, K., et al., *Stromal Cell-Derived Factor 1 Regulates the Actin Organization of Chondrocytes and Chondrocyte Hypertrophy.* PLoS ONE, 2012. **7**(5): p. e37163.

262. Tortorella, M.D., et al., *The role of ADAM-TS4 (aggrecanase-1) and ADAM-TS5 (aggrecanase-2) in a model of cartilage degradation.* Osteoarthritis Cartilage, 2001. **9**(6): p. 539-52.

263. Boeuf, S., et al., *Regulation of aggrecanases from the ADAMTS family and aggrecan neoepitope formation during in vitro chondrogenesis of human mesenchymal stem cells.* Eur Cell Mater, 2012. **23**: p. 320-32.

264. Pais, H., et al., *Analyzing mRNA expression identifies Smad3 as a microRNA-140 target regulated only at protein level.* RNA, 2010. **16**(3): p. 489-94.

265. Sugihara, K., et al., *The exocyst complex binds the small GTPase RalA to mediate filopodia formation.* Nat Cell Biol, 2002. **4**(1): p. 73-8.

266. Matsuzaki, T., et al., *Regulation of endocytosis of activin type II receptors by a novel PDZ protein through Ral/Ral-binding protein 1-dependent pathway.* J Biol Chem, 2002. **277**(21): p. 19008-18.

267. Wang, L., G. Li, and S. Sugita, *RalA-exocyst interaction mediates GTP-dependent exocytosis.* J Biol Chem, 2004. **279**(19): p. 19875-81.

268. Lin, E., et al., *miR-199a*, a bone morphogenic protein 2 responsive microRNA, regulates chondrogenesis via direct targeting to Smad1*. J Biol Chem, 2009.

269. Retting, K.N., et al., *BMP canonical Smad signaling through Smad1 and Smad5 is required for endochondral bone formation.* Development, 2009. **136**(7): p. 1093-1104.

270. Zhong, N., et al., *MicroRNA-337 is associated with chondrogenesis through regulating TGFBR2 expression.* Osteoarthritis and Cartilage. **20**(6): p. 593-602.

271. Spagnoli, A., et al., *TGF-beta signaling is essential for joint morphogenesis.* J Cell Biol, 2007. **177**(6): p. 1105-17.
272. Lee, S., et al., *microRNA-495 inhibits chondrogenic differentiation in human mesenchymal stem cells by targeting Sox9.* Stem Cells Dev, 2014. **23**(15): p. 1798-808.
273. Guérit, D., et al., *Inhibitory effect of miR-29A on the chondrogenic differentiation of mesenchymal stem cells.* Osteoarthritis and Cartilage, 2012. **20**: p. S52.
274. Guerit, D., et al., *FOXO3A regulation by miRNA-29a Controls chondrogenic differentiation of mesenchymal stem cells and cartilage formation.* Stem Cells Dev, 2014. **23**(11): p. 1195-205.
275. Guérit, D., et al., *Sox9-Regulated miRNA-574-3p Inhibits Chondrogenic Differentiation of Mesenchymal Stem Cells.* PLoS ONE, 2013. **8**(4): p. e62582.
276. Glass, C.K. and M.G. Rosenfeld, *The coregulator exchange in transcriptional functions of nuclear receptors.* Genes Dev, 2000. **14**(2): p. 121-41.
277. Salbert, G., et al., *Retinoic acid receptors and retinoid X receptor-alpha down-regulate the transforming growth factor-beta 1 promoter by antagonizing AP-1 activity.* Mol Endocrinol, 1993. **7**(10): p. 1347-56.
278. Tanaka, T. and L.M. De Luca, *Therapeutic potential of "rexinoids" in cancer prevention and treatment.* Cancer Res, 2009. **69**(12): p. 4945-7.
279. Lin, X., et al., *MiR-335-5p promotes chondrogenesis in mouse mesenchymal stem cells and is regulated through two positive feedback loops.* J Bone Miner Res, 2014. **29**(7): p. 1575-85.
280. Woods, A., G. Wang, and F. Beier, *RhoA/ROCK signaling regulates Sox9 expression and actin organization during chondrogenesis.* J Biol Chem, 2005. **280**(12): p. 11626-34.
281. Habas, R., Y. Kato, and X. He, *Wnt/Frizzled Activation of Rho Regulates Vertebrate Gastrulation and Requires a Novel Formin Homology Protein Daam1*. Cell. **107**(7): p. 843-854.
282. Tian, Y., et al., *MicroRNA-30a promotes chondrogenic differentiation of mesenchymal stem cells through inhibiting Delta-like 4 expression.* Life Sci, 2016. **148**: p. 220-8.
283. Radtke, F., et al., *Notch regulation of lymphocyte development and function.* Nat Immunol, 2004. **5**(3): p. 247-53.
284. Mead, T.J. and K.E. Yutzey, *Notch pathway regulation of chondrocyte differentiation and proliferation during appendicular and axial skeleton development.* Proceedings of the National Academy of Sciences, 2009. **106**(34): p. 14420-14425.
285. Tian, Y., et al., *Notch inhibits chondrogenic differentiation of mesenchymal progenitor cells by targeting Twist1*. Molecular and cellular endocrinology, 2015. **403**: p. 30-38.
286. Zhang, Z., et al., *MiR-455-3p regulates early chondrogenic differentiation via inhibiting Runx2.* FEBS Letters, 2015. **589**(23): p. 3671-3678.
287. Ueta, C., et al., *Skeletal Malformations Caused by Overexpression of Cbfa1 or Its Dominant Negative Form in Chondrocytes.* The Journal of Cell Biology, 2001. **153**(1): p. 87-100.

288. Dudek, K.A., et al., *Type II collagen expression is regulated by tissue-specific miR-675 in human articular chondrocytes.* J Biol Chem, 2010. **285**(32): p. 24381-7.
289. Zhang, Z., et al., *Expression of microRNAs during chondrogenesis of human adipose-derived stem cells.* Osteoarthritis Cartilage, 2012. **20**(12): p. 1638-46.
290. Hou, C., et al., *MiR-193b regulates early chondrogenesis by inhibiting the TGF-beta2 signaling pathway.* FEBS Lett, 2015. **589**(9): p. 1040-7.
291. Hinck, A.P., *Structural studies of the TGF-βs and their receptors – insights into evolution of the TGF-β superfamily.* FEBS Letters, 2012. **586**(14): p. 1860-1870.
292. Seo, H.S. and R. Serra, *Deletion of Tgfbr2 in Prx1-cre expressing mesenchyme results in defects in development of the long bones and joints.* Dev Biol, 2007. **310**(2): p. 304-16.
293. Kim, D., J. Song, and E.-J. Jin, *MicroRNA-221 Regulates Chondrogenic Differentiation through Promoting Proteosomal Degradation of Slug by Targeting Mdm2.* The Journal of Biological Chemistry, 2010. **285**(35): p. 26900-26907.
294. Wang, S.P., et al., *p53 controls cancer cell invasion by inducing the MDM2-mediated degradation of Slug.* Nat Cell Biol, 2009. **11**(6): p. 694-704.
295. Lolli, A., et al., *Pro-chondrogenic effect of miR-221 and slug depletion in human MSCs.* Stem Cell Rev, 2014. **10**(6): p. 841-55.
296. Kim, D., et al., *MicroRNA-34a modulates cytoskeletal dynamics through regulating RhoA/Rac1 cross-talk in chondroblasts.* J Biol Chem, 2012. **287**(15): p. 12501-9.
297. Woods, A., et al., *Rac1 signaling stimulates N-cadherin expression, mesenchymal condensation, and chondrogenesis.* J Biol Chem, 2007. **282**(32): p. 23500-8.
298. Hu, S., et al., *Novel microRNA prosurvival cocktail for improving engraftment and function of cardiac progenitor cell transplantation.* Circulation, 2011. **124**(11 Suppl): p. S27-34.
299. Cui, L., et al., *A set of microRNAs mediate direct conversion of human umbilical cord lining-derived mesenchymal stem cells into hepatocytes.* Cell Death Dis, 2013. **4**: p. e918.
300. Chen, J.J. and S.H. Zhou, *Mesenchymal stem cells overexpressing MiR-126 enhance ischemic angiogenesis via the AKT/ERK-related pathway.* Cardiol J, 2011. **18**(6): p. 675-81.
301. Chen, L., et al., *MicroRNA-34a Inhibits Osteoblast Differentiation and In Vivo Bone Formation of Human Stromal Stem Cells.* STEM CELLS, 2014. **32**(4): p. 902-912.
302. Eskildsen, T., et al., *MicroRNA-138 regulates osteogenic differentiation of human stromal (mesenchymal) stem cells in vivo.* Proc Natl Acad Sci U S A, 2011. **108**(15): p. 6139-44.
303. Livak, K.J. and T.D. Schmittgen, *Analysis of relative gene expression data using Real-Time quantitative PCR and the 2-ΔΔCt method.* Methods, 2001. **25**.
304. Loeser, R.F., et al., *Osteoarthritis: a disease of the joint as an organ.* Arthritis Rheum, 2012. **64**(6): p. 1697-707.
305. Cui, S., et al., *Molecular mechanisms of osteoarthritis using gene microarrays.* Acta Histochemica, 2015. **117**(1): p. 62-68.

306. Le, L.T.T., T.E. Swingler, and I.M. Clark, *Review: The Role of MicroRNAs in Osteoarthritis and Chondrogenesis.* Arthritis & Rheumatism, 2013. **65**(8): p. 1963-1974.
307. Taganov, K., et al., *NF-kappaB-dependent induction of microRNA miR-146, an inhibitor targeted to signaling proteins of innate immune responses.* Proc Natl Acad Sci USA, 2006. **103**: p. 12481 - 6.
308. Wang, Z., *MicroRNAs and Cardiovascular Disease*. 2010: Bentham Science Publishers.
309. Li, J., et al., *MiR-429 is an independent prognostic factor in colorectal cancer and exerts its anti-apoptotic function by targeting SOX2.* Cancer Lett, 2012.
310. Nakasa, T., et al., *Expression of microRNA-146 in rheumatoid arthritis synovial tissue.* Arthritis Rheum, 2008. **58**: p. 1284 - 92.
311. Perry, M.M., et al., *Rapid changes in microRNA-146a expression negatively regulate the IL-1beta-induced inflammatory response in human lung alveolar epithelial cells.* J Immunol, 2008. **180**(8): p. 5689-98.
312. Stanczyk, J., et al., *Altered expression of MicroRNA in synovial fibroblasts and synovial tissue in rheumatoid arthritis.* Arthritis Rheum, 2008. **58**: p. 1001 - 1009.
313. Bhaumik, D., et al., *MicroRNAs miR-146a/b negatively modulate the senescence-associated inflammatory mediators IL-6 and IL-8.* Aging (Albany NY), 2009. **1**(4): p. 402-11.
314. Lukiw, W.J., Y. Zhao, and J.G. Cui, *An NF-kappaB-sensitive micro RNA-146a-mediated inflammatory circuit in Alzheimer disease and in stressed human brain cells.* J Biol Chem, 2008. **283**(46): p. 31315-22.
315. Pauley, K., et al., *Upregulated miR-146a expression in peripheral blood mononuclear cells from rheumatoid arthritis patients.* Arthritis Res Ther, 2008. **10**: p. R101.
316. Liu, Z., et al., *Up-regulated microRNA-146a negatively modulate Helicobacter pylori-induced inflammatory response in human gastric epithelial cells.* Microbes Infect, 2010. **12**(11): p. 854-63.
317. Iyer, A., et al., *MicroRNA-146a: A Key Regulator of Astrocyte-Mediated Inflammatory Response.* PLoS ONE, 2012. **7**(9): p. e44789.
318. Kutty, R.K., et al., *Differential regulation of microRNA-146a and microRNA-146b-5p in human retinal pigment epithelial cells by interleukin-1beta, tumor necrosis factor-alpha, and interferon-gamma.* Mol Vis, 2013. **19**: p. 737-50.
319. Shi, C., et al., *IL-6 and TNF-alpha induced obesity-related inflammatory response through transcriptional regulation of miR-146b.* J Interferon Cytokine Res, 2014. **34**(5): p. 342-8.
320. Meisgen, F., et al., *MiR-146a Negatively Regulates TLR2-Induced Inflammatory Responses in Keratinocytes.* J Invest Dermatol, 2014. **134**(7): p. 1931-1940.
321. Cheng, H.S., et al., *MicroRNA-146 represses endothelial activation by inhibiting pro-inflammatory pathways.* EMBO Mol Med, 2013. **5**(7): p. 949-66.

322. Park, H., et al., *MicroRNA-146a and microRNA-146b regulate human dendritic cell apoptosis and cytokine production by targeting TRAF6 and IRAK1 proteins.* J Biol Chem, 2015. **290**(5): p. 2831-41.

323. Weber, A., P. Wasiliew, and M. Kracht, *Interleukin-1 (IL-1) pathway.* Sci Signal, 2010. **3**(105): p. cm1.

324. Fernandes, J.C., J. Martel-Pelletier, and J.P. Pelletier, *The role of cytokines in osteoarthritis pathophysiology.* Biorheology, 2002. **39**(1-2): p. 237-46.

325. van de Loo, A.A. and W.B. van den Berg, *Effects of murine recombinant interleukin 1 on synovial joints in mice: measurement of patellar cartilage metabolism and joint inflammation.* Ann Rheum Dis, 1990. **49**(4): p. 238-45.

326. van Beuningen, H.M., et al., *Transforming growth factor-beta 1 stimulates articular chondrocyte proteoglycan synthesis and induces osteophyte formation in the murine knee joint.* Lab Invest, 1994. **71**(2): p. 279-90.

327. van Beuningen, H.M., et al., *Osteoarthritis-like changes in the murine knee joint resulting from intra-articular transforming growth factor-beta injections.* Osteoarthritis Cartilage, 2000. **8**(1): p. 25-33.

328. Thompson, C.C., P.D. Clegg, and S.D. Carter, *Differential regulation of gelatinases by transforming growth factor beta-1 in normal equine chondrocytes.* Osteoarthritis Cartilage, 2001. **9**(4): p. 325-31.

329. van Beuningen, H.M., et al., *Protection from interleukin 1 induced destruction of articular cartilage by transforming growth factor beta: studies in anatomically intact cartilage in vitro and in vivo.* Ann Rheum Dis, 1993. **52**(3): p. 185-91.

330. Chandrasekhar, S. and A.K. Harvey, *Transforming growth factor-beta is a potent inhibitor of IL-1 induced protease activity and cartilage proteoglycan degradation.* Biochem Biophys Res Commun, 1988. **157**(3): p. 1352-9.

331. Redini, F., et al., *Transforming growth factor beta exerts opposite effects from interleukin-1 beta on cultured rabbit articular chondrocytes through reduction of interleukin-1 receptor expression.* Arthritis Rheum, 1993. **36**(1): p. 44-50.

332. Smith, P., et al., *Genetic enhancement of matrix synthesis by articular chondrocytes: comparison of different growth factor genes in the presence and absence of interleukin-1.* Arthritis Rheum, 2000. **43**(5): p. 1156-64.

333. Wu, H. and J.R. Arron, *TRAF6, a molecular bridge spanning adaptive immunity, innate immunity and osteoimmunology.* Bioessays, 2003. **25**(11): p. 1096-105.

334. Curtale, G., et al., *Negative regulation of Toll-like receptor 4 signaling by IL-10-dependent microRNA-146b.* Proc Natl Acad Sci U S A, 2013. **110**(28): p. 11499-504.

335. Chassin, C., et al., *miR-146a Mediates Protective Innate Immune Tolerance in the Neonate Intestine.* Cell Host & Microbe. **8**(4): p. 358-368.

336. Cheng, G. and D. Baltimore, *TANK, a co-inducer with TRAF2 of TNF- and CD 40L-mediated NF-kappaB activation.* Genes Dev, 1996. **10**(8): p. 963-73.

337. Saba, R., et al., *MicroRNA 146a (miR-146a) is over-expressed during prion disease and modulates the innate immune response and the microglial activation state.* PLoS One, 2012. **7**(2): p. e30832.

338. Medzhitov, R., P. Preston-Hurlburt, and C.A. Janeway, Jr., *A human homologue of the Drosophila Toll protein signals activation of adaptive immunity.* Nature, 1997. **388**(6640): p. 394-7.

339. Fitzgerald, K.A., et al., *Mal (MyD88-adapter-like) is required for Toll-like receptor-4 signal transduction.* Nature, 2001. **413**(6851): p. 78-83.

340. Starczynowski, D.T., et al., *Identification of miR-145 and miR-146a as mediators of the 5q- syndrome phenotype.* Nat Med, 2010. **16**(1): p. 49-58.

341. Marques, R.E., et al., *Targeting CCL5 in inflammation.* Expert Opin Ther Targets, 2013. **17**(12): p. 1439-60.

342. Barnes, B.J., P.A. Moore, and P.M. Pitha, *Virus-specific activation of a novel interferon regulatory factor, IRF-5, results in the induction of distinct interferon alpha genes.* J Biol Chem, 2001. **276**(26): p. 23382-90.

343. Tang, Y., et al., *MicroRNA-146A contributes to abnormal activation of the type I interferon pathway in human lupus by targeting the key signaling proteins.* Arthritis Rheum, 2009. **60**(4): p. 1065-75.

344. Ryu, S.W. and E. Kim, *Apoptosis induced by human Fas-associated factor 1, hFAF1, requires its ubiquitin homologous domain, but not the Fas-binding domain.* Biochem Biophys Res Commun, 2001. **286**(5): p. 1027-32.

345. Li, J., et al., *Altered microRNA expression profile with miR-146a upregulation in CD4(+)T cells from patients with rheumatoid arthritis.* Arthritis Research & Therapy, 2010. **12**(3): p. R81-R81.

346. Greenfield, E.A., K.A. Nguyen, and V.K. Kuchroo, *CD28/B7 costimulation: a review.* Crit Rev Immunol, 1998. **18**(5): p. 389-418.

347. Gauna, A.E., et al., *Dysregulated co-stimulatory molecule expression in a Sjogren's syndrome mouse model with potential implications by microRNA-146a.* Mol Immunol, 2015. **68**(2 Pt C): p. 606-16.

348. Ricciotti, E. and G.A. FitzGerald, *Prostaglandins and Inflammation.* Arteriosclerosis, thrombosis, and vascular biology, 2011. **31**(5): p. 986-1000.

349. Li, G., et al., *Modulation of inflammatory markers by miR-146a during replicative senescence in trabecular meshwork cells.* Invest Ophthalmol Vis Sci, 2010. **51**(6): p. 2976-85.

350. Sato, T., et al., *Reduced miR-146a increases prostaglandin E(2)in chronic obstructive pulmonary disease fibroblasts.* Am J Respir Crit Care Med, 2010. **182**(8): p. 1020-9.

351. Comer, B.S., et al., *MicroRNA-146a and microRNA-146b expression and anti-inflammatory function in human airway smooth muscle.* American Journal of Physiology - Lung Cellular and Molecular Physiology, 2014. **307**(9): p. L727-L734.

352. Wang, L., et al., *Card10 is a novel caspase recruitment domain/membrane-associated guanylate kinase family member that interacts with BCL10 and activates NF-kappa B.* J Biol Chem, 2001. **276**(24): p. 21405-9.

353. Crone, S.G., et al., *microRNA-146a inhibits G protein-coupled receptor-mediated activation of NF-kappaB by targeting CARD10 and COPS8 in gastric cancer.* Mol Cancer, 2012. **11**: p. 71.

354. Garbacki, N., et al., *MicroRNAs Profiling in Murine Models of Acute and Chronic Asthma: A Relationship with mRNAs Targets.* PLoS ONE, 2011. **6**(1): p. e16509.

355. Li, S., et al., *IRAK-4: A novel member of the IRAK family with the properties of an IRAK-kinase.* Proceedings of the National Academy of Sciences, 2002. **99**(8): p. 5567-5572.

356. Kanamori, M., et al., *T2BP, a novel TRAF2 binding protein, can activate NF-kappaB and AP-1 without TNF stimulation.* Biochem Biophys Res Commun, 2002. **290**(3): p. 1108-13.

357. Takatsuna, H., et al., *Identification of TIFA as an adapter protein that links tumor necrosis factor receptor-associated factor 6 (TRAF6) to interleukin-1 (IL-1) receptor-associated kinase-1 (IRAK-1) in IL-1 receptor signaling.* J Biol Chem, 2003. **278**(14): p. 12144-50.

358. Ea, C.K., et al., *TIFA activates IkappaB kinase (IKK) by promoting oligomerization and ubiquitination of TRAF6.* Proc Natl Acad Sci U S A, 2004. **101**(43): p. 15318-23.

359. Ohto, U., H. Tanji, and T. Shimizu, *Structure and function of toll-like receptor 8.* Microbes and Infection, 2014. **16**(4): p. 273-282.

360. Novick, D., B. Cohen, and M. Rubinstein, *The human interferon α β receptor: Characterization and molecular cloning.* Cell. **77**(3): p. 391-400.

361. Kwa, M.Q., et al., *Interferon Regulatory Factor 6 Differentially Regulates Toll-like Receptor 2-dependent Chemokine Gene Expression in Epithelial Cells.* The Journal of Biological Chemistry, 2014. **289**(28): p. 19758-19768.

362. McIlwain, D.R., T. Berger, and T.W. Mak, *Caspase functions in cell death and disease.* Cold Spring Harb Perspect Biol, 2013. **5**(4): p. a008656.

363. Vasilevko, V., et al., *CD80 (B7-1) and CD86 (B7-2) are functionally equivalent in the initiation and maintenance of CD4+ T-cell proliferation after activation with suboptimal doses of PHA.* DNA Cell Biol, 2002. **21**(3): p. 137-49.

364. Ruefli-Brasse, A.A., D.M. French, and V.M. Dixit, *Regulation of NF-kappaB-dependent lymphocyte activation and development by paracaspase.* Science, 2003. **302**(5650): p. 1581-4.

365. Elgueta, R., et al., *Molecular mechanism and function of CD40/CD40L engagement in the immune system.* Immunol Rev, 2009. **229**(1): p. 152-72.

366. Ignatov, A., et al., *RANTES stimulates Ca2+ mobilization and inositol trisphosphate (IP3) formation in cells transfected with G protein-coupled receptor 75.* British Journal of Pharmacology, 2006. **149**(5): p. 490-497.

367. Muniz, V.S., P.F. Weller, and J.S. Neves, *Eosinophil crystalloid granules: structure, function, and beyond.* Journal of Leukocyte Biology, 2012. **92**(2): p. 281-288.

368. Martin, L.B., et al., *Eosinophils in allergy: role in disease, degranulation, and cytokines.* Int Arch Allergy Immunol, 1996. **109**(3): p. 207-15.

369. Bouchier-Hayes, L., et al., *CARDINAL, a novel caspase recruitment domain protein, is an inhibitor of multiple NF-kappa B activation pathways.* J Biol Chem, 2001. **276**(47): p. 44069-77.

370. Nelson, F., et al., *Evidence for altered synthesis of type II collagen in patients with osteoarthritis.* J Clin Invest, 1998. **102**(12): p. 2115-25.

371. Garofalo, S., et al., *Assembly of cartilage collagen fibrils is disrupted by overexpression of normal type II collagen in transgenic mice.* Proceedings of the National Academy of Sciences, 1993. **90**(9): p. 3825-3829.

372. Mitchell, P.G., et al., *Cloning, expression, and type II collagenolytic activity of matrix metalloproteinase-13 from human osteoarthritic cartilage.* The Journal of Clinical Investigation, 1996. **97**(3): p. 761-768.

373. Reboul, P., et al., *The new collagenase, collagenase-3, is expressed and synthesized by human chondrocytes but not by synoviocytes. A role in osteoarthritis.* The Journal of Clinical Investigation, 1996. **97**(9): p. 2011-2019.

374. Singh, A., et al., *Collagenase-3 (MMP-13) deficiency protects C57BL/6 mice from antibody-induced arthritis.* Arthritis Research & Therapy, 2013. **15**(6): p. R222.

375. Fanjul-Fernández, M., et al., *Matrix metalloproteinases: Evolution, gene regulation and functional analysis in mouse models.* Biochimica et Biophysica Acta (BBA) - Molecular Cell Research, 2010. **1803**(1): p. 3-19.

376. Stove, J., et al., *Interleukin-1beta induces different gene expression of stromelysin, aggrecan and tumor-necrosis-factor-stimulated gene 6 in human osteoarthritic chondrocytes in vitro.* Pathobiology, 2000. **68**(3): p. 144-9.

377. Tardif, G., et al., *NFAT3 and TGF-beta/SMAD3 regulate the expression of miR-140 in osteoarthritis.* Arthritis Res Ther, 2013. **15**(6): p. R197.

378. Li, X., et al., *MicroRNA-146a is linked to pain-related pathophysiology of osteoarthritis.* Gene, 2011. **480**(1-2): p. 34-41.

379. Rydziel, S., S. Varghese, and E. Canalis, *Transforming growth factor beta1 inhibits collagenase 3 expression by transcriptional and post-transcriptional mechanisms in osteoblast cultures.* J Cell Physiol, 1997. **170**(2): p. 145-52.

380. Chen, C.G., et al., *Chondrocyte-intrinsic Smad3 represses Runx2-inducible matrix metalloproteinase 13 expression to maintain articular cartilage and prevent osteoarthritis.* Arthritis Rheum, 2012. **64**(10): p. 3278-89.

381. Yang, B., et al., *Effect of microRNA-145 on IL-1beta-induced cartilage degradation in human chondrocytes.* FEBS Lett, 2014. **588**(14): p. 2344-52.

382. Martinez-Sanchez, A., K.A. Dudek, and C.L. Murphy, *Regulation of human chondrocyte function through direct inhibition of cartilage master regulator SOX9 by microRNA-145 (miRNA-145).* J Biol Chem, 2012. **287**(2): p. 916-24.

383. Long, X. and J.M. Miano, *Transforming growth factor-beta1 (TGF-beta1) utilizes distinct pathways for the transcriptional activation of microRNA 143/145 in human coronary artery smooth muscle cells.* J Biol Chem, 2011. **286**(34): p. 30119-29.

384. Matagrano, L.B., J.A. Magida, and D.W. McGee, *Transforming growth factor-beta1 enhances the secretion of monocyte chemoattractant protein-1 by the IEC-18 intestinal epithelial cell line.* In Vitro Cell Dev Biol Anim, 2003. **39**(3-4): p. 183-6.

385. Yoshimura, H., et al., *Transforming growth factor-beta stimulates IL-1beta-induced monocyte chemoattractant protein-1 expression in human synovial cells via the ERK/AP-1 pathway.* Inflamm Res, 2006. **55**(12): p. 543-9.

386. Rebane, A., et al., *MicroRNA-146a alleviates chronic skin inflammation in atopic dermatitis through suppression of innate immune responses in keratinocytes.* J Allergy Clin Immunol, 2014. **134**(4): p. 836-847 e11.

387. Kuppner, M.C., S. McKillop-Smith, and J.V. Forrester, *TGF-beta and IL-1 beta act in synergy to enhance IL-6 and IL-8 mRNA levels and IL-6 production by human retinal pigment epithelial cells.* Immunology, 1995. **84**(2): p. 265-71.

388. Mirmalek-Sani, S.H., et al., *Characterization and multipotentiality of human fetal femur-derived cells: implications for skeletal tissue regeneration.* Stem Cells, 2006. **24**(4): p. 1042-53.

389. Guillot, P.V., et al., *Human first-trimester fetal MSC express pluripotency markers and grow faster and have longer telomeres than adult MSC.* Stem Cells, 2007. **25**(3): p. 646-54.

390. Gotherstrom, C., et al., *Difference in gene expression between human fetal liver and adult bone marrow mesenchymal stem cells.* Haematologica, 2005. **90**(8): p. 1017-26.

391. Kim, D., et al., *MicroRNA-34a regulates migration of chondroblast and IL-1β-induced degeneration of chondrocytes by targeting EphA5.* Biochemical and Biophysical Research Communications, 2011. **415**(4): p. 551-557.

392. Cheung, K.S.C., et al., *MicroRNA-146a Regulates Human Foetal Femur Derived Skeletal Stem Cell Differentiation by Down-Regulating SMAD2 and SMAD3.* PLoS ONE, 2014. **9**(6): p. e98063.

393. Imoto, I., et al., *Amplification and Overexpression of TGIF2, a Novel Homeobox Gene of the TALE Superclass, in Ovarian Cancer Cell Lines.* Biochemical and Biophysical Research Communications, 2000. **276**(1): p. 264-270.

394. Melhuish, T.A., C.M. Gallo, and D. Wotton, *TGIF2 interacts with histone deacetylase 1 and represses transcription.* J Biol Chem, 2001. **276**(34): p. 32109-14.

395. Glenisson, W., V. Castronovo, and D. Waltregny, *Histone deacetylase 4 is required for TGFβ1-induced myofibroblastic differentiation.* Biochimica et Biophysica Acta (BBA) - Molecular Cell Research, 2007. **1773**(10): p. 1572-1582.

396. Krzeszinski, J.Y., et al., *miR-34a blocks osteoporosis and bone metastasis by inhibiting osteoclastogenesis and Tgif2.* Nature, 2014. **advance online publication**.

397. Hu, Y., et al., *MicroRNA-34a inhibits tumor invasion and metastasis in gastric cancer by targeting Tgif2.* International Journal of Clinical and Experimental Pathology, 2015. **8**(8): p. 8921-8928.

398. Gothard, D., et al., *Regionally-derived cell populations and skeletal stem cells from human foetal femora exhibit specific osteochondral and multi-lineage differentiation capacity in vitro and ex vivo.* Stem Cell Research & Therapy, 2015. **6**: p. 251.

399. Tuddenham, L., et al., *The cartilage specific microRNA-140 targets histone deacetylase 4 in mouse cells.* FEBS Lett, 2006. **580**(17): p. 4214-7.

400. Nicolas, F.E., et al., *Experimental identification of microRNA-140 targets by silencing and overexpressing miR-140.* RNA, 2008. **14**(12): p. 2513-20.

401. Nicolas, F.E., et al., *mRNA expression profiling reveals conserved and non-conserved miR-140 targets.* RNA Biol, 2011. **8**(4): p. 607-15.

402. Yang, J., et al., *MiR-140 is co-expressed with Wwp2-C transcript and activated by Sox9 to target Sp1 in maintaining the chondrocyte proliferation.* FEBS Lett, 2011. **585**(19): p. 2992-7.

403. Nakamura, Y., et al., *Chondrocyte-specific microRNA-140 regulates endochondral bone development and targets Dnpep to modulate bone morphogenetic protein signaling.* Mol Cell Biol, 2011. **31**(14): p. 3019-28.

404. Legendre, M., et al., *Differential repression of alternative transcripts: a screen for miRNA targets.* PLoS Comput Biol, 2006. **2**(5): p. e43.

405. Hon, L.S. and Z. Zhang, *The roles of binding site arrangement and combinatorial targeting in microRNA repression of gene expression.* Genome Biol, 2007. **8**(8): p. R166.

406. Mayorga, M.E. and M.S. Penn, *miR-145 is differentially regulated by TGF-β(1) and ischaemia and targets Disabled-2 expression and wnt/β-catenin activity.* Journal of Cellular and Molecular Medicine, 2012. **16**(5): p. 1106-1113.

407. Davis-Dusenbery, B.N., et al., *down-regulation of Kruppel-like factor-4 (KLF4) by microRNA-143/145 is critical for modulation of vascular smooth muscle cell phenotype by transforming growth factor-beta and bone morphogenetic protein 4.* J Biol Chem, 2011. **286**(32): p. 28097-110.

408. Yang, S., et al., *miR-145 regulates myofibroblast differentiation and lung fibrosis.* The FASEB Journal, 2013. **27**(6): p. 2382-2391.

409. Zhou, Y., et al., *Secreted fibroblast-derived miR-34a induces tubular cell apoptosis in fibrotic kidney.* J Cell Sci, 2014. **127**(Pt 20): p. 4494-506.

410. Kim, D., J. Song, and E.J. Jin, *MicroRNA-221 regulates chondrogenic differentiation through promoting proteosomal degradation of slug by targeting Mdm2.* J Biol Chem, 2010. **285**(35): p. 26900-7.

411. Nakajima, M., et al., *p21Cip-1/SDI-1/WAF-1 expression via the mitogen-activated protein kinase signaling pathway in insulin-induced chondrogenic differentiation of ATDC5 cells.* Biochemical and Biophysical Research Communications, 2004. **320**(4): p. 1069-1075.

412. Tuli, R., et al., *Transforming growth factor-beta-mediated chondrogenesis of human mesenchymal progenitor cells involves N-cadherin and mitogen-activated protein kinase and Wnt signaling cross-talk.* J Biol Chem, 2003. **278**(42): p. 41227-36.

413. Caplan, A.I., *Adult mesenchymal stem cells for tissue engineering versus regenerative medicine.* J Cell Physiol, 2007. **213**(2): p. 341-7.

414. Le Blanc, K., et al., *HLA expression and immunologic properties of differentiated and undifferentiated mesenchymal stem cells.* Exp Hematol, 2003. **31**(10): p. 890-6.

415. Klyushnenkova, E., et al., *T cell responses to allogeneic human mesenchymal stem cells: immunogenicity, tolerance, and suppression.* J Biomed Sci, 2005. **12**(1): p. 47-57.

416. Tse, W.T., et al., *Suppression of allogeneic T-cell proliferation by human marrow stromal cells: implications in transplantation.* Transplantation, 2003. **75**(3): p. 389-97.

417. Brittberg, M., et al., *Treatment of deep cartilage defects in the knee with autologous chondrocyte transplantation.* N Engl J Med, 1994. **331**(14): p. 889-95.

418. Tare, R.S., et al., *Isolation, differentiation, and characterisation of skeletal stem cells from human bone marrow in vitro and in vivo.* Methods Mol Biol, 2012. **816**: p. 83-99.

419. Bauge, C. and K. Boumediene, *Use of Adult Stem Cells for Cartilage Tissue Engineering: Current Status and Future Developments.* Stem Cells Int, 2015. **2015**: p. 438026.

420. Wu, C., et al., *MicroRNAs play a role in chondrogenesis and osteoarthritis (review).* Int J Mol Med, 2014. **34**(1): p. 13-23.

421. McAlinden, A., et al., *Differentially Expressed MicroRNAs in Chondrocytes from Distinct Regions of Developing Human Cartilage.* PLoS ONE, 2013. **8**(9): p. e75012.

422. Zhang, J., et al., *Smad4 is required for the normal organization of the cartilage growth plate.* Developmental Biology, 2005. **284**(2): p. 311-322.

423. Ikeda, T., et al., *Distinct roles of Sox5, Sox6, and Sox9 in different stages of chondrogenic differentiation.* J Bone Miner Metab, 2005. **23**(5): p. 337-40.

424. Thomas, J.T., et al., *The human collagen X gene: complete primary sequence and re-expression in osteoarthritis.* Biochem Soc Trans, 1991. **19**(4): p. 804-8.

425. Mueller, M.B. and R.S. Tuan, *Functional Characterization of Hypertrophy in Chondrogenesis of Human Mesenchymal Stem Cells.* Arthritis and rheumatism, 2008. **58**(5): p. 1377-1388.

426. Eyre, D., *Articular cartilage and changes in Arthritis: Collagen of articular cartilage.* Arthritis Research, 2002. **4**(1): p. 30-35.

427. Walker, G.D., et al., *Expression of type-X collagen in osteoarthritis.* J Orthop Res, 1995. **13**(1): p. 4-12.

428. Benazet, J.D., et al., *Smad4 is required to induce digit ray primordia and to initiate the aggregation and differentiation of chondrogenic progenitors in mouse limb buds.* Development, 2012. **139**(22): p. 4250-60.

429. Geraldo, M.V., A.S. Yamashita, and E.T. Kimura, *MicroRNA miR-146b-5p regulates signal transduction of TGF-beta by repressing SMAD4 in thyroid cancer.* Oncogene, 2012. **31**(15): p. 1910-22.

430. Khanna, N., Y. Ge, and J. Chen, *MicroRNA-146b Promotes Myogenic Differentiation and Modulates Multiple Gene Targets in Muscle Cells.* PLoS One, 2014. **9**(6): p. e100657.

431. Maier, T., M. Güell, and L. Serrano, *Correlation of mRNA and protein in complex biological samples.* FEBS Letters, 2009. **583**(24): p. 3966-3973.

432. Vogel, C. and E.M. Marcotte, *Insights into the regulation of protein abundance from proteomic and transcriptomic analyses.* Nature reviews. Genetics, 2012. **13**(4): p. 227-232.

433. Rossi, J.J., *RNAi and the P-body connection.* Nat Cell Biol, 2005. **7**(7): p. 643-644.

434. Bhattacharyya, S.N., et al., *Stress-induced reversal of microRNA repression and mRNA P-body localization in human cells.* Cold Spring Harb Symp Quant Biol, 2006. **71**: p. 513-21.

435. Androsavich, J.R. and B.N. Chau, *Non-inhibited miRNAs shape the cellular response to anti-miR.* Nucleic Acids Research, 2014. **42**(11): p. 6945-6955.

436. Henrotin, Y.E., et al., *Modulation of human chondrocyte metabolism by recombinant human interferon.* Osteoarthritis Cartilage, 2000. **8**(6): p. 474-82.

437. Goldring, M.B., et al., *Immune interferon suppresses levels of procollagen mRNA and type II collagen synthesis in cultured human articular and costal chondrocytes.* J Biol Chem, 1986. **261**(19): p. 9049-55.

438. McGee, D.W., et al., *Transforming growth factor-beta and IL-1 beta act in synergy to enhance IL-6 secretion by the intestinal epithelial cell line, IEC-6.* J Immunol, 1993. **151**(2): p. 970-8.

439. Bender, S., et al., *Interleukin-1 beta induces synthesis and secretion of interleukin-6 in human chondrocytes.* FEBS Lett, 1990. **263**(2): p. 321-4.

440. Zhou, J., et al., *MiR-146a regulated IL-6 expression promotes monocyte proliferation in sepsis patients.* The Journal of Immunology, 2012. **188**(Meeting Abstracts 1): p. 117.22.

441. He, Y., et al., *MiR-146a regulates IL-6 production in lipopolysaccharide-induced RAW264.7 macrophage cells by inhibiting Notch1.* Inflammation, 2014. **37**(1): p. 71-82.

442. Derynck, R. and Y.E. Zhang, *Smad-dependent and Smad-independent pathways in TGF-beta family signalling.* Nature, 2003. **425**(6958): p. 577-84.

443. Proudfoot, N.J., *Ending the message: poly(A) signals then and now.* Genes Dev, 2011. **25**(17): p. 1770-82.

444. An, J., et al., *A dynamic interplay between alternative polyadenylation and microRNA regulation: Implications for cancer (Review).* International journal of oncology, 2013. **43**(4): p. 995-1001.

445. Tian, B., et al., *A large-scale analysis of mRNA polyadenylation of human and mouse genes.* Nucleic Acids Res, 2005. **33**(1): p. 201-12.

446. Wang, E.T., et al., *Alternative isoform regulation in human tissue transcriptomes.* Nature, 2008. **456**(7221): p. 470-6.

447. Zhang, H., J.Y. Lee, and B. Tian, *Biased alternative polyadenylation in human tissues.* Genome Biol, 2005. **6**(12): p. R100.

448. Katayama, S., et al., *Antisense transcription in the mammalian transcriptome.* Science, 2005. **309**(5740): p. 1564-6.

449. Faghihi, M.A., et al., *Expression of a noncoding RNA is elevated in Alzheimer's disease and drives rapid feed-forward regulation of beta-secretase.* Nat Med, 2008. **14**(7): p. 723-30.

450. Faghihi, M.A., et al., *Evidence for natural antisense transcript-mediated inhibition of microRNA function.* Genome Biol, 2010. **11**(5): p. R56.

451. Barreau, C., L. Paillard, and H.B. Osborne, *AU-rich elements and associated factors: are there unifying principles?* Nucleic Acids Res, 2005. **33**(22): p. 7138-50.

452. Connerty, P., A. Ahadi, and G. Hutvagner, *RNA Binding Proteins in the miRNA Pathway.* Int J Mol Sci, 2015. **17**(1).

453. Jacobsen, A., et al., *Signatures of RNA binding proteins globally coupled to effective microRNA target sites.* Genome Res, 2010. **20**(8): p. 1010-9.

454. Bhattacharyya, S.N., et al., *Relief of microRNA-mediated translational repression in human cells subjected to stress.* Cell, 2006. **125**(6): p. 1111-24.

455. Ji, Z., et al., *Progressive lengthening of 3′ untranslated regions of mRNAs by alternative polyadenylation during mouse embryonic development.* Proceedings of the National Academy of Sciences, 2009. **106**(17): p. 7028-7033.

456. Boutet, S.C., et al., *Alternative polyadenylation mediates microRNA regulation of muscle stem cell function.* Cell Stem Cell, 2012. **10**(3): p. 327-36.

457. Spangenberg, L., et al., *Role of Alternative Polyadenylation during Adipogenic Differentiation: An <italic>In Silico</italic> Approach.* PLoS ONE, 2013. **8**(10): p. e75578.

458. Ebert, M.S., J.R. Neilson, and P.A. Sharp, *MicroRNA sponges: competitive inhibitors of small RNAs in mammalian cells.* Nat Methods, 2007. **4**(9): p. 721-6.

459. Haraguchi, T., Y. Ozaki, and H. Iba, *Vectors expressing efficient RNA decoys achieve the long-term suppression of specific microRNA activity in mammalian cells.* Nucleic Acids Res, 2009. **37**(6): p. e43.

460. Lolli, A., et al., *Silencing of Antichondrogenic MicroRNA-221 in Human Mesenchymal Stem Cells Promotes Cartilage Repair In Vivo.* Stem Cells, 2016. **34**(7): p. 1801-11.